

Aus dem Institut für Klinische Neurowissenschaften und Medizinische Psychologie  
Direktor: Univ.-Prof. Dr. med. Alfons Schnitzler

***The rhythm of perception:  
Neuronal oscillatory activity  
underlying perceptual processes***

Habilitationsschrift

zur Erlangung der Venia Legendi für das Fach

Kognitive Neurowissenschaften

an der Hohen Medizinischen Fakultät der Heinrich-Heine-Universität Düsseldorf

Vorgelegt von

Dr. rer. nat. Joachim Lange

Düsseldorf 2020

### **Eidesstattliche Erklärung:**

Hiermit versichere ich an Eides statt, dass ich die vorliegende Habilitationsschrift ohne unerlaubte Hilfe angefertigt und das benutzte Schrifttum vollständig erwähnt habe.

Zudem versichere ich, dass es keine anderen eingeleiteten oder erfolglos beendeten Habilitationsverfahren gibt.

Bei den wissenschaftlichen Untersuchungen, die Gegenstand dieser schriftlichen Habilitationsleistung sind, wurden ethische Grundsätze und die jeweils gültigen Empfehlungen zur Sicherung guter wissenschaftlicher Praxis eingehalten.

A handwritten signature in black ink, appearing to read 'J. Lange'. The signature is fluid and cursive, with a long horizontal stroke extending to the right.

Dr. rer. nat. Joachim Lange

Düsseldorf, November 2020

## I. Zusammenfassung

Unser alltägliches Leben wird zu einem Großteil von Rhythmen bestimmt. Diese Rhythmen sind mannigfaltig und können auf unterschiedlichen Ebenen unser Leben sehr unterschiedlich beeinflussen. Man denke zum Beispiel an den Tag und Nacht-Rhythmus oder den ungleich schnelleren Rhythmus des Herzschlags. Darüber hinaus können auch Neuronen rhythmisch aktiv sein. Dieser Rhythmus wird *neuronale Oszillation* genannt. Neuronal Oszillationen kommen in vielen Gehirnarealen und in unterschiedlichen Frequenzen vor. Auf der einen Seite ist seit langem bekannt, dass diese neuronalen Oszillationen unser Verhalten, Handlung und Wahrnehmung beeinflussen. Auf der anderen Seite sind die genauen Prozesse nicht vollständig verstanden und werden teils kontrovers diskutiert.

In der vorliegenden Arbeit wurde die Rolle der neuronalen Oszillationen für die Wahrnehmung untersucht. Aber auch Wahrnehmung selbst ist nicht konstant, sondern kann über die Zeit rhythmisch fluktuieren. Diese rhythmischen Fluktuationen der Wahrnehmung wurden in den vorliegenden Arbeiten untersucht, um die neuronalen Mechanismen der Wahrnehmung besser zu verstehen.

Die vorliegenden Arbeiten bedienen sich einem weiten Spektrum an Methoden. Neuronale Oszillationen wurden nicht-invasiv mittels Magnetenzephalographie (MEG) untersucht, während die Wahrnehmung in Verhaltensstudien erfasst wurde. Darüber hinaus wurden mittels transkranieller Wechselstromstimulation (tACS; vom englischen *transcranial alternating current stimulation*) neuronale Oszillationen nicht-invasiv manipuliert. Zusätzlich wurde mittels Magnetresonanztomographie (MRS) die Rolle des Neurotransmitters  $\gamma$ -Aminobuttersäure (GABA, vom englischen  *$\gamma$ -aminobutyric-acid*) für neuronale Oszillationen und Wahrnehmung untersucht.

Die Ergebnisse der Studien zeigen, dass neuronale Oszillationen eine fundamentale Rolle spielen für die funktionale Interaktion innerhalb und zwischen neuronalen Gruppen. Diese Interaktion wiederum beeinflusst die Wahrnehmung. Zweitens konnte gezeigt werden, dass neuronale Oszillationen bereits vor einer Stimulation Wahrnehmung beeinflussen, indem sie die Erregbarkeit der Neuronen modulieren und so die kortikale Verarbeitung und damit Wahrnehmung beeinflussen. Drittens konnte gezeigt werden, dass Wahrnehmung selbst ein rhythmischer Prozess ist. Dies liefert Evidenzen, dass Wahrnehmung in diskreten, diskontinuierlichen Schritten verläuft. Zuletzt konnte gezeigt werden, dass Patienten mit hepatischer Enzephalopathie (HE) in ihrer Wahrnehmung beeinträchtigt sind und diese Beeinträchtigung potenziell als Marker der HE dienen kann. Untersuchungen der neuronalen Oszillationen konnten zudem neue Einblicke in die Pathophysiologie der HE geben.

Zusammengefasst liefern die Studien der vorliegenden Arbeit neue Erkenntnisse in die funktionale Rolle der neuronalen Oszillationen für neuronale Prozesse und Wahrnehmung. Die Ergebnisse liefern zudem Evidenzen, dass - im Gegensatz zum subjektiven Empfinden - Wahrnehmung ein diskreter, diskontinuierlicher Prozess ist. Pathophysiologische neuronale Oszillationen beeinträchtigen somit Wahrnehmung. In zukünftigen Studien könnte die Untersuchung von neuronalen Oszillationen somit weitere Einblicke in die pathophysiologischen Gehirnprozesse liefern.

## II. Summary

Rhythms are an omnipresent phenomenon in everyday life. These rhythms can be present on different levels and time scales, such as the circadian rhythm or the rhythm of the heartbeat. Also, neuronal activity can fluctuate in a rhythmic pattern – so-called neuronal oscillations. These neuronal oscillations have been shown to influence behaviour, action, and perception. In addition to intrinsic neuronal oscillations, perception itself can fluctuate over time and show rhythmic patterns. While these rhythmic patterns are well known, the role of neuronal oscillations for perception and the cause for the rhythmic patterns of perception are not well understood and controversially discussed.

The common aim of the studies of the present thesis is to shed further light on the role of neuronal oscillations for perception. Furthermore, the inherent oscillations of perception were investigated to elucidate the underlying mechanisms of perception.

To accomplish this goal, the studies used a spectrum of complementary methods. Neuronal oscillations of the human brain were measured non-invasively by means of magnetoencephalography (MEG), while perception was assessed in behavioural tasks. In addition, neuronal oscillations were non-invasively modulated with transcranial alternating current stimulation (tACS). Finally, to elucidate the underlying mechanisms of neuronal oscillations and perception on the level of neurotransmitters,  $\gamma$ -aminobutyric-acid (GABA) was measured by means of magnetic resonance spectroscopy (MRS).

The studies of the present thesis revealed new insights in the functional interaction of neuronal groups and their functional role for perception. This functional interaction was mediated by neuronal oscillations in specific frequency bands. Secondly, the studies revealed that neuronal oscillations prior to stimulation define brain states that substantially influence perception. Thirdly, it was demonstrated that the rhythmic processes of perception provide evidence for a discrete nature of perception. Finally, studies on groups of patients suffering from hepatic encephalopathy (HE) revealed that impaired perception can act as a marker of HE and that studying neuronal oscillations provides insights into the pathophysiology of HE.

In sum, the studies of the present thesis provide new evidence for a fundamental and functional role of neuronal oscillations for neuronal processing, interaction, and eventually perception. Furthermore, these results suggest that due to the inherent rhythmic neuronal processes, perception itself is a discrete and rhythmic process. Consequently, aberrant neuronal oscillations lead to impaired perception and behaviour. The results of the present studies suggest that studying neuronal oscillations might provide a window into pathophysiological processes of the brain.

### III. Selected research articles published in this thesis

- 1) Wittenberg, M. A., Morr, M., Schnitzler, A., & Lange, J. (2019).  
10 Hz tACS over somatosensory cortex does not modulate supra-threshold tactile temporal discrimination in humans.  
*Frontiers in Neuroscience*, *13*, 311.
- 2) Wittenberg, M. A., Baumgarten, T. J., Schnitzler, A., & Lange, J. (2018).  
U-shaped relation between prestimulus alpha-band and poststimulus gamma-band power in temporal tactile perception in the human somatosensory cortex.  
*Journal of Cognitive Neuroscience*, *30*(4), 552–564.
- 3) Lazar, M., Butz, M., Baumgarten, T. J., Füllenbach, N.-D., Jördens, M. S., Häussinger, D., Schnitzler, A., & Lange, J. (2018).  
Impaired tactile temporal discrimination in patients with hepatic encephalopathy.  
*Frontiers in Psychology*, *9*, 2059.
- 4) Baumgarten, T. J., Neugebauer, J., Oeltzschner, G., Füllenbach, N.-D., Kircheis, G., Häussinger, D., Lange, J., Wittsack, H.-J., Butz, M., & Schnitzler, A. (2018).  
Connecting Occipital Alpha Band Peak Frequency, Visual Temporal Resolution, and Occipital GABA Levels in Healthy Participants and Hepatic Encephalopathy Patients.  
*NeuroImage: Clinical*, *20*, 347-356.
- 5) Baumgarten, T. J., Königs, S., Schnitzler, A., & Lange, J. (2017a).  
Subliminal stimuli modulate somatosensory perception rhythmically and provide evidence for discrete perception.  
*Scientific Reports*, *7*:43937. <https://doi.org/10.1038/srep43937>
- 6) Baumgarten, T. J., Schnitzler, A., & Lange, J. (2017b).  
Beyond the Peak—Tactile Temporal Discrimination Does Not Correlate with Individual Peak Frequencies in Somatosensory Cortex.  
*Frontiers in Psychology*, *8*, 421. <https://doi.org/10.3389/fpsyg.2017.00421>
- 7) Baumgarten, T. J., Oeltzschner, G., Hoogenboom, N., Wittsack, H.-J., Schnitzler, A., & Lange, J. (2016a).  
Beta peak frequencies at rest correlate with endogenous GABA<sup>+</sup>/Cr concentrations in sensorimotor cortex areas.  
*PloS One*, *11*(6), e0156829.
- 8) Baumgarten, T. J., Schnitzler, A., & Lange, J. (2016b).  
Prestimulus Alpha Power Influences Tactile Temporal Perceptual Discrimination and Confidence in Decisions.  
*Cerebral Cortex (New York, N.Y.: 1991)*, *26*(3), 891–903.
- 9) Baumgarten, T. J., Schnitzler, A., & Lange, J. (2015).  
Beta oscillations define discrete perceptual cycles in the somatosensory domain.  
*Proceedings of the National Academy of Sciences*, *112*(39), 12187–12192.
- 10) Lange, J., Pavlidou, A., & Schnitzler, A. (2015).  
Lateralized modulation of beta-band power in sensorimotor areas during action observation.  
*Frontiers in Integrative Neuroscience*, *9*.
- 11) Pavlidou, A., Schnitzler, A., & Lange, J. (2014a).  
Distinct spatio-temporal profiles of beta-oscillations within visual and sensorimotor areas

during action recognition as revealed by MEG.  
*Cortex*, 54, 106–116.

- 12) Pavlidou, A., Schnitzler, A., & Lange, J. (2014b).  
Interactions between visual and motor areas during the recognition of plausible actions as revealed by magnetoencephalography.  
*Human brain mapping*, 35(2), 581-592.
- 13) Lange, J., Christian, N., & Schnitzler, A. (2013a).  
Audio–visual congruency alters power and coherence of oscillatory activity within and between cortical areas.  
*NeuroImage*, 79, 111–120.
- 14) Lange, J., Oostenveld, R., & Fries, P. (2013b).  
Reduced occipital alpha power indexes enhanced excitability rather than improved visual perception.  
*The Journal of Neuroscience: The Official Journal of the Society for Neuroscience*, 33(7), 3212–3220.
- 15) Lange, J., Halacz, J., van Dijk, H., Kahlbrock, N., & Schnitzler, A. (2012).  
Fluctuations of prestimulus oscillatory power predict subjective perception of tactile simultaneity.  
*Cerebral Cortex (New York, N.Y.: 1991)*, 22(11), 2564–2574.
- 16) Lange, J., Oostenveld, R., & Fries, P. (2011).  
Perception of the touch-induced visual double-flash illusion correlates with changes of rhythmic neuronal activity in human visual and somatosensory areas.  
*NeuroImage*, 54(2), 1395–1405.

Ich weise darauf hin, dass die in der vorliegenden Habilitationsschrift zusammengefassten Publikationen Baumgarten et al. 2015, 2016a, 2016b sowie Pavlidou et al. 2014a, 2014b in abgeschlossene Promotionen der Mathematisch-Naturwissenschaftlichen Fakultät der Heinrich-Heine-Universität eingegangen sind. Die Publikationen Wittenberg et al. 2018 und 2019 sind Teil eines derzeit noch laufenden Promotionsverfahrens der Mathematisch-Naturwissenschaftlichen Fakultät der Heinrich-Heine-Universität. Die Publikation Lazar et al. 2018 ist in eine abgeschlossene Promotion an der Medizinischen Fakultät der Heinrich-Heine-Universität eingegangen. Darüber hinaus sind Teile der Publikation Lange et al. 2013a in eine Masterarbeit der Mathematisch-Naturwissenschaftlichen Fakultät der Heinrich-Heine-Universität eingegangen.

<b><i>I. Zusammenfassung</i></b> .....	<b><i>II</i></b>
<b><i>II. Summary</i></b> .....	<b><i>III</i></b>
<b><i>III. Selected research articles published in this thesis</i></b> .....	<b><i>IV</i></b>
<b>1 State of the art</b> .....	<b>1</b>
<b>1.1 Periodicity and rhythms</b> .....	<b>1</b>
<b>1.2 Neuronal Oscillations</b> .....	<b>2</b>
<b>1.3 Frequency bands</b> .....	<b>3</b>
1.3.1 Alpha (~8-12 Hz).....	4
1.3.2 Beta (~13-30 Hz).....	4
1.3.3 Gamma (~30-150 Hz) .....	5
1.3.4 Theta (~3-7 Hz).....	6
<b>1.4 Measuring neuronal oscillations with MEG</b> .....	<b>6</b>
<b>1.5 Perception and (neuronal) oscillations</b> .....	<b>8</b>
1.5.1 Multisensory integration and neuronal oscillations.....	9
1.5.2 Brain states and neuronal oscillations .....	10
<b>1.6 Rhythmic perception</b> .....	<b>11</b>
1.6.1 Rhythmic patterns of perception .....	11
1.6.2 Perceptual cycles of perception .....	12
<b>2 Summary of selected research articles</b> .....	<b>13</b>
<b>2.1 Neuronal oscillatory activity correlates with neuronal integration processes</b> .....	<b>13</b>
2.1.1 Multisensory integration.....	13
2.1.2 Visuo-motor integration.....	15
<b>2.2 Prestimulus neuronal oscillations index cortical states and influence perception</b> .....	<b>17</b>
<b>2.3 Perceptual cycles and rhythmic perception</b> .....	<b>21</b>
<b>2.4 Aberrant neuronal oscillations and perception</b> .....	<b>24</b>
<b>3 General Discussion</b> .....	<b>27</b>
<b>3.1 Intra- and crossmodal neuronal interactions underlying perception</b> .....	<b>27</b>
<b>3.2 Perceptual cycles</b> .....	<b>28</b>
<b>3.3 Aberrant neuronal oscillation and impaired perception</b> .....	<b>29</b>
<b>4 Outlook</b> .....	<b>30</b>
<b>4.1 Potential future directions in cognitive sciences</b> .....	<b>30</b>
<b>4.2 Potential future studies directions in clinical research</b> .....	<b>31</b>
<b>5 Conclusion</b> .....	<b>32</b>
<b>6 Bibliography</b> .....	<b>33</b>
<b>7 Danksagung</b> .....	<b>43</b>
<b>8 Appendix</b> .....	<b>44</b>

# 1 State of the art

## 1.1 Periodicity and rhythms

Periodicity refers to a repeating pattern across space and time. Periodic patterns are ubiquitous in nature and can be found at many different levels of time and space: planets rotate around their central star with a constant periodicity, clocks tick regularly and with constant rhythm, music typically inherits rhythms, and our everyday life is strongly influenced by the periodic change of light caused by the constant rotation of earth around its own axis, i.e. the circadian rhythm.

The circadian rhythm is just one of several rhythms that influence human behaviour and functioning. These rhythms can occur on different time scales and have different functions. Rhythms can originate from the outside world, but rhythmic patterns can also be generated by the human body itself, such as heartbeat or the respiratory rhythm. Since the seminal work by Hans Berger (1929), it is known that also the brain can generate rhythmic patterns of neuronal activity. Since Berger's discovery, neuronal rhythms at different frequencies have been described in almost all parts of the brain (Buzsáki et al., 2013). The selective occurrence or modulation of neuronal oscillations during different cognitive, perceptual, and motor tasks suggests that they are functionally relevant. The functions, however, are controversially discussed and a unifying framework for the role of neuronal rhythms is still not found (see chapter 1.3 Frequency bands).

In addition to intrinsic brain rhythms, human behaviour, actions, and perception show rhythmic patterns. For example, speech is known to be structured at different time scales and thus contains different rhythms ( e.g., for consonants, syllables, words, semantics; Rosen et al., 1992). Also, normal and pathological movements reveal specific rhythmic patterns (Schnitzler et al., 2006). Finally, even sustained attention and perceptual processes are not constant, but show rhythmic waxing and waning over time (VanRullen, 2016; VanRullen et al., 2007; VanRullen & Koch, 2003b).

In summary, rhythmic patterns are omnipresent in brain activity, behaviour, and perception. Their functional role and their interplay, however, is still not well understood. In the present work, I will study the rhythmicity of perception. I will study the role of the brain rhythms for perception by measuring brain activity with magnetencephalography (MEG), as well as the rhythmic patterns of perception itself in behavioural studies. Furthermore, the putative role of rhythmic brain activity for rhythmic perception in healthy participants and pathological rhythms in patients will be studied in a combination of different methods (behavioural studies, MEG, transcranial alternating current stimulation [tACS], and magnetic resonance spectroscopy [MRS]).

## 1.2 Neuronal Oscillations

Since the seminal work by Hans Berger in the 1920s, it is known that brain activity can show rhythmic activity patterns (Berger, 1929). In a series of studies, Berger used electroencephalography (EEG) to record non-invasively neuronal activity outside the brain. Berger realized that the recorded data showed a remarkably regular rhythmic pattern close to a sine wave with “10-11 waves per second” (Figure 2).

Such rhythmic patterns of neuronal activity are nowadays typically termed *neuronal oscillations*. Since Berger’s times, numerous studies have shown that neuronal oscillations are a ubiquitous phenomenon in the brain. They are present in simple and complex systems and on multiple levels of the brain, from subcortical to cortical areas (Buzsáki et al., 2013).

Neuronal oscillations can be found in single neurons and in neuronal populations of neuronal networks. In single neurons, membrane potentials can fluctuate over time. Such fluctuations show oscillatory patterns. Oscillating potentials can be below the threshold to elicit spike activity. Yet, the fluctuating potentials can crucially influence neuronal activity by modulating the probability of spikes.

Single neurons can form functional networks by reciprocally coupling with other neurons. As a result of reciprocal coupling, several classes of specific networks of inhibitory interneurons are formed (Klausberger & Somogyi, 2008). Inhibitory interneurons play a crucial role for the generation of oscillatory activity in neuronal networks. It has been known for a long time that in a network of reciprocally coupled excitatory and inhibitory neurons, fast excitation is followed by slower feedback inhibition. Such reciprocal interplay gives rise to oscillations (e.g., Whittington et al., 1995; Wilson & Cowan, 1972). In addition, it has been shown that oscillatory activity can arise in networks of purely inhibitory neurons (e.g., Van Vreeswijk et al., 1994; Wang & Buzsáki, 1996). These inhibitory properties play a crucial role in the temporal dynamics of the network activity and thus critically contribute to the frequency of the oscillatory activities.

Within such networks neurons tend to synchronize their rhythmic activity, resulting in networks of synchronized neuronal oscillatory activity. Synchronisation here refers to the state in which two systems (e.g., neurons or neuronal networks) display the same frequency. Neuronal synchronisation is often interpreted as an indicator of interaction of the two systems. That is, neuronal groups might be coactivated by the same source or and they co-synchronize their neuronal patterns by intra-network interactions. If these neurons not only temporally align their activity, but are also spatially aligned, their activity can sum up. Eventually, the net activity is strong enough to be measured non-invasively outside the brain by means of MEG or EEG (see chapter 1.4 for details).

To determine the frequency of neuronal oscillations, often the so-called Fourier Transformation is applied on the recorded time-series data. The method of Fourier Transformation was discovered in 1822 by the French mathematician and physicist Jean-Baptiste Joseph Fourier. He revealed that any (periodic) signal can be described as a series of sine waves, which describe regular periodic signals (Figure 1). Hence, Fourier transformation reveals the presence of periodic signals in a recorded signal. Consequently, with the help of

Fourier transformation neuronal oscillations can be detected in brain signals and their frequencies as well as their relative contribution to the signal can be analysed.

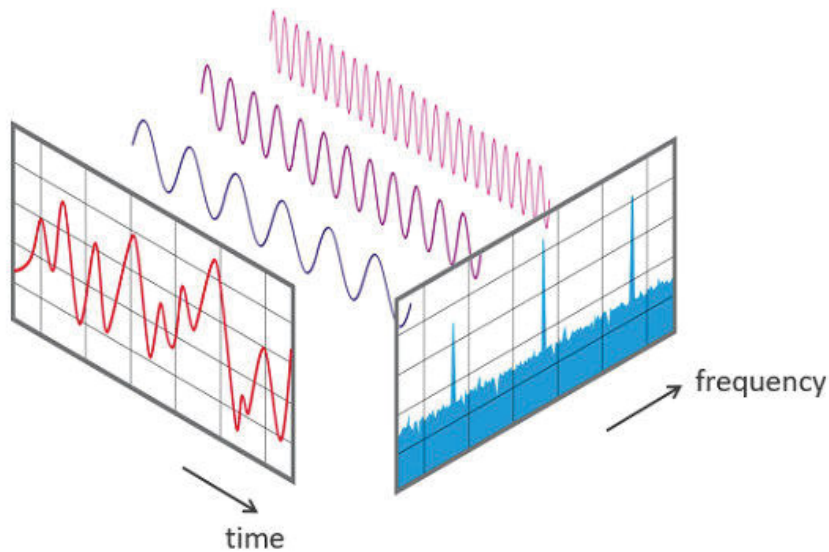


Figure 1: Illustration of the principle of Fourier transformation: A time series signal (red signal, left) can be decomposed into a series of sine waves of different frequencies and amplitudes (purple signals, top). After this decomposition, the time series signal can be represented in the frequency domain (blue signal, right).

Figure by Phonical (<https://commons.wikimedia.org/wiki/File:FFT-Time-Frequency-View.png>), distributed under Creative Commons Attribution-Share Alike 4.0 International license.

The frequencies of neuronal oscillations can range from ultra-slow ( $\sim 0.1$  Hz) to ultrafast ( $\sim 600$  Hz) frequencies. Importantly, these different frequencies do not merely represent a continuum of possible frequencies. Rather, different frequencies (or better: frequency bands) seem to be related to different functions, cognitive states, or neuronal processes.

### 1.3 Frequency bands

In his initial works, Berger observed a regular, rhythmic pattern in his EEG recordings with “10-11 waves per second” (Figure 2; Berger, 1929). Interestingly, the amplitude of this rhythmic activity decreased with attention or intellectual work. This frequency band was later named the *alpha* frequency band. Since then, multiple frequency bands have been identified that are believed to reflect different cognitive, motor, or behavioural states or functions. I will briefly describe below the four frequency bands which play the most important roles for my studies.

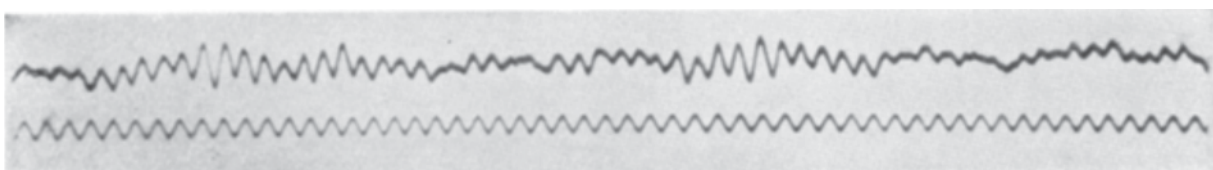


Figure 2: An EEG recording of brain activity showing alpha-band activity as published by Berger (1929). Top row shows 5.5 s of recordings. Note the rhythmic pattern and the modulation of the amplitude (by different cognitive states). Bottom row shows a sine wave with a frequency of 10 Hz as a reference signal. Figure from Berger (1929) adapted and printed with permission from Springer Nature.

### 1.3.1 Alpha (~8-12 Hz)

As described above, the alpha frequency band was first described by Berger (1929). While alpha is most prominent in parietal areas of the cortex, it can be found in many other areas, including sensory areas. As already noticed by Berger, alpha oscillations are present even in the absence of external stimulation. In sensory areas, the power of alpha oscillations decreases after stimulation. But the power of alpha oscillations can be modulated also in the absence of sensory stimulation. For example, alpha power increases if the eyes are closed and decreases with eyes open, even in darkness. In addition, alpha power decreases if the participant is more attentive. This led to the hypothesis that alpha power reflects an idling process, indicating a cortical area is deactivated from the neuronal processing (Pfurtscheller et al., 1996).

Following studies extended the view on the functional role of alpha oscillations. Several studies have shown that spatial attention to one hemifield decreases alpha power in contralateral sensory areas, while alpha power increases in the ipsilateral site (e.g., Haegens et al., 2011; Thut et al., 2006; Worden et al., 2000). From this finding of lateralized increases and decreases, Jensen and Mazaheri (2010) developed the theory that alpha power reflects a gating mechanism for information flow and neuronal processing in the brain. In this theory, cortical sites with increased alpha power are actively blocked from neuronal processing, while information processing is guided to sites with decreased alpha power.

Another theory argues that alpha oscillations reflect a state of excitability of cortical areas. The lower alpha power, the higher the excitability, i.e. the more effective a stimulus will be processed (Romei et al., 2008; Sauseng et al., 2009). Recent studies revealed that at states of low alpha power not only sensitivity to target stimuli is increased – leading to increased hit rates -, but sensitivity is also increased to non-target or noise stimuli – leading to increased false alarms rates. In sum, alpha power would reflect shifts of decision criterion rather than improved perception. With lower alpha power thresholds for perception become more liberal and vice versa (Iemi et al., 2016; Limbach & Corballis, 2016).

### 1.3.2 Beta (~13-30 Hz)

Already in 1929 Berger observed in addition to alpha waves (“10-11 waves per second”) a second rhythm with smaller amplitude and “20-30 waves per second” (Berger, 1929). Later, he named this rhythm “ $\beta$ -waves”; today this frequency band between ~13-30 Hz is named the beta-frequency band. First evidence for a functional separation of alpha and beta frequencies was found by Jaspers and Andrews (1936): While neuronal oscillations in the parieto-occipital alpha-band decreased after visual stimulation, neuronal oscillations in sensorimotor beta-band were found to be unaffected by visual stimulation but to decrease after tactile stimulation (Jasper & Andrews, 1936). In another seminal work, Jasper and Penfield (1949) reported strong neuronal oscillations in the beta-band (~25 Hz) in sensorimotor areas that were mostly present during movement preparation (“readiness”) and diminished during movement execution.

Since these days, neuronal oscillations in the beta-band have been regarded as a rhythm of sensorimotor cortex. Numerous studies have reported beta oscillations in sensorimotor cortex and their modulation by motor-related tasks such as motor preparation, execution, or even imagination of movements (e.g., Pfurtscheller et al., 1998; Schnitzler et al., 1997, 2006; Schnitzler & Gross, 2005). In line with the hypothesis that beta oscillations are crucial in movement, aberrant beta oscillations have been reported in movement disorders like Parkinson's disease (Hammond et al., 2007; Hirschmann et al., 2011; Little & Brown, 2014; Schnitzler & Gross, 2005).

While beta oscillations are most prominent in the sensorimotor system, their role is not limited to the sensorimotor system. Beta power and synchronization in the beta band has also been implicated in broader cognitive processes. For example, beta oscillations seem to play a role in long-range interactions between neuronal groups (Gross et al., 2004). Other studies suggest that interactions in the beta-band predominate in cognitive and perceptual tasks that strongly involve endogenous top-down processes (Buschman & Miller, 2007; Michalareas et al., 2016; Pesaran et al., 2008; Richter et al., 2017). It has been suggested that beta oscillations indicate that the motor or cognitive system is holding its present "status quo", a continuation of the current motor or cognitive state (Engel & Fries, 2010).

### 1.3.3 Gamma (~30-150 Hz)

Gamma oscillations refer to rhythmic neuronal activity within a frequency of ~30-80 (or even up to 150 Hz). Compared to alpha and beta-band activity, gamma oscillations have been in the focus of science relatively late. Although already in 1938 Jasper and Andrews (1938) observed frequencies with 35-45 Hz in the human EEG and suggested to call them "gamma waves", the phrase gamma oscillations became popular only in the 1980s (Bressler & Freeman, 1980). One reason for the lack of interest of research in gamma oscillations might have been that gamma oscillations are more difficult to detect. The power of neuronal oscillations typically decreases with increasing frequencies. Thus, the power of gamma oscillations is much lower than alpha and beta power and thus harder to detect in noisy data. In addition, gamma oscillations typically occur in local networks.

Gamma oscillations are observed in many subcortical and cortical areas across many species (Buzsáki et al., 2013), yet their functions and mechanisms remain a matter of debate. Gamma oscillations are believed to emerge from an interplay of excitatory and inhibitory neurons (Buzsáki & Wang, 2012).

Earlier studies have proposed that gamma oscillations inherit the temporal features to form an efficient mechanism for the binding of object features to a coherent object – the so-called feature binding theory (Eckhorn et al., 1988; Gray et al., 1989; Singer & Gray, 1995). More recent studies have proposed that synchronization of neuronal populations in the gamma frequency might form a more general mechanism for effective signal processing. Signals of multiple neurons converging on another neuron up the hierarchy of stimulus processing are temporally coordinated by synchronisation in the gamma-band – the so-called communication by coherence theory (Fries, 2005, 2015). In addition, studies have linked

gamma oscillations to attention (Bauer et al., 2006; Fries et al., 2001; Hoogenboom et al., 2006; Womelsdorf & Fries, 2007).

#### 1.3.4 Theta (~3-7 Hz)

The theta rhythm (~3-7 Hz) is most prominent in hippocampus and neighbouring structures. Theta oscillations are best known for their role in spatial navigation in rat hippocampus (Bland, 1986; Buzsáki, 2002; Buzsáki & Moser, 2013).

In human cortex, theta oscillations have been found predominantly in frontal areas. The power of theta oscillations was found to correlate with working memory tasks (see Axmacher et al., 2006; Klimesch, 1999 for reviews). In addition, theta oscillations have been found to correlate with error monitoring in anterior cingulate cortex (e.g., Cohen, 2011; Luu et al., 2004; Voloh et al., 2015; Womelsdorf et al., 2010).

Furthermore, cumulative evidence shows that theta oscillations interact with gamma oscillations: The phase of the theta frequency-band (3-7 Hz) modulates power in the gamma-band (80-150 Hz). Such cross-frequency coupling has been shown for memory tasks and in hippocampus (Axmacher et al., 2010; Lisman & Jensen, 2013; Osipova et al., 2006), but also for other cognitive task or resting-state brain activity (Canolty et al., 2006; Florin & Baillet, 2015; Maris et al., 2011).

In summary, frequency bands are distinguished by their different functions for cognition, perception, motor functions. The functions, however, of each frequency band can differ depending on the task or stimulation. To define a unifying framework of the functions within and across frequency bands, further experimental and theoretical studies are required.

### 1.4 Measuring neuronal oscillations with MEG

To analyse neuronal oscillations, the neuronal signal needs to be recorded with high temporal resolution in the order of milliseconds. This high temporal resolution is offered by electroencephalography (EEG) and magnetoencephalography (MEG). Both methods are non-invasive methods to record neuronal activity. In contrast to methods like functional magnetic resonance imaging (fMRI) or positron emission tomography (PET), which rely on the relatively slow changes of blood oxygen levels or glucose metabolism, EEG and MEG offer a more direct, instantaneous measure of brain activity with a temporal resolution of < 1 ms. While EEG measures the electric potentials of the summed neuronal signals, MEG measures the magnetic fields. Since magnetic fields are far less distorted by the tissues, skull, etc. than electric fields, the magnetic fields measured by MEG provide a higher spatial accuracy compared to the electric fields of EEG (Baillet et al., 2001). Under ideal conditions, the spatial accuracy of MEG is in the order of millimetres, while in practice the spatial accuracy is ~1-2 cm, depending on the source of the neuronal signal. The studies presented

in this thesis used MEG to record neuronal activity (Figure 3), thus taking advantage of the excellent temporal resolution and the very good spatial resolution of MEG.



*Figure 3: Picture of the 306-channel whole-head MEG device (MEGIN Oy, Helsinki, Finland) at the Institute of Clinical Neuroscience and Medical Psychology, Heinrich Heine University Düsseldorf, which was used in this thesis to record neuronal activity. (Photo taken by author).*

The following paragraphs will provide a more detailed insight in the functioning of MEG.

In any active neuron, membrane potentials are constantly polarized and depolarized, leading to transmembrane current flows. These transmembrane currents cause intra- and extracellular electromagnetic fields. Such electromagnetic fields could be measured if an electrode were placed in the vicinity of the neuron(s) creating the electromagnetic field. This measurement requires, however, an invasive technique. To be eventually strong enough to be measured non-invasively outside the skull, the electromagnetic fields of populations of neurons need to sum up. Effective summation of the electromagnetic fields requires a high temporal coincidence of the single neuronal signals, but also spatial alignment of neurons. If neurons are not spatially aligned, closed fields will be produced that do not reach the outside of the skull (Figure 4A). Only neurons that are aligned in the same direction are able to produce open fields (Figure 4A). Although in principal all neurons might show such spatial alignment, the main contribution to the extracellular electromagnetic fields measured with EEG and MEG is made by pyramidal neurons (Hämäläinen et al., 1993; Hansen et al., 2010). These neurons possess characteristically shaped and orientated long apical dendrites. Pyramidal neurons are arranged parallel to each other and the cells are oriented perpendicular to the cortical surface. This geometry allows for the efficient superposition of synchronously active neurons (Buzsáki et al., 2012; Hämäläinen et al., 1993).

Given that magnetic fields are orientated orthogonally to the underlying currents, sources orientated tangentially to the cortex surface will produce magnetic fields that are maximally

strong outside the skull (Figure 4). In contrast, radially oriented sources produce magnetic fields that cannot be measured with detectors above the source (but to a weaker extent with detectors orthogonal to the source - which in turn is typically farther away from the source; Hämäläinen et al., 1993). Consequently, the orientation of the neuronal source plays an important role for the strength of the measured magnetic field, with maximum activity arising from cortical fissures (Hämäläinen et al., 1993; Hansen et al., 2010).

It is assumed that  $> 10^6$  neurons are necessary to produce magnetic field strengths that are detectable outside the skull (Hämäläinen et al., 1993). Even with such a large number of neurons, the magnetic field strength measured at the skull is only in the order of Femtotesla (fT,  $10^{-15}$  T). Thus, the magnetic fields to be measured with MEG are at the magnitude of the external, non-neuronal noise (like electrical devices, heartbeat, muscle activity, etc.). The small signals require extremely sensitive detectors, shielding of the chamber against external noise sources, and post-hoc artifact detection and removal from the recorded signals.

The extremely sensitive detectors are realized by so-called super-conducting quantum interference devices (SQUIDS). One major principle of SQUIDS is their superconductivity. Superconductivity is achieved by cooling the detectors with liquid helium to temperatures below 4.2 K (Hämäläinen et al., 1993; Zimmerman et al., 1970). A new generation of magnetometers, which do not rely on superconductivity but can work at room temperature, is currently developed (Boto et al., 2017, 2018). Since these devices were not used in my studies, I refrain from a detailed description of these devices.

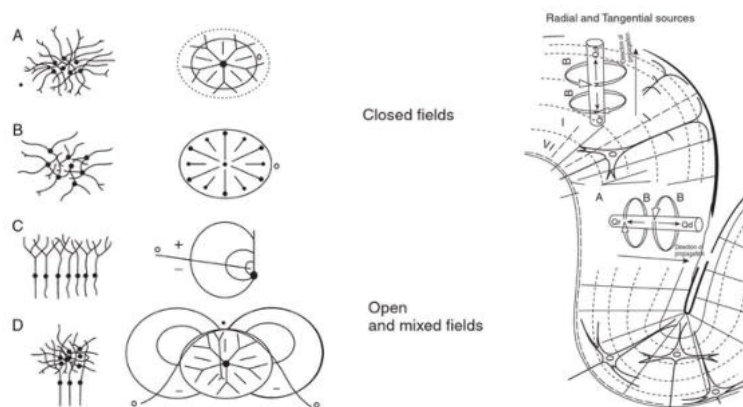


Figure 4: A) Examples of closed and open fields. Left side: Schematic drawing of neuronal populations with different orientations of the single neurons. Right side: Schematic drawings of the resulting closed, open, or mixed magnetic fields. B) A schematic drawing of a part of gyrus. Cylinders illustrate cells with intracellular current flow and extracellular induced magnetic fields. The cylinder at the top induces a radial field, which is invisible for MEG detectors above the source. The source in the middle of the gyrus induces a tangential field, which can be detected by MEG sensors. Figures adapted from Hansen et al., (2010) adapted and printed with permission from Oxford Publishing Limited (Academic).

## 1.5 Perception and (neuronal) oscillations

If information from the environment enters the human body, this information is first processed in the receptor cells. Various receptor types exist, each sensitive to specific features of a stimulus, e.g., photoreceptors of the retina are sensitive to electromagnetic waves of a certain wavelength (i.e., light); mechanoreceptors in the skin are sensitive to

pressure or distortion, etc. Sensory pathways carry the information from the receptor cells to the cerebral cortex. Part of the stimulus properties are encoded in specific, single cells, other features or the interpretation of features is encoded in the population code of many neurons, especially be neurons in the cerebral cortex (Kandel et al., 2000).

Since the work of Weber and Fechner in the 19<sup>th</sup> century, it is clear that the subjective perception of stimulus properties is not necessarily a 1:1 copy of the physical properties of an object or stimulus. Moreover, in contrast to our subjective experience the information entering the sensory system is incomplete and imperfect. For example, if two target stimuli are presented in rapid succession, the second target is often missed, a phenomenon known as the “attentional blink” (Shapiro et al., 1997). So-called ambiguous or bi-stable figures are another striking example that show that perception is more than a mere copy of the environment. In these stimuli the image consists of two separate images – e.g., a face and a vase in the “Rubin vase” example (Kornmeier & Bach, 2012). The two images (face or vase), however, are typically seen not together, but the visual system “favours” and perceives one image and treats the other image as background. Although the visual input remains unchanged, the visual perception alternates over time. Such ambiguous or bi-stable figures demonstrate that perception does not merely rely on the input but also on internal brain states, prior knowledge, expectation, etc., to interpret information, create predictions or fill in missing information.

When the information from external stimuli enters cortex, the signal can elicit neuronal oscillations or modulate existing, ongoing neuronal oscillations. As outlined above, specific frequency bands can be associated with specific neuronal processes or functions. Studying neuronal oscillations in response to specific stimuli can thus provide information about the neuronal process underlying the processing of these stimuli. Moreover, it has been shown that not only the neuronal responses are rhythmical, but also the perceptual process themselves (e.g., VanRullen, 2016).

The following sections will give a brief overview about the role of neuronal oscillations for uni- and multisensory perception.

### 1.5.1 Multisensory integration and neuronal oscillations

When information is received by the sensory receptors, the signal is initially forwarded and processed in unisensory cortical areas. For example, the first cortical area for signals from the photoreceptors is the primary visual cortex in occipital cortex. Typically, natural stimuli bear multimodal information. For example, a car passing by provides visual and auditory information. These auditory and visual information will be processed in the brain initially in different cortical areas (i.e., primary auditory and visual cortex). For a coherent multisensory perception, these separately processed unisensory information needs to be integrated. While traditionally multisensory integration has been assumed to take place in higher, multisensory association areas, where the signals from unisensory areas converge (Stein & Meredith, 1993), more recent studies reported effects of multisensory integration or crossmodal interaction in sensory specific cortical areas (Ghazanfar & Schroeder, 2006; Macaluso & Driver, 2005).

Neuronal oscillations have been shown to play a crucial role for multisensory perception and integration. For example, studies have demonstrated increased gamma band power for multisensory signals compared to the sum of unisensory signals (Sakowitz et al., 2001; Senkowski et al., 2005). This finding is consistent with the early theory that gamma band oscillations reflect binding of stimulus features (Gray et al., 1989). In addition, studies revealed multisensory or crossmodal modulation of neuronal oscillations in primary sensory cortices. For example, Lakatos et al. (2007) revealed that somatosensory stimulation induces a phase reset of ongoing neuronal oscillations in primary auditory cortex. As a result, auditory signals arrive during a phase of high excitability and thus produce amplified neuronal responses. Similarly, visually induced resets of the phase of neuronal oscillations were found to modulate auditory evoked activity (Kayser et al., 2008).

Taken together, studies suggest two possible mechanisms of multisensory integration by neuronal oscillations: (i) a crossmodal phase reset of neuronal oscillations in primary sensory areas resulting in higher excitability for sensory stimuli. (ii) modulation of neuronal oscillations in primary sensory and higher, putative multisensory integration reflecting enhanced neuronal processing of integrated multisensory stimuli.

### 1.5.2 Brain states and neuronal oscillations

Perception is more than a mere 1:1 representation of the physical input to the sensory organs. For example, ambiguous or multistable visual stimuli such as the Rubin vase are perceived differently over time despite constant physical stimulation. Such phenomena impressively demonstrate that perception not only relies on the external input but also depends on intrinsic functional neuronal patterns, so called “brain states”. These brain states are not constant but fluctuate over time. Consequently, a sensory input impinges on different brain states at different time points, and so does perception of a given sensory input vary over time. It has become clear that fluctuations of brain states are more than noise fluctuations.

Studies have demonstrated that ongoing neuronal oscillations may reflect brain states. Already decades ago, Bishop (1932) reported that in visual cortex of rabbits evoked responses could be elicited only at certain intervals in the cycle of the ongoing alpha oscillation. Also in humans, several earlier EEG studies reported that brain states in form of neuronal oscillations influence perception (e.g., Callaway & Yeager, 1960; Nunn & Osselson, 1974).

In recent years, neuroscience has rediscovered the importance of brain states and especially ongoing neuronal oscillation for perception. Studies have revealed higher detection rates for visual stimuli near perceptual threshold if the power of prestimulus parieto-occipital alpha oscillations prior to the stimulus was low (Hanslmayr et al., 2007; Mathewson et al., 2009; Van Dijk et al., 2008). Similarly, perception of near-threshold tactile stimuli depends on the power of ongoing alpha oscillations in somatosensory cortex (Linkenkaer-Hansen et al., 2004).

These neuronal oscillations reflecting brain states can also be influenced, e.g. by attention. When attention is directed towards the location of a stimulus, power of alpha oscillations decreases in visual, auditory, or somatosensory cortex, respectively, contralateral to the (covertly) attended site and increases in ipsilateral sites (e.g., Haegens et al., 2011; Worden et al., 2000). Such modulations of prestimulus neuronal oscillations can substantially influence the perception of upcoming stimuli (e.g., Haegens et al., 2011; Thut et al., 2006).

In addition to power, the phase of prestimulus neuronal oscillations has been shown to influence perception. For example, near-threshold visual stimuli are better detected at certain phases of an alpha oscillation (Dugué et al., 2011; Mathewson et al., 2009).

## 1.6 Rhythmic perception

Subjective experience implies that perception is a constant and seamless continuously ongoing and smooth process. And yet, despite these strong subjective experiences, perception might not be continuous, but rather a discrete or cyclic process (for a review see e.g., VanRullen, 2016). In this view, perception is mediated by discrete temporal “snapshots” of our environment, similar to the functioning of a video camera. The subjective experience of continuous perception would then be an illusion, a temporal ‘filling-in’ created by our brain to cover the temporal gaps of perception, similar to the spatial filling in of visual perception to overcome the spatial gap of the “blind spot” in the retina.

The question whether perception is a continuous or discrete process is a long-standing question in neuroscience, psychology, as well as in philosophy (Busch & VanRullen, 2014). However, as outlined in detail below, the neurophysiological mechanisms underlying the putative discrete perception are unclear and controversially discussed.

One prominent candidate neuronal mechanism that might underlie variations of brain states and the putative discrete or cyclic perception - and putatively perception in general - are neuronal oscillations. The following chapters will summarize the state of the art regarding rhythmic perception and the putative underlying mechanisms.

### 1.6.1 Rhythmic patterns of perception

While subjective experience suggests that perception is a smooth and continuous process, cumulative evidence indicates that processing of incoming information is a fundamentally rhythmic process. When we explore the environment, we constantly redirect attention to different locations or objects. Recent evidence indicates that even when covert attention is sustained to one location, the attentional processes still show rhythmical patterns. Cumulative evidence suggests that the intrinsic rhythm of attentional modulation of perceptual measures is around 4-7 Hz, i.e. in the theta frequency band. For example, in tasks that cued attention, detection rates or reaction times varied rhythmically with a periodicity in the theta frequency range (Fiebelkorn et al., 2013; Landau & Fries, 2012; Song et al., 2014). In addition, it has been demonstrated that perceptual outcome varies as a function of the theta phase even in states of sustained spatial attention (Helfrich et al., 2018).

Also in the absence of attentional modulations, perception is rhythmically modulated. Studies have shown that the phase of neuronal oscillation in occipital cortex influences the likelihood of detecting a visual target that was presented with intensities near around the threshold for detection (Busch et al., 2009; Mathewson et al., 2009). Consequently, visual perception is modulated with a rhythmic pattern, depending on the actual phase of the intrinsic neuronal oscillations (Chakravarthi & VanRullen, 2012; VanRullen et al., 2014). Furthermore, perception in one modality has been shown to be modulated rhythmically also by crossmodal input from another modality. Lakatos et al. (2007) revealed in monkey cortex that somatosensory stimulation resets the phase of neuronal oscillations in primary auditory cortex (A1). Depending on the phase at which auditory signals reached A1, neuronal processing was amplified or deteriorated. Romei et al. (2012) demonstrated in humans that a brief sound induced a periodic pattern of improved/impaired visual perception depending on the time interval between auditory and visual stimuli. These and other studies led to the hypothesis that neuronal oscillations provide temporal windows for cross-modal influences. These temporal windows result in periodic or rhythmic patterns of perception (Bauer et al., 2020).

### 1.6.2 Perceptual cycles of perception

As outlined above, rather than being a uniform process, attention and perception alternate periodically, arguing for a periodic modulation of brain states. As brain states can be reflected by neuronal oscillations, researchers linked neuronal oscillations to the question whether perception is a discrete or continuous process (VanRullen, 2016; VanRullen & Koch, 2003b). The hypothesis of discrete perception argues that incoming stimuli are processed in a succession of single perceptual cycles or snapshots. The theory of perceptual cycles poses that a cycle of a neuronal oscillations provides the basis unit of temporal perception. If two stimuli fall within the same cycle, they will be perceptually fused and perceived as only one stimulus. If two stimuli fall in two separate cycles, they will be processed and perceived separately. Cumulative evidence suggests that these perceptual cycles operate at a ~10 Hz rhythm in the visual domain (Cecere et al., 2015; Samaha & Postle, 2015; VanRullen & Koch, 2003a). For example, Samaha and Postle (2015) showed that participants' temporal visual discrimination thresholds correlated with their individual alpha peak frequencies, providing evidence for a link of alpha frequency to visual perceptual cycles.

While these studies provide evidence for discrete sampling of visual perception, a drawback is their mainly correlative nature, while a causal link between the phase of occipital neuronal oscillations and perception is less established (but see Cecere et al., 2015). Furthermore, while there is substantial evidence for perceptual cycles in the visual modality, evidence for perceptual cycles in the auditory and tactile modality is almost absent (VanRullen, 2016; VanRullen et al., 2014).

## 2 Summary of selected research articles

The central hypothesis of my studies presented in this thesis is that rhythmicity is an essential part of perception. Rhythmicity can be found in patterns of neuronal activity. These are typically termed neuronal oscillations. But also perception itself can show rhythmic patterns.

The role of rhythmicity for perception was studied in four parts:

**In the first part**, the role of rhythmic patterns of neuronal activity for sensory integration in response to stimulation was investigated. I will show in five studies that neuronal oscillations, especially in the beta-band, index the integration of the visual and the motor system during the perception of human movements. In addition, neuronal oscillations in several frequency-bands play a role for multisensory integration processes during audio-visual and visuo-tactile integration.

Neuronal oscillations can be found also in the absence of sensory input – so-called ongoing or prestimulus neuronal oscillations. **In the second part**, the role of ongoing neuronal oscillations for visual, tactile, and visuo-tactile perception was investigated. I will demonstrate in five studies that neuronal oscillations provide insights in the cortical state before a stimulus is presented. In addition, I will show that ongoing fluctuations of these prestimulus neuronal oscillations critically influence perception of subsequent stimuli, within and across sensory modalities.

**In the third part**, the rhythmicity of perception itself was investigated. I will study the long-standing question whether perception is a continuous or discrete process. In three studies, I will provide evidence that perception itself is a rhythmic process. In addition, I will show that neuronal oscillations in the beta-band form the underlying cortical mechanism for discrete and rhythmic perception.

**Finally**, I will show in three studies on healthy participants and patients with hepatic encephalopathy (HE) that aberrant neuronal oscillations and aberrant perception provide information about pathophysiological processes in HE and the role of the neurotransmitter GABA for temporal perception.

### 2.1 Neuronal oscillatory activity correlates with neuronal integration processes

#### 2.1.1 Multisensory integration

Neuronal oscillations have been demonstrated to play a role in multisensory integration. In the present thesis, two multisensory paradigms were used to further elucidate the role of neuronal oscillations for audio-visual and visuo-tactile integration.

The first study (Lange et al., 2011) used a multisensory illusion that was first described in the audio-visual modality (Shams et al., 2000). In this illusion, a briefly presented visual stimulus is accompanied by two brief auditory stimuli. If the stimuli are presented within a time window of ~70 ms, the observers frequently observed an additional, illusory second visual stimulus. Obviously, the illusion relies on multisensory integration of the stimuli. The exact

mechanisms, however, are unknown. The illusion offers thus an excellent opportunity to study the mechanisms of multisensory integration.

In this study, the visuo-tactile variant of the illusion (i.e., a visual stimulus accompanied by two tactile stimuli) was used to study the role of neuronal oscillations for the perception of the illusion – and multisensory integration in general. Twenty-two participants were presented with the paradigm to induce the illusion while we measured the neuronal activity with MEG.

When participants perceived the illusory second stimulus, an increase of occipital gamma-band (80–140 Hz) power was observed relative to trials in which no illusion was perceived (Figure 5A). In addition, in somatosensory areas an increase of power for low frequencies (5–17.5 Hz) and a decrease of power in the 22.5–30 Hz range was observed (Figure 5B). In summary, the results demonstrate that the rhythmic neuronal activity plays an important role for variable subjective experience despite constant physical stimulation.

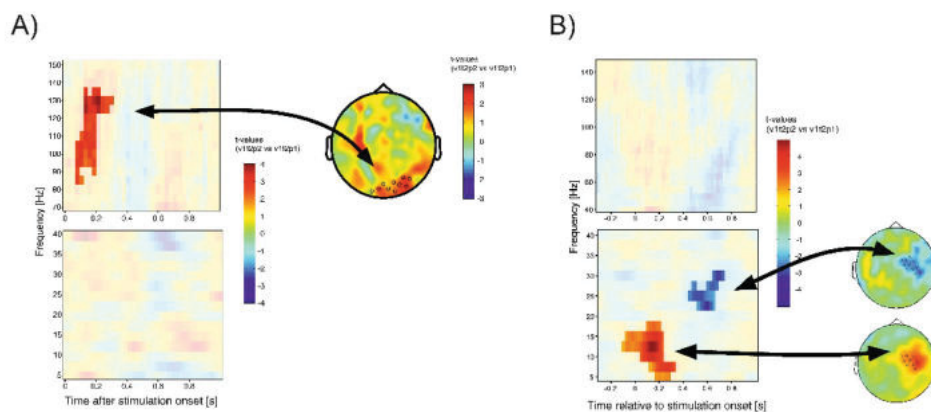


Figure 5: Power of neuronal oscillations in response to visuo-tactile stimulation. A) Left: Time frequency representation of statistical comparison of power between conditions “illusion” vs. “no illusion” perceived averaged across sensors over right visual cortex. Right: Topographical illustration of the significant effect in left plot. B) Same as A), but now for sensors over somatosensory cortex. Significant clusters are highlighted by stronger colours. Red colours indicate higher power in “illusion” trials, blue colours indicate higher power in “no illusion” trials.  $t = 0$  indicates the onset of stimulation. Figure adapted from Lange et al., (2011), adapted and printed with permission from Elsevier.

In a second study (Lange et al., 2013a), the role of neuronal oscillations in audio–visual integration during speech perception was investigated. Participants viewed audio–visual articulations of vowels. In these stimuli, the audio–visual information could be either congruent (visual and auditory information match) or incongruent (modified versions in which visual and auditory signals mismatched). Participants rated whether the stimuli were congruent or incongruent stimuli while their neuronal activity was recorded with MEG.

The contrast of perception of congruent vs. incongruent stimulation revealed an increase of power in theta and alpha frequencies (4–12 Hz) around left auditory cortex, an increase of power in the beta-band (20–30 Hz) in supramarginal gyrus, and an increase of power in the high gamma (120–140 Hz)-band in inferior frontal gyrus (Figure 6A). By analysing coherence (i.e., the relation of phases of the neuronal oscillations in different areas), we were able to reveal a functional coupling between auditory cortex and inferior frontal gyrus. This coupling

was only found for congruent stimuli, while coherence decreased for incongruent stimuli (Figure 6B).

The results demonstrate that neuronal oscillations correlate with the processing of matching audio-visual speech on a large spatio-temporal scale. Neuronal oscillations were also found to indicate a coupling of neuronal groups that mediate audio-visual integration during speech perception.

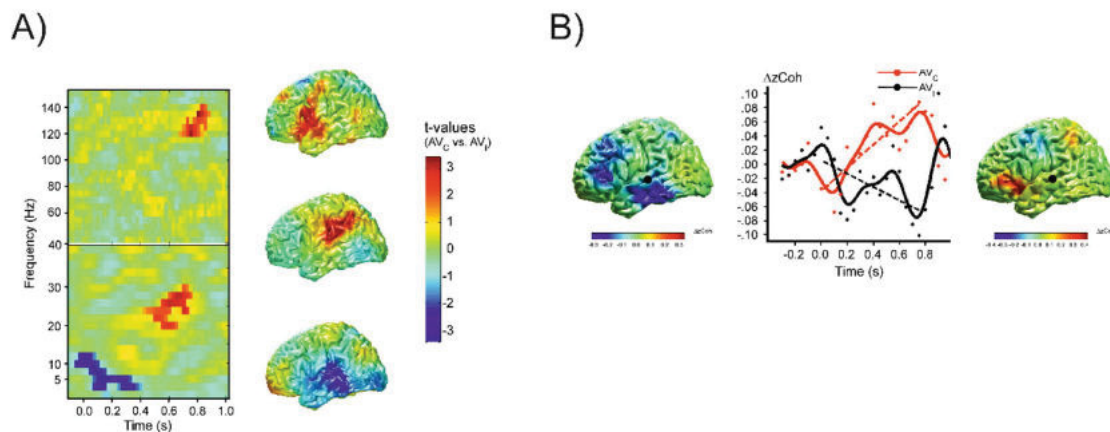


Figure 6: Modulations of neuronal oscillations in response to audio-visual speech stimuli. A) Left: Time-frequency representation of statistical comparison of power between congruent vs. incongruent audio-visual speech stimuli. Significant clusters are highlighted by stronger colours.  $t=0$  indicates onset of stimulation. Right: source reconstruction of the significant effects. Red colours indicate stronger power in congruent stimuli, blue stronger power in incongruent stimuli. B) Results of coherence analysis for congruent and incongruent stimuli. Coherence is shown in relation to auditory cortex (black dot). Left: source reconstruction of coherence at onset of auditory stimulation, middle: temporal evolution of coherence in inferior frontal cortex for congruent and incongruent stimuli, right: same as left, but now for offset of auditory stimulation. Figure adapted from Lange et al., (2013a), adapted and printed with permission from Elsevier.

### 2.1.2 Visuo-motor integration

The perception of human movements is crucial for the interaction with other people. For effective interaction, it is essential to recognize the direction of the movement, the gestures or mimics, or the identity of the moving person. Visual perception and recognition of human movements was for long believed to be a visual process alone. Earlier studies thus focused on the visual features of the movement stimuli or the neuronal activation the stimuli induced in the visual system and adjacent areas of the brain of humans and monkeys (Grossman et al., 2000; Johansson, 1973; Mather et al., 1992; Oram & Perrett, 1994). Only with the discovery of the mirror neuron system, research realized that also – among other areas - the motor premotor areas are involved in movement recognition (Buccino et al., 2001; Gallese et al., 1996). Consequently, studies found also an involvement of (pre)motor areas in the perception of human movements (Saygin, 2007; Saygin et al., 2004).

In three studies (Lange et al., 2015; Pavlidou et al., 2014a, 2014b), we investigated a specific role of non-visual areas, mainly premotor and motor areas for the perception of human movements. The focus was on the question whether visual and non-visual areas show differential activation during the perception of naturalistic and non-naturalistic human movements. As neuronal oscillations in the beta-band are known as a specific marker of

activity in the sensorimotor system (Engel & Fries, 2010; Pfurtscheller et al., 1998; Schnitzler & Gross, 2005), we specifically focused on neuronal oscillatory activity in the beta-band.

The first study (Pavlidou et al., 2014b) investigated whether human movements and non-movements differentially activate visual areas and parts of the mirror neuron system.

Twelve participants viewed naturalistic human movements and distorted versions of the movements while their neuronal activity was recorded with Magnetencephalography (MEG). The human movements were recorded from real movements of persons and displayed as point-light displays (Johansson, 1973). In point-light displays, light dots are attached to the major joints (head, shoulders, elbows, wrists, hips, knees, and feet) of the recorded person. These point-light stimuli were additionally manipulated by repositioning the single point-lights by adding random offsets to their coordinates. This way, stimuli were created that inherit identical low-level features (like intact movement of single point-lights), but which do not display a human movement anymore.

Neuronal oscillations were computed in response to naturalistic point-light movements and in response to the random, non-movement stimuli. Finally, the neuronal oscillations of the two conditions were contrasted.

Results revealed a complex pattern of differential activations across frequency-bands, time points, and cortical areas. In a nutshell, the contrast revealed a stronger response in the parieto-occipital gamma-band activity for naturalistic movements, followed by higher beta-band power in bilateral sensorimotor areas, and higher alpha-band power in left temporal areas. At later time points ( $> 1.0$  s after stimulus onset), higher power for scrambled movements was observed in the right temporal gamma-band and in parieto-occipital alpha/beta-bands. Interestingly, there was a significant positive correlation between sensorimotor beta-band power and parieto-occipital gamma-band on the one hand and temporal alpha-band power on the other hand. This trial-by-trial correlation of power was only present for naturalistic stimuli, but not for the random non-movements (Figure 7A).

While the above mentioned study investigated the neuronal patterns for human movements as opposed to random dot movements, the second study (Pavlidou et al., 2014a) took a more fine-grained look at human movement perception. Humans can quickly recognize movements of others and also easily detect small deviations from natural, realistic movements, e.g., limping. The second study investigated whether neuronal oscillations could reveal the neuronal mechanisms that differentiate between naturalistic and unnaturalistic movements. To this end, participants viewed point-light displays of naturalistic and of modified, unnaturalistic human movements.

The results revealed a significant difference of the power of neuronal oscillations in the alpha ( $\sim 5$ -11 Hz) and especially in the lower beta-band ( $\sim 13$ -21 Hz) between naturalistic and unnaturalistic movements (Figure 7B). This difference was found in temporal, parieto-occipital, and sensorimotor areas at distinct time intervals. Interestingly, sensorimotor beta power correlated with temporal beta power, but only for naturalistic movements (Figure 7B).

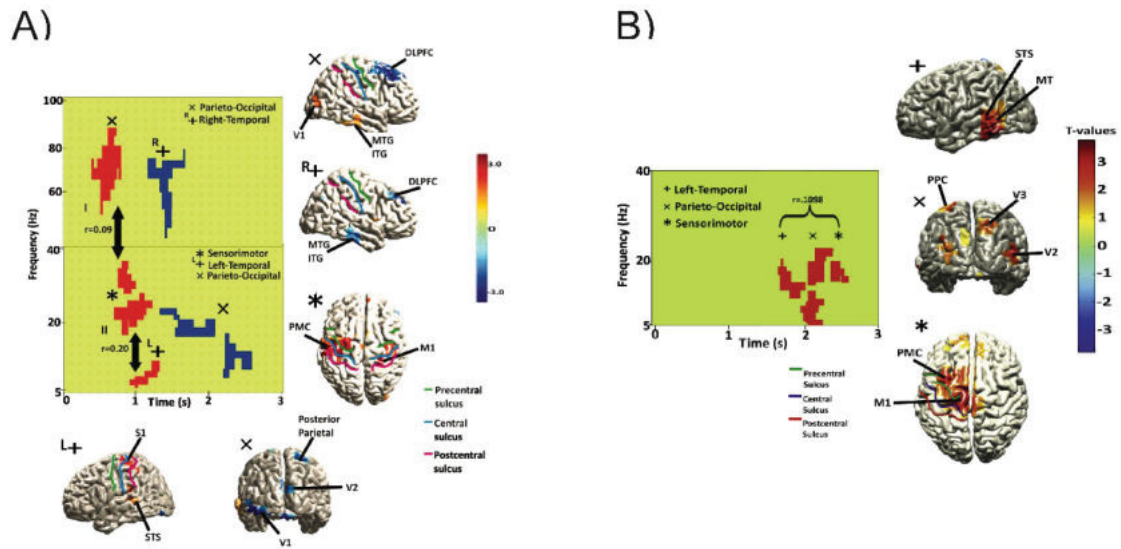


Figure 7: Neuronal oscillations in response to human movements. A) Time-frequency illustration of significant differences between conditions human movements vs. random dot movements. The plot illustrates significant clusters for different regions of interest. Black arrows indicate significant correlations between regions of interest for the human movement conditions. Source reconstructions of the effects in the significant time-frequency windows. Red colours indicate positive, blue colours negative effects. B) Same as A) but now for the contrast naturalistic vs. unnaturalistic human movements. Figure adapted from Pavlidou et al. (2014b, A) and Pavlidou et al. (2014a, B). Adapted and printed with permission from Elsevier and John Wiley & Sons Books.

Finally, a third study (Lange et al., 2015) found that beta-band oscillation in (pre)motor areas show lateralized patterns of activity. That is, human movements facing to the right or to the left elicit differential activations in left and right (pre)motor areas.

In summary, by analysing the rhythmic patterns of neuronal activity the study could provide evidence for an involvement of sensorimotor areas in the perception of human movements. Specifically, the power of beta-band oscillations plays an important role as it indexes the involvement of sensorimotor areas, shows differential activation for naturalistic vs. random, non-movements, and finally reveals putative interaction patterns between sensorimotor and parieto-temporo-occipital areas.

## 2.2 Prestimulus neuronal oscillations index cortical states and influence perception

Even if the brain receives no sensory input, it is still active. Consequently, neuronal oscillations can be observed in the absence of external stimulation – frequently named ongoing neuronal oscillations. For a long time, however, most research assumed that fluctuations of ongoing neuronal oscillations represent “noise” and are irrelevant for stimulus processing, perception, or behaviour. Only in the past decade(s), it has been demonstrated that such relatively “spontaneous” fluctuations of neuronal oscillations can influence stimulus processing and perception. While studies have revealed an influence of prestimulus alpha-band oscillations on near-threshold stimuli (Hanslmayr et al., 2007; Van Dijk et al., 2008), it remains elusive whether ongoing neuronal oscillations play a role for the

perception of suprathreshold stimuli. Consequently, the precise function of ongoing neuronal oscillations is still under debate.

In five studies, the role of ongoing neuronal oscillations in the prestimulus period for temporal perception of suprathreshold stimuli in the visual, tactile, and visuo-tactile modality was investigated (Baumgarten et al., 2016b; Lange et al., 2012, 2013b; Wittenberg et al., 2018, 2019).

To study the role of ongoing neuronal oscillations for visual temporal perception, two brief stimuli at the same location, separated by a brief interstimulus interval (ISI) of ~30-100 ms were presented to the participants while their neuronal activity was measured with MEG (Lange et al., 2013b). The ISI was chosen so that participants perceived the veridical two visual stimuli only in ~50% of all trials, while they perceived only one stimulus in the remaining 50% of trials. The results demonstrated that the power of alpha oscillations was predictive about the varying perception of the subjects despite their constant stimulation: The lower the power of alpha oscillations in parieto-occipital areas was, the higher was the probability that participants perceived the two veridical stimuli. Vice versa, the higher prestimulus alpha power, the more often they missed one visual stimulus (Figure 8A).

A similar pattern of neuronal activity was found when we studied visuo-tactile temporal integration (Lange et al., 2013b). To this end, the visuo-tactile illusion we had used in our previous study described above was employed (Lange et al., 2011). Again, the results show that the power of parieto-occipital oscillations in the alpha-band predicted the perception of the illusion: The lower the power of alpha oscillations was, the more often subjects perceived two visual stimuli (Figure 8B). Interestingly, the results also demonstrated that power correlations in the beta-band between occipital and somatosensory areas correlated with the perception of the illusion (Figure 8C). These results argue for a stronger interaction of visual and somatosensory areas during illusion perceptions mediated by beta-band oscillations.

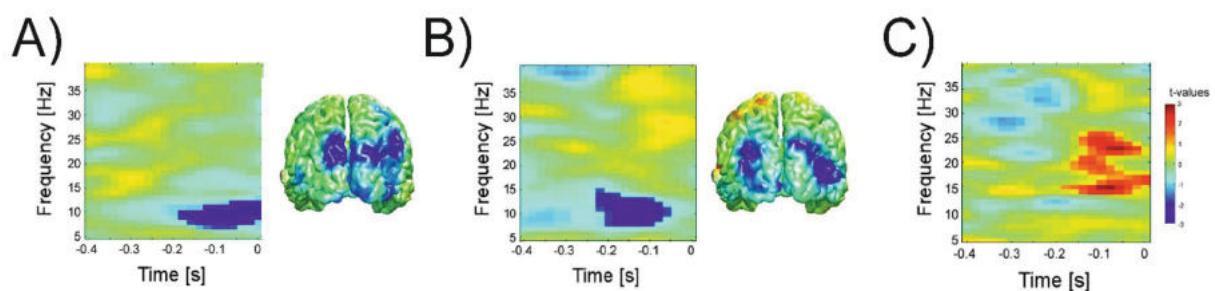


Figure 8: Brain states: Power of neuronal oscillations in visual and visuo-tactile temporal discrimination tasks A) Left: Time-frequency representations of statistical comparison of power for the contrast two vs. one visual stimulus perceived. Significant cluster is highlighted by stronger colours. Right: source reconstruction of the significant effect in the alpha band. B) Same as A) but now for the contrast illusion vs. no illusion perceived. C) Time-frequency representations of the power correlation of visual and somatosensory for the contrast illusion vs. no illusion perceived. Significant cluster is highlighted by stronger colours.  $t = 0$  indicates the onset of the first stimulation. Red colours indicate greater power in trials when subjects perceived two visual stimuli / the illusion compared with trials in which they perceived one stimulus / no illusion. Figures adapted from Lange et al. (2013b). Adapted and printed with permission from Society of Neuroscience under CC-BY-NC-SA.

Two additional studies (Baumgarten et al., 2016b; Lange et al., 2012) investigated temporal perception in the somatosensory modality.

In the first study, temporal perception in one hemifield, i.e. presented two tactile stimuli on the same finger, was investigated (Baumgarten et al., 2016b). In line with our previous studies in the visual and visuo-tactile modality, two tactile stimuli with an SOA were presented, for which participants perceived the stimulation as two stimulations in ~50% of the trials and as one stimulation in the remaining 50% of trials.

Similar to the results of the above described studies in the visual and visuo-tactile modality (Lange et al., 2013b), the results reveal that prestimulus power of alpha oscillations (8-12 Hz) in somatosensory areas correlated with participants' varying perception: The lower alpha power, the more often participants reported to perceive two stimulations (Figure 9A).

In another study, stimulation was applied to both fingers with varying SOAs and participants had to report whether stimulation was simultaneous on both fingers (Lange et al., 2012). With stimulation on both fingers, temporal perception could be analysed within one modality, but across both hemifields. Power of neuronal oscillations between simultaneous and non-simultaneous trials. Unlike in our previous within-hemifield studies, where we found significant effects in the alpha band, we now found that power in the beta band (~20 to 40 Hz) in somatosensory cortex prior to the electrical stimulation predicted participants' reports of simultaneity (Figure 9B).

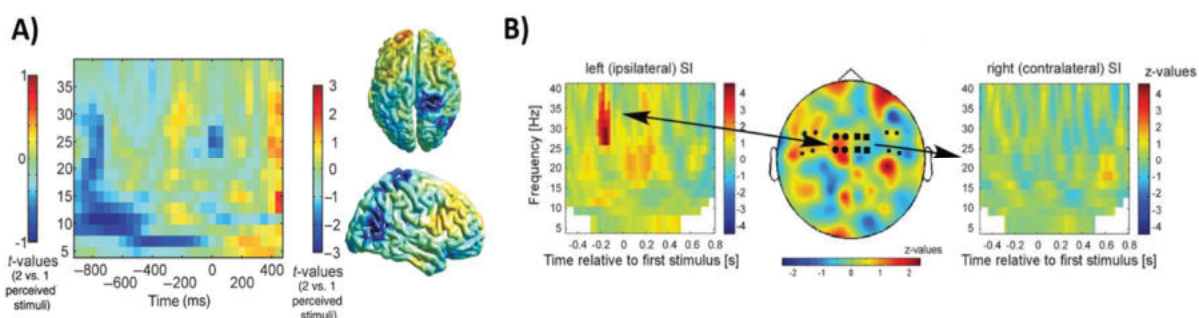


Figure 9: Brain states: Power of prestimulus neuronal oscillations in tactile temporal discrimination tasks. A) Unilateral tactile stimulation on the left hand. Left: Time-frequency representation of statistical comparison of power of neuronal oscillations between conditions two vs. one tactile stimulus perceived. Right: Source reconstruction of the significant effect in the alpha band. B) Bilateral tactile stimulation on left and right hand. Left: Time-frequency representation of statistical comparison of power of neuronal oscillations between conditions simultaneity vs. non-simultaneity averaged over sensors over left S1. Significant cluster is highlighted by stronger colours. Right: Same as Left, but for sensors over right S1. No significant clusters were found. Middle: Topographical representation of the significant cluster in the left time-frequency representation. Red colours indicate higher power in trials with perceived two / simultaneous stimulation compared to one / non-simultaneous stimulation.  $t = 0$  indicates onset of stimulation.

Figures adapted from Baumgarten et al. (2016b, A) and Lange et al. (2012, B). Adapted and printed with permission from Oxford University Press.

In summary, the results of these three studies indicate that fluctuations of ongoing neuronal oscillations in the alpha- and beta-bands shape subjective perception of physically identical stimulation. The evidence we found is of correlative nature. To establish a causal link between prestimulus neuronal oscillations and participants' subjective perception, it is necessary to modulate prestimulus neuronal oscillations and measure its impact on perception. To this end, the method of transcranial alternating current stimulation (tACS)

was employed. With tACS, an alternating current is applied on the participants' skull. This externally applied alternating current is believed to interact with endogenous ongoing neuronal oscillations. This way, neuronal oscillations can be modulated and their (causal) impact on perception can be measured (e.g., Cecere et al., 2015; Helfrich et al., 2014).

In our study (Wittenberg et al., 2019), a causal link between neuronal oscillations and perception should be established by modulating the ongoing alpha oscillations with tACS and measure whether this modulation alters perception. tACS with 10 Hz (i.e., in the alpha-band) on the somatosensory cortex was applied while participants performed the tactile temporal discrimination task which we had used in our previous study (Baumgarten et al., 2016b). In contrast to our hypothesis, perception was unaffected by tACS. It remains speculative, however, why we could not establish a causal link between tACS and perception. It might be that the stimulation parameters were not ideally chosen so that alpha oscillations were not effectively modulated. Alternatively, it might be that alpha power and (temporal) perception are just not causally linked. Rather, both measures might be correlated by a third, latent variable. Our negative results, however, line up in a series of other studies which did not find any effects of tACS on neuronal oscillations or perception (e.g., Asamoah et al., 2019; Veniero et al., 2017).

In a final study on the role of prestimulus neuronal oscillations, the relationship between power of prestimulus alpha oscillations and power of poststimulus gamma oscillations was investigated (Wittenberg et al., 2018). Previous studies found diametrical patterns of prestimulus alpha and poststimulus gamma power with respect to attention or perception (e.g., Bauer et al., 2006; Thut et al., 2006; Womelsdorf & Fries, 2007). While these and other findings suggest a negative linear relationship between prestimulus alpha and poststimulus gamma power, such a relationship has never been investigated before. In our study, we used data from our previous study (Baumgarten et al., 2016b) to study a potential linear relationship between prestimulus alpha and poststimulus gamma power.

First, the results confirmed previous findings that prestimulus alpha power correlated negatively with subjects' perception (Figure 10A). That is, the lower prestimulus alpha power, the more often participants perceived the veridical two stimuli. With regard to our main hypothesis, we found a quadratic, "u-shaped" correlation between prestimulus alpha power and poststimulus gamma power (Figure 10B). That is, poststimulus gamma power was high when prestimulus alpha power was either low or high. For intermediate levels of prestimulus alpha power, poststimulus gamma power was low. This result was confirmed by a subsequent study (Hirschmann et al., 2020).

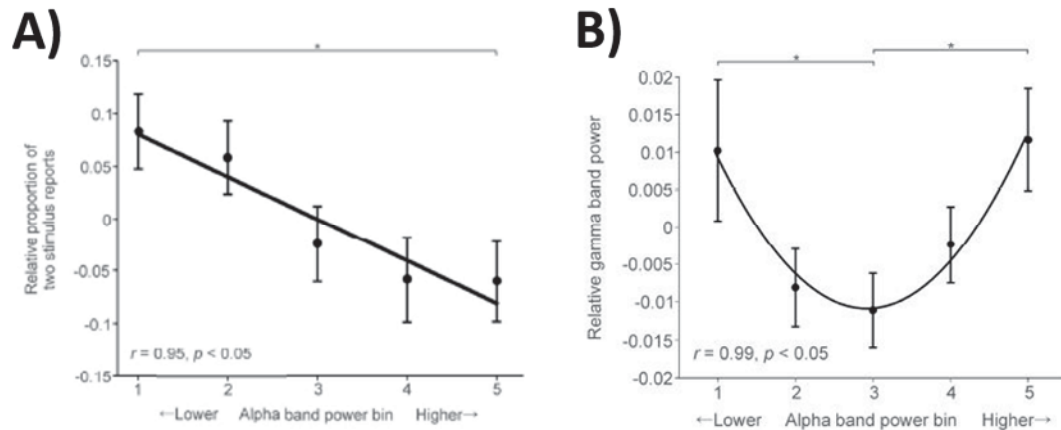


Figure 10: Brain states: Power of prestimulus neuronal oscillations in relation to perception and poststimulus power. A) Prestimulus power of alpha-band neuronal oscillations correlates negatively with tactile temporal perception. B) Prestimulus power of alpha-band neuronal oscillations shows a u-shaped relation to poststimulus gamma-band power. Alpha power was sorted and divided in bins. Higher bins indicate higher averaged power. Error bars indicated 1 SEM. Figure adapted from Wittenberg et al. (2018). Adapted and printed with permission from MIT Press.

In summary, the results of these studies demonstrate a correlation between prestimulus neuronal oscillations and temporal perception. The results indicate that alpha oscillations seem to be relevant if stimuli are presented within one hemifield and modality. Beta oscillations might be relevant if stimuli are presented across hemifields or within multiple modalities. Prestimulus oscillations are related to poststimulus gamma band activity. However, a causal relationship between alpha band oscillations and perception could not be demonstrated. The reasons need to be investigated in future studies.

### 2.3 Perceptual cycles and rhythmic perception

An intriguing, long-standing, yet unsolved question in neuroscience as well as in philosophy is whether perception is a continuous or discrete process. Our subjective experience implies that perception is a continuously ongoing stream. There is, however, evidence that perception might work like a video camera and capture discrete, static images of our environment. In this view, discrete perception constitutes of a succession of single perceptual cycles or snapshots.

In recent years, studies have provided new evidence for perceptual cycles. These studies indicate these perceptual cycles operate at a  $\sim 10$  Hz rhythm in the visual domain (Cecere et al., 2015; Samaha & Postle, 2015; VanRullen & Koch, 2003a). Furthermore, these studies suggest that neuronal oscillations might be the neuronal correlate of perceptual cycles, also working at a  $\sim 10$  Hz rhythm (i.e., in the alpha band). While there is cumulative evidence for

discrete perception in the visual modality, evidence for perceptual cycles in other modalities is largely missing (VanRullen et al., 2014).

In a series of three studies (Baumgarten et al., 2017a, 2015, 2017b), we studied discrete perception and putative perceptual cycles in the somatosensory domain.

In a first study (Baumgarten et al., 2015), we employed the tactile temporal discrimination task described above (Baumgarten et al., 2016b) while neuronal activity was measured with MEG. The results demonstrated that the phase of neuronal oscillations in the primary somatosensory cortex in the alpha- and beta-band (8-20 Hz) differed for perceptions of “1” or “2” stimuli (Figure 11A,B). Notably, this effect was found only in the prestimulus period (−0.53 to −0.09 s). From these results we developed model that described the relationship of neuronal oscillations and perceptual cycles in the somatosensory domain (Figure 11C). The model proposes that a cycle of a beta-band oscillation defines a perceptual cycle. If two stimuli fall within one cycle, they are perceived as “1”; when they fall in two cycles, they are perceived as two stimuli.

These results argue against a continuous process for somatosensory perception. Rather, the results provided the first evidence that somatosensory perception operates in a discrete mode, with sensory input being sampled by discrete perceptual cycles in the alpha band and, in particular, the lower beta band (8–20 Hz). The results indicate that perceptual cycles in the somatosensory modality work on a different time scale than in the visual modality (~20 Hz vs. 10 Hz).

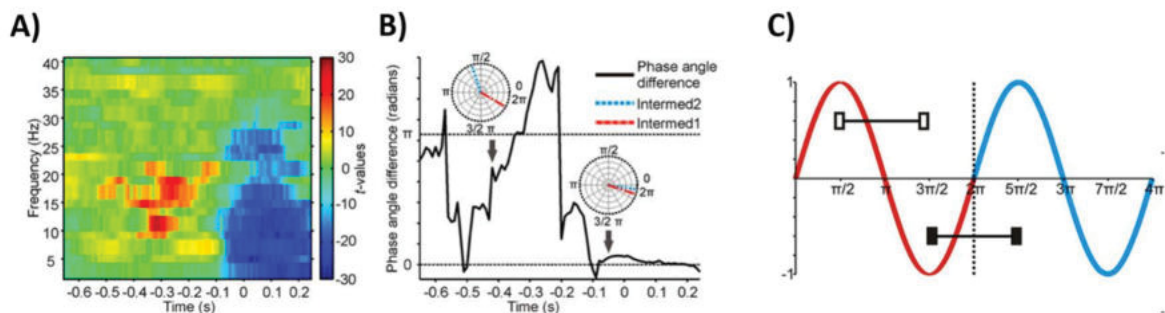


Figure 11: Perceptual cycles: Phase analyses and model for perceptual cycles. A) Time-frequency representation of the statistical analysis of phase angle differences between perceived two vs. one stimuli. Red colors indicate higher phase differences compared with random phases.  $t = 0$  indicates onset of stimulation. Statistically significant clusters are highlighted by stronger colours. B) Temporal evolution of phase differences between perceived two vs one for the exemplary 14 Hz frequency. Insets shows phases for perceived two and one for exemplary time points as indicated by arrows. C) Model for perceptual cycles. Red and blue colours illustrate two cycles of neuronal oscillations (i.e., perceptual cycles). If two stimuli fall into one cycle, they will be perceived as one stimulus (white rectangles), if they fall into two cycles, they will be perceived as two stimuli (black rectangles).

Figure adapted with permission from Baumgarten et al. (2015). Adapted and printed with permission of National Academy of Sciences.

While this study provided first evidence for perceptual cycles and discrete perception in the somatosensory modality, the evidence was only of correlative nature. A follow-up study aimed to provide causal evidence for perceptual cycles by testing predictions of the model of perceptual cycles.

In this study (Baumgarten et al., 2017a), again the established tactile temporal discrimination task was applied (Baumgarten et al., 2015, 2016b). The critical variation of this study was that the tactile target stimuli were preceded by a subliminal (i.e., below perceptual threshold) stimulus. Although not consciously perceived, subliminal stimuli are known to modulate the phase of ongoing neuronal oscillations (Palva et al., 2005). We hypothesized that the subliminal stimulus modulates the ongoing phase of neuronal oscillations in primary somatosensory cortex and thus modulates the onset of perceptual cycles (Figure 11C). By systematically modulating the interstimulus interval between subliminal and supraliminal target stimuli, we should systematically modify the impact of perceptual cycle on perception and induce a rhythmical modulation of perception.

The results confirm the hypothesis: The subliminal stimulus critically influenced perception in the discrimination task. Perception was modulated rhythmically, i.e., the subliminal stimulus improved or deteriorated perception rhythmically as a function of interstimulus interval between subliminal and supraliminal stimuli (Figure 12A). The frequency of the rhythmic modulations corresponds to the beta-band (13–18 Hz; Figure 12B). This result supports the model of discrete perceptual cycles and provides further, causal evidence for discrete perception in the somatosensory modality.

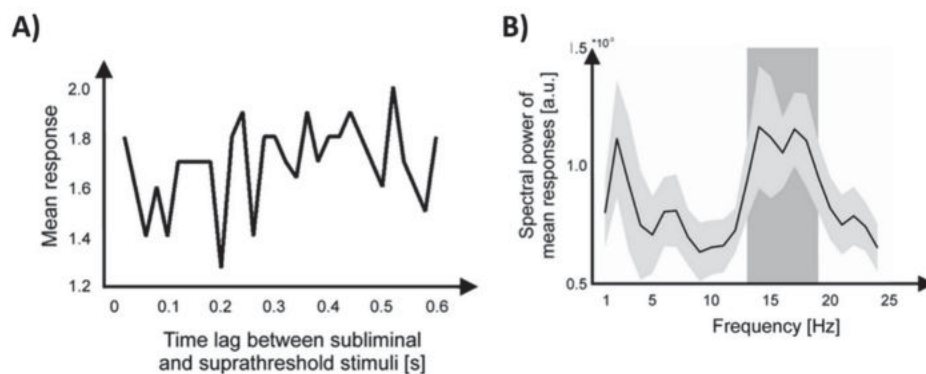


Figure 12: Perceptual cycles: Rhythmic modulation of perception. A) Behavioural data of one exemplary participant showing mean perception across trials in a tactile temporal discrimination tasks as a function of time lag between subliminal stimulus and suprathreshold target stimuli.  $t = 0$  denotes onset of the subliminal stimulus. B) Individual data of each participant were Fourier-transformed, averaged across participants, and statistically tested. The shaded box highlights frequencies with significantly increased amplitudes ( $p = 0.002$ , corrected for multiple comparisons). The grey shading around the black line (mean across participants) represents the SEM.

Figure adapted from Baumgarten et al. (2017a). Adapted and printed with permission from Springer Nature under CC-BY.

The third study investigated whether the perceptual cycles of discrete perception correlate with the peak frequency of neuronal oscillations (Baumgarten et al., 2017b). Studies from the visual modality suggest that the frequency of neuronal oscillations showing the highest amplitude (i.e. the peak frequency) correlates with temporal resolution in visual discrimination tasks (Cecere et al., 2015; Samaha & Postle, 2015). These results indicate that the peak frequency might constitute the neuronal correlate of perceptual cycles.

This third study investigated whether such a correlation of peak frequency and temporal discrimination holds also for the somatosensory modality. We used data from our previous study (Baumgarten et al., 2016b) and analysed the peak frequencies in somatosensory

cortex. Next, we determined the resolution thresholds of the behavioural tactile temporal discrimination task. Finally, in line with previous work from the visual modality, we correlated the neuronal (peak frequency) and the behavioural (behavioural thresholds) measures. In contrast to the results from the visual modality, we could not find a correlation between the two measures. Bayesian statistics provided evidence that there is no correlation between peak frequencies and temporal resolution in the somatosensory modality. We thus suggest that also other frequencies in the beta-band apart from the peak frequency play an important role for (discrete) perception.

In summary, these studies provide the first evidence for perceptual cycles in the somatosensory domain, mediate by neuronal oscillations in the beta-band. Importantly, a follow-up study could provide causal evidence for discrete, rhythmic patterns of perception.

#### 2.4 Aberrant neuronal oscillations and perception

Neuronal oscillations possess several functions in the healthy human brain. Consequently, numerous diseases like Parkinson's disease or schizophrenia have been associated with aberrant neuronal oscillations (Schnitzler et al., 2006; Uhlhaas & Singer, 2010). On the one hand, such aberrant neuronal oscillations can be informative about the cause and origins of diseases. On the other hand, aberrant neuronal oscillations can be informative about functional role of neuronal oscillations in the healthy brain.

In two studies (Baumgarten et al., 2018; Lazar et al., 2018), neuronal oscillations and perception was investigated in patients with hepatic encephalopathy (HE). HE is a common complication in patients with liver cirrhosis (Häussinger & Schliess, 2008). The liver cirrhosis impairs the detoxification function of the liver, which leads to increased ammonia levels in the blood. Eventually, the increased ammonia levels can cause impairments in neuronal processing (Häussinger & Schliess, 2008). The altered neuronal processing is known to induce slowed neuronal oscillations in HE patients, e.g. in the visual or somatosensory system (Butz et al., 2013; Kahlbrock et al., 2012; May et al., 2014). HE patients also show impairments on the behavioural level. For example, it is well known that the critical flicker frequency (CFF) is decreased in HE patients (Kircheis et al., 2002). The CFF is defined as the specific frequency at which a flickering light that is presented with a decreasing frequency is first perceived as a discrete flicker. The CFF serves as an objective clinical parameter to detect and monitor HE (Kircheis et al., 2002).

In summary, HE patients are known to be impaired in their visual temporal perception (CFF) and they show slowed neuronal oscillations. The exact relationship between the behavioural and physiological measures are not well understood. In addition, it is unknown whether the slowed temporal perception is specific for the visual system or whether it generalizes to other modalities. We investigated these experimental questions in two studies (Baumgarten et al., 2018; Lazar et al., 2018).

For the generation of neuronal oscillations, synaptic inhibition mediated by  $\gamma$ -Aminobutyric acid (GABA) neurons seems to be a key factor. Specifically, GABA seems to play an essential role for the generation of beta-band oscillations (Hall et al., 2010; Roopun et al., 2006; Yamawaki et al., 2008). Therefore, we additionally studied the relationship of GABA and neuronal oscillations in healthy participants and HE patients (Baumgarten et al., 2016a, 2018).

The first study (Baumgarten et al., 2016a) investigated whether GABA concentrations in the healthy brain correlate with peak frequencies. GABA concentrations were measured with magnetic resonance spectroscopy (MRS) and neuronal oscillations with MEG. The results revealed a positive correlation between peak frequencies and GABA concentrations in sensorimotor cortex (Figure 13A).

The second study (Baumgarten et al., 2018) found that GABA levels, peak frequencies and visual temporal perception correlate in healthy participants and HE patients. The lower the GABA concentrations in parieto-occipital cortex, the lower the peak frequencies in parieto-occipital areas (Figure 13B). Interestingly, also the peak frequency in the parieto-occipital alpha band correlated with the CFF (Figure 13C). That is, the lower the peak frequency, the worse the visual temporal discrimination ability. This finding is in line with the model of neuronal oscillations as the correlate of temporal perception mediated by perceptual cycles, as described above (Figure 11C; Baumgarten et al., 2017, 2015).

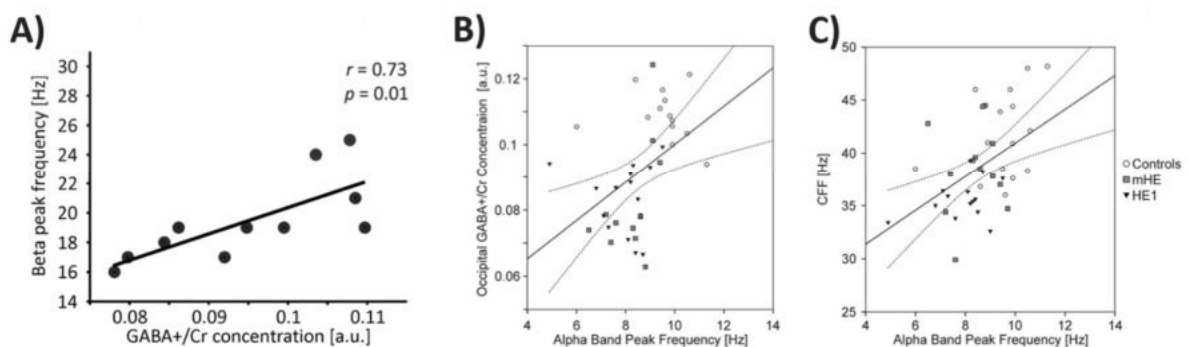


Figure 13: Aberrant neuronal oscillations and perception: Relation of GABA, peak frequencies, and temporal perception. A) Linear relation between GABA and beta-band peak frequencies in sensorimotor cortex of healthy participants. B) Linear relation between GABA and alpha-band peak frequencies in visual cortex of healthy participants and HE patients. C) Linear relationship between alpha-band peak frequencies and visual temporal discrimination (measured by CFF). Figures adapted from Baumgarten et al. (2016a, A) and Baumgarten et al. (2018, B and C). Adapted and printed with permission from Public Library of Science under CC-BY and Elsevier.

Our model also predicts that the slowed oscillations in somatosensory cortex of HE patients (May et al., 2014) lead to impaired tactile temporal perception in HE patients. Neuronal oscillations in HE patients are thus an ideal model to test the hypothesis that temporal tactile perception is mediated by discrete perceptual cycles in the beta-band.

This prediction was tested in a third study (Lazar et al., 2018). Here, HE patients and healthy controls performed the above described tactile temporal discrimination task in which participants receive two tactile stimuli and have to report their subjective perception (Baumgarten et al., 2015, 2016b). In line with our hypothesis, the results demonstrate that HE patients needed a significant longer time interval between the two tactile stimuli to perceive them as two separate events (Figure 14).

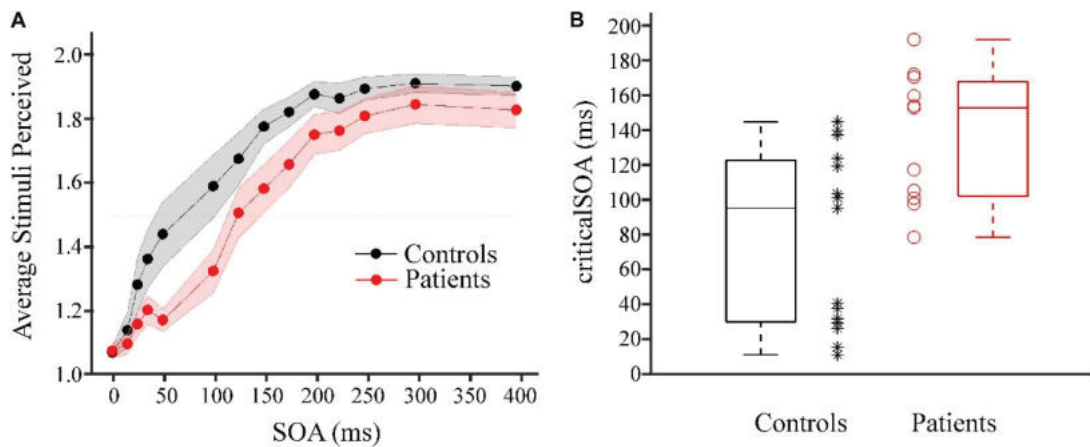


Figure 14: Aberrant neuronal oscillations and perception: Impaired tactile temporal discrimination in HE. A) Average perception as a function of SOA between the two target stimuli for HE patients (red) and healthy controls (black). Shaded areas around dots indicate  $\pm 1$  SEM. The dotted horizontal line indicates mean perception rate of 1.5. B) Individual data and box plots for the perceptual thresholds (i.e. SOA with balanced “1” and “2” reports) for HE patients (red) and healthy controls (black) Both groups differed significantly ( $p = 0.005$ ).

Figure adapted from Lazar et al. (2018). Adapted and printed with permission from Frontiers Media under CC BY.

In summary, the studies of this chapter demonstrate that in HE pathophysiologically impaired perception and aberrant modulations of neuronal activity are associated. This association could be shown for the visual and for the somatosensory system. The results confirm recent theories of slowed oscillatory activity in HE (Butz et al., 2013) and that this slowing should result in impaired perception (Baumgarten et al., 2015). In addition, the studies could demonstrate a correlation between neuronal oscillations, perception, and GABA, thereby corroborating the role of GABA for the generation of neuronal oscillations and the putative relevance of aberrant GABA levels and aberrant neuronal oscillations in HE.

### 3 General Discussion

The studies of the present thesis investigated the role of rhythmicity for perception. Rhythmicity can be found in the patterns of neuronal activity – so-called neuronal oscillations. In addition, perception is not stable over time but can show rhythmic patterns. By studying these different rhythmic patterns of perception, the studies summarized in the present thesis revealed new insights in the neuronal mechanisms underlying perception. In summary, the studies revealed that local changes of neuronal oscillations as well as interactions between neuronal groups reveal new insights in the functional interaction of neuronal groups and their functional role for perception. Secondly, the studies revealed that neuronal oscillations prior to stimulation define brain states that substantially influence perception. Thirdly, it was demonstrated that the rhythmic processes of perception provide evidence for a discrete nature of perception. Finally, studies on patient groups revealed that impaired perception can act as a marker of disease and that studying neuronal oscillations can provide insights into the pathophysiology of the disease.

#### 3.1 Intra- and crossmodal neuronal interactions underlying perception

Studies 1-10 investigated how neuronal oscillations define brain states and mediate the integration of different, spatially and functionally distinct cortical areas for perception. The studies demonstrated that neuronal oscillation in the prestimulus period and modulations in the poststimulus period are important for perception.

The results of these studies provide several new insights into the role of rhythmicity for perception. It could be demonstrated that neuronal oscillations in the prestimulus period can modulate the perception of subsequent stimuli. While it was known that the power of parieto-occipital alpha oscillations modulates visual detection abilities of weak, near-threshold stimuli (Thut et al., 2006; van Dijk et al., 2008), the studies of the present thesis could demonstrate that alpha oscillations also play a role for *temporal* perception of *supra-threshold* visual (Lange et al., 2013b), tactile (Baumgarten et al., 2016b), and visuo-tactile (Lange et al., 2013b) stimuli. In addition, we could demonstrate that local alpha band power in primary visual cortex - which was believed for long to process only unisensory visual stimuli - influences the perception of crossmodal stimuli (Lange et al., 2013b). The results suggest that prestimulus oscillations define the momentary state of the respective part of cortex. The lower the prestimulus power the higher the excitability of the cortex. As a consequence, unisensory stimuli are more effectively processed and multisensory stimuli are more effectively integrated, leading typically to more veridical perception. In rare case, such as the double-flash illusion, however, higher excitability and better integration can also lead to higher rate of illusory perception (Lange et al., 2013b).

In line with our studies discussed above, several other previous studies highlighted the role of alpha-band oscillations for local networks, primarily in sensory cortex (e.g., Haegens et al., 2011; Linkenkaer-Hansen et al., 2004; Romei et al., 2008; van Dijk et al., 2008). Two of the studies in the present thesis investigated additionally the role of prestimulus neuronal oscillations for an interaction of spatially distinct local networks (Lange et al., 2012, 2013b). The results show a modulation of beta-band oscillations if the interaction of distinct networks is required for successful perception. Such correlations of prestimulus beta-band

power with perception have been shown for bilateral tactile perception (Lange et al., 2012) and for visuo-tactile perception (Lange et al., 2013b).

While alpha-band power seems relevant mostly in local networks, our studies indicate that prestimulus beta-band power becomes relevant if communication between distinct networks becomes relevant for perception (Lange et al., 2012, 2013b). Beta-band power might thus reflect a long-range interaction mechanisms, functional coupling of spatially distinct areas, or effective top-down control of (multisensory) perception (Buschman & Miller, 2007; Gross et al., 2004; Richter et al., 2017).

By studying modulations of neuronal oscillations in the poststimulus period, it could be demonstrated that local modulations of neuronal oscillations provide information about the subjective perception of stimuli (Lange et al., 2011, 2013a). Interestingly, when studying multisensory perception, multisensory integration patterns could be demonstrated already in early sensory areas, which were believed for long to process only unisensory stimuli (Lange et al., 2011, 2013a). These results are in line with previous work in humans and monkeys showing multisensory interactions in early primary cortices (Lakatos et al., 2007; Romei et al., 2012).

In addition, studying poststimulus neuronal oscillations during perception of human movements provided information about the functional coupling of spatially distinct neuronal groups. The functional coupling was found predominantly in the beta-band (~13-30 Hz), for visuo-motor integration (Lange et al., 2015; Pavlidou et al., 2014a, 2014b), as well as for visuo-tactile integration (Lange et al., 2013b). Most interestingly, visual and (pre)motor areas are functionally coupled only during the perception of realistic human movements (Lange et al., 2015; Pavlidou et al., 2014a, 2014b).

In conclusion, the studies 1-10 could extend previous knowledge about the role of prestimulus neuronal oscillations by showing their importance for suprathreshold, temporal perception. Extending previous theories for alpha-band power as an idling or gating mechanism (Jensen & Mazaheri, 2010; Klimesch, 1999), the findings suggest that local alpha-band power indexes excitability of (primary) sensory cortex, relevant for perception of uni- but also multisensory stimuli. While alpha-band power seems relevant mostly in local networks, our studies indicate (prestimulus) beta-band power becomes relevant if communication between distinct networks becomes relevant for perception (Buschman & Miller, 2007; Gross et al., 2004; Richter et al., 2017).

### 3.2 Perceptual cycles

Studies 11-13 investigated the rhythmicity of perception itself and the underlying neuronal mechanisms. These studies shed new light on the long-standing question whether perception is a continuous or discrete process (Allport, 1968; VanRullen & Koch, 2003b). Previous studies indicated that visual perception is mediated by discrete perceptual cycles and that alpha-band oscillations are the neuronal correlate of perceptual cycles (e.g., Cecere

et al., 2015; Samaha & Postle, 2015). Evidence for discrete perception apart from the visual modality, however, remains sparse or even absent (VanRullen, 2016; VanRullen et al., 2014).

For the first time, we were able to demonstrate discrete perceptual mechanism in the somatosensory modality. These perceptual cycles are mediated by neuronal oscillations in the beta-band (Baumgarten et al., 2015). In addition, the rhythmic and discrete processes of perception in the beta-band could be confirmed in a behavioural study (Baumgarten et al., 2017a). While alpha-band seems relevant for the visual modality, our results show that beta-band oscillations are the relevant frequency band in the somatosensory modality. We conclude that neuronal oscillations in the beta-band form the basic unit for temporal perception in the somatosensory modality. These results are in line with the higher temporal resolution of the tactile modality compared to the visual modality.

While studies in the visual modality suggested that the dominant frequency in parieto-occipital cortex (i.e., the peak frequency) also mediates perceptual cycles (e.g., Samaha & Postle, 2015), the present study provides evidence that the peak frequencies in the beta-band do not correlate with the perceptual cycles (Baumgarten et al., 2017b).

### 3.3 Aberrant neuronal oscillation and impaired perception

Finally, studies 14-16 investigated impaired tactile temporal perception and aberrant neuronal oscillations in patients with hepatic encephalopathy (HE) and healthy participants. The results demonstrated that HE patients show aberrant neuronal oscillations: Compared to healthy subjects the frequency of alpha oscillations is decreased (Baumgarten et al., 2018). Thereby, the results are in line with findings that neuronal oscillations are slowed in HE patients (Butz et al., 2013; Götz et al., 2013).

The theory of perceptual cycles predicts that with slower neuronal oscillations (i.e., longer cycles of neuronal oscillations) participants should need a longer time gap between two stimuli to perceive them correctly as two stimuli (Baumgarten et al., 2015; Samaha & Postle, 2015). In line with this theory, Baumgarten et al. (2018) demonstrated that the frequency neuronal oscillations correlates with participants' visual temporal discrimination abilities. Our studies demonstrated that in addition to visual tactile perception also tactile temporal perception is impaired in HE patients (Lazar et al., 2018). The results suggest that impaired (temporal) perception might be a general deficit in HE, not restricted to the visual modality.

In addition, our study revealed a correlation between the concentrations of the neurotransmitter GABA with the frequency of neuronal oscillations and temporal perception in HE patients and healthy controls in parieto-occipital cortex (Baumgarten et al., 2018). In addition, we could show that GABA levels in healthy participants correlate with sensorimotor peak frequencies (Baumgarten et al., 2016a). These results confirm previous studies suggesting a functional role of GABA for the generation of neuronal oscillations (e.g., Hall et al., 2010; Lozano-Soldevilla et al., 2014). In addition, these results suggest that aberrant GABA levels might constitute a crucial factor underlying aberrant neuronal oscillations and impaired temporal perception in HE.

## 4 Outlook

The studies presented in this thesis critically extend the knowledge about the role of rhythmicity for perception. At the same time, the results pose new questions for future studies.

### 4.1 Potential future directions in cognitive sciences

The present studies demonstrated a novel relation between neuronal oscillations and temporal perception. A drawback of these studies – and this drawback applies to most other studies – is their correlative nature, while causal evidence is largely missing. That is, future studies need to establish a causal link between neuronal oscillations and perception by actively manipulating neuronal oscillations (power, phase, or frequency) and measuring the impact of these manipulations on temporal perception. In one of our studies, we attempted to manipulate neuronal oscillation by transcranial alternating current stimulation (tACS). However, this tACS approach did not alter temporal perception in our participants (Wittenberg et al., 2019). This negative finding is in line with several recent reports of negative findings when applying tACS to alter neuronal oscillations and behaviour (e.g., Asamoah et al., 2019; Veniero et al., 2017). The evidence for the effectiveness of tACS, however, is mixed. While several studies failed to find effects, several studies reported significant modulatory effects of tACS (e.g., Cecere et al., 2015; Helfrich et al., 2014). Thus, future research needs to further elucidate the mechanisms underlying tACS and its effectiveness to modulate neuronal oscillations. Alternatively, future studies might use other methods to modulate neuronal oscillations, e.g., by external stimulation (Baumgarten et al., 2017a; Spaak et al., 2014).

The present studies also extended the knowledge about a relation between GABA, neuronal oscillations, and temporal perception. Again, future research needs to go beyond the correlative level and provide causal evidence for a crucial role of GABA for neuronal oscillations and temporal perception. A potential approach might be to modulate GABA levels by pharmacological intervention, e.g., by applying medications that modulate GABA concentrations or the effectiveness of GABAergic-receptors and measure the impact on neuronal oscillations and perception (e.g., Hall et al., 2010; Lozano-Soldevilla et al., 2014)

While there is cumulative evidence for perceptual cycles in the visual modality. Evidence for perceptual cycles in other modalities was largely missing (VanRullen, 2016; VanRullen et al., 2014). The present studies provided the first evidence for perceptual cycles in the somatosensory modality (Baumgarten et al., 2017a, 2015). An obvious research question for future studies is to study perceptual cycles in the auditory modality. Given that the theory of perceptual cycles applies to all sensory modalities and neuronal oscillations are found in all sensory modalities, it seems surprising that evidence for perceptual cycles in the auditory modality is sparse or even absent (Baltus & Herrmann, 2015; VanRullen et al., 2014). The analyses used in our studies in the somatosensory modality (Baumgarten et al., 2017a, 2015) offer elegant approaches to study perceptual cycles without a priori hypothesis about the frequency of the relevant neuronal oscillations. Thus, these approaches might offer promising approaches to study perceptual cycles in the auditory modality.

## 4.2 Potential future studies directions in clinical research

The present studies have established a crucial role for neuronal oscillations for temporal perception. We could demonstrate that these aberrant neuronal oscillations are associated with impaired visual temporal perception (Baumgarten et al., 2018). In addition, it was demonstrated that HE patients show impaired tactile temporal perception (Lazar et al., 2018). The link between impaired tactile perception and aberrant neuronal oscillations so far is only hypothetically and needs to be established in future studies.

Aberrant neuronal oscillations have been shown to correlate with dysfunctions in several diseases, like Schizophrenia and Parkinson's disease (Schnitzler & Gross, 2005; Uhlhaas & Singer, 2010). Future studies might thus study whether temporal perception is impaired also in other diseases showing aberrant neuronal oscillations. For example, studies have demonstrated that temporal perception is impaired in patients with Parkinson's disease (Artieda et al., 1992; Conte et al., 2016). A direct link between impaired perception and altered neuronal oscillations, however, has not been studied so far. Results from such a study might provide further insights into other diseases and provide potential insights in common underlying pathophysiological mechanisms across diseases.

One potential mechanism underlying temporal perception might rely on the neurotransmitter GABA. The measurement of GABA concentrations by means of magnetic resonance spectroscopy (MRS) in HE patients and healthy participants offered new insights into the underlying mechanisms of HE, but also the mechanisms of temporal perception and the generation of neuronal oscillations (Baumgarten et al., 2016a, 2018). The results suggest that aberrant GABA levels might play a major functional role for impaired temporal perception in HE. Future studies might investigate whether aberrant GABA correlate with impaired temporal perception in other diseases like Parkinson's disease (Conte et al., 2013, 2016).

It has been shown that tactile temporal perception in healthy participants can be non-pharmacologically altered by means of repetitive somatosensory stimulation (Erro et al., 2016). RSS might thus provide an elegant, non-invasive and non-pharmacological tool to improve tactile temporal perception in diseases like HE and Parkinson's disease. Furthermore, it has been shown that RSS alters GABA levels in sensorimotor cortex (Heba et al., 2016). Future studies might thus use RSS to non-pharmacologically improve temporal perception and thereby further investigate the putative link between GABA, temporal perception, and neuronal oscillations (Baumgarten et al., 2018).

Finally, future studies might rely on the presented studies to develop behavioural markers for diseases, e.g. in HE. An important behavioural parameter in the clinical routine for classification of HE patients is the critical flicker frequency (CFF, Kircheis et al., 2002). The CFF is a measure of temporal discrimination abilities. HE patients show decreased frequencies and the decrease correlates with the severity of the HE symptoms (Kircheis et al., 2002). We could demonstrate that the impaired temporal perception is not restricted to the visual domain but extends to the somatosensory domain. Measuring tactile temporal discrimination levels might thus be an alternative measurement in clinical routine if patients are unable to perform visual tasks, e.g. due to blindness.

## 5 Conclusion

In the studies of the presented thesis, I investigate the role of rhythmicity for perception. The studies revealed that rhythmic patterns of neuronal activity – so-called neuronal oscillations – are tightly linked to the subjective experience of perception. On the behavioural level, the temporal course of perception shows rhythmic patterns. These rhythmic patterns provide insights into the underlying mechanisms of perception and indicate that perception is a discrete process – in contrast to the subjectively experienced continuous perception. Finally, the studies revealed that aberrant neuronal oscillations are linked to impaired perception in HE. These studies offer new insights into the pathophysiology of HE and open new experimental questions for future studies.

In conclusion, perception is an intrinsically rhythmic process and studying the rhythm of perception opens a window into the physiological and pathophysiological brain.

## 6 Bibliography

- Allport, D. A. (1968). Phenomenal simultaneity and the perceptual moment hypothesis. *British Journal of Psychology*, 59(4), 395–406.
- Artieda, J., Pastor, M. A., Lacruz, F., & Obeso, J. A. (1992). Temporal discrimination is abnormal in Parkinson's disease. *Brain*, 115(1), 199–210.
- Asamoah, B., Khatoun, A., & Mc Laughlin, M. (2019). TACS motor system effects can be caused by transcutaneous stimulation of peripheral nerves. *Nature Communications*, 10(1), 1–16.
- Axmacher, N., Henseler, M. M., Jensen, O., Weinreich, I., Elger, C. E., & Fell, J. (2010). Cross-frequency coupling supports multi-item working memory in the human hippocampus. *Proceedings of the National Academy of Sciences*, 107(7), 3228–3233.
- Axmacher, N., Mormann, F., Fernández, G., Elger, C. E., & Fell, J. (2006). Memory formation by neuronal synchronization. *Brain Research Reviews*, 52(1), 170–182.
- Baillet, S., Mosher, J. C., & Leahy, R. M. (2001). Electromagnetic brain mapping. *IEEE Signal Processing Magazine*, 18(6), 14–30.
- Baltus, A., & Herrmann, C. S. (2015). Auditory temporal resolution is linked to resonance frequency of the auditory cortex. *International Journal of Psychophysiology*, 98(1), 1–7.
- Bauer, A.-K. R., Debener, S., & Nobre, A. C. (2020). Synchronisation of Neural Oscillations and Cross-modal Influences. *Trends in Cognitive Sciences*, 24(6), 481–495.  
<https://doi.org/10.1016/j.tics.2020.03.003>
- Bauer, M., Oostenveld, R., Peeters, M., & Fries, P. (2006). Tactile spatial attention enhances gamma-band activity in somatosensory cortex and reduces low-frequency activity in parieto-occipital areas. *Journal of Neuroscience*, 26(2), 490–501.
- Baumgarten, T. J., Königs, S., Schnitzler, A., & Lange, J. (2017a). Subliminal stimuli modulate somatosensory perception rhythmically and provide evidence for discrete perception. *Scientific Reports*, 7:43937. <https://doi.org/10.1038/srep43937>
- Baumgarten, T. J., Neugebauer, J., Oeltzschner, G., Füllenbach, N.-D., Kircheis, G., Häussinger, D., Lange, J., Wittsack, H.-J., Butz, M., & Schnitzler, A. (2018). Connecting Occipital Alpha Band Peak Frequency, Visual Temporal Resolution, and Occipital GABA Levels in Healthy Participants and Hepatic Encephalopathy Patients. *NeuroImage: Clinical*, 20, 347–356.
- Baumgarten, T. J., Oeltzschner, G., Hoogenboom, N., Wittsack, H.-J., Schnitzler, A., & Lange, J. (2016a). Beta peak frequencies at rest correlate with endogenous GABA+/Cr concentrations in sensorimotor cortex areas. *PLoS One*, 11(6), e0156829.
- Baumgarten, T. J., Schnitzler, A., & Lange, J. (2015). Beta oscillations define discrete perceptual cycles in the somatosensory domain. *Proceedings of the National Academy of Sciences of the United States of America*, 112(39), 12187–12192. <https://doi.org/10.1073/pnas.1501438112>
- Baumgarten, T. J., Schnitzler, A., & Lange, J. (2016b). Prestimulus Alpha Power Influences Tactile Temporal Perceptual Discrimination and Confidence in Decisions. *Cerebral Cortex (New York, N.Y.: 1991)*, 26(3), 891–903. <https://doi.org/10.1093/cercor/bhu247>
- Baumgarten, T. J., Schnitzler, A., & Lange, J. (2017b). Beyond the Peak—Tactile Temporal Discrimination Does Not Correlate with Individual Peak Frequencies in Somatosensory Cortex. *Frontiers in Psychology*, 8, 421. <https://doi.org/10.3389/fpsyg.2017.00421>

- Berger, H. (1929). Über das elektrenkephalogramm des menschen. *European Archives of Psychiatry and Clinical Neuroscience*, 87(1), 527–570.
- Bishop, G. H. (1932). Cyclic changes in excitability of the optic pathway of the rabbit. *American Journal of Physiology–Legacy Content*, 103(1), 213–224.
- Bland, B. H. (1986). The physiology and pharmacology of hippocampal formation theta rhythms. *Progress in Neurobiology*, 26(1), 1–54.
- Boto, E., Holmes, N., Leggett, J., Roberts, G., Shah, V., Meyer, S. S., Muñoz, L. D., Mullinger, K. J., Tierney, T. M., Bestmann, S., Barnes, G. R., Bowtell, R., & Brookes, M. J. (2018). Moving magnetoencephalography towards real-world applications with a wearable system. *Nature*, 555(7698), 657–661. <https://doi.org/10.1038/nature26147>
- Boto, E., Meyer, S. S., Shah, V., Alem, O., Knappe, S., Kruger, P., Fromhold, T. M., Lim, M., Glover, P. M., Morris, P. G., Bowtell, R., Barnes, G. R., & Brookes, M. J. (2017). A new generation of magnetoencephalography: Room temperature measurements using optically-pumped magnetometers. *NeuroImage*, 149, 404–414. <https://doi.org/10.1016/j.neuroimage.2017.01.034>
- Bressler, S. L., & Freeman, W. J. (1980). Frequency analysis of olfactory system EEG in cat, rabbit, and rat. *Electroencephalography and Clinical Neurophysiology*, 50(1–2), 19–24.
- Buccino, G., Binkofski, F., Fink, G. R., Fadiga, L., Fogassi, L., Gallese, V., Seitz, R. J., Zilles, K., Rizzolatti, G., & Freund, H.-J. (2001). Action observation activates premotor and parietal areas in a somatotopic manner: An fMRI study. *European Journal of Neuroscience*, 13(2), 400–404.
- Busch, N. A., Dubois, J., & VanRullen, R. (2009). The phase of ongoing EEG oscillations predicts visual perception. *The Journal of Neuroscience*, 29(24), 7869–7876.
- Busch, N. A., & VanRullen, R. (2014). Is visual perception like a continuous flow or a series of snapshots? In *Subjective time: The philosophy, psychology, and neuroscience of temporality* (pp. 161–178). MIT Press.
- Buschman, T. J., & Miller, E. K. (2007). Top-down versus bottom-up control of attention in the prefrontal and posterior parietal cortices. *Science*, 315(5820), 1860–1862.
- Butz, M., May, E. S., Häussinger, D., & Schnitzler, A. (2013). The slowed brain: Cortical oscillatory activity in hepatic encephalopathy. *Archives of Biochemistry and Biophysics*, 536(2), 197–203. <https://doi.org/10.1016/j.abb.2013.04.004>
- Buzsáki, G. (2002). Theta Oscillations in the Hippocampus. *Neuron*, 33(3), 325–340. [https://doi.org/10.1016/S0896-6273\(02\)00586-X](https://doi.org/10.1016/S0896-6273(02)00586-X)
- Buzsáki, G., Anastassiou, C. A., & Koch, C. (2012). The origin of extracellular fields and currents—EEG, ECoG, LFP and spikes. *Nature Reviews Neuroscience*, 13(6), 407–420. <https://doi.org/10.1038/nrn3241>
- Buzsáki, G., Logothetis, N., & Singer, W. (2013). Scaling Brain Size, Keeping Timing: Evolutionary Preservation of Brain Rhythms. *Neuron*, 80(3), 751–764. <https://doi.org/10.1016/j.neuron.2013.10.002>
- Buzsáki, G., & Moser, E. I. (2013). Memory, navigation and theta rhythm in the hippocampal-entorhinal system. *Nature Neuroscience*, 16(2), 130–138.
- Buzsáki, G., & Wang, X.-J. (2012). Mechanisms of gamma oscillations. *Annual Review of Neuroscience*, 35, 203–225.

- Callaway, E., & Yeager, C. L. (1960). Relationship between reaction time and electroencephalographic alpha phase. *Science*, *132*(3441), 1765–1766.
- Canolty, R. T., Edwards, E., Dalal, S. S., Soltani, M., Nagarajan, S. S., Kirsch, H. E., Berger, M. S., Barbaro, N. M., & Knight, R. T. (2006). High Gamma Power Is Phase-Locked to Theta Oscillations in Human Neocortex. *Science*, *313*(5793), 1626–1628.  
<https://doi.org/10.1126/science.1128115>
- Cecere, R., Rees, G., & Romei, V. (2015). Individual differences in alpha frequency drive crossmodal illusory perception. *Current Biology*, *25*(2), 231–235.
- Chakravarthi, R., & VanRullen, R. (2012). Conscious updating is a rhythmic process. *Proceedings of the National Academy of Sciences*, *109*(26), 10599–10604.  
<https://doi.org/10.1073/pnas.1121622109>
- Cohen, M. X. (2011). Error-related medial frontal theta activity predicts cingulate-related structural connectivity. *Neuroimage*, *55*(3), 1373–1383.
- Conte, A., Khan, N., Defazio, G., Rothwell, J. C., & Berardelli, A. (2013). Pathophysiology of somatosensory abnormalities in Parkinson disease. *Nature Reviews Neurology*, *9*(12), 687–697. <https://doi.org/10.1038/nrneurol.2013.224>
- Conte, A., Leodori, G., Ferrazzano, G., De Bartolo, M. I., Manzo, N., Fabbrini, G., & Berardelli, A. (2016). Somatosensory temporal discrimination threshold in Parkinson’s disease parallels disease severity and duration. *Clinical Neurophysiology*, *127*(9), 2985–2989.  
<https://doi.org/10.1016/j.clinph.2016.06.026>
- Dugué, L., Marque, P., & VanRullen, R. (2011). The phase of ongoing oscillations mediates the causal relation between brain excitation and visual perception. *The Journal of Neuroscience*, *31*(33), 11889–11893.
- Eckhorn, R., Bauer, R., Jordan, W., Brosch, M., Kruse, W., Munk, M., & Reitboeck, H. J. (1988). Coherent oscillations: A mechanism of feature linking in the visual cortex? *Biological Cybernetics*, *60*(2), 121–130.
- Engel, A. K., & Fries, P. (2010). Beta-band oscillations—Signalling the status quo? *Current Opinion in Neurobiology*, *20*(2), 156–165. <https://doi.org/10.1016/j.conb.2010.02.015>
- Erro, R., Rocchi, L., Antelmi, E., Palladino, R., Tinazzi, M., Rothwell, J., & Bhatia, K. P. (2016). High frequency repetitive sensory stimulation improves temporal discrimination in healthy subjects. *Clinical Neurophysiology*, *127*(1), 817–820.
- Fiebelkorn, I. C., Saalmann, Y. B., & Kastner, S. (2013). Rhythmic Sampling within and between Objects despite Sustained Attention at a Cued Location. *Current Biology*, *23*(24), 2553–2558.  
<https://doi.org/10.1016/j.cub.2013.10.063>
- Florin, E., & Baillet, S. (2015). The brain’s resting-state activity is shaped by synchronized cross-frequency coupling of neural oscillations. *NeuroImage*, *111*, 26–35.  
<https://doi.org/10.1016/j.neuroimage.2015.01.054>
- Fries, P. (2005). A mechanism for cognitive dynamics: Neuronal communication through neuronal coherence. *Trends in Cognitive Sciences*, *9*(10), 474–480.  
<https://doi.org/10.1016/j.tics.2005.08.011>
- Fries, P. (2015). Rhythms for Cognition: Communication through Coherence. *Neuron*, *88*(1), 220–235.  
<https://doi.org/10.1016/j.neuron.2015.09.034>

- Fries, P., Reynolds, J. H., Rorie, A. E., & Desimone, R. (2001). Modulation of Oscillatory Neuronal Synchronization by Selective Visual Attention. *Science*, *291*(5508), 1560–1563. <https://doi.org/10.1126/science.1055465>
- Gallese, V., Fadiga, L., Fogassi, L., & Rizzolatti, G. (1996). Action recognition in the premotor cortex. *Brain*, *119*(2), 593–610.
- Ghazanfar, A. A., & Schroeder, C. E. (2006). Is neocortex essentially multisensory? *Trends in Cognitive Sciences*, *10*(6), 278–285.
- Götz, T., Huonker, R., Kranczoch, C., Reuken, P., Witte, O. W., Günther, A., & Debener, S. (2013). Impaired evoked and resting-state brain oscillations in patients with liver cirrhosis as revealed by magnetoencephalography. *NeuroImage: Clinical*, *2*, 873–882.
- Gray, C. M., König, P., Engel, A. K., & Singer, W. (1989). Oscillatory responses in cat visual cortex exhibit inter-columnar synchronization which reflects global stimulus properties. *Nature*, *338*(6213), 334–337.
- Gross, J., Schmitz, F., Schnitzler, I., Kessler, K., Shapiro, K., Hommel, B., & Schnitzler, A. (2004). Modulation of long-range neural synchrony reflects temporal limitations of visual attention in humans. *Proceedings of the National Academy of Sciences*, *101*(35), 13050–13055.
- Grossman, E., Donnelly, M., Price, R., Pickens, D., Morgan, V., Neighbor, G., & Blake, R. (2000). Brain areas involved in perception of biological motion. *Journal of Cognitive Neuroscience*, *12*(5), 711–720.
- Haegens, S., Händel, B. F., & Jensen, O. (2011). Top-down controlled alpha band activity in somatosensory areas determines behavioral performance in a discrimination task. *The Journal of Neuroscience*, *31*(14), 5197–5204.
- Hall, S. D., Barnes, G. R., Furlong, P. L., Seri, S., & Hillebrand, A. (2010). Neuronal network pharmacodynamics of GABAergic modulation in the human cortex determined using pharmaco-magnetoencephalography. *Human Brain Mapping*, *31*(4), 581–594.
- Hämäläinen, M., Hari, R., Ilmoniemi, R. J., Knuutila, J., & Lounasmaa, O. V. (1993). Magnetoencephalography—Theory, instrumentation, and applications to noninvasive studies of the working human brain. *Reviews of Modern Physics*, *65*(2), 413–497. <https://doi.org/10.1103/RevModPhys.65.413>
- Hammond, C., Bergman, H., & Brown, P. (2007). Pathological synchronization in Parkinson's disease: Networks, models and treatments. *Trends in Neurosciences*, *30*(7), 357–364.
- Hansen, P., Kringelbach, M., & Salmelin, R. (2010). *MEG: An Introduction to Methods*. Oxford University Press.
- Hanslmayr, S., Aslan, A., Staudigl, T., Klimesch, W., Herrmann, C. S., & Bäuml, K.-H. (2007). Prestimulus oscillations predict visual perception performance between and within subjects. *Neuroimage*, *37*(4), 1465–1473.
- Häussinger, D., & Schliess, F. (2008). Pathogenetic mechanisms of hepatic encephalopathy. *Gut*, *57*(8), 1156–1165. <https://doi.org/10.1136/gut.2007.122176>
- Heba, S., Puts, N. A., Kalisch, T., Glaubitz, B., Haag, L. M., Lenz, M., Dinse, H. R., Edden, R. A., Tegenthoff, M., & Schmidt-Wilcke, T. (2016). Local GABA concentration predicts perceptual improvements after repetitive sensory stimulation in humans. *Cerebral Cortex*, *26*(3), 1295–1301.

- Helfrich, R. F., Fiebelkorn, I. C., Szczepanski, S. M., Lin, J. J., Parvizi, J., Knight, R. T., & Kastner, S. (2018). Neural Mechanisms of Sustained Attention Are Rhythmic. *Neuron*, *99*(4), 854-865.e5. <https://doi.org/10.1016/j.neuron.2018.07.032>
- Helfrich, R. F., Knepper, H., Nolte, G., Strüber, D., Rach, S., Herrmann, C. S., Schneider, T. R., & Engel, A. K. (2014). Selective Modulation of Interhemispheric Functional Connectivity by HD-tACS Shapes Perception. *PLoS Biol*, *12*(12), e1002031. <https://doi.org/10.1371/journal.pbio.1002031>
- Hirschmann, J., Baillet, S., Woolrich, M., Schnitzler, A., Vidaurre, D., & Florin, E. (2020). Spontaneous network activity < 35 Hz accounts for variability in stimulus-induced gamma responses. *Neuroimage*, *207*, 116374.
- Hirschmann, J., Özkurt, T. E., Butz, M., Homburger, M., Elben, S., Hartmann, C. J., Vesper, J., Wojtecki, L., & Schnitzler, A. (2011). Distinct oscillatory STN-cortical loops revealed by simultaneous MEG and local field potential recordings in patients with Parkinson's disease. *NeuroImage*, *55*(3), 1159–1168. <https://doi.org/10.1016/j.neuroimage.2010.11.063>
- Hoogenboom, N., Schoffelen, J.-M., Oostenveld, R., Parkes, L. M., & Fries, P. (2006). Localizing human visual gamma-band activity in frequency, time and space. *NeuroImage*, *29*(3), 764–773. <https://doi.org/10.1016/j.neuroimage.2005.08.043>
- Iemi, L., Chaumon, M., Crouzet, S. M., & Busch, N. A. (2016). Spontaneous neural oscillations bias perception by modulating baseline excitability. *Journal of Neuroscience*, 1432–16. <https://doi.org/10.1523/JNEUROSCI.1432-16.2016>
- Jasper, & Andrews, H. L. (1936). Human brain rhythms: I. Recording techniques and preliminary results. *The Journal of General Psychology*, *14*(1), 98–126.
- Jasper, & Andrews, H. L. (1938). ELECTRO-ENCEPHALOGRAPHY: III. NORMAL DIFFERENTIATION OF OCCIPITAL AND PRECENTRAL REGIONS IN MAN. *Archives of Neurology & Psychiatry*, *39*(1), 96–115. <https://doi.org/10.1001/archneurpsyc.1938.02270010106010>
- Jasper, H., & Penfield, W. (1949). Electrocorticograms in man: Effect of voluntary movement upon the electrical activity of the precentral gyrus. *Archiv Für Psychiatrie Und Nervenkrankheiten*, *183*(1), 163–174. <https://doi.org/10.1007/BF01062488>
- Jensen, O., & Mazaheri, A. (2010). Shaping functional architecture by oscillatory alpha activity: Gating by inhibition. *Frontiers in Human Neuroscience*, *4*, 186. <https://doi.org/10.3389/fnhum.2010.00186>
- Johansson, G. (1973). Visual perception of biological motion and a model for its analysis. *Perception & Psychophysics*, *14*(2), 201–211. <https://doi.org/10.3758/BF03212378>
- Kahlbrock, N., Butz, M., May, E. S., & Schnitzler, A. (2012). Sustained gamma band synchronization in early visual areas reflects the level of selective attention. *NeuroImage*, *59*(1), 673–681. <https://doi.org/10.1016/j.neuroimage.2011.07.017>
- Kandel, E. R., Schwartz, J. H., Jessell, T. M., Siegelbaum, S. A., Hudspeth, A. J., & others. (2000). *Principles of neural science* (Vol. 5). McGraw-hill New York. [http://www.academia.edu/download/29551329/neuroscience\\_syllabus.pdf](http://www.academia.edu/download/29551329/neuroscience_syllabus.pdf)
- Kayser, C., Petkov, C. I., & Logothetis, N. K. (2008). Visual modulation of neurons in auditory cortex. *Cerebral Cortex*, *18*(7), 1560–1574.

- Kircheis, G., Wettstein, M., Timmermann, L., Schnitzler, A., & Häussinger, D. (2002). Critical flicker frequency for quantification of low-grade hepatic encephalopathy. *Hepatology*, *35*(2), 357–366. <https://doi.org/10.1053/jhep.2002.30957>
- Klausberger, T., & Somogyi, P. (2008). Neuronal Diversity and Temporal Dynamics: The Unity of Hippocampal Circuit Operations. *Science*, *321*(5885), 53–57. <https://doi.org/10.1126/science.1149381>
- Klimesch, W. (1999). EEG alpha and theta oscillations reflect cognitive and memory performance: A review and analysis. *Brain Research Reviews*, *29*(2), 169–195.
- Kornmeier, J., & Bach, M. (2012). Ambiguous Figures – What Happens in the Brain When Perception Changes But Not the Stimulus. *Frontiers in Human Neuroscience*, *6*. <https://doi.org/10.3389/fnhum.2012.00051>
- Lakatos, P., Chen, C.-M., O’Connell, M. N., Mills, A., & Schroeder, C. E. (2007). Neuronal oscillations and multisensory interaction in primary auditory cortex. *Neuron*, *53*(2), 279–292. <https://doi.org/10.1016/j.neuron.2006.12.011>
- Landau, A. N., & Fries, P. (2012). Attention samples stimuli rhythmically. *Current Biology*, *22*(11), 1000–1004.
- Lange, J., Christian, N., & Schnitzler, A. (2013a). Audio–visual congruency alters power and coherence of oscillatory activity within and between cortical areas. *NeuroImage*, *79*, 111–120. <https://doi.org/10.1016/j.neuroimage.2013.04.064>
- Lange, J., Halacz, J., van Dijk, H., Kahlbrock, N., & Schnitzler, A. (2012). Fluctuations of prestimulus oscillatory power predict subjective perception of tactile simultaneity. *Cerebral Cortex (New York, N.Y.: 1991)*, *22*(11), 2564–2574. <https://doi.org/10.1093/cercor/bhr329>
- Lange, J., Oostenveld, R., & Fries, P. (2011). Perception of the touch-induced visual double-flash illusion correlates with changes of rhythmic neuronal activity in human visual and somatosensory areas. *NeuroImage*, *54*(2), 1395–1405. <https://doi.org/10.1016/j.neuroimage.2010.09.031>
- Lange, J., Oostenveld, R., & Fries, P. (2013b). Reduced occipital alpha power indexes enhanced excitability rather than improved visual perception. *The Journal of Neuroscience: The Official Journal of the Society for Neuroscience*, *33*(7), 3212–3220. <https://doi.org/10.1523/JNEUROSCI.3755-12.2013>
- Lange, J., Pavlidou, A., & Schnitzler, A. (2015). Lateralized modulation of beta-band power in sensorimotor areas during action observation. *Frontiers in Integrative Neuroscience*, *9*.
- Lazar, M., Butz, M., Baumgarten, T. J., Füllenbach, N.-D., Jördens, M. S., Häussinger, D., Schnitzler, A., & Lange, J. (2018). Impaired tactile temporal discrimination in patients with hepatic encephalopathy. *Frontiers in Psychology*, *9*, 2059.
- Limbach, K., & Corballis, P. M. (2016). Prestimulus alpha power influences response criterion in a detection task. *Psychophysiology*, *53*(8), 1154–1164. <https://doi.org/10.1111/psyp.12666>
- Linkenkaer-Hansen, K., Nikulin, V. V., Palva, S., Ilmoniemi, R. J., & Palva, J. M. (2004). Prestimulus oscillations enhance psychophysical performance in humans. *The Journal of Neuroscience*, *24*(45), 10186–10190.
- Lisman, J. E., & Jensen, O. (2013). The Theta-Gamma Neural Code. *Neuron*, *77*(6), 1002–1016. <https://doi.org/10.1016/j.neuron.2013.03.007>

- Little, S., & Brown, P. (2014). The functional role of beta oscillations in Parkinson's disease. *Parkinsonism & Related Disorders*, *20*, S44–S48. [https://doi.org/10.1016/S1353-8020\(13\)70013-0](https://doi.org/10.1016/S1353-8020(13)70013-0)
- Lozano-Soldevilla, D., ter Huurne, N., Cools, R., & Jensen, O. (2014). GABAergic modulation of visual gamma and alpha oscillations and its consequences for working memory performance. *Current Biology*, *24*(24), 2878–2887.
- Luu, P., Tucker, D. M., & Makeig, S. (2004). Frontal midline theta and the error-related negativity: Neurophysiological mechanisms of action regulation. *Clinical Neurophysiology*, *115*(8), 1821–1835.
- Macaluso, E., & Driver, J. (2005). Multisensory spatial interactions: A window onto functional integration in the human brain. *Trends in Neurosciences*, *28*(5), 264–271.
- Maris, E., van Vugt, M., & Kahana, M. (2011). Spatially distributed patterns of oscillatory coupling between high-frequency amplitudes and low-frequency phases in human iEEG. *NeuroImage*, *54*(2), 836–850. <https://doi.org/10.1016/j.neuroimage.2010.09.029>
- Mather, G., Radford, K., & West, S. (1992). Low-level visual processing of biological motion. *Proceedings of the Royal Society of London B: Biological Sciences*, *249*(1325), 149–155.
- Mathewson, K. E., Gratton, G., Fabiani, M., Beck, D. M., & Ro, T. (2009). To see or not to see: Prestimulus  $\alpha$  phase predicts visual awareness. *The Journal of Neuroscience*, *29*(9), 2725–2732.
- May, E. S., Butz, M., Kahlbrock, N., Brenner, M., Hoogenboom, N., Kircheis, G., Häussinger, D., & Schnitzler, A. (2014). Hepatic encephalopathy is associated with slowed and delayed stimulus-associated somatosensory alpha activity. *Clinical Neurophysiology*, *125*(12), 2427–2435. <https://doi.org/10.1016/j.clinph.2014.03.018>
- Michalareas, G., Vezoli, J., van Pelt, S., Schoffelen, J.-M., Kennedy, H., & Fries, P. (2016). Alpha-Beta and Gamma Rhythms Subserve Feedback and Feedforward Influences among Human Visual Cortical Areas. *Neuron*, *89*(2), 384–397. <https://doi.org/10.1016/j.neuron.2015.12.018>
- Nunn, C. M. H., & Osselton, J. W. (1974). The influence of the EEG alpha rhythm on the perception of visual stimuli. *Psychophysiology*, *11*(3), 294–303.
- Oram, M. W., & Perrett, D. I. (1994). Responses of Anterior Superior Temporal Polysensory (STPa) Neurons to “Biological Motion” Stimuli. *Journal of Cognitive Neuroscience*, *6*(2), 99–116. <https://doi.org/10.1162/jocn.1994.6.2.99>
- Osipova, D., Takashima, A., Oostenveld, R., Fernández, G., Maris, E., & Jensen, O. (2006). Theta and Gamma Oscillations Predict Encoding and Retrieval of Declarative Memory. *Journal of Neuroscience*, *26*(28), 7523–7531. <https://doi.org/10.1523/JNEUROSCI.1948-06.2006>
- Palva, S., Linkenkaer-Hansen, K., Näätänen, R., & Palva, J. M. (2005). Early Neural Correlates of Conscious Somatosensory Perception. *The Journal of Neuroscience*, *25*(21), 5248–5258. <https://doi.org/10.1523/JNEUROSCI.0141-05.2005>
- Pavlidou, A., Schnitzler, A., & Lange, J. (2014a). Interactions between visual and motor areas during the recognition of plausible actions as revealed by magnetoencephalography. *Human Brain Mapping*, *35*(2), 581–592. <https://doi.org/10.1002/hbm.22207>
- Pavlidou, A., Schnitzler, A., & Lange, J. (2014b). Distinct spatio-temporal profiles of beta-oscillations within visual and sensorimotor areas during action recognition as revealed by MEG. *Cortex*, *54*, 106–116. <https://doi.org/10.1016/j.cortex.2014.02.007>

- Pesaran, B., Nelson, M. J., & Andersen, R. A. (2008). Free choice activates a decision circuit between frontal and parietal cortex. *Nature*, *453*(7193), 406–409.
- Pfurtscheller, G., Stancak Jr, A., & Neuper, C. (1996). Event-related synchronization (ERS) in the alpha band—an electrophysiological correlate of cortical idling: A review. *International Journal of Psychophysiology*, *24*(1–2), 39–46.
- Pfurtscheller, G., Zalaudek, K., & Neuper, C. (1998). Event-related beta synchronization after wrist, finger and thumb movement. *Electroencephalography and Clinical Neurophysiology/Electromyography and Motor Control*, *109*(2), 154–160.  
[https://doi.org/10.1016/S0924-980X\(97\)00070-2](https://doi.org/10.1016/S0924-980X(97)00070-2)
- Richter, C. G., Thompson, W. H., Bosman, C. A., & Fries, P. (2017). Top-Down Beta Enhances Bottom-Up Gamma. *Journal of Neuroscience*, *37*(28), 6698–6711.  
<https://doi.org/10.1523/JNEUROSCI.3771-16.2017>
- Romei, V., Gross, J., & Thut, G. (2012). Sounds reset rhythms of visual cortex and corresponding human visual perception. *Current Biology: CB*, *22*(9), 807–813.  
<https://doi.org/10.1016/j.cub.2012.03.025>
- Romei, V., Rihs, T., Brodbeck, V., & Thut, G. (2008). Resting electroencephalogram alpha-power over posterior sites indexes baseline visual cortex excitability. *Neuroreport*, *19*(2), 203–208.  
<https://doi.org/10.1097/WNR.0b013e3282f454c4>
- Roopun, A. K., Middleton, S. J., Cunningham, M. O., LeBeau, F. E., Bibbig, A., Whittington, M. A., & Traub, R. D. (2006). A beta2-frequency (20–30 Hz) oscillation in nonsynaptic networks of somatosensory cortex. *Proceedings of the National Academy of Sciences*, *103*(42), 15646–15650.
- Rosen, S., Carlyon, R. P., Darwin, C. J., & Russell, I. J. (1992). Temporal information in speech: Acoustic, auditory and linguistic aspects. *Philosophical Transactions of the Royal Society of London. Series B: Biological Sciences*, *336*(1278), 367–373.  
<https://doi.org/10.1098/rstb.1992.0070>
- Sakowitz, O. W., Quiroga, R. Q., Schürmann, M., & Başar, E. (2001). Bisensory stimulation increases gamma-responses over multiple cortical regions. *Cognitive Brain Research*, *11*(2), 267–279.
- Samaha, J., & Postle, B. R. (2015). The speed of alpha-band oscillations predicts the temporal resolution of visual perception. *Current Biology*, *25*(22), 2985–2990.
- Sauseng, P., Klimesch, W., Gerloff, C., & Hummel, F. C. (2009). Spontaneous locally restricted EEG alpha activity determines cortical excitability in the motor cortex. *Neuropsychologia*, *47*(1), 284–288.
- Saygin, A. P. (2007). Superior temporal and premotor brain areas necessary for biological motion perception. *Brain*, *130*(9), 2452–2461.
- Saygin, A. P., Wilson, S. M., Hagler, D. J., Bates, E., & Sereno, M. I. (2004). Point-light biological motion perception activates human premotor cortex. *The Journal of Neuroscience*, *24*(27), 6181–6188.
- Schnitzler, A., & Gross, J. (2005). Normal and pathological oscillatory communication in the brain. *Nature Reviews Neuroscience*, *6*(4), 285–296. <https://doi.org/10.1038/nrn1650>
- Schnitzler, A., Salenius, S., Salmelin, R., Jousmäki, V., & Hari, R. (1997). Involvement of Primary Motor Cortex in Motor Imagery: A Neuromagnetic Study. *NeuroImage*, *6*(3), 201–208.  
<https://doi.org/10.1006/nimg.1997.0286>

- Schnitzler, A., Timmermann, L., & Gross, J. (2006). Physiological and pathological oscillatory networks in the human motor system. *Journal of Physiology-Paris*, *99*(1), 3–7. <https://doi.org/10.1016/j.jphysparis.2005.06.010>
- Senkowski, D., Talsma, D., Herrmann, C. S., & Woldorff, M. G. (2005). Multisensory processing and oscillatory gamma responses: Effects of spatial selective attention. *Experimental Brain Research*, *166*(3–4), 411–426.
- Shams, L., Kamitani, Y., & Shimojo, S. (2000). Illusions. What you see is what you hear. *Nature*, *408*(6814), 788. <https://doi.org/10.1038/35048669>
- Shapiro, K. L., Raymond, J. E., & Arnell, K. M. (1997). The attentional blink. *Trends in Cognitive Sciences*, *1*(8), 291–296. [https://doi.org/10.1016/S1364-6613\(97\)01094-2](https://doi.org/10.1016/S1364-6613(97)01094-2)
- Singer, W., & Gray, C. M. (1995). Visual feature integration and the temporal correlation hypothesis. *Annual Review of Neuroscience*, *18*(1), 555–586.
- Song, K., Meng, M., Chen, L., Zhou, K., & Luo, H. (2014). Behavioral Oscillations in Attention: Rhythmic  $\alpha$  Pulses Mediated through  $\theta$  Band. *The Journal of Neuroscience*, *34*(14), 4837–4844. <https://doi.org/10.1523/JNEUROSCI.4856-13.2014>
- Spaak, E., de Lange, F. P., & Jensen, O. (2014). Local entrainment of alpha oscillations by visual stimuli causes cyclic modulation of perception. *The Journal of Neuroscience*, *34*(10), 3536–3544.
- Stein, B. E., & Meredith, M. A. (1993). *The merging of the senses* (pp. xv, 211). The MIT Press.
- Thut, G., Nietzel, A., Brandt, S. A., & Pascual-Leone, A. (2006).  $\alpha$ -Band electroencephalographic activity over occipital cortex indexes visuospatial attention bias and predicts visual target detection. *The Journal of Neuroscience*, *26*(37), 9494–9502.
- Uhlhaas, P. J., & Singer, W. (2010). Abnormal neural oscillations and synchrony in schizophrenia. *Nature Reviews Neuroscience*, *11*(2), 100–113.
- Van Dijk, H., Schoffelen, J.-M., Oostenveld, R., & Jensen, O. (2008). Prestimulus oscillatory activity in the alpha band predicts visual discrimination ability. *The Journal of Neuroscience*, *28*(8), 1816–1823.
- van Dijk, H., Schoffelen, J.-M., Oostenveld, R., & Jensen, O. (2008). Prestimulus oscillatory activity in the alpha band predicts visual discrimination ability. *The Journal of Neuroscience: The Official Journal of the Society for Neuroscience*, *28*(8), 1816–1823. <https://doi.org/10.1523/JNEUROSCI.1853-07.2008>
- Van Vreeswijk, C., Abbott, L. F., & Ermentrout, G. B. (1994). When inhibition not excitation synchronizes neural firing. *Journal of Computational Neuroscience*, *1*(4), 313–321.
- VanRullen, R. (2016). Perceptual cycles. *Trends in Cognitive Sciences*, *20*(10), 723–735. <https://doi.org/10.1016/j.tics.2016.07.006>
- VanRullen, R., Carlson, T., & Cavanagh, P. (2007). The blinking spotlight of attention. *Proceedings of the National Academy of Sciences*, *104*(49), 19204–19209. <https://doi.org/10.1073/pnas.0707316104>
- VanRullen, R., & Koch, C. (2003a). Is perception discrete or continuous? *Trends in Cognitive Sciences*, *7*(5), 207–213.
- VanRullen, R., & Koch, C. (2003b). Is perception discrete or continuous? *Trends in Cognitive Sciences*, *7*(5), 207–213. [https://doi.org/10.1016/S1364-6613\(03\)00095-0](https://doi.org/10.1016/S1364-6613(03)00095-0)

- VanRullen, R., Zoefel, B., & Ilhan, B. (2014). On the cyclic nature of perception in vision versus audition. *Philosophical Transactions of the Royal Society B: Biological Sciences*, *369*(1641), 20130214.
- Veniero, D., Benwell, C. S., Ahrens, M. M., & Thut, G. (2017). Inconsistent effects of parietal  $\alpha$ -tACS on Pseudoneglect across two experiments: A failed internal replication. *Frontiers in Psychology*, *8*, 952.
- Voloh, B., Valiante, T. A., Everling, S., & Womelsdorf, T. (2015). Theta–gamma coordination between anterior cingulate and prefrontal cortex indexes correct attention shifts. *Proceedings of the National Academy of Sciences*, *112*(27), 8457–8462.
- Wang, X.-J., & Buzsáki, G. (1996). Gamma oscillation by synaptic inhibition in a hippocampal interneuronal network model. *Journal of Neuroscience*, *16*(20), 6402–6413.
- Whittington, M. A., Traub, R. D., & Jefferys, J. G. (1995). Synchronized oscillations in interneuron networks driven by metabotropic glutamate receptor activation. *Nature*, *373*(6515), 612–615.
- Wilson, H. R., & Cowan, J. D. (1972). Excitatory and inhibitory interactions in localized populations of model neurons. *Biophysical Journal*, *12*(1), 1–24.
- Wittenberg, M. A., Baumgarten, T. J., Schnitzler, A., & Lange, J. (2018). U-shaped relation between prestimulus alpha-band and poststimulus gamma-band power in temporal tactile perception in the human somatosensory cortex. *Journal of Cognitive Neuroscience*, *30*(4), 552–564.
- Wittenberg, M. A., Morr, M., Schnitzler, A., & Lange, J. (2019). 10 Hz tACS over somatosensory cortex does not modulate supra-threshold tactile temporal discrimination in humans. *Frontiers in Neuroscience*, *13*, 311.
- Womelsdorf, T., & Fries, P. (2007). The role of neuronal synchronization in selective attention. *Current Opinion in Neurobiology*, *17*(2), 154–160.  
<https://doi.org/10.1016/j.conb.2007.02.002>
- Womelsdorf, T., Johnston, K., Vinck, M., & Everling, S. (2010). Theta-activity in anterior cingulate cortex predicts task rules and their adjustments following errors. *Proceedings of the National Academy of Sciences*, *107*(11), 5248–5253.
- Worden, M. S., Foxe, J. J., Wang, N., & Simpson, G. V. (2000). Anticipatory biasing of visuospatial attention indexed by retinotopically specific alpha-band electroencephalography increases over occipital cortex. *The Journal of Neuroscience: The Official Journal of the Society for Neuroscience*, *20*(6), RC63.
- Yamawaki, N., Stanford, I. M., Hall, S. D., & Woodhall, G. L. (2008). Pharmacologically induced and stimulus evoked rhythmic neuronal oscillatory activity in the primary motor cortex in vitro. *Neuroscience*, *151*(2), 386–395.
- Zimmerman, J. E., Thiene, P., & Harding, J. T. (1970). Design and Operation of Stable rf-Biased Superconducting Point-Contact Quantum Devices, and a Note on the Properties of Perfectly Clean Metal Contacts. *Journal of Applied Physics*, *41*(4), 1572–1580.  
<https://doi.org/10.1063/1.1659074>

## 7 Danksagung

Mein größter Dank gilt Prof. Dr. Alfons Schnitzler, der mir die Möglichkeit gegeben hat, den Großteil der hier beschriebenen Studien an dem von ihm geleiteten Institut anzufertigen. Danke für die Unterstützung in all den Jahren, die großartigen Voraussetzungen für spannende Wissenschaft, die ich im Institut vorgefunden habe, dein Vertrauen in mich und den Freiraum, mich weiterzuentwickeln zu können und ein eigenes wissenschaftliches Profil im Rahmen dieses Instituts entwickeln zu können.

Darüber hinaus gilt ein großer Dank Prof. Dr. Pascal Fries. Obwohl MEG und neuronale Oszillationen damals für mich absolutes Neuland waren, hast du mich in deine Arbeitsgruppe in Nijmegen aufgenommen. Danke für das Vertrauen und die Möglichkeit, so viel erlernen zu können. Diese zwei Jahre waren im positivsten Sinne sehr prägend für mein weiteres wissenschaftliches Arbeiten.

Danke auch an all meine Ko-Autoren ohne die die hier genannten Studien nicht möglich gewesen wären. Wissenschaft ist nahezu immer Teamarbeit und ich hatte Glück, mit vielen großartigen Teams zusammen zu arbeiten.

Weiter danke ich allen ehemaligen und heutigen Mitgliedern meiner Arbeitsgruppe für die schöne und erfolgreiche Zusammenarbeit. Insbesondere möchte ich mich bei den Masteranden und Doktoranden bedanken, deren Arbeiten zu dieser Habilitationsschrift beigetragen haben. Danke Anastasia, Johanna, Marc, Moritz, Nadine, Thomas!

Danke an die weiteren Kollegen in Düsseldorf und Nijmegen, die mich in all den Jahren begleitet und unterstützt haben.

All diese Arbeit und das Erreichte wären nicht möglich gewesen, wenn ich nicht auch großartige Unterstützung außerhalb der Wissenschaft gehabt hätte: Danke an meine Eltern für die langjährige Unterstützung. Und zu guter Letzt ein großer Dank an meine Familie, die mich all die Jahre unterstützt und nicht zuletzt immer wieder motiviert hat, die hier vorliegende Arbeit zu vollenden!

## 8 Appendix

All papers are published with permission of the publishers (Elsevier, Oxford University Press, MIT Press, John Wiley & Sons Books, National Academy of Sciences, Frontiers Media, Public Library of Science, Society of Neuroscience, Springer Nature) or under Creative Common licence CC BY.

- 1) Wittenberg, M. A., Morr, M., Schnitzler, A., & Lange, J. (2019).  
10 Hz tACS over somatosensory cortex does not modulate supra-threshold tactile temporal discrimination in humans.  
*Frontiers in Neuroscience, 13*, 311.  
Impact Factor (2019): 3.707  
Published with permission.



# 10 Hz tACS Over Somatosensory Cortex Does Not Modulate Supra-Threshold Tactile Temporal Discrimination in Humans

Marc A. Wittenberg<sup>1</sup>, Mitjan Morr<sup>1,2</sup>, Alfons Schnitzler<sup>1</sup> and Joachim Lange<sup>1\*</sup>

<sup>1</sup> Institute of Clinical Neuroscience and Medical Psychology, Medical Faculty, Heinrich-Heine-Universität Düsseldorf, Düsseldorf, Germany, <sup>2</sup> Division of Medical Psychology, University of Bonn, Bonn, Germany

## OPEN ACCESS

### Edited by:

Gregor Thut,  
University of Glasgow,  
United Kingdom

### Reviewed by:

Philipp Ruhnau,  
Universitätsklinikum Magdeburg,  
Germany  
Christopher Gundlach,  
Leipzig University, Germany

### \*Correspondence:

Joachim Lange  
Joachim.Lange@  
med.uni-duesseldorf.de

### Specialty section:

This article was submitted to  
Perception Science,  
a section of the journal  
Frontiers in Neuroscience

**Received:** 07 January 2019

**Accepted:** 19 March 2019

**Published:** 03 April 2019

### Citation:

Wittenberg MA, Morr M,  
Schnitzler A and Lange J (2019) 10 Hz  
tACS Over Somatosensory Cortex  
Does Not Modulate Supra-Threshold  
Tactile Temporal Discrimination  
in Humans. *Front. Neurosci.* 13:311.  
doi: 10.3389/fnins.2019.00311

Perception of physical identical stimuli can differ over time depending on the brain state. One marker of this brain state can be neuronal oscillations in the alpha band (8–12 Hz). A previous study showed that the power of prestimulus alpha oscillations in the contralateral somatosensory area negatively correlate with the ability to temporally discriminate between two subsequent tactile suprathreshold stimuli. That is, with high alpha power subjects were impaired in discriminating two stimuli and more frequently reported to perceive only one stimulus. While this previous study found correlative evidence for a role of alpha oscillations on tactile temporal discrimination, here, we aimed to study the causal influence of alpha power on tactile temporal discrimination by using transcranial alternating current stimulation (tACS). We hypothesized that tACS in the alpha frequency should entrain alpha oscillations and thus modulate alpha power. This modulated alpha power should alter temporal discrimination ability compared to a control frequency or sham. To this end, 17 subjects received one or two electrical stimuli to their left index finger with different stimulus onset asynchronies (SOAs). They reported whether they perceived one or two stimuli. Subjects performed the paradigm before (pre), during (peri), and 25 min after tACS (post). tACS was applied to the contralateral somatosensory-parietal area with either 10, 5 Hz or sham on three different days. We found no significant difference in discrimination abilities between 10 Hz tACS and the control conditions, independent of SOAs. In addition to choosing all SOAs as the independent variable, we chose individually different SOAs, for which we expected the strongest effects of tACS. Again, we found no significant effects of 10 Hz tACS on temporal discrimination abilities. We discuss potential reasons for the inability to modulate tactile temporal discrimination abilities with tACS.

**Keywords:** transcranial alternate current stimulation, tactile discrimination, alpha oscillations, somatosensory, supra-threshold

## INTRODUCTION

Perception does not only depend on the incoming stimuli, but also on intrinsic neuronal activity (or so called brain states). This intrinsic neuronal activity fluctuates over time and from trial to trial. Recent studies have shown that such fluctuations of neuronal activity can substantially influence perception. Specifically, fluctuations of neuronal oscillatory activity in the alpha band

(~8–12 Hz) correlate with perception of physical identical stimuli over time. For example, the ability to detect visual near-threshold stimuli improved with lower posterior prestimulus alpha band power (Hanslmayr et al., 2007; van Dijk et al., 2008). Similarly in the somatosensory domain, lower prestimulus alpha band power was related to better perception or discrimination of tactile stimuli (Linkenkaer-Hansen et al., 2004; Haegens et al., 2011; Lange et al., 2012; Baumgarten et al., 2016). Alpha oscillations are therefore interpreted as reflecting the excitability of a brain area, a decision bias or active inhibition of brain areas (Thut et al., 2006; Klimesch et al., 2007; Jensen and Mazaheri, 2010; Lange et al., 2013, 2014; Iemi et al., 2017; Limbach and Corballis, 2017). The evidence for a role of prestimulus alpha power, however, is mostly correlative. To provide causal evidence for an influence of alpha power on perception it is required to modulate alpha power and measure its impact on perception.

One potential method to modulate neuronal oscillations is transcranial alternating current stimulation (tACS). tACS is a method to non-invasively stimulate the brain with electrical activity of a given frequency (Antal and Paulus, 2013). It has been suggested that tACS with 10 Hz entrains the endogenous alpha band power in the stimulated brain area during stimulation (Helfrich et al., 2014b; Ruhnau et al., 2016). Alterations in alpha power have also been shown to outlast tACS, such that alpha power was increased after tACS (Zaehle et al., 2010; Neuling et al., 2013; Kasten et al., 2016). However, these studies were not conducted in the somatosensory domain. Recently, a study in the somatosensory cortex showed a decrease in alpha power after tACS (Gundlach et al., 2017). This opens the possibility to study the causal influence of alpha oscillations on brain functions. tACS over the sensory area areas has been used successfully to elicit sensations in the respective sensory domains (Abd Hamid et al., 2015). For example, Feurra et al. (2011b) used tACS to stimulate the primary somatosensory cortex and could elicit tactile sensations in the contralateral hand. Also, tACS has been successfully used to modulate performance in motor (Pogosyan et al., 2009; Feurra et al., 2011a; Joundi et al., 2012), perceptual (Laczó et al., 2012; Neuling et al., 2012; Helfrich et al., 2014a; Kar and Krekelberg, 2014), and higher cognitive function tasks (Santarnecchi et al., 2013).

Here, we aimed to use tACS to study a putative causal impact of alpha oscillations on tactile temporal perception. A recent study has shown that prestimulus alpha band (~8–12 Hz) power significantly negatively correlated with subjects' ability to perceive two electro-tactile stimuli as two separate stimuli (rather than one single stimulus; Baumgarten et al., 2016). To this end, we stimulated the somatosensory cortex with tACS at 10 Hz (i.e., in the alpha band) while subjects performed a tactile temporal discrimination task (Baumgarten et al., 2016). We hypothesized that 10 Hz tACS entrains intrinsic alpha oscillations and thus modulates the power of these alpha oscillations. Subsequently, discrimination of two subsequent tactile supra-threshold stimuli is expected to be altered with 10 Hz tACS compared to sham stimulation and stimulation with a control frequency (5 Hz). We tested this hypothesis during stimulation and 25 min after stimulation had ended.

## MATERIALS AND METHODS

### Subjects

We measured 17 subjects (nine female; age:  $25.4 \pm 1.4$  years; mean  $\pm$  SEM; range: 18 to 41 years). All subjects were right-handed according to the Edinburgh Handedness Inventory ( $87.0 \pm 3.4$ ; mean  $\pm$  SEM; Oldfield, 1971).

Exclusion criteria were history or family history of epilepsy, history of loss of consciousness, brain related injury, or other neurological or psychiatric disorders, high blood pressure, cardiac pacemaker or intracranial metal implantation, tinnitus, intake of central nervous system-affective medication, pregnancy, and impairments of the peripheral nerves in the left arm.

The experiment was conducted in accordance with the Declaration of Helsinki and approved by the local ethics committee of the Heinrich-Heine-Universität Düsseldorf, Germany (Study No. 4965R). Prior to the experiment, subjects gave written informed consent.

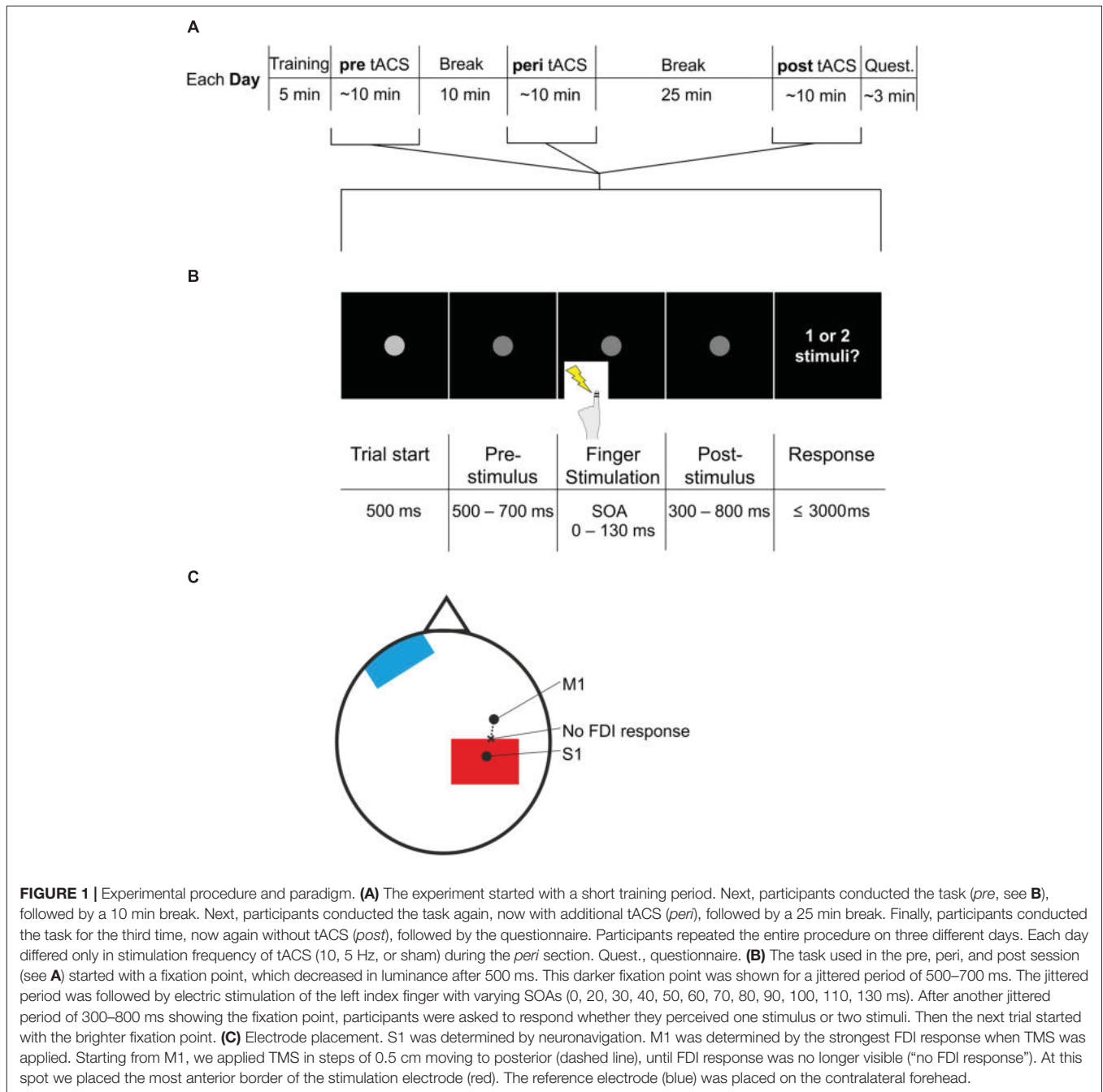
Subjects were naïve with respect to the hypotheses and stimulation conditions. Subjects received 50€ after completion of the entire experiment.

### Paradigm

The paradigm was modified after Baumgarten et al. (2016). Subjects received one or two electrical stimuli with different stimulus onset asynchronies (SOAs) on their left index finger. Subjects were asked to respond whether they perceived one or two stimuli.

Each trial began with a fixation dot which decreased in luminance after 500 ms, indicating the upcoming application of the stimuli (**Figure 1B**). After a jittered period of 500–700 ms, subjects received one or two stimulations to the left index finger (stimulation duration: 0.3 ms each) while viewing the fixation dot. Amplitude of the stimuli was individually determined such that subjects could clearly perceive the stimuli without being painful ( $2.1 \pm 0.2$  mA; mean  $\pm$  SEM). After another jittered period of 300–800 ms showing the fixation dot, subjects were asked by written instruction on the screen to respond with their right hand by button press. In nine subjects, button press with the right index finger related to perception of two stimuli and button press with the right middle finger related to perception of one stimulus. In the other subjects, button press pattern was reversed such that a press with the right index finger related to perception of one stimulus and button press with the right middle finger related to perception of two stimuli.

We used the following SOAs: 0 (i.e., only one stimulus applied), 20, 30, 40, 50, 60, 70, 80, 90, 100, 110, 130 ms. Trials with SOAs 0, 110, and 130 ms were each presented in 10 trials whereas each of the other SOAs was presented in 20 trials. SOAs with only 10 trials were added so that subjects responded to SOAs that clearly allowed for a perception of either 1 or 2 stimuli. The lower number of stimuli was chosen to keep the duration of the experiment within the time limit for tACS safety conditions (see below). The different SOAs were presented in pseudo-random order.



Subjects were asked to perform the experiment on 3 days, each separated by 1 week. On each day a different tACS frequency was applied: 10, 5 Hz, or sham. The order of tACS frequencies was randomized across subjects and double-blinded. For the double blinding, a person naïve to the experiment randomly selected the tACS frequency in each session and operated the DC stimulator during the experiment while the participants and the main experimenter who performed and analyzed the tACS experiment and communicated with the participants were unaware of the tACS frequency. Main experimenter and participants learned

of the used tACS frequencies only after all three frequencies had been applied.

During each day, subjects performed the paradigm three times: pre (before tACS), peri (during tACS), and post (after tACS). The peri session started 10 min after pre session ended; the post-session started 25 min after the peri session ended (**Figure 1A**). The pre session was included as baseline performance of the paradigm. The post-session was included because it was shown that tACS effects can outlast the end of stimulation (Veniero et al., 2015). There is no consistent pattern, however, regarding the latency and duration of post-stimulation

tACS effects (Veniero et al., 2015). While some studies report aftereffects a few minutes after the end of stimulation (e.g., Helfrich et al., 2014b), other studies report that aftereffects of 10 Hz tACS can last for 30 min (Neuling et al., 2013) or even start only 30 min after stimulation (Wach et al., 2013; see Veniero et al., 2015 for an overview). Most of these studies investigated tACS in the visual domain. Here, we aimed to investigate whether post-stimulation effects might be obtained in the somatosensory domain. Previous studies in the sensorimotor domain reported no effects of 10 Hz tACS directly after stimulation (Wach et al., 2013; Gundlach et al., 2016) and that aftereffects were visible only 30 min after stimulation (Wach et al., 2013). Therefore, we chose to study potential post-stimulation effects 25 min after tACS.

One session including all SOAs and repetitions lasted ~8–10 min.

A training phase of 5 min was included at the beginning of each day to let subjects familiarize with the paradigm. This training phase included SOAs 0, 20, 40, 60, 80, 100, 130, 150 ms. 0 and 150 ms appeared three times as often as the other SOAs to familiarize subjects with the clear perception of 1 or 2 stimuli, respectively.

The paradigm was presented with the Presentation software (Neurobehavioral Systems, Albany, NY, United States). Electrical stimuli at the left index finger were delivered by a stimulus current generator (DeMeTec GmbH, Langgöns, Germany).

In summary, our study included three independent variables: *frequency* (sham, 5, 10 Hz), *session* (pre, peri, post), *SOAs* (0–130 ms).

The post-session of each day was followed by a short questionnaire. In this questionnaire, subjects were interviewed if they felt a sensation during the tACS. Also, they were asked whether they thought stimulation or sham was applied and how confident they were with their answer on a scale from 1 (“very unsure”) to 10 (“very sure”). If they answered that stimulation had happened, then subjects were asked on their subjective impression of the stimulation frequency and their confidence in their judgment on a scale from 1 (“very unsure”) to 10 (“very sure”).

## Transcranial Alternating Current Stimulation (tACS)

Transcranial alternating current stimulation was applied with two saline-soaked sponge electrodes (7 cm × 5 cm) on the skin surface (DC Stimulator Plus, NeuroConn, Ilmenau, Germany). The electrodes were held in place with a rubber band covering the whole electrode. One electrode was placed over the right somatosensory cortex similar to the area found in Baumgarten et al. (2016). The other electrode was placed over the left orbit. tACS was applied at 10 or 5 Hz with a current of 1 mA (peak-to-peak amplitude, sinusoidal waveform) for a maximum of 10 min leading to a current density of 28.57  $\mu\text{A}/\text{cm}^2$  and a total charge of 0.017 C/cm<sup>2</sup>. Impedance was kept below 5 k $\Omega$ . These settings are within the boundary conditions of established safety protocols for transcranial direct current stimulation (Nitsche et al., 2003). Sham stimulation consisted of only 30 s stimulation with either 10 or 5 Hz. Each stimulation session included 10 s fade-in and 10 s fade-out time. If subjects finished the paradigm

before 10 min, the stimulation was terminated, resulting in an average stimulation time of  $8.2 \pm 0.13$  min (mean  $\pm$  SEM).

## Localization of Right Primary Motor and Somatosensory Cortex

Since Baumgarten et al. (2016) found a significant correlation between alpha power and tactile temporal discrimination in primary somatosensory cortex (S1) contralateral to stimulation, we aimed to stimulate contralateral (i.e., right) S1 with tACS.

To this end, the right S1 was localized by using neuronavigation (LOCALITE, Sankt Augustin, Germany) based on a standard MRI brain (MNI coordinates  $x = 36$  mm,  $y = -36$  mm,  $z = 48$  mm; Bingel et al., 2004).

After locating S1 with neuronavigation, the tACS electrode can be placed differently on the located spot (i.e., electrode centered above spot or spot at the border of the electrode). We sought to place the electrode to minimally overlap with motor cortex to avoid stimulation of the finger muscle which might be misjudged for a stimulus from the finger electrodes and thus interfere with the task (Figure 1C). To this end, we localized the right primary motor cortex (M1) with TMS.

Right M1 was localized by inducing muscle twitching in the first dorsal interosseus (FDI) by means of TMS. TMS of the right motor cortex was performed using a standard figure of eight coil (MC-B70) connected to a MagPro stimulator (Medtronic, Minneapolis, MN, United States). We located the right FDI by placing the coil tangentially to the scalp with the handling pointing backward. We began by placing the coil 45° away from the head midline and vertical to the right periauricular point. Moving the coil anterior, posterior, medial, and lateral in ~0.5 cm steps led to the localization with the maximal FDI motor response. This spot was determined as M1.

From M1 we applied TMS again posterior in ~0.5 cm steps until hand twitching stopped. This point we determined as the posterior end of M1. Here, we placed the anterior border of the electrode.

S1 localized by neuronavigation was  $2.8 \pm 0.2$  cm posterior to M1.

## Data Analysis and Statistics

For data analysis we used custom MATLAB (The MathWorks, Natick, MA, United States) scripts.

For each frequency (5, 10 Hz, sham), session (pre, peri, post), SOA and subject, we determined mean responses across all repetitions. Next, for each frequency, session and SOA, individual mean responses were averaged across subjects.

In our main statistical analysis, we applied three-way repeated-measures ANOVA (rmANOVA, Trujillo-Ortiz, 2006) with factors *Frequency*, *Session* and *SOAs*, after testing for normality of the data by means of Shapiro–Wilk tests (BenSaida, 2009, all  $p$ -values  $> 0.42$ ). The main hypothesis was to test whether subjects' responses showed significant main effects of *Frequency* and/or *Session*, or significant interaction effects.

Since our main analysis did not reveal any relevant significant effects (see section “Results”), we performed additional statistical tests. These tests were performed to exclude the possibility that

the non-significant results of the main analysis were caused by too low statistical power, by “noise” in the data due to the inclusion of data points that are irrelevant with respect to the hypothesis, or by too high intra- or inter-individual variability of responses.

The normalization was done in two different ways. In the first additional analysis, we normalized the data to minimize intra-individual variability.

The first normalization was based on the potential problem that individual performance might differ between different days in terms of absolute performance. We aimed to reduce intra-individual differences across days by normalizing the responses in the peri and post-sessions with respect to the pre session according to the formula:

$$r_{normFreq,Session}(SOA) = \frac{r_{Freq,Session}(SOA) - r_{Freq,pre}(SOA)}{r_{Freq,pre}(SOA)} \quad (1)$$

with  $r_{norm}$  being the individual normalized mean response as a function of SOA for a given tACS frequency  $Freq$  (10, 5 Hz, Sham) and paradigm  $Session$  (pre, peri, post).  $r$  denotes the non-normalized response as a function of SOA for a given  $Freq$  and  $Session$ . This normalization results in a measure that can be described as “responses relative to the pre session.”

In a second normalization, we sought to reduce inter-individual differences by transforming individual mean responses on a scale between 0 and 1 according to the following formula

$$r_{normFreq,Session}(SOA) = \frac{r_{Freq,Session}(SOA) - r_{minFreq,Session}}{r_{maxFreq,Session} - r_{minFreq,Session}} \quad (2)$$

with  $r_{norm}$  being the individual normalized mean response as a function of SOA for a given tACS frequency  $Freq$  (10, 5 Hz, Sham) and paradigm  $Session$  (pre, peri, post).  $r$  denotes the non-normalized response as a function of SOA for a given  $Freq$  and  $Session$ .  $r_{min}$  and  $r_{max}$  denote the non-normalized minimum and maximum, respectively, responses across all SOAs for a given  $Freq$  and  $Session$ . As mentioned above, this normalization results in responses normalized between 0 and 1.

As for the main analysis, we applied three-way repeated-measures ANOVA (rmANOVA, Trujillo-Ortiz, 2006) with factors  $Frequency$ ,  $Session$  and  $SOAs$  on individual and normalized mean responses, again after confirming normality by means of Shapiro–Wilk tests (BenSaïda, 2009, all  $p$ -values > 0.12).

In the third and final analysis, we focused on *a priori* hypotheses for chosen SOAs for the statistical analysis. The *a priori* chosen SOAs were based on results of one of our previous studies (Baumgarten et al., 2016). This MEG study found an influence of alpha power on perception for intermediate SOAs at ~25 ms. We speculated therefore that the effect of alpha power on perception is specific for SOAs of ~25 ms, while all other SOAs are unaffected by changes in alpha power. To this end, we selected from our study only those SOAs that are close to 25 ms. That is, we chose the responses of the SOA at 20

and 30 ms, either separately or averaged across both SOAs. For statistical analyses, we applied either planned  $t$ -tests or Wilcoxon sign-ranked tests, depending on whether or not input data were normally distributed (again tested by means of Shapiro–Wilk tests; BenSaïda, 2009).

Alternatively, the effect of alpha power on response rates might not be specific for SOAs of 25 ms *per se*, but rather for individual intermediate SOAs (intermediate SOAs and SOAs of ~25 ms coincide in Baumgarten et al., 2016). In the present study, the intermediate SOA was  $54.1 \pm 7.7$  ms (mean  $\pm$  SEM). If the influence of alpha power is specific for intermediate SOAs, we might expect an influence at ~54 ms (the intermediate SOA). In this analysis, we therefore chose to analyze the effect of tACS on mean responses for the individual intermediate SOA.

In line with the statistical analyses above, we applied either planned  $t$ -tests or Wilcoxon sign-ranked tests, depending on whether or not input data were normally distributed (again tested by means of Shapiro–Wilk tests; BenSaïda, 2009).

For the statistical analysis of specific SOAs, we applied left-tailed tests when comparing mean responses at peri 10 Hz tACS against mean responses pre 10 Hz tACS, peri 5 Hz tACS, or peri sham tACS, respectively.

We used two-tailed tests when comparing mean responses at post 10 Hz tACS against mean responses pre 10 Hz tACS, post 5 Hz tACS, or post-sham tACS, respectively.

In addition, we used Bayesian statistics to test whether our data is in favor of the null hypothesis that there is no difference between 10 Hz tACS and control conditions. For all Bayesian tests we used the program JASP (JASP Team, 2018).

For non-normalized and normalized data, we calculated Bayesian repeated measures ANOVAs with factors  $Frequency$ ,  $Session$ , and  $SOAs$ . For the interactions  $Frequency \times Session$ ,  $Frequency \times SOAs$ ,  $Session \times SOAs$  and  $Frequency \times Session \times SOAs$  we calculated the Bayes Inclusion Factor ( $BF_{Inclusion}$ ) based on matched models in JASP.

For our hypotheses for specific SOAs, we calculated Bayesian paired sample  $t$ -tests. As with our frequentist approach, we calculated left-tailed tests for peri tACS at 10 Hz vs. control conditions (i.e., mean responses at 10 Hz tACS smaller than mean responses at control conditions), and two-tailed tests for post-tACS at 10 Hz vs. control conditions. All Bayesian statistics were estimated based on a uniform prior distribution.

As an additional analysis we tested whether subjects that reported a flicker during tACS at 10 Hz showed a behavioral effect. To this end, we compared mean responses for peri tACS at 10 Hz vs. peri tACS at sham in line with above described analyses, but now only for subjects that reported a flicker sensation.

Given that tACS can have after-effects due to neuro-plastic changes (Veniero et al., 2015), we compared the first and the second half of the trials for peri tACS at 10 Hz by means of two-way repeated measures ANOVAs for non-normalized and normalized data with factors  $SOAs$  and  $Half$  (i.e., first or second half of the trials). Beforehand, we tested data for normality by means of Shapiro–Wilk tests. All data were normally distributed (all  $p > 0.10$ ). Additionally, we calculated Bayesian repeated measures ANOVAs with factors  $SOAs$  and  $Half$ .

We also tested the first half against the second half of the trials for peri tACS at 10 Hz for the aforementioned specific SOAs. Depending on normality (tested by Shapiro–Wilk tests) we applied either planned *t*-tests or planned Wilcoxon sign-ranked tests. Additionally, we calculated Bayesian *t*-tests.

## RESULTS

### Questionnaire

All subjects tolerated tACS and TMS well. Four subjects felt a tingling sensation under the electrodes at the start of the stimulation. Four subjects reported a light burning under an electrode at the beginning of the stimulation while one of them felt the burning during the whole stimulation at 10 Hz. Two subjects reported a warming under an electrode.

Five subjects had a flickering effect in their visual field at 10 Hz tACS. Two subjects had the flickering only at the beginning of the stimulation while three subjects during the whole stimulation.

When 10 Hz tACS was applied, two of the 17 subjects correctly identified the 10 Hz frequency with a confidence rating of  $7.0 \pm 0.3$  (mean  $\pm$  SEM), only one of them reporting the flickering effect.

For the 5 Hz tACS frequency, five of the 17 subjects identified correctly the 5 Hz frequency with a confidence rating of  $3.2 \pm 0.9$ . For sham tACS, six of the 17 subjects identified correctly that sham tACS was applied with a confidence rating of  $5.8 \pm 0.6$ . Since all these values are below chance level, we evaluated the blinding procedure as successful.

### General Effects of 10 Hz tACS on Tactile Perception

We measured perceptual responses in a temporal tactile discrimination task where subjects had to decide whether they perceived one or two electrical stimuli. We employed tACS at three different stimulation conditions: 10, 5 Hz, and sham. For each tACS frequency, subjects performed the paradigm three times: pre-, peri-, and post-tACS. Mean responses are shown in **Figure 2**. We tested the hypothesis that tACS at 10 Hz should modulate subjects' perception.

Three-way repeated measures ANOVA (rmANOVA) with factors *Frequency* (sham, 5, 10 Hz), *Session* (pre, peri, post), and SOAs (0–130 ms) revealed no significant main effects of *Frequency* [ $F(2,32) = 0.78$ ,  $p = 0.47$ ], *Session* [ $F(2,32) = 1.67$ ,  $p = 0.20$ ], nor interaction effects for *Frequency*  $\times$  *Session* [ $F(4,64) = 0.64$ ,  $p = 0.64$ ], *Frequency*  $\times$  SOAs [ $F(22,352) = 0.44$ ,  $p = 0.99$ ], and *Frequency*  $\times$  *Session*  $\times$  SOAs [ $F(44,704) = 0.72$ ,  $p = 0.91$ ]. There was a significant main effect of SOAs [ $F(11,176) = 59.59$ ,  $p < 0.01$ ] which indicates that mean responses increase with increasing SOAs (**Figure 2**). There was also a significant interaction *Session*  $\times$  SOAs [ $F(22,352) = 2.29$ ,  $p < 0.01$ ] which indicates that the increase of mean responses over SOAs differs between sessions independent of tACS frequency. However, the aim of our study was to investigate an effect of tACS frequency. Therefore, these two significant effects are irrelevant with respect to the main goal and will thus not further be discussed.

Bayesian repeated measures ANOVA with factors *Frequency*, *Session*, and SOAs revealed Bayes factors in favor of the null hypothesis that there is no difference in mean responses for the relevant main factors *Frequency* and *Session* and the interactions (*Frequency*:  $BF_{10} = 0.11$ , *Session*:  $BF_{10} = 0.07$ , *Frequency*  $\times$  *Session*:  $BF_{Inclusion} = 0.01$ , *Frequency*  $\times$  SOAs:  $BF_{Inclusion} = 6.37 \times 10^{-6}$ , *Session*  $\times$  SOAs:  $BF_{Inclusion} = 3.93 \times 10^{-5}$ , *Frequency*  $\times$  *Session*  $\times$  SOAs:  $BF_{Inclusion} = 8.89 \times 10^{-6}$ ). Only the factor SOAs revealed strong evidence for the alternative hypothesis ( $BF_{10} = 6.50 \times 10^{346}$ ), indicating that the factor SOA is an explanatory factor for the observed pattern of the data. Since this factor is of no relevance for the hypothesis of our study, we will not further discuss this finding.

Since the most relevant effects in the above analyses were not significant, we conducted further analyses to exclude several factors that might have hampered the main analyses. Our approaches included normalization approaches (to reduce intra- and inter-subjective variability) or using specific *a priori* hypotheses based on previous results (Baumgarten et al., 2016; see section “Materials and Methods”).

### Normalized Response Rates

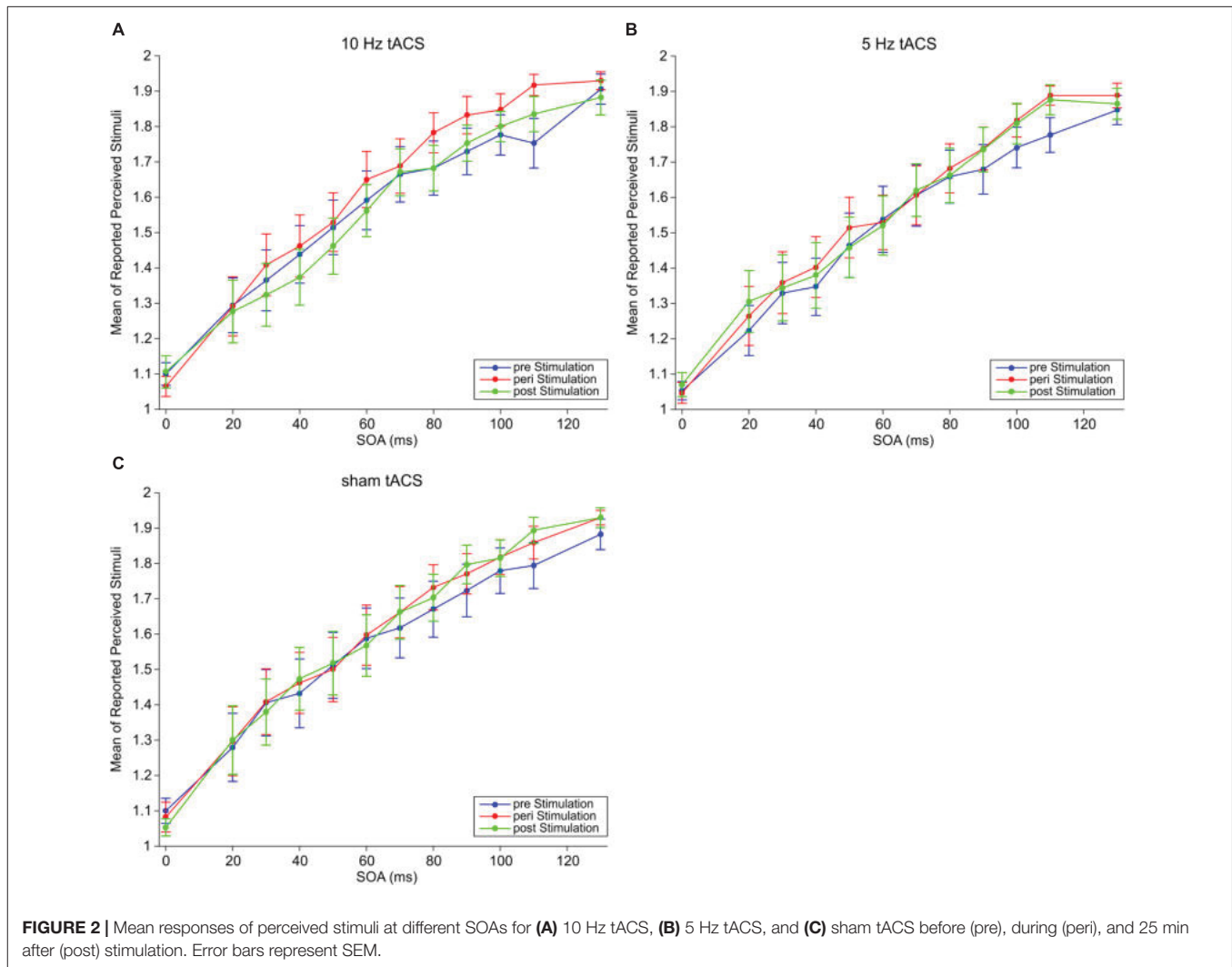
We normalized data in two ways: in a first approach, we normalized individual mean responses relative to the pre session for each tACS frequency. In the second approach, we normalized individual mean responses relative to individual minimum and maximum mean responses.

Similar to the main analysis of non-normalized response rates, we only obtained significant results for the main factor SOAs [relative to pre:  $F(11,176) = 2.83$ ,  $p < 0.01$ ; relative to minimum-maximum:  $F(11,176) = 61.56$ ,  $p < 0.01$ ] and the interaction factor *Session*  $\times$  SOA [relative to pre:  $F(22,352) = 2.14$ ,  $p < 0.01$ ; relative to minimum-maximum:  $F(22,352) = 1.67$ ,  $p = 0.03$ ]. Again, because these results are not relevant for our main goal, no *post hoc* analyses were carried out here.

We did not obtain significant results for main factors *Frequency* and *Session* nor for the interactions *Frequency*  $\times$  *Session*, *Frequency*  $\times$  SOAs, or *Frequency*  $\times$  *Session*  $\times$  SOAs (relative to pre: all  $p > 0.08$ ; relative to minimum-maximum: all  $p > 0.15$ ).

When data were normalized to the pre session, we obtained large Bayes factors for *Session* ( $BF_{10} = 29913.82$ ) and SOAs ( $BF_{10} = 3.80$ ). The large Bayes factor for the main factor *Session* most likely indicates a trivial result. Due to the normalization, all values in the pre session are set to “0” whereas the values in the peri and post-session are non-zeros. Bayesian analysis states that the model “*Session*” explains this difference better than a randomized model between all values. However, in this case this does not reveal a true difference between sessions *per se* but rather this is a result of our normalization procedure.

The main factor *Frequency* provides evidence for no difference between tACS frequencies ( $BF_{10} = 0.02$ ). Also, the Bayes factors for the interactions provided strong evidence in favor of no effects (*Frequency*  $\times$  *Session*:  $BF_{Inclusion} = 0.06$ , *Frequency*  $\times$  SOAs:  $BF_{Inclusion} = 4.83 \times 10^{-5}$ , *Session*  $\times$  SOAs:



$BF_{\text{Inclusion}} = 9.00 \times 10^{-4}$ ,  $\text{Frequency} \times \text{Session} \times \text{SOAs}$ :  $BF_{\text{Inclusion}} = 2.82 \times 10^{-5}$ ).

When data was normalized relative to minimum-maximum, Bayesian repeated measures ANOVA revealed again Bayes factors in favor of the null hypothesis that there is no difference in mean responses for the relevant factors ( $\text{Frequency}$ :  $BF_{10} = 0.02$ ,  $\text{Session}$ :  $BF_{10} = 0.02$ ,  $\text{Frequency} \times \text{Session}$ :  $BF_{\text{Inclusion}} < 0.01$ ,  $\text{Frequency} \times \text{SOAs}$ :  $BF_{\text{Inclusion}} = 1.75 \times 10^{-5}$ ,  $\text{Session} \times \text{SOAs}$ :  $BF_{\text{Inclusion}} = 1.77 \times 10^{-5}$ ,  $\text{Frequency} \times \text{Session} \times \text{SOAs}$ :  $BF_{\text{Inclusion}} = 9.82 \times 10^{-6}$ ). Only the factor  $\text{SOAs}$  provided strong evidence for an effect ( $\text{SOAs}$ :  $BF_{10} = 1.31 \times 10^{399}$ ), indicating again that the factor  $\text{SOAs}$  is an explanatory factor for the observed pattern of the data. Since this factor is of no relevance for the hypothesis of our study, we will not further discuss this finding.

### Comparison Between the First and Second Half of the Trials for 10 Hz tACS

To test whether tACS duration influences perception (e.g., due to neuro-plastic changes), we compared the

first and the second half of the trials for the peri session of tACS at 10 Hz.

A two-way repeated measures ANOVA revealed neither a significant main effect for *Half* nor an interaction effect for  $\text{SOAs} \times \text{Half}$  (all  $p > 0.22$  for normalized and non-normalized data and for *a priori* chosen SOAs).

Bayesian statistics provided evidence for no difference between halves (all  $BF_{10} < 0.20$ , for normalized and non-normalized data). Results for the interaction  $\text{SOAs} \times \text{Half}$  provided evidence for no interaction effects (all  $BF_{\text{Inclusion}} \leq 0.23$ ).

### *A priori* Hypotheses for the Effect of 10 Hz tACS on Tactile Perception at Intermediate SOAs

Here, we test the hypothesis that 10 Hz tACS might affect specifically intermediate SOA (i.e., SOAs for which subjects had mean responses of  $\sim 1.5$ , i.e., no clear bias toward perception of “1” or “2”).

Mean responses at peri 10 Hz tACS did not differ significantly from mean responses at pre 10 Hz tACS, peri Sham tACS or peri 5 Hz tACS (all  $p > 0.54$ ; **Figure 3**). Bayesian statistics provided evidence for the null hypothesis of no effect of tACS (all  $BF_{10} < 0.23$ ).

Likewise, mean responses at post 10 Hz tACS did not differ significantly from mean responses at pre 10 Hz tACS, post-Sham tACS or post 10 Hz tACS (all  $p > 0.34$ ; **Figure 3**). Bayesian statistics provided either inconclusive results or evidence for the null hypothesis of no effect of tACS (all  $BF_{10}$  between 0.25 and 0.44).

### Hypotheses for the Effect of 10 Hz tACS on Tactile Perception at SOAs 20 and 30 ms

A previous study reported a correlation of alpha power and perception at SOAs of  $\sim 25$  ms (Baumgarten et al., 2016). Therefore, we tested in this analysis that the causal effect of 10 Hz oscillations on temporal tactile perception might not be related to the intermediate SOA *per se*, but rather to an SOA of 20 to 30 ms.

Mean responses at peri 10 Hz tACS did not differ significantly from pre 10 Hz tACS, peri Sham tACS or peri 5 Hz tACS at an SOA of 20, 30 ms, or when responses of the SOAs at 20 and 30 ms were combined (all  $p > 0.38$ ). Bayesian statistics provided evidence in favor of the null hypothesis (all  $BF_{10} < 0.27$ ).

Likewise, mean responses at post 10 Hz tACS did not differ significantly from mean responses at pre 10 Hz tACS, post-Sham tACS or post 10 Hz tACS (all  $p > 0.22$ ). Bayesian statistics provided either inconclusive results or evidence for the null hypothesis of no effect of tACS (all  $BF_{10}$  between 0.26 and 0.48).

### Additional Analyses Only for Subjects That Reported a Flicker Sensation

When comparing mean responses for peri tACS at 10 Hz vs. peri tACS at sham only for subjects that

reported a flicker sensation, there was no behavioral effect (all  $p > 0.21$ ).

## DISCUSSION

We stimulated the somatosensory cortex with transcranial tACS while subjects performed a tactile discrimination task. Based on previous findings that reported a correlation between alpha power and tactile discrimination abilities (Baumgarten et al., 2016), we hypothesized that 10 Hz tACS would affect subjects' tactile perception. This way, we would provide evidence for a causal role of alpha power for tactile perception and add on the numerous studies reporting a correlation between (prestimulus) alpha power and perception. However, we found no significant effects of 10 Hz tACS on perceptual performance, neither when applied while subjects performed the task (i.e., peri tACS) nor did we find any aftereffects of stimulation (post-tACS).

That is, we did not find evidence for a causal role of alpha oscillations for tactile temporal discrimination. Bayesian statistics revealed that there is moderate to strong evidence in favor of the null hypothesis that mean responses with tACS at 10 Hz do not differ from control conditions. That is, our results are in favor that tACS at 10 Hz did not modulate tactile temporal discrimination. However, we do not conclude that 10 Hz or alpha power is not causally involved in tactile temporal discrimination. For such a conclusion there are still many factors to be considered as discussed below.

We will discuss in the following potential reasons and implications of this null result.

One potential reason might be that tACS at 10 Hz did not entrain neuronal oscillations. Since we did not measure neuronal activity in our study, we cannot exclude this possibility. Several previous studies, however, have shown that tACS in the alpha-band modulates neuronal oscillations. These studies have shown that alpha power is typically increased during tACS (Helfrich et al., 2014b; Ruhnau et al., 2016) as well as after tACS (Zaehle et al., 2010; Neuling et al., 2013; Kasten et al., 2016). In contrast to our study, these studies were not conducted in the somatosensory domain. In the somatosensory domain, recently, a decrease of alpha power after tACS at alpha frequencies was reported (Gundlach et al., 2017). One might argue that the current density we used may have been too low to entrain neuronal oscillations. Several studies, however, were able to entrain brain oscillations using similar current densities as we did (Moliadze et al., 2012; Neuling et al., 2015; Ruhnau et al., 2016). Since these studies were conducted in the visual domain, it might still be that in the somatosensory domain stronger current densities are needed to induce behavioral relevant entrainment. However, we refrained from using higher current densities because Feurra et al. (2011b) showed that tACS with a higher current density over S1 at alpha frequency elicited tactile sensations in the contralateral hand. Therefore, we used lower current density to minimize the possibility of inducing tactile sensations interfering with the task.

Another potential problem might be spatial inaccuracies in the stimulation so that our tACS did not entrain neuronal oscillations

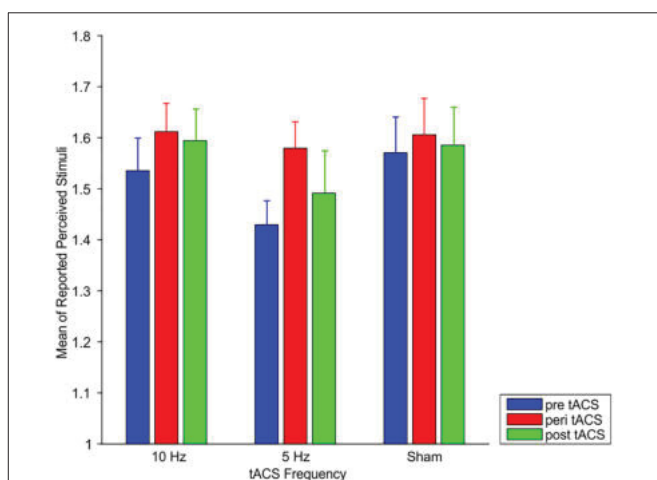


**FIGURE 3** | Mean responses of perceived stimuli at the individual intermediate SOA for 10 Hz tACS, 5 Hz tACS, and sham tACS before (pre), during (peri), and 25 min after (post) stimulation. Error bars represent SEM.

in S1. To exclude such a problem, we located S1 with two independent criteria (neuronavigation and no motor response with TMS) and we applied a large stimulation electrode. It seems thus unlikely that a putative entrainment did not affect S1.

In sum, although we have no direct measure of entrainment, we are confident that we entrained neuronal oscillations in the same area in which alpha power correlated with tactile discrimination in our previous study (Baumgarten et al., 2016).

Previous studies reported no unequivocal effects of tACS on perception. On the one hand, studies reported that tACS modulates perception (Neuling et al., 2012; Brignani et al., 2013; Gundlach et al., 2016; Veniero et al., 2017). On the other hand, several studies did not find an effect of tACS on perception (Brignani et al., 2013; Gundlach et al., 2016; Veniero et al., 2017; Sheldon and Mathewson, 2018). Specifically in the somatosensory domain, results are not clear. For example, Sliva et al. (2018) reported that tACS at alpha frequencies over somatosensory cortex lead to a decrease of performance in a tactile detection task of near-threshold stimuli. This decrease was reported for baseline corrected detection rates, but not for absolute detection rates. Thus, the putative effect of tACS may at least partially be explained by differences in baseline performances. In contrast, Gundlach et al. (2016) reported for a similar task that tACS at alpha frequencies did not affect mean detection rates. However, they reported that detection rates varied in a phasic manner, i.e., depending on the phase of tACS. Notably, these studies used detection tasks in which subjects had to report whether a stimulus near perceptual threshold was perceived. In our study, however, we used a discrimination task in which stimulation was always above perceptual threshold and subjects had to report whether they perceived one or two stimuli. Detection and discrimination tasks might be influenced by different processes. For example, our previous studies have shown that tactile discrimination tasks are influenced by power in the alpha frequencies, but the phase of beta frequencies (Baumgarten et al., 2015, 2016). Therefore, we focused our analysis on power modulations. In line with this hypothesis, Brignani et al. (2013) reported an effect of tACS at alpha frequencies in a visual detection task, while they could not find an effect of 10 Hz tACS in a visual discrimination task. Future studies might explore the differences between detection and discrimination tasks and how tACS might affect these tasks in more detail.

There is no clear consensus which frequency to use when tACS with “alpha frequencies” is applied. Whereas some studies used individual alpha frequencies, based on individual peak frequencies of neuronal oscillations in the alpha band (Cecere et al., 2015; Gundlach et al., 2016), others used a fixed frequency for all subjects (Brignani et al., 2013; Kar and Krekelberg, 2014; Sheldon and Mathewson, 2018). In the present study, we used a fixed frequency of tACS for all subjects. While this approach is easier to perform, especially since we did not measure neuronal oscillations, a fixed frequency might bear the downside that tACS does not match the “optimal” frequency in all subjects. According to the Arnold’s tongue principle, low stimulation intensities only entrain the endogenous frequency in

a small frequency band, whereas higher stimulation intensities can entrain a wider frequency band around the endogenous frequency (Herrmann et al., 2016; Kurmann et al., 2018). Therefore, it could be that we did not entrain alpha power in those subjects whose endogenous peak alpha frequency differs too much from 10 Hz to be entrained at the low stimulation intensity. However, Baumgarten et al. (2017) showed that tactile temporal discrimination does not correlate with individual alpha frequency of neuronal oscillations. In addition, several studies found an effect of tACS on detection using fixed frequencies (e.g., Brignani et al., 2013; Kar and Krekelberg, 2014). Finally, Baumgarten et al. (2016) reported an effect of alpha power on discrimination performances for one frequency, averaged across all subjects, rather than individual frequencies for each subject. Therefore, it seemed feasible for us to expect an effect of a fixed frequency for tACS. On the other hand, it could be that the mechanisms underlying tactile discrimination are not modulated by 10 Hz but other, neighboring frequencies within the alpha band. Given our low stimulation intensity, this potential alpha frequency might not be entrained due to the Arnold’s tongue principle. As mentioned above, however, we were restricted to 1 mA stimulation intensities, because a higher stimulation intensity could have produced tactile sensations (Feurra et al., 2011b), which might be misjudged for a stimulus from the finger electrode and thus distort behavioral results.

One might argue that the control frequency of 5 Hz might affect alpha power similarly to 10 Hz stimulation (de Graaf et al., 2013). Given that we found no effect of tACS in our study at all, this limitation does not change the conclusion of this study.

Given that tACS can produce after-effects due to neuro-plastic changes (Veniero et al., 2015), we also investigated whether tACS at 10 Hz might have an effect only at a later time segment during the stimulation. To this end, we compared the first half of the trials to the second half of the trials during peri tACS at 10 Hz. We found no differences between the first and the second half of the trials. This result suggests that longer stimulation duration did not lead to stronger results.

In summary, in our study we were unable to modulate tactile discrimination by applying tACS at alpha frequencies contralateral to the tactile stimulation. Consequently, we were unable to provide evidence for a causal role of somatosensory alpha oscillations in tactile discrimination tasks. tACS experiments comprise many degrees of freedom (e.g., electrode placements, stimulation frequency, stimulation current density, task and combinations of all factors). Another problem is that tACS can have different effects on different individuals due to anatomical differences such as the gyral depth or the thickness of the skull (Nitsche et al., 2008; Opitz et al., 2015). These factors result in a large search space for optimal parameters for the tACS experiment, making it difficult to decide for the optimal setup with regard to the question investigated (Kar and Krekelberg, 2014). And even with identical parameters, sometimes results of an tACS experiment cannot be replicated, even within one study (Veniero et al., 2017).

We are, however, confident that we used a reasonable parameter space for the stimulation parameters to expect a modulation of discrimination abilities. Thus, we might conclude that this specific combination of experimental factors is unable to modulate tactile temporal discrimination, but that we cannot conclude whether alpha power has a causal role on tactile temporal discrimination. This null effect should thus offer new insights and increase knowledge about an adequate setup of tACS experiments and to further understand difficulties and sometimes inconsistent results in tACS studies. Nevertheless, additional studies are needed to investigate a potential causal role of somatosensory alpha oscillations in tactile discrimination tasks.

## DATA AVAILABILITY

The datasets generated for this study are available on request to the corresponding author.

## REFERENCES

- Abd Hamid, A. I., Gall, C., Speck, O., Antal, A., and Sabel, B. A. (2015). Effects of alternating current stimulation on the healthy and diseased brain. *Front. Neurosci.* 9:391. doi: 10.3389/fnins.2015.00391
- Antal, A., and Paulus, W. (2013). Transcranial alternating current stimulation (tACS). *Front. Hum. Neurosci.* 7:317. doi: 10.3389/fnhum.2013.00317
- Baumgarten, T. J., Schnitzler, A., and Lange, J. (2015). Beta oscillations define discrete perceptual cycles in the somatosensory domain. *Proc. Natl. Acad. Sci. U.S.A.* 112, 12187–12192. doi: 10.1073/pnas.1501438112
- Baumgarten, T. J., Schnitzler, A., and Lange, J. (2016). Prestimulus alpha power influences tactile temporal perceptual discrimination and confidence in decisions. *Cereb. Cortex N.Y.* 26, 891–903. doi: 10.1093/cercor/bhu247
- Baumgarten, T. J., Schnitzler, A., and Lange, J. (2017). Beyond the peak - tactile temporal discrimination does not correlate with individual peak frequencies in somatosensory cortex. *Front. Psychol.* 8:421. doi: 10.3389/fpsyg.2017.00421
- BenSaïda, A. (2009). *Shapiro-Wilk and Shapiro-Francia Normality Tests*. Available at: <https://de.mathworks.com/matlabcentral/fileexchange/13964-shapiro-wilk-and-shapiro-francia-normality-tests> (accessed November 15, 2016).
- Bingel, U., Lorenz, J., Glauche, V., Knab, R., Gläscher, J., Weiller, C., et al. (2004). Somatotopic organization of human somatosensory cortices for pain: a single trial fMRI study. *NeuroImage* 23, 224–232. doi: 10.1016/j.neuroimage.2004.05.021
- Brignani, D., Ruzzoli, M., Mauri, P., and Miniussi, C. (2013). Is transcranial alternating current stimulation effective in modulating brain oscillations? *PLoS One* 8:e56589. doi: 10.1371/journal.pone.0056589
- Cecere, R., Rees, G., and Romei, V. (2015). Individual differences in alpha frequency drive crossmodal illusory perception. *Curr. Biol.* 25, 231–235. doi: 10.1016/j.cub.2014.11.034
- de Graaf, T. A., Gross, J., Paterson, G., Rusch, T., Sack, A. T., and Thut, G. (2013). Alpha-band rhythms in visual task performance: phase-locking by rhythmic sensory stimulation. *PLoS One* 8:e60035. doi: 10.1371/journal.pone.0060035
- Feurra, M., Bianco, G., Santarnecchi, E., Del Testa, M., Rossi, A., and Rossi, S. (2011a). Frequency-dependent tuning of the human motor system induced by transcranial oscillatory potentials. *J. Neurosci.* 31, 12165–12170. doi: 10.1523/JNEUROSCI.0978-11.2011
- Feurra, M., Paulus, W., Walsh, V., and Kanai, R. (2011b). Frequency specific modulation of human somatosensory cortex. *Front. Psychol.* 2:13. doi: 10.3389/fpsyg.2011.00013
- Gundlach, C., Müller, M. M., Nierhaus, T., Villringer, A., and Sehm, B. (2016). Phasic modulation of human somatosensory perception by transcranially applied oscillating currents. *Brain Stimulat.* 9, 712–719. doi: 10.1016/j.brs.2016.04.014
- Gundlach, C., Müller, M. M., Nierhaus, T., Villringer, A., and Sehm, B. (2017). Modulation of somatosensory alpha rhythm by transcranial alternating current stimulation at mu-frequency. *Front. Hum. Neurosci.* 11:432. doi: 10.3389/fnhum.2017.00432
- Haegens, S., Nächer, V., Luna, R., Romo, R., and Jensen, O. (2011).  $\alpha$ -Oscillations in the monkey sensorimotor network influence discrimination performance by rhythmical inhibition of neuronal spiking. *Proc. Natl. Acad. Sci. U.S.A.* 108, 19377–19382. doi: 10.1073/pnas.1117190108
- Hanslmayr, S., Aslan, A., Staudigl, T., Klimesch, W., Herrmann, C. S., and Bäuml, K.-H. (2007). Prestimulus oscillations predict visual perception performance between and within subjects. *NeuroImage* 37, 1465–1473. doi: 10.1016/j.neuroimage.2007.07.011
- Helfrich, R. F., Knepper, H., Nolte, G., Strüber, D., Rach, S., Herrmann, C. S., et al. (2014a). Selective modulation of interhemispheric functional connectivity by HD-tACS shapes perception. *PLoS Biol.* 12:e1002031. doi: 10.1371/journal.pbio.1002031
- Helfrich, R. F., Schneider, T. R., Rach, S., Trautmann-Lengsfeld, S. A., Engel, A. K., and Herrmann, C. S. (2014b). Entrainment of brain oscillations by transcranial alternating current stimulation. *Curr. Biol.* 24, 333–339. doi: 10.1016/j.cub.2013.12.041
- Herrmann, C. S., Murray, M. M., Ionta, S., Hutt, A., and Lefebvre, J. (2016). Shaping intrinsic neural oscillations with periodic stimulation. *J. Neurosci.* 36, 5328–5337. doi: 10.1523/JNEUROSCI.0236-16.2016
- Iemi, L., Chaumon, M., Crouzet, S. M., and Busch, N. A. (2017). Spontaneous neural oscillations bias perception by modulating baseline excitability. *J. Neurosci.* 37, 807–819. doi: 10.1523/JNEUROSCI.1432-16.2016
- Jensen, O., and Mazaheri, A. (2010). Shaping functional architecture by oscillatory alpha activity: gating by inhibition. *Front. Hum. Neurosci.* 4:186. doi: 10.3389/fnhum.2010.00186
- Joundi, R. A., Jenkinson, N., Brittain, J.-S., Aziz, T. Z., and Brown, P. (2012). Driving oscillatory activity in the human cortex enhances motor performance. *Curr. Biol.* 22, 403–407. doi: 10.1016/j.cub.2012.01.024
- Kar, K., and Krekelberg, B. (2014). Transcranial alternating current stimulation attenuates visual motion adaptation. *J. Neurosci.* 34, 7334–7340. doi: 10.1523/JNEUROSCI.5248-13.2014
- Kasten, F. H., Dowsett, J., and Herrmann, C. S. (2016). Sustained Aftereffect of  $\alpha$ -tACS lasts up to 70 min after stimulation. *Front. Hum. Neurosci.* 10:245. doi: 10.3389/fnhum.2016.00245
- Klimesch, W., Sauseng, P., and Hanslmayr, S. (2007). EEG alpha oscillations: the inhibition-timing hypothesis. *Brain Res. Rev.* 53, 63–88. doi: 10.1016/j.brainresrev.2006.06.003
- Kurmann, R., Gast, H., Schindler, K., and Fröhlich, F. (2018). Rational design of transcranial alternating current stimulation: identification, engagement, and

## AUTHOR CONTRIBUTIONS

MW and JL designed the study and analyzed the data. MW and MM collected the data. MW, MM, AS, and JL wrote the manuscript.

## FUNDING

JL was supported by the German Research Foundation (Grant No. LA 2400/4-1).

## ACKNOWLEDGMENTS

We would like to thank Vanessa Krause, Mareike Heller, Thomas Baumgarten, Konstantin Weltersbach, and Ariane Keitel for help with the tACS experiments.

- validation of network oscillations as treatment targets. *Clin. Transl. Neurosci.* 2:2514183X18793515.
- Laczó, B., Antal, A., Niebergall, R., Treue, S., and Paulus, W. (2012). Transcranial alternating stimulation in a high gamma frequency range applied over V1 improves contrast perception but does not modulate spatial attention. *Brain Stimulat.* 5, 484–491. doi: 10.1016/j.brs.2011.08.008
- Lange, J., Halacz, J., van Dijk, H., Kahlbrock, N., and Schnitzler, A. (2012). Fluctuations of prestimulus oscillatory power predict subjective perception of tactile simultaneity. *Cereb. Cortex N.Y.* 1991, 2564–2574. doi: 10.1093/cercor/bhr329
- Lange, J., Keil, J., Schnitzler, A., van Dijk, H., and Weisz, N. (2014). The role of alpha oscillations for illusory perception. *Behav. Brain Res.* 271, 294–301. doi: 10.1016/j.bbr.2014.06.015
- Lange, J., Oostenveld, R., and Fries, P. (2013). Reduced occipital alpha power indexes enhanced excitability rather than improved visual perception. *J. Neurosci.* 33, 3212–3220. doi: 10.1523/JNEUROSCI.3755-12.2013
- Limbach, K., and Corballis, P. M. (2017). Alpha-power modulation reflects the balancing of task requirements in a selective attention task. *Psychophysiology* 54, 224–234. doi: 10.1111/psyp.12774
- Linkenkaer-Hansen, K., Nikulin, V. V., Palva, S., Ilmoniemi, R. J., and Palva, J. M. (2004). Prestimulus oscillations enhance psychophysical performance in humans. *J. Neurosci.* 24, 10186–10190. doi: 10.1523/JNEUROSCI.2584-04.2004
- Moliadze, V., Atalay, D., Antal, A., and Paulus, W. (2012). Close to threshold transcranial electrical stimulation preferentially activates inhibitory networks before switching to excitation with higher intensities. *Brain Stimulat.* 5, 505–511. doi: 10.1016/j.brs.2011.11.004
- Neuling, T., Rach, S., and Herrmann, C. S. (2013). Orchestrating neuronal networks: sustained after-effects of transcranial alternating current stimulation depend upon brain states. *Front. Hum. Neurosci.* 7:161. doi: 10.3389/fnhum.2013.00161
- Neuling, T., Rach, S., Wagner, S., Wolters, C. H., and Herrmann, C. S. (2012). Good vibrations: oscillatory phase shapes perception. *NeuroImage* 63, 771–778. doi: 10.1016/j.neuroimage.2012.07.024
- Neuling, T., Ruhnau, P., Fuscà, M., Demarchi, G., Herrmann, C. S., and Weisz, N. (2015). Friends, not foes: Magnetoencephalography as a tool to uncover brain dynamics during transcranial alternating current stimulation. *NeuroImage* 118, 406–413. doi: 10.1016/j.neuroimage.2015.06.026
- Nitsche, M. A., Cohen, L. G., Wassermann, E. M., Priori, A., Lang, N., Antal, A., et al. (2008). Transcranial direct current stimulation: State of the art 2008. *Brain Stimulat.* 1, 206–223. doi: 10.1016/j.brs.2008.06.004
- Nitsche, M. A., Liebetanz, D., Lang, N., Antal, A., Tergau, F., and Paulus, W. (2003). Safety criteria for transcranial direct current stimulation (tDCS) in humans. *Clin. Neurophysiol.* 114, 2220–2222; author reply 2222–2223.
- Oldfield, R. C. (1971). The assessment and analysis of handedness: the edinburgh inventory. *Neuropsychologia* 9, 97–113.
- Opitz, A., Paulus, W., Will, S., Antunes, A., and Thielscher, A. (2015). Determinants of the electric field during transcranial direct current stimulation. *NeuroImage* 109, 140–150. doi: 10.1016/j.neuroimage.2015.01.033
- Pogosyan, A., Gaynor, L. D., Eusebio, A., and Brown, P. (2009). Boosting cortical activity at beta-band frequencies slows movement in humans. *Curr. Biol.* 19, 1637–1641. doi: 10.1016/j.cub.2009.07.074
- Ruhnau, P., Neuling, T., Fuscà, M., Herrmann, C. S., Demarchi, G., and Weisz, N. (2016). Eyes wide shut: transcranial alternating current stimulation drives alpha rhythm in a state dependent manner. *Sci. Rep.* 6:27138. doi: 10.1038/srep27138
- Santaracchi, E., Polizzotto, N. R., Godone, M., Giovannelli, F., Feurra, M., Matzen, L., et al. (2013). Frequency-dependent enhancement of fluid intelligence induced by transcranial oscillatory potentials. *Curr. Biol.* 23, 1449–1453. doi: 10.1016/j.cub.2013.06.022
- Sheldon, S. S., and Mathewson, K. E. (2018). Does 10-Hz cathodal oscillating current of the parieto-occipital lobe modulate target detection? *Front. Neurosci.* 12:83. doi: 10.3389/fnins.2018.00083
- Sliva, D. D., Black, C. J., Bowary, P., Agrawal, U., Santoyo, J. F., Philip, N. S., et al. (2018). A prospective study of the impact of transcranial alternating current stimulation on eeg correlates of somatosensory perception. *Front. Psychol.* 9:2117. doi: 10.3389/fpsyg.2018.02117
- JASP Team (2018). *JASP (Version 0.9)[Computer software]*.
- Thut, G., Nietzel, A., Brandt, S. A., and Pascual-Leone, A. (2006). Alpha-band electroencephalographic activity over occipital cortex indexes visuospatial attention bias and predicts visual target detection. *J. Neurosci.* 26, 9494–9502. doi: 10.1523/JNEUROSCI.0875-06.2006
- Trujillo-Ortiz, A. (2006). *RMAOV33*. Available at: <https://de.mathworks.com/matlabcentral/fileexchange/9638-rmaov33> (accessed March 20, 2017).
- van Dijk, H., Schoffelen, J.-M., Oostenveld, R., and Jensen, O. (2008). Prestimulus oscillatory activity in the alpha band predicts visual discrimination ability. *J. Neurosci.* 28, 1816–1823. doi: 10.1523/JNEUROSCI.1853-07.2008
- Veniero, D., Benwell, C. S. Y., Ahrens, M. M., and Thut, G. (2017). Inconsistent effects of parietal  $\alpha$ -tACS on pseudoneglect across two experiments: a failed internal replication. *Front. Psychol.* 8:952. doi: 10.3389/fpsyg.2017.00952
- Veniero, D., Vossen, A., Gross, J., and Thut, G. (2015). Lasting EEG/MEG aftereffects of rhythmic transcranial brain stimulation: level of control over oscillatory network activity. *Front. Cell. Neurosci.* 9:477. doi: 10.3389/fncel.2015.00477
- Wach, C., Krause, V., Moliadze, V., Paulus, W., Schnitzler, A., and Pollok, B. (2013). Effects of 10 Hz and 20 Hz transcranial alternating current stimulation (tACS) on motor functions and motor cortical excitability. *Behav. Brain Res.* 241, 1–6. doi: 10.1016/j.bbr.2012.11.038
- Zaehle, T., Rach, S., and Herrmann, C. S. (2010). Transcranial alternating current stimulation enhances individual alpha activity in human EEG. *PloS One* 5:e13766. doi: 10.1371/journal.pone.0013766

**Conflict of Interest Statement:** The authors declare that the research was conducted in the absence of any commercial or financial relationships that could be construed as a potential conflict of interest.

Copyright © 2019 Wittenberg, Morr, Schnitzler and Lange. This is an open-access article distributed under the terms of the Creative Commons Attribution License (CC BY). The use, distribution or reproduction in other forums is permitted, provided the original author(s) and the copyright owner(s) are credited and that the original publication in this journal is cited, in accordance with accepted academic practice. No use, distribution or reproduction is permitted which does not comply with these terms.

- 2) Wittenberg, M. A., Baumgarten, T. J., Schnitzler, A., & **Lange, J.** (2018).  
U-shaped relation between prestimulus alpha-band and poststimulus gamma-band  
power in temporal tactile perception in the human somatosensory cortex.  
*Journal of Cognitive Neuroscience*, 30(4), 552–564.  
Impact Factor (2018): 3.029

# U-shaped Relation between Prestimulus Alpha-band and Poststimulus Gamma-band Power in Temporal Tactile Perception in the Human Somatosensory Cortex

Marc André Wittenberg, Thomas J. Baumgarten, Alfons Schnitzler, and Joachim Lange

## Abstract

■ Neuronal oscillations are a ubiquitous phenomenon in the human nervous system. Alpha-band oscillations (8–12 Hz) have been shown to correlate negatively with attention and performance, whereas gamma-band oscillations (40–150 Hz) correlate positively. Here, we studied the relation between prestimulus alpha-band power and poststimulus gamma-band power in a suprathreshold tactile discrimination task. Participants received two electrical stimuli to their left index finger with different SOAs (0 msec, 100 msec, intermediate SOA, intermediate SOA  $\pm$  10 msec). The intermediate SOA was individually determined so that stimulation was bistable, and participants perceived one stimulus in half of the trials and two stimuli in the other half. We measured neuronal activity with magnetoencephalography (MEG). In trials with intermediate SOAs, behavioral performance correlated inversely

with prestimulus alpha-band power but did not correlate with poststimulus gamma-band power. Poststimulus gamma-band power was high in trials with low and high prestimulus alpha-band power and low for intermediate prestimulus alpha-band power (i.e., U-shaped). We suggest that prestimulus alpha activity modulates poststimulus gamma activity and subsequent perception: (1) low prestimulus alpha-band power leads to high poststimulus gamma-band power, biasing perception such that two stimuli were perceived; (2) intermediate prestimulus alpha-band power leads to low gamma-band power (interpreted as inefficient stimulus processing), consequently, perception was not biased in either direction; and (3) high prestimulus alpha-band power leads to high poststimulus gamma-band power, biasing perception such that only one stimulus was perceived. ■

## INTRODUCTION

Even in the absence of external sensory input, the brain is constantly active. Thus, neuronal activity is constantly fluctuating (Buzsáki & Draguhn, 2004). Incoming stimuli can therefore impinge on different levels of neuronal activity (i.e., brain states) at different times. These brain states can influence the processing of stimuli (Iemi, Chaumon, Crouzet, & Busch, 2017; Lange, Keil, Schnitzler, van Dijk, & Weisz, 2014; Weisz et al., 2014; Keil, Müller, Ihssen, & Weisz, 2012; Jensen & Mazaheri, 2010).

One prominent marker of brain states is neuronal oscillation. Neuronal oscillations refer to rhythmic changes in activity of neuronal populations (Buzsáki & Watson, 2012). Thus, fluctuations of brain states can be reflected in fluctuations of these neuronal oscillations. Two prominent frequency bands are the alpha (8–12 Hz) and gamma band (40–150 Hz). It has been found that fluctuations in prestimulus alpha-band power correlate with varying perception despite physically identical stimulation (Lange,

Halacz, van Dijk, Kahlbrock, & Schnitzler, 2012; van Dijk, Schoffelen, Oostenveld, & Jensen, 2008; Linkenkaer-Hansen, Nikulin, Palva, Ilmoniemi, & Palva, 2004). For example, lower parieto-occipital alpha-band power increased participants' ability to detect near-threshold visual stimuli (van Dijk et al., 2008; Hanslmayr et al., 2007). Similarly, prestimulus alpha-band power in contralateral somatosensory-posterior areas was lower when participants could discriminate veridically between two subsequent tactile stimuli compared with trials where participants perceived stimulation as one single stimulus (Baumgarten, Schnitzler, & Lange, 2016). Given these results, it was suggested that prestimulus alpha oscillations reflect the excitability of a brain area, which in turn influences the neuronal processing and perception of ambiguous stimuli (Lange et al., 2014; Lange, Oostenveld, & Fries, 2013; Thut, Nietzel, Brandt, & Pascual-Leone, 2006). In addition, alpha-band power has been related to active inhibition of brain areas (Jensen & Mazaheri, 2010; Klimesch, Sauseng, & Hanslmayr, 2007). In line with the inhibition hypothesis, prestimulus alpha-band power is modulated by spatial attention, and such modulations of

alpha-band power have been shown to affect perception (Thut et al., 2006; Worden, Foxe, Wang, & Simpson, 2000; Foxe, Simpson, & Ahlfors, 1998). In addition to prestimulus alpha-band power, the power of poststimulus gamma oscillations is also modulated by attention. In visuospatial attention tasks, poststimulus gamma-band power increases in the visual area contralateral to the stimulus (e.g., Händel, Haarmeier, & Jensen, 2011; Fries, Womelsdorf, Oostenveld, & Desimone, 2008; Siegel, Donner, Oostenveld, Fries, & Engel, 2008; Müller, Gruber, & Keil, 2000). Similarly, poststimulus gamma power in tactile spatial attention tasks increases in somatosensory areas contralateral to the attended side and can affect perception (Haegens, Nächer, Hernández, et al., 2011; Haegens, Osipova, Oostenveld, & Jensen, 2010; Bauer, Oostenveld, Peeters, & Fries, 2006). Finally, it was found that poststimulus gamma oscillations and behavioral performance are linked. For example, high gamma-band power in visual cortex relates to faster RTs (Hoogenboom, Schoffelen, Oostenveld, & Fries, 2010; Womelsdorf, Fries, Mitra, & Desimone, 2006). In the somatosensory domain, higher poststimulus gamma-band power in contralateral primary somatosensory cortex (S1) relates to increased stimulus detection (Siegle, Pritchett, & Moore, 2014; Meador, Ray, Echauz, Loring, & Vachtsevanos, 2002). Generally, gamma oscillations are discussed as the neuronal underpinnings of cortical information processing (Fries, 2005, 2009, 2015).

In summary, both prestimulus alpha and poststimulus gamma oscillations are associated with attention, neuronal processing, and behavioral performance. Prestimulus alpha-band power typically decreases with higher attention, and low alpha-band power is associated with higher behavioral performance. By contrast, poststimulus gamma-band power typically increases with higher attention and high gamma-band power is associated with higher behavioral performance. Given these similar, but also diametrical effects of prestimulus alpha-band power and poststimulus gamma-band power, we speculated that prestimulus alpha-band power and poststimulus gamma-band power are directly (negatively) correlated.

To this end, we studied the relation of prestimulus alpha-band power, poststimulus gamma-band power, and tactile perception in a suprathreshold tactile discrimination task. We hypothesized that poststimulus gamma-band power in primary somatosensory cortex (S1) is positively correlated with perception, whereas prestimulus alpha-band power is negatively correlated with perception. Consequently, when comparing alpha- and gamma-band power directly, we hypothesized to find a negative correlation between prestimulus alpha-band power and poststimulus gamma-band power.

## METHODS

We used data recorded by Baumgarten et al. (2016). Here, we give a concise description. More details on

paradigm, participants and recordings can be found in Baumgarten et al. (2016).

## Participants

We included 12 of the 16 right-handed participants (four men, mean = 26.0 years,  $SD = 5.3$  years) measured by Baumgarten et al. (2016; see below for reasons for excluding four participants). Participants gave written informed consent in accordance with the Declaration of Helsinki and the Ethical Committee of the Medical Faculty, Heinrich-Heine-University Düsseldorf before participating in the experiment.

Participants had no known neurological disorders, no somatosensory deficits, and normal or corrected-to-normal vision.

## Paradigm

Each trial began with a fixation dot in the center of the participant's visual field projected on the backside of a translucent screen (60 Hz refresh rate) positioned 60 cm in front of the participant. After 500 msec, this fixation dot decreased in luminance, indicating that the stimulation is about to be applied after a jittered period (900–1100 msec). Then, participants received two electrical stimuli (duration: 0.3 msec each) with different SOAs. Electrical stimuli were applied by electrodes located between the two distal joints of the left index finger. The amplitude of the pulses was individually determined so that stimulation was clearly perceived, but without being painful (stimulus amplitude: mean = 4.1,  $SD = 1.4$  mA). In a premeasurement, the individual SOA was determined for which a participant veridically perceived two stimuli in ~50% of the trials (intermediate SOA, mean = 24.6 msec,  $SD = 6.2$  msec). During the task, participants received stimulation with five different SOAs: 0 msec, 100 msec, intermediate SOA, intermediate SOA  $\pm 10$  msec. After stimulation, the fixation dot remained visible for another jittered period (500–1200 msec) to minimize motor preparation effects. By written instruction on the screen, participants were asked to report the number of perceived stimuli (either one or two) within 3000 msec via button press with the right index or middle finger. Again, to minimize motor preparation effects, configuration of the response buttons was randomized for each trial.

Each SOA was used in 50 trials. Only the intermediate SOA was used in 200 trials, resulting in 400 trials in total. Stimuli were presented in blocks. Each block consisted of 80 trials: 40 trials with intermediate SOA and 10 trials for each of the remaining SOAs. After each block, a self-paced break (~2 min) was included.

To familiarize participants with the task, a 5-min training phase with all five SOAs preceded the actual measurement. Before the measurement, participants received

information about the task, but not about the purpose of the study or the different SOAs.

Presentation of the stimuli was done with Presentation software (Neurobehavioral Systems, Albany, NY).

### Magnetoencephalography Measurement

A 306-channel whole-head magnetoencephalography (MEG; Neuromag Elekta Oy, Helsinki, Finland) was used to record brain activity at a sampling rate of 1000 Hz while participants performed the task. The MEG consisted of 102 pairs of orthogonal gradiometers and 102 magnetometers. For the analysis, only the gradiometers were taken into account. EOGs were measured to detect eye movements. EOG electrodes were placed at the outer sides of both eyes and above and below the left eye.

### Data Preprocessing

Data were analyzed with custom-made scripts using Fieldtrip (Oostenveld, Fries, Maris, & Schoffelen, 2011) and Matlab (The MathWorks, Natick, MA).

Continuously recorded data were divided into trials. A trial started with the appearance of the fixation dot and ended with the press of the response button. The total number of trials was 400 with an average trial length of ~6 sec (4–8.6 sec). Power line noise at 50 Hz and its harmonics at 100 and 150 Hz were removed by a band-stop filter, and data were bandpass filtered between 2 and 250 Hz. For the filters, we used the default options implemented in FieldTrip, that is, we used an infinite impulse response zero-phase Butterworth filter of fourth order. A mean of 5.1 ( $SEM = 0.5$ ) noisy channels were removed and reconstructed by interpolation of neighboring channels. Artifacts (muscle or eye movement, SQUID jumps) were removed semiautomatically by means of a  $z$ -score-based algorithm implemented in FieldTrip, followed by an additional visual inspection to remove artifacts (e.g., extensively noisy channels or channels still containing nondetected squid jumps, etc.). A mean of 104.1 ( $SEM = 9.1$ ) trials were removed due to artifacts.

Other preprocessing steps were conducted according to the respective analyses (see below).

### Overview of Analysis Steps

We aimed to analyze the relation between prestimulus alpha-band power, poststimulus gamma-band power, and perception. Details on the analyses will be provided below. Here, we give a concise overview of the analysis steps performed. First, for each single trial prestimulus alpha-band power was determined by averaging power in a priori defined sensors, time range, and frequency band based on results of our previous study (Baumgarten et al., 2016). Second, for each single trial poststimulus gamma-band power was determined similarly by averag-

ing power across sensors, time, and frequency. Here, sensors of interest were determined based on the topography of the M50, and frequency ranges were determined individually.

After performing these two steps, we could determine per participant and for each single trial one value for prestimulus alpha-band power, poststimulus gamma-band power, and perception, respectively. This enabled us to sort individual trials with respect to alpha-band power or gamma-band power. Then, we combined trials to bins, computed mean gamma-band power and/or mean perception in these bins. Finally, we tested by means of first- and second-order regression analyses a putative relation between the two variables (i.e., alpha- or gamma-band power, respectively, on the one side, and gamma-band power or perception, respectively, on the other side).

### Time-Frequency Analysis

Time-frequency analysis (TFA) was performed for frequencies in the alpha (8–12 Hz) and gamma band (40–150 Hz) by means of discrete Fourier transformation on sliding time windows. For the following analyses, we only used trials with intermediate SOA. Before TFA, we removed the mean of the respective time period and the linear trend. We combined each pair of gradiometers by summing the spectral power of orthogonal gradiometers. The TFA was performed on 3000-msec data segments (–1000 to 2000 msec). If the data in a trial were shorter than 3000 msec (e.g., due to removed artifacts), the corresponding trial was zero-padded to 3000 msec.

The alpha-band (8–12 Hz) power was analyzed in steps of 1 Hz with a time window  $\Delta t$  of seven cycles of the respective frequency  $f$  ( $\Delta t = 7/f$ ), moved in steps of 50 msec (Baumgarten et al., 2016). We used a single Hanning taper on each time window, resulting in spectral smoothing of  $1/\Delta t$ .

In our previous study, we found a significant effect of prestimulus alpha-band power on perception in a specific set of sensors and in the prestimulus time period (–0.9 to –0.25 sec, with 0 msec being the time point in which the first electrical stimulus occurred; Baumgarten et al., 2016). Here, we thus analyzed alpha-band power in the same sensors and the same time period. As in Baumgarten et al. (2016), we averaged alpha-band power from 8 to 12 Hz in this time window and in these sensors. These sensors are as follows: MEG1042+1043, MEG1112+1113, MEG1122+1123, MEG1312+1313, MEG0712+0713, MEG0722+0723, MEG1142+1143, MEG1132+1133, MEG1342+1343, MEG2212+2213, MEG2412+2413, MEG2422+2423, MEG2642+2643, MEG1832+1833, MEG2242+2243, MEG2232+2233, MEG2012+2013, MEG2442+2443, MEG2432+2433, MEG2522+2523, MEG2312+2313, MEG2322+2323, MEG2512+2513, MEG2342+2343, MEG2022+2023, MEG2212+2213, MEG2612+2613, MEG2222+2223.

The gamma band (40–150 Hz) was analyzed in steps of 5 Hz with a time window of 100 msec, moved in steps of 20 msec. Here, we used three Slepian tapers on each time window, resulting in spectral smoothing of  $\pm 20$  Hz. We focused our analysis of gamma-band power on the right primary somatosensory cortex (S1 contralateral to stimulation site) by identifying five sensors showing maximum amplitude of the M50 (MEG1122+1123, MEG1132+1133, MEG1312+1313, MEG1342+1343, MEG1332+1333; see below for details on sensor selection). In the following analyses, we averaged gamma-band power over these five sensors. Furthermore, we only used trials with intermediate SOAs.

For the analysis of gamma-band power, we first determined individual frequencies showing maximal power. To this end, we calculated for each participant, for each time point between 0 and 200 msec, and for each frequency between 40 and 150 Hz the power relative to an averaged prestimulus baseline ( $-600$  to  $-200$  msec) by means of an independent  $t$  test.

Next, we averaged for each frequency the  $t$  values across all poststimulus time points (0–200 msec; Baumgarten, Schnitzler, & Lange, 2017; Cousijn et al., 2014). Individual gamma-band peaks were identified using Matlab's built-in function *findpeaks* (Baumgarten et al., 2017). Gamma ranges with maximum power were determined by taking the width of the gamma-band peak at its half height (as implemented in the function *findpeaks*; Figure 1A).

We used two inclusion criteria for a frequency to be identified as a peak frequency: First, to ensure that gamma-band activity was not just a broadband signal in response to stimulation onset but a clear narrow-band range, we defined a minimum peak height relative to neighboring points (i.e., setting in *findpeaks* the *MinPeakProminence* to a  $t$  value of 0.5). By this criterion, we had to exclude one participant because we could not ensure that a seeming gamma range was actually a broadband response across a wider range of frequencies, including the beta band (20–40 Hz, Participant 8 excluded; see Figure 1A). Second, to ensure that gamma ranges with highest power were sufficiently strong to be not confused with noise fluctuations, we set an absolute threshold of  $t = 1$  (i.e., setting in *findpeaks* the *MinPeakHeight* to a  $t$  value of 1). By this criterion, we had to exclude three participants from further analyses (Participants 5, 13, and 15; see Figure 1A).

### **Selection of Sensors of Interest (Event-related Field Analysis)**

We focused our analysis of gamma-band power on the right primary somatosensory cortex (S1 contralateral to stimulation site). To this end, we determined sensors showing maximum amplitude of the M50 component of the event-related field. The M50 component is known to originate from S1 after tactile stimulation (Iguchi, Hoshi, Tanosaki, Taira, & Hashimoto, 2005). To identify the

M50, we first averaged the time domain data for each gradiometer and each participant separately. Next, gradiometer pairs were combined by adding the signal of all trials to the two orthogonal sensors using Pythagoras' rule. The evoked responses were then averaged across participants. We identified the M50 component by focusing on the time window 0.025–0.120 sec after stimulation. Finally, we determined five sensor pairs showing maximum amplitude of the M50 (MEG1122+1123, MEG1132+1133, MEG1312+1313, MEG1342+1343, MEG1332+1333).

### **Regression Analyses**

For each participant, we sorted the trials with intermediate SOA from low to high power, either for the gamma band or the alpha band. Then, we divided the trials in five bins with equal number of trials in each bin. There were  $30.0 \pm 0.1$  trials per bin. Note that the sum of trials in all bins is not 200 due to trials being removed in the preprocessing steps.

To determine a potential relation between oscillatory power and perception, we determined for each bin the mean responses per participant by averaging the number of "1" and "2" responses.

For each bin, we normalized mean responses according to the following procedure (Baumgarten et al., 2016; Lange et al., 2012; Jones et al., 2010; Linkenkaer-Hansen et al., 2004): We calculated the mean response for each participant for (a) each single bin and (b) across all bins. Then, for each single bin, we subtracted the mean response across all bins from the mean response from a single bin. The obtained result was then divided by the mean response across all bins.

Finally, we calculated for each bin mean responses (and *SEM*) across participants.

To reproduce the results of Baumgarten et al. (2016), we performed linear regression analysis between alpha-band power and perceptual responses. To determine a potential relation between prestimulus alpha-band power and poststimulus gamma-band power, we performed regression analyses (Baumgarten et al., 2016; Lange et al., 2012; Linkenkaer-Hansen et al., 2004). Because we a priori expected a linear relationship, we first performed a linear regression. In addition, we performed a post hoc quadratic regression analysis.

To determine a potential relation between alpha-band and gamma-band power, we determined for each alpha-band power bin the average gamma-band power per participant. Next, we normalized for each participant the mean gamma-band power relative to the mean gamma-band power across all bins. Finally, we calculated for each alpha-band power bin mean gamma-band power (and *SEM*) across participants.

To exclude the possibility that a correlation between alpha-band power and gamma-band power was induced by covarying noise levels in both frequency bands across

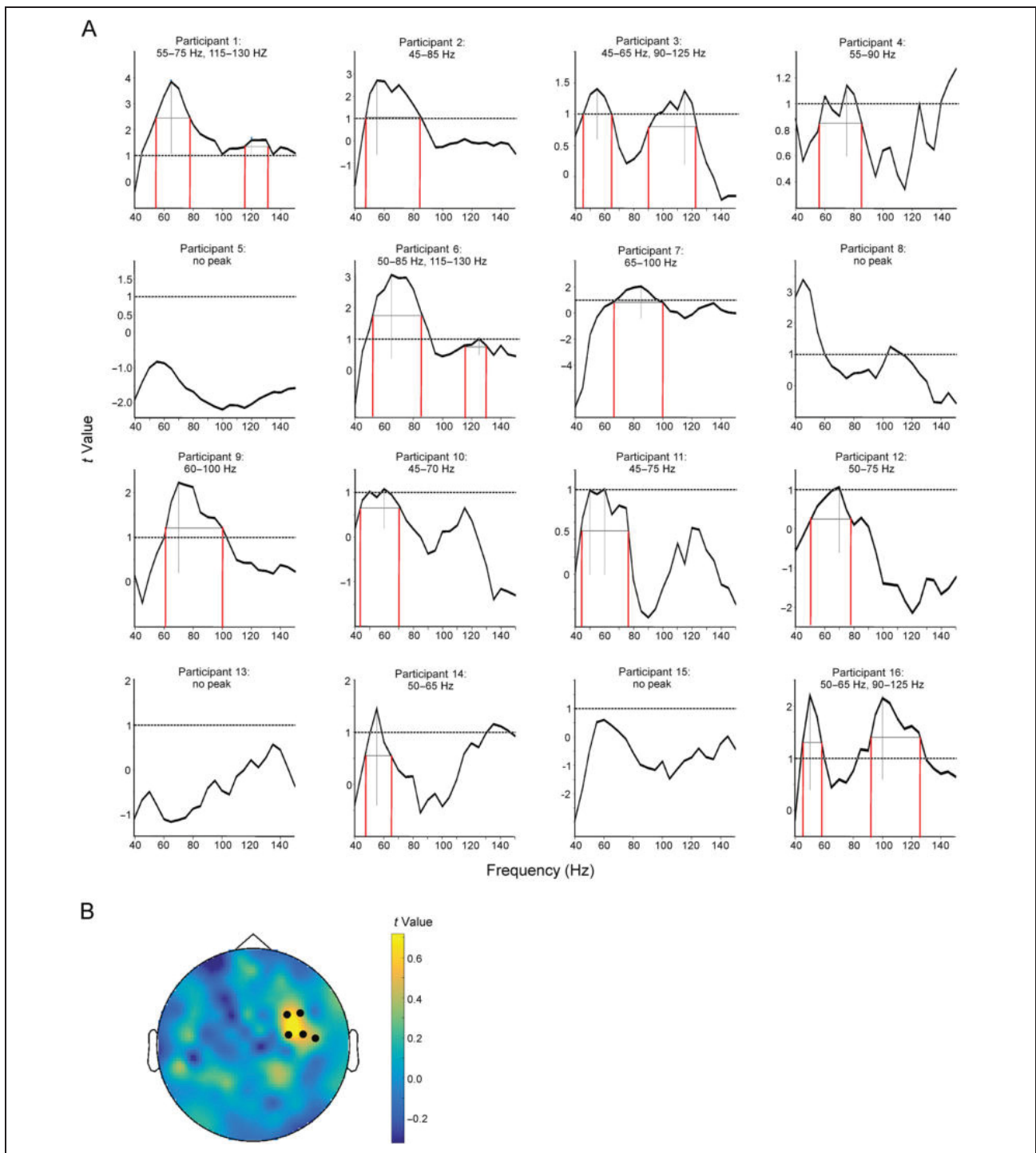


**Figure 1.** Poststimulus gamma-band activity. (A) Individual spectra in the gamma-band range (40–150 Hz). Spectra were determined by computing for each frequency (40–150 Hz) and time point (0–200 msec)  $t$  values (poststimulus vs. prestimulus activity) and then averaging  $t$  values across 0–200 msec. Peaks of each spectrum were determined using the Matlab function *findpeaks*. Dashed horizontal lines indicate the threshold ( $t = 1$ ) for a peak to be recognized. Instead of peak frequencies, our analysis relied on narrow-band frequency ranges. Frequency ranges were determined by computing the width of the peak at its half height. Smaller gray lines indicate the relative height of the peak (Prominence in Matlab function *findpeaks*) and the width (Width at half prominence in Matlab function *findpeaks*). Red vertical lines indicate the frequencies at the half height, which determine the upper and lower limits of the gamma-band range used for subsequent analyses. Note that Participants 5, 13, and 15 had to be excluded from further analyses because their gamma peaks were below the threshold. Participant 8 had to be excluded from further analyses, because increased activity extended also to lower frequencies (not shown) so that we could not excluded that this activity was actually a broadband response to stimulation. (B) Topographical representation of gamma-band activity averaged across participants. For each participant,  $t$  values in the individual gamma-band ranges (see A) were averaged for each sensor. Next, the  $t$  values were averaged across participants. Black dots indicate the sensors of interest for gamma-band analysis, which were determined beforehand.

trials, we performed additional control analyses. To this end, we repeated the abovementioned analysis, but now with gamma-band power averaged across a different time window (but with identical length), for which we did not expect modulations of gamma-band power but just noise fluctuations (−500 to −300 msec).

Second, we computed signal-to-noise ratios (SNRs) by dividing for each participant and trial poststimulus gamma-band power (i.e., between 0 and 200 msec) and prestimulus gamma-band power (i.e., “noise” between −500 and −300 msec). Then, we repeated the abovementioned analysis for the SNRs.

All regression analyses were carried out using the Matlab built-in function *regstats*.

### Statistical Analysis

We statistically compared perception across alpha- and gamma-band power bins, respectively. Likewise, we statistically compared gamma-band power across alpha-band power bins. First, we applied a Kolmogorov–Smirnov test to test for normality of the data for each bin. Kolmogorov–Smirnov tests showed that data in all bins significantly differed from a normal distribution (all  $p$ s < .05). To confirm and strengthen the significant linear or quadratic regression, we additionally performed planned post hoc Wilcoxon signed-ranked tests on the most extreme values, respectively. That is, for the significant linear regression between alpha-band power and perception, we compared Bins 1 and 5. For the significant quadratic regression between alpha-band power and gamma-band power, gamma-band power should be lower in alpha-band power Bin 3 relative to Bins 1 and 5. To this end, we applied one-sided Wilcoxon signed-ranked tests to compare Bin 3 versus Bin 1 and Bin 3 versus Bin 5.

## RESULTS

To investigate the relationship between prestimulus alpha-band power, poststimulus gamma-band power, and perception, we measured MEG while participants performed a tactile temporal discrimination task.

### Behavioral Data

Participants received one or two stimuli with varying SOAs and had to report the number of perceived stimuli. When only one stimulus was presented, participants reported one stimulus in  $94.3 \pm 0.4\%$  of all trials. When two stimuli were presented with an SOA of 100 msec, participants reported two stimuli in  $97.0 \pm 0.3\%$  of all trials. In addition, we presented stimuli with a predetermined individual SOA for which participants were supposed to perceive half of the trials as one stimulus and the other half as two stimuli (intermediate SOA, mean = 24.6 msec,  $SD = 6.2$  msec). As intended, participants perceived trials with this intermediate SOA as two

stimuli in  $59.9 \pm 0.9\%$  of the trials. Finally, stimuli with an intermediate SOA+10 msec were perceived as two stimuli in  $82.1 \pm 1.3\%$  and stimuli with an intermediate SOA−10 msec were perceived as two stimuli in  $27.2 \pm 1.5\%$ .

### Individual Gamma Ranges with Highest Power

We analyzed for each participant’s gamma ranges with highest power within 40–150 Hz. Twelve of the 16 participants showed narrow-banded gamma-band activity within the range of 40–150 Hz (Figure 1A). Four participants showed two different gamma ranges with highest power. Three participants had to be excluded because their gamma-band activity never reached the threshold of  $t = 1$ . One participant had to be excluded because of a broadband response that extended into lower frequencies. Thus, for this participant, we could not distinguish a clear narrow-banded range of gamma-band activity.

### Relation of Prestimulus Alpha and Poststimulus Gamma-band Power to Perception

We divided all trials with the intermediate SOA in five bins with respect to prestimulus alpha-band or poststimulus gamma-band power, respectively, and computed mean perception rates per bin. We found a significant negative correlation between prestimulus alpha-band power bins and perception,  $r(3) = 0.92$ ,  $p = .03$  (Figure 2A).

That is, with lower prestimulus alpha-band power, participants more likely reported to perceive two stimuli. Wilcoxon sign-ranked tests showed a significant difference in perception between alpha-band power Bin 1 and Bin 5 ( $z = 2.20$ ,  $p = .03$ ).

By contrast, we found no significant correlation between poststimulus gamma-band power and perception for both linear,  $r(3) = 0.04$ ,  $p = .95$  (Figure 2B), and quadratic,  $r(2) = 0.44$ ,  $p = .80$ , regression analyses.

### Relation of Prestimulus Alpha and Poststimulus Gamma-band Power

We divided all trials with the intermediate SOA in five bins with respect to prestimulus alpha-band power and computed mean gamma-band power per bin. Regression analysis did not demonstrate a significant linear relationship between prestimulus alpha-band power and poststimulus gamma-band power,  $r(2) = 0.22$ ,  $p = .72$ . However, regression analysis demonstrated a significant quadratic relationship between prestimulus alpha-band power and poststimulus gamma-band power,  $r(2) = 0.98$ ,  $p = .04$  (Figure 3).

That is, trials with high and low prestimulus alpha-band power showed the highest poststimulus gamma-band power. Trials with intermediate prestimulus alpha-band power showed the lowest poststimulus gamma-band power.

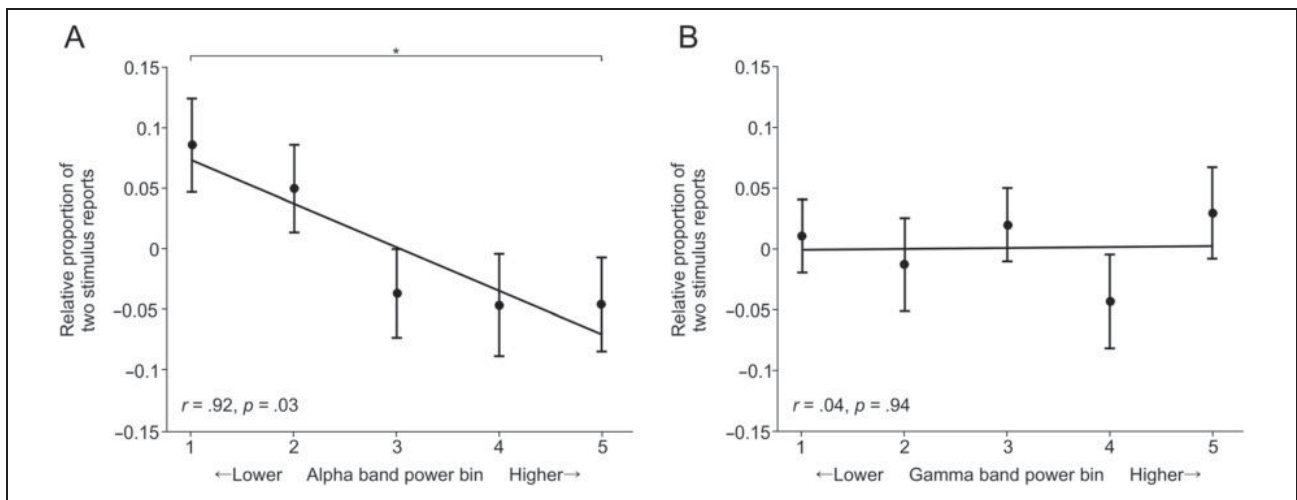


**Figure 2.** Regression analyses of oscillatory power and normalized temporal perceptual discrimination rate for (A) binned prestimulus alpha-band power (8–12 Hz, Bin 1 vs. Bin 5,  $p = .03$ ) and (B) binned poststimulus gamma range with highest power. Insets show results of linear regression analyses (black lines). Higher number bins indicate higher spectral power. Error bars represent SEM.

Wilcoxon signed-rank tests revealed a significant difference in gamma-band power between alpha-band power Bins 1 and 3 ( $z = -2.00$ ,  $p = .02$ ), that is, bins with low prestimulus alpha-band power showed significantly higher poststimulus gamma-band power than trials with intermediate prestimulus alpha-band power. Wilcoxon sign-ranked tests also revealed a significant difference of poststimulus gamma-band power between alpha-band power Bins 3 and 5 ( $z = -1.84$ ,  $p = .03$ ), that is, bins with high prestimulus alpha-band power showed significantly higher poststimulus gamma power than trials with intermediate prestimulus alpha-band power. Gamma-band power in the intermediate alpha-band power bin is therefore significantly lower than in the bin with highest or lowest alpha-band power, respectively.

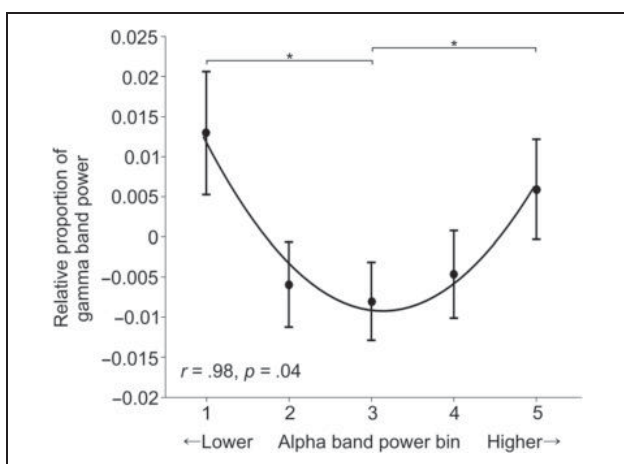


**Figure 3.** Regression analysis of binned prestimulus alpha-band power (8–12 Hz) and poststimulus gamma range with highest power. Inset shows result of quadratic regression analysis (black line). Higher number bins indicate higher spectral power. Error bars represent SEM. Bin 3 vs. Bin 1,  $p = .02$ ; Bin 3 vs. Bin 5,  $p = .03$ .

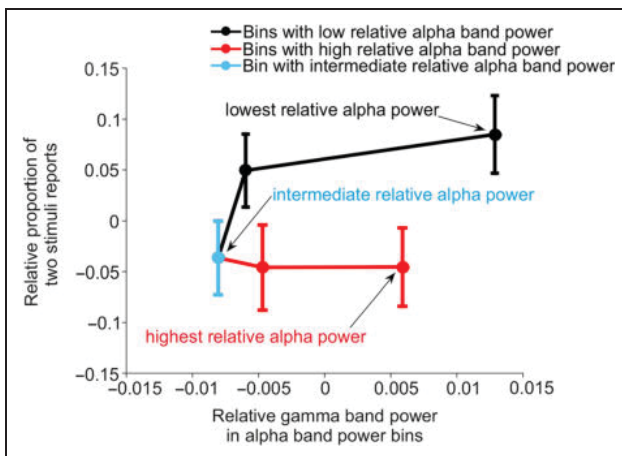
Control analyses revealed that this result could not be explained by common noise fluctuations in the alpha and gamma bands (Figure A1).

Figure 4 combines and summarizes the results above; with low prestimulus alpha and high poststimulus gamma-band power, participants more often perceived two stimuli. By contrast, with high poststimulus gamma-band power but with high prestimulus, alpha-band power participants more often perceived one stimulus. Finally, with intermediate alpha-band power and low poststimulus gamma-band power, participants had no clear preference for either perception (Figure 4).

## DISCUSSION

We analyzed data from a previous temporal tactile discrimination task in which participants received one or two tactile stimuli with varying SOAs (Baumgarten et al., 2016). We analyzed neuronal activity recorded with MEG with respect to the relation of prestimulus alpha-band power, poststimulus gamma-band power, and tactile perception. We found a significant linear relationship between prestimulus alpha-band power and tactile perception. However, we did not find a significant correlation between poststimulus gamma-band power and tactile perception (Figure 2). Finally, we found a significant U-shaped relation between prestimulus alpha-band power and poststimulus gamma-band power (Figure 3). That is, for both lowest and highest prestimulus alpha-band power, we found the highest poststimulus gamma-band power. For intermediate prestimulus alpha-band power, we found the lowest poststimulus gamma-band power.

As in our original study (with 16 participants; Baumgarten et al., 2016), we also found a significant correlation between prestimulus alpha-band power and perception for the 12 participants in our present study. Our results are also in line with other studies reporting a linear relationship between



**Figure 4.** Combination and summary of results. Low prestimulus alpha-band power (8–12 Hz) and high poststimulus gamma-band power lead to increased perception of two stimuli. High prestimulus alpha-band power and high poststimulus gamma-band power lead to increased perception of one stimuli. Intermediate alpha-band power and low gamma-band power lead to no clear preference for either perception.

prestimulus alpha-band power in somatosensory areas and tactile perception (Lange et al., 2012; Jones et al., 2010).

Prestimulus alpha-band power and poststimulus gamma-band power were analyzed in predefined sensors of interest. Prestimulus alpha-band power was analyzed in sensors showing a significant effect of prestimulus alpha power on perception in our previous study (Baumgarten et al., 2016). Poststimulus gamma-band power was analyzed in sensors defined by the M50 component of evoked fields. Because we performed our analyses on sensor level, we can only indirectly infer the underlying cortical sources. In our previous study, we found that the alpha effect on perception originates from somatosensory and parietal cortical regions (Baumgarten et al., 2016). In addition, the M50 component is known to originate from primary somatosensory cortex (S1; Iguchi et al., 2005). Because the poststimulus gamma response in our task strongly overlapped with the sensors defined by the M50 component (Figure 1B), it seems likely that the effect of poststimulus gamma-band activity has the same origin as the M50 event-related field component, namely, S1. This interpretation is in line with previous studies showing that poststimulus gamma-band activity in response to tactile stimulation is typically found in (primary) somatosensory areas or in sensors putatively overlying somatosensory areas (Cheng et al., 2016; Siegle et al., 2014; Lange, Oostenveld, & Fries, 2011; Gross, Schnitzler, Timmermann, & Ploner, 2007; Bauer et al., 2006). In summary, this suggests that the cortical sources of prestimulus alpha-band power and poststimulus gamma-band power might overlap but also demonstrate differences.

We focused our analysis of poststimulus gamma-band power on the time period of 0–200 msec. This time window temporally coincides with evoked activity. Such

evoked activity could induce broadband activity in the frequency domain that might be misinterpreted as gamma-band activity. However, except for one participant, our analysis of the individual gamma-band ranges revealed narrow-band poststimulus gamma-band power increases that did not extend into lower frequencies (Figure 1A). We are thus confident that our gamma-band activity is not due to broadband evoked responses.

Three participants did not show a reliable range of gamma-band activity and were thus excluded from the analyses. We can only speculate about the reason for the missing gamma-band activity. One reason might be a SNR of gamma-band activity too low to be detected. Moreover, these participants showed a decrease of gamma-band power in almost all frequencies. Such a decrease is highly unusual as it indicates increased prestimulus gamma-band power relative to the poststimulus period in almost all frequencies. Because of the unusual gamma-band activity and missing gamma range with highest power (according to our criteria, see above), we thus decided to exclude these participants from further analyses.

We have analyzed gamma-band activity in the range of 40–150 Hz. Many studies have used an upper limit lower than 150 Hz for gamma oscillations (Fries, Nikolić, & Singer, 2007; Bauer et al., 2006; Hoogenboom, Schoffelen, Oostenveld, Parkes, & Fries, 2006). However, several studies have shown that gamma-band activity can extend up to 150 Hz (Lange et al., 2011; Ray, Niebur, Hsiao, Sinai, & Crone, 2008; Tallon-Baudry, Bertrand, Hénaff, Isnard, & Fischer, 2005). Therefore, we included gamma-band activity up to 150 Hz to not miss potentially important effects in the higher frequencies of the gamma band.

There has been an ongoing discussion about the nature of gamma-band oscillations. Several studies report increases of gamma-band power in narrow frequency bands in response to sensory stimulation (Krebbber, Harwood, Spitzer, Keil, & Senkowski, 2015; Fries et al., 2007; Gross et al., 2007; Hoogenboom et al., 2006), arguing that gamma-band power reflects oscillatory activity. Other studies reported increases of gamma-band power in broadbands, spanning almost the entire gamma band (40 up to 200 Hz; e.g., Hermes, Miller, Wandell, & Winawer, 2015; Crone, Korzeniewska, & Franaszczuk, 2011). These studies often argue that the broadband response is unlikely of oscillatory nature but rather reflects asynchronous neuronal firing. In line with previous MEG/EEG studies, we found in our study poststimulus gamma-band responses in comparably narrow frequency bands. It seems interesting that narrow band gamma responses are often found in MEG and EEG studies, whereas broadband gamma responses are often reported in ECoG studies (e.g., Hermes et al., 2015; Lachaux et al., 2005). The nature of gamma-band power is thus far from conclusive, and thus, it is interesting and important to further elucidate the nature of gamma-band activity.

Previous studies reported increased somatosensory poststimulus gamma-band power in relation to improved

tactile or nociceptive somatosensory perception (Siegle et al., 2014; Gross et al., 2007; Meador et al., 2002). Therefore, we hypothesized that poststimulus gamma-band power might correlate with perception in our tactile discrimination task. Contrary to our hypothesis, however, we did not find a significant correlation between poststimulus gamma-band power and perception. The reason for the apparent discrepancy between our study and previous studies might be found in the stimuli and tasks. Stimulus detection tasks can be near-threshold or suprathreshold. In near-threshold tasks, participants typically report whether or not they perceive a stimulus near perceptual threshold (e.g., Siegle et al., 2014; Weisz et al., 2014; van Dijk et al., 2008; Linkenkaer-Hansen et al., 2004). In suprathreshold tasks, stimuli are always above perceptual threshold, and thus, participants always perceive a stimulus but typically have to discriminate between different stimuli or perceptual states (e.g., Baumgarten et al., 2016; Peng, Hautus, Oey, & Silcock, 2016; Sato, Nagai, Kuriki, & Nakauchi, 2016; Lange et al., 2012).

Notably, the studies reporting a positive relation between poststimulus gamma-band power and perception used near-threshold stimuli and tasks. For example, detection of tactile near-threshold stimuli improved when participants exhibited higher poststimulus gamma-band power in contralateral S1 (Meador et al., 2002). Also, perceived pain around the pain threshold was accompanied by higher gamma-band power in S1 compared with unperceived pain stimuli (Gross et al., 2007). Entraining peristimulus neocortical gamma-band power optogenetically led to increased tactile stimulus detection in mice in a near-threshold detection task (Siegle et al., 2014). By contrast, we used a suprathreshold discrimination task. That is, participants always perceived a stimulus but their perception varied on a trial-by-trial basis between perceiving one or two stimuli. It has been suggested that neuronal oscillations in the gamma band are a fundamental process of neuronal communication and stimulus processing (e.g., Fries, 2005, 2015). Gamma oscillations are believed to be instrumental for efficient neuronal processing. That is, neuronal synchronization in the gamma band leads to efficient transmission of the sensory signal in the neuronal network and hence to an efficient stimulus processing (e.g., Womelsdorf & Fries, 2007). By contrast, lower gamma-band activity would then indicate that the sensory signal is transmitted less efficiently across the neuronal network and hence the signal is less efficiently processed, leading potentially to a less clear and potentially even ambiguous perception. In line with this hypothesis, low gamma-band power in a near-threshold detection task might indicate that the stimulus is insufficiently processed and thus not perceived. By contrast, high gamma-band power indicates efficient stimulus processing, leading to successful detection of the near-threshold stimulus (Siegle et al., 2014; Gross et al., 2007). In suprathreshold tasks, a stimulus is always strong enough to be sufficiently processed to result in successful

perception. Therefore, a suprathreshold task should display high gamma-band power for all stimuli.

In our study, we used stimuli with identical physical characteristics (two suprathreshold stimuli with intermediate SOA), which differed only in participants' subjective perception. Gamma-band power was present in all trials, indicating efficient stimulus processing. However, the lack of a significant difference in gamma-band power between perceiving one or two stimuli suggests that the stimulus processing in S1 is largely independent of subjective perception in suprathreshold tasks. Subjective perception might be processed in other, higher cortical areas. For example, studies using working memory tasks in humans and monkeys found that vibrotactile stimulation induced gamma-band power in somatosensory areas. Somatosensory gamma-band power, however, did not differ between correctly and incorrectly perceived trials. Such differences between subjective perception and gamma-band power were found in higher areas (Haegens, Nacher, Hernández, et al., 2011; Haegens et al., 2010).

An alternative explanation for the lack of a significant correlation between poststimulus gamma-band power and perception might be that a potential correlation between gamma-band power and subjective perception might be too small to be detected with our paradigm or analysis approach. In addition, differences in gamma-band power might occur at different frequencies than analyzed in our study. However, we focused our analysis on individual frequency bands showing gamma-band power in response to stimulation, whereas other frequency bands showed only negligible gamma-band power, at all.

In contrast to our study in the somatosensory domain, studies in the visual domain reported that poststimulus gamma-band power correlated with subjective perception in suprathreshold tasks. These differences in gamma-band power, however, were typically found in higher visual areas, other than primary visual cortex. For example, if participants receive one visual stimulus accompanied by two tactile stimuli, they frequently perceive a second illusory visual stimulus (Shams, Kamitani, & Shimojo, 2000).

Studies have shown that, despite identical physical stimulation, poststimulus gamma-band power in parieto-occipital cortex correlated with participants' subjective perception of the illusion (Balz et al., 2016; Lange et al., 2011; Bhattacharya, Shams, & Shimojo, 2002). Moreover, poststimulus gamma-band power in somatosensory cortices was larger for congruent compared with incongruent visuotactile stimuli and correlated with shorter RTs (Kreber et al., 2015). Future studies might thus further investigate how gamma-band power correlates with tactile perception in suprathreshold tasks by studying other cortical areas or using methodological approaches that allow a finer spatial resolution, such as intracranial EEG or local field potential recording.

The main focus of our study was to study a potential relationship between prestimulus alpha and poststimulus

gamma-band power. It has been shown that attention correlates negatively with prestimulus alpha-band power and positively with poststimulus gamma-band power in somatosensory areas (Haegens, Luther, & Jensen, 2012; Haegens, Nacher, Luna, Romo, & Jensen, 2011; Bauer et al., 2006). In addition, higher behavioral performance is associated with lower prestimulus alpha-band power and higher poststimulus gamma-band power (e.g., Baumgarten et al., 2016; Siegle et al., 2014). We thus hypothesized that prestimulus alpha and poststimulus gamma-band power negatively correlate on a trial-by-trial basis, a question that to our knowledge has never been directly investigated. In contrast to our hypothesis, we did not find a significant linear relationship. Rather, we found that prestimulus alpha and poststimulus gamma-band power show a quadratic relationship. That is, low but also high prestimulus alpha-band power was associated with high poststimulus gamma-band power, whereas intermediate levels of prestimulus alpha-band power were associated with low levels of poststimulus gamma-band power. In addition, in trials with low prestimulus alpha/high poststimulus gamma-band power, participants more often perceived two stimuli, whereas in trials with high prestimulus alpha/high poststimulus gamma-band power, participants perceived more often one stimulus (Figure 4). Furthermore, in trials with intermediate prestimulus alpha/low poststimulus gamma-band power, participants showed no preference for either perception.

Although this quadratic relation was shown to be significant, the overall effect sizes seem rather small. We can only speculate about the size of the effects. It might be that only a small fraction of neurons that elicit gamma-band activity are involved in the perception process and are modulated by prestimulus alpha-band power. This would lead to a comparably low SNR and thus small effect sizes. Another potential reason might be found in the overall lower SNR for higher frequencies. Such a low SNR might reduce potential effects. The effect sizes in our study are, however, comparable in size to effect sizes of gamma-band effects in other MEG studies (Yuan, Li, Liu, Yuan, & Huang, 2016; Krebber et al., 2015; Haegens et al., 2010).

We propose that low prestimulus alpha-band power reflects states of high excitability (Jemi et al., 2017; Lange et al., 2013; Thut et al., 2006). Therefore, stimuli will be efficiently processed during states of low prestimulus alpha-band power, resulting in the perception of two stimuli (Baumgarten et al., 2016).

The lower prestimulus alpha-band power, the higher was participants' confidence in their decision. In other words, stronger or more efficient processing of "two" stimuli is accompanied by lower alpha-band power (Baumgarten et al., 2016).

Such efficient stimulus processing should be reflected in high poststimulus gamma-band power (Fries, 2005, 2009).

Hence, we propose that low prestimulus alpha-band power will lead to high poststimulus gamma-band power,

resulting in the perception of two stimuli (Figure 4, upper curve). On the other hand, high prestimulus alpha-band power reflects lower excitability or pulsed inhibition (Jensen & Mazaheri, 2010; Mathewson, Gratton, Fabiani, Beck, & Ro, 2009), leading to the perception of only one stimulus (Baumgarten et al., 2016).

The higher prestimulus alpha-band power, the higher was participants' confidence in their decision of "one" stimulus. In other words, stronger or more efficient processing of "one" stimuli was accompanied by higher alpha-band power (Baumgarten et al., 2016). Again, such efficient stimulus processing (despite leading to erroneous perception) should be reflected in high poststimulus gamma-band power (Fries, 2005, 2009). Thus, we propose that high prestimulus alpha-band power should also lead to high poststimulus gamma-band power. This way, however, high gamma-band power will result in the perception of one stimulus (Figure 4, lower curve). Finally, intermediate level of prestimulus alpha-band power will not bias perception in either direction, leading to lower or inefficient forwarding of the stimulus, which will be reflected in lower levels of gamma-band power.

This proposed model offers an alternative explanation why we did not find a significant correlation between gamma-band power and perception (Figure 2B). If prestimulus alpha-band power determines whether high poststimulus gamma-band power reflects the perception of one or two stimuli, then averaging across all prestimulus alpha states (as done in Figure 2B) will also average across both perceptions. Thus, ignoring the prestimulus alpha state and simply looking at poststimulus gamma states might give the wrong impression of no correlation between poststimulus gamma-band power and perception.

In conclusion, we found that prestimulus alpha-band and poststimulus gamma-band power show a quadratic relationship with both low and high prestimulus alpha power, leading to high poststimulus gamma-band power. Notably, the two states of high poststimulus gamma-band power are related to different states of perception. We propose a model in which prestimulus alpha-band power determines the computational and perceptual fate of a stimulus. If prestimulus alpha-band power is low, stimuli are efficiently processed, leading to more veridical perception in suprathreshold temporal discrimination tasks or near-threshold detection tasks. In such cases, poststimulus gamma-band power will be high, indicating efficient stimulus processing. If prestimulus alpha-band power is high, stimuli are inefficiently processed, leading to more incorrect perceptions in suprathreshold temporal discrimination tasks and no perception in near-threshold detection tasks. In suprathreshold temporal discrimination tasks, stimuli will still be processed, leading to high gamma-band power. In near-threshold detection task, nonperceived stimuli will not be processed, leading to no poststimulus gamma-band power.

## APPENDIX

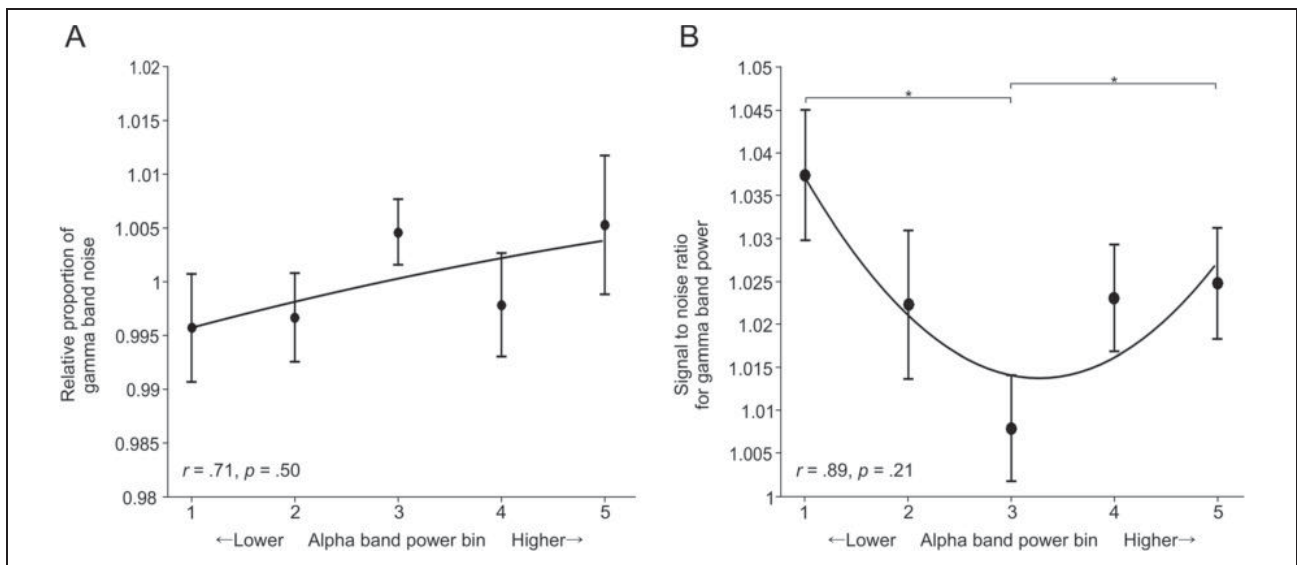


**Figure A1.** Regression analysis of binned prestimulus alpha-band power (8–12 Hz) and (A) prestimulus gamma-band noise or (B) SNR of gamma-band power. Inset shows results of quadratic regression analyses (black line). Higher number bins indicate higher spectral power. Error bars represent *SEM*. For (A): Bin 1 versus Bin 3,  $p = .95$ ; Bin 3 versus Bin 5,  $p = .48$ . For (B): Bin 3 versus Bin 1,  $p = .026$ ; Bin 3 versus Bin 5,  $p = .002$ .

## Acknowledgments

J. L. was supported by the German Research Foundation (LA 2400/4-1).

Reprint requests should be sent to Marc André Wittenberg, Institute of Clinical Neuroscience and Medical Psychology, Medical Faculty, Heinrich-Heine-University Düsseldorf, Universitätsstrasse 1, Düsseldorf, 40225, Germany, or via e-mail: marc.wittenberg@hhu.de.

## REFERENCES

- Balz, J., Keil, J., Roa Romero, Y., Meckle, R., Schubert, F., Aydin, S., et al. (2016). GABA concentration in superior temporal sulcus predicts gamma power and perception in the sound-induced flash illusion. *NeuroImage*, *125*, 724–730.
- Bauer, M., Oostenveld, R., Peeters, M., & Fries, P. (2006). Tactile spatial attention enhances gamma-band activity in somatosensory cortex and reduces low-frequency activity in parieto-occipital areas. *Journal of Neuroscience*, *26*, 490–501.
- Baumgarten, T. J., Schnitzler, A., & Lange, J. (2016). Prestimulus alpha power influences tactile temporal perceptual discrimination and confidence in decisions. *Cerebral Cortex*, *26*, 891–903.
- Baumgarten, T. J., Schnitzler, A., & Lange, J. (2017). Beyond the peak—Tactile temporal discrimination does not correlate with individual peak frequencies in somatosensory cortex. *Frontiers in Psychology*, *8*, 421.
- Bhattacharya, J., Shams, L., & Shimojo, S. (2002). Sound-induced illusory flash perception: Role of gamma band responses. *NeuroReport*, *13*, 1727–1730.
- Buzsáki, G., & Draguhn, A. (2004). Neuronal oscillations in cortical networks. *Science*, *304*, 1926–1929.
- Buzsáki, G., & Watson, B. O. (2012). Brain rhythms and neural syntax: Implications for efficient coding of cognitive content

and neuropsychiatric disease. *Dialogues in Clinical Neuroscience*, *14*, 345–367.

- Cheng, C.-H., Chan, P.-Y. S., Niddam, D. M., Tsai, S.-Y., Hsu, S.-C., & Liu, C.-Y. (2016). Sensory gating, inhibition control and gamma oscillations in the human somatosensory cortex. *Scientific Reports*, *6*, 20437.
- Cousijn, H., Haegens, S., Wallis, G., Near, J., Stokes, M. G., Harrison, P. J., et al. (2014). Resting GABA and glutamate concentrations do not predict visual gamma frequency or amplitude. *Proceedings of the National Academy of Sciences, U.S.A.*, *111*, 9301–9306.
- Crone, N. E., Korzeniewska, A., & Franaszczuk, P. J. (2011). Cortical  $\gamma$  responses: Searching high and low. *International Journal of Psychophysiology*, *79*, 9–15.
- Foxe, J. J., Simpson, G. V., & Ahlfors, S. P. (1998). Parieto-occipital approximately 10 Hz activity reflects anticipatory state of visual attention mechanisms. *NeuroReport*, *9*, 3929–3933.
- Fries, P. (2005). A mechanism for cognitive dynamics: Neuronal communication through neuronal coherence. *Trends in Cognitive Sciences*, *9*, 474–480.
- Fries, P. (2009). Neuronal gamma-band synchronization as a fundamental process in cortical computation. *Annual Review of Neuroscience*, *32*, 209–224.
- Fries, P. (2015). Rhythms for cognition: Communication through coherence. *Neuron*, *88*, 220–235.
- Fries, P., Nikolić, D., & Singer, W. (2007). The gamma cycle. *Trends in Neurosciences*, *30*, 309–316.
- Fries, P., Womelsdorf, T., Oostenveld, R., & Desimone, R. (2008). The effects of visual stimulation and selective visual attention on rhythmic neuronal synchronization in macaque area V4. *Journal of Neuroscience*, *28*, 4823–4835.
- Gross, J., Schnitzler, A., Timmermann, L., & Ploner, M. (2007). Gamma oscillations in human primary somatosensory cortex reflect pain perception. *PLoS Biology*, *5*, e133.
- Haegens, S., Luther, L., & Jensen, O. (2012). Somatosensory anticipatory alpha activity increases to suppress distracting input. *Journal of Cognitive Neuroscience*, *24*, 677–685.

- Haegens, S., Nacher, V., Hernández, A., Luna, R., Jensen, O., & Romo, R. (2011). Beta oscillations in the monkey sensorimotor network reflect somatosensory decision making. *Proceedings of the National Academy of Sciences, U.S.A.*, *108*, 10708–10713.
- Haegens, S., Nacher, V., Luna, R., Romo, R., & Jensen, O. (2011).  $\alpha$ -Oscillations in the monkey sensorimotor network influence discrimination performance by rhythmical inhibition of neuronal spiking. *Proceedings of the National Academy of Sciences, U.S.A.*, *108*, 19377–19382.
- Haegens, S., Osipova, D., Oostenveld, R., & Jensen, O. (2010). Somatosensory working memory performance in humans depends on both engagement and disengagement of regions in a distributed network. *Human Brain Mapping*, *31*, 26–35.
- Händel, B. F., Haarmeier, T., & Jensen, O. (2011). Alpha oscillations correlate with the successful inhibition of unattended stimuli. *Journal of Cognitive Neuroscience*, *23*, 2494–2502.
- Hanslmayr, S., Aslan, A., Staudigl, T., Klimesch, W., Herrmann, C. S., & Bäuml, K.-H. (2007). Prestimulus oscillations predict visual perception performance between and within subjects. *Neuroimage*, *37*, 1465–1473.
- Hermes, D., Miller, K. J., Wandell, B. A., & Winawer, J. (2015). Stimulus dependence of gamma oscillations in human visual cortex. *Cerebral Cortex*, *25*, 2951–2959.
- Hoogenboom, N., Schoffelen, J.-M., Oostenveld, R., & Fries, P. (2010). Visually induced gamma-band activity predicts speed of change detection in humans. *Neuroimage*, *51*, 1162–1167.
- Hoogenboom, N., Schoffelen, J.-M., Oostenveld, R., Parkes, L. M., & Fries, P. (2006). Localizing human visual gamma-band activity in frequency, time and space. *Neuroimage*, *29*, 764–773.
- Iemi, L., Chaumon, M., Crouzet, S. M., & Busch, N. A. (2017). Spontaneous neural oscillations bias perception by modulating baseline excitability. *Journal of Neuroscience*, *37*, 807–819.
- Iguchi, Y., Hoshi, Y., Tanosaki, M., Taira, M., & Hashimoto, I. (2005). Attention induces reciprocal activity in the human somatosensory cortex enhancing relevant- and suppressing irrelevant inputs from fingers. *Clinical Neurophysiology*, *116*, 1077–1087.
- Jensen, O., & Mazaheri, A. (2010). Shaping functional architecture by oscillatory alpha activity: Gating by inhibition. *Frontiers in Human Neuroscience*, *4*, 186.
- Jones, S. R., Kerr, C. E., Wan, Q., Pritchett, D. L., Hämäläinen, M., & Moore, C. I. (2010). Cued spatial attention drives functionally relevant modulation of the mu rhythm in primary somatosensory cortex. *Journal of Neuroscience*, *30*, 13760–13765.
- Keil, J., Müller, N., Ihssen, N., & Weisz, N. (2012). On the variability of the McGurk effect: Audiovisual integration depends on prestimulus brain states. *Cerebral Cortex*, *22*, 221–231.
- Klimesch, W., Sauseng, P., & Hanslmayr, S. (2007). EEG alpha oscillations: The inhibition-timing hypothesis. *Brain Research Reviews*, *53*, 63–88.
- Kreber, M., Harwood, J., Spitzer, B., Keil, J., & Senkowski, D. (2015). Visuotactile motion congruence enhances gamma-band activity in visual and somatosensory cortices. *Neuroimage*, *117*, 160–169.
- Lachaux, J.-P., George, N., Tallon-Baudry, C., Martinerie, J., Hugueville, L., Minotti, L., et al. (2005). The many faces of the gamma band response to complex visual stimuli. *Neuroimage*, *25*, 491–501.
- Lange, J., Halacz, J., van Dijk, H., Kahlbrock, N., & Schnitzler, A. (2012). Fluctuations of prestimulus oscillatory power predict subjective perception of tactile simultaneity. *Cerebral Cortex*, *22*, 2564–2574.
- Lange, J., Keil, J., Schnitzler, A., van Dijk, H., & Weisz, N. (2014). The role of alpha oscillations for illusory perception. *Behavioural Brain Research*, *271*, 294–301.
- Lange, J., Oostenveld, R., & Fries, P. (2011). Perception of the touch-induced visual double-flash illusion correlates with changes of rhythmic neuronal activity in human visual and somatosensory areas. *Neuroimage*, *54*, 1395–1405.
- Lange, J., Oostenveld, R., & Fries, P. (2013). Reduced occipital alpha power indexes enhanced excitability rather than improved visual perception. *Journal of Neuroscience*, *33*, 3212–3220.
- Linkenkaer-Hansen, K., Nikulin, V. V., Palva, S., Ilmoniemi, R. J., & Palva, J. M. (2004). Prestimulus oscillations enhance psychophysical performance in humans. *Journal of Neuroscience*, *24*, 10186–10190.
- Mathewson, K. E., Gratton, G., Fabiani, M., Beck, D. M., & Ro, T. (2009). To see or not to see: Prestimulus alpha phase predicts visual awareness. *Journal of Neuroscience*, *29*, 2725–2732.
- Meador, K. J., Ray, P. G., Echaz, J. R., Loring, D. W., & Vachtsevanos, G. J. (2002). Gamma coherence and conscious perception. *Neurology*, *59*, 847–854.
- Müller, M. M., Gruber, T., & Keil, A. (2000). Modulation of induced gamma band activity in the human EEG by attention and visual information processing. *International Journal of Psychophysiology*, *38*, 283–299.
- Oostenveld, R., Fries, P., Maris, E., & Schoffelen, J.-M. (2011). FieldTrip: Open source software for advanced analysis of MEG, EEG, and invasive electrophysiological data. *Computational Intelligence and Neuroscience*, *2011*, 156869.
- Peng, M., Hautus, M. J., Oey, I., & Silcock, P. (2016). Is there a generalized sweetness sensitivity for an individual? A psychophysical investigation of inter-individual differences in detectability and discriminability for sucrose and fructose. *Physiology & Behavior*, *165*, 239–248.
- Ray, S., Niebur, E., Hsiao, S. S., Sinai, A., & Crone, N. E. (2008). High-frequency gamma activity (80–150Hz) is increased in human cortex during selective attention. *Clinical Neurophysiology*, *119*, 116–133.
- Sato, T., Nagai, T., Kuriki, I., & Nakauchi, S. (2016). Dissociation of equilibrium points for color-discrimination and color-appearance mechanisms in incomplete chromatic adaptation. *Journal of the Optical Society of America. A, Optics, Image Science, and Vision*, *33*, A150–A163.
- Shams, L., Kamitani, Y., & Shimojo, S. (2000). Illusions. What you see is what you hear. *Nature*, *408*, 788.
- Siegel, M., Donner, T. H., Oostenveld, R., Fries, P., & Engel, A. K. (2008). Neuronal synchronization along the dorsal visual pathway reflects the focus of spatial attention. *Neuron*, *60*, 709–719.
- Siegle, J. H., Pritchett, D. L., & Moore, C. I. (2014). Gamma-range synchronization of fast-spiking interneurons can enhance detection of tactile stimuli. *Nature Neuroscience*, *17*, 1371–1379.
- Tallon-Baudry, C., Bertrand, O., Hénaff, M.-A., Isnard, J., & Fischer, C. (2005). Attention modulates gamma-band oscillations differently in the human lateral occipital cortex and fusiform gyrus. *Cerebral Cortex*, *15*, 654–662.
- Thut, G., Nietzel, A., Brandt, S. A., & Pascual-Leone, A. (2006). Alpha-band electroencephalographic activity over occipital cortex indexes visuospatial attention bias and predicts visual target detection. *Journal of Neuroscience*, *26*, 9494–9502.
- van Dijk, H., Schoffelen, J.-M., Oostenveld, R., & Jensen, O. (2008). Prestimulus oscillatory activity in the alpha band predicts visual discrimination ability. *Journal of Neuroscience*, *28*, 1816–1823.
- Weisz, N., Wühle, A., Monittola, G., Demarchi, G., Frey, J., Popov, T., et al. (2014). Prestimulus oscillatory power and

- connectivity patterns predispose conscious somatosensory perception. *Proceedings of the National Academy of Sciences, U.S.A.*, *111*, E417–E425.
- Womelsdorf, T., & Fries, P. (2007). The role of neuronal synchronization in selective attention. *Current Opinion in Neurobiology*, *17*, 154–160.
- Womelsdorf, T., Fries, P., Mitra, P. P., & Desimone, R. (2006). Gamma-band synchronization in visual cortex predicts speed of change detection. *Nature*, *439*, 733–736.
- Worden, M. S., Foxe, J. J., Wang, N., & Simpson, G. V. (2000). Anticipatory biasing of visuospatial attention indexed by retinotopically specific alpha-band electroencephalography increases over occipital cortex. *Journal of Neuroscience*, *20*, RC63.
- Yuan, X., Li, H., Liu, P., Yuan, H., & Huang, X. (2016). Pre-stimulus beta and gamma oscillatory power predicts perceived audiovisual simultaneity. *International Journal of Psychophysiology*, *107*, 29–36.

- 3) Lazar, M., Butz, M., Baumgarten, T. J., Füllenbach, N.-D., Jördens, M. S., Häussinger, D., Schnitzler, A., & **Lange, J.** (2018). Impaired tactile temporal discrimination in patients with hepatic encephalopathy. *Frontiers in Psychology, 9*, 2059.  
Impact factor (2018): 2.129



# Impaired Tactile Temporal Discrimination in Patients With Hepatic Encephalopathy

Moritz Lazar<sup>1</sup>, Markus Butz<sup>1</sup>, Thomas J. Baumgarten<sup>1,2</sup>, Nur-Deniz Füllenbach<sup>3</sup>, Markus S. Jördens<sup>3</sup>, Dieter Häussinger<sup>3</sup>, Alfons Schnitzler<sup>1</sup> and Joachim Lange<sup>1\*</sup>

<sup>1</sup> Institute of Clinical Neuroscience and Medical Psychology, Medical Faculty, Heinrich Heine University Düsseldorf, Düsseldorf, Germany, <sup>2</sup> Neuroscience Institute, Langone Medical Center, New York University, New York, NY, United States, <sup>3</sup> Department of Gastroenterology, Hepatology and Infectious Diseases, Medical Faculty, Heinrich Heine University Düsseldorf, Düsseldorf, Germany

## OPEN ACCESS

### Edited by:

Gregor Thut,  
University of Glasgow,  
United Kingdom

### Reviewed by:

Julian Keil,  
Christian-Albrechts-Universität zu Kiel,  
Germany  
Andi Wutz,  
University of Salzburg, Austria

### \*Correspondence:

Joachim Lange  
joachim.lange@med.uni-  
duesseldorf.de

### Specialty section:

This article was submitted to  
Perception Science,  
a section of the journal  
Frontiers in Psychology

**Received:** 03 August 2018

**Accepted:** 05 October 2018

**Published:** 30 October 2018

### Citation:

Lazar M, Butz M, Baumgarten TJ,  
Füllenbach N-D, Jördens MS,  
Häussinger D, Schnitzler A and  
Lange J (2018) Impaired Tactile  
Temporal Discrimination in Patients  
With Hepatic Encephalopathy.  
Front. Psychol. 9:2059.  
doi: 10.3389/fpsyg.2018.02059

The sensory system constantly receives stimuli from the external world. To discriminate two stimuli correctly as two temporally distinct events, the temporal distance or stimulus onset asynchrony (SOA) between the two stimuli has to exceed a specific threshold. If the SOA between two stimuli is shorter than this specific threshold, the two stimuli will be perceptually fused and perceived as one single stimulus. Patients with hepatic encephalopathy (HE) are known to show manifold perceptual impairments, including slowed visual temporal discrimination abilities as measured by the critical flicker frequency (CFF). Here, we hypothesized that HE patients are also impaired in their tactile temporal discrimination abilities and, thus, require a longer SOA between two tactile stimuli to perceive the stimuli as two temporally distinct events. To test this hypothesis, patients with varying grades of HE and age-matched healthy individuals performed a tactile temporal discrimination task. All participants received two tactile stimuli with varying SOA applied to their left index finger and reported how many distinct stimuli they perceived (“1” vs. “2”). HE patients needed a significantly longer SOA ( $138.0 \pm 11.3$  ms) between two tactile stimuli to perceive the stimuli as two temporally distinct events than healthy controls ( $78.6 \pm 13.1$  ms;  $p < 0.01$ ). In addition, we found that the temporal discrimination ability in the tactile modality correlated positively with the temporal discrimination ability in the visual domain across all participants (i.e., negative correlation between tactile SOA and visual CFF:  $r = -0.37$ ,  $p = 0.033$ ). Our findings provide evidence that temporal tactile perception is substantially impaired in HE patients. In addition, the results suggest that tactile and visual discrimination abilities are affected in HE in parallel. This finding might argue for a common underlying pathophysiological mechanism. We argue that the known global slowing of neuronal oscillations in HE might represent such a common mechanism.

**Keywords:** behavioral, perception, somatosensory, liver cirrhosis, integration window

## INTRODUCTION

The human brain constantly receives multiple signals from external sources through the senses. Precise neuronal processing of these signals and their temporal relationships is crucial for perception and behavior. If two signals arrive with sufficiently long temporal interval between both stimuli (stimulus onset asynchrony, SOA), they are readily perceived as two temporally separate

events. However, the temporal resolution necessary to discriminate the two stimuli is limited and with decreasing SOA, subjects will perceive two stimuli only as one single stimulus with increasing probability. The threshold for which two stimuli can be successfully discriminated is altered in several diseases. For example, patients with motor impairments, such as Parkinson's disease or dystonia, need longer time intervals to perceive two tactile stimuli as two separate events (Antelmi et al., 2017; Lee et al., 2018). This alteration has been assigned to impairments in the basal ganglia, which are believed to play a role in temporal perception (Lacruz et al., 1991; Pastor et al., 2004; Conte et al., 2016). Recent studies in healthy individuals additionally highlighted the role of primary somatosensory cortex (S1) for temporal perception of tactile stimuli (Hannula et al., 2008; Conte et al., 2012; Rocchi et al., 2016). In addition, Baumgarten et al. (2015, 2016) recently showed that neuronal oscillations in S1 correlate with temporal perception of tactile stimuli. Neuronal oscillations in the beta-band (~15–20 Hz) predicted whether subjects perceived one or two stimuli. These studies suggested that neuronal oscillations in the beta-band of S1 form the basis of temporal perception in the tactile domain (Baumgarten et al., 2015, 2017a). In more detail, this model for temporal perception proposes that cycles of neuronal oscillations form temporal windows for neuronal integration of incoming information (see VanRullen, 2016 for a review). If these two stimuli fall into different cycles, they are processed separately and hence perceived as two separate stimuli. Previous studies suggest that in the somatosensory domain these integration windows are reflected in cycles of neuronal oscillations in the beta-band in S1 (Baumgarten et al., 2015, 2017a). Similarly, studies have proposed that such integration windows also exist in the visual modality and for audio-visual integration with cycles of the alpha rhythm (~8–12 Hz) forming the temporal integration windows (e.g., VanRullen et al., 2006; Wutz et al., 2014; Cecere et al., 2015; VanRullen, 2016). These models of temporal perception state that temporal perception is mediated by the length of the cycles of neuronal oscillations. Consequently, if subjects show altered neuronal oscillations, these models would predict altered temporal perception.

In the present study, we studied tactile temporal perception in patients with hepatic encephalopathy (HE). HE patients are known to have slowed oscillatory activity (e.g., Butz et al., 2013) and thus are an ideal model to test the hypothesis that temporal tactile perception is mediated by discrete perceptual cycles in the beta-band. HE is a common complication in patients with liver cirrhosis and can serve as a model for slowed cortical oscillatory activity (Butz et al., 2013). In this patient population, the presence of liver cirrhosis restricts the detoxification function of the liver, which then leads to increased ammonia levels in the blood. The rise in ammonia levels are thought to lead to a low-grade cerebral edema, causing alterations in signal transduction, neurotransmission, and synaptic plasticity (Häussinger and Schliess, 2008; Prakash and Mullen, 2010; Felipo, 2013). Moreover, a slowing of oscillatory activity in visual and motor systems was observed (Timmermann et al., 2008; Kahlbrock et al., 2012; Butz et al., 2013; Götz et al., 2013). Likewise, slowed oscillatory activity was also reported for the

somatosensory cortex of patients with HE (May et al., 2014). In the light of this works, it has been suggested that a global slowing of oscillatory activity spanning across the different cortical subsystems and across the different frequency bands forms a key mechanism underlying altered behavior and neuropsychiatric symptoms occurring in HE patients (Timmermann et al., 2008; Butz et al., 2013). Consequently, HE comprises a great variety of neuropsychiatric symptoms, including cognitive, vigilance, and motor impairments (Häussinger and Sies, 2013). Also the visual temporal perception is impaired in patients with HE, which is represented in a decreased critical flicker frequency (CFF; Kircheis et al., 2002). The CFF is defined as the specific frequency at which a flickering light that is presented with a decreasing frequency is first perceived as a discrete flicker. The CFF serves as an objective clinical parameter to detect and monitor HE. Moreover, decreases in CFF correlated with slowing of neuronal oscillations in the visual cortex (Götz et al., 2013; Baumgarten et al., 2018).

In summary, patients with HE show slowed oscillatory activity and impaired visual temporal perception. Based on the findings that demonstrated slowed oscillatory activity also in somatosensory cortex, we hypothesized in the present study that HE patients should also show impaired tactile temporal perception. We used an established paradigm to test temporal perception of tactile stimuli (Baumgarten et al., 2015, 2016, 2017a,b). Related to the slowed CFF in the visual system, we proposed that HE patients demonstrate slowed temporal perception in the tactile system and thus, need longer SOAs compared to healthy subjects to detect two separate stimuli.

## MATERIALS AND METHODS

### Participants

Fifteen healthy controls (CON) and 16 patients (PAT) diagnosed with varying grades of HE due to liver cirrhosis participated in the experiment. Two PAT were excluded from analyses due to exclusively "1" reports regardless of SOA (see below for details). Three additional PAT were excluded from analyses due to unreliable fits of the behavioral data (see below for details). For details on the remaining 11 (14, respectively) PAT and 15 CON see **Table 1**.

Patients were diagnosed with HE by means of clinical assessment in combination with the CFF (see below) and computer psychometry (Vienna test system, Dr. Schuhfried GmbH, Mödling, Austria). Computer psychometry tested for an age corrected skill set of cognitive, motoric, reaction time, and attention competencies.

Patients were categorized in two groups: (1) Minimal HE (labeled mHE), i.e., patients without overt clinical symptoms but lowered CFF and/or deficits in psychometric testing (Kircheis et al., 2002). (2) Manifest HE (labeled HE), i.e., patients with clinically visible symptoms of HE (e.g., tiredness, reduced attention, or flapping tremor), graded as HE1 ( $n = 7$ ) or HE2 ( $n = 2$ ) according to the *West-Haven-Criteria*, which are commonly used to classify patients with overt symptoms into four stages (Ferenzi et al., 2002).

**TABLE 1** | Characteristics of patient and control groups.

	Controls	mHE	HE
N (f/m)	15 (5/10)	5 (2/3)	6 (1/5) [9 (2/7)]
Age (y; median (first, third quartile))	65.0 (52.0, 69.8)	57.0 (46.0, 71.3)	64.5 (58.0, 75.0) [66.0 (60.8, 76)]
CFF (Hz; median (first, third quartile))	42.6 (40.5, 43.3)	39.5 (37.6, 40.3)	36.7 (34.7, 37.9) [37.1 (34.7, 37.9)]
Stimulation amplitude (mA, median (first, third quartile))	3.2 (3.0, 4.2)	2.3 (2.0, 3.3)	3.4 (2.8, 3.8) [3.3 (2.7, 3.9)]
Etiology of cirrhosis	–	4 ALC, 1 overlap	4 ALC, 1NASH, 1 HCV, 1 CRYP, 1 NT, 1 AI

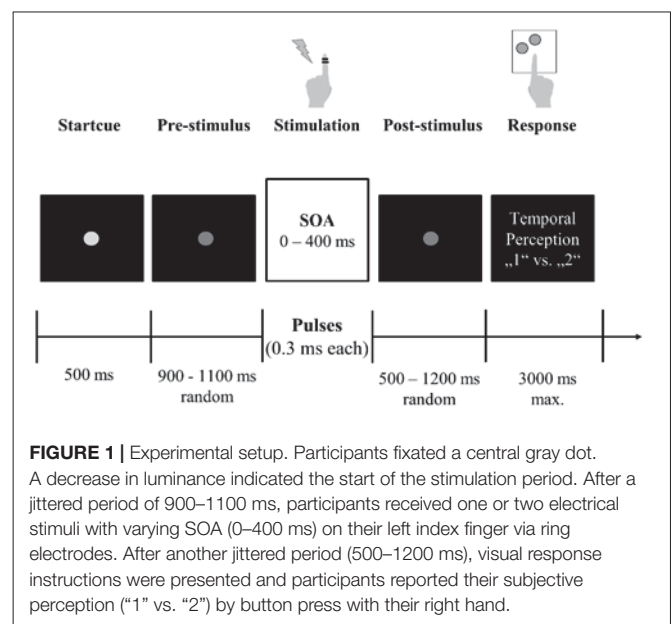
Data are presented for those participants that entered the main analyses (see **Figures 2, 3**) because their behavioral data could be successfully fitted (see **Supplementary Figure S2**). The column HE shows additionally (in square brackets []) the data for all patients that successfully completed the task, e.g., including three patients that did not enter the main analyses due to non-successful fits (see **Supplementary Figures S1, S2C**). mHE, minimal hepatic encephalopathy; HE, manifest hepatic encephalopathy; CFF, critical flicker frequency; ALC, alcoholic; Overlap, overlap syndrome; NASH, non-alcoholic steatohepatitis; HCV, hepatitis C virus; CRYP, cryptogenic, NT, nutritive toxic; AI, autoimmune hepatitis.

The CFF is typically used to detect patients with HE with a cutoff frequency of 39.0 Hz (Kircheis et al., 2002). In our study, three mHE patients showed a CFF > 39.0 Hz (39.5; 39.6; 42.2 Hz). Despite a CFF > 39.0 Hz, mHE was diagnosed in these patients by their deficits in the psychometric testing (Kircheis et al., 2002). Liver cirrhosis in all patients was confirmed by biopsy or Fibroscan/ARFI.

Exclusion criteria were psychiatric or neurological diseases apart from HE or abuse of alcohol or psychoactive drugs within the last 4 weeks. Also, patients with HE grade 3 or 4 were excluded from the study. All participants reported normal or corrected-to-normal vision and no tactile impairments. All patients were recruited from the Department of Gastroenterology, Hepatology and Infectious Diseases of the University Hospital Düsseldorf. All participants gave their written informed consent prior to the experiments. Healthy controls were financially reimbursed, patients received no financial reimbursement. The study was approved by the ethics committee of the University Hospital Düsseldorf (study no. 5779).

## Experimental Design and Paradigm

We adapted an established experimental task, which was designed to study tactile temporal perceptual discrimination in healthy humans (Baumgarten et al., 2015, 2016, 2017a,b). Participants were comfortably seated in a dimmed and sound-attenuated room. The start of every trial was signaled by a bright central fixation dot, serving as start cue (duration 500 ms; **Figure 1**). The following prestimulus period (duration randomized between 900 and 1100 ms) was indicated by a decreasing luminance of the cue. Next, the participants received either 1 or 2 short (0.3 ms) electrical pulses, applied by two ring electrodes placed at the distal phalanx of the left index finger. Electrical current was generated by a Stimulus Current Generator (DeMeTec GmbH, Langgöns, Germany). The amplitude of the pulses was adjusted individually to 150% of the subjective individual perception threshold. Subjective reports confirmed that stimulation at this level was clearly felt but below pain thresholds. The electrical pulses were applied with different SOAs ranging from 0 ms (i.e., only one stimulus was applied) to 400 ms with 12 steps in-between (15, 25, 35, 50, 100, 125, 150, 175, 200, 225, 250, and 300 ms). Next, the poststimulus period (duration randomized between 500 and 1200 ms) followed, during which only the fixation dot was visible. Durations of pre- and poststimulus epoch



were randomized in every trial to reduce temporal expectation effects in the prestimulus period and motor preparation effects in the poststimulus period. The poststimulus period was followed by a written instruction, which marked the start of the response window (duration max. 3000 ms). Then, participants reported whether they perceived the stimulation either as 1 single or 2 temporally separated sensations, giving feedback by button-presses with their index or middle finger of the right hand. Button configurations were randomized between participants but kept constant within each individual. If no answer was given after 3000 ms or if participants responded before the instruction text was presented, a warning text appeared and the respective trial was discarded from analysis and repeated at the end of the block. After button press, the next trial started. The experiment was subdivided in blocks. Each block consisted of 50 trials. Between blocks participants had the chance to take a self-paced break of up to 2 min. All 14 SOAs were presented in a pseudo-randomized order. This pseudo-randomized order changed after each presentation of all 14 SOAs. Total duration of the experiment was limited to 30 min. Due to differences in reaction times and length of self-paced breaks this resulted in

a varying total number of 350–450 trials (i.e., 7–9 blocks) per participant. Five patients ended the experiment earlier due to fatigue (duration of recorded data: ~10–25 min, resulting in 100–300 trials). All controls finished the entire 30 min period.

Stimulus presentation was controlled using Presentation software (Neurobehavioral Systems, Albany, NY, United States). Each participant received instructions of the task but remained naïve to the purpose of the experiment and the different SOAs used. Standardized instructions on the task were given prior to the start of the experiment in form of an information sheet and verbal instructions, as well as in form of written instructions presented on screen. After instructions were given and before recording, every participant underwent a training phase of ~5 min containing all possible SOAs to familiarize participants with the paradigm. Except the aforementioned warning text no further feedback was given during the actual test. Instructions and visual stimuli were presented via a projector on the backside of a translucent screen with a 60 Hz refresh rate positioned 60 cm in front of the participants.

Simultaneously to the behavioral study, we recorded neuronal activity with magnetoencephalography (MEG). The MEG data will be analyzed in future studies, in the present study we solely focus on the analysis of the behavioral data.

## Psychometric Fitting Function

As a measure for evaluating the individual tactile temporal discrimination abilities of each participant, we calculated the criticalSOA. The criticalSOA defines the specific SOA for which participants theoretically should exhibit a balanced response distribution (i.e., an equal amount of responses indicating a perception of one single stimulus and responses indicating two separate stimuli; Cecere et al., 2015; Baumgarten et al., 2017b). To account for potential lapse rates and response biases, we defined the criticalSOA as the SOA for which response rates reached the individual mean between the minimum and maximum mean response (**Supplementary Figure S2**).

To determine the criticalSOA of each participant, we fitted a sigmoid function to the individual raw behavioral data (Baumgarten et al., 2017b). Fitting procedure was conducted using the Palamedes toolbox for Matlab (Prins and Kingdom, 2009). As the independent variable we chose the SOAs (0, 15, 25, 35, 50, 100, 125, 150, 175, 200, 225, 250, 300, and 400 ms), whereas the average stimulus perception (averaged across trials, ranging from 1 to 2) at each SOA was chosen as the dependent variable. The fitting algorithm estimated four parameters of the logistic function: threshold, slope, guess rate, and lapse rate. We estimated the goodness of fit by computing the deviance and corresponding *p*-values. Only *p*-values >0.05 were estimated as a reliable fit of the experimental data and therefore included in further analysis (**Supplementary Figure S2**; Baumgarten et al., 2017b). For three PAT no reliable fit could be determined (**Supplementary Figure S2C**).

## Critical Flicker Frequency

The CFF is defined as the specific frequency at which a flickering light that is presented with a decreasing frequency is first perceived as a discrete flicker as opposed to a continuous light

(Kircheis et al., 2002). The CFF was shown to be decreased in patients even with mild forms of HE, with a critical cut-off frequency of 39 Hz separating patients with HE from healthy controls (Kircheis et al., 2014; Barone et al., 2018).

Critical flicker frequency was assessed by an experienced psychologist (NDF) using the HEPAtonorm<sup>TM</sup>-Analyzer (NEVOLab, Maierhöfen, Germany) on the day of the tactile temporal perceptual discrimination task before experimental testing took place. The CFF was determined by presenting a flickering small red dot foveally with a starting frequency of 60 Hz. At this frequency, the flickering dot is always perceived as a constant light. Next, the frequency was decreased and subjects responded by button press as soon as they perceived the light as flickering. After standardized verbal instruction and a short training period, the CFF value was determined eight times per participant and the average value was taken as the individual CFF (see also Kircheis et al., 2002, 2014).

## Correlation Analysis, Effect Sizes, and Statistics

To test for significant differences in CFF, age, and electrical stimulation amplitudes between the three groups (controls, mHE, HE), we applied non-parametric Kruskal–Wallis tests. For *post hoc* pairwise comparisons and to test whether the criticalSOA differed across groups (CON and PAT; mHE, and HE), non-parametric Mann–Whitney *U*-tests were applied. From the resulting *z*-values effect sizes (*r*) were calculated:

$$r = \text{abs}\left(\frac{z}{\sqrt{N}}\right)$$

with *N* denoting the sample size (Fritz et al., 2012).

To analyze a potential correlation between the criticalSOA and the CFF, we computed the one-sided Pearson partial correlation coefficient between criticalSOA and CFF, controlling for age as a covariant, since the CFF is known to correlate with age (Kircheis et al., 2014). Additionally, we computed Pearson correlation coefficients within each group (controls and patients). 95% confidence intervals were estimated using bootstrapping approach (1000 repetitions). Correlation analysis was conducted in SPSS Statistics (IBM, Armonk, NY, United States).

All other statistical analyses were conducted in Matlab (Mathworks, Natick, MA, United States).

## RESULTS

The following statistical tests are performed on only those 15 controls and 11 patients (5 mHE and 6 HE) that finally were included in the analyses (see section “Materials and Methods” and below for details on exclusion criteria).

A Kruskal–Wallis test revealed highly significant differences between groups (controls, mHE, HE, see **Table 1**) for the CFF [ $\chi^2(2) = 14.83$ ,  $p = 0.0006$ ]. *Post hoc* Mann–Whitney *U*-tests showed that the CFF significantly differed between controls and mHE ( $z = 2.36$ ,  $p = 0.009$ ; effect size  $r = 0.53$ ), between controls and HE ( $z = 3.31$ ,  $p = 0.0005$ ;  $r = 0.51$ ), and between mHE and HE ( $z = 1.83$ ,  $p = 0.03$ ;  $r = 0.55$ ).

No significant differences between groups were found for age [ $\chi^2(2) = 1.14$ ,  $p = 0.57$ ; pairwise comparisons: all  $p > 0.37$ ,  $r \leq 0.25$ ] and amplitude of the electrical stimulation [ $\chi^2(2) = 2.94$ ,  $p = 0.23$ ; pairwise comparisons: all  $p > 0.08$ ,  $r \leq 0.40$ ].

## Behavioral Results and Fitting Procedure

Participants received one or two short electrical pulses with varying stimulus onset asynchronies (SOAs) to their left index finger (Figure 1). In a two-alternative forced choice tactile temporal discrimination task, they reported their subjective perception of the stimulation (“1” vs. “2” stimuli).

On average, for both groups (PAT and CON) mean perception rates increased with increasing SOA (Figure 2A). To quantify the individual temporal discrimination abilities, we fitted a sigmoid function to the individual behavioral data and estimated from this curve the criticalSOA (see section “Materials and Methods” and Supplementary Figures S2A,B for details). Three patients (2 HE1 and 1 HE2) had to be excluded from further analysis due to unreliable fits (Supplementary Figure S2C). Supplementary Figure S1 illustrates the corresponding behavioral data with these three individuals excluded. Notably, these three patients exhibited low overall perception rates not reaching mean perception of 1.5 even for largest SOAs. In addition, two additional patients had been excluded from all analyses because they always responded “1,” regardless of SOA. Of these five patients, four belonged to the HE-group and only one belonged to the mHE-group.

Averaged across individuals, the median criticalSOA was 96.8 ms (first quartile; 31.4 ms, third quartile: 124.1 ms) for the CON group and 154.4 ms (first quartile; 103.5 ms, third quartile: 169.3 ms) for the PAT group (Figure 2B). Statistical analysis revealed a highly significant difference between both groups ( $z = 2.60$ ,  $p = 0.005$ ,  $r = 0.51$ ). Additionally, we split the PAT group into mHE and HE patients and tested whether criticalSOAs differed between these groups. No significant difference was found between these groups ( $z = 0.46$ ,  $p = 0.68$ ,  $r = 0.14$ ).

## Correlation of CriticalSOA and CFF

Correlation analysis revealed a significant negative linear relationship between CFF and criticalSOA, corrected for age ( $r = -0.37$ , 95% confidence intervals:  $[-0.69, -0.05]$ ,  $N = 26$ ,  $p = 0.033$ , Figure 3). That is, decreasing CFF is associated with increasing criticalSOA. This result indicates a positive correlation between visual and tactile temporal discrimination abilities.

Additionally, we computed correlation coefficients between CFF and criticalSOA, corrected for age, within each group (controls and patients). We did not find significant correlations for the group controls ( $r = 0.15$ , 95% CI:  $[-0.47, 0.64]$ ,  $N = 15$ ,  $p = 0.62$ ) nor for the group patients ( $r = -0.08$ , CI:  $[-0.75, 0.66]$ ,  $N = 11$ ,  $p = 0.83$ ).

## DISCUSSION

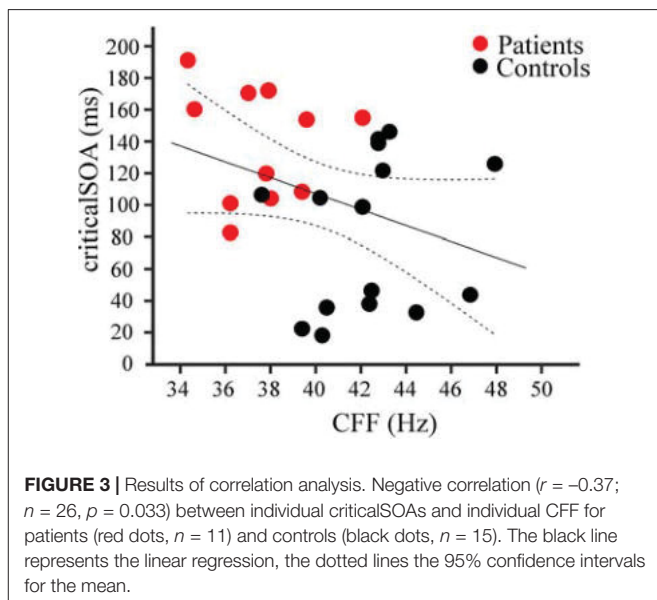
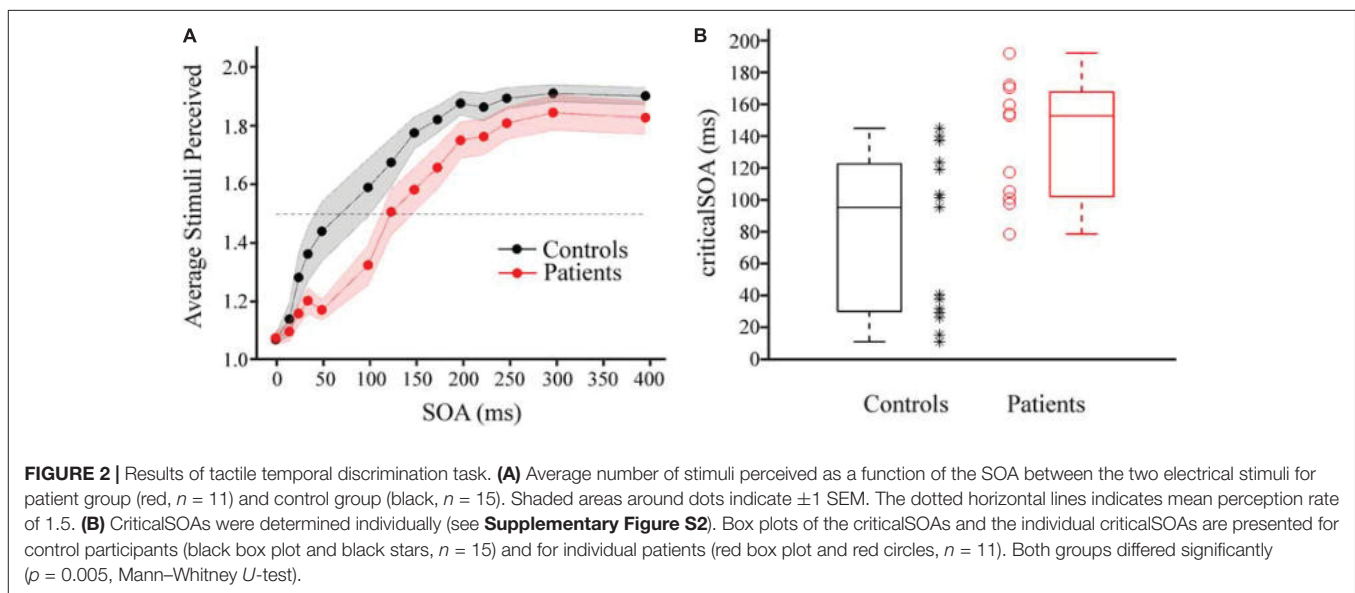
In this study, we investigated the hypothesis that tactile temporal discrimination is impaired in patients with HE. To this end, HE

patients and healthy controls received two subsequent electrical stimuli to their index finger with varying SOAs and had to report their subjective perception (“1” vs. “2” stimuli). We found that the SOA for which participants perceived the two stimuli as “2” in 50% of all trials and as “1” in the remaining 50% of all trials (denoted “criticalSOA”) was significantly prolonged in HE patients compared to healthy controls. The effect size of  $r = 0.51$  indicates a strong effect (Fritz et al., 2012). In addition, we found that across all participants the criticalSOA correlated negatively with the CFF.

Patients with HE are known to reveal impairments in their visual temporal discrimination abilities. In particular, the CFF is slowed in HE patients compared to healthy participants and the CFF decreases with increasing severity of HE (Romero-Gómez et al., 2007; Torlot et al., 2013; Kircheis et al., 2014). Our results demonstrate that this disease-related impairment does also span the somatosensory modality, and particularly the temporal discrimination of tactile stimuli. This finding tallies with early work showing both sensory impairments on the behavioral level in HE (Brenner et al., 2015) and slowing of cortical oscillatory activity within the somatosensory system in this patient population (May et al., 2014). Moreover, the correlation of CFF and criticalSOA implies that the severity of the impairment of tactile temporal perception parallels the impairments of visual temporal perception. This implies a progression according to the clinical severity of HE.

We did not find a significant difference between the mHE group and the HE group. It should be noted, however, that five patients had to be excluded from analyses: either due to exclusive “1” reports or due to unreliable fits (with average perception  $< 1.5$  for the highest SOA, see Supplementary Figure S2C). Of these five patients, four belonged to the HE-group and only one belonged to the mHE-group. Thus, the non-significant result might partially be due to exclusion of the most severely impaired participants. In addition, both patients with the most severe HE (graded as HE2) were also strongly impaired in their tactile temporal perception so that they just reached an average perception of 1.0 (patient excluded from analysis) and 1.3 for the highest SOA. Despite the non-significant difference of the criticalSOA between mHE and HE groups, these results argue in favor of increased impairments in tactile temporal discrimination with increasing disease severity. Moreover, these results may reflect that the pathological mechanism underlying impaired tactile temporal perception already occurs in initial mild forms of HE. Other studies reported that mHE and HE groups significantly differ in terms of CFF (e.g., Kircheis et al., 2002; Oeltzschner et al., 2015). The most likely reason for the lack of difference might be the comparably small sample size especially in the HE2 group. For future studies in addition to increasing the number of severely impaired patients, we might also refine the parameters to differentiate between patient groups, e.g., by increasing duration of the SOAs further, so that also the most strongly impaired patients might be included.

One possible concern might be that our paradigm cannot differentiate whether the prolonged SOAs are caused by impairments on the sensory, decisional, or cognitive level. That is, patients’ prolonged SOAs might be due to impaired perceptual



abilities, due to altered processes in the decision process (e.g., shifted decision criterions; see, e.g., Iemi et al., 2016; Limbach and Corballis, 2016) or cognitive impairments (patients simply did not understand the task). Notably, this concern would equally hold for the CFF. For example, the result that some patients predominantly reported “1” even for the largest SOA might be due to the fact that their criticalSOA was larger than 400 ms, or they had a strong bias toward reporting “1” or they did not understand the task and simply always pressed the “1” button. If patients did not understand the task, however, they might with equal probability have pressed always the “2” button, especially as the response buttons were counterbalanced across participants. A response pattern of always “2,” however, was never reported, speaking against impairment on a purely cognitive level. Also,

some patients verbally reported after the experiment that they indeed simply always felt “1,” which might argue for a process on sensory rather than decisional level. Future studies are needed both in the visual and tactile modality to further elucidate the level of the impairments.

The correlation between impairments in visual (CFF) and tactile temporal discrimination (criticalSOA) suggests a common underlying mechanism across modalities. Recent studies proposed that temporal perception relies on discrete “perceptual cycles” mediated by cycles of neuronal oscillations (Baumgarten et al., 2015, 2017a; Cecere et al., 2015; VanRullen, 2016). These models postulate a cycle of a neuronal oscillation as the basic unit of temporal stimulus processing and perception. Two stimuli can only be perceptually distinguished if they fall into two separate cycles of a neuronal oscillation, while they will be perceptually fused to a single sensation if both stimuli fall within one cycle. Several studies have demonstrated that HE patients show slowed oscillatory activity in sensorimotor, visual, and somatosensory areas (Kullmann et al., 2001; Olesen et al., 2011; Butz et al., 2013; Götz et al., 2013; May et al., 2014; Baumgarten et al., 2018). According to the model of perceptual cycles, for slower oscillations, two stimuli are more likely to fall into one cycle. Thus, these patients should need longer SOAs to successfully discriminate two stimuli. Our results confirm this prediction on a behavioral level. In addition, studies found a correlation between parieto-occipital alpha oscillations and visual discrimination abilities (Götz et al., 2013; Baumgarten et al., 2018). To date, the direct mechanistic link between slowed somatosensory neuronal oscillations and impaired tactile temporal discrimination, however, is missing. Thus, it remains unclear whether similar pathophysiological processes underlie impaired visual and tactile discrimination. We did not find, however, significant correlations between CFF and criticalSOA within groups (patients and controls). This might be due to the low number of subjects entering the separate groups. On the other hand, for both groups, the

correlation coefficient was close to zero, indicating that the correlation across all participants is mainly mediated by the groups. Similarly, Baumgarten et al. (2018) reported a significant correlation between CFF and alpha frequencies in visual cortex. This correlation was significant only across groups (HE patients and controls), but not within groups. These results indicate that correlations do not primarily rely on individual differences in CFF and criticalSOA. The individual measures might be too noisy or variable and reliable correlations can be detected only when taking larger intervals of the CFF and criticalSOA into account, i.e., by pooling controls and patients. Future analysis of the MEG data might provide further insights whether slowed neuronal oscillations represent the pathophysiological mechanisms underlying impaired tactile temporal discrimination in HE and linking it to visual impairments.

In addition to differences in prestimulus ongoing neuronal oscillations, also peri- or poststimulus effects might account for our results. For example, peri- or poststimulus phase resets might reset temporal integration windows (Wutz et al., 2014; Baumgarten et al., 2017a). In this view, stronger phase resets in controls compared to patients might lead to more consistent resets of integration windows and thus higher precision for temporal perception of subsequent stimuli. Again, future analysis of the MEG data might provide further insights in the neuronal mechanisms.

An alternative explanation for the impaired tactile temporal discrimination abilities might be found in the power of somatosensory alpha oscillations. Previous studies in healthy individuals reported that tactile temporal discrimination abilities correlate with prestimulus power of alpha oscillation (~8–12 Hz) in somatosensory cortex, with higher alpha power leading to more “1” reports (Jones et al., 2010; Lange et al., 2012; Baumgarten et al., 2016; Craddock et al., 2017). Other studies suggested that alpha power modulates the decision criterion, with high alpha power biasing decisions to “missing” stimuli (Iemi et al., 2016; Limbach and Corballis, 2016). Increased power of alpha oscillations in HE patients might thus lead to more “1” reports. Indeed, some studies reported increased alpha power in HE patients, either in resting state activity in visual cortex (Götz et al., 2013) or in poststimulus activity in somatosensory cortex (May et al., 2014). However, none of the studies has linked somatosensory alpha power to tactile temporal perception in HE patients so far. Again, future analysis of the MEG data might help to disentangle the underlying pathophysiological mechanisms which might consist of one of the previous or a combination of both explanations.

Finally, it has been shown in numerous studies that attention influences perception. It seems therefore likely that attention also influences temporal perception. In fact, attention has been shown to rhythmically modulate perception and behavior (Landau and Fries, 2012; Song et al., 2014). In line with the abovementioned connection between temporal perception and oscillatory activity, several studies suggest that attention modulates neuronal oscillations (e.g., Calderone et al., 2014; Landau et al., 2015). However, in our present study, we did not explicitly modulate attention. In addition, HE patients seem to be specifically impaired in their visual and tactile temporal

perception. Other perceptual abilities that are also affected by attention modulations seem less affected by HE. In sum, while we cannot exclude an influence of attention on our results, it seems unlikely to us that the impaired tactile temporal perception can be explained by attention alone.

In summary, we found that HE patients are significantly impaired in their tactile temporal discrimination abilities compared to a healthy control group. HE patients required a longer SOA between two tactile stimuli to veridically perceive them as two temporally separate events. To the best of our knowledge, this is the first study to extend findings of impairments of temporal perception in HE patients to the somatosensory domain. These behavioral results are in line with a model of discrete tactile temporal perception (Baumgarten et al., 2015, 2017a). Furthermore, we found that tactile temporal perception correlated with visual temporal perception, arguing for a global impairment in HE affecting the different sub-systems in parallel. While the behavioral results confirm predictions from previous models, further neuroscientific studies are needed to unravel the pathophysiological mechanisms underlying the impaired tactile temporal perception in patients with HE.

## AUTHOR CONTRIBUTIONS

MB, TB, AS, and JL conceived the study. MB, TB, and JL designed the study. ML, TB, and JL collected the data. ML and JL analyzed the data and drafted the manuscript. N-DF and MJ recruited, tested, and categorized the patients. All authors critically revised the draft and approved the final version.

## FUNDING

This work was supported by the German Research Foundation (DFG, SFB 974, Project B07). ML was supported by a scholarship of the Integrated Research Training Group (iGK) of the SFB 974. TB has received funding from the European Union’s Horizon 2020 research and innovation programme under the Marie Skłodowska-Curie grant agreement number 795998 (MSCA-IF-GF).

## SUPPLEMENTARY MATERIAL

The Supplementary Material for this article can be found online at: <https://www.frontiersin.org/articles/10.3389/fpsyg.2018.02059/full#supplementary-material>

**FIGURE S1** | Same as **Figure 2A**, but including the patients for which the data could not be fitted (see **Supplementary Figure S2C**; controls:  $n = 15$ ; patients:  $n = 14$ ).

**FIGURE S2** | Results of the fitting procedure. **(A)** Psychometric functions were fitted to the individual mean responses as a function of SOA for the control group. Black horizontal lines indicate the criticalSOA, black vertical lines the corresponding SOA. **(B)** Same as panel **(A)**, but now for the patient group. **(C)** Individual mean responses for three individual patients for which the data could not be reliably fitted. These subjects were excluded from analyses and **Figures 2, 3**, but included in **Supplementary Figure S1**.

## REFERENCES

- Antelmi, E., Erro, R., Rocchi, L., Liguori, R., Tinazzi, M., Di Stasio, F., et al. (2017). Neurophysiological correlates of abnormal somatosensory temporal discrimination in dystonia. *Mov. Disord.* 32, 141–148. doi: 10.1002/mds.26804
- Barone, M., Shahini, E., Iannone, A., Viggiani, M. T., Corvace, V., Principi, M., et al. (2018). Critical flicker frequency test predicts overt hepatic encephalopathy and survival in patients with liver cirrhosis. *Dig. Liver Dis.* 50, 496–500. doi: 10.1016/j.dld.2018.01.133
- Baumgarten, T. J., Königs, S., Schnitzler, A., and Lange, J. (2017a). Subliminal stimuli modulate somatosensory perception rhythmically and provide evidence for discrete perception. *Sci. Rep.* 7:43937. doi: 10.1038/srep43937
- Baumgarten, T. J., Schnitzler, A., and Lange, J. (2017b). Beyond the peak–tactile temporal discrimination does not correlate with individual peak frequencies in somatosensory cortex. *Front. Psychol.* 8:421. doi: 10.3389/fpsyg.2017.00421
- Baumgarten, T. J., Neugebauer, J., Oeltzschner, G., Füllenbach, N.-D., Kircheis, G., Häussinger, D., et al. (2018). Connecting occipital alpha band peak frequency, visual temporal resolution, and occipital GABA levels in healthy participants and hepatic encephalopathy Patients. *Neuroimage Clin.* 20, 347–356. doi: 10.1016/j.nicl.2018.08.013
- Baumgarten, T. J., Schnitzler, A., and Lange, J. (2015). Beta oscillations define discrete perceptual cycles in the somatosensory domain. *Proc. Natl. Acad. Sci. U.S.A.* 112, 12187–12192. doi: 10.1073/pnas.1501438112
- Baumgarten, T. J., Schnitzler, A., and Lange, J. (2016). Prestimulus alpha power influences tactile temporal perceptual discrimination and confidence in decisions. *Cereb. Cortex* 26, 891–903. doi: 10.1093/cercor/bhu247
- Brenner, M., Butz, M., May, E. S., Kahlbrock, N., Kircheis, G., Häussinger, D., et al. (2015). Patients with manifest hepatic encephalopathy can reveal impaired thermal perception. *Acta Neurol. Scand.* 132, 156–163. doi: 10.1111/ane.12376
- Butz, M., May, E. S., Häussinger, D., and Schnitzler, A. (2013). The slowed brain: cortical oscillatory activity in hepatic encephalopathy. *Arch. Biochem. Biophys.* 536, 197–203. doi: 10.1016/j.abb.2013.04.004
- Calderone, D. J., Lakatos, P., Butler, P. D., and Castellanos, F. X. (2014). Entrainment of neural oscillations as a modifiable substrate of attention. *Trends Cogn. Sci.* 18, 300–309. doi: 10.1016/j.tics.2014.02.005
- Cecere, R., Rees, G., and Romei, V. (2015). Individual differences in alpha frequency drive crossmodal illusory perception. *Curr. Biol.* 25, 231–235. doi: 10.1016/j.cub.2014.11.034
- Conte, A., Leodori, G., Ferrazzano, G., De Bartolo, M. I., Manzo, N., Fabbrini, G., et al. (2016). Somatosensory temporal discrimination threshold in Parkinson's disease parallels disease severity and duration. *Clin. Neurophysiol.* 127, 2985–2989. doi: 10.1016/j.clinph.2016.06.026
- Conte, A., Rocchi, L., Nardella, A., Dispenza, S., Scontrini, A., Khan, N., et al. (2012). Theta-burst stimulation-induced plasticity over primary somatosensory cortex changes somatosensory temporal discrimination in healthy humans. *PLoS One* 7:e32979. doi: 10.1371/journal.pone.0032979
- Craddock, M., Poliakoff, E., El-dereby, W., Klepousniotou, E., and Lloyd, D. M. (2017). Pre-stimulus alpha oscillations over somatosensory cortex predict tactile misperceptions. *Neuropsychologia* 96, 9–18. doi: 10.1016/j.neuropsychologia.2016.12.030
- Felipo, V. (2013). Hepatic encephalopathy: effects of liver failure on brain function. *Nat. Rev. Neurosci.* 14:851. doi: 10.1038/nrn3587
- Ferenci, P., Lockwood, A., Mullen, K., Tarter, R., Weissenborn, K., and Blei, A. T. (2002). Hepatic encephalopathy—definition, nomenclature, diagnosis, and quantification: final report of the working party at the 11th World Congresses of Gastroenterology. Vienna, 1998. *Hepatology* 35, 716–721. doi: 10.1053/jhep.2002.31250
- Fritz, C. O., Morris, P. E., and Richler, J. J. (2012). Effect size estimates: current use, calculations, and interpretation. *J. Exp. Psychol.* 141:2. doi: 10.1037/a0024338
- Götz, T., Huonker, R., Kranczioch, C., Reuken, P., Witte, O. W., Günther, A., et al. (2013). Impaired evoked and resting-state brain oscillations in patients with liver cirrhosis as revealed by magnetoencephalography. *NeuroImage* 2, 873–882. doi: 10.1016/j.nicl.2013.06.003
- Hannula, H., Neuvonen, T., Savolainen, P., Tukiainen, T., Salonen, O., Carlson, S., et al. (2008). Navigated transcranial magnetic stimulation of the primary somatosensory cortex impairs perceptual processing of tactile temporal discrimination. *Neurosci. Lett.* 437, 144–147. doi: 10.1016/j.neulet.2008.03.093
- Häussinger, D., and Schliess, F. (2008). Pathogenetic mechanisms of hepatic encephalopathy. *Gut* 57, 1156–1165. doi: 10.1136/gut.2007.122176
- Häussinger, D., and Sies, H. (2013). Hepatic encephalopathy: clinical aspects and pathogenetic concept. *Arch. Biochem. Biophys.* 536, 97–100. doi: 10.1016/j.abb.2013.04.013
- Iemi, L., Chaumon, M., Crouzet, S. M., and Busch, N. A. (2016). Spontaneous neural oscillations bias perception by modulating baseline excitability. *J. Neurosci.* 37, 807–819. doi: 10.1523/JNEUROSCI.1432-16.2016
- Jones, S. R., Kerr, C. E., Wan, Q., Pritchett, D. L., Hämäläinen, M., and Moore, C. I. (2010). Cued spatial attention drives functionally relevant modulation of the Mu rhythm in primary somatosensory cortex. *J. Neurosci.* 30, 13760–13765. doi: 10.1523/JNEUROSCI.2969-10.2010
- Kahlbrock, N., Butz, M., May, E. S., Brenner, M., Kircheis, G., Häussinger, D., et al. (2012). Lowered frequency and impaired modulation of gamma band oscillations in a bimodal attention task are associated with reduced critical flicker frequency. *NeuroImage* 61, 216–227. doi: 10.1016/j.neuroimage.2012.02.063
- Kircheis, G., Hilger, N., and Häussinger, D. (2014). Value of critical flicker frequency and psychometric hepatic encephalopathy score in diagnosis of low-grade hepatic encephalopathy. *Gastroenterology* 146, 961–969. doi: 10.1053/j.gastro.2013.12.026
- Kircheis, G., Wettstein, M., Timmermann, L., Schnitzler, A., and Häussinger, D. (2002). Critical flicker frequency for quantification of low-grade hepatic encephalopathy. *Hepatology* 35, 357–366. doi: 10.1053/jhep.2002.30957
- Kullmann, F., Hollerbach, S., Lock, G., Holstege, A., Dierks, T., and Schölmerich, J. (2001). Brain electrical activity mapping of EEG for the diagnosis of (sub) clinical hepatic encephalopathy in chronic liver disease. *Eur. J. Gastroenterol. Hepatol.* 13, 513–522. doi: 10.1097/00042737-200105000-00009
- Lacruz, F., Artieda, J., Pastor, M. A., and Obeso, J. A. (1991). The anatomical basis of somesthetic temporal discrimination in humans. *J. Neurol. Neurosurg. Psychiatry* 54, 1077–1081. doi: 10.1136/jnnp.54.12.1077
- Landau, A. N., and Fries, P. (2012). Attention samples stimuli rhythmically. *Curr. Biol.* 22, 1000–1004. doi: 10.1016/j.cub.2012.03.054
- Landau, A. N., Schreyer, H. M., van Pelt, S., and Fries, P. (2015). Distributed attention is implemented through theta-rhythmic gamma modulation. *Curr. Biol.* 25, 2332–2337. doi: 10.1016/j.cub.2015.07.048
- Lange, J., Halacz, J., van Dijk, H., Kahlbrock, N., and Schnitzler, A. (2012). Fluctuations of prestimulus oscillatory power predict subjective perception of tactile simultaneity. *Cereb. Cortex* 22, 2564–2574. doi: 10.1093/cercor/bhr329
- Lee, M. S., Lee, M. J., Conte, A., and Berardelli, A. (2018). Abnormal somatosensory temporal discrimination in Parkinson's disease: pathophysiological correlates and role in motor control deficits. *Clin. Neurophysiol.* 129, 442–447. doi: 10.1016/j.clinph.2017.11.022
- Limbach, K., and Corballis, P. M. (2016). Prestimulus alpha power influences response criterion in a detection task. *Psychophysiology* 53, 1154–1164. doi: 10.1111/psyp.12666
- May, E. S., Butz, M., Kahlbrock, N., Brenner, M., Hoogenboom, N., Kircheis, G., et al. (2014). Hepatic encephalopathy is associated with slowed and delayed stimulus-associated somatosensory alpha activity. *Clin. Neurophysiol.* 125, 2427–2435. doi: 10.1016/j.clinph.2014.03.018
- Oeltzschner, G., Butz, M., Baumgarten, T. J., Hoogenboom, N., Wittsack, H.-J., and Schnitzler, A. (2015). Low visual cortex GABA levels in hepatic encephalopathy: links to blood ammonia, critical flicker frequency, and brain osmolytes. *Metab. Brain Dis.* 30, 1429–1438. doi: 10.1007/s11011-015-9729-2
- Olesen, S. S., Graversen, C., Hansen, T. M., Blauenfeldt, R. A., Hansen, J. B., Steimle, K., et al. (2011). Spectral and dynamic electroencephalogram abnormalities are correlated to psychometric test performance in hepatic encephalopathy. *Scand. J. Gastroenterol.* 46, 988–996. doi: 10.3109/00365521.2011.579160
- Pastor, M. A., Day, B. L., Macaluso, E., Friston, K. J., and Frackowiak, R. S. J. (2004). The functional neuroanatomy of temporal discrimination. *J. Neurosci.* 24, 2585–2591. doi: 10.1523/JNEUROSCI.4210-03.2004
- Prakash, R., and Mullen, K. D. (2010). Mechanisms, diagnosis and management of hepatic encephalopathy. *Nat. Rev. Gastroenterol. Hepatol.* 7, 515–525. doi: 10.1038/nrgastro.2010.116
- Prins, N., and Kingdom, F. A. A. (2009). *Palamedes: Matlab Routines for Analyzing Psychophysical Data*. Available at: <http://www.palamedestoolbox.org>

- Rocchi, L., Casula, E., Tocco, P., Berardelli, A., and Rothwell, J. (2016). Somatosensory temporal discrimination threshold involves inhibitory mechanisms in the primary somatosensory area. *J. Neurosci.* 36, 325–335. doi: 10.1523/JNEUROSCI.2008-15.2016
- Romero-Gómez, M., Córdoba, J., Jover, R., Del Olmo, J. A., Ramírez, M., Rey, R., et al. (2007). Value of the critical flicker frequency in patients with minimal hepatic encephalopathy. *Hepatology* 45, 879–885. doi: 10.1002/hep.21586
- Song, K., Meng, M., Chen, L., Zhou, K., and Luo, H. (2014). Behavioral oscillations in attention: rhythmic  $\alpha$  pulses mediated through  $\theta$  band. *J. Neurosci.* 34, 4837–4844. doi: 10.1523/JNEUROSCI.4856-13.2014
- Timmermann, L., Butz, M., Gross, J., Ploner, M., Südmeyer, M., Kircheis, G., et al. (2008). Impaired cerebral oscillatory processing in hepatic encephalopathy. *Clin. Neurophysiol.* 119, 265–272. doi: 10.1016/j.clinph.2007.09.138
- Torlot, F. J., McPhail, M. J. W., and Taylor-Robinson, S. D. (2013). Meta-analysis: the diagnostic accuracy of critical flicker frequency in minimal hepatic encephalopathy. *Aliment. Pharmacol. Therap.* 37, 527–536. doi: 10.1111/apt.12199
- VanRullen, R. (2016). Perceptual cycles. *Trends Cogn. Sci.* 20, 723–735. doi: 10.1016/j.tics.2016.07.006
- VanRullen, R., Reddy, L., and Koch, C. (2006). The continuous wagon wheel illusion is associated with changes in electroencephalogram power at approximately 13 Hz. *J. Neurosci.* 26, 502–507. doi: 10.1523/JNEUROSCI.4654-05.2006
- Wutz, A., Weisz, N., Braun, C., and Melcher, D. (2014). Temporal windows in visual processing: “prestimulus brain state” and “poststimulus phase reset” segregate visual transients on different temporal scales. *J. Neurosci.* 34, 1554–1565. doi: 10.1523/JNEUROSCI.3187-13.2014

**Conflict of Interest Statement:** DH belongs to a group of patent holders for the HEPATonorm™-Analyzer (device determining the critical flicker frequency).

The remaining authors declare that the research was conducted in the absence of any commercial or financial relationships that could be construed as a potential conflict of interest.

Copyright © 2018 Lazar, Butz, Baumgarten, Füllenbach, Jördens, Häussinger, Schnitzler and Lange. This is an open-access article distributed under the terms of the Creative Commons Attribution License (CC BY). The use, distribution or reproduction in other forums is permitted, provided the original author(s) and the copyright owner(s) are credited and that the original publication in this journal is cited, in accordance with accepted academic practice. No use, distribution or reproduction is permitted which does not comply with these terms.

- 4) Baumgarten, T. J., Neugebauer, J., Oeltzschner, G., Füllenbach, N.-D., Kircheis, G., Häussinger, D., **Lange, J.**, Wittsack, H.-J., Butz, M., & Schnitzler, A. (2018). Connecting Occipital Alpha Band Peak Frequency, Visual Temporal Resolution, and Occipital GABA Levels in Healthy Participants and Hepatic Encephalopathy Patients. *NeuroImage: Clinical*, 20, 347-356.
- Impact Factor (2018): 3.943



# Connecting occipital alpha band peak frequency, visual temporal resolution, and occipital GABA levels in healthy participants and hepatic encephalopathy patients

Thomas J. Baumgarten<sup>a,b,\*</sup>, Julia Neugebauer<sup>a</sup>, Georg Oeltzschner<sup>c,d</sup>, Nur-Deniz Füllenbach<sup>e</sup>, Gerald Kircheis<sup>e</sup>, Dieter Häussinger<sup>e</sup>, Joachim Lange<sup>a</sup>, Hans-Jörg Wittsack<sup>f</sup>, Markus Butz<sup>a</sup>, Alfons Schnitzler<sup>a</sup>

<sup>a</sup> Institute of Clinical Neuroscience and Medical Psychology, Medical Faculty, Heinrich Heine University Düsseldorf, 40225 Düsseldorf, Germany

<sup>b</sup> Neuroscience Institute, New York University Langone Medical Center, New York, NY, USA

<sup>c</sup> Russell H. Morgan Department of Radiology and Radiological Science, The Johns Hopkins University School of Medicine, Baltimore, MD, USA

<sup>d</sup> F.M. Kirby Center for Functional Brain Imaging, Kennedy Krieger Institute, Baltimore, MD, USA

<sup>e</sup> Department of Gastroenterology, Hepatology and Infectiology, Medical Faculty, Heinrich Heine University Düsseldorf, 40225 Düsseldorf, Germany

<sup>f</sup> Department of Diagnostic and Interventional Radiology, Medical Faculty, Heinrich Heine University Düsseldorf, 40225 Düsseldorf, Germany

## ARTICLE INFO

### Keywords:

Hepatic encephalopathy  
Magnetoencephalography  
Alpha oscillations  
Peak frequency  
Magnetic resonance spectroscopy  
GABA

## ABSTRACT

Recent studies have proposed a connection between the individual alpha band peak frequency and the temporal resolution of visual perception in healthy human participants. This connection rests on animal studies describing oscillations in the alpha band as a mode of phasic thalamocortical information transfer for low-level visual stimuli, which critically relies on GABAergic interneurons.

Here, we investigated the interplay of these parameters by measuring occipital alpha band peak frequency by means of magnetoencephalography, visual temporal resolution by means of behavioral testing, and occipital GABA levels by means of magnetic resonance spectroscopy. Importantly, we investigated a sample of healthy participants and patients with varying grades of hepatic encephalopathy, which are known to exhibit decreases in the investigated parameters, thus providing an increased parameter space.

We found that occipital alpha band peak frequency and visual temporal resolution were positively correlated, i.e., higher occipital alpha band peak frequencies were on average related to a higher temporal resolution. Likewise, occipital alpha band peak frequency correlated positively with occipital GABA levels. However, correlations were significant only when both healthy participants and patients were included in the analysis, thereby indicating a connection of the measures on group level (instead of the individual level). These findings provide new insights into neurophysiological and neurochemical underpinnings of visual perception.

## 1. Introduction

Neuronal oscillatory activity has received increasing attention within the neuroscientific community during the last two decades (Buzsáki and Draguhn, 2004). Neuronal oscillations presumably represent a dynamic functional link for neuronal communication. In this role, neuronal oscillations are centered between the relatively invariant dimension of anatomical connections on the one side and the highly

flexible dimension of behavioral output on the other side (Buzsáki and Watson, 2012; Singer and Lazar, 2016). Historically, the brain was interpreted as operating in a passive stimulus-driven mode substantially focused on bottom-up serial processing of stimulus properties (e.g., Hubel and Wiesel, 1965; Thorpe et al., 1996). In contrast, current theories emphasize the role of dynamic internal brain states which affect stimulus processing in a largely stimulus-independent top-down direction. In this context, neuronal oscillations are considered to be

**Abbreviations:** CFF, Critical flicker frequency; CSD, Cross-spectral density; EC, Eyes-closed; ECG, Electro-cardiogram; EO, Eyes-open; EOG, Electro-oculogram; GABA,  $\gamma$ -aminobutyric acid; GABA +/Cr, GABA-to creatine -ratio; HE, Hepatic encephalopathy; HE1, Clinically manifest HE grade 1; HPI, Head position indication; ICA, Independent component analysis; MEG, Magnetoencephalography; mHE, Minimal HE; MNI, Montreal Neurological Institute; MRS, Magnetic resonance spectroscopy

\* Corresponding author at: Neuroscience Institute, New York University Langone Medical Center, New York, NY, USA.

E-mail address: [Thomas.Baumgarten@nyumc.org](mailto:Thomas.Baumgarten@nyumc.org) (T.J. Baumgarten).

<https://doi.org/10.1016/j.nicl.2018.08.013>

Received 8 March 2018; Received in revised form 24 July 2018; Accepted 8 August 2018

Available online 09 August 2018

2213-1582/ © 2018 The Authors. Published by Elsevier Inc. This is an open access article under the CC BY-NC-ND license (<http://creativecommons.org/licenses/by-nc-nd/4.0/>).

critical for the implementation of top-down processes (Engel et al., 2001; Hipp et al., 2011).

The functional impact of neuronal oscillations is specifically well documented for the alpha band (~7–14 Hz, Haegens et al., 2014). Alpha band oscillations are most prominent in parieto-occipital cortex areas (Hari et al., 1997) and are both predictive (Hanslmayr et al., 2007; van Dijk et al., 2008) and causally relevant (Romei et al., 2010) for neuronal processing and perception of visual stimuli. Mechanistically, the connection between cortical alpha band oscillations and visual stimulus perception rests on the synchronization of alpha band oscillations to periodic activity in thalamic relay neurons (Lőrincz et al., 2009). Thus, alpha band oscillations likely reflect a mode of phasic information transfer within a thalamocortical network (Bollimunta et al., 2011; Vijayan and Kopell, 2012). This phasic pattern relies heavily on pulsed inhibition mediated by GABAergic interneurons (Lőrincz et al., 2009). Both the phasic patterns of information transfer as well as the alpha cycle length predetermine alpha band activity to shape the temporal structure of perception (Busch et al., 2009; Mathewson et al., 2009).

This temporal dimension of perception is closely linked to the concept of perceptual cycles (Varela et al., 1981; Vanrullen and Koch, 2003; Vanrullen, 2016; Baumgarten et al., 2015; Baumgarten et al., 2017). Perceptual cycles constitute discrete temporal windows for neuronal stimulus processing, which temporally sample incoming stimuli. While experimental evidence for this concept and its connection to oscillatory alpha band activity has been first provided by a seminal study of Varela et al. (1981), multiple attempts to replicate this finding have remained unsuccessful (see Vanrullen and Koch, 2003; Vanrullen et al., 2014). Nonetheless, recent findings demonstrate that perceptual sampling of visual stimuli is primarily determined by the frequency of individual alpha band activity (Dugué et al., 2011; Chakravarthi and Vanrullen, 2012; Cecere et al., 2015; Samaha and Postle, 2015). Some studies aimed to connect individual markers of alpha band activity to individual perceptual performance levels. Such approaches targeting individual oscillatory parameters mostly focus on the peak frequency of a specific predetermined frequency band. Here, peak frequency is defined as the specific frequency within a predefined band exhibiting the highest spectral power (i.e., the power-dominant frequency). Recent studies reported correlations between the individual alpha band peak frequency and the speed of temporal sampling in the visual (Samaha and Postle, 2015) and audio-visual domain (Cecere et al., 2015). The theory of perceptual cycles and the abovementioned findings provide the hypothesis of a positive linear correlation between alpha band peak frequency and visual temporal resolution. Individuals with a low alpha band peak frequency should exhibit a low visual temporal resolution. However, testing this hypothesis is hindered because, in healthy subjects, alpha band peak frequencies are distributed only across a limited range (Haegens et al., 2014). Therefore, it can be beneficial to include groups showing systematic shifts of alpha band activity, which consequently increases alpha band frequency ranges measurable in the overall study sample.

Such frequency shifts have been repeatedly reported in patients with hepatic encephalopathy (HE). HE describes changes in neurological function as a consequence of liver dysfunction (Häussinger and Schliess, 2008). This patient group is known to exhibit a global slowing of oscillatory activity (Kullmann et al., 2001; Timmermann et al., 2005; Olesen et al., 2011; Butz et al., 2013), with especially prominent effects found for the alpha band peak frequency (Kullmann et al., 2001; Marchetti et al., 2011; Olesen et al., 2011; Götz et al., 2013). In addition to alpha band peak frequency decreases, topographical changes of peak frequency generators have been repeatedly shown in HE patient samples. Early electrophysiological studies mention topographical shifts in peak frequency sources from the occipito-parietal to parieto-central areas (Sagalés et al. (1990), Kullmann et al. (2001), Montagnese et al. (2007), Olesen et al. (2011)). Although most of these results remain on the descriptive level, this repeatedly published effect has been labeled

“anteriorization” of peak frequency activity. A recent MEG study likewise addressed this topic and reported a spatial blurring of oscillatory sources in HE patients compared to healthy controls (Götz et al., 2013).

HE patients also demonstrate a variety of neuropsychological impairments, including deficits in visual perception (Häussinger et al., 2007; Götz et al., 2013). These visual perceptual impairments are reflected in a decreased critical flicker frequency (CFF). The CFF assesses the temporal resolution of the visual sensory system by presenting a red light with an initial frequency of 60 Hz, which is gradually and linearly decreasing in frequency. While initially being perceived as a steady and continuous light, subjects indicate the time point at which they perceive the light as a discontinuous flicker (Kircheis et al., 2002). The CFF can be used to differentiate subclinical disease stages from overt clinical HE manifestation (Romero-Gómez et al., 2007; Sharma et al., 2007; Torlot et al., 2013) and further correlates with the disease severity in HE patients (Kircheis et al., 2002).

Regarding neurotransmitter concentration levels, HE patients show disease-related changes in  $\gamma$ -aminobutyric acid (GABA) levels. However, so far results have been inconsistent. Whereas classical theories advocated a generally increased GABAergic tone in HE patients (Schafer and Jones, 1982), recent studies put forward a more complex picture of regionally specific changes in GABA levels (e.g., Cauli et al., 2009a; Cauli et al., 2009b; Llansola et al., 2015). Moreover, our group reported a significant decrease in the occipital GABA-to-creatine ratio (GABA+/Cr) for HE patients compared to healthy controls (Oeltzschner et al., 2015). Although first investigations of healthy subjects have not demonstrated a relationship between occipital alpha band peak frequency and occipital GABA levels (Baumgarten et al., 2016), connections remain unknown for HE patients. Given such a connection, occipital GABA levels could represent a critical parameter linking disease-related changes in oscillatory activity and disease-related sensory impairments in HE.

The present study investigated the relationship between individual electrophysiological (occipital alpha band peak frequency), perceptual (CFF), and neurochemical (occipital GABA+/Cr levels) parameters in patients with varying grades of HE (minimal HE / manifest HE) and healthy controls. With this approach, we aimed to assess if neuronal oscillatory activity acts as a connecting factor between the perceptual visual sampling rate and occipital GABA+/Cr levels. By specifically including a patient sample for which perceptual impairments and regionally specific decreases in GABA+/Cr levels were known, the present investigation goes beyond previous studies, which examined only healthy subjects and only single connections (i.e., only the connection between alpha band peak frequency and CFF or GABA+/Cr levels). This way, the hypothesized connections can be tested within an increased parameter space of the investigated metrics, as compared to the investigation of healthy subjects alone. In accordance with previous findings (e.g., Kullmann et al., 2001; Olesen et al., 2011; Götz et al., 2013), we hypothesized that HE subjects demonstrate decreased occipital alpha band peak frequency and that this decrease worsens with progressing disease state. Given the comparatively high spatial resolution provided by MEG measures of neural activity, we additionally investigated if the topographical distribution of alpha band peak frequency differs between HE patients and healthy controls. Here, the main aim was to specify effects of peak frequency anteriorization previously reported by electroencephalographic studies. Further, we hypothesized a positive connection between occipital alpha band peak frequency and temporal visual perception as measured by the CFF in accordance with current models of perceptual cycles. Finally, we hypothesized that occipital alpha band peak frequency is correlated positively with occipital GABA+/Cr ratios.

**Table 1**

Demographic data for all participants separated by group. Data is presented as mean  $\pm$  SD.

	Sex (male/female)	Age (years)	CFF (Hz)
Controls (n = 15)	7/8	59.9 $\pm$ 9.0	41.8 $\pm$ 4.1
mHE (n = 14)	9/5	53.6 $\pm$ 10.8	38.7 $\pm$ 4.0
HE1 (n = 14)	11/3	60.7 $\pm$ 7.3	35.7 $\pm$ 1.9

## 2. Materials & methods

### 2.1. Participants

43 participants (16 females, age: 58.1  $\pm$  9.5 years (mean  $\pm$  SD)) were included in the present study after providing prior written informed consent in accordance with the Declaration of Helsinki and the Ethical Committee of the Medical Faculty, Heinrich Heine University Düsseldorf (study number: 3644). The present sample was previously described in Oeltzschner et al. (2015). Specifically, 28 patients with hepatic encephalopathy (HE) and 15 healthy controls were included in the study (see Table 1 for demographic details of the respective groups). Patient inclusion criteria were a clinically confirmed liver cirrhosis and the diagnosis of either a minimal HE (mHE) or a clinically relevant HE (HE1; see below for the respective diagnosis criteria). The age-matched healthy participants were recruited as a control group. Data from all subjects (i.e., patients and healthy subjects) was used for the respective correlation analyses. All participants had normal or corrected to normal vision. Exclusion criteria for both patients and controls included severe intestinal, neurological, or psychiatric diseases excluding the diagnosis of HE for the patient group, the use of any medication acting on the central nervous system, blood clotting dysfunction, pregnancy, and diagnosed peripheral/retinal neuropathy. Further, patients had to confirm alcohol abstinence for at least 4 weeks prior to measurement. In addition, patients underwent a standard blood examination on the day of the measurement, which included an assessment of current blood alcohol levels.

Grading of HE disease severity consisted of a combination of the West-Haven criteria (Ferenci et al., 2002), the critical flicker frequency (CFF; Kircheis et al., 2002; Kircheis et al., 2014), a clinical assessment of the mental state and consciousness by an experienced clinician, and psychometric testing with the computer-based neuropsychological test battery from the Vienna Test System (Dr. Schuhfried GmbH, Mödling, Austria). Patients were classified as minimal HE when they did not exhibit manifest HE-related clinical symptoms but showed test score deviations of at least one standard deviation to the tests control cohort in more than two psychometric tests. CFFs were measured with a mobile measurement device, the HEPATonorm™-Analyzer (nevoLAB, Maierhöfen, Germany). To assess the individual CFF, a flickering light is presented to the participants. The light starts to flicker with a frequency of 60 Hz, which is perceived as a continuous light. Then, the frequency by which the light flickers steadily decreases and participants are requested to report when they first perceive the light as clearly flickering, instead of a continuous light. Importantly, the CFF was shown to decrease depending on HE disease severity, with 39 Hz suggested as a cut-off to detect manifest HE patients (Kircheis et al., 2002; Kircheis et al., 2014). Individual CFFs were assessed on the day of the MEG/MRS measurement.

### 2.2. MEG Data

Individual magnetoencephalography (MEG) data was assessed on the same day as the respective individual CFF and magnetic resonance spectroscopy (MRS) data, whereas MEG measurements were always performed prior to MRS measurements to avoid contamination of the magnetic brain signal.

#### 2.2.1. Paradigm

Participants were seated in the MEG. All visual stimuli were projected on a translucent screen (60 Hz refresh rate) positioned 57 cm in front of the participant. Neuromagnetic activity was recorded during two sessions with a respective duration of 5 min each. For the first session, participants were instructed to focus a dimmed fixation dot (0.5° diameter) presented in the center of the screen, subsequently labeled eyes-open condition (EO). In the second session, subjects were visually and verbally instructed to close their eyes but remain awake. This condition is labeled eyes-closed condition (EC). During both sessions, participants were instructed to relax and refrain from any additional cognitive or motor activity. The intention for recording neuromagnetic activity for both the EO and EC condition was that oscillatory alpha band power is known to be increased during eyes-closed conditions (Adrian and Matthews, 1934; Ahveninen et al., 2007). Based on this, we expected to be able to record alpha band peak frequency more robustly in the EC condition. Stimulus presentation was controlled using Presentation software (Neurobehavioral Systems, Albany, NY, USA).

#### 2.2.2. Data recording and preprocessing

Continuous spontaneous neuromagnetic brain activity was recorded with a 306-channel whole head MEG system (Elekta Oy, Helsinki, Finland) including 102 magnetometers and 204 planar gradiometers (102 pairs of orthogonal gradiometers) at a sampling rate of 1 kHz. Unless stated otherwise, data analysis was restricted to the planar gradiometers. To account for an offline rejection of artifacts introduced by eye movements, additional electro-oculograms (EOGs) were recorded. Electrodes were applied above and below the left eye as well as on the outer canthi of each eye. In addition, an electro-cardiogram (ECG) was recorded for offline artifact rejection of cardiac artifacts with two electrodes placed on the left collarbone and the lowest left rib. Individual head position during the MEG measurement was assessed using four head position indication (HPI) coils placed at the subjects' forehead and behind both ears. To obtain individual full-brain high-resolution standard T<sub>1</sub>-weighted structural magnetic resonance images, subjects were measured in a 3 T whole-body MRI scanner (Siemens MAGNETOM Trio A TIM System, Siemens Healthcare AG, Erlangen, Germany). Structural MRIs were aligned offline with the MEG coordinate system based on the HPI coils and prominent anatomical landmarks (nasion, left and right preauricular points).

Offline analysis of MEG data was performed using custom-made Matlab scripts (The Mathworks Inc., Natick/MA, USA) and the Matlab-based open source toolbox FieldTrip (<http://www.fieldtriptoolbox.org/>; Oostenveld et al., 2011). Continuous MEG data were separated into EO and EC epochs. To this end, each epoch was defined from 3 s after beginning of the respective condition to 3 s before the end of the respective condition. Subsequently, epochs were semi-automatically and visually inspected for artifacts caused by SQUID jumps, muscle activity, and eye movements. Corresponding artifacts were identified by means of a z-score based algorithm implemented in FieldTrip. Linear trends and the mean power of each epoch were removed from the respective data set. Data sets were band-pass filtered at 1 Hz to 200 Hz and power line noise components were removed by using a band-stop filter encompassing the 50 Hz, 100 Hz, and 150 Hz components. Data epochs were segmented into trials of 1 s duration, which were defined with a 0.25 s overlap. Excessively noisy channels and trials were then removed after visual inspection. Further removal of cardiac and eye-movement related artifacts was achieved by means of an independent component analysis (ICA). To this end, mutual information between the respective ICA components and the EOG and ECG data was computed (Liu et al., 2012; Abbasi et al., 2015). Components were sorted according to the level of mutual information and visually examined regarding the topography and time course. Those components that showed a high level of mutual information as well as topographies and time courses characteristic for eye-movement or cardiac activity were removed

manually. Subsequently, ICA data was back-projected to the channel level. Previously removed channels were reconstructed by an interpolation of neighboring channels. For the EO condition,  $62.3 \pm 8.6$  s (mean  $\pm$  SEM; range: 30.5–116.8 s)/ $20.4 \pm 2.6\%$  of the total EO recording (range: 10.0–38.3%) of data were removed due to artifact contamination in the control group. In the mHE group,  $52.6 \pm 6.2$  s (21.2–90.8 s)/ $17.3 \pm 2.0\%$  (7.0–29.8%) were removed. In the HE1 group,  $46.8 \pm 4.8$  s (12.7–86.4 s)/ $15.4 \pm 1.6\%$  (4.2–28.3%) were removed. For the EC condition,  $65.3 \pm 9.3$  s (29.0–135.2 s)/ $22.1 \pm 2.9\%$  (9.8–45.8%) of data were removed in the control group. In the mHE group,  $46.0 \pm 4.9$  s (20.5–86.6 s)/ $15.6 \pm 1.7\%$  (7.0–29.4%) were removed. In the HE1 group,  $42.4 \pm 4.4$  s (21.4–75.9 s)/ $14.4 \pm 1.4\%$  (7.3–25.2%) were removed. On average,  $322.2 \pm 29.3$  (mean  $\pm$  SD) trials in the EO condition and  $313.9 \pm 28.5$  in the EC condition entered subsequent analyses, which were performed separately for the EO and EC condition.

### 2.2.3. Peak frequency determination

Individual alpha band peak frequencies were determined by applying a frequency analysis on time series data. As we hypothesized that HE patients exhibit a reduced peak frequency (i.e., the peak frequency would be located in lower frequencies compared to healthy subjects), we chose a frequency range for analysis that is substantially broader than the classical alpha frequency band. Thus, we determined peak frequencies between 4 and 14 Hz, whereas the alpha band typically is defined between 7 and 14 Hz (e.g., Haegens et al., 2014). Single trials were zero-padded to a length of 10 s in order to achieve a frequency resolution of 0.1 Hz. Subsequently, a Fourier transformation with a single Hanning taper was applied for the entire trial duration. For each condition (i.e., EO, EC), spectral power was averaged over all trials for each frequency separately, independently for each of the 204 gradiometers. Subsequently, gradiometer pairs were combined by summing spectral power across each pair of orthogonal gradiometers, resulting in 102 channel pairs. Since the present study specifically investigates occipital alpha band activity, ten medial channel pairs covering the occipital cortex were selected for further processing (van Dijk et al., 2010; Fig. S1). Individual alpha-band peak frequencies were defined as those frequencies with maximal power between 4 and 14 Hz and detected by means of the Matlab function ‘*findpeaks.m*’. Additionally, the power value of a potential peak frequency had to exhibit an amplitude increase of at least 10% relative to neighboring peaks (i.e., the option ‘*MinPeakProminence*’ was set to 10% of the respective peak amplitude; see also Baumgarten et al., 2017). By this, it was guaranteed that spontaneous power fluctuations and the 1/f power distribution would not be mistaken as frequency peaks and that selected peak frequencies would show a sufficient peak size relative to neighboring frequencies.

### 2.2.4. Source analysis

To localize the main source of the respective individual alpha band peak frequency, we calculated source-level power estimates using an adaptive spatial filtering technique (DICS; Gross et al., 2001). Therefore, a regular spaced 3D grid with 0.5 cm resolution was applied to the Montreal Neurological Institute (MNI) template brain. Subject-wise individual grids were computed by nonlinearly warping the subject-specific structural MRI on the MNI template grid and then applying the inverse of this warp to the MNI template grid. For each grid point, a lead-field matrix was computed using a realistically shaped single-shell volume conduction model (Nolte, 2003). The cross-spectral density (CSD) matrix was computed between all MEG gradiometer pairs for the respective individual sensor-level alpha band peak frequency by applying a Fourier transformation on the entire trial duration. For each individual grid point, spatial filters were constructed by using the CSD and lead-field matrix. CSD matrices of all single trials were then projected through these spatial filters and subsequently averaged across trials, resulting in across-trial-averages of estimated source power for the respective individual alpha band peak frequencies. To correct for

differing signal-to-noise ratios across grid points, grid-point-specific source power estimates were divided by grid-point-specific noise estimates. The resulting individual peak frequency source power distributions were statistically compared across groups by means of a non-parametric randomization test (Maris and Oostenveld, 2007) implemented within the FieldTrip toolbox. To this end, peak frequency source power estimates were compared across groups with an independent samples F-test. F-values of spatially adjacent grid points exceeding an a priori-defined threshold ( $p < 0.05$ ) were combined to a cluster and F-values within a cluster were summed up and entered in the second-level cluster statistic. Subsequently, a reference distribution was computed by randomly permuting the data, assuming no differences between groups and thus exchangeability of the data. Random assignments were repeated 1000 times, resulting in a summed cluster F-value for each repetition. The proportion of elements in the reference distribution exceeding the observed maximum cluster-level test statistic was used to derive a p-value for each cluster. Importantly, this approach effectively controls for the Type I error rate due to multiple comparisons.

### 2.3. Magnetic resonance spectroscopy data

Magnetic resonance spectroscopy (MRS) measures were performed on a clinical 3 T whole-body MRI scanner (Siemens MAGNETOM Trio A TIM System, Siemens Healthcare AG, Erlangen, Germany) using a 12-channel head matrix coil. For target volume localization and segmentation purposes, high-resolution 3D anatomical transversal  $T_1$ -weighted magnetization prepared gradient echo (MP RAGE) scans were performed (TR/TE = 1950/4.6 ms, FoV  $256 \times 192$  mm,  $256 \times 192$  matrix within-slice, 176 slices, slice thickness 1 mm, resulting in isotropic resolution of 1 mm). MRS data analyzed in the present study were computed for spectroscopic volumes placed in the central occipital lobe (please see Fig. 3A in Oeltzschner et al., 2015 for an exemplary spectroscopic volume placement). Volumes were manually aligned to include as much of the visual area as possible with caudal boundaries aligned along the *cerebellar tentorium*, while minimizing lipid contamination of the spectra by including portions of the skull in the volume. Subsequent to  $T_1$ -weighted planning sequences and the localization of the target volumes, MEGA PRESS (Mescher et al., 1998) spectra were acquired (number of excitations = 192, TR = 1500 ms, TE = 68 ms,  $V = 3 \times 3 \times 3$  cm<sup>3</sup>, bandwidth = 1200 Hz, 1024 data points). Editing of the spectra was conducted by J-refocusing pulses irradiated at 1.9 ppm (‘On’ resonance) and 7.5 ppm (‘Off’ resonance) using Gaussian pulses with a bandwidth of 44 Hz. In total, 192 averages (96 On spectra, 96 Off spectra) were acquired, resulting in a total measurement time of 4.8 min per session.

The MATLAB-based tool GANNET 2.0 (Edden et al., 2014) was used to process MRS spectral data. This postprocessing included individual frequency and phase correction of the single acquisitions. Fitting of the 3 ppm GABA resonance was performed in the frequency domain with a single Gaussian, whereas the 3 ppm creatine peak was modeled as a single Lorentzian peak. For subsequent analyses, the GABA-to-creatine ratio (GABA + /Cr) was used (see also Mullins et al., 2014; Oeltzschner et al., 2015).

### 2.4. Data analysis & statistical evaluation

To assess group level differences of alpha band peak frequency, CFF, and GABA + /Cr the following analysis steps were performed. Group level differences were investigated by means of a one-factor-repeated-measures ANOVA and post-hoc Tukey’s range tests (i.e., a post-hoc *t*-tests correcting for the family-wise error-rate). Prior to computing the ANOVA, a Levene test was performed to ensure homoscedasticity. If no homoscedasticity was given, the robust Brown-Forsythe test was performed instead of an ANOVA. Furthermore, if a Shapiro-Wilk test indicated a departure from normality for the respective parameter, a non-

parametric Kruskal-Wallis test was computed instead of the one-factor-repeated-measures ANOVA, and Dunn-Bonferroni post-hoc tests were computed instead of post-hoc Tukey's range tests.

The present study aimed at elucidating connections between individual alpha band peak frequencies and different markers related to HE disease severity. To this end, individual alpha band peak frequencies of all participants (i.e., healthy controls and patients) were linearly correlated (Pearson) with the individual CFF measure and occipital GABA+/Cr levels. In order to compare correlation coefficients for the correlation between CFF and alpha band peak frequency in both EO and EC condition, we applied the Meng Z-test (Meng et al., 1992). However, certain parameters investigated in this study are known to be influenced by different demographic or measurement-related factors. For example, alpha band peak frequency is known to decrease with older age (Lindsley, 1939; Aurlieu et al., 2004) and MRS derived GABA estimates vary depending on the amount of gray matter inclusion in the MRS voxel (Simister et al., 2003). Therefore, we accordingly corrected measures of correlation by computing partial correlations (Pearson) between alpha band peak frequency and CFF corrected for age. Further, the correlation between alpha band peak frequency and occipital GABA+/Cr was corrected for age and gray matter volume within the occipital MRS voxel. Previous analyses reported significant correlations between CFF and occipital GABA+/Cr ratios in the present data set (Oeltzschner et al., 2015). To determine if any potential correlation present between alpha-band peak frequency and occipital GABA+/Cr would be mediated only by the variance of the CFF values, we further corrected the correlation between alpha-band peak frequency and occipital GABA+/Cr for age, gray matter volume, and CFF. Correction for multiple comparisons was performed by means of the Benjamini-Hochberg method in order to control the false discovery rate at  $Q = 0.05$ . Statistical comparison of group level differences as well as correlation analyses were performed with SPSS Statistics 24.

### 3. Results

A summary of the measured target variables separated by group is presented in Table 2.

#### 3.1. Alpha band peak frequencies

Alpha band peak frequencies could be successfully determined in 38 of 43 participants in the eyes-open (EO) condition and in 42 of 43 participants in the eyes-closed (EC) condition. Distribution of alpha band peak frequencies significantly deviated from normality only for the control group in the EC condition ( $W(15) = 0.87$ ,  $p < 0.05$ ). Thus, the group level comparison of mean alpha band peak frequencies in the EC condition was performed by means of a non-parametric Kruskal-Wallis test. For the EO condition, no significant deviations from homoscedasticity ( $F(2,35) = 2.81$ ,  $p = 0.07$ ) were observed. Group level average alpha band peak frequencies were significantly different for the EO condition ( $F(2,35) = 9.37$ ,  $p < 0.01$ ), with significant post-hoc differences between the control group and the mHE group ( $p < 0.01$ ) and between the control group and the HE1 group ( $p < 0.01$ ). Likewise, group level average alpha band peak frequencies also differed significantly for the EC condition ( $\chi^2(2) = 15.4$ ,  $p < 0.01$ , with median peak frequencies of 9.8 (first quartile: 8.9 Hz, third quartile: 10.5 Hz) for controls, 8.6 (first quartile: 7.55 Hz, third

quartile: 9.17 Hz) for mHE patients, and 8.2 (first quartile: 7.25 Hz, third quartile: 8.55 Hz) for HE1 patients; Fig. 1A), with significant post-hoc differences between the control group and the mHE group ( $p < 0.05$ ) and between the control group and the HE1 group ( $p < 0.01$ ).

#### 3.2. Source level alpha band peak frequencies

Group-wise peak frequency source power distributions for the EO and the EC condition (Fig. 2) were displayed on the MNI template brain. Statistical comparison of peak frequency source power distributions across groups revealed no significant differences in source power distribution for the EO and the EC condition (all  $p > 0.05$ ).

#### 3.3. CFF

Visual temporal resolution as measured with the CFF could be successfully determined in all participants. For all groups, the distribution did not significantly deviate from normality ( $p > 0.2$  for all groups). However, the variable CFF significantly deviated from homoscedasticity ( $F = 4.41$ ,  $p < 0.05$ ). Group level CFF significantly differed between groups ( $F(2,32.3) = 11.12$ ,  $p < 0.01$ ; Fig. 1B). Post-hoc tests showed significant differences between controls and HE1 patients ( $p < 0.01$ ), a trend between controls and mHE patients ( $p = 0.06$ ), and a trend between mHE patients and HE1 patients ( $p = 0.07$ ).

#### 3.4. GABA+/Cr levels

Occipital GABA+/Cr levels could be successfully determined in 40 of 43 participants. GABA+/Cr levels significantly differed from normal distribution for the mHE group ( $W(12) = 0.8$ ,  $p = 0.01$ ). Therefore, group level comparisons of GABA+/Cr levels were performed by means of a non-parametric Kruskal-Wallis test. Group level GABA+/Cr levels significantly differed between groups ( $\chi^2(2) = 15.1$ ,  $p < 0.01$ , with median GABA+/Cr levels of 0.108 for controls, 0.077 for mHE patients and 0.087 for HE1 patients; Fig. 1C). Post-hoc tests showed significant differences between controls and mHE patients ( $p < 0.01$ ) as well as between controls and HE1 patients ( $p < 0.01$ ).

#### 3.5. Correlations

In order to investigate potential relations between occipital alpha band peak frequency (EO and EC), CFF, and occipital GABA+/Cr levels, we computed partial linear (Pearson) correlations. Correlations between alpha band peak frequency and CFF were corrected for age, whereas correlations between alpha band peak frequency and occipital GABA+/Cr levels were corrected for age and gray matter fraction within the occipital MRS voxel. Since a previous study found significant correlations between CFF and occipital GABA+/Cr levels in the present data set (Oeltzschner et al., 2015), we additionally corrected the correlation between alpha band peak frequency and occipital GABA+/Cr levels for CFF. Correction for multiple comparisons was performed by means of the Benjamini-Hochberg method, with both unadjusted and adjusted  $p$ -values provided subsequently.

A significant positive linear correlation between alpha band peak frequency and CFF was found for the EO condition ( $r = 0.33$ ,  $p < 0.05$ , adjusted  $p = 0.048$ ) and for the EC condition ( $r = 0.49$ ,  $p < 0.01$ ,

**Table 2**

Target variables separated by group. Data is presented as mean (median)  $\pm$  SD.

	Age (years)	Alpha Band Peak Frequency – EO (Hz)	Alpha Band Peak Frequency – EC (Hz)	CFF (Hz)	GABA+/Cr Levels (a.u.)
Controls	59.9 (59.0) $\pm$ 9.0	9.9 (9.9) $\pm$ 0.9	9.5 (9.8) $\pm$ 1.2	41.8 (41) $\pm$ 4.1	0.107 (0.108) $\pm$ 0.011
mHE	53.6 (56.0) $\pm$ 10.8	8.5 (8.4) $\pm$ 1.2	8.4 (8.6) $\pm$ 0.9	38.7 (38.9) $\pm$ 4.0	0.088 (0.077) $\pm$ 0.026
HE1	60.7 (61.0) $\pm$ 7.3	8.5 (8.5) $\pm$ 0.7	7.9 (8.2) $\pm$ 1.1	35.7 (35.5) $\pm$ 1.9	0.084 (0.087) $\pm$ 0.011

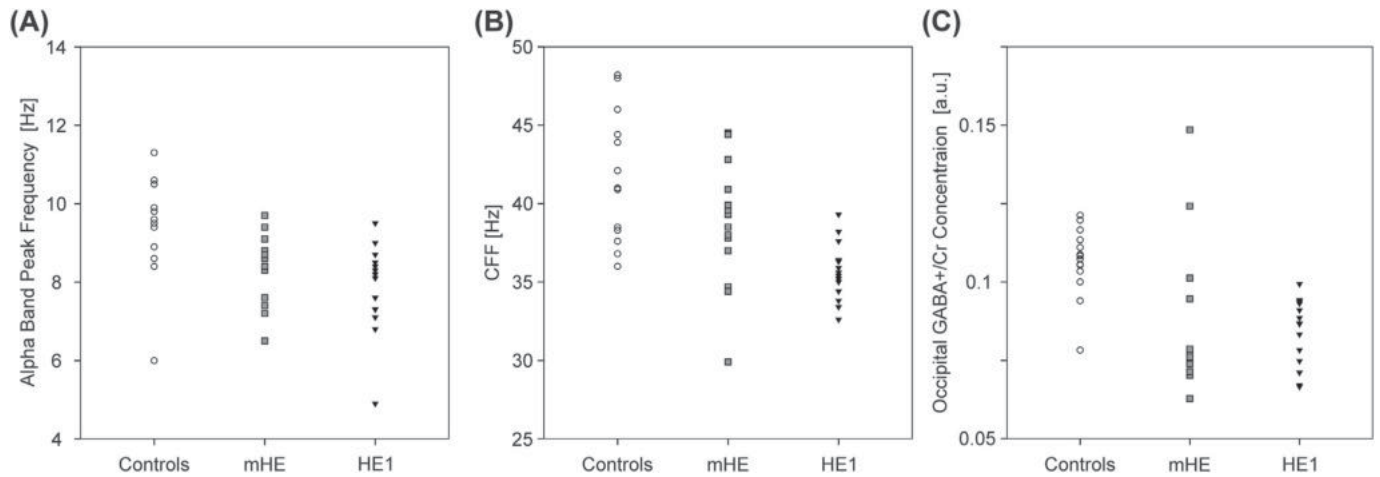


Fig. 1. Individual occipital alpha band peak frequencies in the eyes-closed (EC) condition (A), CFF (B) and occipital GABA +/Cr levels (C) separated by group. Each data point represents data for a single subject.

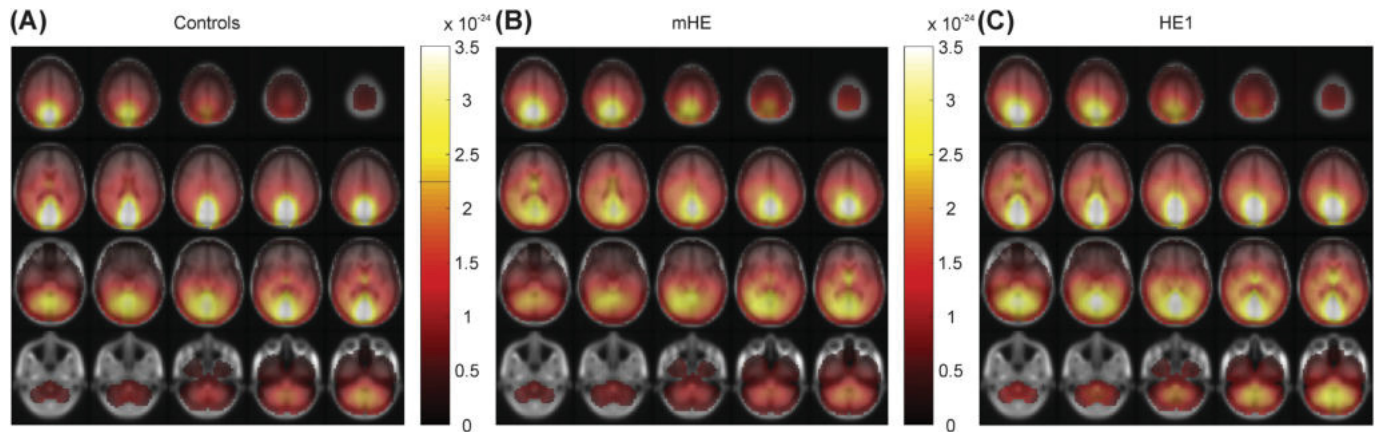


Fig. 2. Group-level average alpha band peak frequency source power distributions for the eyes-closed (EC) condition displayed on the MNI template brain for healthy controls (A), mHE patients (B), and HE1 patients (C). Source power estimates at each grid point are corrected for the noise estimate of the respective grid point (please see the Materials and methods part for further details). Color bars depict arbitrary units (a.u.) and uniformly apply to all three images.

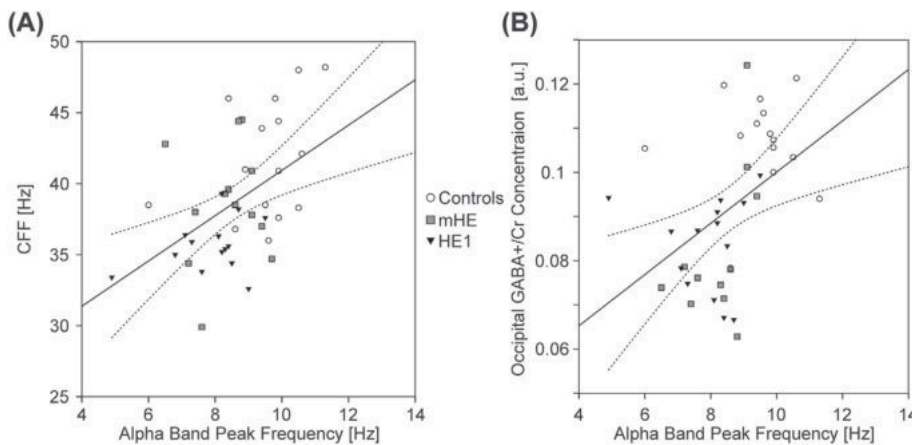


Fig. 3. Scatterplots for individual occipital alpha band peak frequency for the eyes-closed (EC) condition as a function of CFF (A) and occipital GABA +/Cr levels (B). Correlations between occipital alpha band peak frequency and CFF were corrected for age. Correlations between occipital alpha band peak frequency and occipital GABA +/Cr levels were corrected for age and gray matter volume within the occipital MRS voxel. Insets show the regression line (straight line) and the 95% confidence intervals for the mean (dotted lines).

adjusted  $p = 0.003$ ; Fig. 3A). No significant difference was found comparing the correlation coefficients between CFF and alpha band peak frequency in the EO and the EC condition ( $z = 1.25$ ,  $p = 0.1$ ). For correlations between alpha band peak frequency and occipital GABA +/Cr levels, significant positive linear correlations were observed for the EO condition ( $r = 0.55$ ,  $p < 0.01$ , adjusted  $p = 0.003$ ) and the EC condition ( $r = 0.44$ ,  $p < 0.01$ , adjusted  $p = 0.009$ ; Fig. 3B). If CFF was included as an additional control variable, correlations remained

significant for both the EO ( $r = 0.5$ ,  $p < 0.01$ , adjusted  $p = 0.006$ ) and the EC condition ( $r = 0.34$ ,  $p < 0.05$ , adjusted  $p = 0.048$ ).

#### 4. Discussion

The present study investigated connections between occipital alpha band peak frequencies, visual temporal resolution assessed by means of the Critical Flicker Frequency (CFF), and occipital GABA-to-creatine

(GABA+/Cr) levels. In accordance with our hypothesis, patients with manifest HE (i.e., HE1 patients) showed a significant reduction in alpha band peak frequency (Fig. 1A), CFF (Fig. 1B), and occipital GABA+/Cr levels (Fig. 1C) compared to healthy controls. For patients with minimal HE (mHE), alpha band peak frequency and the occipital GABA+/Cr concentration but not CFF were significantly different from healthy controls. No significant changes between patient groups and healthy controls were found regarding the topographical distribution of the alpha band peak frequency sources. Further, we could determine positive linear correlations between alpha band peak frequency recorded for the eyes-open condition (EO) and eyes-closed condition (EC), and the CFF (Fig. 3A). Thus, subjects exhibiting a higher visual temporal resolution, also on average exhibited a higher alpha band peak frequency. Although correlation coefficients were higher for correlations between CFF and alpha band peak frequency in the EC condition compared to the EO condition, this difference was not significant. Presumably, the higher correlation coefficient for the EC condition can be explained by a higher signal-to-noise ratio for alpha band power during closing of the eyes (Adrian and Matthews, 1934; Ahveninen et al., 2007), which allows for a more robust peak frequency determination. Finally, significant positive linear correlations were also present between alpha band peak frequency recorded for both experimental conditions, and occipital GABA+/Cr levels (Fig. 3B). Here, individuals with higher occipital alpha band peak frequencies also on average possessed a higher occipital GABA+/Cr ratio.

Contrary to previous studies, no significant differences in CFF were found between both healthy controls and mHE patients, as well as between mHE patients and HE1 patients. Although at first glance these null findings might suggest a reduced sensitivity for the CFF parameter, we would like to highlight that the CFF has been repeatedly shown to be a sensitive and diagnostically valuable parameter to distinguish healthy individuals from those with pre-clinical forms of HE (e.g., Sharma et al., 2007), as well as to distinguish between different HE disease stages (Kircheis et al., 2002). Further support for this notion is provided by the comparatively large sample sizes provided by these studies (approx. 90–150 patients). Due to the extensive MEG and MRS measurements presented here, the present study was not able to include a patient sample of comparable size. Thus, we interpret the present null findings rather as an effect of low statistical power resulting from a limited sample size, instead of indicating low sensitivity of the CFF as diagnostic tool. In line with this, the present paper does not aim to promote peak frequency measurements in sensory cortices or local GABA+/Cr concentrations as a diagnostic marker superior to CFF. Despite the potential of peak frequency measurements and GABA+/Cr concentrations as an additional predictor of disease state, practical consideration in terms of measurement effort, time, and financial costs necessary to acquire these parameters have to be taken into account.

Although GABA+/Cr levels differed significantly between healthy controls and both patient groups, no significant difference could be found between mHE and HE1 patient groups. This might partially be due to the relatively high variance of GABA+/Cr levels in mHE patients. Presumably, the broad distribution of GABA+/Cr levels in mHE patients is a result of the rather coarse mHE diagnosis criteria, which is based on performance decreases in a specific number of different psychometrical tests. In contrast, HE1 categorization is based on more neuropsychiatric impairments (Ferenci et al., 2002). Since decreases in test performance represent a behavioral output measure, it can be assumed that such performance decreases can result from multiple different neuronal sources. Thus, GABA+/Cr levels might already be altered in some mHE patients, whereas other in mHE patients GABA+/Cr levels might be within the normal range, but test performance is impaired due to different factors. In addition, the present results are in agreement with an earlier MRS study investigating a large mHE sample (Singhal et al., 2010), which likewise reported substantially higher standard deviations for occipital GABA+/Cr levels in mHE patients compared to healthy controls.

Most studies assessing neurophysiological parameters in patient groups aim to operationalize the respective parameters as disease-specific diagnostic biomarker. Although this has previously been performed for peak frequencies in HE (e.g., Van der Rijt et al., 1984; Kullmann et al., 2001; Marchetti et al., 2011; Olesen et al., 2011; Schiff et al., 2016), this was not the primary intention of the present study. Rather, we wanted to investigate the connections between three different parameters (i.e., electrophysiological, perceptual, and neurochemical variables) connected by previous models of perceptual sampling and experimental evidence derived from both human and animal studies. By additionally including a patient group for which a general decrease of oscillatory frequency and perceptual sampling is well documented (see Butz et al., 2013 for a review on this topic), we were able to test the predictions about the connection between peak frequencies and visual perceptual sampling based on a broader distribution of the investigated parameters.

The present correlational results support a group-dependent effect. Significant correlations between alpha band peak frequency and CFF, as well as alpha band peak frequency and occipital GABA+/Cr levels were present when all participants (i.e., healthy individuals and patients) were analyzed. Additional analyses focusing solely on one specific group (i.e., separate analyses for the control, mHE, and HE1 group) yielded no significant results. Although the general consequence of a smaller sample size should be mentioned here, it is unlikely that smaller sample sizes are the only reason for the results. Rather, the results point in the direction that the respective correlations do not primarily rest on individual differences in the measured parameters, but more on differences between the groups. This interpretation is further supported by the distribution of the subsamples on the correlation plots (Fig. 3A, B). Instead of the majority of single subjects clustering on the linear regression line, rather the 3 different subsamples are located close to the linear fit, with the in-group subjects following a more random distribution. Notably, this finding stands in contrast to previous studies relating resting state peak frequency to CFF in HE patients (Götz et al., 2013; May et al., 2014). However, the study of May and colleagues assessed alpha band peak frequencies originated from the primary somatosensory cortex (May et al., 2014), thereby recording oscillatory activity from cortical regions not primarily associated with visual stimulus processing. Likewise, Götz and colleagues (Götz et al., 2013) used a spatially unspecific peak frequency determination without any spatial or sensor restrictions. Therefore, the analyzed peak frequencies might have originated from other cortical areas than the occipital cortex.

The finding of a correlation between occipital alpha band peak frequency and CFF across groups (instead of within groups) does not suggest that the individual occipital alpha band peak frequency precisely indicates the individual temporal visual resolution. In contrast, recent studies reported a correlation of individual alpha band peak frequency and temporal resolution of perception in healthy participants (Cecere et al., 2015; Samaha and Postle, 2015). However, these studies used a very different experimental approach along with substantially younger participants. Samaha and Postle (2015) tasked their participants to discriminate two spatially overlapping, successively flashing lights from a single flashing light, with the interstimulus interval between the two stimuli being determined by individual perceptual thresholds. In contrast, the present study presented subjects with a flickering light which steadily decreased in frequency, with subjects asked to indicate at which frequency they perceived the light as flickering (i.e., not as a continuously light). We point out that the paradigm used by Samaha and Postle assesses visual temporal perception in a more indirect way, i.e., by means of a comparison of flash durations. The CFF on the other hand aims to determine the frequency for which one perceives the light as flickering and non-continuous directly. Cecere et al. (2015) implemented a multimodal audio-visual integration task, with subjects performing the sound-induced double-flash illusion task. Here, subjects had to report if they perceived either one single or two

successive visual flashes, while a single flash was temporally paired with two auditory beeps presented at a different time delay. Although this paradigm likewise focusses on perceptual resolution, the approach is generally multimodal and thus focuses on the temporal binding of stimulation in different modalities. In addition, the samples of both studies consisted entirely of healthy and young participants. Although we corrected for the factor age by adding age as a covariate in the partial correlation, general age-related differences between the respective samples cannot be ruled out. For example, there are reports of alpha band peak frequencies shifting to more frontal positions with increasing age, whereas it is unknown if posterior alpha power is decreasing or frontal alpha power is increasing (Chiang et al., 2011). This shift in weight could result in the measurement of different generators of alpha power activity for samples of young and old age, which could not be compensated by partial correlation.

The first main result that the correlation between alpha band peak frequency and CFF were mainly driven by group differences merits further discussion. Although it currently remains unclear how alpha band peak frequency, visual perceptual sampling, and local GABAergic activity are interlinked, we provide a short speculation on potentially underlying mechanisms. The connection between visual temporal resolution and alpha band activity can be explained by current models of perceptual cycles (Vanrullen and Koch, 2003; Baumgarten et al., 2015; Vanrullen, 2016). Here, ongoing neuronal oscillations in sensory cortices constitute an electrophysiological correlate of perceptual windows. It is hypothesized that multiple temporally distinct stimuli that fall within such a single window are fused and thus perceived as single percept. In contrast, if multiple temporally distinct stimuli fall within two distinct perceptual windows, they are perceived as two temporally distinct percepts. Probabilities for multiple temporally distinct stimuli to either fall within one or two cycles are determined by both the temporal distance between the distinct stimuli and the cycle length of the neuronal oscillation. The respective cycle length is directly related to the frequency of the ongoing neuronal oscillation. Given the definition of peak frequency as the local power dominant frequency, peak frequencies index the current cycle length of ongoing oscillatory activity, by which the length of a perceptual window can be inferred. Thus, a higher peak frequency indexes a shorter cycle length, which in turn points towards a higher perceptual resolution and a denser perceptual sampling. Since an exact individual mapping between peak frequency and perceptual resolution was not found, the present results indicate a rather coarse and stochastic connection between occipital alpha peak frequency and visual temporal resolution. In addition, it has to be taken into account that HE goes along with multiple other symptoms which potentially impede CFF performance. Thus, although CFF reliably indexes disease severity in HE patients, there presumably are also other factors besides alpha band activity which contribute to impairments in visual temporal resolution. For example, flexible deployment of attention and underlying gamma band activity have been reported to be impaired in HE patients. Importantly, these impairments were likewise related to visual temporal resolution as measured by CFF (Kahlbrock et al., 2012).

The second main finding of the present study is a significant positive linear correlation between occipital alpha band peak frequencies and occipital GABA +/Cr levels. Similar to the correlation between alpha band peak frequency and CFF, connections seem to rely mostly on the group level and not on the individual level. In general, the inhibitory effects mediated by GABAergic interneurons are thought essential for the rigid temporal coding necessary for the generation of oscillatory neuronal activity (Lozano-Soldevilla et al., 2014). So far, individual occipital GABA levels have been mostly related to frequencies within the gamma band (Bartos et al., 2007). For example, Muthukumaraswamy et al. (2009) reported a positive connection between occipital GABA +/Cr and occipital gamma peak frequency (but see Cousijn et al., 2014 for a contradictory finding). Balz et al. (2016) reported connections between GABA levels in the superior temporal

sulcus as measured by MRS and oscillatory gamma band power. Importantly, GABA levels also correlated with the perceptual parameters in an audiovisual perception task. In contrast, the connection between oscillatory alpha band activity and occipital GABA +/Cr levels remains speculative. Animal studies suggest that phasic GABAergic inhibition temporally shapes the output of thalamocortical neurons, which in turn is deemed crucial for discretely constraining the temporal neuronal activity within occipital cortex areas and thus influences the processing of low-level visual information (Lőrincz et al., 2009). In humans, a reasonable number of studies show effects of pharmacological GABAergic modulation on occipital oscillatory alpha band activity (e.g., Schreckenberger et al., 2004; Ahveninen et al., 2007). However, these studies almost exclusively focus on oscillatory power (reviewed by Lozano-Soldevilla, 2018), whereas modulations of peak frequency are rarely reported (but see Liley et al., 2003). Mechanistic models of thalamic generators driving the frequency of cortical alpha band activity by means of GABA-mediated conductance changes at 10 Hz have been recently put forward and related to visual stimulus processing (Gips et al., 2016). Here, multiple cycles of gamma band activity locked to alpha band phase are interpreted as a mechanism of temporal structuring for visual stimulus information, which relates to the abovementioned concept of perceptual cycles. Alpha band activity is seen as a mechanism of pulsed physiological inhibition, which separates incoming stimulus information in discrete sequential cycles. However, the location of GABAergic inhibition in this model lies within the thalamus, whereas the present study estimated GABA +/Cr levels in occipital cortical areas. Given the evidence of changes within the thalamo-cortical network connections due to GABAergic manipulation (Schreckenberger et al., 2004), it can be assumed that disease-related GABAergic concentration imbalances between these regions could critically affect the generation of alpha band oscillations, including shifts in peak frequency. Nonetheless, to obtain a clearer picture of the GABAergic influence on peak frequencies in sensory cortices, novel studies focusing specifically on this topic are necessary. Here, either human EEG/MEG studies investigating pharmacodynamical effects of GABAergic modulators on peak frequency changes in sensory cortices or animal studies directly investigating effects of GABAergic modulators on the presumed thalamo-cortical connection would be specifically valuable.

Nonetheless, it has to be kept in mind that GABA measurements by means of MRS can be considered a relatively coarse estimate of neurochemical concentrations. This owes to the relatively large voxel size, as well as to the inability to differentiate between synaptic and extrasynaptic GABA concentrations (Stagg, 2014). While the extracellular synaptic GABA levels are the most relevant to neurotransmission, MRS generally measures the total bulk tissue content of a metabolite, and therefore rather reflects the general GABAergic tone (Rae, 2014). As a quantitative measure of the local ability to exert and maintain inhibitory activity, GABA MRS levels are nevertheless of high functional relevance, and have been associated with numerous indicators of behavior and brain function (see e.g., Puts and Edden, 2012 for an overview).

The present findings of decreased alpha band peak frequencies in HE patients can further be related to reported changes in resting state functional connectivity within this patient group. A common result emerging from this line of research is the decline in clustering of functional nodes and an increased randomness in the topography of functional networks, which progressively worsens with increasing disease level (Jao et al., 2015). Specific functional connectivity decreases located in visual sensory areas for HE patients compared to healthy controls were recently reported by Zhang and colleagues (Zhang et al., 2017). Given that multiple theories presume functional integration between different cortex areas by means of alpha band synchronization (e.g., Jensen et al., 2012) and recent experimental evidence demonstrates top-down mediated alpha band phase adjustment between frontal and visual cortex areas (Solís-Vivanco et al., 2018), this suggests

that disease-related alterations in alpha band activity could be closely related to the broadly replicated changes of functional activity in HE. However, a direct connection between decreases in local oscillatory alpha band peak frequency and functional connectivity decreases in visual sensory areas remains to be shown in HE patients.

The present study found no significant differences in the topographical distribution of the alpha band peak frequency sources. Although multiple previous studies reported a general anteriorization of alpha band peak frequencies in HE patient samples (Sagalés et al. (1990), Kullmann et al. (2001), Montagnese et al. (2007), Olesen et al. (2011)), most of these studies only provided descriptive evidence without further statistical analysis. The present source distributions suggest alpha peak frequency sources to be more focally centered in the occipital cortex in healthy controls compared to both HE patient groups (Fig. 2). This would be in accordance with a recent MEG study (Götz et al., 2013), which similarly mentioned a spatial blurring of oscillatory sources in HE patients compared to healthy controls.

The broad distribution of alpha band peak frequencies might be considered a potential shortcoming of the present study, in the sense that the question arises if we really assessed peak frequencies for the alpha band in all participants. However, despite the significant differences in the mHE and HE1 samples, it can be safely assumed that our analysis approach yielded a reliable assessment of alpha band peak frequencies. First, the determined peak frequencies in the patient sample consisted of clearly discernible occipital frequency peaks (Fig. S2) present at rest (i.e., during the EO/EC condition), which supports the view that these peaks resemble the classical alpha band peak, albeit with decreased frequency. Further, alpha band peak frequency significantly differed depending on experimental condition (i.e., EO vs. EC,  $t(37) = 2.14$ ,  $p < 0.05$ ) and could be determined more reliably and in more subjects in the EC condition, which also represents a characteristic of the classical alpha rhythm (Berger, 1929; Götz et al., 2013).

Taken together, the present study demonstrates a connection between occipital alpha band peak frequency and temporal visual resolution as measured with the CFF. This connection is determined on group level (i.e., across subsamples) and not on the single subject level. Consequently, occipital alpha band activity does not seem to indicate the individual perceptual resolution, but rather seems to be decisively altered across varying disease stages of HE. The same holds true for the connection between occipital alpha band peak frequency and occipital GABA + /Cr levels. Thus, the present study reveals functional connections between electrophysiological, perceptual and neurochemical variables, with disease-related alterations in these variables declining in parallel.

## Funding

This work was supported by the German Research Foundation [Sonderforschungsbereich (SFB) 974 Project B07]. This project has received funding from the European Union's Horizon 2020 research and innovation programme under the Marie Skłodowska-Curie grant agreement No 795998 (MSCA-IF-GF awarded to T.J.B.). The funding sources had no involvement in the study design, collection, analysis, and interpretation of the presented data.

## Conflict of interest

G.K. and D.H. belong to a group of patent holders for the bedside measurement device determining the critical flicker frequency.

## Acknowledgements

The authors would like to express their gratitude to Erika Rädisch (Department of Diagnostic and Interventional Radiology, University Hospital Düsseldorf) for support with MR measurements and to Dr.

Nienke Hoogenboom for her help with the MEG measurements.

## Appendix A. Supplementary data

Supplementary data to this article can be found online at <https://doi.org/10.1016/j.nicl.2018.08.013>.

## References

- Abbasi, O., Dammers, J., Arrubla, J., Warbrick, T., Butz, M., Neuner, I., Shah, N.J., 2015. Time-frequency analysis of resting state and evoked EEG data recorded at higher magnetic fields up to 9.4T. *J. Neurosci. Methods* 255, 1–11.
- Adrian, E.D., Matthews, B.H., 1934. The Berger rhythm: potential changes from the occipital lobes in man. *Brain* 57, 355–385.
- Ahveninen, J., Lin, F.H., Kivisaari, R., Autti, T., Hämäläinen, M., Stufflebeam, S., Belliveau, J.W., Kähkönen, S., 2007. MRI-constrained spectral imaging of benzodiazepine modulation of spontaneous neuromagnetic activity in human cortex. *NeuroImage* 35, 577–582.
- Aurlin, H., Gjerde, I., Aarseth, J., Eldøen, G., Karlsen, B., Skeidsvoll, H., Gilhus, N., 2004. EEG background activity described by a large computerized database. *Clin. Neurophysiol.* 115, 665–673.
- Balz, J., Keil, J., Roa Romero, Y., Mekle, R., Schubert, F., Aydin, S., Ittermann, B., Gallinat, J., Senkowski, D., 2016. GABA concentration in superior temporal sulcus predicts gamma power and perception in the sound-induced flash illusion. *NeuroImage* 125, 724–730.
- Bartos, M., Vida, I., Jonas, P., 2007. Synaptic mechanisms of synchronized gamma oscillations in inhibitory interneuron networks. *Nat. Rev. Neurosci.* 8, 45.
- Baumgarten, T.J., Schnitzler, A., Lange, J., 2015. Beta oscillations define discrete perceptual cycles in the somatosensory domain. *Proc. Natl. Acad. Sci.* 112, 12187–12192.
- Baumgarten, T.J., Oeltzschner, G., Hoogenboom, N., Wittsack, H.-J., Schnitzler, A., Lange, J., 2016. Beta peak frequencies at rest correlate with endogenous GABA + /Cr concentrations in sensorimotor cortex areas. *PLoS One* 11, e0156829.
- Baumgarten, T.J., Königs, S., Schnitzler, A., Lange, J., 2017. Subliminal stimuli modulate somatosensory perception rhythmically and provide evidence for discrete perception. *Sci. Rep.* 7.
- Berger, H., 1929. Über das Elektrenkephalogramm des Menschen. *Archiv. für. Psychiatrie und Nervenkrankheiten* 87, 527–570.
- Bollimunta, A., Mo, J., Schroeder, C.E., Ding, M., 2011. Neuronal mechanisms and attentional modulation of Corticothalamic alpha oscillations. *J. Neurosci.* 31, 4935–4943.
- Busch, N.A., Dubois, J., Vanrullen, R., 2009. The phase of ongoing EEG oscillations predicts visual perception. *J. Neurosci.* 29, 7869–7876.
- Butz, M., May, E.S., Häußinger, D., Schnitzler, A., 2013. The slowed brain: cortical oscillatory activity in hepatic encephalopathy. *Hepatic Encephalopathy* 536, 197–203.
- Buzsáki, G., Draguhn, A., 2004. Neuronal oscillations in cortical networks. *Science* 304, 1926–1929.
- Buzsáki, G., Watson, B.O., 2012. Brain rhythms and neural syntax: implications for efficient coding of cognitive content and neuropsychiatric disease. *Dialogues Clin. Neurosci.* 14, 345–367.
- Cauli, O., Mansouri, M.T., Agusti, A., Felipo, V., 2009a. Hyperammonemia increases GABAergic tone in the cerebellum but decreases it in the rat cortex. *Gastroenterology* 136, 1359–1367.e2.
- Cauli, O., Rodrigo, R., Llansola, M., Montoliu, C., Monfort, P., Piedrafita, B., el Mlili, N., Boix, J., Agustí, A., Felipo, V., 2009b. Glutamatergic and gabaergic neurotransmission and neuronal circuits in hepatic encephalopathy. *Metab. Brain Dis.* 24, 69–80.
- Cecere, R., Rees, G., Romei, V., 2015. Individual differences in alpha frequency drive crossmodal illusory perception. *Curr. Biol.* 25, 231–235.
- Chakravarthi, R., Vanrullen, R., 2012. Conscious updating is a rhythmic process. *Proc. Natl. Acad. Sci.* 109, 10599–10604.
- Chiang, A., Rennie, C.J., Robinson, P.A., van Albada, S.J., Kerr, C.C., 2011. Age trends and sex differences of alpha rhythms including split alpha peaks. *Clin. Neurophysiol.* 122, 1505–1517.
- Cousijn, H., Haegens, S., Wallis, G., Near, J., Stokes, M.G., Harrison, P.J., Nobre, A.C., 2014. Resting GABA and glutamate concentrations do not predict visual gamma frequency or amplitude. *Proc. Natl. Acad. Sci.* 111, 9301–9306.
- der Rijt, Van, Carin, C.D., Schalm, S.W., de Groot, G.H., de Vlieger, M., 1984. Objective measurement of hepatic encephalopathy by means of automated EEG analysis. *Electroencephalogr. Clin. Neurophysiol.* 57, 423–426.
- Dugué, L., Marque, P., Vanrullen, R., 2011. The phase of ongoing oscillations mediates the causal relation between brain excitation and visual perception. *J. Neurosci.* 31, 11889.
- Edden, R.A., Puts, N.A., Harris, A.D., Barker, P.B., Evans, C.J., 2014. Gannet: a batch-processing tool for the quantitative analysis of gamma-aminobutyric acid-edited MR spectroscopy spectra. *J. Magn. Reson. Imaging* 40, 1445–1452.
- Engel, A.K., Fries, P., Singer, W., 2001. Dynamic predictions: oscillations and synchrony in top-down processing. *Nat. Rev. Neurosci.* 2, 704–716.
- Ferenci, P., Lockwood, A., Mullen, K., Tarter, R., Weissenborn, K., Blei, A.T., 2002. Hepatic encephalopathy—definition, nomenclature, diagnosis, and quantification: final report of the working party at the 11th world congresses of gastroenterology, Vienna, 1998. *Hepatology* 35, 716–721.
- Gips, B., Erden, J.P., Jensen, O., 2016. A biologically plausible mechanism for neuronal coding organized by the phase of alpha oscillations. *Eur. J. Neurosci.* 44, 2147–2161.

- Götz, T., Huonker, R., Kranczioch, C., Reuken, P., Witte, O.W., Günther, A., Debener, S., 2013. Impaired evoked and resting-state brain oscillations in patients with liver cirrhosis as revealed by magnetoencephalography. *NeuroImage* 2, 873–882.
- Gross, J., Kujala, J., Hamalainen, M., Timmermann, L., Schnitzler, A., Salmelin, R., 2001. Dynamic imaging of coherent sources: studying neural interactions in the human brain. *Proc. Natl. Acad. Sci.* 98, 694–699.
- Haegens, S., Cousijn, H., Wallis, G., Harrison, P.J., Nobre, A.C., 2014. Inter- and intra-individual variability in alpha peak frequency. *NeuroImage* 92, 46–55.
- Hanslmayr, S., Aslan, A., Staudigl, T., Klimesch, W., Herrmann, C.S., Bäuml, K.-H., 2007. Prestimulus oscillations predict visual perception performance between and within subjects. *NeuroImage* 37, 1465–1473.
- Hari, R., Salmelin, R., Mäkelä, J.P., Salenius, S., Helle, M., 1997. Magnetoencephalographic cortical rhythms. *Int. J. Psychophysiol.* 26, 51–62.
- Häussinger, D., Schliess, F., 2008. Pathogenetic mechanisms of hepatic encephalopathy. *Gut* 57, 1156–1165.
- Häussinger, D., Blei, A.T., Rodes, J., Benhamou, J.P., Reichen, J., Rizzetto, M., 2007. *The Textbook of Hepatology: From Basic Science to Clinical Practise*. Wiley-Blackwell, Oxford.
- Hipp, J.F., Engel, A.K., Siegel, M., 2011. Oscillatory synchronization in large-scale cortical networks predicts perception. *Neuron* 69, 387–396.
- Hubel, D.H., Wiesel, T.N., 1965. Receptive fields and functional architecture in two nonstriate visual areas (18 and 19) of the cat. *J. Neurophysiol.* 28, 229.
- Jao, T., Schröter, M., Chen, C.L., Cheng, Y.F., Lo, C.Y.Z., Chou, K.H., Patel, A.X., Lin, W.C., Lin, C.P., Bullmore, E.T., 2015. Functional brain network changes associated with clinical and biochemical measures of the severity of hepatic encephalopathy. *NeuroImage* 122, 332–344.
- Jensen, O., Bonnefond, M., Vanrullen, R., 2012. An oscillatory mechanism for prioritizing salient unattended stimuli. *Trends Cogn. Sci.* 16, 200–206.
- Kahlbrock, N., Butz, M., May, E.S., Brenner, M., Kircheis, G., Häussinger, D., Schnitzler, A., 2012. Lowered frequency and impaired modulation of gamma band oscillations in a bimodal attention task are associated with reduced critical flicker frequency. *NeuroImage* 61, 216–227.
- Kircheis, G., Wettstein, M., Timmermann, L., Schnitzler, A., Häussinger, D., 2002. Critical flicker frequency for quantification of low-grade hepatic encephalopathy. *Hepatology* 35, 357–366.
- Kircheis, G., Hilger, N., Häussinger, D., 2014. Value of critical flicker frequency and psychometric hepatic encephalopathy score in diagnosis of low-grade hepatic encephalopathy. *Gastroenterology* 146, 961–969.e11.
- Kullmann, F., Hollerbach, S., Lock, G., Holstege, A., Dierks, T., Schölmerich, J., 2001. Brain electrical activity mapping of EEG for the diagnosis of (sub) clinical hepatic encephalopathy in chronic liver disease. *Eur. J. Gastroenterol. Hepatol.* 13, 513–522.
- Liley, D.T., Cadusch, P.J., Gray, M., Nathan, P.J., 2003. Drug-induced modification of the system properties associated with spontaneous human electroencephalographic activity. *Phys. Rev. E* 68, 051906.
- Lindsley, D.B., 1939. A longitudinal study of the occipital alpha rhythm in normal children: frequency and amplitude standards. *Pedagogical Seminary J. Genet. Psychol.* 55, 197–213.
- Liu, Z., de Zwart, J.A., van Gelderen, P., Kuo, L.-W., Duyn, J.H., 2012. Statistical feature extraction for artifact removal from concurrent fMRI-EEG recordings. *NeuroImage* 59, 2073–2087.
- Llansola, M., Montoliu, C., Agusti, A., Hernandez-Rabaza, V., Cabrera-Pastor, A., Gomez-Gimenez, B., Malaguarnera, M., Dadsetan, S., Belghiti, M., Garcia-Garcia, R., Balzano, T., 2015. Interplay between glutamatergic and GABAergic neurotransmission alterations in cognitive and motor impairment in minimal hepatic encephalopathy. *Neurochem. Int.* 88, 15–19.
- Lőrincz, M.L., Kékesi, K.A., Juhász, G., Crunelli, V., Hughes, S.W., 2009. Temporal framing of thalamic relay-mode firing by phasic inhibition during the alpha rhythm. *Neuron* 63, 683–696.
- Lozano-Soldevilla, D., 2018. On the physiological modulation and potential mechanisms underlying Parieto-occipital alpha oscillations. *Front. Comput. Neurosci.* 12, 23.
- Lozano-Soldevilla, D., ter Huurne, N., Cools, R., Jensen, O., 2014. GABAergic modulation of visual gamma and alpha oscillations and its consequences for working memory performance. *Curr. Biol.* 24, 2878–2887.
- Marchetti, P., D'Avanzo, C., Orsato, R., Montagnese, S., Schiff, S., Kaplan, P.W., Piccione, F., Merkel, C., Gatta, A., Sparacino, G., Toffolo, G.M., Amodio, P., 2011. Electroencephalography in patients with cirrhosis. *Gastroenterology* 141, 1680–1689.e2.
- Maris, E., Oostenveld, R., 2007. Nonparametric statistical testing of EEG- and MEG-data. *J. Neurosci. Methods* 164, 177–190.
- Mathewson, K.E., Gratton, G., Fabiani, M., Beck, D.M., Ro, T., 2009. To see or not to see: prestimulus alpha phase predicts visual awareness. *J. Neurosci.* 29, 2725–2732.
- May, E.S., Butz, M., Kahlbrock, N., Brenner, M., Hoogenboom, N., Kircheis, G., Häussinger, D., Schnitzler, A., 2014. Hepatic encephalopathy is associated with slowed and delayed stimulus-associated somatosensory alpha activity. *Clin. Neurophysiol.* 125, 2427–2435.
- Meng, X.L., Rosenthal, R., Rubin, D.B., 1992. Comparing correlated correlation coefficients. *Psychol. Bull.* 111, 172–175.
- Mescher, M., Merkle, H., Kirsch, J., Garwood, M., Gruetter, R., 1998. Simultaneous in vivo spectral editing and water suppression. *NMR Biomed.* 11, 266–272.
- Montagnese, S., Jackson, C., Morgan, M.Y., 2007. Spatio-temporal decomposition of the electroencephalogram in patients with cirrhosis. *J. Hepatol.* 46, 447–458.
- Mullins, P.G., McGonigle, D.J., O'Gorman, R.L., Puts, N.A., Vidyasagar, R., Evans, C.J., Edden, R.A., 2014. Current practice in the use of MEGA-PRESS spectroscopy for the detection of GABA. *NeuroImage* 86, 43–52.
- Muthukumaraswamy, S.D., Edden, R.A., Jones, D.K., Swettenham, J.B., Singh, K.D., 2009. Resting GABA concentration predicts peak gamma frequency and fMRI amplitude in response to visual stimulation in humans. *Proc. Natl. Acad. Sci.* 106, 8356–8361.
- Nolte, G., 2003. The magnetic lead field theorem in the quasi-static approximation and its use for magnetoencephalography forward calculation in realistic volume conductors. *Phys. Med. Biol.* 48, 3637.
- Oeltzschner, G., Butz, M., Baumgarten, T., Hoogenboom, N., Wittsack, H.-J., Schnitzler, A., 2015. Low visual cortex GABA levels in hepatic encephalopathy: links to blood ammonia, critical flicker frequency, and brain osmolytes. *Metab. Brain Dis.* 1–10.
- Olesen, S.S., Graversen, C., Hansen, T.M., Blauenfeldt, R.A., Hansen, J.B., Steimle, K., Drewes, A.M., 2011. Spectral and dynamic electroencephalogram abnormalities are correlated to psychometric test performance in hepatic encephalopathy. *Scand. J. Gastroenterol.* 46, 988–996.
- Oostenveld, R., Fries, P., Maris, E., Schoffelen, J.-M., 2011. FieldTrip: open source software for advanced analysis of MEG, EEG, and invasive electrophysiological data. *Comput. Intell. Neurosci.* 2011, 9.
- Puts, N.A., Edden, R.A., 2012. In vivo magnetic resonance spectroscopy of GABA: a methodological review. *Prog. Nucl. Magn. Reson. Spectrosc.* 60, 29.
- Rae, C., 2014. A guide to the metabolic pathways and function of metabolites observed in human brain 1H magnetic resonance spectra. *Neurochem. Res.* 39, 1–36.
- Romei, V., Gross, J., Thut, G., 2010. On the role of Prestimulus alpha rhythms over Occipito-parietal areas in visual input regulation: correlation or causation? *J. Neurosci.* 30, 8692.
- Romero-Gómez, M., Córdoba, J., Jover, R., del Olmo, J.A., Ramírez, M., Rey, R., de Madaria, E., Montoliu, C., Nuñez, D., Flavia, M., Compañy, L., Rodrigo, J.M., Felipe, V., 2007. Value of the critical flicker frequency in patients with minimal hepatic encephalopathy. *Hepatology* 45, 879–885.
- Sagalés, T., Gimeno, V., de la Calzada, M.D., Casellas, F., Dolores Macià, M., Villar Soriano, M., 1990. Brain mapping analysis in patients with hepatic encephalopathy. *Brain Topogr.* 2, 221–228.
- Samaha, J., Postle, B.R., 2015. The speed of alpha-band oscillations predicts the temporal resolution of visual perception. *Curr. Biol.* 25, 2985–2990.
- Schafer, D., Jones, E.A., 1982. Hepatic encephalopathy and the  $\gamma$ -aminobutyric-acid neurotransmitter system. *Lancet* 319, 18–20.
- Schiff, S., Casa, M., Di Caro, V., Aprile, D., Spinelli, G., de Rui, M., Angeli, P., Amodio, P., Montagnese, S., 2016. A low-cost, user-friendly electroencephalographic recording system for the assessment of hepatic encephalopathy. *Hepatology* 63, 1651–1659.
- Schreckenberger, M., Lange-Asschenfeld, C., Lochmann, M., Mann, K., Siessmeier, T., Buchholz, H.G., Bartenstein, P., Gründer, G., 2004. The thalamus as the generator and modulator of EEG alpha rhythm: a combined PET/EEG study with lorazepam challenge in humans. *NeuroImage* 22, 637–644.
- Sharma, P., Sharma, B.C., Puri, V., Sarin, S.K., 2007. Critical flicker frequency: diagnostic tool for minimal hepatic encephalopathy. *J. Hepatol.* 47, 67–73.
- Simister, R.J., McLean, M.A., Barker, G.J., Duncan, J.S., 2003. A proton magnetic resonance spectroscopy study of metabolites in the occipital lobes in epilepsy. *Epilepsia* 44, 550–558.
- Singer, W., Lazar, A., 2016. Does the cerebral cortex exploit high-dimensional, non-linear dynamics for information processing? *Front. Comput. Neurosci.* 10, 99.
- Singhal, A., Nagarajan, R., Hinkin, C.H., Kumar, R., Sayre, J., Elderkin-Thompson, V., Huda, A., Gupta, R.K., Han, S.H., Thomas, M.A., 2010. Two-dimensional MR spectroscopy of minimal hepatic encephalopathy and neuropsychological correlates in vivo. *J. Magn. Reson. Imaging* 32, 35–43.
- Solis-Vivanco, R., Jensen, O., Bonnefond, M., 2018. Top-down control of alpha phase adjustment in anticipation of temporally predictable visual stimuli. *J. Cogn. Neurosci.* 1–13.
- Stagg, C.J., 2014. Magnetic resonance spectroscopy as a tool to study the role of GABA in motor-cortical plasticity. *NeuroImage* 86, 19–27.
- Thorpe, S., Fize, D., Marlot, C., 1996. Speed of processing in the human visual system. *Nature* 381, 520–522.
- Timmermann, L., Butz, M., Gross, J., Kircheis, G., Häussinger, D., Schnitzler, A., 2005. Neural synchronization in hepatic encephalopathy. *Metab. Brain Dis.* 20, 337–346.
- Torlot, F.J., McPhail, M.J.W., Taylor-Robinson, S.D., 2013. Meta-analysis: the diagnostic accuracy of critical flicker frequency in minimal hepatic encephalopathy. *Aliment. Pharmacol. Ther.* 37, 527–536.
- van Dijk, H., Schoffelen, J.-M., Oostenveld, R., Jensen, O., 2008. Prestimulus oscillatory activity in the alpha band predicts visual discrimination ability. *J. Neurosci.* 28, 1816–1823.
- van Dijk, H., van der Werf, J., Mazaheri, A., Medendorp, W.P., Jensen, O., 2010. Modulations in oscillatory activity with amplitude asymmetry can produce cognitively relevant event-related responses. *Proc. Natl. Acad. Sci.* 107, 900–905.
- Vanrullen, R., 2016. Perceptual cycles. *Trends Cogn. Sci.* 20, 723–735.
- Vanrullen, R., Koch, C., 2003. Is perception discrete or continuous? *Trends Cogn. Sci.* 7, 207–213.
- Vanrullen, R., Zoefel, B., Ilhan, B., 2014. On the cyclic nature of perception in vision versus audition. *Philosophical transactions of the royal society of London. Series B. Biol. Sci.* 369, 20130214.
- Varela, F.J., Toro, A., John, E.R., Schwartz, E.L., 1981. Perceptual framing and cortical alpha rhythm. *Neuropsychologia* 19, 675–686.
- Vijayan, S., Kopell, N.J., 2012. Thalamic model of awake alpha oscillations and implications for stimulus processing. *Proc. Natl. Acad. Sci.* 109, 18553–18558.
- Zhang, G., Cheng, Y., Liu, B., 2017. Abnormalities of voxel-based whole-brain functional connectivity patterns predict the progression of hepatic encephalopathy. *Brain Imaging Behav.* 11, 784–796.

- 5) Baumgarten, T. J., Königs, S., Schnitzler, A., & **Lange, J.** (2017a).  
Subliminal stimuli modulate somatosensory perception rhythmically and provide  
evidence for discrete perception.  
*Scientific Reports*, 7:43937. <https://doi.org/10.1038/srep43937>  
Impact factor (2017): 4.122

# SCIENTIFIC REPORTS



OPEN

## Subliminal stimuli modulate somatosensory perception rhythmically and provide evidence for discrete perception

Received: 17 August 2016

Accepted: 31 January 2017

Published: 09 March 2017

Thomas J. Baumgarten<sup>1</sup>, Sara Königs<sup>2</sup>, Alfons Schnitzler<sup>1</sup> & Joachim Lange<sup>1</sup>

Despite being experienced as continuous, there is an ongoing debate if perception is an intrinsically discrete process, with incoming sensory information treated as a succession of single perceptual cycles. Here, we provide causal evidence that somatosensory perception is composed of discrete perceptual cycles. We used in humans an electrotactile temporal discrimination task preceded by a subliminal (i.e., below perceptual threshold) stimulus. Although not consciously perceived, subliminal stimuli are known to elicit neuronal activity in early sensory areas and modulate the phase of ongoing neuronal oscillations. We hypothesized that the subliminal stimulus indirectly, but systematically modulates the ongoing oscillatory phase in S1, thereby rhythmically shaping perception. The present results confirm that, without being consciously perceived, the subliminal stimulus critically influenced perception in the discrimination task. Importantly, perception was modulated rhythmically, in cycles corresponding to the beta-band (13–18 Hz). This can be compellingly explained by a model of discrete perceptual cycles.

Although perception appears smooth and continuous in our subjective experience, it has been discussed whether the nature of sensory information processing is intrinsically discrete. Within such a framework, incoming sensory information would be grouped in consecutive separated perceptual cycles or snapshots<sup>1–3</sup>. A snapshot or perceptual cycle, thus, forms the temporal unit of perceptual experience, leading to rhythmic or cyclic perception<sup>4</sup>. While the ongoing debate whether perception is continuous or discrete has been put forward at least a century ago<sup>5,6</sup>, the hypothesis of discrete perception has only recently regained new support from neuroimaging studies. These studies have shown that the periodic modulation of subjects' perception was related to the phase of ongoing neuronal oscillations in the alpha and beta band located in the parieto-occipital or primary somatosensory cortex (S1)<sup>7–9</sup>. Said neuronal oscillations might thus form the neurophysiological basis of periodic modulations of perception, suggesting that neuronal oscillations in specific frequencies define perceptual cycles. However, current experimental evidence for discrete perception and its putative underlying neuronal mechanisms is mostly of correlative nature, while causal evidence remains scarce<sup>10,11</sup>. Consequently, the theory of discrete perception remains controversially discussed<sup>12,13</sup>. To advance this discussion, it would be necessary to causally modulate the rhythmic patterns of perception (i.e., the perceptual cycles). Here, we use the term causal to define a process in which an independent variable (e.g., the onset of a putative perceptual cycle on behavioral level or the phase of neuronal oscillations on neurophysiological level) is experimentally and systematically modulated while measuring the corresponding changes on the dependent variable (i.e., rhythmic perception). This causal approach stands in contrast to the simultaneous measurement of both variables without systematic variation, which would result in correlative evidence. The causal approach would allow for the possibility to gather experimental evidence for or against the theory of discrete perception and shed light on the patterns of perceptual cycles. We assessed this relationship by using an electrotactile temporal discrimination task which was preceded by a subliminal (i.e., below perceptual threshold) stimulus. Operationally, the use of subliminal stimuli is advantageous compared to the use of supra-threshold stimuli. Because subliminal stimuli intensities are insufficient to initiate global network activity<sup>14,15</sup> and these stimuli are not consciously perceived, the risk of perceptually confusing preceding subliminal stimuli

<sup>1</sup>Institute of Clinical Neuroscience and Medical Psychology, Medical Faculty, Heinrich-Heine-University, Düsseldorf 40225, Germany. <sup>2</sup>Department of Experimental Psychology, Faculty of Mathematics and Natural Sciences, Heinrich-Heine-University, Düsseldorf 40225, Germany. Correspondence and requests for materials should be addressed to J.L. (email: Joachim.Lange@med.uni-duesseldorf.de)

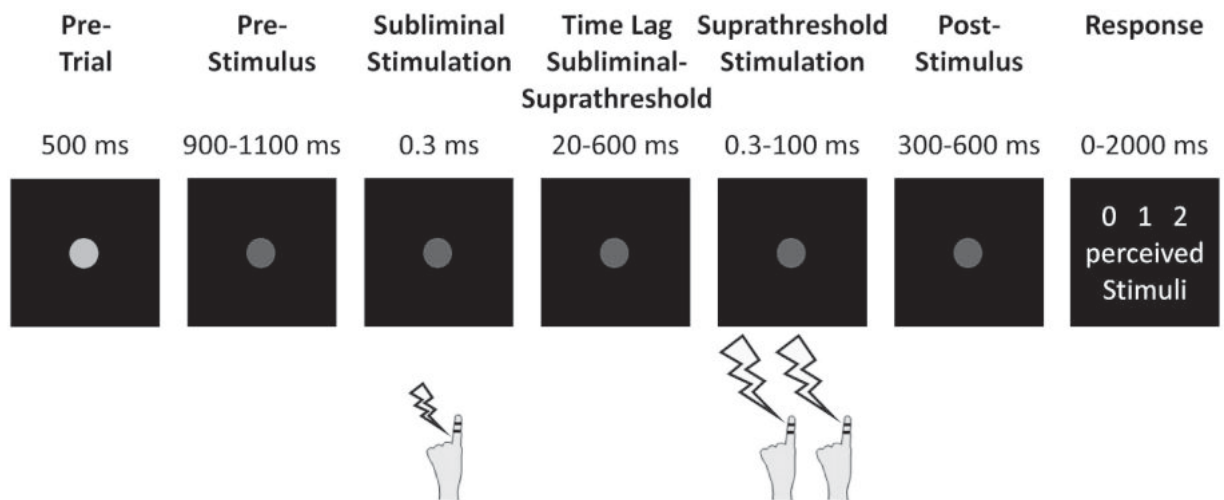


**Figure 1. Experimental setup.** Subjects fixated a central grey dot. After a jittered pre-stimulus period, they received one subliminal electro-tactile stimulus (i.e., below perceptual threshold) on their left index finger, followed by a time lag (20–600 ms) in which only the fixation dot was present. Then subjects received two suprathreshold electro-tactile stimuli with varying SOA. After another jittered time period (300–600 ms), written instructions prompted the subjects to report their perception.

with the subsequent target stimuli of the temporal discrimination task or masking the target stimuli is minimized. In addition, suprathreshold stimuli might attract exogenous (i.e., task-independent) and conscious attention. Conscious attention has been utilized in previous studies to induce a reset event. These studies have shown that conscious attention can trigger rhythmical patterns of behavior and neuronal activity<sup>7,16,17</sup>, which might interfere with the proposed cycles of perception. While we cannot exclude that a subliminal stimulus also triggers (unconscious) attentional mechanisms, the subliminal stimulus enables us to exclude conscious attention mechanisms and investigate how an unconsciously perceived event modulates perception. Despite not being consciously perceived, subliminal stimuli trigger neuronal activity in early sensory areas<sup>15,18,19</sup>. Other studies report subliminal stimuli to elicit weak evoked responses in somatosensory areas<sup>19,20</sup> and fMRI BOLD decreases related to functional inhibition<sup>19,21</sup>. Albeit not being consciously perceived, subliminal stimuli have been shown to affect the perception of subsequently presented stimuli<sup>22</sup>. This effect on perception is presumably mediated by the modulation of phase of ongoing neuronal oscillations in sensory areas (e.g., refs 23, 24). This process of phase resetting is well documented within and across sensory modalities for suprathreshold stimuli<sup>25–28</sup>, whereas reports on subthreshold stimuli remain scarce<sup>20</sup>. We hypothesized that by presenting the subliminal stimulus at systematically varying time points relative to the discrimination task, the phase of ongoing neuronal oscillations and consequently the starting point of a perceptual cycle would be modulated systematically (though indirectly; see ref. 24 for a similar paradigm in the visual domain). Accordingly, perception in the discrimination task should vary rhythmically. Such results would provide valuable evidence for discrete perception which would go beyond studies that report correlative evidence for perceptual cycles.

## Results

Subjects performed a temporal perceptual discrimination task (see Materials and Methods section for details) in which they received either zero, one or two suprathreshold electro-tactile target stimuli separated by specific stimulus onset asynchronies (SOAs; Fig. 1)<sup>9,29</sup>. Crucially, these target stimuli were preceded by a subliminal electro-tactile stimulus. The time lag between the subliminal stimulus and the first target stimulus was systematically varied (20–600 ms). After presentation of the target stimuli, subjects had to report the amount of perceived electro-tactile stimuli (i.e., zero, one, or two stimuli).

When no target stimuli were presented, but only the subliminal stimulus (i.e., the control condition), subjects on average perceived  $0.03 \pm 0.03$  stimuli [mean  $\pm$  SD] (Fig. 2A), demonstrating that the subliminal stimuli were not perceived as target stimuli. After presentation of one target stimulus, subjects perceived  $1.04 \pm 0.08$  stimuli, averaged across all time lags between subliminal and target stimuli. When two target stimuli were presented, subjects' responses increased monotonically with increasing SOA between the two stimuli (Fig. 2A; see Materials and Methods section for details). A repeated measures ANOVA revealed highly significantly different responses across conditions ( $F(5,95) = 666.5$ ,  $p < 0.01$ ). Post-hoc pairwise t-tests revealed highly significant differences between all SOAs ( $p < 0.01$  for all comparisons).

Next, we investigated potential periodic relationships between subjects' response rates and the time lag between subliminal stimulus and target stimuli by applying Fourier transformation on perceptual response rates (see Fig. 2B,C for exemplary single subject data, see Supplementary Figure 1 for an overview of all single subject data; see Fig. 2D for the group-level average data). The spectra showed a highly significant peak between 13–18 Hz ( $p < 0.01$ ) and a second peak between 1–2 Hz which, however, did not reach statistical significance ( $p = 0.11$ ; Fig. 2D). To assess whether the rhythmic modulation of perception was phase-locked, i.e., whether the

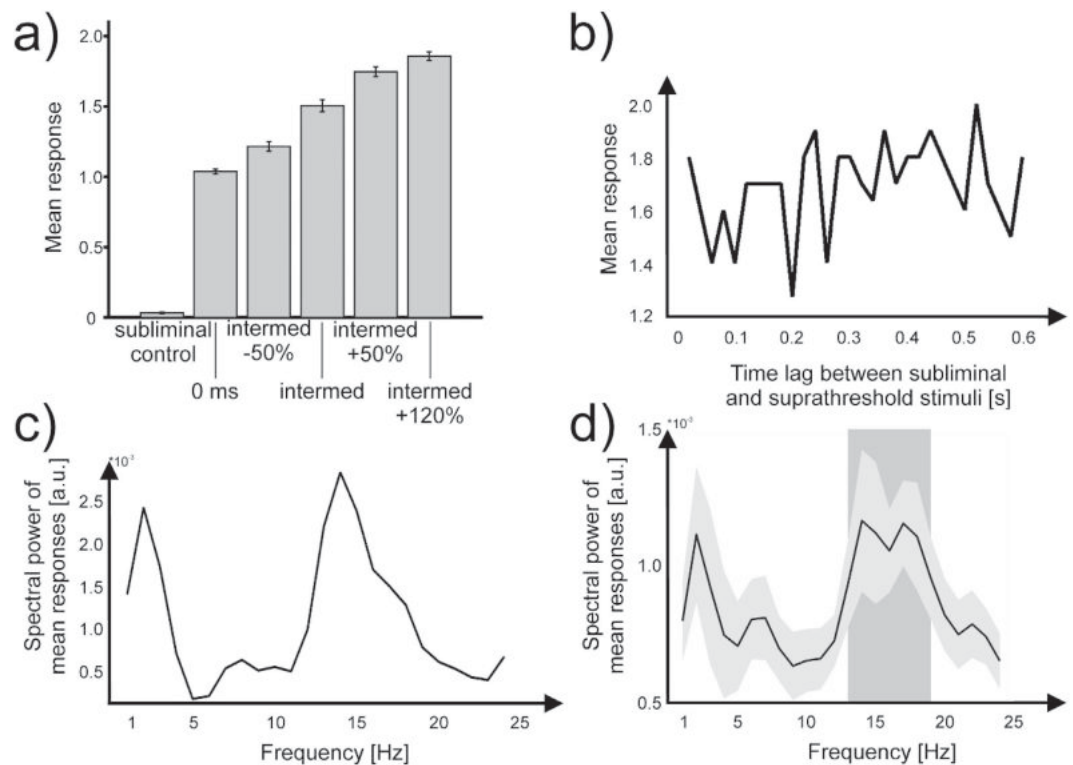


**Figure 2. Behavioral data.** (a) Average number of perceived suprathreshold stimuli displayed separately for all conditions (i.e., different SOAs) averaged across all subjects and time lags between subliminal and suprathreshold stimuli. Data are presented as mean  $\pm$  SEM. (b) Exemplary single subject average number of perceived suprathreshold stimuli of the intermed-condition as a function of time lag between subliminal and suprathreshold stimuli.  $t=0$  denotes the onset of the subliminal stimulus. Time points indicate the time lag between subliminal stimulus and first suprathreshold target stimulus. (c) Spectral decomposition of the exemplary single subject data in (b). (d) Same as (c), but now averaged across all subjects. The shaded box highlights frequencies with significantly increased amplitudes ( $p=0.002$ , corrected for multiple comparisons). The grey shading represents the SEM.

subliminal stimulus induced a phase resetting, we computed the average phase angle across the entire interval between subliminal stimulus and the first target stimulus for each subject. For each subject, we selected the phase angle of the specific frequency within the beta-band (13–24 Hz) showing the highest amplitude. The selected phase angles ( $-1.92 \pm 1.03$  radians [mean  $\pm$  SD]) significantly differed from a uniform distribution (Rayleigh test for non-uniformity across subjects;  $z=4.485$ ,  $p < 0.01$ ). In addition, phase consistency computed for each frequency separately (i.e., without a-priori selection of the individual frequency) across subjects showed a peak of phase consistency between  $\sim 12$ – $16$  Hz, which however did not differ significantly from a uniform distribution.

## Discussion

We investigated if perception in an electro-tactile temporal discrimination task is influenced by a preceding subliminal stimulus. Despite not being perceived consciously, the subliminal stimulus modulated perception rhythmically with a periodicity of 13–18 Hz. Furthermore, phase angles within the beta-band across subjects significantly differed from a uniform distribution, indicating consistent phase across subjects.

We propose an explanation of the results based on our recent findings in an MEG study<sup>9</sup>. Here, subjects received two electro-tactile stimuli (similar to the present study, but without any subliminal stimuli). Subjects' perception varied between one or two perceived stimuli from trial to trial. Perceptual variability depended on the phase of ongoing neuronal oscillations in the alpha and lower beta frequency band (8–20 Hz) in S1. We have proposed a model stating that if the two electro-tactile stimuli fall within one cycle of the 8–20 Hz oscillations, they are perceived as a single stimulus, but if they fall within separate cycles, they are perceived as two distinct stimuli (Fig. 3). Accordingly, our model states that cycles of neuronal oscillations in the alpha-/beta-band define discrete perceptual cycles in the somatosensory domain. We propose that this model explains the present results: In ongoing neuronal oscillations, the phases - and thus the perceptual cycles - are randomly distributed with respect to the to-be-perceived target stimuli. Consequently, also subjects' perception varies randomly from trial to trial (provided that the SOA is smaller than the cycle length). In the present study, the subliminal stimulus presumably resets the phase of ongoing neuronal oscillations<sup>20</sup>, which is supported by the finding of consistent phase across subjects within the beta-band. Depending on the time-lag between subliminal stimulus and the first target stimulus, this phase reset determines if the two target stimuli fall within one or two cycles, leading to the perception of one or two stimuli, respectively (Fig. 3). Accordingly, the frequency of the rhythmic variation

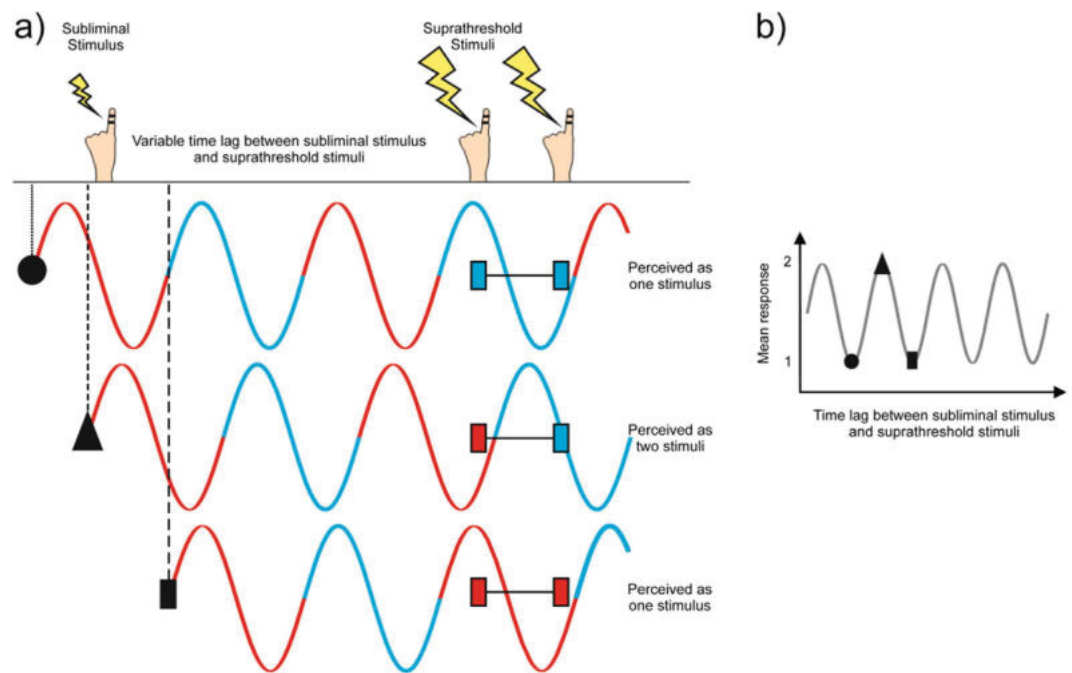


**Figure 3. Model for perceptual cycles.** (a) Three illustrative trials with different time lags between subliminal stimulus and suprathreshold stimuli. Each subliminal stimulus resets neuronal oscillations (indicated by black circle, triangle and rectangle). Perceptual cycles in neuronal oscillations are represented by red and blue lines. Different time lags result in suprathreshold stimuli falling in either one (black circle and rectangle) or two (black triangle) perceptual cycles, which results in perception of either one stimulus (black circle and rectangle) or two separate stimuli (black triangle). (b) Schematic representation of periodic relation between number of perceived suprathreshold stimuli and the time lag between subliminal stimulus and suprathreshold stimuli as a result of the model in (a).

in perception is determined by the cycle length of those neuronal oscillations that define the discrete perceptual cycles. Based on the MEG data, we proposed that the perceptual cycles are defined by neuronal oscillations in the 8–20 Hz frequency band<sup>9</sup>. This proposition is confirmed by the 13–18 Hz fluctuation of perception induced by the subliminal stimulus (Fig. 2D). However, since the present effect is located at the lower end of the classical beta band and in between the “classical” centers of somatosensory alpha (~10 Hz) and beta (~20 Hz) oscillations (or mu-rhythm<sup>30,31</sup>), a clear distinction from the alpha frequency band remains difficult. Accordingly, in our previous MEG study, we found a significant phase difference between perceiving “2” and “1” stimuli in the frequency range 8–20 Hz, thus encompassing the classical alpha- as well as the lower beta-band (albeit more strongly pronounced in the beta-band<sup>9</sup>). Although the behavioral effects in our present study do not show a peak in the classical alpha-band (8–12 Hz), it still remains not fully clear which frequency band(s) the effect might be assigned to. Future MEG/EEG studies investigating the neurophysiological basis of a phase resetting, might clarify this question.

Most previous studies providing evidence for a causal influence of neuronal oscillations on perception modulated neuronal oscillations by inducing an external rhythm to the brain<sup>10,11,25</sup>. In contrast, we do not induce an external rhythm to the brain nor does our single subliminal stimulus contain a temporal structure. Thus, any rhythmicity in the data cannot be explained by an externally induced rhythm but is putatively due to reset of ongoing neuronal oscillations<sup>16</sup>.

Recent studies reported rhythmic modulations of behavioral performance following within-modality or crossmodal reset stimuli<sup>16,26</sup>. While these studies investigated visual perception, our results provide novel evidence for rhythmic patterns of somatosensory perception. Furthermore, these studies often found low frequency rhythms in the delta to alpha range (<1 to 12 Hz) and assigned the rhythmic pattern to rhythmic fluctuations of visual attention<sup>16</sup>. In contrast, we find the significant rhythmic fluctuations in the beta-band in the somatosensory domain. Most importantly, these studies did not address the question of whether perception is a continuous or discrete process. In addition to the few studies providing evidence for discrete perceptual cycles in the visual and somatosensory domain, our results critically extend these studies by demonstrating that perception can be systematically modulated as predicted by a model of perceptual cycles<sup>9</sup>.

Subliminal stimulation intensities were selected for the preceding stimulus in order to guarantee that performance in the temporal discrimination task relied solely on the suprathreshold target stimuli (i.e., that the preceding stimulus would not be perceptually confused with the target stimuli). One might expect that a suprathreshold preceding stimulus would likewise, or even more likely, elicit a phase reset and thus lead to similar results. A suprathreshold stimulus might, however, additionally trigger conscious attentional sampling mechanisms<sup>7,16,17</sup>. Such conscious attentional sampling mechanisms might interfere with our proposed perceptual cycles. While we

cannot exclude that the subliminal stimulus also triggers (unconscious) attentional mechanisms, we were able to study a phase reset that is unnoticed by subjects. In addition, a preceding suprathreshold stimulus could perceptually mask the subsequent target stimuli. This would affect the perception of the target stimuli and could even render the target stimuli near invisible for short intervals between preceding and target stimuli (see ref. 16 for a similar effect). Thus, by using a subliminal stimulus, the results are less likely confounded by other, unintentional processes. In addition, we believe that our results are even more intriguing due to the fact that subliminal stimulation can modulate perception.

In line with studies demonstrating phase resets in response to suprathreshold stimuli (e.g., refs 26–28), there is evidence that subliminal tactile stimuli can induce oscillatory phase resets in the somatosensory cortex<sup>20</sup> and the finding of consistent phase across subjects likewise suggests such a phase reset. Nonetheless, it should be noted that our behavioral approach provides no direct measure of oscillatory phase. Thus, although the theory of phase resets has been brought forward by other studies (e.g., refs 23, 24) and is compelling and offers an elegant explanation for our results, future MEG/EEG studies should aim to confirm the present hypothesis of a phase reset of neuronal oscillations as the underlying process of our results. To conclude, our findings demonstrate a rhythmic modulation in the beta-band (13–18 Hz) of perception by subliminal, i.e., not consciously perceived stimuli. The findings support a model of perceptual cycles in the somatosensory domain<sup>9</sup>. The results provide novel causal evidence for discrete and cyclic perception.

## Materials and Methods

**Subjects.** Twenty-five healthy subjects participated in the study after providing written informed consent in accordance with the Declaration of Helsinki. The study and methods were approved by the Ethical Committee of the Medical Faculty, Heinrich-Heine-University Düsseldorf, and in line with the guidelines of the Declaration of Helsinki. All subjects had normal or corrected-to-normal vision and reported no sensory impairments, known history of neurological disorders or use of neuro-modulatory medication. Two subjects had to be excluded because they perceived the subliminal stimulation even at minimal stimulation amplitude. Three subjects (#4, #9, #22) were excluded from further analysis because they either perceived subliminal stimulation or because they showed a bottom or ceiling effects in their response distribution (see Analysis section for a detailed explanation of the exclusion criteria). Thus, twenty subjects (13 females, age:  $27.6 \pm 5.6$  years [mean  $\pm$  SD]) remained for further analysis.

**Stimuli and Procedure.** Subjects were seated in a dimmed and sound-attenuated room. Visual instructions were projected on a translucent screen (60 Hz refresh rate), which was centrally positioned 57 cm in front of the subjects. Each trial started with the presentation of a light grey dot in the middle of the screen for 500 ms (Fig. 1). Next, the light grey dot decreased in luminance, signaling the start of the stimulation period. After a jittered time period of 900–1100 ms in which only the fixation dot was present, subjects received electro-tactile stimuli on their left index finger. First, subjects were stimulated with one subliminal stimulus (i.e., stimulation with subthreshold amplitude levels) followed by zero, one, or two suprathreshold target stimuli (see below for details on stimulation parameters). The subliminal stimulus was applied by means of an electrode pair located at the base of the left index finger. Current amplitudes of the subliminal stimulation ( $1.2 \pm 0.3$  mA [mean  $\pm$  SD]) were determined individually for each subject prior to the experiment and set to 85% of the individual perceptual threshold, so that subjects did not consciously perceive this stimulus. Target stimuli were applied by means of an electrode pair located at the tip of the left index finger. Target stimuli amplitudes ( $2.5 \pm 0.5$  mA) were individually set to a level where subjects could clearly perceive stimulation, but below pain threshold. The time lag between the subliminal stimulus and the first target stimulus were pseudo-randomly varied from 20 to 600 ms in steps of 20 ms. All electro-tactile stimuli were applied for 0.3 ms and generated by a Stimulus Current Generator (DeMeTec GmbH, Langgöns, Germany). After stimulation, the fixation dot was present for a jittered time period between 300–600 ms before written instructions were presented. Subjects had to report their perception of the target stimuli, i.e., if they perceived either zero, one single or two temporally separate stimuli. If subjects did not respond within 2 seconds or responded before the presentation of the instructions, a warning was presented visually and the trial was repeated at the end of the block. Responses were given by button press with the index, middle and ring finger of the right hand. Button configurations for reporting one or two stimuli were randomized from trial to trial between the right index and middle finger. The perception of zero stimuli was always reported by a button press with the right ring finger. No further feedback was given.

Prior to each experiment, we presented to each subject suprathreshold target stimuli (without subliminal stimuli) with varying stimulus onset asynchronies (SOA). This way, we determined in a staircase procedure the individual SOA for which the respective subject perceived stimulation with two suprathreshold electrical stimuli as two separate stimuli in 50% of all trials and as one stimulus in the other 50% of trials (subsequently labeled intermediate SOA;  $31.9 \pm 15.7$  ms; average difference  $8.2 \pm 15.1$  ms (mean  $\pm$  SD) across blocks). In the following main experiment, subjects were stimulated with two target stimuli separated by this intermediate SOA in 300 trials. In addition, subjects were stimulated with two target stimuli separated by an SOA with  $\pm 50\%$  length of the intermediate SOA in 90 trials, respectively. Furthermore, trials with a predetermined SOA of 0 ms (i.e., only one stimulus was presented) and trials with long SOA (+120% intermediate SOA length) were presented in 60 trials, respectively. Finally, in on average 60 trials no target stimuli were presented. This condition served as a control condition (subsequently labeled subliminal control) to guarantee that the subjects did not perceive the subliminal stimulation. In summary, subjects received 660 trials presented in randomized order.

The experiment consisted of two identical blocks. Each block began with the staircase procedure in order to determine the individual intermediate SOA, followed by the main experiment containing 660 trials as described above. After 200 trials, subjects had the possibility to take self-paced breaks. In addition, subjects were offered a break between the two blocks. Each block had a duration of ~20 min.

Stimulus presentation was controlled by means of Presentation software (Neurobehavioral Systems, Albany, NY, USA). Before beginning the experiment, each subject received instructions of the experimental task but remained naïve to the purpose of the experiment.

**Analysis.** Behavioral data were first analyzed with regard to perceptual response rates (i.e., perceived zero, one or two stimuli) for each condition (subliminal control, 0 ms SOA, intermediate SOA,  $\pm 50\%$  intermediate SOA, and 120% intermediate SOA), pooled across all time lags between subliminal and target stimuli. Perceptual response rates were averaged across both blocks and across subjects and compared across conditions by means of a repeated measures ANOVA and post-hoc paired t-tests. For the analysis of perceptual response rates as a function of the time lag between subliminal stimulation and the first target stimulus, only trials with intermediate SOA were analyzed. All other conditions (subliminal control, 0 ms SOA,  $\pm 50\%$  intermediate SOA, and 120% intermediate SOA,) served only as control conditions and/or to mask the main condition in order to minimize learning effects or perceptual biases. Subliminal control trials (i.e., trials in which only the subliminal stimulus was presented, without target stimuli) were used as a control condition to guarantee that subjects did not perceive the subliminal stimulation. Blocks in which subjects reported to perceive  $>10\%$  of subliminal control trials were discarded from further analysis (6 blocks rejected). Blocks in which response rates showed bottom or ceiling effects (mean perception of either “1” or “2” in two or more adjacent time lags in trials with intermediate SOA) were discarded from analysis, because these bottom or ceiling effects would have affected the spectral decomposition (6 blocks rejected).

For all trials with intermediate SOA, we computed for each block mean response rates for each subject as a function of time lag between subliminal and target stimuli. To this end, individual mean response rates were computed for each 20 ms shift of the subliminal stimulus relative to the target stimuli (i.e., subliminal stimulus presented 600 ms vs. 580 ms vs. 560 ms ... vs. 20 ms before the first target stimulus), resulting in a temporal resolution of 20 ms (i.e., 50 Hz, resulting in a Nyquist frequency of 25 Hz). To investigate potential periodic relationships between perceptual response rates and the time lag between subliminal stimulation and the first target stimulus, we computed a Fourier transformation on the perceptual response rates within each block. Perceptual reports were zero padded (1000 ms trial length) and multiplied with a single Hanning taper before Fourier transformation. Spectral analysis was performed for frequencies between 1 and 24 Hz (i.e., below the Nyquist frequency) in steps of 1 Hz. Subsequently, we averaged for each subject the results of the two Fourier transformations (one per block).

Statistical analysis of the spectral amplitudes was performed using a nonparametric randomization approach<sup>32</sup>. The null hypothesis states that perceptual reports are independent of the time lag between subliminal stimulation and target stimuli. Since regarding to the null hypothesis, there is no periodicity or other temporal structure in the perceptual performance, time points are exchangeable. Thus, we randomly exchanged time points 1000 times to generate a randomization distribution against which observed data were compared<sup>16</sup>. These randomizations were performed for each subject individually (i.e., for each subject and for each block separately). For each randomization, we performed the same analysis as for the observed data as described above. This procedure resulted in 1000 spectra for each subject and block, which constituted the null distribution per subject and block. Then, we combined per subject the null distributions of the two blocks to achieve one null distribution per subject for further analysis. Next, we statistically tested for each frequency independently the observed data against the null distribution across subjects by means of a nonparametric permutation approach<sup>16,32</sup>. First, we took the median of the null distribution and computed t-values between observed data and the median value by means of an independent t-test. This approach resulted in t-values (not corrected for multiple comparisons) for each frequency. Secondly, we applied a non-parametric cluster-based permutation approach to correct for multiple comparisons<sup>32</sup>. To this end, we thresholded the t-values at  $t = 1.96$  ( $p < 0.05$ ). This resulted in clusters of adjacent frequencies. Cluster-level test statistics were calculated by taking the sum of the t-values within a cluster. Next, we computed a cluster-level null distribution by re-computing the frequency t-maps after randomly permuting the data (under the null hypothesis of no difference, and thus exchangeability, between observed data and shuffled data). This process of random permutation was repeated 1000 times. For each repetition, we re-computed the cluster-level statistics as described above, which served as the cluster-level null distribution. The proportion of elements in the null distribution exceeding the observed cluster-level test statistic was used to estimate a p-value for each cluster. This statistical approach effectively controls for multiple comparisons across time points and channels (see ref. 32 for a detailed discussion on cluster-based nonparametric tests) and has been used for statistical control of similar behavioral data (e.g., refs 16, 17). This analysis corresponds to a random effects analysis<sup>16</sup>.

Analysis of phase was based on the complex output of the Fourier transformation of the perceptual response rates per block. Fourier transformation parameters were equal to the spectral analysis (see above). For each block of each subject, phase angles were computed for each frequency (1–24 Hz), then normalized by their amplitude and averaged over blocks. For each subject, we determined the frequency showing the highest amplitude within the beta-band range (13–24 Hz) based on the across-block averaged Fourier transformations. Average phase angles for this individual frequency were selected for each subject, respectively, and statistically compared against a uniform distribution by means of a Rayleigh test.

We also computed phase consistency across subjects for all frequencies (i.e., without a-priori selection of the individual frequency). To this end, we computed the complex output of the fast Fourier transformation (FFT) of the perceptual response rates per block (see Material and Methods for parameters of the FFT above). For each block of each subject, phase angles were computed for each frequency (1–24 Hz), then normalized by their amplitude and averaged over blocks. Finally, we averaged the phase angles per frequency across subjects.

All data analysis was performed using Matlab (Mathworks inc., Natick, MA, USA) and the FieldTrip toolbox<sup>33</sup> (www.fieldtriptoolbox.org). Circular data analysis was performed using the CircStat toolbox<sup>34</sup>.

## References

1. Stroud, J. M. In *Information theory in psychology: problems and methods* (Free Press, New York, NY, US), pp. 174–207 (1956).
2. Harter, M. R. Excitability cycles and cortical scanning: A review of two hypotheses of central intermittency in perception. *Psychol Bull.* **68**, 47–58 (1967).
3. VanRullen, R. & Koch, C. Is perception discrete or continuous? *Trends Cogn Sci.* **7**, 207–213 (2003).
4. VanRullen, R. Perceptual Cycles. *Trends Cogn Sci.* **20**, 723–735 (2016).
5. von Baer, K. E. In *Aus baltischer Geistesarbeit. Reden und Aufsätze*. Vol. 1, edited by Alexander, Keyserling (Jonck and Poliewsky, Riga, 1908).
6. Bergson, H. *Creative evolution* (Henry Holt, New York, NY, US, 1911).
7. Busch, N. A. & VanRullen, R. Spontaneous EEG oscillations reveal periodic sampling of visual attention. *Proc Natl Acad Sci USA* **107**, 16048–16053 (2010).
8. Chakravarthi, R. & VanRullen, R. Conscious updating is a rhythmic process. *Proc Natl Acad Sci USA* **109**, 10599–10604 (2012).
9. Baumgarten, T. J., Schnitzler, A. & Lange, J. Beta oscillations define discrete perceptual cycles in the somatosensory domain. *Proc Natl Acad Sci USA* **112**, 12187–12192 (2015).
10. Cecere, R., Rees, G. & Romei, V. Individual differences in alpha frequency drive crossmodal illusory perception. *Curr Biol.* **25**, 231–235 (2015).
11. Gundlach, C., Müller, M. M., Nierhaus, T., Villringer, A. & Sehm, B. Phasic modulation of human somatosensory perception by transcranially applied oscillating currents. *Brain Stimul.* (2016).
12. Holcombe, A. O., Clifford, C. W., Eagleman, D. M. & Pakarian, P. Illusory motion reversal in tune with motion detectors. *Trends Cogn Sci.* **9**, 559–560 (2005).
13. Kline, K. A. & Eagleman, D. M. Evidence against the temporal subsampling account of illusory motion reversal. *J Vis.* **8**, 13 (2008).
14. Dehaene, S., Changeux, J.-P., Naccache, L., Sackur, J. & Sergent, C. Conscious, preconscious, and subliminal processing: a testable taxonomy. *Trends Cogn Sci.* **10**, 204–211 (2006).
15. Weisz, N. *et al.* Prestimulus oscillatory power and connectivity patterns predispose conscious somatosensory perception. *Proc Natl Acad Sci USA* **111**, E417–E425 (2014).
16. Landau, A. N. & Fries, P. Attention samples stimuli rhythmically. *Curr Biol.* **22**, 1000–1004 (2012).
17. Landau, A. N., Schreyer, H. M., van Pelt, S. & Fries, P. Distributed attention is implemented through theta-rhythmic gamma modulation. *Curr Biol.* **25**, 2332–2337 (2015).
18. Ress, D. & Heeger, D. J. Neuronal correlates of perception in early visual cortex. *Nat Neurosci.* **6**, 414–420 (2003).
19. Nierhaus, T. *et al.* Imperceptible somatosensory stimulation alters sensorimotor background rhythm and connectivity. *J Neurosci.* **35**, 5917–5925 (2015).
20. Palva, S., Linkenkaer-Hansen, K., Näätänen, R. & Palva, J. M. Early neural correlates of conscious somatosensory perception. *J Neurosci.* **25**, 5248–5258 (2005).
21. Blankenburg, F. *et al.* Imperceptible stimuli and sensory processing impediment. *Science* **299**, 1864 (2003).
22. Bauer, F., Cheadle, S. W., Parton, A., Müller, H. J. & Usher, M. Gamma flicker triggers attentional selection without awareness. *Proc Natl Acad Sci USA* **106**, 1666–1671 (2009).
23. Diederich, A., Schomburg, A., Colonius, H. & Hamed, S. B. Saccadic reaction times to audiovisual stimuli show effects of oscillatory phase reset. *PLoS One* **7**, e44910 (2012).
24. Drewe, J., Zhu, W., Wutz, A. & Melcher, D. Dense sampling reveals behavioral oscillations in rapid visual categorization. *Sci Rep.* **5**, 16290 (2015).
25. Lakatos, P., Karmos, G., Mehta, A. D., Ulbert, I. & Schroeder, C. E. Entrainment of neuronal oscillations as a mechanism of attentional selection. *Science* **320**, 110–113 (2008).
26. Romei, V., Gross, J. & Thut, G. Sounds reset rhythms of visual cortex and corresponding human visual perception. *Curr Biol.* **22**, 807–813 (2012).
27. Fiebelkorn, I. C., Saalman, Y. B. & Kastner, S. Rhythmic sampling within and between objects despite sustained attention at a cued location. *Curr Biol.* **23**, 10.1016/j.cub.2013.10.063 (2013).
28. Mercier, M. R. *et al.* Neuro-oscillatory phase alignment drives speeded multisensory response times: an electro-corticographic investigation. *J Neurosci.* **35**, 8546–8557 (2015).
29. Baumgarten, T. J., Schnitzler, A. & Lange, J. Prestimulus alpha power influences tactile temporal perceptual discrimination and confidence in decisions. *Cereb Cor.* **26**, 891–903 (2016).
30. Salmelin, R. & Hari, R. Spatiotemporal characteristics of sensorimotor neuromagnetic rhythms related to thumb movement. *Neuroscience* **60**, 537–550 (1994).
31. Salenius, S., Portin, K., Kajola, M., Salmelin, R. & Hari, R. Cortical control of human motoneuron firing during isometric contraction. *J Neurophysiol* **77**, 3401–3405 (1997).
32. Maris, E. & Oostenveld, R. Nonparametric statistical testing of EEG- and MEG-data. *J Neurosci Methods.* **164**, 177–190 (2007).
33. Oostenveld, R., Fries, P., Maris, E. & Schoffelen, J.-M. FieldTrip: Open source software for advanced analysis of MEG, EEG, and invasive electrophysiological data. *Comput Intell Neurosci* **2011**, 156869 (2010).
34. Berens, P. CircStat: A MATLAB toolbox for circular statistics. *J Stat Softw.* **31**, 1–21 (2009).

## Acknowledgements

This work was supported by the German Research Foundation (Grant LA 2400/4-1 to J.L. and SFB 974, B07 to T.J.B.).

## Author Contributions

Designed Research: J.L.; Performed research: T.J.B., S.K., J.L.; Analyzed and interpreted data: T.J.B., J.L.; Wrote article: T.J.B., A.S., J.L.

## Additional Information

**Supplementary information** accompanies this paper at <http://www.nature.com/srep>

**Competing Interests:** The authors declare no competing financial interests.

**How to cite this article:** Baumgarten, T. J. *et al.* Subliminal stimuli modulate somatosensory perception rhythmically and provide evidence for discrete perception. *Sci. Rep.* **7**, 43937; doi: 10.1038/srep43937 (2017).

**Publisher's note:** Springer Nature remains neutral with regard to jurisdictional claims in published maps and institutional affiliations.



This work is licensed under a Creative Commons Attribution 4.0 International License. The images or other third party material in this article are included in the article's Creative Commons license, unless indicated otherwise in the credit line; if the material is not included under the Creative Commons license, users will need to obtain permission from the license holder to reproduce the material. To view a copy of this license, visit <http://creativecommons.org/licenses/by/4.0/>

© The Author(s) 2017

- 6) Baumgarten, T. J., Schnitzler, A., & **Lange, J.** (2017b).  
Beyond the Peak–Tactile Temporal Discrimination Does Not Correlate with Individual  
Peak Frequencies in Somatosensory Cortex.  
*Frontiers in Psychology*, 8, 421. <https://doi.org/10.3389/fpsyg.2017.00421>  
Impact factor (2017): 2.089



# Beyond the Peak – Tactile Temporal Discrimination Does Not Correlate with Individual Peak Frequencies in Somatosensory Cortex

Thomas J. Baumgarten, Alfons Schnitzler and Joachim Lange\*

*Institute of Clinical Neuroscience and Medical Psychology, Medical Faculty, University of Düsseldorf, Düsseldorf, Germany*

## OPEN ACCESS

### Edited by:

W. Pieter Medendorp,  
Radboud University Nijmegen,  
Netherlands

### Reviewed by:

Saskia Haegens,  
Columbia University, USA  
Niko Busch,  
Westfälische Wilhelms-Universität  
Münster, Germany

### \*Correspondence:

Joachim Lange  
joachim.lange@med.uni-  
duesseldorf.de

### Specialty section:

This article was submitted to  
Perception Science,  
a section of the journal  
Frontiers in Psychology

**Received:** 25 August 2016

**Accepted:** 06 March 2017

**Published:** 22 March 2017

### Citation:

Baumgarten TJ, Schnitzler A and  
Lange J (2017) Beyond the Peak –  
Tactile Temporal Discrimination Does  
Not Correlate with Individual Peak  
Frequencies in Somatosensory  
Cortex. *Front. Psychol.* 8:421.  
doi: 10.3389/fpsyg.2017.00421

The human sensory systems constantly receive input from different stimuli. Whether these stimuli are integrated into a coherent percept or segregated and perceived as separate events, is critically determined by the temporal distance of the stimuli. This temporal distance has prompted the concept of temporal integration windows or perceptual cycles. Although this concept has gained considerable support, the neuronal correlates are still discussed. Studies suggested that neuronal oscillations might provide a neuronal basis for such perceptual cycles, i.e., the cycle lengths of alpha oscillations in visual cortex and beta oscillations in somatosensory cortex might determine the length of perceptual cycles. Specifically, recent studies reported that the peak frequency (the frequency with the highest spectral power) of alpha oscillations in visual cortex correlates with subjects' ability to discriminate two visual stimuli. In the present study, we investigated whether peak frequencies in somatosensory cortex might serve as the correlate of perceptual cycles in tactile discrimination. Despite several different approaches, we were unable to find a significant correlation between individual peak frequencies in the alpha- and beta-band and individual discrimination abilities. In addition, analysis of Bayes factor provided evidence that peak frequencies and discrimination thresholds are unrelated. The results suggest that perceptual cycles in the somatosensory domain are not necessarily to be found in the peak frequency, but in other frequencies. We argue that studies based solely on analysis of peak frequencies might thus miss relevant information.

**Keywords:** beta, alpha, MEG, oscillations, perceptual cycles, temporal integration

## INTRODUCTION

The human sensory system is constantly excited by numerous stimuli originating from multiple sources. These stimuli often impinge on the sensory system within short time delays. Depending on the particular stimuli or situation, the sensory system needs to either integrate these stimuli into a temporally coherent percept or segregate these stimuli and treat them as temporally separate stimuli. Whether stimuli are perceived as temporally coherent or separated depends – among other factors – to a great part on the temporal distance between the stimuli. The role of temporal distance for perceptual integration has prompted the idea of 'temporal integration windows,' 'perceptual cycles,' or 'perceptual moments' (von Baer, 1908; Harter, 1967; VanRullen and Koch, 2003; VanRullen et al., 2014; Baumgarten et al., 2015; Cecere et al., 2015; Wutz et al., 2016).

The concept of temporal integration windows or perceptual cycles states that the sensory system integrates input over a certain time window or cycle. Hence, stimuli falling within a certain time interval are perceptually integrated into one coherent percept. Vice versa, stimuli falling in two temporal windows are perceived as two distinct events. Although this concept is intriguing, computationally beneficial (Busch et al., 2009; Jensen et al., 2014) and has gained substantial evidence from behavioral studies (e.g., Sugita and Suzuki, 2003; Van Wassenhove et al., 2007), evidence for potential underlying neuronal mechanisms has been sparse.

One potential mechanism that has been repeatedly suggested as the neuronal concept of temporal integration windows are neuronal oscillations (VanRullen et al., 2014; Cecere et al., 2015; Landau et al., 2015). Several studies have shown that the phase of neuronal oscillations is linked to perception and behavior (Busch et al., 2009; Dugué et al., 2011; Landau et al., 2015; Gundlach et al., 2016). Phases of neuronal oscillations repeat periodically. Accordingly, several behavioral studies have shown that perception and behavior follow periodical and rhythmic patterns (Landau and Fries, 2012; Song et al., 2014; Huang et al., 2015). In addition, recent studies using EEG/MEG in humans have suggested that cycles of specific neuronal oscillations form the potential mechanism for temporal integration/segregation windows and correlate with perceptual reports. This could be shown, for example, in the visual cortex employing the wagon wheel illusion (VanRullen et al., 2006). In this paradigm, a wheel, although constantly rotating in one direction, is sometimes perceived as spontaneously reversing its direction of rotation. VanRullen et al. (2006) could show that the wagon wheel illusion correlates with cycles in the alpha (8–12 Hz) band oscillation in occipital areas. Furthermore, a study combining EEG and transcranial alternating current stimulation (tACS) provided causal evidence for alpha oscillations acting as temporal integration windows in an audio-visual illusion (Cecere et al., 2015). The study used the so-called double-flash illusion, where two auditory stimuli presented with one visual stimulus repeatedly induce the percept of a second, illusory visual stimulus if the three stimuli are presented with short temporal delays (typically < 100 ms; Shams et al., 2000). Cecere et al. (2015) showed that the individual temporal window for the audio-visual illusion correlated with the individual's peak frequency of an alpha oscillation (i.e., those frequencies with the highest spectral power within the alpha-band) in parieto-occipital areas. More importantly, they showed that non-invasively manipulating the peak frequency and thus the length of the individual alpha cycles by means of tACS correlated with an increase or decrease, respectively, of the behavioral temporal integration windows.

In addition, a recent EEG study suggested that the peak frequency of parieto-occipital alpha oscillations might also represent a mechanism for temporal discrimination of visual stimuli (Samaha and Postle, 2015). The authors presented two visual stimuli separated by a blank gap or one visual stimulus with an identical overall temporal length, with subjects asked to report if they perceived stimulation as one single stimulus or two temporally separate stimuli. The authors showed that the

individual length of the stimulus necessary for the respective subject to segregate two stimuli from one stimulus correlated with the subjects' individual alpha peak frequency derived from occipital sensors.

Although the majority of studies on perceptual cycles focus on the visual domain, recent studies investigated mechanisms of temporal discrimination in the somatosensory domain. Baumgarten et al. (2015) used two electrotactile stimuli and determined neuronal correlates of the time windows perceptually separating the two presented stimuli. The study revealed that beta (13–20 Hz) and to a lesser degree also alpha (8–12 Hz) oscillations act as temporal integration windows (or perceptual cycles) in the somatosensory domain. This finding is consistent with the higher temporal resolution of touch compared to vision and the prominent role of beta band oscillations in the somatosensory domain (Jones et al., 2010; Haegens et al., 2011). In contrast to previous studies focusing on the visual domain (Cecere et al., 2015; Samaha and Postle, 2015), however, Baumgarten et al. (2015) did not explicitly analyze peak frequencies but phase differences between all frequencies from 5 to 40 Hz. Thus, it remains unclear whether the peak frequency of neuronal oscillations in the somatosensory domain also might act as a correlate for perceptual cycles.

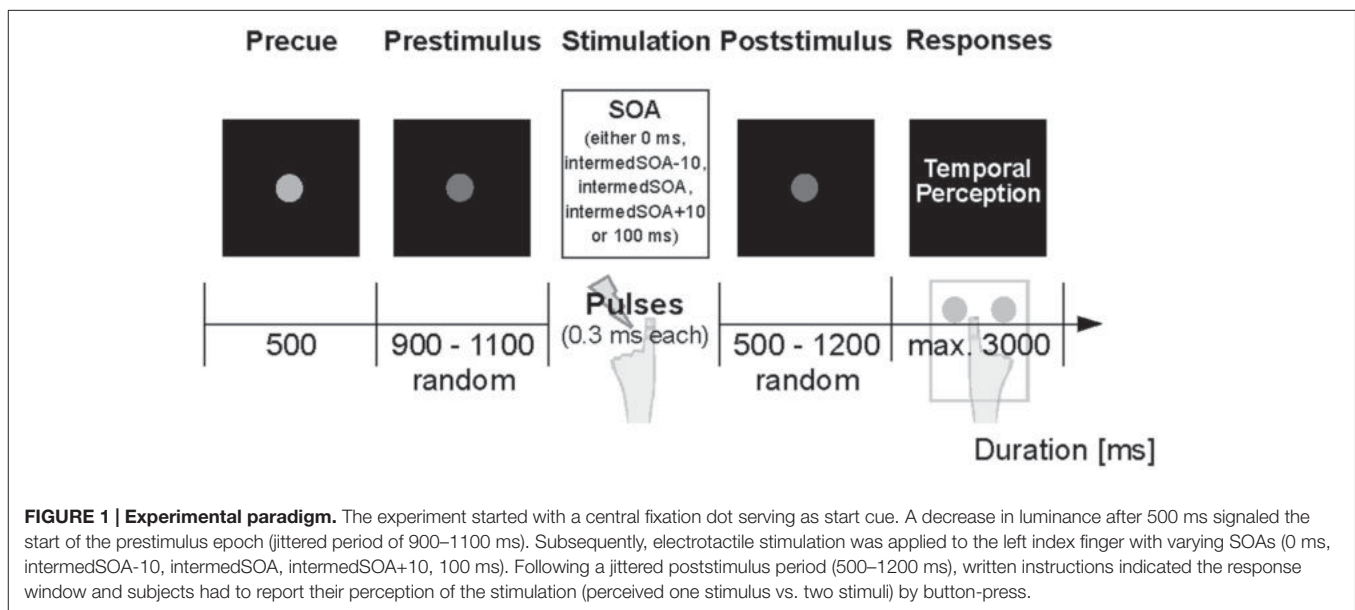
In summary, recent studies provided novel evidence for the hypothesis that neuronal oscillations represent a putative neuronal mechanism for perceptual cycles in the visual and somatosensory domain. Studies on visual (Samaha and Postle, 2015) and audio-visual (Cecere et al., 2015) tasks suggest that the peak frequency of alpha oscillations in parieto-occipital areas represents the best estimate. However, it is unknown whether similar mechanisms hold true for the somatosensory domain, i.e., whether the peak frequency of the alpha- or beta-band is the best representation of the perceptual cycles in somatosensory regions. Similar to a study focusing on the visual domain (Samaha and Postle, 2015), the present study aimed to investigate this question by investigating whether somatosensory peak frequencies correlate with perceptual discrimination thresholds in a tactile temporal discrimination task. We hypothesized to find a negative correlation between individual discrimination thresholds and individual peak frequencies. That is, shorter discrimination thresholds should correlate with higher frequencies, i.e., shorter perceptual cycles/temporal integration windows.

## MATERIALS AND METHODS

The subjects, experimental paradigm and MEG data investigated in the present study were previously reported in Baumgarten et al. (2015, 2016b). Here, we present a concise overview.

### Subjects

Sixteen right-handed volunteers [7 males, age:  $26.1 \pm 4.7$  years (mean  $\pm$  SD)] participated in the experiment after providing written informed consent in accordance with the Declaration of Helsinki and the Ethical Committee of the Medical Faculty, Heinrich Heine University Düsseldorf. Subjects reported normal



or corrected-to-normal vision and no somatosensory and/or neurological disorders.

## Experimental Paradigm

The present experimental paradigm is illustrated in **Figure 1** and described in Baumgarten et al. (2015, 2016b). Seated within the MEG, subjects were presented with electro-tactile stimulation while visual instructions were projected on the backside of a translucent screen centrally positioned in front of the subjects. Trials began with a short precue period (500 ms; **Figure 1**), followed by a jittered prestimulus period (900–1100 ms). After the prestimulus period, either one or two electrical pulses were applied to the left index finger. Pulse amplitude was determined individually in a pre-measurement and set to a level above subjective perceptual threshold, but below pain threshold [ $4.1 \pm 1.2$  mA (mean  $\pm$  SD)]. Pulses were separated by a specific stimulus onset asynchrony (SOA), which varied between 0 ms (i.e., only one pulse was presented) and 100 ms. Importantly, in the main condition subjects received pulses separated by an individually determined intermediate SOA [labeled *intermedSOA*;  $25.9 \pm 1.9$  ms (mean  $\pm$  SEM)] for which subjects reported a balanced perception of one stimulus or two stimuli (i.e., 50% of the trials were perceived as one stimulus, whereas the other 50% of the trials were perceived as two stimuli). In addition, two SOAs encompassed the *intermedSOA* by  $\pm 10$  ms (labeled *intermedSOA-10* and *intermedSOA+10*, respectively). Subsequent to stimulation, a jittered poststimulus period (500–1200 ms) was presented, after which subjects were indicated to report their respective perception (i.e., one or two stimuli) with a button press of the right hand. No feedback regarding the response was given.

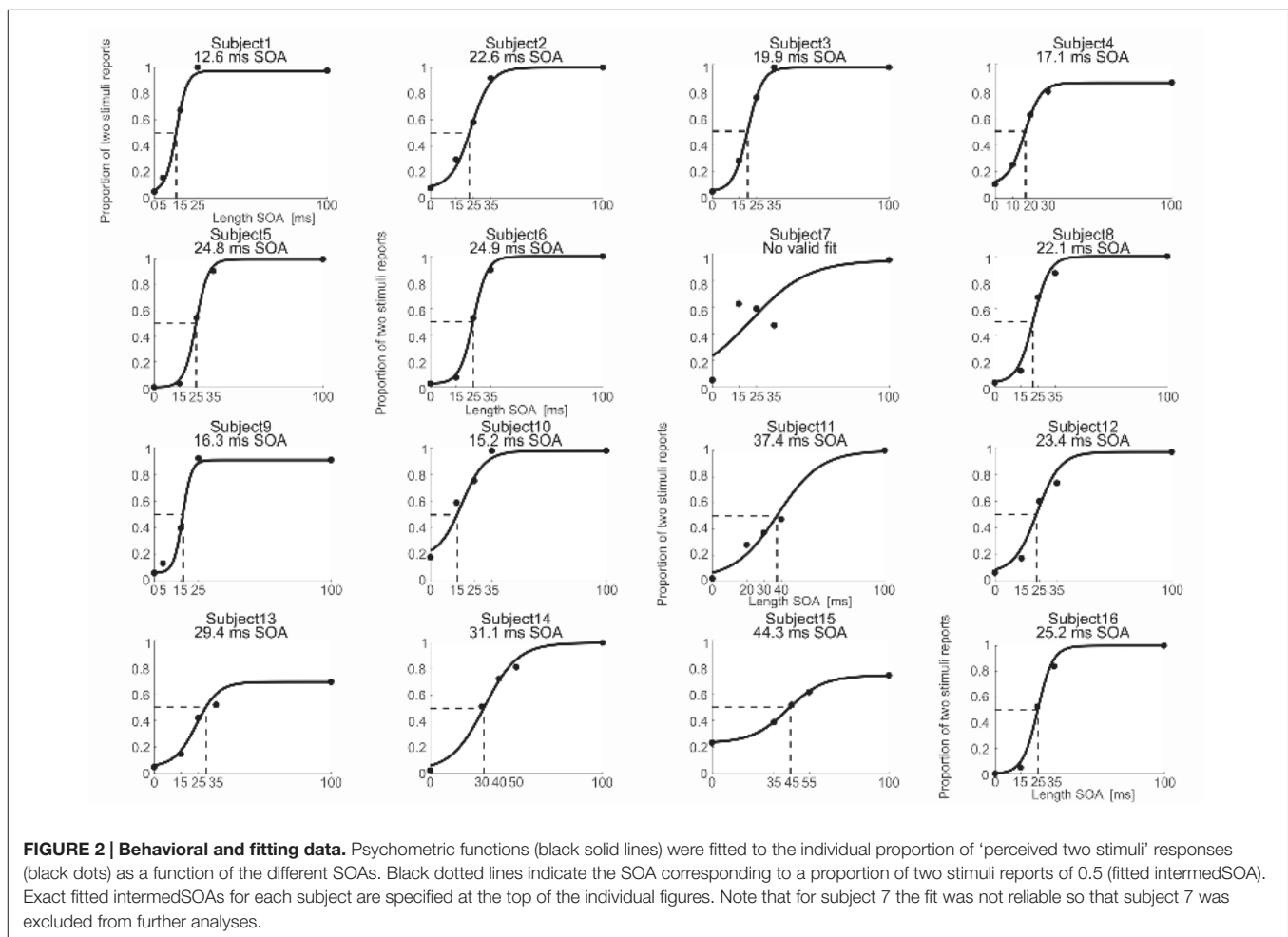
## Psychometric Fitting Function

The *intermedSOA* experimentally determined in the pre-experiment yielded naturally not an exactly equal distribution of

perceived one and two stimuli in the main experiment, but some deviations. To determine the theoretical individual thresholds for which subjects achieve an equal distribution for the perception of one vs. two stimuli (the theoretical *intermedSOA*), we fitted psychometric functions to the experimental data of the main experiment (Cecere et al., 2015; Samaha and Postle, 2015). We fitted a sigmoid function to the data using the Palamedes toolbox for Matlab (Prins and Kingdom, 2009). The different experimental SOA lengths (i.e., 0 ms SOA, *intermedSOA-10*, *intermedSOA*, *intermedSOA+10*, 100 ms) were chosen as independent variable, whereas the individual proportion of ‘perceived two stimuli’ responses at each condition was chosen as dependent variable. The fit estimated four parameters: threshold, slope, guess rate, and lapse rate. Individual guess rates were set to the proportion of two stimuli percepts when actually one stimulus was presented (SOA 0 ms) and individual lapse rates to the proportion of one stimuli percepts when actually two stimuli with an SOA of 100 ms were presented. The goodness of fit was estimated by computing the deviance and corresponding *p*-values. *p*-values  $> 0.05$  indicate a reliable fit of the experimental data. Only for one subject we found high deviance ( $p < 0.05$ ), indicating that the data could not be reliably fitted (**Figure 2**, subject 7). This subject was excluded from further analyses. From the Palamedes toolbox, we determined thresholds at which subjects showed an equal distribution of perceiving one and two stimuli (**Figure 2**) and the corresponding error of the threshold.

## MEG Data Recording and Analysis

During the task, electromagnetic brain activity was continuously recorded by means of a 306-channel, whole-head MEG system (Neuromag Elekta Oy, Helsinki, Finland). Data was recorded with a sampling rate of 1 kHz. Only gradiometer data was analyzed for the present study. Since gradiometers are ordered in pairs of sensors measuring activity in mainly orthogonal directions, we offline combined these pairs of sensors to one



sensor pair. This combination of orthogonal sensors resulted in 102 pairs of sensors. Offline analysis of the data was performed with custom-made MATLAB (Mathworks, Natick, MA, USA) scripts and the FieldTrip toolbox<sup>1</sup> (Oostenveld et al., 2010).

Continuously recorded MEG data were segmented into trials, which started with the beginning of the precue period and ended with the subject's response. Trials were visually and semi-automatically inspected for artifacts. Artifacts due to muscle activity, eye movements or technical reasons were removed semi-automatically by means of a z-score-based algorithm implemented in FieldTrip. Excessively noisy or dead channels were removed and reconstructed by an interpolation of neighboring channels. Power line noise was removed by applying a band-stop filter encompassing the 50, 100, and 150 Hz components. Furthermore, the linear trend and mean of every trial was removed from the data. Only trials with intermedSOA entered the subsequent analysis, which resulted in an average of  $145 \pm 19$  trials with intermediate SOA (mean  $\pm$  SD) after preprocessing.

We were interested in how the individual prestimulus alpha- (8–12 Hz) or beta- (14–30 Hz) band peak frequencies are related

to the individual tactile temporal resolution. Thus, subsequent analyses focused on neuronal oscillations in sensorimotor areas during the prestimulus epoch of the respective trials (i.e., before any task- or response-related components). To analyze neuronal oscillations, data epochs from  $-900$  to  $0$  ms relative to the onset of the first electro tactile stimuli were multiplied with a single hanning window, zero padded to a length of 10000 ms and fast Fourier transformed for frequencies from 5 to 40 Hz with a frequency resolution of 0.1 Hz. Gradiometer pairs were combined by summing spectral power across the two orthogonal channels, resulting in 102 channels.

In order to focus the analysis on channels representing neural activity of the somatosensory cortex, the sensors of interest (SOI) were functionally determined by means of poststimulus event-related fields (ERFs) in response to electro tactile stimulation. ERFs were computed based on trials with intermedSOA. Trials were baseline corrected by subtracting the mean of the prestimulus period immediately preceding stimulus presentation ( $-200$  to  $0$  ms). To focus on channels representing different components of activity from somatosensory cortex, we selected those time windows known to be critical for the different processing stages of somatosensory stimuli, i.e., the M50 of the ERF (known to originate mainly from S1) and M100 (known

<sup>1</sup>fieldtriptoolbox.org

to originate mainly from S2; Suk et al., 1991; Iguchi et al., 2005). Therefore, amplitude values from 0.025 to 0.075 ms (labeled M50), 0.075–0.125 ms (labeled M100), and 0.025–0.125 (labeled M50+100) were averaged over all channels. Subsequently, those channels which amplitude values surpassed the respective average across all 102 channels by at least 1 SD were determined as the sensor-space for the respective somatosensory component (Supplementary Figure S1). The resulting channels included (MEG1122+23, MEG1132+33, MEG1312+13, MEG1322+23, MEG1332+33, MEG1342+43, MEG1442+43, MEG2022+23, MEG2222+23, MEG2232+33, MEG2242+43, MEG2412+13) for the M50 component (Figure 3A), (MEG0232+33, MEG1122+23, MEG1132+33, MEG1142+43, MEG1222+23, MEG1232+33, MEG1312+13, MEG1322+23, MEG1332+33, MEG1342+43, MEG1442+43, MEG2212+13) for the M100 component and (MEG0232+33, MEG1122+23, MEG1132+33, MEG1142+43, MEG1222+23, MEG1312+13, MEG1322+23, MEG1332+33, MEG1342+43, MEG1442+43, MEG2212+13) for the M50+100 component.

Similar to the approach Samaha and Postle (2015) chose for the visual domain, we defined two approaches to determine the individual peak frequencies. For the first approach, we selected the single channel-pair within the previously predetermined SOI showing on group level maximum prestimulus (–900 to 0 ms) alpha (8–12 Hz) or beta power (14–30 Hz), respectively. The rationale of this approach was that the channel-pair showing the maximum prestimulus power should provide the best estimate of peak frequency. Since the predetermined SOI slightly differed for the M50, M100, and M50+100 components, channels showing maximum power likewise differed across the respective components. The resulting maximum power channels for the beta-band were MEG2222+23 for the M50 component (Figure 3A), MEG0232+33 for the M100 component and MEG0232+33 for the M50+100 component. The resulting maximum power channels for alpha-band were MEG2022+23 for the M50 component (Figure 3A), MEG0232+33 for the M100 component and MEG0232+33 for the M50+100 component. Then we determined individual peak frequencies in these sensors (see below).

For the second approach, we determined the individual peak frequencies (see below) in the sensor showing on individual, single-subject level maximum prestimulus alpha or beta band power, again within the previously predetermined SOI. If no valid peak frequency could be found, peak frequency was determined in the sensor showing the second highest prestimulus power levels, and so on.

In addition to Samaha and Postle (2015), we also determined peak frequencies on source level by means of a “virtual sensor” approach. Here, we will give a concise description of the computation of virtual sensor data. For a detailed description of the procedure see Baumgarten et al. (2015). The virtual sensor was functionally determined by localizing the individual sources of the M50 or M100 component. Source localization was performed by means of an LCMV beamformer on individual 3D grids with a resolution of 1 cm. The grid points with maximal M50 or M100 activity were selected as the location of the virtual sensor (Supplementary Figure S2). In addition, we anatomically

determined a virtual sensor for S1 based on the AFNI atlas implemented in FieldTrip, resulting in four neighbouring grid points (Supplementary Figure S2).

Next, we constructed spatial filters for the selected grid points. We projected single trial MEG sensor time series data through this spatial filter to obtain the time series data on source level. These time series data were then used as input to the frequency and peak detection analyses as described above. For the M50 and M100 defined virtual sensors, analysis was performed on single grid points, respectively. For the four atlas-defined virtual sensors, we performed spectral analysis separately for each sensor and then averaged spectral activity across the four grid points.

Individual alpha and beta peak frequency (IAFs and IBFs) were defined as the frequencies showing maximal power within the respective frequency band (8–12 Hz or 14–30 Hz). Peak frequencies were detected using the Matlab function `findpeaks.m`. In addition, to represent a peak, the power value of a potential peak frequency had to show an amplitude increase of at least 10% (i.e., `MinPeakProminence` was set to 10% of the amplitude of the peak). This method prevented peak frequency selection to be influenced by spontaneous power fluctuations and guaranteed that only peaks of sufficient size were selected as peak frequency.

To obtain a measure of the reliability of the peak estimate, we performed a bootstrapping approach and recomputed the peak frequency 100 times. From this distribution of peak frequencies, we computed the interquartile range (Figure 4).

We additionally determined for each subject the theoretically expected frequency based on the models of perceptual cycles (Baumgarten et al., 2015, 2017; Samaha and Postle, 2015). According to these models, the cycle length of the theoretically relevant frequency should be determined by the `intermedSOA`:

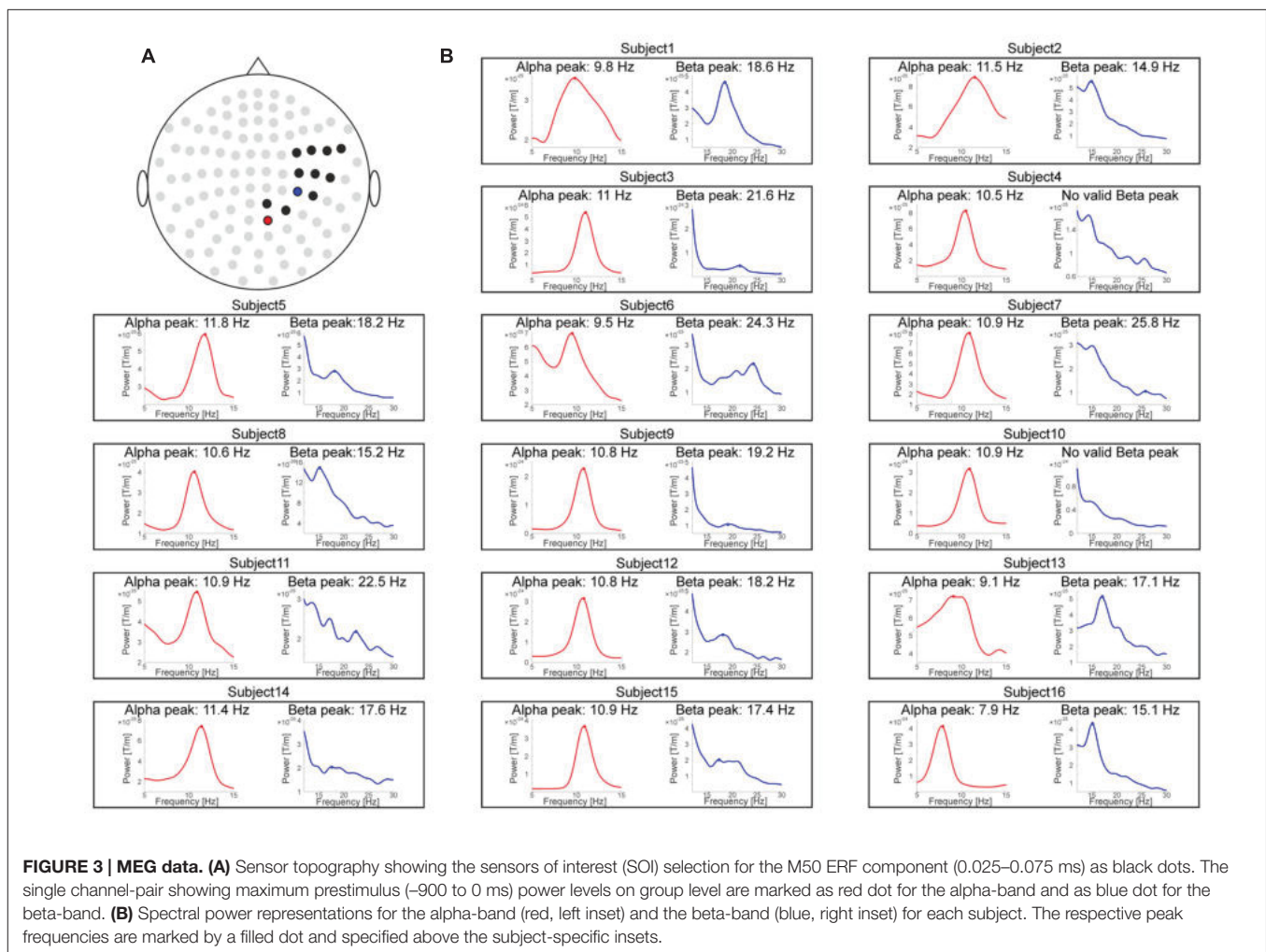
$$\text{Freq}_{\text{theoretical}} = 1000 / (2 * \text{intermedSOA})$$

Finally, to test the hypothesis whether alpha- and beta-band frequencies are related (e.g., beta-band peak frequencies might be harmonics of the alpha-band peak frequencies), we investigated whether peak frequencies in the alpha- and beta-band are correlated by applying a Pearson correlation.

## Correlation Analysis and Bayes Factor Analysis

Correlations between IAFs and IBFs and individual theoretical `intermedSOA` were assessed by means of a Pearson correlation. The correlations were performed separately for each frequency band, SOIs and approach to determine the individual frequencies (group or single subject approach on sensor level or source level approaches).

In our study, we asked whether subjects' temporal discrimination thresholds correlate with their individual peak frequencies. Using conventional inference statistics, however, it is only possible to provide evidence in favor of the H1-Hypotheses (i.e., correlation) by rejecting the H0-Hypotheses (no correlation). If the H0 cannot be rejected, this does not mean that the H0 (no correlation) is true. To test our two hypotheses of “no correlation” and “correlation” directly, we used Bayes factor (BF) analysis (Dienes, 2014; Iemi et al., 2016). In a nutshell, BF



analysis tests whether the experimental data provide stronger evidence for the H0 or H1 hypothesis. A  $BF > 1$  indicates more evidence for the H1, while  $BF < 1$  indicates more evidence for H0. However, BF-values of 1/3–3 are regarded as inconclusive and only BF-values  $> 3$  or  $< 1/3$  are regarded as providing sufficient evidence for H1 or H0. We computed the BF by forwarding the data of the correlation analysis to the BF analysis in the software JASP<sup>2</sup>.

## RESULTS

### Behavioral Data (Temporal Resolution Thresholds)

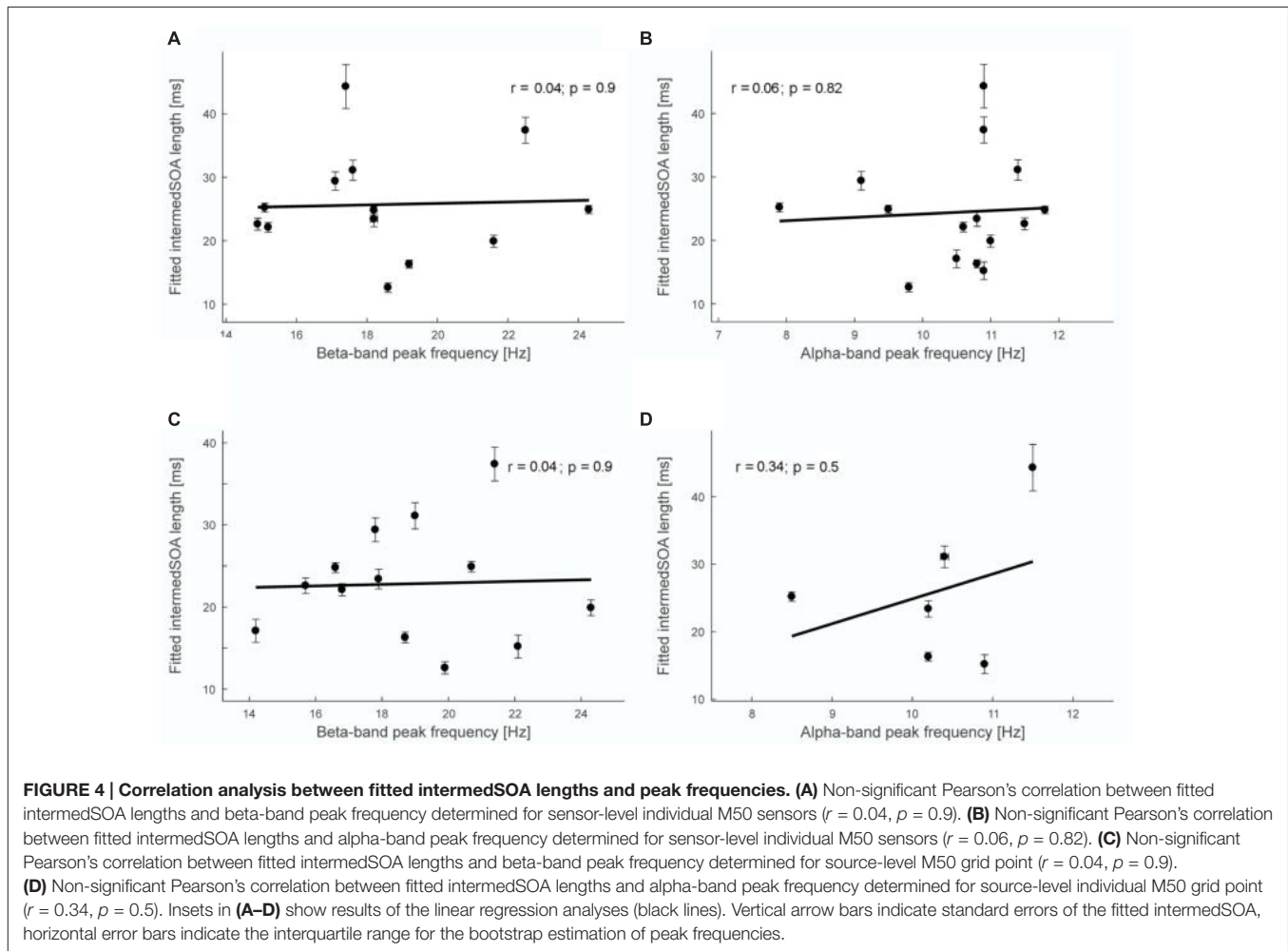
In a pre-measurement, we determined the SOA for which subjects perceived two electrocutaneous stimuli as one stimulus in 50% of the trials, whereas in the other 50% of the trials the stimulation was perceived as two stimuli (labeled *intermedSOA*; **Figure 1**). In addition, trials with 0 ms SOA, *intermedSOA*-10,

*intermedSOA*+10, 100 ms SOA were presented (see Materials and Methods for details).

On average, subjects perceived stimulation as two stimuli in  $6.8 \pm 1.5\%$  (mean  $\pm$  SEM) for trials with 0 ms SOA, in  $25.8 \pm 4.7\%$  for trials with *intermedSOA*-10, in  $58.0 \pm 3.1\%$  for trials with *intermedSOA*, in  $79.4 \pm 4.5\%$  for trials with *intermedSOA*+10 and in  $94.3 \pm 2.4\%$  for trials with 100 ms SOA.

Since in the main MEG experiment the *intermedSOA* did not yield a perfect equal distribution of “one” and “two” percepts, we fitted psychometric functions to the individual experimental data and computed the time point for which subjects theoretically perceived two successively presented stimuli as two stimuli in 50% of the trials and as one stimulus in 50% of the trials (**Figure 2**). The fitting procedure provided reliable fits for 15 out of the 16 subjects. The one subject showing a too high deviance ( $p < 0.05$ ) and thus an unreliable fit was excluded from further analyses (subject 7, see **Figure 2**). The average *intermedSOA* across the 15 remaining subjects determined by the fitting procedure was  $24.4 \pm 2.2$  ms (mean  $\pm$  SEM; range 13–44 ms). We used these individual theoretically determined *intermedSOA* for the subsequent correlation analyses (see Correlations between *IntermedSOAs* and Peak Frequency and Bayes Factor Analyses).

<sup>2</sup><https://jasp-stats.org>, version 0.8.0.1



## MEG Data (Peak Frequencies)

Individual alpha (8–12 Hz) and beta-band (14–30 Hz) peak frequencies were determined on sensor and on source level. On sensor level, we defined three functionally defined somatosensory SOI: M50, M100, M50+100 (see Materials and Methods for SOI definition and **Figure 3A** and Supplementary Figure S1 for illustration of the M50 SOI), in order to cover a wide range of potentially relevant sensors. We employed two different approaches for channel selection [i.e., group level analysis vs. single subject analysis (Samaha and Postle, 2015); see Materials and Methods for details].

For the single-subject analysis, valid beta-band peak frequencies could be determined in 13 out of the remaining 15 subjects for the M50 SOI and in all subjects in the M100 and M50+100 SOI. The average beta-band peak frequency was  $18.5 \pm 0.7$  Hz (mean  $\pm$  SEM) for the M50 SOI (see **Figure 3B** for individual spectra),  $19.1 \pm 0.8$  Hz for the M100 channel selection and  $19.1 \pm 0.8$  Hz for the M50+100 SOI. Valid alpha peak frequencies could be determined in all subjects for the M50, M100, and M50+100 SOI. The average alpha-band peak frequency was  $10.5 \pm 0.3$  Hz for the M50 SOI and  $10.3 \pm 0.2$  Hz for the M100 and M50+100 SOI.

Visual inspection of the spectra confirmed the results of the automatic peak detection procedure for all reported peaks. In one case [M50 SOI, single-subject analysis of the beta-band (**Figure 3B**)], visual inspection might suggest an additional broad peak in one subject which was not detected by the automatic procedure. Including this subject based on peak definition by visual inspection, however, had only a negligible quantitative (absolute  $r$ -values became slightly smaller) and no qualitative effect on the correlation analysis. We will report the correlation analysis, however, only for the results of the objective peak detection procedure, thus excluding this single subject/peak from the respective correlation analysis.

For the group level analysis, valid beta-band peak frequencies could be determined in 9 out of 15 subjects for the M50 SOI and in 9 out of 15 subjects in the M100 and M50+100 SOI. The average beta-band peak frequency was  $18.2 \pm 0.6$  Hz (mean  $\pm$  SEM) for the M50 SOI and  $18.6 \pm 0.6$  Hz for the M100 and M50+100 SOI. Valid alpha peak frequencies could be determined in all 15 subjects for the M50, M100, and M50+100 SOI. The average alpha-band peak frequency was  $10.7 \pm 0.2$  Hz for the M50 SOI and  $10.3 \pm 0.2$  Hz for the M100 and M50+100 SOI.

On source level, we defined regions of interest either based on the source localization of the M50 and M100 components or based on the AFNI atlas (see Materials and Methods for details).

Valid beta-band peak frequencies could be determined in 13 out of 15 subjects in the region defined by the M50 component, in 14 out of 15 subjects in the region defined by the M100 component and in 13 out of 15 subjects in the atlas-defined region. The average beta-band peak frequency was  $18.9 \pm 0.7$  Hz (mean  $\pm$  SEM) for the M50-defined region,  $19.2 \pm 0.9$  Hz for the M100-defined region and  $18.5 \pm 0.7$  for the atlas-defined region.

Valid alpha-band peak frequencies could be determined in 6 out of 15 subjects in each of the three regions. The average alpha-band peak frequency was  $10.3 \pm 0.3$  Hz (mean  $\pm$  SEM) for the M50-defined region,  $10.9 \pm 0.3$  Hz for the M100-defined region and  $10.1 \pm 0.05$  Hz for the atlas-defined region.

To test whether alpha- and beta-band peak frequencies are related (e.g., beta-peak frequencies being harmonics of the alpha-band peak frequencies), we performed a correlation analysis. None of the nine correlation analyses revealed a significant correlation between alpha- and beta-band frequencies ( $r < 0.27$ ;  $p > 0.30$ ).

## Correlations between IntermedSOAs and Peak Frequency and Bayes Factor Analyses

To determine any potential relationship between the temporal resolution of somatosensory perception and the alpha- or beta-band peak frequencies, we performed a correlation analysis between individual intermedSOAs from the fitting procedure [see Behavioral Data (Temporal Resolution Thresholds) and **Figure 2**] and the respective individual peak frequencies [MEG Data (Peak Frequencies) and **Figure 3B**].

**Figure 4** shows exemplary results for the correlation analyses. For the single subject analysis, no significant correlations were found on sensor level (M50 SOI) between intermedSOA and neither beta-band nor alpha-band peak frequencies (beta:  $r = 0.04$ ,  $p = 0.90$ ; alpha:  $r = 0.06$ ,  $p = 0.82$ ; **Figures 4A,B**). In addition, no significant correlations between intermedSOA and beta- or alpha-band peak frequencies were found on source level (M50 defined grid point; beta:  $r = 0.04$ ,  $p = 0.90$ ; alpha:  $r = 0.34$ ,  $p = 0.5$ ). The results of all correlation analyses are provided in detail in **Table 1**. In summary, none of the correlations revealed a significant correlation between intermedSOAs and peak frequencies.  $r$ -values varied between  $-0.19$  and  $0.35$  ( $p > 0.22$ ) for the beta-band and between  $-0.14$  and  $0.34$  ( $p > 0.5$ ) for the alpha-band, with  $r$ -values for the correlations on source level all being positive.

**Table 1** also provides the results of BF analysis. In summary, the BF analysis revealed that for all correlations BF-values were  $< 1$ , thus providing stronger evidence for the H0 hypothesis (i.e., there is no correlation) than for the H1 (i.e., there is a correlation). For the beta-band on sensor level, 2 out of 6 analyses provided strong evidence in favor of the H0 (BF  $< 1/3$ ), while on source level, all three analyses provided strong evidence for the H0 (BF  $< 1/3$ , i.e., no correlation). For the alpha-band on sensor-level, 5 out of 6 analyses provided strong evidence for the H0,

while on source level for one analysis BF was  $< 1/3$  while the other two BF-values were still  $\leq 0.42$  (note that on source level alpha peaks could be detected only for a small number of subjects).

Finally, to test whether experimentally and theoretically determined frequencies (see Materials and Methods and arrows in Supplementary Figure S3) are related to each other, we performed a correlation analysis. None of the correlations revealed a significant correlation ( $r < 0.27$ ;  $p > 0.31$ ).

## DISCUSSION

It has long been debated whether perception is organized as a continuous process or in discrete perceptual cycles (or temporal integration windows), where two stimuli falling within one cycle are perceptually integrated to one stimulus and two stimuli falling in two separate cycles are perceived as two separate stimuli (von Baer, 1908; Harter, 1967; Allport, 1968; VanRullen and Koch, 2003). Recent studies have suggested that the peak frequency (i.e., the frequency with the maximal power) of alpha-band (8–12 Hz) oscillations in parieto-occipital areas serves as the neuronal correlate of such perceptual cycles in the (audio-) visual domain (Cecere et al., 2015; Samaha and Postle, 2015). Here, we studied in a tactile temporal discrimination task whether peak frequencies might likewise serve as a correlate for perceptual cycles in the somatosensory domain. However, we were unable to demonstrate a significant correlation between subjects' individual peak frequencies and their perceptual temporal discrimination thresholds. This lack of correlation was true for the alpha- (8–12 Hz) and the beta- (14–30 Hz) band over several regions of interest in the somatosensory cortex on sensor level as well as on source level. Since from a lack of significant correlation it does not necessarily follow that the null hypothesis (i.e., there is actually no correlation) is true, we additionally performed an analysis of BF. The BF analysis revealed that for all tested correlations evidence was stronger in favor of the H0 (no correlation) compared to the H1 (correlation) as indicated in BF-values  $< 1$ . Importantly, most of the BF provided strong evidence for the H0 (BF-values  $< 1/3$ ), especially those on source level.

We have performed our peak frequency detections on sensor and on source level. The reason to perform the analysis on sensor level was to keep the analyses as close as possible to previous studies which have performed their analyses on sensor level as well (Samaha and Postle, 2015; Cecere et al., 2015). This way, we ought to ensure that methodological approaches are similar, facilitating the comparability across studies. A disadvantage of the analysis on sensor level is the problem of spatial smearing. That is, sensors do not only measure activity from the region directly below them, but easily can pick up activity from more distant areas. For example, sensors over somatosensory areas might not only measure somatosensory alpha activity but also pick up alpha activity from parieto-occipital regions. Such activity might potentially deteriorate the analysis. Our source level analyses support this concern. While we found clear alpha peaks for all subjects on sensor level, only a minority of subjects showed alpha peaks on source level. These different results for sensor and source level analyses suggest that sensor and source data contain

TABLE 1 | Summary of the correlation analyses.

Frequency band of interest	Analysis on sensor or source level	Approach to define sensors of interest	No. subjects showing valid peak frequencies	r-value	p-value	Bayes-factor
Alpha	Sensor	Individual M50	15	0.06	0.82	0.27*
	Sensor	Individual M100	15	0.08	0.77	0.26*
	Sensor	Individual M150	15	0.08	0.77	0.26*
	Sensor	Group M50	15	-0.14	0.61	0.49
	Sensor	Group M100	15	0.15	0.58	0.22*
	Sensor	Group M150	15	0.15	0.58	0.22*
	Source	M50	6	0.34	0.50	0.33*
	Source	M100	6	0.33	0.52	0.34
	Source	Atlas	6	0.14	0.80	0.42
Beta	Sensor	Individual M50	13	0.04	0.90	0.31*
	Sensor	Individual M100	15	-0.19	0.50	0.58
	Sensor	Individual M150	15	-0.19	0.50	0.58
	Sensor	Group M50	9	0.26	0.50	0.27*
	Sensor	Group M100	9	0.02	0.96	0.39
	Sensor	Group M150	9	0.02	0.96	0.39
	Source	M50	13	0.04	0.90	0.31*
	Source	M100	14	0.35	0.22	0.17*
	Source	Atlas	12	0.19	0.55	0.24*

Peak frequencies were determined separately for the alpha- and beta-band (column 1) on either source or sensor level (column 2). The regions of interest in which peak frequencies were determined, were based on different approaches (column 3, see Materials and Methods for details). Column 4 shows for how many subjects peak frequencies could be determined. Results of the correlation analysis (r- and p-values are presented in columns 5 and 6. Finally column 7 shows the result of the Bayes factor analyses for each correlation. \*Indicates strong evidence in favour of the null hypothesis of no correlation (i.e.,  $BF < 1/3$ ).

different signals with sensor level analysis being more prone to potential parieto-occipital alpha-band activity. Thus, we believe that while sensor level analyses ensure better comparability to previous studies, source level analyses are closer related to the actual somatosensory neuronal activity. Importantly, the correlation and BF analyses on source level demonstrated stronger evidence in favor of the H0 of no correlation ( $BF < 0.31$  for all beta-band analyses;  $BF < 0.42$  for all data analyses, please note the overall low number of subjects for alpha-band analyses), while the sensor level provided evidence for H0 but BF values were mostly in the “inconclusive” range ( $1/3 < BF < 3$ ).

Importantly, it should be noted that this non-significant result does not imply that in the somatosensory system perceptual cycles do not exist. Rather, a previous study has shown that the phase of neuronal oscillations in the primary somatosensory cortex in the alpha-/beta- (8–20 Hz) band correlates with subjects’ perception, in line with the idea of perceptual cycles in the somatosensory domain (Baumgarten et al., 2015). Thus, while there is evidence for perceptual cycles, the present results state that the carrying frequency of the perceptual cycles in somatosensory areas is not necessarily equivalent to the peak frequency of a frequency band.

On the other hand, studies in the visual domain reported a significant correlation between alpha peak frequencies and perception or discrimination performance (Cecere et al., 2015; Samaha and Postle, 2015). This raises the question where these discrepancies between results in the visual and somatosensory domain originate from? One reason might be found in methodological differences between studies or in inapt parameters for the analyses. For example, too low statistical power due to a low number of subjects might account for a

non-significant result. Our hypothesis was to find a negative correlation of individual perceptual thresholds and individual peak frequencies. That is, shorter thresholds should result in higher frequencies, i.e., shorter cycles. While we found a small, but non-significant negative correlation in a few correlations, it is unlikely that the correlation becomes significant with a higher number of subjects. This is mainly due to the reason that BF values provided stronger evidence for the null hypothesis of no correlation. While for a few regions of interest in which we analyzed spectral activity, BF-values are strictly speaking inconclusive ( $1/3 < BF < 3$ ), other regions of interest show strong evidence in favor of the “no correlation” hypothesis. This is mostly evident for the correlation analyses on source level. As discussed above, we argue that source level analyses of peak frequencies should be more reliable than sensor level analyses. In addition, subjects showed a rather high variability with no obvious and consistent relationship between perceptual thresholds and individual peak frequencies. Also, we did not find a significant correlation between the experimentally determined peak frequencies and the relevant frequencies predicted by the models of perceptual cycles (Baumgarten et al., 2015, 2017; Samaha and Postle, 2015). Moreover, for most subjects, no clear peak could be detected at frequencies predicted by the model. This finding is difficult to explain by low statistical power alone. Moreover, the number of subjects in our study is comparable to the number of subjects in other studies that found a significant correlation in visual areas for alpha peak frequencies (Samaha and Postle, 2015). Secondly, we cannot exclude, of course, that with different parameters or a more fine-grained analysis, the hypothesized negative correlation can be found. However, we specifically chose our parameters to cover different regions and

frequency bands of interest and different approaches to analyze peak frequencies (e.g., based on individual or group level). Furthermore, we tried to keep our analyses as close as possible to analyses of a previous study that reported to succeed in finding a significant result (Samaha and Postle, 2015). There are some differences, however, that might explain at least to some degree differences in the results. While we analyzed subjects' perception of two short stimuli directly (i.e., if subjects perceived two stimuli separated by a specific SOA as one single stimulus or two separate stimuli), Samaha and Postle (2015) analyzed subjects' ability to discriminate two rather long stimuli separated by a temporal gap from a single stimulus matching the duration of both stimuli and the respective temporal gap. It might be that this paradigm measures subjects' ability to detect the gap between the two stimuli to a certain degree. However, this is only indirectly related to the perception of two discrete stimuli. Furthermore, the length of the stimuli differs considerably between both studies (i.e., a flash in the study from Samaha and Postle lasted 40 ms, whereas an electrotactile pulse in the present study lasted 0.3 ms). The to-be-expected differences in stimulus processing might therefore further hamper a comparison of the results. In another study that found a significant correlation between individual peak frequencies and temporal integration windows, Cecere et al. (2015) used a paradigm in which auditory and visual stimuli need to be integrated to induce a visual illusion. Their paradigm might thus focus stronger on the integration of crossmodal stimuli while our study focuses on the temporal segregation of unimodal stimuli. Such integration processes across sensory modalities might correlate more strongly with the peak frequencies in the alpha-band. Finally, definition of regions of interest differed slightly between studies. For example, while sensors were chosen in regions expected to be most directly related to prestimulus or stimulation effects in our study and by Cecere et al. (2015), Samaha and Postle (2015) chose SOI in a wider spatial range, potentially covering some sensors not directly related to stimulus processing (e.g., potentially ipsilateral to processing sites). However, while these methodological differences might explain some differences of the results, they cannot fully explain the lack of significant correlations in our study. This is mainly due to the fact that the methodological differences also partly exist between Cecere et al. (2015) and Samaha and Postle (2015), yet both studies found significant correlations in the visual domain.

One simple argument to explain the differences might be that neuronal oscillations in visual and somatosensory regions have different characteristics. While alpha-band activity is mostly characterized by one strong and more or less clearly defined peak, beta-band activity is sometimes characterized by multiple, weaker peaks (see **Figure 3B**) or even no clear peak, at all. In line with these results, we did not find a significant correlation between alpha and beta band peak frequencies. Thus, we feel safe to exclude that beta-band peak frequencies might be simply harmonics of the alpha-band activity (see also Haegens et al., 2014). In addition, we found that some subjects did not show a reliably detectable peak in the alpha band on source level, although a peak in the beta-band could be reliably determined. Thus, it might be that not the peak with the highest power is the carrier frequency of perceptual cycles, but other peaks

with overall lower power. Additionally, it should be noted that although several effects and/or functions seem to be reflected in the peak frequency (Salmelin and Hari, 1994; Haegens et al., 2011; Baumgarten et al., 2016a), functionally significant effects do not need to be necessarily reflected in the peak frequency (e.g., Pavlidou et al., 2014; Tucciarelli et al., 2015). Thus, it might well be that the carrier frequency is not reflected in any peak, e.g., potentially because the carrier frequency is characterized more strongly by phase rather than power (Baumgarten et al., 2015).

Despite the lack of a significant correlation between peak frequencies and perceptual performances in our study in the somatosensory domain and thus the discrepancy to other recent studies in the visual domain (Cecere et al., 2015; Samaha and Postle, 2015), there is increasing evidence for neuronal oscillations as the correlate of discrete perceptual cycles (VanRullen et al., 2014; Baumgarten et al., 2015). The studies arguing in favor of perceptual cycles commonly agree on the hypothesis that the length of a cycle of a neuronal oscillation determines a perceptual cycle for integration or segregation. The discrepancy seems to be which frequency determines the relevant oscillation and how the frequency can be determined. We suggest that the phase of a neuronal oscillation is a critical measure that determines the perceptual cycle (Baumgarten et al., 2015). The critical role of phase is supported by recent studies which reported a correlation between the phase of neuronal oscillations and perception or behavior (Busch et al., 2009; Mathewson et al., 2009; Busch and VanRullen, 2010; Dugué et al., 2011; Schyns et al., 2011; VanRullen et al., 2011; Landau and Fries, 2012; Landau et al., 2015). The phase might determine the beginning and end of a perceptual cycle. The phase and the power of an oscillation might carry different information and thus act independently or in different frequencies (Schyns et al., 2011). Thus, effects of phase might be independent of power and thus might be found in frequencies that do not show the maximal power (e.g., Baumgarten et al., 2015). On the other hand, phase and power effects might be found in the same frequency, especially if there is only one frequency active in a certain neuronal system (e.g., presumably the alpha oscillations in the visual system). We thus suggest that analyzing the power or peak frequency is a relevant tool for determining perceptual cycles and their carrier frequency. This approach might, however, sometimes miss relevant information which is coded in the phase of an oscillation. This might be an explanation why we found evidence for perceptual cycles when analyzing the phase of beta oscillations in the somatosensory domain (Baumgarten et al., 2015) but not in the present study when analyzing the peak frequencies. We thus suggest broadening analyses of spectral power to phases in broader frequency bands rather than focusing purely on peak frequencies.

Future studies might also use more strongly modulatory techniques to establish a causal link between putative perceptual cycles, oscillations and perception. tACS might be used to non-invasively modulate the length of perceptual cycles (Cecere et al., 2015). In addition, studies have demonstrated that beta oscillations can be pharmacologically modulated

(Hall et al., 2011; Muthukumaraswamy et al., 2013). Such modulations might be used to modulate beta oscillations in somatosensory cortex and measure the effect on putative perceptual cycles and consequently perception.

## CONCLUSION

There is cumulative evidence for perceptual cycles in visual and somatosensory cortex resulting in discrete and cyclic perception. While some studies on the visual domain argue that the peak frequency acts as the neuronal correlate of perceptual cycles, we were unable to demonstrate such a correlation between peak frequencies and perception in the somatosensory domain in the present study. We argue that this discrepancy does not speak against perceptual cycles, at all, but for an analysis that goes beyond analyses of power and peak frequencies, taking the phase of neuronal oscillations into account.

## REFERENCES

- Allport, D. A. (1968). Phenomenal simultaneity and the perceptual moment hypothesis. *Br. J. Psychol.* 59, 395–406. doi: 10.1111/j.2044-8295.1968.tb01154.x
- Baumgarten, T. J., Königs, S., Schnitzler, A., and Lange, J. (2017). Subliminal stimuli modulate somatosensory perception rhythmically and provide evidence for discrete perception. *Sci. Rep.* 7:43937. doi: 10.1038/srep43937
- Baumgarten, T. J., Oeltzschner, G., Hoogenboom, N., Wittsack, H.-J., Schnitzler, A., and Lange, J. (2016a). Beta peak frequencies at rest correlate with endogenous GABA+/Cr concentrations in sensorimotor cortex areas. *PLoS ONE* 11:e0156829. doi: 10.1371/journal.pone.0156829
- Baumgarten, T. J., Schnitzler, A., and Lange, J. (2015). Beta oscillations define discrete perceptual cycles in the somatosensory domain. *Proc. Natl. Acad. Sci. U.S.A.* 112, 12187–12192. doi: 10.1073/pnas.1501438112
- Baumgarten, T. J., Schnitzler, A., and Lange, J. (2016b). Prestimulus alpha power influences tactile temporal perceptual discrimination and confidence in decisions. *Cereb. Cortex* 26, 891–903. doi: 10.1093/cercor/bhu247
- Busch, N. A., Dubois, J., and VanRullen, R. (2009). The phase of ongoing EEG oscillations predicts visual perception. *J. Neurosci.* 29, 7869–7876. doi: 10.1523/JNEUROSCI.0113-09.2009
- Busch, N. A., and VanRullen, R. (2010). Spontaneous EEG oscillations reveal periodic sampling of visual attention. *Proc. Natl. Acad. Sci. U.S.A.* 107, 16048–16053. doi: 10.1073/pnas.1004801107
- Cecere, R., Rees, G., and Romei, V. (2015). Individual differences in alpha frequency drive crossmodal illusory perception. *Curr. Biol.* 25, 231–235. doi: 10.1016/j.cub.2014.11.034
- Dienes, Z. (2014). Using Bayes to get the most out of non-significant results. *Front. Psychol.* 5:781. doi: 10.3389/fpsyg.2014.00781
- Dugué, L., Marque, P., and VanRullen, R. (2011). The phase of ongoing oscillations mediates the causal relation between brain excitation and visual perception. *J. Neurosci.* 31, 11889–11893. doi: 10.1523/JNEUROSCI.1161-11.2011
- Gundlach, C., Müller, M. M., Nierhaus, T., Villringer, A., and Sehm, B. (2016). Phasic modulation of human somatosensory perception by transcranially applied oscillating currents. *Brain Stimul.* 9, 712–719. doi: 10.1016/j.brs.2016.04.014
- Haegens, S., Cousijn, H., Wallis, G., Harrison, P. J., and Nobre, A. C. (2014). Inter- and intra-individual variability in alpha peak frequency. *Neuroimage* 92, 46–55. doi: 10.1016/j.neuroimage.2014.01.049
- Haegens, S., Nächer, V., Hernández, A., Luna, R., Jensen, O., and Romo, R. (2011). Beta oscillations in the monkey sensorimotor network reflect somatosensory decision making. *Proc. Natl. Acad. Sci. U.S.A.* 108, 10708–10713. doi: 10.1073/pnas.1107297108
- Hall, S. D., Stanford, I. M., Yamawaki, N., McAllister, C. J., Rönqvist, K. C., Woodhall, G. L., et al. (2011). The role of GABAergic modulation in

## AUTHOR CONTRIBUTIONS

JL conceived the study, TB and JL designed the study, TB collected the data, TB and JL analyzed the data, TB, AS, and JL wrote the article.

## FUNDING

This work was supported by the German Research Foundation (DFG; SFB 974 TP B07 to TB and AS, LA 2400/4-1 to JL).

## SUPPLEMENTARY MATERIAL

The Supplementary Material for this article can be found online at: <http://journal.frontiersin.org/article/10.3389/fpsyg.2017.00421/full#supplementary-material>

- motor function related neuronal network activity. *Neuroimage* 56, 1506–1510. doi: 10.1016/j.neuroimage.2011.02.025
- Harter, M. R. (1967). Excitability cycles and cortical scanning: a review of two hypotheses of central intermittency in perception. *Psychol. Bull.* 68, 47–58. doi: 10.1037/h0024725
- Huang, Y., Chen, L., and Luo, H. (2015). Behavioral oscillation in priming: competing perceptual predictions conveyed in alternating theta-band rhythms. *J. Neurosci.* 35, 2830–2837. doi: 10.1523/JNEUROSCI.4294-14.2015
- Iemi, L., Chaumon, M., Crouzet, S. M., and Busch, N. A. (2016). Spontaneous neural oscillations bias perception by modulating baseline excitability. *J. Neurosci.* doi: 10.1523/jneurosci.1432-16.2016 [Epub ahead of print].
- Iguchi, Y., Hoshi, Y., Tanosaki, M., Taira, M., and Hashimoto, I. (2005). Attention induces reciprocal activity in the human somatosensory cortex enhancing relevant and suppressing irrelevant inputs from fingers. *Clin. Neurophysiol.* 116, 1077–1087. doi: 10.1016/j.clinph.2004.12.005
- Jensen, O., Gips, B., Bergmann, T. O., and Bonnefond, M. (2014). Temporal coding organized by coupled alpha and gamma oscillations prioritize visual processing. *Trends Neurosci.* 37, 357–369. doi: 10.1016/j.tins.2014.04.001
- Jones, S. R., Kerr, C. E., Wan, Q., Pritchett, D. L., Hämäläinen, M., and Moore, C. I. (2010). Cued spatial attention drives functionally relevant modulation of the mu rhythm in primary somatosensory cortex. *J. Neurosci.* 30, 13760–13765. doi: 10.1523/JNEUROSCI.2969-10.2010
- Landau, A. N., and Fries, P. (2012). Attention samples stimuli rhythmically. *Curr. Biol.* 22, 1000–1004. doi: 10.1016/j.cub.2012.03.054
- Landau, A. N., Schreyer, H. M., van Pelt, S., and Fries, P. (2015). Distributed attention is implemented through theta-rhythmic gamma modulation. *Curr. Biol.* 25, 2332–2337. doi: 10.1016/j.cub.2015.07.048
- Mathewson, K. E., Gratton, G., Fabiani, M., Beck, D. M., and Ro, T. (2009). To see or not to see: prestimulus alpha phase predicts visual awareness. *J. Neurosci.* 29, 2725–2732. doi: 10.1523/JNEUROSCI.3963-08.2009
- Muthukumaraswamy, S. D., Myers, J. F., Wilson, S. J., Nutt, D. J., Lingford-Hughes, A., Singh, K. D., et al. (2013). The effects of elevated endogenous GABA levels on movement-related network oscillations. *Neuroimage* 66, 36–41. doi: 10.1016/j.neuroimage.2012.10.054
- Oostenveld, R., Fries, P., Maris, E., and Schoffelen, J.-M. (2010). FieldTrip: open source software for advanced analysis of MEG, EEG, and invasive electrophysiological data. *Comput. Intell. Neurosci.* 2011:e156869. doi: 10.1155/2011/156869
- Pavlidou, A., Schnitzler, A., and Lange, J. (2014). Interactions between visual and motor areas during the recognition of plausible actions as revealed by magnetoencephalography. *Hum. Brain Mapp.* 35, 581–592. doi: 10.1002/hbm.22207
- Prins, N., and Kingdom, F. A. A. (2009). *Palamedes: Matlab Routines for Analyzing Psychophysical Data*. Available at: <http://www.palamedestoolbox.org>

- Salmelin, R., and Hari, R. (1994). Spatiotemporal characteristics of sensorimotor neuromagnetic rhythms related to thumb movement. *Neuroscience* 60, 537–550. doi: 10.1016/0306-4522(94)90263-1
- Samaha, J., and Postle, B. R. (2015). The speed of alpha-band oscillations predicts the temporal resolution of visual perception. *Curr. Biol.* 25, 2985–2990. doi: 10.1016/j.cub.2015.10.007
- Schyns, P. G., Thut, G., and Gross, J. (2011). Cracking the code of oscillatory activity. *PLoS Biol.* 9:e1001064. doi: 10.1371/journal.pbio.1001064
- Shams, L., Kamitani, Y., and Shimojo, S. (2000). Illusions. What you see is what you hear. *Nature* 408, 788. doi: 10.1038/35048669
- Song, K., Meng, M., Chen, L., Zhou, K., and Luo, H. (2014). Behavioral oscillations in attention: rhythmic  $\alpha$  pulses mediated through  $\theta$  band. *J. Neurosci.* 34, 4837–4844. doi: 10.1523/JNEUROSCI.4856-13.2014
- Sugita, Y., and Suzuki, Y. (2003). Audiovisual perception: implicit estimation of sound-arrival time. *Nature* 421, 911–911. doi: 10.1038/421911a
- Suk, J., Ribary, U., Cappell, J., Yamamoto, T., and Llinas, R. (1991). Anatomical localization revealed by MEG recordings of the human somatosensory system. *Electroencephalogr. Clin. Neurophysiol.* 78, 185–196. doi: 10.1016/0013-4694(91)90032-Y
- Tucciarelli, R., Turella, L., Oosterhof, N. N., Weisz, N., and Lingnau, A. (2015). MEG multivariate analysis reveals early abstract action representations in the lateral occipitotemporal cortex. *J. Neurosci.* 35, 16034–16045. doi: 10.1523/JNEUROSCI.1422-15.2015
- Van Wassenhove, V., Grant, K. W., and Poeppel, D. (2007). Temporal window of integration in auditory-visual speech perception. *Neuropsychologia* 45, 598–607. doi: 10.1016/j.neuropsychologia.2006.01.001
- VanRullen, R., Busch, N., Drewes, J., and Dubois, J. (2011). Ongoing EEG phase as a trial-by-trial predictor of perceptual and attentional variability. *Front. Psychol.* 2:60. doi: 10.3389/fpsyg.2011.00060
- VanRullen, R., and Koch, C. (2003). Is perception discrete or continuous? *Trends Cogn. Sci.* 7, 207–213.
- VanRullen, R., Reddy, L., and Koch, C. (2006). The continuous wagon wheel illusion is associated with changes in electroencephalogram power at approximately 13 Hz. *J. Neurosci.* 26, 502–507. doi: 10.1523/JNEUROSCI.4654-05.2006
- VanRullen, R., Zoefel, B., and Ilhan, B. (2014). On the cyclic nature of perception in vision versus audition. *Philos. Trans. R. Soc. B Biol. Sci.* 369:20130214. doi: 10.1098/rstb.2013.0214
- von Baer, K. E. (1908). *Welche Auffassung der Lebenden Natur ist die Richtige? (1908). Riga: Jonck und Poliewsky.* Available at: <http://caliban.mpipz.mpg.de/baer/baltisch/> [accessed August 8, 2016].
- Wutz, A., Muschter, E., van Koningsbruggen, M. G., Weisz, N., and Melcher, D. (2016). *Temporal Integration Windows in Neural Processing and Perception Aligned to Saccadic Eye Movements.* Available at: <http://www.sciencedirect.com/science/article/pii/S096098221630464X> [accessed August 2, 2016].

**Conflict of Interest Statement:** The authors declare that the research was conducted in the absence of any commercial or financial relationships that could be construed as a potential conflict of interest.

Copyright © 2017 Baumgarten, Schnitzler and Lange. This is an open-access article distributed under the terms of the Creative Commons Attribution License (CC BY). The use, distribution or reproduction in other forums is permitted, provided the original author(s) or licensor are credited and that the original publication in this journal is cited, in accordance with accepted academic practice. No use, distribution or reproduction is permitted which does not comply with these terms.

- 7) Baumgarten, T. J., Oeltzschner, G., Hoogenboom, N., Wittsack, H.-J., Schnitzler, A., & **Lange, J.** (2016a).  
Beta peak frequencies at rest correlate with endogenous GABA+/Cr concentrations in sensorimotor cortex areas.  
*PloS One*, *11*(6), e0156829.  
Impact factor (2016): 2.806

RESEARCH ARTICLE

# Beta Peak Frequencies at Rest Correlate with Endogenous GABA+/Cr Concentrations in Sensorimotor Cortex Areas

Thomas J. Baumgarten<sup>1\*</sup>, Georg Oeltzschner<sup>1,2,3,4</sup>, Nienke Hoogenboom<sup>1</sup>, Hans-Jörg Wittsack<sup>4</sup>, Alfons Schnitzler<sup>1</sup>, Joachim Lange<sup>1</sup>

**1** Institute of Clinical Neuroscience and Medical Psychology, Medical Faculty, Heinrich-Heine-University Düsseldorf, Düsseldorf, Germany, **2** Russell H. Morgan Department of Radiology and Radiological Science, The Johns Hopkins University School of Medicine, Baltimore, Maryland, United States of America, **3** F.M. Kirby Center for Functional Brain Imaging, Kennedy Krieger Institute, Baltimore, Maryland, United States of America, **4** Department of Diagnostic and Interventional Radiology, Medical Faculty, Heinrich-Heine-University Düsseldorf, Düsseldorf, Germany

\* [Thomas.Baumgarten@med.uni-duesseldorf.de](mailto:Thomas.Baumgarten@med.uni-duesseldorf.de)



 OPEN ACCESS

**Citation:** Baumgarten TJ, Oeltzschner G, Hoogenboom N, Wittsack H-J, Schnitzler A, Lange J (2016) Beta Peak Frequencies at Rest Correlate with Endogenous GABA+/Cr Concentrations in Sensorimotor Cortex Areas. PLoS ONE 11(6): e0156829. doi:10.1371/journal.pone.0156829

**Editor:** Blake Johnson, ARC Centre of Excellence in Cognition and its Disorders (CCD), AUSTRALIA

**Received:** October 20, 2015

**Accepted:** May 21, 2016

**Published:** June 3, 2016

**Copyright:** © 2016 Baumgarten et al. This is an open access article distributed under the terms of the [Creative Commons Attribution License](https://creativecommons.org/licenses/by/4.0/), which permits unrestricted use, distribution, and reproduction in any medium, provided the original author and source are credited.

**Data Availability Statement:** Privacy protection restrictions set out in the authors' Ethical Committee permission prohibit them from making subject raw data publicly available. However, the minimal data set (i.e., the individual spectroscopy results and individual peak frequencies in graphical and tabular form) on which the findings of the present manuscript are based and which are necessary to reproduce the results are stated in the present paper and its Supporting Information files.

**Funding:** This work was supported by Deutsche Forschungsgemeinschaft (SFB974 B07, Grant LA

## Abstract

Neuronal oscillatory activity in the beta band (15–30 Hz) is a prominent signal within the human sensorimotor cortex. Computational modeling and pharmacological modulation studies suggest an influence of GABAergic interneurons on the generation of beta band oscillations. Accordingly, studies in humans have demonstrated a correlation between GABA concentrations and power of beta band oscillations. It remains unclear, however, if GABA concentrations also influence beta peak frequencies and whether this influence is present in the sensorimotor cortex at rest and without pharmacological modulation. In the present study, we investigated the relation between endogenous GABA concentration (measured by magnetic resonance spectroscopy) and beta oscillations (measured by magnetoencephalography) at rest in humans. GABA concentrations and beta band oscillations were measured for left and right sensorimotor and occipital cortex areas. A significant positive linear correlation between GABA concentration and beta peak frequency was found for the left sensorimotor cortex, whereas no significant correlations were found for the right sensorimotor and the occipital cortex. The results show a novel connection between endogenous GABA concentration and beta peak frequency at rest. This finding supports previous results that demonstrated a connection between oscillatory beta activity and pharmacologically modulated GABA concentration in the sensorimotor cortex. Furthermore, the results demonstrate that for a predominantly right-handed sample, the correlation between beta band oscillations and endogenous GABA concentrations is evident only in the left sensorimotor cortex.

2400/4-1). The funders had no role in study design, data collection and analysis, decision to publish, or preparation of the manuscript.

**Competing Interests:** The authors have declared that no competing interests exist.

## Introduction

Oscillatory activity in the beta (15–30 Hz) frequency range is a prominent signal in the human sensorimotor cortex, both at rest and during motor activity [1–4]. Beta band activity differs across areas and depends on motor output (see [5] for a review). For example, beta band power in sensorimotor cortex decreases during movement, whereas beta band power increases following movement [6].

The majority of studies on beta band activity investigated the role of power (e.g., [7, 8]). In addition to power, there is increasing evidence that beta peak frequency (i.e., the frequency within the beta band with the highest power) is an important and functionally relevant parameter of oscillatory activity [9]. Beta peak frequency differs across distinct recording sites within the sensorimotor cortex [1]. Furthermore, beta peak frequency differs during movement and stimulation of lower and upper limbs, thereby distinguishing between different somatotopic representations [10]. Finally, beta peak frequency seems to be an important factor for the communication between cortical areas and muscles during movement. For example, neuronal activity in the motor cortex and electromyographic activity during movement is coherently coupled at ~20 Hz [11]. This 20 Hz motor cortical activity is thought to optimize motor output by maximal recruitment of motor neurons at a minimum discharge in the pyramidal tract [11].

Animal and modeling studies provide evidence for an essential role of GABAergic interneuronal activity for the generation of beta oscillations in the sensorimotor cortex [12–14]. For example, a study using modeled neuronal networks found increases in the power of beta band oscillations to result from an increase in the synaptic conductance of GABA<sub>A</sub>-mediated inhibition [12]. Further, studies demonstrated increases in human beta power [7, 8, 12, 15, 16] as well as decreases in beta peak frequency [12] (but see [16, 17]) as a result of pharmacological GABAergic modulation. Such modulations of beta power were evident at rest [7, 12] as well as after motor output [8, 15, 17].

While the abovementioned studies demonstrated a causal link between GABA administration and changes in beta band power and peak frequencies, the concentration of GABA and its direct modulation in the sensorimotor cortex was not measured. Thus, the quantitative relation remains unclear. Magnetic resonance spectroscopy (MRS) offers a non-invasive method for *in vivo* quantification of endogenous neurotransmitter concentrations in spatially restricted cortical regions [18]. While this approach has initially been applied to estimate GABA concentrations especially in occipital cortical areas (e.g., [19, 20]), recent studies also focused on the sensorimotor cortex (e.g., [16, 21, 22]). These studies demonstrated a linear relationship between sensorimotor GABA concentration and post-movement oscillatory beta power. In contrast, no relationship could be demonstrated between sensorimotor GABA concentration and post-movement oscillatory beta peak frequency [16]. Taken together, there are consistent results supporting a general relationship between GABA concentration and beta power in sensorimotor cortex areas. Contrarily, the results concerning beta peak frequency are less consistent. Therefore, the question remains whether beta peak frequency is related to GABA concentrations and if such a potential relation is present at rest (i.e., without movement) and for endogenous (i.e., non-modulated) GABA concentrations.

Here, we investigated whether the peak frequency of ongoing beta band oscillations is correlated to endogenous GABA concentration in the sensorimotor cortex at rest. Beta peak frequencies were determined by magnetoencephalography (MEG) and individual GABA concentrations were measured by means of MRS. Peak frequencies were determined for the left and right sensorimotor cortex, as well as for a control region in the occipital cortex. For these three regions of interest (ROIs), we linearly related peak frequencies to GABA concentrations estimated for analogue cortical areas.

## Materials and Methods

### Subjects

15 subjects (7 male, age:  $59.9 \pm 9$  years (mean  $\pm$  SD)) participated after providing written informed consent in accordance with the Declaration of Helsinki and the Ethical Committee of the Medical Faculty, Heinrich-Heine-University Düsseldorf. All participants had normal or corrected to normal vision and reported no sensory impairments, known history of neurological disorders or use of neuro-modulatory medication. The subjects were selected from the healthy controls of a sample that was previously reported in [23].

### Behavioral data

Individual handedness was assessed by comparing bi-manual performance (hand dominance test (HDT), [24]). Categorization based on the performance measure resulted in 12 clearly right-handed subjects (HDT score:  $29.8 \pm 8.1$  (mean  $\pm$  SD)) and 3 subjects with no clear hand preference (HDT score:  $-6.8 \pm 9.7$ ).

### Magnetic resonance spectroscopy (MRS) data

MRS data were recorded using a 3T whole-body MRI scanner (Siemens MAGNETOM Trio A TIM System, Siemens Healthcare AG, Erlangen, Germany) in connection with a 12-channel head matrix coil. Subjects were instructed to lie in the scanner, relax and refrain from any further activity. For the determination of neurotransmitter concentrations, MRS voxels ( $3 \times 3 \times 3 \text{ cm}^3$ ) were placed in left and right sensorimotor cortices and occipital cortex (Fig 1A). For both sensorimotor cortices, voxels were centered on the respective 'hand knob' within the *Gyrus praecentralis* [25], thus covering both motor and somatosensory cortex. The occipital MRS voxel was medially centered on the occipital lobe with the inferior boundary of the voxel aligned with the *Tentorium cerebelli*. For all subjects, voxel placement was performed with the focus to include a maximum portion of cortical volume, as well as a minimal volume of non-cerebral tissues to avoid any additional lipid contamination of the spectra. MRS voxels will be addressed as MRS ROIs (in contrast to MEG ROIs) subsequently.

After the localization of target volumes by means of  $T_1$ -weighted planning sequences, MEGA-PRESS spectra [26] were acquired (TR = 1500 ms, TE = 68 ms, V =  $3 \times 3 \times 3 \text{ cm}^3$ , spectral width = 1200 Hz, 1024 data points). Spectral editing was performed by frequency selective Gaussian refocusing pulses with a bandwidth of 44 Hz. These pulses were irradiated at 1.9 ppm ('On' resonance) and 7.5 ppm ('OFF' resonance) in alternating fashion. 96 ON and 96 OFF

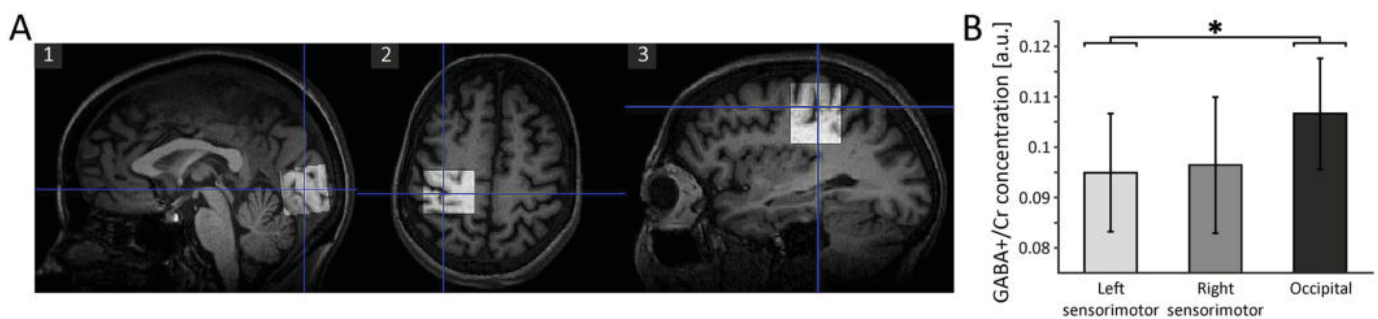


**Fig 1. Localization of MRS ROIs and average GABA+/Cr concentrations across MRS ROIs.** A) Placement of the occipital voxel in the sagittal plane (1), placement of the left sensorimotor voxel, centered on the hand knob, in the axial (2) and sagittal (3) planes. B) Average GABA+/Cr concentrations for the left and right sensorimotor and occipital MRS ROIs. Error bars represent standard deviations. \*:  $p = 0.047$ .

doi:10.1371/journal.pone.0156829.g001

spectra were acquired to give a total of 192 averages (total measurement time: 4.8 minutes per acquisition). Postprocessing and fitting of MEGA-PRESS data was performed with the MATLAB-based tool GANNET 2.0 [27], a software package specifically designed for the analysis of GABA-edited spectra. Postprocessing steps included individual frequency and phase correction of the single acquisitions [28] to reduce potential effects of thermal scanner frequency drift such as linebroadening and subtraction artefacts [29]. Fitting was performed in the frequency domain, with the 3 ppm GABA resonance being modelled as a single Gaussian, and the 3 ppm creatine peak as a single Lorentzian peak. For subsequent analyses, the GABA-to-creatine ratio (GABA+/Cr) was used [30].

GABA+/Cr estimates were not available for every MRS ROI in each subject (see [results](#) section for further details). To assess potential differences in GABA+/Cr concentrations across MRS ROIs, GABA+/Cr concentrations were compared across the left, right and occipital MRS ROIs by means of a one-factor repeated-measures ANOVA and post-hoc *t*-tests. To account for the effect of age and handedness, individual values for age and HDT handedness scores were added as covariates to the one-factor repeated-measures ANOVA. In order to ensure that any potential effects would not result from differences in individual cortical grey matter volume across the respective MRS ROIs, we calculated correlations between the individual grey matter volume and the GABA+/Cr concentrations for each MRS ROI, respectively. The rationale of this approach was that, since individual grey matter volume presumably differs across MRS ROIs, it is not feasible to include individual grey matter volume as a covariate in the one-factor repeated-measures ANOVA comparing GABA+/Cr concentrations across MRS ROIs. Although the present approach represents only an indirect control of the influence of individual grey matter volume on GABA+/Cr concentrations, an influence of individual grey matter volume on GABA+/Cr concentration can be deemed implausible if there is no significant correlation between individual grey matter volume and GABA+/Cr concentration in the respective MRS ROI.

## MEG data

**Experimental design.** Subjects were seated in the MEG with all visual stimuli projected on the backside of a translucent screen (60 Hz refresh rate) positioned 57 cm in front of the subjects. Resting-state neuromagnetic activity was recorded during two sessions with a respective duration of 5 minutes, with subjects being instructed to relax and refrain from any additional activity. In the first session, subjects had to focus a dimmed fixation dot (diameter: 0.5 degree) presented in the middle of the translucent screen (eyes open condition (EO)). After completing the first session, subjects were verbally informed regarding the beginning and the instructions of the second session. In the second session, subjects had to close their eyes (eyes closed condition (EC)) but remain awake during the measurement. Stimulus presentation was controlled using Presentation software (Neurobehavioral Systems, Albany, NY, USA).

**Data recording and preprocessing.** Continuous neuromagnetic brain activity was recorded at a sampling rate of 1000 Hz using a 306-channel whole head MEG system (Neuro-mag Elekta Oy, Helsinki, Finland), including 204 planar gradiometers (102 pairs of orthogonal gradiometers) and 102 magnetometers. Data analysis in the present study was restricted to the planar gradiometers. Electro-oculograms (EOGs) were recorded for offline artifact rejection by applying electrodes above and below the left eye as well as on the outer sides of each eye. Further, an electro-cardiogram (ECG) was recorded for offline artifact rejection by means of two electrodes placed on the left collarbone and the lowest left rib.

Data were offline analyzed using custom-made Matlab (The Mathworks Inc., Natick/MA, USA) scripts and the Matlab-based open source toolbox FieldTrip (<http://fieldtriptoolbox.org>; [31]). Continuously recorded data were divided into two epochs according to the respective

session (EO and EC), starting 3 s after beginning and ending 3 seconds before the end of the respective task. Data were band-pass filtered at 1 Hz to 200 Hz and power line noise was removed by using a band-stop filter encompassing the 50, 100, and 150 Hz components. Data were detrended and the mean of every epoch was subtracted. Continuous data were segmented into trials of 1 s duration with a 0.25 s overlap. Subsequently, trials were semi-automatically and visually inspected for artifacts. Artifacts caused by muscle activity, eye movements or SQUID jumps were removed semi-automatically using a z-score based algorithm implemented in FieldTrip. Excessively noisy channels were removed. To further eliminate cardiac and ocular artifacts, an independent component analysis was computed. Mutual information was calculated between the resulting components and the EOG and ECG channels [32, 33]. Components were sorted according to their level of mutual information and subsequently visually examined regarding their topography and time course. Those components showing high mutual information with EOG and ECG channels as well as topographies and time courses typical for cardiac and ocular artifacts were rejected. Afterwards, removed channels were reconstructed by an interpolation of neighboring channels. After artifact rejection,  $292 \pm 34.5$  (mean  $\pm$  SD) trials in the EO condition and  $304 \pm 35.4$  trials in the EC condition remained for further analysis. Subsequent analyses were performed separately for the EO and EC condition as well as for a combined data set created by appending the EO and EC condition (EC+EO).

**Frequency analysis and peak frequency determination.** To determine individual peak frequencies, we performed a frequency analysis encompassing all frequencies of the beta band (15 to 30 Hz; [6, 34]) by applying a Fourier transformation over the entire trial duration. Trials were tapered with a single Hanning taper, resulting in a spectral resolution of 1 Hz. Within each condition, spectral power was averaged over all trials for each frequency separately. Power was estimated independently for each of the 204 gradiometers. Subsequently, gradiometer pairs were combined by summing spectral power across the two orthogonal channels, resulting in 102 pairs of gradiometers.

Since GABA-concentrations were assessed for three different MRS ROIs (left and right sensorimotor cortex, occipital cortex; see Fig 1A and methods section (Magnetic resonance spectroscopy (MRS) data) for details), we determined corresponding MEG ROIs by selecting 6 sensor pairs in the left and 6 sensor pairs in the right hemisphere covering the respective sensorimotor cortices (Fig 2A). The selection of sensors was based on previous studies [35, 36]. In addition, we selected 6 posterior sensor pairs covering the occipital cortex [37].

Individual beta peak frequencies were determined semi-automatically within each MEG ROI separately for each subject. For each subject, the frequency showing the maximum power within the predefined beta band (15–30 Hz) was algorithmically selected as the individual peak frequency. Beta peak frequencies were statistically compared between the three MEG ROIs and the three conditions by means of a two-factor repeated-measures ANOVA (main factors: MEG ROI (left sensorimotor, right sensorimotor, occipital) and condition (EO, EC, EC+EO)). Similar to the comparison of GABA+/Cr concentrations, age and HDT handedness scores were included in the analysis as covariates. In case of violations of sphericity, Greenhouse-Geisser corrected values were reported.

To ensure that the peak frequencies determined for the respective sensor selections originate from cortex areas corresponding to the respective MRS ROIs, we additionally computed the respective cortical sources (see S1 Text materials & methods section for details). Subsequently, source level power distributions (S1 and S2 Figs) were visually compared with the location of the MRS ROIs (Fig 1A).

In addition to beta peak frequencies, we performed a control analysis for peak frequencies in the alpha band (8–12 Hz; see S1 Text and S3 and S4 Figs for details on the alpha peak frequency analysis and the corresponding results).

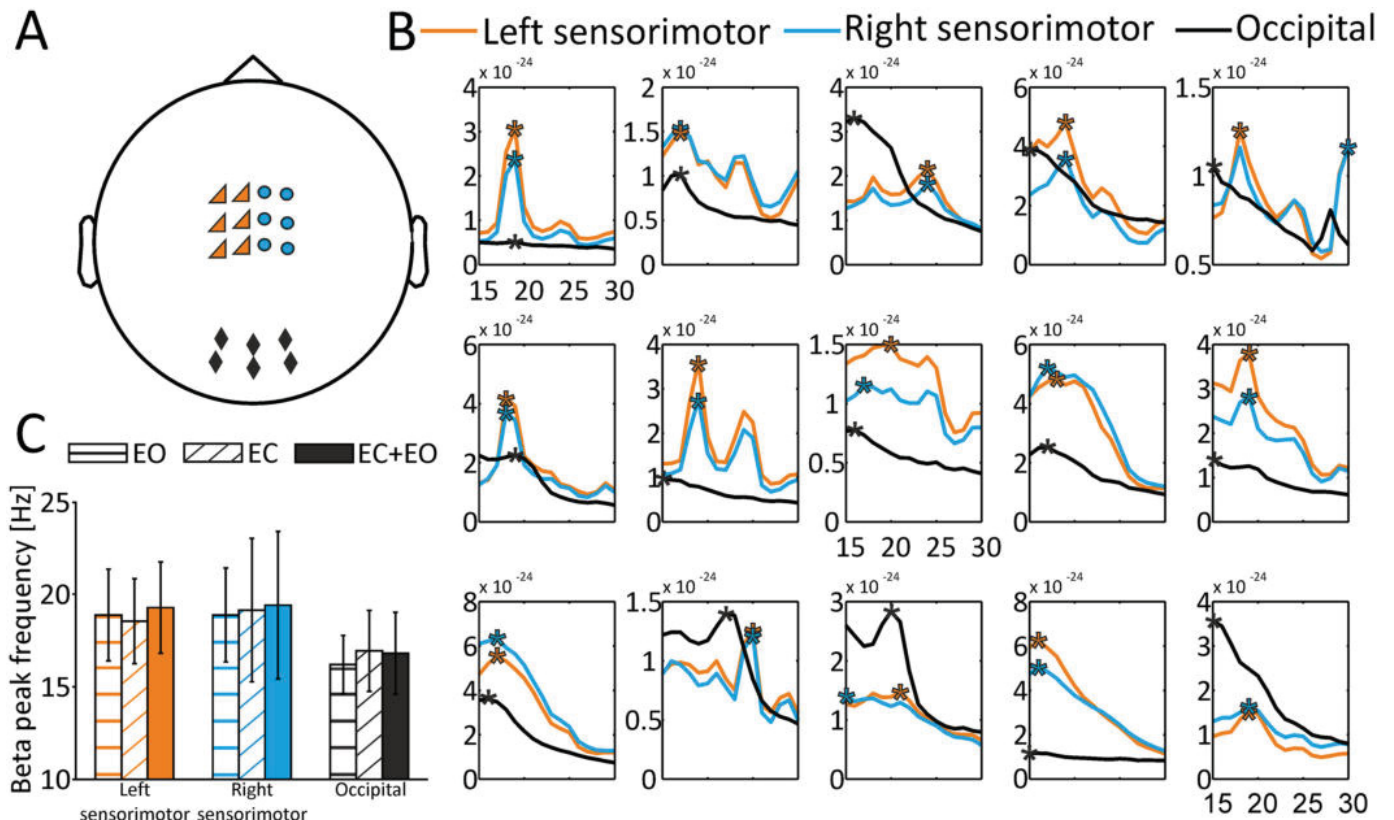


**Fig 2. Sensor selection for respective MEG ROIs, individual beta peak frequencies and average beta peak frequencies across MEG ROIs.** A) Sensors for left sensorimotor MEG ROI (orange triangles), right sensorimotor MEG ROI (blue dots) and occipital MEG ROI (black diamonds). B) Individual beta peak frequencies for all 15 subjects (EC+EO condition) for left sensorimotor MEG ROI (orange lines), right sensorimotor MEG ROI (blue lines) and occipital MEG ROI (black lines). Individual beta peak frequencies are highlighted by asterisks. C) Average beta peak frequencies separately for all conditions (EO, EC, EC+EO) and all MEG ROIs. Error bars represent standard deviations.

doi:10.1371/journal.pone.0156829.g002

### Correlation of MRS and MEG data

In order to examine the relationship between GABA+/Cr concentrations and resting-state neuro-magnetic brain activity, we linearly correlated individual GABA+/Cr concentrations within the respective MRS ROIs with the beta band peak frequencies determined for the corresponding MEG ROIs. We computed correlations (Pearson) within each ROI (e.g., between left sensorimotor MRS ROI and left sensorimotor MEG ROI), thus resulting in 3 correlations for each condition (EO, EC, EC+EO). In addition, we corrected the respective correlations for age, the HDT handedness scores and the individual cortical grey matter volume within the respective MRS ROI by means of partial correlation (Pearson).

### Results

#### GABA+/Cr concentrations

GABA+/Cr values were determined in left sensorimotor, right sensorimotor and occipital MRS ROIs (Fig 1). Due to cancellation of the measurements or distorted spectra, GABA+/Cr concentrations could not be estimated for the left sensorimotor, right sensorimotor and occipital MRS ROI in 4, 2, and 1 subjects, respectively (see Table 1 for a summary of GABA+/Cr estimates). For the remaining subjects, a one-factor repeated-measures ANOVA including age and

**Table 1. GABA+/Cr values per MRS ROI.**

Subject	GABA+/Cr Left Sensori-motor	Right Sensori-motor	Occipital
1	0.1097	0.1083	0.1054
2	0.0798	0.0713	0.1197
3	0.1035		0.1087
4	0.0995	0.1011	0.1056
5	0.0844	0.0886	0.0940
6		0.0914	0.1213
7		0.0730	0.1134
8		0.1004	0.1166
9			0.1110
10	0.0948	0.1045	0.1073
11	0.0920	0.1187	0.1083
12	0.1078	0.0962	
13	0.1085	0.1014	0.1034
14	0.0781	0.0908	0.0783
15	0.0862	0.1079	0.1000
<b>Mean</b>	0.0949	0.0964	0.1066
<b>SD</b>	0.0117	0.0135	0.0110

doi:10.1371/journal.pone.0156829.t001

individual HDT handedness scores as covariates yielded a significant difference between GABA+/Cr concentrations in the 3 MRS ROIs ( $F(2,12) = 4.024, p = 0.046, 95\% \text{ CI}$  [left sensorimotor: 0.084, 0.101; right sensorimotor: 0.09, 0.108; occipital: 0.093, 0.112]). Post-hoc  $t$ -tests revealed significant differences in GABA+/Cr concentration between left sensorimotor and occipital MRS ROIs ( $t(9) = -2.29, p = 0.047, 95\% \text{ CI}$  [-0.019, 0.0001]; Fig 1B). To ensure that any differences between GABA+/Cr concentrations across MRS ROIs did not result from differences in individual cortical grey matter volume, correlations between the individual grey matter volume and the GABA+/Cr concentrations were computed for each MRS ROI. For all three MRS ROIs, no significant correlation between individual grey matter volume and GABA+/Cr concentration could be found (left sensorimotor:  $r = -0.225, p = 0.532$ ; right sensorimotor:  $r = -0.112, p = 0.729$ ; occipital:  $r = 0.123, p = 0.69$ ).

### MEG data

Beta peak frequencies could be determined in all subjects (Fig 2B; Table 2). A two-factor repeated measures ANOVA comparing beta peak frequencies for the factors MEG ROI (left sensorimotor, right sensorimotor, occipital) and condition (EO, EC, EC+EO), with age and individual HDT handedness score included as covariates, yielded no significant main effects for MEG ROI ( $F(2,24) = 0.979, p = 0.39, 95\% \text{ CI}$  [left sensorimotor: 17.591, 20.187, right sensorimotor: 17.473, 20.794, occipital: 15.626, 17.663]) or condition ( $F(2,24) = 1.462, p = 0.252, 95\% \text{ CI}$  [EO: 17.142, 18.813, EC: 17.066, 19.334, EC+EO: 17.365, 19.613]). Likewise, there was no significant interaction between the factors ROI and condition ( $F(1.905, 22.86) = 0.63, p = 0.534$ ; Fig 2C). Since no significant results could be found for the factor condition, we chose the combined condition EC+EO for visualization purposes in Fig 2B.

Source-level analyses of the power distributions for the peak frequencies determined for the left and right sensorimotor MEG ROIs confirmed that the center of activity was centered near the ‘hand knob’ within the *Gyrus praecentralis*, which was selected as the center of the sensorimotor MRS ROIs (see S1 and S2 Figs).

Table 2. Beta peak frequencies per MEG ROI and condition.

Beta peak frequency (Hz)									
Subject	Left Sensorimotor			Right Sensorimotor			Occipital		
	EO	EC	ECEO	EO	EC	ECEO	EO	EC	ECEO
1	19	19	19	19	19	19	19	19	19
2	17	17	17	18	16	17	17	17	17
3	24	18	24	24	18	24	15	17	16
4	19	16	19	19	19	19	16	15	15
5	18	18	18	18	30	30	15	15	15
6	18	18	18	18	18	18	17	19	19
7	19	19	19	19	19	19	15	15	15
8	18	19	20	18	17	17	16	15	16
9	17	18	18	17	20	17	17	17	17
10	19	19	19	19	19	19	15	15	15
11	17	17	17	15	17	17	16	16	16
12	25	25	25	25	25	25	15	22	22
13	18	21	21	18	15	15	20	20	20
14	16	15	16	17	15	16	15	17	15
15	19	19	19	19	20	19	15	15	15
Mean	18.87	18.53	19.27	18.87	19.13	19.4	16.2	16.93	16.8
SD	2.47	2.29	2.46	2.53	3.87	3.98	1.57	2.17	2.21

doi:10.1371/journal.pone.0156829.t002

### Correlation of MRS and MEG data

We computed linear correlations between GABA+/Cr concentrations determined in MRS ROIs and beta peak frequencies determined in MEG ROIs, separately for each of the three ROIs (left sensorimotor cortex, right sensorimotor cortex, occipital cortex). Correlation analyses revealed significant linear correlations in the left sensorimotor ROI (EO:  $r = 0.616$ ,  $p = 0.043$ , EC:  $r = 0.621$ ,  $p = 0.0414$ , EC+EO:  $r = 0.735$ ,  $p = 0.01$ ; Fig 3A). No significant correlations were found in the right sensorimotor ROI (EO:  $r = -0.139$ ,  $p = 0.65$ , EC:  $r = -0.067$ ,  $p = 0.827$ , EC+EO:  $r = -0.134$ ,  $p = 0.662$ ; Fig 3B). Similarly, no significant correlations were found in the occipital ROI (EO:  $r = 0.235$ ,  $p = 0.418$ , EC:  $r = 0.086$ ,  $p = 0.771$ , EC+EO:  $r = 0.35$ ,  $p = 0.23$ ).

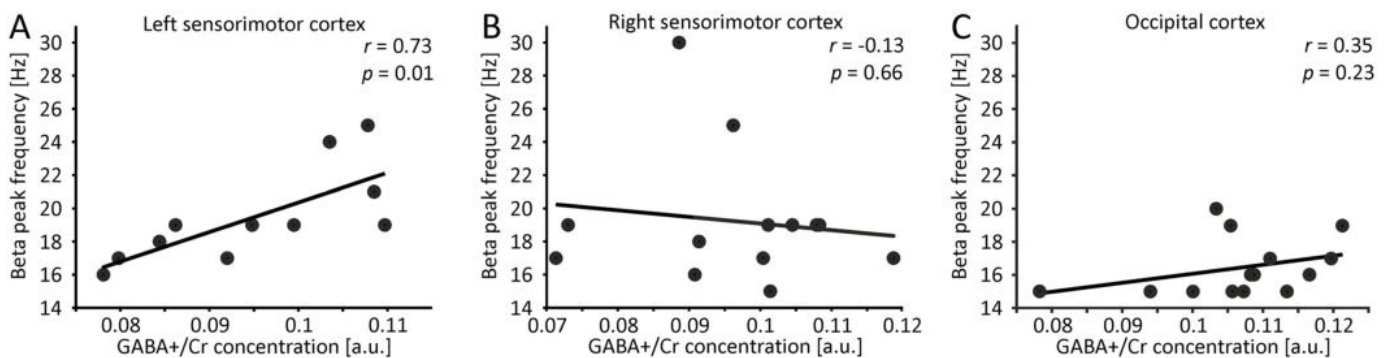


Fig 3. Correlation of beta peak frequencies and GABA+/Cr concentration. (A) Beta peak frequencies calculated for the left sensorimotor MEG ROI and the EC+EO condition correlated with GABA+/Cr estimates from the left sensorimotor MRS ROI. (B) Same as (A), but now for right sensorimotor MEG and MRS ROI. (C) Same as (A), but now for occipital MEG and MRS ROI.

doi:10.1371/journal.pone.0156829.g003

$r = 0.345$ ,  $p = 0.228$ ; Fig 3C). For all correlations, we additionally partialized out the effect of age, HDT handedness score and respective individual cortical grey matter volume. In line with the uncorrected analyses, corrected correlation analyses revealed significant linear correlations in the left sensorimotor ROI for the EC and the EC+EO condition (EC:  $r = 0.758$ ,  $p = 0.048$ , EC+EO:  $r = 0.816$ ,  $p = 0.025$ ). For the EO condition, a strong trend could be demonstrated ( $r = 0.724$ ,  $p = 0.066$ ). No significant correlations were found for the right sensorimotor (EO:  $r = -0.139$ ,  $p = 0.721$ , EC:  $r = -0.084$ ,  $p = 0.829$ , EC+EO:  $r = -0.108$ ,  $p = 0.783$ ) and occipital cortex (EO:  $r = 0.125$ ,  $p = 0.731$ , EC:  $r = -0.08$ ,  $p = 0.826$ , EC+EO:  $r = 0.296$ ,  $p = 0.407$ ).

Since, within each ROI, correlations were highly similar across conditions, we selected the combined condition EC+EO for visualization purposes in Fig 3. Further, correlations within the respective ROIs statistically remained highly similar when correlations were restricted to those subjects for whom valid MRS spectra could be determined for all 3 MRS ROIs (see section MRS data above).

## Discussion

Using magnetoencephalography (MEG) and magnetic resonance spectroscopy (MRS) in healthy human subjects, we investigated the relationship between beta peak frequencies at rest and endogenous (i.e., non-modulated) GABA+/Cr concentrations in the left and right sensorimotor and occipital cortex. The results show significant positive linear correlations between peak frequencies in the beta band (15–30 Hz) and GABA+/Cr concentrations for the left sensorimotor cortex (i.e., higher beta peak frequency was related to a higher GABA+/Cr concentration).

The connection of neuronal oscillatory activity in the beta band and in vivo GABA concentrations has been the topic of various scientific publications. Previous studies that have addressed the general question if sensorimotor beta activity is related to the GABAergic system, applied pharmacological GABAergic modulators [7, 8, 12, 15, 17] and/or investigated movement-related sensorimotor beta activity [8, 15–17]. To our knowledge, the present work is the first study to investigate the connection between beta peak frequency at rest (i.e., without movement or a movement-related task) and non-modulated GABA+/Cr values in the sensorimotor cortex. By focusing exclusively on non-modulated parameters (i.e., no movement-related and pharmaco-induced manipulation), the present study was able to show a correlation between GABA+/Cr concentrations and beta peak frequency at rest.

The analysis of neuromagnetic activity did not demonstrate significant differences in beta peak frequencies across MEG ROIs or conditions. While left and right sensorimotor cortices showed clear peaks in the beta band in all subjects (Fig 2B), beta peaks were less prominent in the occipital cortex, with six subjects showing no clear peak. This is in agreement with the specific role of beta band activity for the sensorimotor cortex [1, 4], while beta band activity in occipital regions is less common. Although the analysis of beta peak frequencies in occipital areas proves to be difficult, we included the occipital MEG ROI as a control condition in order to demonstrate that potential correlations between beta band peak frequency and GABA+/Cr concentrations are not ubiquitously present throughout the cortex, but spatially restricted to sensorimotor cortex areas. Less clear peaks in the beta band for the occipital ROI might be a reason why correlations between GABA+/Cr concentrations and beta peak frequencies were only found for the sensorimotor cortex. This interpretation, however, cannot account for the lack of a significant correlation in right sensorimotor areas, since we found clear peaks in the right sensorimotor cortex for all subjects.

Although the analysis of GABA+/Cr concentrations encompassing all MRS ROIs yielded a significant result, this effect was driven by differences between the left sensorimotor and the

occipital MRS ROIs. Since the post-hoc tests showed no significant differences between both sensorimotor MRS ROIs, it is unlikely that hemispherical differences between GABA+/Cr concentrations are responsible for the significant correlation between beta peak frequency and GABA+/Cr concentrations only in the left sensorimotor cortex. Because 12 of 15 subjects in the present study were classified as right-handed, handedness might be an explanation for the unilateral correlation. However, correlations largely remained significant even after correcting for handedness. This finding suggests that handedness alone is unlikely to account for the differences between left and right sensorimotor cortices. Handedness, however, is known to lead to asymmetries with respect to hand representations in the sensorimotor cortex [38–40]. Such asymmetries might lead to regional differences in GABA+/Cr concentration and/or generators of beta frequencies in left and right sensorimotor areas. The results of the correlation analysis further remained virtually unchanged after correcting for age and individual cortical grey matter volume. This excludes the possibility that the unilateral correlation arises as an epiphenomenon due to demographic or neuroanatomical variables. The rather large size of the MRS ROIs poses an additional challenge, since for such voxel sizes it is not possible to separately measure GABA+/Cr concentrations for motor and somatosensory cortex. Although smaller voxel sizes are possible [21], they result in extended measurement time for a comparable signal to noise ratio. Thus, although GABA+/Cr concentrations did not significantly differ between left and right sensorimotor MRS ROIs, our method might have measured more GABA+/Cr concentrations that are unrelated to beta frequency generations in right sensorimotor cortex (i.e., more “noise”). More fined-grained analyses might resolve this problem and shed further light on the relation between GABA concentration and beta peak frequencies. In addition, the sample size of the present study has to be taken into account. Although 15 subjects is a considerable sample size for an MEG/MRS study (i.e., see [12, 16, 19]), an increased sample size would have been preferable. In line with this, it would be interesting to assess both left and right-handed populations of sufficient sample size in future studies to further elucidate the effect of handedness on GABAergic concentrations in sensorimotor cortices.

A general limitation of GABA measurements via MRS is that this method is unable to differentiate between synaptic and extra-synaptic GABA concentrations [22]. Nonetheless, GABA concentrations measured by MRS might primarily reflect extra-cellular GABA concentrations, i.e., the general GABAergic tone [41]. Contrary to intra-cellular GABA concentrations, extra-cellular GABA concentrations would include synaptic concentrations. Beta band oscillations would be primarily related to synaptic GABA concentrations, since this represents the synaptically active neurotransmitter pool [15]. Thus, our results represent correlations with the overall GABA+/Cr concentration of a given voxel, not exclusively for the synaptically active GABA concentration. Despite all potential limitations, we were able to demonstrate a significant positive correlation between GABA+/Cr concentration and beta peak frequency. In addition, various studies using parameters similar to the present study proved that GABA MRS in sensorimotor and occipital cortices yields feasible results (reviewed in [22]). The general feasibility of GABA MRS is further supported by studies that link MRS-derived neurotransmitter concentrations to functional and behavioral measurements [21].

Neuronal oscillations are thought to depend on the balance between excitatory (i.e., glutamatergic synaptic input) and inhibitory (i.e., GABAergic synaptic input) network components [12, 42, 43]. For beta band activity in the sensorimotor cortex, a connection between GABAergic tone and beta band oscillations is supported by studies reporting increases in somatosensory beta band power as an effect of GABAergic modulation by means of positive allosteric GABAergic modulators (e.g., benzodiazepine) [7, 12, 15, 17]. The relation between GABAergic modulation and beta peak frequencies, however, is less clear. While, Jensen and colleagues [12] reported a small decrease (~1.6 Hz) in resting-state beta peak frequency in bilateral

sensorimotor cortices after the administration of benzodiazepine, Baker and Baker [17] found no modulation of beta peak frequency after the administration of benzodiazepine. Benzodiazepine is considered to enhance the synaptic GABAergic drive [12]. Simplified, an enhanced GABAergic drive could be related to an increased GABAergic concentration, which would contradict the positive correlation between beta peak frequency and GABA+/Cr levels in the left sensorimotor cortex observed in the present study. Yet, various differences between the studies have to be taken into account. First, Jensen et al. [12] and Baker and Baker [17] measured the influence of pharmacological GABA modulations on beta peak frequencies on the within-subject level. The present study measured non-modulated GABA concentrations and investigated correlations on a between-subject level. Further, while we report a correlation for the left sensorimotor cortex, Jensen and colleagues [12] averaged beta peak frequency over bilateral sensorimotor cortices (thereby not investigating lateral differences). Finally, we measured mostly right-handed subjects, so that an influence of handedness cannot be excluded. The abovementioned studies do not report handedness of their subjects, making a direct comparison difficult.

Gaetz and colleagues [16] found no correlation between beta peak frequency during post-movement beta-rebound and endogenous GABA concentrations for the left motor cortex. Post-movement beta-rebound, however, is intrinsically different from resting state beta activity, as measured in our study. Any differences found between our study and Gaetz et al. [16] might thus be related to different tasks. Taken together, the few existing studies focusing on the connection between beta peak frequency and GABA concentrations in sensorimotor cortex areas strongly vary in experimental setting and assessed parameters, thereby complicating a comparison to our results.

For future studies, it would be interesting to determine how sensorimotor beta peak frequency and GABA concentration both relate on a behavioral level. There is evidence that higher sensorimotor GABA concentrations correlate with slower reaction times in a motor sequence learning task [44]. Here, slower reaction has been interpreted as a result of higher levels of inhibition. Furthermore, higher concentrations of sensorimotor GABA have been related to lower discrimination thresholds in a tactile frequency discrimination task [21]. The authors associated higher GABA concentrations with a potentially higher temporal resolution of tactile perception, which would enable neurons to more closely tune their responses to the stimulus cycles. Such an adjustment of neuronal response to stimulus frequency is considered as the underlying mechanism of the connection between sensorimotor GABA levels and frequency discrimination and to result in lower frequency discrimination thresholds. The influence of oscillatory beta activity on behavioral parameters is less clear. Studies relating individual beta peak frequencies to measures of functional performance apart from motor-related tasks are scarce. Differences in the phase of ongoing beta band oscillations in the somatosensory cortex have been shown to predict the temporal perception of subsequently presented tactile stimuli [45]. Here, the specific beta band frequency showing the biggest phase differences predicted the temporal resolution of tactile perception. Perfetti and colleagues [46] found beta power variations to successfully predict mean reaction time in a visually guided motor task, with a decrease of beta power in left sensory-motor areas corresponding to faster reaction times. In line with this, lower beta-power levels during the time of stimulus presentation were related to a faster reaction towards this stimulus [47]. Taken together, these results suggest an involvement of GABA concentrations and beta band activity within the sensorimotor cortex in the temporal dimension of tactile perception. Thus, further research should investigate if GABA concentration and beta band activity show similar connections to behavioral parameters assessed in parallel.

In conclusion, the present study shows a significant linear correlation between beta peak frequency at rest and non-modulated endogenous GABA concentration measured by spectrally

edited MRS. Significant correlations were restricted to the left sensorimotor cortex. While previous studies revealed connections between GABA concentrations and beta band power, our results provide a novel connection between GABA concentrations and peak frequencies in the beta band. In line with previous results from studies using pharmacological modulation of GABA concentrations, these results support a specific role of GABAergic inhibition in the generation of oscillatory beta band activity within the sensorimotor system.

## Supporting Information

**S1 Fig. Source reconstruction of the average power distribution for individual beta peak frequencies determined for the left sensorimotor MEG ROI.** A) Source power projected on the surface of the MNI template brain. The striped square approximates the size and position of the left sensorimotor MRS ROI. B) Source power projected on the sagittal plane of the MNI template brain. Source plots are masked to highlight power maxima.  
(TIF)

**S2 Fig. Source reconstruction of the average power distribution for individual beta peak frequencies determined for the right sensorimotor MEG ROI.** A) Source power projected on the surface of the MNI template brain. The striped square approximates the size and position of the left sensorimotor MRS ROI. B) Source power projected on the sagittal plane of the MNI template brain. Source plots are masked to highlight power maxima.  
(TIF)

**S3 Fig. Sensor selection for respective MEG ROIs, individual alpha peak frequencies and average alpha peak frequencies across MEG ROIs.** A) Sensors for left sensorimotor MEG ROI (orange triangles), right sensorimotor MEG ROI (blue dots) and occipital MEG ROI (black diamonds). B) Individual alpha peak frequencies for all 15 subjects (EC+EO condition) for left sensorimotor MEG ROI (orange lines), right sensorimotor MEG ROI (blue lines) and occipital MEG ROI (black lines). Individual alpha peak frequencies are highlighted by asterisks. C) Average alpha peak frequencies separately for all conditions (EO, EC, EC+EO) and all MEG ROIs. Error bars represent standard deviations.  
(TIF)

**S4 Fig. Correlation of alpha peak frequencies and GABA+/Cr concentration.** (A) Alpha peak frequencies calculated for the left sensorimotor MEG ROI and the EC+EO condition correlated with GABA+/Cr estimates from the left sensorimotor MRS ROI. (B) Same as (A), but now for right sensorimotor MEG and MRS ROI. (C) Same as (A), but now for occipital MEG and MRS ROI.  
(TIF)

**S1 Text. Supporting information materials & methods and results.**  
(DOCX)

## Author Contributions

Conceived and designed the experiments: NH HJW AS JL. Performed the experiments: TJB GO. Analyzed the data: TJB GO JL. Contributed reagents/materials/analysis tools: TJB NH JL. Wrote the paper: TJB GO NH HJW AS JL.

## References

1. Salmelin R, Hari R. Spatiotemporal characteristics of sensorimotor neuromagnetic rhythms related to thumb movement. *Neuroscience*. 1994; 60:537–50. PMID: [8072694](https://pubmed.ncbi.nlm.nih.gov/8072694/)

2. Murthy VN, Fetz EE. Oscillatory activity in sensorimotor cortex of awake monkeys: synchronization of local field potentials and relation to behavior. *Journal of Neurophysiology*. 1996; 76:3949–67. PMID: [8985892](#)
3. Pfurtscheller G, Stancák A Jr., Neuper C. Post-movement beta synchronization. A correlate of an idling motor area? *Electroencephalography and Clinical Neurophysiology*. 1996; 98:281–93. PMID: [8641150](#)
4. Kilavik BE, Zaepffel M, Brovelli A, MacKay WA, Riehle A. The ups and downs of beta oscillations in sensorimotor cortex. *Special Issue: Neuronal oscillations in movement disorders*. 2013; 245:15–26.
5. Neuper C, Pfurtscheller G. Event-related dynamics of cortical rhythms: frequency-specific features and functional correlates. *Thalamo-Cortical Relationships*. 2001; 43:41–58.
6. Jurkiewicz MT, Gaetz WC, Bostan AC, Cheyne D. Post-movement beta rebound is generated in motor cortex: Evidence from neuromagnetic recordings. *NeuroImage*. 2006; 32:1281–89. PMID: [16863693](#)
7. Hall SD, Barnes GR, Furlong PL, Seri S, Hillebrand A. Neuronal network pharmacodynamics of GABAergic modulation in the human cortex determined using pharmaco-magnetoencephalography. *Human Brain Mapping*. 2010; 31:581–94. doi: [10.1002/hbm.20889](#) PMID: [19937723](#)
8. Muthukumaraswamy S, Myers J, Wilson S, Nutt D, Lingford-Hughes A, Singh K, et al. The effects of elevated endogenous GABA levels on movement-related network oscillations. *NeuroImage*. 2013; 66:36–41. doi: [10.1016/j.neuroimage.2012.10.054](#) PMID: [23110884](#)
9. Kilavik BE, Ponce-Alvarez A, Trachel R, Confais J, Takerkart S, Riehle A. Context-related frequency modulations of macaque motor cortical LFP beta oscillations. *Cerebral Cortex*. 2012; 22:2148–59. doi: [10.1093/cercor/bhr299](#) PMID: [22021914](#)
10. Neuper C, Pfurtscheller G. Evidence for distinct beta resonance frequencies in human EEG related to specific sensorimotor cortical areas. *Clinical Neurophysiology*. 2001; 112:2084–97. PMID: [11682347](#)
11. Salenius S, Portin K, Kajola M, Salmelin R, Hari R. Cortical control of human motoneuron firing during isometric contraction. *Journal of Neurophysiology*. 1997; 77:3401–05. PMID: [9212286](#)
12. Jensen O, Goel P, Kopell N, Pohja M, Hari R, Ermentrout B. On the human sensorimotor-cortex beta rhythm: Sources and modeling. *NeuroImage*. 2005; 26:347–55. PMID: [15907295](#)
13. Roopun AK, Middleton SJ, Cunningham MO, LeBeau FEN, Bibbig A, Whittington MA, et al. A beta2-frequency (20–30 Hz) oscillation in nonsynaptic networks of somatosensory cortex. *Proceedings of the National Academy of Sciences*. 2006; 103: 15646–50.
14. Yamawaki N, Stanford IM, Hall SD, Woodhall GL. Pharmacologically induced and stimulus evoked rhythmic neuronal oscillatory activity in the primary motor cortex in vitro. *Neuroscience*. 2008; 151:386–95. PMID: [18063484](#)
15. Hall SD, Stanford IM, Yamawaki N, McAllister CJ, Rönqvist KC, Woodhall GL, et al. The role of GABAergic modulation in motor function related neuronal network activity. *NeuroImage*. 2011; 56:1506–10. doi: [10.1016/j.neuroimage.2011.02.025](#) PMID: [21320607](#)
16. Gaetz W, Edgar J, Wang D, Roberts T. Relating MEG measured motor cortical oscillations to resting  $\gamma$ -Aminobutyric acid (GABA) concentration. *NeuroImage*. 2011; 55:616–21. doi: [10.1016/j.neuroimage.2010.12.077](#) PMID: [21215806](#)
17. Baker MR, Baker SN. The effect of diazepam on motor cortical oscillations and corticomuscular coherence studied in man. *The Journal of Physiology*. 2003; 546:931–42. PMID: [12563016](#)
18. Durst CR, Michael N, Tustison NJ, Patrie JT, Raghavan P, Wintermark M, et al. Noninvasive evaluation of the regional variations of GABA using magnetic resonance spectroscopy at 3 Tesla. *Magnetic Resonance Imaging*. 2015; 33:611–17. doi: [10.1016/j.mri.2015.02.015](#) PMID: [25708260](#)
19. Muthukumaraswamy SD, Edden RA, Jones DK, Swettenham JB, Singh KD. Resting GABA concentration predicts peak gamma frequency and fMRI amplitude in response to visual stimulation in humans. *Proceedings of the National Academy of Sciences*. 2009; 106:8356–61.
20. Cousijn H, Haegens S, Wallis G, Near J, Stokes MG, Harrison PJ, et al. Resting GABA and glutamate concentrations do not predict visual gamma frequency or amplitude. *Proceedings of the National Academy of Sciences*. 2014; 111:9301–06.
21. Puts NAJ, Edden RAE, Evans CJ, McGlone F, McGonigle DJ. Regionally specific human GABA concentration correlates with tactile discrimination thresholds. *The Journal of Neuroscience*. 2011; 31:16556–60. doi: [10.1523/JNEUROSCI.4489-11.2011](#) PMID: [22090482](#)
22. Stagg CJ. Magnetic Resonance Spectroscopy as a tool to study the role of GABA in motor-cortical plasticity. *NeuroImage*. 2014; 86:19–27. doi: [10.1016/j.neuroimage.2013.01.009](#) PMID: [23333699](#)
23. Oeltzschner G, Butz M, Baumgarten T, Hoogenboom N, Wittsack H, Schnitzler A. Low visual cortex GABA levels in hepatic encephalopathy: links to blood ammonia, critical flicker frequency, and brain osmolytes. *Metabolic Brain Disease*. 2015:1–10.

24. Steingrüber H. Hand-Dominanz-Test. Göttingen: Hogrefe; 2011.
25. Yousry TA, Schmid UD, Alkadhi H, Schmidt D, Peraud A, Buettner A, et al. Localization of the motor hand area to a knob on the precentral gyrus. A new landmark. *Brain*. 1997; 120:141–57. PMID: [9055804](#)
26. Mescher M, Merkle H, Kirsch J, Garwood M, Gruetter R. Simultaneous in vivo spectral editing and water suppression. *NMR in Biomedicine*. 1998; 11:266–72. PMID: [9802468](#)
27. Edden RA, Puts NA, Harris AD, Barker PB, Evans CJ. Gannet: A batch-processing tool for the quantitative analysis of gamma-aminobutyric acid-edited MR spectroscopy spectra. *Journal of Magnetic Resonance Imaging*. 2014; 40:1445–52. doi: [10.1002/jmri.24478](#) PMID: [25548816](#)
28. Near J, Edden R, Evans CJ, Paguin R, Harris A, Jezzard P. Frequency and phase drift correction of magnetic resonance spectroscopy data by spectral registration in the time domain. *Magnetic Resonance in Medicine*. 2014; 73:44–50. doi: [10.1002/mrm.25094](#) PMID: [24436292](#)
29. Harris AD, Glaubitz B, Near J, John Evans C, Puts NA, Schmidt-Wilcke T, et al. Impact of frequency drift on gamma-aminobutyric acid-edited MR spectroscopy. *Magnetic Resonance in Medicine*. 2014; 72:941–8. doi: [10.1002/mrm.25009](#) PMID: [24407931](#)
30. Mullins PG, McGonigle DJ, O’Gorman RL, Puts NA, Vidyasagar R, Evans CJ, et al. Current practice in the use of MEGA-PRESS spectroscopy for the detection of GABA. *NeuroImage*. 2014; 86: 43–52. doi: [10.1016/j.neuroimage.2012.12.004](#) PMID: [23246994](#)
31. Oostenveld R, Fries P, Maris E, Schoffelen J. FieldTrip: Open source software for advanced analysis of MEG, EEG, and invasive electrophysiological data. *Computational Intelligence and Neuroscience*. 2011; 2011:9.
32. Liu Z, de Zwart JA, van Gelderen P, Kuo L, Duyn JH. Statistical feature extraction for artifact removal from concurrent fMRI-EEG recordings. *NeuroImage*. 2012; 59:2073–87. doi: [10.1016/j.neuroimage.2011.10.042](#) PMID: [22036675](#)
33. Abbasi O, Dammers J, Arrubla J, Warbrick T, Butz M, Neuner I, et al. Time-frequency analysis of resting state and evoked EEG data recorded at higher magnetic fields up to 9.4T. *Journal of Neuroscience Methods*. 2015.
34. Haegens S, Nacher V, Hernandez A, Luna R, Jensen O, Romo R. Beta oscillations in the monkey sensorimotor network reflect somatosensory decision making. *Proceedings of the National Academy of Sciences*. 2011; 108:10708–13.
35. van Ede F, Jensen O, Maris E. Tactile expectation modulates pre-stimulus  $\beta$ -band oscillations in human sensorimotor cortex. *NeuroImage*. 2010; 51:867–76. doi: [10.1016/j.neuroimage.2010.02.053](#) PMID: [20188186](#)
36. Lange J, Halacz J, van Dijk H, Kahlbrock N, Schnitzler A. Fluctuations of prestimulus oscillatory power predict subjective perception of tactile simultaneity. *Cerebral Cortex*. 2012; 22:2564–74. doi: [10.1093/cercor/bhr329](#) PMID: [22114082](#)
37. van Dijk H, van der Werf J, Mazaheri A, Medendorp WP, Jensen O. Modulations in oscillatory activity with amplitude asymmetry can produce cognitively relevant event-related responses. *Proceedings of the National Academy of Sciences*. 2010; 107:900–05.
38. Volkmann J, Schnitzler A, Witte OW, Freund H. Handedness and asymmetry of hand representation in human motor cortex. *Journal of Neurophysiology*. 1998; 79:2149–54. PMID: [9535974](#)
39. Sörös P, Knecht S, Imai T, Gürtler S, Lütkenhöner B, Ringelstein EB, et al. Cortical asymmetries of the human somatosensory hand representation in right- and left-handers. *Neuroscience Letters*. 1999; 271:89–92. PMID: [10477109](#)
40. Triggs WJ, Subramaniam B, Rossi F. Hand preference and transcranial magnetic stimulation asymmetry of cortical motor representation. *Brain Research*. 1999; 835:324–29. PMID: [10415389](#)
41. Rae C. A guide to the metabolic pathways and function of metabolites observed in human brain 1H magnetic resonance spectra. *Neurochemical Research*. 2014; 39:1–36. doi: [10.1007/s11064-013-1199-5](#) PMID: [24258018](#)
42. Brunel N, Wang X. What determines the frequency of fast network oscillations with irregular neural discharges? I. Synaptic dynamics and excitation-inhibition balance. *Journal of Neurophysiology*. 2003; 90:415–30. PMID: [12611969](#)
43. Buzsáki G. Rhythms of the brain. Oxford, New York: Oxford University Press; 2006.
44. Stagg CJ, Bachtiair V, Johansen-Berg H. The role of GABA in human motor learning. *Current Biology*. 2011; 21:480–84. doi: [10.1016/j.cub.2011.01.069](#) PMID: [21376596](#)
45. Baumgarten TJ, Schnitzler A, Lange J. Beta oscillations define discrete perceptual cycles in the somatosensory domain. *Proceedings of the National Academy of Sciences*. 2015; 112:12187–92.

46. Perfetti B, Moisello C, Landsness EC, Kvint S, Pruski A, Onofrij M, et al. Temporal evolution of oscillatory activity predicts performance in a choice-reaction time reaching task. *Journal of Neurophysiology*. 2011; 105:18–27. doi: [10.1152/jn.00778.2010](https://doi.org/10.1152/jn.00778.2010) PMID: [21047934](https://pubmed.ncbi.nlm.nih.gov/21047934/)
47. Tzagarakis C, Ince NF, Leuthold AC, Pellizzer G. Beta-band activity during motor planning reflects response uncertainty. *Journal of Neuroscience*. 2010; 30:11270–77. doi: [10.1523/JNEUROSCI.6026-09.2010](https://doi.org/10.1523/JNEUROSCI.6026-09.2010) PMID: [20739547](https://pubmed.ncbi.nlm.nih.gov/20739547/)

- 8) Baumgarten, T. J., Schnitzler, A., & **Lange, J.** (2016b).  
Prestimulus Alpha Power Influences Tactile Temporal Perceptual Discrimination and Confidence in Decisions.  
*Cerebral Cortex (New York, N.Y.: 1991)*, 26(3), 891–903.  
Impact factor (2016): 6.599

## ORIGINAL ARTICLE

# Prestimulus Alpha Power Influences Tactile Temporal Perceptual Discrimination and Confidence in Decisions

Thomas J. Baumgarten, Alfons Schnitzler, and Joachim Lange

Institute of Clinical Neuroscience and Medical Psychology, Medical Faculty, Heinrich-Heine-University Düsseldorf, 40225 Düsseldorf, Germany

Address correspondence to Thomas J. Baumgarten, Institute of Clinical Neuroscience and Medical Psychology, Medical Faculty, Heinrich-Heine-University Düsseldorf, 40225 Düsseldorf, Germany. Email: thomas.baumgarten@med.uni-duesseldorf.de

## Abstract

Recent studies have demonstrated that prestimulus alpha-band activity substantially influences perception of near-threshold stimuli. Here, we studied the influence of prestimulus alpha power fluctuations on temporal perceptual discrimination of suprathreshold tactile stimuli and subjects' confidence regarding their perceptual decisions. We investigated how prestimulus alpha-band power influences poststimulus decision-making variables. We presented electrical stimuli with different stimulus onset asynchronies (SOAs) to human subjects, and determined the SOA for which temporal perceptual discrimination varied on a trial-by-trial basis between perceiving 1 or 2 stimuli, prior to recording brain activity with magnetoencephalography. We found that low prestimulus alpha power in contralateral somatosensory and occipital areas predicts the veridical temporal perceptual discrimination of 2 stimuli. Additionally, prestimulus alpha power was negatively correlated with confidence ratings in correctly perceived trials, but positively correlated for incorrectly perceived trials. Finally, poststimulus event-related fields (ERFs) were modulated by prestimulus alpha power and reflect the result of a decisional process rather than physical stimulus parameters around ~150 ms. These findings provide new insights into the link between spontaneous prestimulus alpha power fluctuations, temporal perceptual discrimination, decision making, and decisional confidence. The results suggest that prestimulus alpha power modulates perception and decisions on a continuous scale, as reflected in confidence ratings.

**Key words:** alpha oscillations, MEG, perceptual decision making, prestimulus fluctuations, tactile stimulation

## Introduction

Decision making can be understood as a process in which sensory evidence is accumulated in a decision variable. If sensory evidence is sufficiently strong and available for a sufficiently long time, the decision variable accumulates until a decision bound for either decision is reached (see [Gold and Shadlen 2007](#) for a review). In some situations, however, sensory evidence is ambiguous, providing equal sensory evidence for each decisional option. In other situations, sensory evidence is weak or presented insufficiently long for the decision variable to reach a decision bound. Consequently, decisions have to be made based on incomplete or equivocal sensory evidence, frequently causing incorrect decisions and low confidence in the decision. In addition, decision making is not only determined by sensory evidence,

but also by trial-to-trial fluctuations of neuronal activity, usually interpreted as internal noise ([Ratcliff and McKoon 2007](#); [O'Connell et al. 2012](#)).

Recent studies, however, demonstrated that fluctuations of neuronal activity can have a functional role for the perception of weak and ambiguous stimuli. Specifically neuronal oscillatory activity in the alpha band (~8–12 Hz) has drawn much attention. Prestimulus alpha power is modulated by attention (e.g., [Foxe et al. 1998](#); [Worden et al. 2000](#)) and prestimulus power and phase in early sensory areas are correlated with perception ([Linkenkaer-Hansen et al. 2004](#); [van Dijk et al. 2008](#); [Mazaheri et al. 2009](#); [Wyart and Tallon-Baudry 2009](#); [Jensen and Mazaheri 2010](#); [Romei et al. 2010](#); [Keil et al. 2014](#)). Furthermore, it has been shown that prestimulus oscillatory activity can influence

poststimulus evoked responses (Başar et al. 1984; Brandt and Jansen 1991; Mazaheri and Jensen 2008; Jones et al. 2009, 2010; Anderson and Ding 2011; Lange et al. 2012). The influence of prestimulus oscillatory activity on decision variables remains largely unknown. In addition, the influence of prestimulus oscillatory activity on subjective confidence in perceptual decisions is unknown. Subjective confidence represents a measure of the degree to which a decision maker believes in the correctness of his decisions and thus provides an insight into decisional processes on a fine-grained scale (Kiani and Shadlen 2009). Moreover, it remains unexplained how the brain forms decisions when sensory evidence is insufficient to reach a decision bound, for example, due to sensory ambiguity.

To test how prestimulus alpha-band power biases perceptual decisions and the underlying neuronal decision variable in humans, we presented electrical stimuli with different stimulus onset asynchronies (SOAs) and compared 2 subjectively ambiguous experimental conditions in which physically identical tactile stimuli were perceived differently on a trial-by-trial basis. We used magnetoencephalography (MEG) and a forced-choice temporal perceptual discrimination task to investigate whether fluctuations of prestimulus neuronal oscillatory activity are related to the trial-to-trial variability of decisions and how prestimulus oscillatory activity influences the decision variable. We hypothesized that prestimulus alpha power correlates with temporal perceptual discrimination rate, with lower alpha power levels related to increased veridical temporal perceptual discrimination. Further, we expected that characteristics of the decision-making process would be evident in neural activity in the form of poststimulus event-related fields (ERFs). This should result in differences of neuronal activity for trials with different decisional outcomes, despite identical physical stimulation. Additionally, we hypothesized that prestimulus alpha power would influence this decision-related neuronal activity.

## Materials and Methods

### Subjects

Sixteen, right-handed subjects (7 males, age:  $26.1 \pm 4.7$  years [mean  $\pm$  SD]) participated in the study after providing written informed consent in accordance with the Declaration of Helsinki. All participants had normal or corrected-to-normal vision and

reported no somatosensory deficits or known history of neurological disorders.

### Experimental Design and Paradigm

The experimental task was designed to compare 2 conditions with identical physical stimuli, differing only in the participant's perception. Each trial started with the presentation of a start cue (500 ms; Fig. 1). Next, the cue decreased in luminance, indicating the prestimulus period (900–1100 ms), after which the subjects received either 1 or 2 short (0.3 ms) electrical pulses, applied by 2 electrodes placed between the 2 distal joints of the left index finger. The amplitude of the pulses was determined individually to a level clearly above subjective perception threshold, but below pain threshold ( $4.1 \pm 1.2$  mA [mean  $\pm$  SD]). Note that all comparisons of conditions were performed at the within-subject level. Therefore, only conditions with identical stimulation parameters were compared (for details, see MEG Data Acquisition and Analysis). The electrical pulses were applied with varying SOAs: short (0 ms, i.e., only one stimulus was applied), long (100 ms), and 3 SOAs individually determined in a premeasurement. These 3 individual SOAs included a SOA for which subjects reported to perceive one electrical pulse in  $\sim 50\%$  of the trials, whereas in the other  $\sim 50\%$  of the trials 2 pulses were perceived (SOA:  $25.9 \pm 1.9$  ms [mean  $\pm$  standard error of the mean [SEM]]). Subsequently, this condition will be labeled the intermediate SOA. The remaining 2 SOAs encompassed the intermediate SOA by  $\pm 10$  ms and were included to minimize learning effects and response biases. A training phase of  $\sim 5$  min containing all possible SOAs preceded the experiment to familiarize subjects with the paradigm. The electrical stimulation was followed by a jittered poststimulus period of 500–1200 ms to minimize motor preparation effects, during which the fixation dot remained visible. Next, a written instruction indicated the start of the first response window. Subjects first reported whether they perceived the stimulation as 1 single or 2 temporally separate sensations. Responses were given by button-presses with the index or middle finger of the right hand, while button configurations were randomized from trial to trial to minimize motor preparation effects. Subjects were instructed to report within 3000 ms after presentation of response instructions. Due to the jittered poststimulus epoch (500–1200 ms) which determined the beginning of the subsequent response window, response speed was not taken into

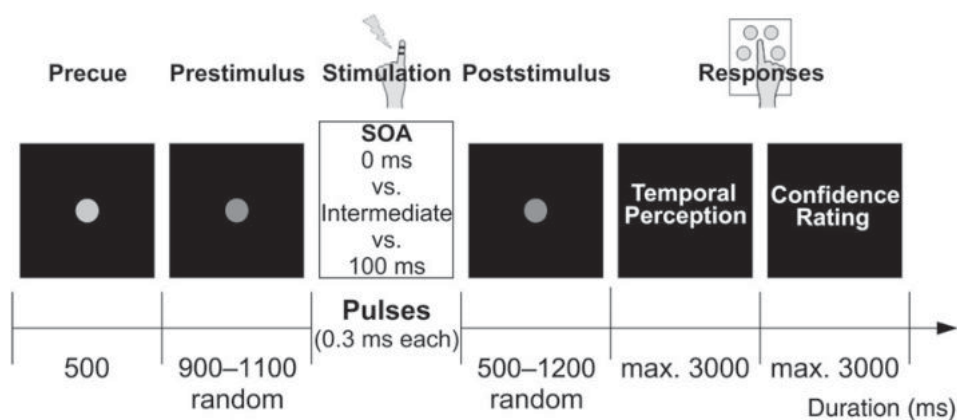


**Figure 1.** Experimental task. Sequence of events: A central fixation dot serves as start cue, after 500 ms a decrease in luminance signals the start of the prestimulus epoch, consisting of a jittered period of 900–1100 ms. Tactile stimulation is applied to the left index finger with varying SOAs (0 ms, intermediate – 10 ms, intermediate, intermediate + 10 ms, 100 ms). After a jittered poststimulus period (500–1200 ms), written instructions indicate the first response window and subjects report their perception of the stimulation by button-press. Subsequently, written instructions indicate the second response window and subjects report their decisional confidence by button-press.

account. If no response was given after 3000 ms or the subject responded before the presentation of the instructions, a warning was presented visually. The respective trial was discarded from analysis and repeated at the end of the block. After reporting their subjective perception, written instructions indicated a second response window. Here, subjects rated their subjective confidence level regarding their first response. The confidence level was assessed via a 4-point rating scale, ranging from “very sure” to “very unsure.” Once both responses were given, the next trial started. With the exception of the aforementioned warning signal, no further feedback was given. All visual stimuli were projected on the backside of a translucent screen (60 Hz refresh rate) positioned 60 cm in front of the subjects.

Each SOA was presented in 50 trials. To increase statistical power, the intermediate SOA was presented 4 times as often as the other SOAs (i.e., 200 trials). 80 trials constituted one block with each block containing 10 repetitions (40 for the intermediate condition) of each SOA presented in pseudorandom order. Blocks were repeated 5 times, interrupted by self-paced breaks of  $\sim 2$  min, resulting in an overall 400 trials. The approximate total duration of the MEG measurement was  $\sim 45$ – $50$  min (400 trials with a trial length of  $\sim 6$  s on average [4–8.6 s], interrupted by up to 4 self-paced breaks of  $\sim 2$  min).

Stimulus presentation was controlled using Presentation software (Neurobehavioral Systems, Albany, NY, USA). Before MEG recording, each subject received instructions of the task but remained naïve to the purpose of the experiment and the different SOAs used.

### Behavioral Data Analysis

Behavioral data were analyzed with regard to correct responses and compared across conditions by means of a paired sample *t*-test. Prior to this, a Kolmogorov–Smirnov test was applied to ensure that the respective distributions did not differ from a Gaussian distribution. Further, we investigated learning/fatigue trends in the perceptual responses and confidence ratings by dividing experimental trials in 12 bins and computing the average temporal perceptual discrimination rate (i.e., perceived 2 stimuli or 1 stimulus) as well as the average confidence rating over subjects for each bin. Subsequently, we fitted a linear regression to the data in order to determine a linear trend.

### MEG Data Acquisition and Analysis

#### Data Recording and Preprocessing

Ongoing neuromagnetic brain activity was continuously recorded at a sampling rate of 1000 Hz using a 306-channel whole head MEG system (Neuromag Elekta Oy, Helsinki, Finland), including 204 planar gradiometers (102 pairs of orthogonal gradiometers) and 102 magnetometers. Data analysis in the present study was restricted to the planar gradiometers. Additionally, electro-oculograms were recorded for offline artifact rejection by applying electrodes above and below the left eye as well as on the outer sides of each eye. Subjects' head position within the MEG helmet was registered by a head position indication system (HPI) built up of 4 coils placed at subjects' forehead and behind both ears. A 3-T MRI scanner (Siemens, Erlangen, Germany) was used to obtain individual full-brain high-resolution standard  $T_1$ -weighted structural magnetic resonance images (MRIs). The MRIs were offline aligned with the MEG coordinate system using the HPI coils and anatomical landmarks (nasion, left and right preauricular points).

Data were offline analyzed using custom-made Matlab (The Mathworks, Natick, MA, USA) scripts, the Matlab-based open source toolbox FieldTrip (<http://fieldtrip.fcdonders.nl>; Oostenveld et al. 2011), and SPM8 (Litvak et al. 2011). Continuously recorded data were segmented into trials, starting with the appearance of the first fixation dot and ending with the second response of the subject. All trials were semiautomatically and visually inspected for artifacts, whereas artifacts caused by muscle activity, eye movements, or SQUID jumps were removed semiautomatically using a z-score-based algorithm implemented in FieldTrip. Excessively noisy channels were removed as well and reconstructed by an interpolation of neighboring channels. In addition, power line noise was removed from the segmented data by using a band-stop filter encompassing the 50, 100, and 150 Hz components. Further preprocessing steps were applied according to the respective analyses.

#### Time–Frequency Analysis

For exploratory reasons, we first performed a time–frequency analysis on all frequencies between 2 and 40 Hz for all time points ( $-900$  to  $500$  ms, Fig. 2A). We focused our analysis on the effects of alpha power (8–12 Hz) in the prestimulus epoch ( $-900$  to  $0$  ms) on perceptual decisions, that is, the responses to the

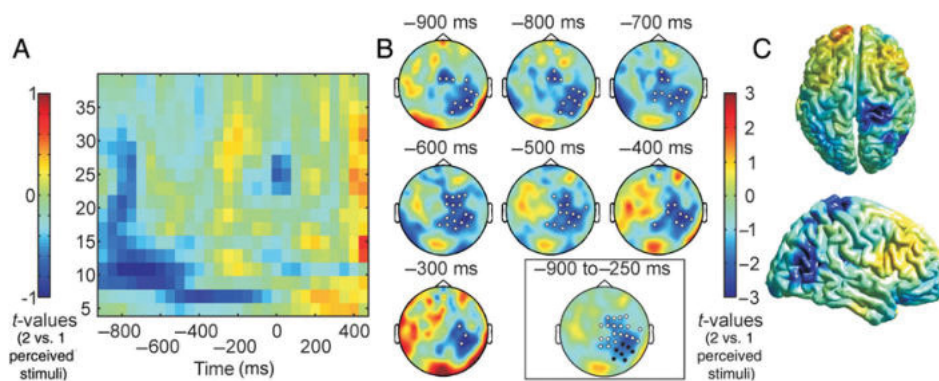


**Figure 2.** Results of the statistical comparison of correctly (perceived 2 stimuli) versus incorrectly (perceived 1 stimulus) perceived trials with intermediate SOA. (A) Time–frequency representation on sensor level averaged over all sensors.  $t = 0$  indicates onset of sensory stimulation. (B) Time series of topographical representations on sensor level averaged over the alpha band (8–12 Hz). Significant sensors ( $P < 0.05$ ) are marked by white circles. The lower right inset illustrates alpha power differences averaged across the whole time window ( $-900$  to  $-250$  ms; white dots represent channels of the anterior/somatosensory sensor-cluster; black crosses represent channels of the parieto-occipital sensor-cluster used for following analyses. See text for details on the separation of the clusters). (C) Source reconstruction projected on the MNI template brain for the significant effect in the alpha band (see B) viewed from the top (top row) and the right (bottom row). Source plots are masked to highlight significant clusters ( $P < 0.05$ ). *P*-values in B and C are cluster corrected to account for multiple comparison corrections. The left color bar applies to A, the right color bar applies to B and C. For both color bars, blue colors indicate lower spectral power in correctly perceived trials compared with incorrectly perceived trials.

temporal perceptual discrimination task. First, the linear trend and mean of every epoch were removed from each trial. Time-frequency representations for each trial were computed by applying a Fourier transformation on adaptive sliding time windows containing 7 full cycles of the respective frequency  $f$  ( $\Delta t = 7/f$ ), moved in steps of 50 ms and 2 Hz (van Dijk et al. 2008; Mazaheri et al. 2009; Lange et al. 2012). Data segments were tapered with a single Hanning taper, resulting in a spectral smoothing of  $1/\Delta t$ . Spectral power was averaged over the alpha band separately for each trial. Alpha power was estimated independently for each of the 204 gradiometers. Subsequently, gradiometer pairs were combined by summing spectral power across the 2 orthogonal channels, resulting in 102 pairs of gradiometers. We sorted the trials with respect to the SOA for each subject separately. For all trials with intermediate SOA, we separated and compared trials with reports of 1 perceived stimulus to trials with 2 perceived stimuli. With this approach, we were able to compare 2 sets of decisional outcomes, which differed only in the subjects' temporal perceptual discrimination of the stimuli, though not regarding their physical properties. Due to the fact that, only for the intermediate condition, a sufficiently high number of trials for both decisional outcomes (perceived 1 stimulus or 2 stimuli) were available, only trials with intermediate SOA entered the analysis. In the following, trials in which stimulation was perceived as 2 temporally separate stimuli will be labeled correctly perceived trials, whereas trials in which stimulation was perceived as 1 single stimulus will be labeled incorrectly perceived trials. To test for statistically significant power differences between sets, we used a cluster-based nonparametric randomization approach (Maris and Oostenveld 2007). In a first step, we compared averaged alpha power between both sets of decisional outcomes (correct and incorrect, i.e., perceived 2 stimuli or 1 stimulus) for each subject independently in all channels and all time points in the prestimulus time window (−900 to 0 ms). Comparison between sets was performed by subtracting the power of both sets and dividing the difference by the variance (equivalent to an independent sample *t*-test). This step serves as a normalization of interindividual differences (Hoogenboom et al. 2010; Lange et al. 2011, 2013). The comparison was done independently for each time sample and channel, resulting in a time-channel map of pseudo-*t*-values for each subject. For group-level statistics, we analyzed the consistency of pseudo-*t*-values over subjects by means of a nonparametric randomization test identifying clusters in time-channel space showing the same effect. Neighboring channels were defined on the basis of spatial adjacency, with spatial clusters requiring a minimum amount of 2 neighboring channels. Spatially and temporally adjacent pseudo-*t*-values exceeding an a priori-defined threshold ( $P < 0.05$ ) were combined to a cluster. *t*-values within a cluster were summed up and used as input for the second-level cluster statistic. Next, we computed a reference distribution by randomly permuting the data, assuming no differences between statistical conditions and exchangeability of the data. This process of random assignment was repeated 1000 times, resulting in a summed cluster *t*-value for each repetition. The proportion of elements in the reference distribution exceeding the observed maximum cluster-level test statistic was used to estimate a *P*-value for each cluster. This statistical approach effectively controls for the Type I error rate due to multiple comparisons across time points and channels (Maris and Oostenveld 2007).

### Source Reconstruction

To identify the cortical sources of the statistically significant effects displayed on sensor level, we calculated source-level

power estimates by means of an adaptive spatial filtering technique (DICS, Gross et al. 2001). To this end, a regular 3D grid with 1 cm resolution was applied to the Montreal Neurological Institute (MNI) template brain. Individual grids for each subject were computed by linearly warping the structural MRI of each subject onto the MNI template brain and applying the inverse of the warp to the MNI template grid. For one subject, no individual structural MRI was available; hence, we used the MNI template brain instead. A lead-field matrix was computed for each grid point employing a realistically shaped single-shell volume conduction model (Nolte 2003). Subsequently, the cross-spectral density (CSD) matrix between all MEG gradiometer sensor pairs was computed for the alpha band by applying a Fourier transformation on time windows of interest. Time windows of interest were based on the significant clusters of the group analysis on sensor level (Fig. 2B). Using the CSD and lead-field matrix, common spatial filters were constructed for each individual grid point. To this end, we pooled trials with intermediate SOA over both sets of decisional outcomes and computed a common spatial filter for each subject. CSD matrices of single trials were projected through those filters, resulting in single-trial estimates of source power (Hoogenboom et al. 2010; Lange et al. 2012), and further sorted according to decisional outcome. In line with the analysis on sensor level, power was contrasted between both sets of decisional outcomes. Similarly to the sensor-level analysis, the resulting individual source parameters were statistically compared across subjects by means of a nonparametric randomization test (Maris and Oostenveld 2007) which effectively controls for the Type I error rate. Group results were displayed on the MNI template brain in form of *t*-values. Finally, cortical sources were identified using the AFNI atlas (<http://afni.nimh.nih.gov/afni>), integrated into FieldTrip.

Since the time–frequency analysis and the source reconstruction demonstrated 2 spatiotemporally different activation clusters (see Results and Fig. 2B,C), we performed the subsequent analyses on 2 different sensor sets. First, we based the analyses on all channels showing a significant alpha power difference between correctly (perceived 2 stimuli) versus incorrectly (perceived 1 stimulus) perceived trials with intermediate SOA (as shown in Fig. 2B). Second, we based the analyses on 2 spatiotemporally separated sensor-clusters (see inset in Fig. 2B), 1 anterior/somatosensory sensor-cluster (MEG-sensors: MEG0712 + 13, MEG0722 + 23, MEG1042 + 43, MEG1112 + 13, MEG1122 + 23, MEG1132 + 33, MEG1142 + 43, MEG1312 + 13, MEG1342 + 43, MEG1832 + 33, MEG2012 + 13, MEG2022 + 23, MEG2212 + 13, MEG2222 + 23, MEG2232 + 33, MEG2242 + 43, MEG2412 + 13, MEG2422 + 23, MEG2612 + 13, MEG2642 + 43), and 1 parieto-occipital sensor-cluster (MEG-sensors: MEG2312 + 13, MEG2322 + 23, MEG2342 + 43, MEG2432 + 33, MEG2442 + 43, MEG2512 + 13, MEG2522 + 23).

### Correlation of Prestimulus Power, Perceptual Decisions, and Confidence Ratings

To examine the relationship between prestimulus power and perceptual decisions, we averaged spectral power over time, frequency, and sensors and correlated averaged power values with perceptual decisions. To this end, we selected the sensors and time points showing a significant difference between decisional outcomes (see above, Fig. 2B). Note that this approach resembles a post hoc statistical analysis in the sense that sensor selection was based on those sensors showing a significant difference in the alpha band (see above, Fig. 2B). Averaging was done separately for each subject and trial, using a fixed time–frequency–sensor triplet resulting from the significant time-channel clusters

derived from group-level statistics and the predetermined alpha frequency (8–12 Hz). Trials of each subject were sorted from low to high alpha power and divided into 5 bins (Linkenkaer-Hansen et al. 2004; Jones et al. 2010; Lange et al. 2012, 2013). For each bin and subject, we calculated the average temporal perceptual discrimination rate and normalized the resulting value for each bin to the individual average temporal perceptual discrimination rate across all bins by first subtracting and then dividing by the individual averaged temporal perceptual discrimination rate across all trials. This resulted in a percentage change relative to the normalized mean across all bins for each subject (Linkenkaer-Hansen et al. 2004; Lange et al. 2012, 2013). For each bin, average power and SEM were computed over all subjects. Linear and quadratic functions were fitted to the data to determine the best fit (Linkenkaer-Hansen et al. 2004; van Dijk et al. 2008; Jones et al. 2010; Lange et al. 2012, 2013). Average temporal perceptual discrimination rates in the respective bins were statistically compared by applying a one-way repeated-measures ANOVA and post hoc *t*-tests.

Additionally, we investigated the correlation of prestimulus power and confidence ratings. The analysis was conducted as stated above, with the following exceptions. To separately determine the relation between prestimulus power and confidence rating for correctly and incorrectly perceived trials, we divided the trials with intermediate SOA regarding their decisional outcome, that is, correctly and incorrectly perceived trials were analyzed separately. For each bin, we calculated the average confidence rating and normalized the result in each bin to the average confidence rating across all trials with the respective decisional outcome. Finally, the average confidence ratings were averaged over subjects. Likewise, linear and quadratic functions were fitted to the data.

Further, we separated the significant channels in 2 clusters (anterior/somatosensory vs. parieto-occipital; see above and inset of Fig. 2B) based on their spatiotemporal characteristics and performed the correlation analysis with power values averaged over the channels of these separated sensor-clusters.

### Relation Between Decision Variable, Prestimulus Power, and Poststimulus ERFs

To examine the neural dynamics of perceptual decision making under conditions with suboptimal evidence accumulation and ambiguous stimulus perception, we studied the relation of poststimulus ERFs, prestimulus alpha power and decisional outcome. Perceptual decisions can be conceptualized as a process in which sensory evidence for a decision accumulates over time in a decision variable until a decision bound is reached, followed by a particular response selection (Gold and Shadlen 2007; Ratcliff and McKoon 2007; Kiani and Shadlen 2009). Recent works in human electrophysiology suggest that such decision variables are reflected in poststimulus event-related potentials (e.g., VanRullen and Thorpe 2001; Philiastides and Sajda 2006; Philiastides et al. 2006; O'Connell et al. 2012). Since event-related potentials/fields resemble a population-based measure of neuronal activity (Hari and Kaukoranta 1985), this is further supported by studies that identify signals from multiple neurons as basis of behavioral decisions (Britten et al. 1996). We hypothesized that, in trials with intermediate SOA, the total accumulation of sensory evidence would remain below any decisional bound due to insufficient sensory information in favor of any decision, therefore requiring forced-choice decisions. We aimed to assess these decision variables in poststimulus ERFs. Additionally, confidence levels should be a function of the distance of the decision variable to

the decision bounds, with closer proximity of the decision variable to the respective decision bound resulting in higher confidence. Moreover, we hypothesized that prestimulus alpha power modulates the distance of the decision variable to the respective decision bounds.

To compute ERFs, preprocessed data were filtered between 2 and 40 Hz, the mean of each epoch was removed from each trial, and these data were averaged across trials. For each subject, ERFs were computed for all sensors that showed a significant difference between decisional outcomes (as shown in Fig. 2B). Additionally, we separated the significant channels in 2 spatial clusters (anterior/somatosensory vs. parieto-occipital, see inset of Fig. 2B) based on their spatiotemporal characteristics and calculated ERFs for all sensors of the respective sensor-cluster separately. To avoid cancelation effects when averaging across sensors and subjects, the signals of the 2 orthogonal sensors of each gradiometer pair were combined by taking the root mean square of the signals in the time domain (e.g., van Dijk et al. 2008; Lange et al. 2012), resulting in 102 gradiometer pairs. Poststimulus ERFs were baseline corrected by subtracting the mean of the prestimulus period (–900 to 0 ms). First, we determined potential poststimulus decision boundaries in the poststimulus ERFs. To this end, we computed ERFs for the 2 conditions with 0 and 100 ms SOA as they provided the most unambiguous perception of 1 and 2 stimuli. Only trials with correct responses (i.e., perceived 1 stimulus for trials with SOA 0 ms and perceived 2 stimuli for trials with SOA 100 ms) were included in this analysis, with conditions subsequently labeled as 0ms-1 and 100ms-2. We statistically compared the ERFs in the poststimulus period (0–300 ms) to identify time periods that maximally discriminated between these 2 reference conditions with 0 and 100 ms SOA. We used a nonparametric statistical test which effectively controls for the Type I error rate due to multiple comparisons across time points in line with the procedure described above (for details, see Time–Frequency Analysis). In brief, we calculated the difference between both ERFs for each subject, followed by a group-level statistic testing the consistency of the differences across subjects against a reference null distribution based on 1000 random sets of permutations regarding the 2 experimental conditions.

Next, we examined whether the ERFs reflect a decision variable that is independent of sensory input, but differing according to subject's decisional outcome. To this end, we sorted trials with intermediate SOA in trials with correct and incorrect responses. We hypothesized that due to their ambiguity and insufficient accumulation of sensory evidence, the decision bounds (i.e., ERFs of conditions 0ms-1 and 100ms-2) will not be reached in trials with intermediate SOA. Nonetheless, because of the implemented forced-choice task, subjects are forced to make the decision with a particular level of uncertainty. We hypothesized that confidence levels should be a function of the distance of the decision variable to the decision bounds, with closer proximity of the decision variable to the respective decision bound resulting in higher confidence. Moreover, we hypothesized that prestimulus alpha power has a distinguishable effect on the decision variable. Since prestimulus alpha power significantly influenced temporal perceptual discrimination and confidence ratings (Fig. 3A,B), an effect of prestimulus alpha power should be visible in the poststimulus decision variable. We hypothesized that prestimulus alpha power modulates the distance of the decision variable to the respective decision bounds (Fig. 4B). To this end, we averaged prestimulus alpha power across those time points and sensors that showed a significant difference between decisional outcomes (see above, Fig. 2B) and grouped the trials with intermediate SOA

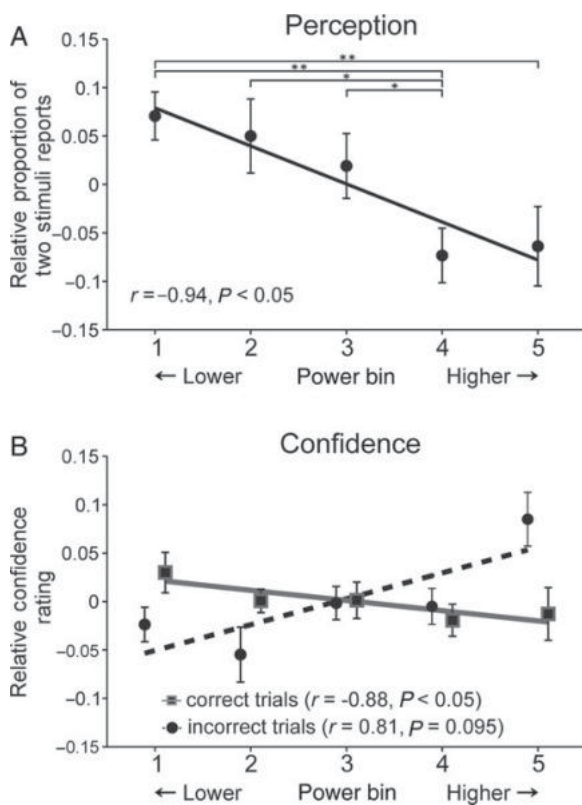


**Figure 3.** Results of the post hoc correlation analyses of averaged prestimulus alpha power (8–12 Hz) for significant sensors (as shown in Fig. 2B) and (A) normalized average temporal perceptual discrimination rate or (B) normalized confidence ratings, separated for correctly and incorrectly perceived trials. Insets show results of the linear regression analyses (black and gray lines). Higher number bins indicate higher spectral power. Error bars represent SEM. \*\* $P < 0.01$ , \* $P < 0.05$ .

into correct and incorrect trials with either high and low prestimulus alpha power. This resulted in 4 different conditions: low prestimulus alpha power and perceived 2 stimuli (subsequently labeled low  $\alpha$ -2), high prestimulus alpha power and perceived 2 stimuli (high  $\alpha$ -2), low prestimulus alpha power and perceived 1 stimulus (low  $\alpha$ -1), high prestimulus alpha power and perceived 1 stimulus (high  $\alpha$ -1). We then computed poststimulus ERFs for each of these conditions.

To quantify the relation between these conditions, we chose 2 parallel approaches to determine a time window of interest. In the first approach, we averaged ERF amplitudes for each condition over those time points showing a significant difference between the conditions 0ms-1 and 100ms-2 (i.e., 145–171 ms; see above and Fig. 4A; see Supplementary Fig. 1 for the complete ERF time courses of all conditions). In the second approach, we determined the time point of maximum amplitude difference between the conditions 0ms-1 and 100ms-2 within those time points showing a significant difference between the conditions (150 ms). Please see the Discussion section for a further discussion on the selection criteria for the time window of interest. We averaged ERF amplitudes for each condition over the 10 ms that precede this time point of maximal difference (i.e., 140–150 ms). The rationale of this approach was that decision variables are thought to increase until a decision bound is reached and decline again afterwards to baseline (Kiani and Shadlen 2009; O’Connell et al. 2012). Thus, the time point of maximal difference between the reference conditions and the preceding time

window should be the best predictor of the decision process (see model in Fig. 4B).

For the additional analyses based on separated sensor-clusters, significant differences between the conditions 0ms-1 and 100ms-2 could be demonstrated from 139 to 172 ms (see Fig. 4D) and the point of maximum amplitude difference was located at 151 ms for the anterior/somatosensory sensor-cluster. For the parieto-occipital cluster, no significant differences between the conditions 0ms-1 and 100ms-2 could be demonstrated (see Fig. 4F). To ensure that the absence of significant differences for the parieto-occipital cluster did not result from low statistical power due to a lower number of channels in this cluster (parieto-occipital cluster: 7 channel pairs, anterior/somatosensory sensor-cluster: 20 channel pairs), we further compared the conditions 0ms-1 and 100ms-2 for a random selection of 7 channel pairs from the anterior/somatosensory sensor-cluster. The results of this analysis reproduced the significant differences between the conditions 0ms-1 and 100ms-2 (139–169 ms; data not shown) as well as a significant negative linear correlation for the ordered averaged ERFs (i.e., 100ms-2, low  $\alpha$ -2, high  $\alpha$ -2, low  $\alpha$ -1, high  $\alpha$ -1, 0ms-1;  $r = -0.96$ ,  $P < 0.01$  for time window 139–169 ms;  $r = -0.87$ ,  $P < 0.05$  for time window 139–149 ms; data not shown). Based on these results, we conclude that the absent significant difference between the conditions 0ms-1 and 100ms-2 for the parieto-occipital cluster cannot be generally explained by the smaller number of channels in this cluster, but instead must be mainly attributed to the absence of decision-related ERF components in the parieto-occipital sensor-cluster.

For both sensor sets (all significant sensors and the anterior/somatosensory sensor-cluster), we subsequently ordered the conditions regarding the expected averaged ERF amplitudes (100ms-2, low  $\alpha$ -2, high  $\alpha$ -2, low  $\alpha$ -1, high  $\alpha$ -1, 0ms-1) and fitted a linear regression to the data to determine a linear trend (Fig. 5). Due to the a priori difference of the conditions 100ms-2 and 0ms-1, we performed an additional analysis in which we excluded these conditions from the regression analysis. Hence, the regression analysis was additionally calculated for the ordered intermediate conditions (low  $\alpha$ -2, high  $\alpha$ -2, low  $\alpha$ -1, high  $\alpha$ -1) only. Averaged ERF amplitudes were statistically compared by applying a one-way repeated-measures ANOVA. Because no time window showing a significant difference between the conditions 0ms-1 and 100ms-2 was found for the parieto-occipital sensor-cluster, we refrained from performing this analysis for the parieto-occipital sensor-cluster.

Finally, we calculated the average confidence ratings per subject for each condition and averaged the mean confidence levels per condition over all subjects. Since confidence levels should be a function of the distance of the decision variable to the respective decision bounds (i.e., low  $\alpha$ -2 and high  $\alpha$ -2 to 100ms-2; low  $\alpha$ -1 and high  $\alpha$ -1 to 0ms-1, see Fig. 4B), we calculated the mean power difference of each intermediate condition (i.e., low  $\alpha$ -2, high  $\alpha$ -2, low  $\alpha$ -1, high  $\alpha$ -1) from the respective decision bounds averaged over the time window showing a significant difference between the conditions 0ms-1 and 100ms-2 (i.e., 145–171 ms) and the time window preceding the point of maximum amplitude difference between the conditions 0ms-1 and 100ms-2 (i.e., 140–150 ms, Fig. 5C). We plotted the distance of the decision variables to the respective decision bounds and related it to the mean confidence levels per condition over all subjects. Subsequently, we fitted a linear regression to the data to determine a linear trend. Additionally, we performed this analysis with amplitude values calculated for the time windows based on the anterior/somatosensory sensor-cluster (i.e., 139–172 ms; 141–151 ms, Fig. 5F). Due to the fact that, for the parieto-occipital sensor-cluster, no

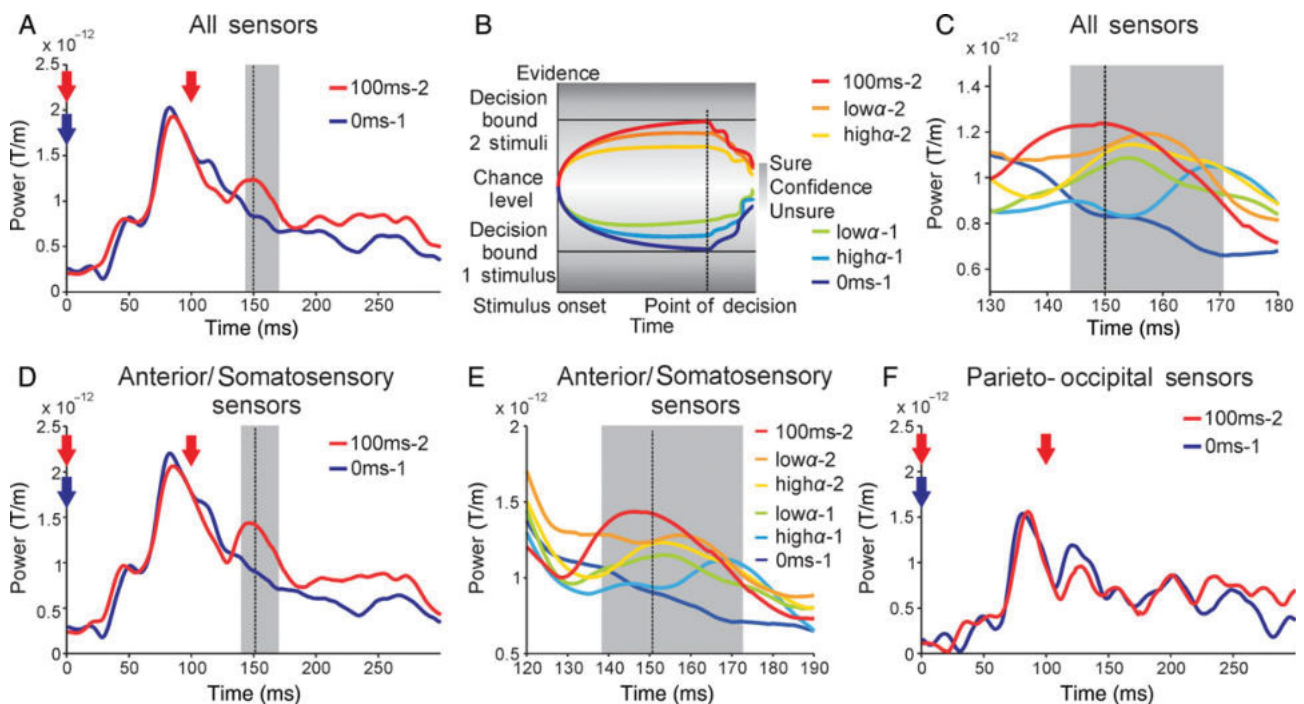


**Figure 4.** Results of the analysis of poststimulus ERFs. (A) Statistical comparison of poststimulus ERF amplitudes (averaged over all significant sensors, as shown in Fig. 2B) of correctly perceived trials with 0 ms (0ms-1) and 100 ms (100ms-2) SOA. Significant differences are indicated by shaded area (145–171 ms). The dashed line represents the point of maximum amplitude difference between the reference conditions 0ms-1 and 100ms-2 (150 ms). The blue arrow highlights the time point of stimulation for the 0ms-1 condition, while the red arrows highlight the time points of stimulation for the 100ms-2 condition. (B) Predicted poststimulus ERFs. Decision model illustrating the hypothesized order of poststimulus ERFs. Conditions 0ms-1 and 100ms-2 reflect the decision bounds for perceiving 1 and 2 stimuli, respectively. The other conditions are predicted to be between these bounds in the presented order. Distance to the bound is hypothesized to reflect confidence in the decision (indicated by gray-shaded background). The dashed line represents the point of maximum amplitude difference between the reference conditions 0ms-1 and 100ms-2. Beyond this point, the decision variables are thought to decline again to baseline. (C) MEG data of poststimulus ERFs. Close-up on the time window of significant difference (145–171 ms; shaded area) between poststimulus ERF amplitudes of 0ms-1 and 100ms-2 (averaged over all significant sensors, as shown in Fig. 2B). Shaded area and dashed line as in A. Color scheme as in B. (D) Same as A, but now for amplitude values averaged over the anterior/somatosensory sensor-cluster (as shown in Fig. 2B; time window: 139–172 ms; time point of maximum amplitude difference: 151 ms). Blue and red arrows as in A. (E) Same as C, but now for amplitude values averaged over the anterior/somatosensory sensor-cluster (as shown in Fig. 2B; time window: 139–172 ms; time point of maximum amplitude difference: 151 ms). Shaded area and dashed line as in D. (F) Same as A, but now for amplitude values averaged over the parieto-occipital sensor-cluster (as shown in Fig. 2B). Blue and red arrows as in A. No statistically significant difference was found. Significance values in A–F are cluster corrected to account for multiple comparison corrections.  $t = 0$  indicates onset of sensory stimulation, that is, the first stimulus of every stimulation.

time window showing a significant difference between the conditions 0ms-1 and 100ms-2 was found, we refrained from performing this analysis for the parieto-occipital sensor-cluster.

## Results

### Behavioral Results

Subjects performed a forced-choice temporal perceptual discrimination task (Fig. 1) and had to report how many electrical stimulations applied to their left index finger they perceived. For SOAs of 0 and 100 ms, subjects made only negligible errors (SOA 0 ms:  $92.3 \pm 1.8\%$  [mean  $\pm$  SD] correct reports; SOA of 100 ms:  $93.8 \pm 2.7\%$  correct reports). For intermediate SOAs, subjects correctly perceived stimulation in approximately half of the trials ( $56.7 \pm 3.2\%$  correct reports). The response distribution of each condition did not significantly differ from a Gaussian distribution ( $P > 0.05$ ). Statistical testing revealed highly significant differences regarding temporal perceptual discrimination rates between the intermediate condition and the 0 ms ( $t_{(15)} = 10.086$ ,  $P < 0.0001$ ) as well as the 100 ms condition ( $t_{(15)} = 11.811$ ,  $P < 0.0001$ ). Overall, the absolute influence of learning/fatigue is negligible. No significant linear trends indicating learning or fatigue effects could be determined for average temporal perceptual discrimination

rate ( $r = 0.49$ ,  $P > 0.05$ , Supplementary Fig. 2A) or confidence ratings ( $r = 0.55$ ,  $P > 0.05$ , Supplementary Fig. 2B).

### Time–Frequency Analysis

We studied the role of prestimulus alpha-band oscillations (8–12 Hz) on temporal perceptual discrimination. We focused on trials with intermediate SOA and compared alpha power in the prestimulus period (–900 to 0 ms) between correctly and incorrectly perceived trials. The exploratory time–frequency analysis confirmed a prominent alpha effect in the prestimulus period (Fig. 2A). Prestimulus alpha power was found to be statistically significantly decreased if subjects correctly perceived the stimulation as 2 stimuli compared with incorrectly perceived trials ( $P < 0.05$ , Fig. 2B). Significant differences were most evident for anterior/somatosensory and parieto-occipital sensors contralateral to stimulation site between –900 and –250 ms. Particularly, the topographical location of the effect shifted over time, with significant decreases in both contralateral anterior/somatosensory and parieto-occipital sensors at the beginning of the prestimulus epoch (–900 to –500 ms), compared with a decrease of power in more posterior sensors in the later prestimulus epoch (–400 to –250 ms). Note that, although both sensor-clusters show a

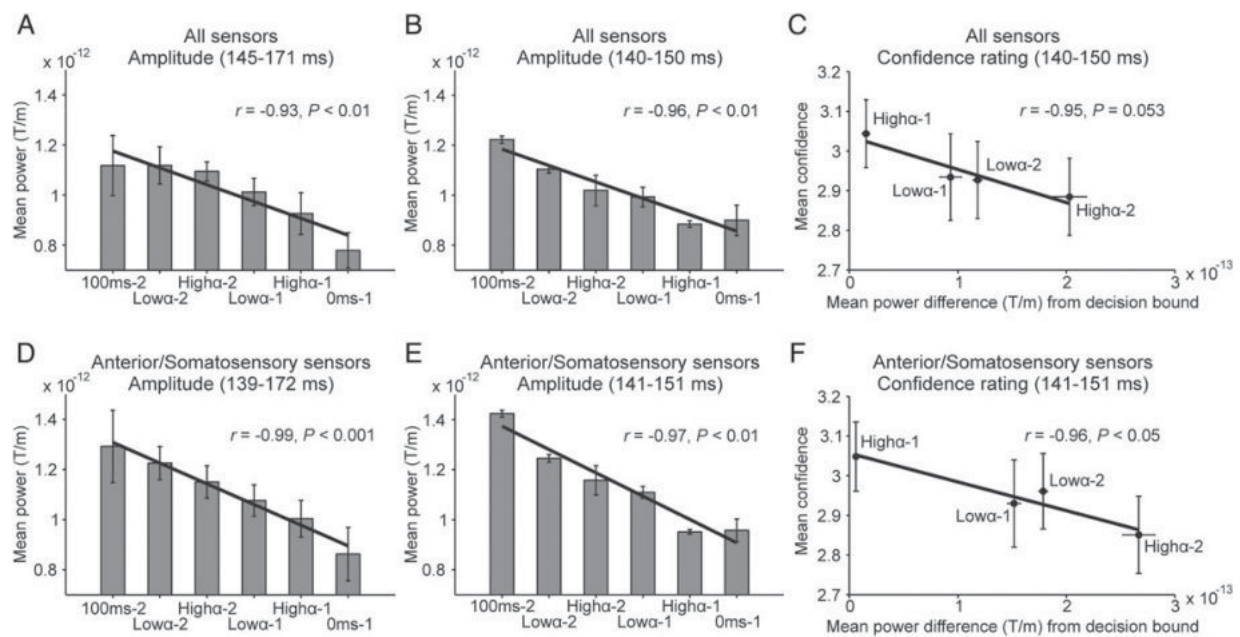


**Figure 5.** Averaged amplitude values and confidence ratings of poststimulus ERFs. (A) Amplitude values (based on all significant sensors, as shown in Fig. 2B) averaged over the time window showing a significant difference between poststimulus ERF amplitudes of 0ms-1 and 100ms-2 (145–171 ms, see Fig. 4A,C). (B) Amplitude values (based on all significant sensors, as shown in Fig. 2B) averaged over the time window preceding the point of maximal amplitude difference (150 ms) between poststimulus ERF amplitudes of 0ms-1 and 100ms-2 (140–150 ms, see Fig. 4A,C). (C) Average confidence ratings per condition in relation to mean power difference to the respective decision bound (based on all significant sensors, as shown in Fig. 2B) for the time window 140 to 150 ms (see Fig. 4A,C). (D) Same as A, but now for amplitude values based on the anterior/somatosensory sensor-cluster (as shown in Fig. 2B; time window: 139–172 ms, Fig. 4D,E). (E) Same as B, but now for amplitude values based on the anterior/somatosensory sensor-cluster (as shown in Fig. 2B; time window: 141–151 ms, Fig. 4D,E). (F) Same as C, but now for mean power difference based on the anterior/somatosensory sensor-cluster (as shown in Fig. 2B; time window 141–151 ms, Fig. 4D,E). In A, B, D, and E conditions are ordered according to the hypothesized decision model (Fig. 4B). Insets in A, B, D, and E show results of the linear regression analyses (black lines) based on all 6 conditions (i.e., 100ms-2, low  $\alpha$ -2, high  $\alpha$ -2, low  $\alpha$ -1, high  $\alpha$ -1, 0ms-1). Note that the additional regression analyses excluding the 100ms-2 and 0ms-1 conditions similarly demonstrate a significant negative linear correlation ( $P < 0.05$ ; regression lines not shown) for the ordered intermediate ERFs (i.e., low  $\alpha$ -2, high  $\alpha$ -2, low  $\alpha$ -1, high  $\alpha$ -1) for all 4 time windows (145–171, 140–150, 139–172, 141–151 ms). Insets in C and F show results of the linear regression analyses (black lines).

significant alpha power decrease in the prestimulus epoch, the decision-related effects of alpha power visible in the poststimulus ERFs could only be demonstrated for the anterior/somatosensory sensor-cluster (see Relation between Decision Variable, Prestimulus Power, and Poststimulus ERFs and Fig. 4).

### Source Reconstruction

To identify the underlying cortical sources of the aforementioned significant effect, we applied a beamforming approach. We identified one source mainly located in contralateral postcentral gyrus (Brodmann area 3, Fig. 2C). A second cluster was found in the contralateral middle occipital region, encompassing Brodmann areas 19, 21, and 39.

### Correlation of Prestimulus Power, Perceptual Decisions, and Confidence Ratings

To determine more precisely the relation of prestimulus alpha power and subjective perception, we performed a correlation analysis. We computed single-trial power averaged over alpha frequencies and significant sensor-time points (time window: –900 to –250 ms, see Fig. 2B). Trials were sorted from low to high power and divided into 5 bins. Response probabilities for each bin were calculated as the percentage change in temporal perceptual discrimination rate from the mean, normalized per subject to the individual mean temporal perceptual discrimination rate over all bins.

We found a significant negative linear relationship between prestimulus alpha power averaged over all sensors showing a significant alpha power difference between correctly (perceived 2 stimuli) versus incorrectly (perceived 1 stimulus) perceived trials with intermediate SOA and subjects' perceptual decisions ( $r = -0.94$ ,  $P < 0.05$ , Fig. 3A). In other words, probability of correctly perceiving the stimulation as 2 temporally separate stimuli was greater during trials with lower prestimulus alpha power. A one-way repeated-measures ANOVA revealed a significant main effect ( $P < 0.05$ ). Post hoc *t*-tests revealed significant differences between bin1 versus bin4 ( $t_{(15)} = 3.049$ ,  $P < 0.01$ ), bin1 versus bin5 ( $t_{(15)} = 3.096$ ,  $P < 0.01$ ), bin2 versus bin4 ( $t_{(15)} = 2.545$ ,  $P < 0.05$ ), and bin3 versus bin4 ( $t_{(15)} = 2.142$ ,  $P < 0.05$ ). No significant quadratic relationship between prestimulus alpha power and subject's perceptual decisions was found ( $r = 0.94$ ,  $P = 0.11$ ). In addition, we performed the same analysis with power values averaged over the sensors of the spatiotemporally separated sensor-clusters (anterior/somatosensory vs. parieto-occipital). For the anterior/somatosensory sensor-cluster, both linear ( $r = -0.97$ ,  $P < 0.01$ ) and quadratic ( $r = 0.99$ ,  $P < 0.05$ ) fits for the relationship between prestimulus alpha power and subjects' perceptual decisions were significant. A one-way repeated-measures ANOVA revealed an effect on trend level ( $P = 0.1$ ). Post hoc *t*-tests revealed significant differences between bin1 versus bin4 ( $t_{(15)} = 2.74$ ,  $P < 0.05$ ), bin1 versus bin5 ( $t_{(15)} = 2.14$ ,  $P < 0.05$ ), and bin2 versus bin4 ( $t_{(15)} = 2.32$ ,  $P < 0.05$ ). Similarly for the parieto-occipital sensor-cluster, both linear ( $r = -0.96$ ,  $P < 0.05$ ) and quadratic ( $r = 0.99$ ,  $P < 0.05$ ) fits for the relationship between prestimulus alpha power and

subjects' perceptual decisions were significant. No significant effect was found by a one-way repeated-measures ANOVA ( $P = 0.15$ ). Post hoc *t*-tests revealed significant differences between bin1 versus bin4 ( $t_{(15)} = 2.47, P < 0.05$ ).

In a similar analysis, we investigated the correlation between prestimulus alpha power and subjects' level of confidence regarding their perceptual decisions. We found a significant negative linear relationship between prestimulus alpha power averaged over all sensors showing a significant alpha power difference between correctly (perceived 1 stimuli) versus incorrectly (perceived 1 stimulus) perceived trials with intermediate SOA and confidence ratings for correctly perceived trials ( $r = -0.88, P < 0.05$ , Fig. 3B) and a strong trend toward a significant positive linear correlation for incorrectly perceived trials ( $r = 0.81, P = 0.095$ ). No significant quadratic relationship between prestimulus alpha power and subjects' confidence ratings was found (correct trials:  $r = 0.95, P = 0.1$ ; incorrect trials:  $r = 0.94, P = 0.11$ ). For the anterior/somatosensory sensor-cluster, a significant negative linear relationship between prestimulus alpha power and confidence ratings for correctly perceived trials ( $r = -0.92, P < 0.05$ ) could be demonstrated, while no significant effect was found for incorrect trials ( $r = 0.6, P = 0.28$ ). For quadratic relationships between prestimulus alpha power and subjects' confidence ratings, no significant fit was found (correct trials:  $r = 0.92, P = 0.14$ ; incorrect trials:  $r = 0.8, P = 0.35$ ). Finally, no significant linear or quadratic relationship between prestimulus alpha power and confidence ratings could be demonstrated for the parieto-occipital cluster, neither for correct (linear:  $r = -0.49, P = 0.41$ ; quadratic:  $r = 0.59, P = 0.65$ ) or incorrect trials (linear:  $r = 0.73, P = 0.17$ ; quadratic:  $r = 0.94, P = 0.11$ ).

### Relation Between Decision Variable, Prestimulus Power, and Poststimulus ERFs

We investigated if poststimulus ERFs show characteristics of a decision variable and the influence of prestimulus alpha power on these variables. We analyzed poststimulus ERFs by applying a boundary-crossing decision-making model (Philiastides et al. 2006; O'Connell et al. 2012). To this end, we estimated decision bounds for the unambiguous perception of 1 and 2 stimuli by calculating poststimulus ERFs from all correct trials of the 0 and 100 ms SOA conditions, subsequently labeled 0ms-1 and 100ms-2. Statistical comparison revealed a significant difference between both ERF amplitudes between 145 and 171 ms ( $P < 0.05$ ), indicating that the 2 signals significantly diverge during this time window (Fig. 4A). The spatial distribution of the stimuli-evoked ERFs for those time points showing a significant difference between the conditions 0ms-1 and 100ms-2 (i.e., 145–171 ms) revealed highly similar patterns of activity over conditions (Supplementary Fig. 3).

According to our hypothesis, these ERFs should reflect the lower and upper boundaries for decisions toward 1 and 2 stimuli, respectively. ERFs of trials with intermediate SOA should be located in between these boundaries and the distance toward the respective boundary should reflect the perceptual decision as well as the confidence in the decision (Fig. 4B). The results demonstrate that, despite physically identical stimulation, the ERFs of trials with intermediate SOA differ with respect to subjects' perception and prestimulus alpha power (Fig. 4C). In line with our hypothesis, we found a significant negative linear correlation for the ordered averaged ERFs (i.e., 100ms-2, low  $\alpha$ -2, high  $\alpha$ -2, low  $\alpha$ -1, high  $\alpha$ -1, 0ms-1), indicating a monotonic decrease in amplitude from the 100ms-2 condition to the 0ms-1 condition ( $r = -0.93, P < 0.01$  for time window 145–171 ms, Fig. 5A;  $r = -0.96,$

$P < 0.01$  for time window 140–150 ms, Fig. 5B). An additional regression analysis which excluded the 100ms-2 and 0ms-1 conditions also revealed a significant negative linear correlation for the ordered averaged intermediate ERFs (i.e., low  $\alpha$ -2, high  $\alpha$ -2, low  $\alpha$ -1, high  $\alpha$ -1), indicating a monotonic decrease in amplitude from the low  $\alpha$ -2 condition to the high  $\alpha$ -1 condition ( $r = -0.97, P < 0.05$  for time window 145–171 ms, see also captions Fig. 5;  $r = -0.98, P < 0.05$  for time window 140–150 ms, see also captions Fig. 5). A one-way repeated-measures ANOVA revealed a strong trend toward a significant main effect ( $P = 0.065$ ) for the analysis of the time window 145–171 ms. No significant effect was found for the time window 140–150 ms.

For the additional regression analysis performed on the anterior/somatosensory sensor-cluster (Fig. 4D,E), a significant negative linear correlation for the ordered averaged ERFs (i.e., 100ms-2, low  $\alpha$ -2, high  $\alpha$ -2, low  $\alpha$ -1, high  $\alpha$ -1, 0ms-1) could be demonstrated ( $r = -0.99, P < 0.001$  for time window 139–172 ms, Fig. 5D;  $r = -0.97, P < 0.01$  for time window 141–151 ms, Fig. 5E). The negative linear correlations remained significant under exclusion of the 100ms-2 and 0ms-1 conditions ( $r = -0.99, P < 0.001$  for time window 139–172 ms, see also captions Fig. 5;  $r = -0.97, P < 0.05$  for time window 141–151 ms, see also captions Fig. 5). A one-way repeated-measures ANOVA revealed a significant main effect for both time windows ( $P < 0.05$  for time window 139–172 ms;  $P < 0.05$  for time window 141–151 ms). Because no time window showing a significant difference between the conditions 0ms-1 and 100ms-2 was found for the parieto-occipital sensor-cluster (see Fig. 4F), we refrained from performing the regression analysis for the parieto-occipital sensor-cluster.

We further related the average confidence ratings per condition to the distance of the decision variables to the respective decision bounds. According to our hypothesis, the average confidence ratings per condition should increase with closer proximity of the decision variables to the respective decision bounds (see Fig. 4B). While for the time window from 145 to 171 ms, no significant linear relation between confidence ratings and distance of the decision variables to the respective decision bounds could be demonstrated ( $r = 0.43, P = 0.57$ ), a strong trend toward a significant negative linear relation ( $r = -0.95, P = 0.053$ ) was evident for the time window from 140 to 150 ms (Fig. 5C). For the critical time windows based on the anterior/somatosensory sensor-cluster, a significant negative linear relation could only be demonstrated for the time window from 141 to 151 ms ( $r = -0.96, P < 0.05$ , Fig. 5F). For the time window from 139 to 172 ms, no significant linear fit was found ( $r = -0.24, P = 0.84$ ). Regarding the time windows before the point of maximum amplitude difference (140–150 ms for all significant sensors, 141–151 ms for the anterior/somatosensory sensor-cluster), in agreement with our hypothesis a closer distance to the reference conditions resulted in higher confidence ratings. Because no time window showing a significant difference between the conditions 0ms-1 and 100ms-2 was found for the parieto-occipital sensor-cluster, we refrained from performing this analysis for the parieto-occipital sensor-cluster.

### Discussion

We investigated the influence of prestimulus alpha activity on the temporal perceptual discrimination of suprathreshold tactile stimuli, the confidence in perceptual decisions and the underlying neuronal decision variable. Subjects received 1 or 2 tactile stimuli with different SOAs. In a forced-choice task, subjects reported their perceptual decision and their confidence in this decision.

Subjects frequently misperceived stimulation as 1 stimulus for trials with intermediate SOA, indicating perceptual ambiguity despite physically identical stimulation. For these trials with intermediate SOA, correct perception of 2 separate stimuli was correlated with a decrease of alpha power (8–12 Hz) relative to incorrectly perceived trials. This effect was evident before onset of stimulation (–900 to –250 ms) mainly in the contralateral postcentral gyrus (presumably primary somatosensory cortex) and the contralateral middle occipital region. Additionally, prestimulus alpha power correlated with subjects' confidence ratings. For correctly perceived trials, high confidence ratings correlated with low prestimulus alpha power. Contrarily, for incorrectly perceived trials, high confidence ratings correlated with high prestimulus alpha power. Finally, poststimulus ERFs at ~150 ms revealed characteristics of a decision variable. In summary, we found: 1) Poststimulus ERFs at ~150 ms reflect perceptual decisions and subjects' confidence in their decisions rather than pure sensory evidence. 2) ERFs for all conditions were in line with an accumulation-to-bound model in which sensory evidence is accumulated in a decision variable (Gold and Shadlen 2007). In trials with ambiguous, intermediate SOA, ERFs of correctly perceived trials were closer to the putative categorical decision bound for perceiving 2 stimuli while incorrectly perceived trials were closer to the categorical decision bound for perceiving 1 stimulus. 3) Due to their perceptual ambiguity, stimuli with intermediate SOA provided only incomplete sensory evidence, resulting in incomplete evidence accumulation and hence ERFs did not cross the decision bound. 4) Incomplete evidence accumulation resulted in lower confidence as reflected in the ERFs. 5) The variability of ERFs, decisions, and confidence ratings is biased by fluctuations of prestimulus alpha power. 6) Finally, the above-mentioned results could be replicated only for the anterior/somatosensory sensor-cluster after separating the sensors of interest. Therefore, it appears that mainly the somatosensory cortex areas account for the decision-related components visible at ~150 ms.

We estimated the poststimulus categorical decision boundaries by calculating significant differences between ERFs of the reference conditions 0ms-1 and 100ms-2. One might argue that these conditions differ not only by subjects' decisions but also by sensory evidence (1 stimulus vs. 2 stimuli), and thus, our putative decision variable might reflect sensory input rather than decisional processes. However, we demonstrate that ERFs around ~150 ms for trials with intermediate SOA, that is, with constant stimulation, correlate with perceptual decisions rather than sensory input.

Several studies have reported an inverted U-shaped relationship between prestimulus alpha power and perceptual performance, with intermediate alpha levels resulting in best performance levels (Linkenkaer-Hansen et al. 2004; Zhang and Ding 2009; Lange et al. 2012). On the contrary, other studies emphasize a linear relationship, with lower power levels being related to better performance (Thut et al. 2006; Hanslmayr et al. 2007; Schubert et al. 2008; van Dijk et al. 2008; Mathewson et al. 2009; Jones et al. 2010). In the present study, linear as well as quadratic fits were applied to the data. For most analyses, both linear and quadratic fits were significant for the correlation of prestimulus alpha power and perceptual decisions for the anterior/somatosensory and the parieto-occipital sensor-cluster. This demonstration of both linear and quadratic dependencies hinders a final conclusion on this matter. It remains to be seen if future studies can clarify the relevant factors in terms of neuroanatomical region or experimental conditions favoring one dependency over the other.

Notably, the majority of previous studies used near-threshold stimuli and relied on conditions where stimuli are either perceived or not perceived. Thus, subjects had to report whether or not stimulation is perceived, irrespective of its content. Here, we contrasted 2 different perceptual qualities with suprathreshold intensities, since subjects had to report whether they perceived 1 stimulus or 2 stimuli. Our paradigm therefore focuses on temporal discrimination and employs temporal ambiguity, with identical suprathreshold stimulation resulting in varying perceptual decisions. Hence, the present study provides critical extensions to the aforementioned studies.

Our results are in line with several studies reporting a correlation of prestimulus alpha power and detection or discrimination of near-threshold stimuli (e.g., Linkenkaer-Hansen et al. 2004; Zhang and Ding 2009; Jones et al. 2010). We critically extend these studies by demonstrating that alpha power influences also the temporal resolution of perception. Although formerly interpreted as correlate of cortical idling (Pfurtscheller et al. 1996), alpha activity has recently been suggested to gate neuronal processing by functional inhibition of task-irrelevant areas (Jensen and Mazaheri 2010; Jensen et al. 2012) and/or by modulating cortical excitability (Thut et al. 2006; Romei, Brodbeck et al. 2008; Romei, Rihs et al. 2008; Lange et al. 2013), resulting in more efficient neuronal stimulus processing in task-related neuronal groups. By using 2 clearly suprathreshold stimuli, we demonstrate that prestimulus alpha power extends the role of a simple binary switch between inhibition and processing. Rather, it modulates the quantity (1 stimulus or 2 stimuli, e.g., Lange et al. 2013; Keil et al. 2014) and the subjective quality (i.e., confidence) of perception continuously. This continuous modulation is reflected in confidence ratings, providing a more fine-grained scale of the decision process.

Prestimulus alpha power can be modulated by attention or expectation (Foxe et al. 1998; Worden et al. 2000; Jones et al. 2010; Anderson and Ding 2011; Haegens et al. 2012). In line with these results, recent studies demonstrated that prestimulus alpha power is predictive of perceptual performance in attention-based tasks (Kelly et al. 2009; O'Connell et al. 2009). While we did not explicitly modulate attention in our study, we suggest that spontaneous fluctuations of attention or arousal modulate prestimulus alpha power and thus influence perception and confidence. Further, it seems that such fluctuations are distinguishable from general training effects, since we did not find significant learning/fatigue trends for either perception or confidence.

We found alpha power to differ significantly in the prestimulus period in the contralateral postcentral gyrus and contralateral middle occipital region. Differential alpha-band activity in the postcentral gyrus (presumably primary somatosensory areas) has been found for other tactile tasks (e.g., Zhang and Ding 2009; Jones et al. 2010; Lange et al. 2012). Here, we extend the role of the postcentral gyrus to temporal perceptual discrimination of 2 subsequently presented stimuli. Since we applied only tactile stimuli and a tactile decision task, the significant alpha-band effect in visual areas might seem surprising. However, our results are in line with findings from a tactile spatial attention task, showing that in the absence of visual stimulation, attention to tactile stimulation resulted in suppression of alpha-band power in occipital areas (Bauer et al. 2006). Similarly, a recent study indicates that task-relevant spatial attention in one sensory domain affects oscillatory activity in other domains (Bauer et al. 2012). In accordance to these findings, a recent study demonstrated that parieto-occipital activation in the alpha band is linked to spatial attention across modalities (Banerjee et al. 2011).

In line with these results, the power differences in the contralateral middle occipital region can also be interpreted as correlate of global attention, thus not restricted to the somatosensory domain. This is supported by classical findings which localize the central generator of alpha rhythms in parieto-occipital areas (e.g., Salmelin and Hari 1994; Manshanden et al. 2002), independent of task requirements. The explanation is further strengthened by our findings that the decision-related ERF components could only be found for the anterior/somatosensory sensor-cluster, but not in the parieto-occipital cluster. This indicates that the parieto-occipital sensor-cluster, although showing significant power differences between perceptual conditions, is not central for decision-related processes. The influence of prestimulus alpha on decision variables is also in line with a recent EEG study (Lou et al. 2014). In this study, the influence of prestimulus activity is seen as top-down attention-based modulation, indicating that the sensory evidence is comprised of stimulus information and attentional state.

We demonstrate that prestimulus alpha power does not only correlate with perceptual decisions, but also with the subjective quality of such decisions. If alpha power was low, subjects were more confident with their decisions, but notably only for correctly perceived stimuli. Contrarily, if stimulation was perceived incorrectly, low alpha power correlated with low confidence. This seemingly contradictory result can be explained by a decision model. It has been proposed that sensory evidence is accumulated over time in a decision variable until a decision bound is reached (e.g., Shadlen and Newsome 2001). Here, we used such a decision-to-bound model to examine poststimulus decision variables. We hypothesized that due to the ambiguity of sensory evidence the decision variable does not cross a decision bound. Further, fluctuations of prestimulus alpha power should influence the decision variable and the confidence in perceptual decisions, if sensory evidence was insufficient to reach a decision bound. We identified this proposed pattern of a decision variable in poststimulus ERFs at  $\sim 150$  ms. Despite identical stimulation, poststimulus ERFs of trials with intermediate SOA differed according to the decisional outcome. While neither condition reached the categorical decision bound, the distance of the decision variable to the respective decision bounds determined the decisional outcome.

We identified perceptual decision-related components in the somatosensory domain, that is, differences in ERF amplitudes for conditions with physically similar stimulation parameters that discriminated between perceptual reports, as early as  $\sim 150$  ms. Other recent studies addressing perceptual decision making in the visual domain report decision-related neural activity at later time points ( $\sim 300$  ms) and relate earlier components to low-level stimulus processing mechanisms (Philiastides et al. 2006; Lou et al. 2014). Such stimulus processing mechanisms can hardly fully explain our results, since our stimulation parameters remained constant for trials with intermediate SOA. An early decision-related component is further supported by studies where early components around  $\sim 75$ – $80$  ms were shown to discriminate between high-level properties such as semantic category and components around  $\sim 150$  ms discriminate between target and nontarget conditions (and hence task-specific decision-related demands), independent of visual category (VanRullen and Thorpe 2001). In line with these results, the present components around  $\sim 150$  ms can be interpreted as a correlate of the subjects' perceptual recognition and subsequent decision, not merely as stimulus-related bottom-up processing. However, it is important to keep in mind that somatosensory processing presumably does not end after

the aforementioned component, but it appears that at this time point sufficient information for a perceptual decision is accumulated.

Kiani and Shadlen (2009) recorded neuronal activity in monkey lateral intraparietal cortex during a decision-making task. If the monkey chose to opt out, that is, at low confidence levels, neural activity was at an intermediate level between decision bounds. We used a more detailed confidence rating and found that subjects' confidence correlated with the distance to a decision bound. This suggests that categorical decision making and confidence estimation can be a simple and fast inherent property of the same process (e.g., Kepecs et al. 2008; Kiani and Shadlen 2009), rather than a serial process requiring additional steps or higher (meta) cognitive functions (e.g., Grinband et al. 2006; Yeung and Summerfield 2012).

Additionally, we found poststimulus ERFs to interact with prestimulus alpha levels. Low prestimulus alpha levels shifted the decision variable towards the decision bound for 2 perceived stimuli, independent of decisional outcome. For correctly perceived intermediate SOA trials, low prestimulus alpha power increased confidence, because the distance between the decision variable and the decision bound for 2 perceived stimuli decreased. Contrarily, for incorrectly perceived intermediate SOA trials, low prestimulus alpha power decreased confidence, because the distance between the decision variable and the decision boundary for 1 perceived stimulus increased. The influence of prestimulus alpha power on poststimulus ERFs is in line with recent studies (Jones et al. 2009, 2010; Anderson and Ding 2011; Lange et al. 2012). The influence of prestimulus activity on decisions and the underlying decision variable is also in line with a recent study demonstrating that prestimulus firing rates bias decisions (Carnevale et al. 2012). While this study considers prestimulus activity as noise fluctuations, we argue that prestimulus alpha power is a functionally relevant marker of cortical excitability that can fluctuate over time or that can be endogenously or exogenously modulated by, for example, attention, arousal, or expectation (e.g., Foxe et al. 1998; Worden et al. 2000; Thut et al. 2006; Jones et al. 2010; Anderson and Ding 2011; de Lange et al. 2011).

In line with a recent study (de Lange et al. 2013), we suggest that prestimulus alpha power biases the starting point of the decision variable. Thus, the decision variable is the combination of the internal brain state (prestimulus activity) and the sensory evidence provided by the stimulus. If sensory evidence is weak or ambiguous, prestimulus activity can effectively bias decisions and confidence ratings by shifting the decision variable closer to either decision bound. The fact that prestimulus activity influences the decisional process implies that the decision-making process starts before stimulus presentation (Carnevale et al. 2012; de Lange et al. 2013). Such prestimulus fluctuations can also explain why decisions, confidence ratings, or response times can vary despite physically identical stimulation.

In conclusion, our results demonstrate that the brain state, characterized by alpha power, substantially modulates temporal perceptual discrimination of tactile stimuli despite identical physical stimulation, as well as confidence in perceptual decisions. Moreover, these fluctuations in prestimulus alpha power are visible in poststimulus ERFs mainly determined by somatosensory areas, reflecting the physiological correlate of evidence accumulation in a decision variable for perceptual decisions based on insufficient and suboptimal evidence. We conclude that alpha-band activity continuously modulates the quality of processing underlying perceptual decisions, resulting in differences in temporal perceptual discrimination.

## Supplementary Material

Supplementary material can be found at: <http://www.cercor.oxfordjournals.org/>.

## Funding

J.L. was supported by the German Research Foundation (LA 2400/4-1).

## Notes

We thank Erika Rädisch for help with the MRI recordings. *Conflict of Interest*: None declared.

## References

- Anderson KL, Ding M. 2011. Attentional modulation of the somatosensory mu rhythm. *Neuroscience*. 180:165–180.
- Banerjee S, Snyder AC, Molholm S, Foxe JJ. 2011. Oscillatory alpha-band mechanisms and the deployment of spatial attention to anticipated auditory and visual target locations: supramodal or sensory-specific control mechanisms? *J Neurosci*. 31:9923–9932.
- Başar E, Başar-Eroglu C, Rosen B, Schütt A. 1984. A new approach to endogenous event-related potentials in man: relation between EEG and P300-Wave. *Int J Neurosci*. 24:1–21.
- Bauer M, Kennett S, Driver J. 2012. Attentional selection of location and modality in vision and touch modulates low-frequency activity in associated sensory cortices. *J Neurophysiol*. 107:2342–2351.
- Bauer M, Oostenveld R, Peeters M, Fries P. 2006. Tactile spatial attention enhances gamma-band activity in somatosensory cortex and reduces low-frequency activity in parieto-occipital areas. *J Neurosci*. 26:490–501.
- Brandt ME, Jansen BH. 1991. The relationship between prestimulus alpha amplitude and visual evoked potential amplitude. *Int J Neurosci*. 61:261–268.
- Britten KH, Newsome WT, Shadlen MN, Celebrini S, Movshon JA. 1996. A relationship between behavioral choice and the visual responses of neurons in macaque MT. *Vis Neurosci*. 13:87–100.
- Carnevale F, de Lafuente V, Romo R, Parga N. 2012. Internal signal correlates neural populations and biases perceptual decision reports. *Proc Nat Acad Sci USA*. 109:18938–18943.
- de Lange FP, Rahnev DA, Donner TH, Lau H. 2013. Prestimulus oscillatory activity over motor cortex reflects perceptual expectations. *J Neurosci*. 33:1400–1410.
- de Lange FP, van Gaal S, Lamme VAF, Dehaene S. 2011. How awareness changes the relative weights of evidence during human decision-making. *PLoS Biol*. 9:e1001203.
- Foxe JJ, Simpson GV, Ahlfors SP. 1998. Parieto-occipital ~10 Hz activity reflects anticipatory state of visual attention mechanisms. *Neuroreport*. 9:3929–3933.
- Gold JI, Shadlen MN. 2007. The neural basis of decision making. *Annu Rev Neurosci*. 30:535–574.
- Grinband J, Hirsch J, Ferrera VP. 2006. A neural representation of categorization uncertainty in the human brain. *Neuron*. 49:757–763.
- Gross J, Kujala J, Hamalainen M, Timmermann L, Schnitzler A, Salmelin R. 2001. Dynamic imaging of coherent sources: studying neural interactions in the human brain. *Proc Nat Acad Sci USA*. 98:694–699.
- Haegens S, Luther L, Jensen O. 2012. Somatosensory anticipatory alpha activity increases to suppress distracting input. *J Cogn Neurosci*. 24:677–685.
- Hanslmayr S, Aslan A, Staudigl T, Klimesch W, Herrmann CS, Bäuml K. 2007. Prestimulus oscillations predict visual perception performance between and within subjects. *Neuroimage*. 37:1465–1473.
- Hari R, Kaukoranta E. 1985. Neuromagnetic studies of somatosensory system: principles and examples. *Prog Neurobiol*. 24:233–256.
- Hoogenboom N, Schoffelen J, Oostenveld R, Fries P. 2010. Visually induced gamma-band activity predicts speed of change detection in humans. *Neuroimage*. 51:1162–1167.
- Jensen O, Bonnefond M, VanRullen R. 2012. An oscillatory mechanism for prioritizing salient unattended stimuli. *Trends Cogn Sci*. 16:200–206.
- Jensen O, Mazaheri A. 2010. Shaping functional architecture by oscillatory alpha activity: gating by inhibition. *Front Hum Neurosci*. 4:186.
- Jones SR, Pritchett DL, Sikora MA, Stufflebeam SM, Hämäläinen M, Moore CI. 2009. Quantitative analysis and biophysically realistic neural modeling of the MEG mu rhythm: rhythmogenesis and modulation of sensory-evoked responses. *J Neurophysiol*. 102:3554–3572.
- Jones SR, Kerr CE, Wan Q, Pritchett DL, Hamalainen M, Moore CI. 2010. Cued spatial attention drives functionally relevant modulation of the mu rhythm in primary somatosensory cortex. *J Neurosci*. 30:13760–13765.
- Keil J, Müller N, Hartmann T, Weisz N. 2014. Prestimulus beta power and phase synchrony influence the sound-induced flash illusion. *Cereb Cortex*. 24:1278–1288.
- Kelly SP, Gomez-Ramirez M, Foxe JJ. 2009. The strength of anticipatory spatial biasing predicts target discrimination at attended locations: a high-density EEG study. *Eur J Neurosci*. 30:2224–2234.
- Kepecs A, Uchida N, Zariwala HA, Mainen ZF. 2008. Neural correlates, computation and behavioural impact of decision confidence. *Nature*. 455:227–231.
- Kiani R, Shadlen MN. 2009. Representation of confidence associated with a decision by neurons in the parietal cortex. *Science*. 324:759–764.
- Lange J, Halacz J, van Dijk H, Kahlbrock N, Schnitzler A. 2012. Fluctuations of prestimulus oscillatory power predict subjective perception of tactile simultaneity. *Cereb Cortex*. 22:2564–2574.
- Lange J, Oostenveld R, Fries P. 2011. Perception of the touch-induced visual double-flash illusion correlates with changes of rhythmic neuronal activity in human visual and somatosensory areas. *Neuroimage*. 54:1395–1405.
- Lange J, Oostenveld R, Fries P. 2013. Reduced occipital alpha power indexes enhanced excitability rather than improved visual perception. *J Neurosci*. 33:3212–3220.
- Linkenkaer-Hansen K, Nikulin VV, Palva S, Ilmoniemi RJ, Palva JM. 2004. Prestimulus oscillations enhance psychophysical performance in humans. *J Neurosci*. 24:10186–10190.
- Litvak V, Mattout J, Kiebel S, Phillips C, Henson R, Kilner J, Barnes G, Oostenveld R, Daunizeau J, Flandin G, et al. 2011. EEG and MEG data analysis in SPM8. *Comput Intell Neurosci*. 2011:852961.
- Lou B, Li Y, Philiastides MG, Sajda P. 2014. Prestimulus alpha power predicts fidelity of sensory encoding in perceptual decision making. *Neuroimage*. 87:242–251.
- Manshanden I, de Munck JC, Simon NR, Lopes da Silva FH. 2002. Source localization of MEG sleep spindles and the relation to

- sources of alpha band rhythms. *Clin Neurophysiol.* 113: 1937–1947.
- Maris E, Oostenveld R. 2007. Nonparametric statistical testing of EEG- and MEG-data. *J Neurosci Methods.* 164:177–190.
- Mathewson KE, Gratton G, Fabiani M, Beck DM, Ro T. 2009. To see or not to see: prestimulus  $\alpha$  phase predicts visual awareness. *J Neurosci.* 29:2725–2732.
- Mazaheri A, Jensen O. 2008. Asymmetric amplitude modulations of brain oscillations generate slow evoked responses. *J Neurosci.* 28:7781–7787.
- Mazaheri A, Nieuwenhuis ILC, van Dijk H, Jensen O. 2009. Prestimulus alpha and mu activity predicts failure to inhibit motor responses. *Hum Brain Mapp.* 30:1791–1800.
- Nolte G. 2003. The magnetic lead field theorem in the quasi-static approximation and its use for magnetoencephalography forward calculation in realistic volume conductors. *Phys Med Biol.* 48:3637–3652.
- O’Connell RG, Dockree PM, Kelly SP. 2012. A supramodal accumulation-to-bound signal that determines perceptual decisions in humans. *Nat Neurosci.* 15:1729–1735.
- O’Connell RG, Dockree PM, Robertson IH, Bellgrove MA, Foxe JJ, Kelly SP. 2009. Uncovering the neural signature of lapsing attention: electrophysiological signals predict errors up to 20 s before they occur. *J Neurosci.* 29:8604–8611.
- Oostenveld R, Fries P, Maris E, Schoffelen J. 2011. FieldTrip: open source software for advanced analysis of MEG, EEG, and invasive electrophysiological data. *Comput Intell Neurosci.* 2011:156869.
- Pfurtscheller G, Stancák A Jr, Neuper C. 1996. Event-related synchronization (ERS) in the alpha band—an electrophysiological correlate of cortical idling: a review. *Int J Psychophysiol.* 24:39–46.
- Philiastides MG, Ratcliff R, Sajda P. 2006. Neural representation of task difficulty and decision making during perceptual categorization: a timing diagram. *J Neurosci.* 26: 8965–8975.
- Philiastides MG, Sajda P. 2006. Temporal characterization of the neural correlates of perceptual decision making in the human brain. *Cereb Cortex.* 16:509–518.
- Ratcliff R, McKoon G. 2007. The diffusion decision model: theory and data for two-choice decision tasks. *Neural Comput.* 20:873–922.
- Romei V, Brodbeck V, Michel C, Amedi A, Pascual-Leone A, Thut G. 2008. Spontaneous fluctuations in posterior  $\alpha$ -band EEG activity reflect variability in excitability of human visual areas. *Cereb Cortex.* 18:2010–2018.
- Romei V, Gross J, Thut G. 2010. On the role of prestimulus alpha rhythms over occipito-parietal areas in visual input regulation: correlation or causation? *J Neurosci.* 30:8692–8697.
- Romei V, Rihs T, Brodbeck V, Thut G. 2008. Resting electroencephalogram alpha-power over posterior sites indexes baseline visual cortex excitability. *Neuroreport.* 19:203–208.
- Salmelin R, Hari R. 1994. Characterization of spontaneous MEG rhythms in healthy adults. *Electroencephalogr Clin Neurophysiol.* 91:237–248.
- Schubert R, Haufe S, Blankenburg F, Villringer A, Curio G. 2008. Now you’ll feel it, now you won’t: EEG rhythms predict the effectiveness of perceptual masking. *J Neurosci.* 21:2407–2419.
- Shadlen MN, Newsome WT. 2001. Neural basis of a perceptual decision in the parietal cortex (Area LIP) of the rhesus monkey. *J Neurophysiol.* 86:1916–1936.
- Thut G, Nietzel A, Brandt SA, Pascual-Leone A. 2006.  $\alpha$ -band electroencephalographic activity over occipital cortex indexes visuospatial attention bias and predicts visual target detection. *J Cogn Neurosci.* 26:9494–9502.
- van Dijk H, Schoffelen J, Oostenveld R, Jensen O. 2008. Prestimulus oscillatory activity in the alpha band predicts visual discrimination ability. *J Neurosci.* 28:1816–1823.
- VanRullen R, Thorpe SJ. 2001. The time course of visual processing: from early perception to decision-making. *J Cogn Neurosci.* 13:454–461.
- Worden MS, Foxe JJ, Wang N, Simpson GV. 2000. Anticipatory biasing of visuospatial attention indexed by retinotopically specific  $\alpha$ -band electroencephalography increases over occipital cortex. *J Neurosci.* 20:RC63.
- Wyart V, Tallon-Baudry C. 2009. How ongoing fluctuations in human visual cortex predict perceptual awareness: baseline shift versus decision bias. *J Neurosci.* 29:8715–8725.
- Yeung N, Summerfield C. 2012. Metacognition in human decision-making: confidence and error monitoring. *Philos Trans R Soc Lond B Biol Sci.* 367:1310–1321.
- Zhang Y, Ding M. 2009. Detection of a weak somatosensory stimulus: role of the prestimulus mu rhythm and its top-down modulation. *J Cogn Neurosci.* 22:307–322.

- 9) Baumgarten, T. J., Schnitzler, A., & **Lange, J.** (2015).  
Beta oscillations define discrete perceptual cycles in the somatosensory domain.  
*Proceedings of the National Academy of Sciences*, 112(39), 12187–12192.  
Impact factor (2015): 9.423

# Beta oscillations define discrete perceptual cycles in the somatosensory domain

Thomas J. Baumgarten<sup>1</sup>, Alfons Schnitzler, and Joachim Lange

Institute of Clinical Neuroscience and Medical Psychology, Medical Faculty, Heinrich-Heine-University Düsseldorf, 40225 Düsseldorf, Germany

Edited by Ranulfo Romo, Universidad Nacional Autónoma de México, Mexico City, D.F., Mexico, and approved July 31, 2015 (received for review January 22, 2015)

Whether seeing a movie, listening to a song, or feeling a breeze on the skin, we coherently experience these stimuli as continuous, seamless percepts. However, there are rare perceptual phenomena that argue against continuous perception but, instead, suggest discrete processing of sensory input. Empirical evidence supporting such a discrete mechanism, however, remains scarce and comes entirely from the visual domain. Here, we demonstrate compelling evidence for discrete perceptual sampling in the somatosensory domain. Using magnetoencephalography (MEG) and a tactile temporal discrimination task in humans, we find that oscillatory alpha- and low beta-band (8–20 Hz) cycles in primary somatosensory cortex represent neurophysiological correlates of discrete perceptual cycles. Our results agree with several theoretical concepts of discrete perceptual sampling and empirical evidence of perceptual cycles in the visual domain. Critically, these results show that discrete perceptual cycles are not domain-specific, and thus restricted to the visual domain, but extend to the somatosensory domain.

somatosensory perception | beta oscillations | MEG | oscillatory phase

The sensory system continuously receives and processes numerous stimuli. Subjective experience implies that conscious perception, and thus cortical processing, of this stimulation is also continuous. This view of continuous cortical processing, however, has been challenged by several studies proposing that the brain operates discontinuously within a framework of discretely sampled “perceptual cycles” (1–4). This process of perceptual cycles is thought to create a temporally defined window, with discrete stimuli falling inside this window being consciously perceived as a single event (4). Discrete sampling of sensory information allows for the possibility of transforming perceptual input into temporal code (5, 6), metabolic efficiency (7), and the efficient organization of information, thereby preventing information overload (6). Over the past decades, however, there has been an ongoing discussion about the nature of perception. Several studies have argued against the theory of discontinuous perceptual cycles (8, 9). In recent years, the hypothesis of a discontinuous cyclic perception received new support by electroencephalography (EEG) and magnetoencephalography (MEG) studies investigating neuronal oscillations. This novel support is attributable to the theory that serial perceptual sampling is thought to depend on the temporal relationship between external stimuli and some ongoing internal neurophysiological process (4) providing a temporal reference frame (5), with neuronal oscillations representing a probable candidate measure for this underlying process.

There is growing evidence that oscillatory power and phase influence cortical processing (10, 11) and perception (3, 12–14). Most of these studies investigated perception of single near-threshold stimuli. Although these studies demonstrate that neuronal oscillations play a critical role in defining neuronal states, which, in turn, influence perception and neuronal processing (5, 15, 16), these studies do not provide direct evidence for or against the theory of perceptual cycles. Recent studies, however, argued that parietooccipital alpha oscillations (~8–12 Hz) might define cycles of perception (6, 15, 17–19). However, they only provide evidence for discrete perceptual sampling in the visual domain. To claim that discrete perception is not domain-specific, it

is critical to demonstrate discrete and cyclic perception also for other sensory modalities and whether different modalities work via the same mechanism (e.g., whether alpha cycles generally define critical perceptual cycles for all modalities). Because sensory modalities work on different time scales, there is some indication that the mechanisms might differ.

We investigated whether discrete perceptual cycles exist in the somatosensory domain. Contrary to most studies in the visual domain, we used discrete rather than continuous stimuli, which differed only in perceptual impact, yet not in physical stimulation parameters. By this method, we could study whether two successively presented stimuli are perceived as either one single or two separate sensory events, depending on their temporal relationship to discrete perceptual cycles defined by the ongoing neuronal oscillatory phase. This setup allowed us to test the theory of discrete perceptual sampling critically in the somatosensory domain, and thus whether cycles of perception represent a mechanism of conscious perception that exists beyond the visual domain.

## Results

**Behavioral Results.** Subjects received one or two electrical pulses separated by a specific stimulus onset asynchrony (SOA; nomenclature is provided in *Materials and Methods*) and had to perform a forced-choice temporal perceptual discrimination task (Fig. 1), wherein they had to report whether they perceived one or two stimuli. Subjects made negligible errors for the conditions 0 ms and 100 ms [SOA 0 ms:  $97.7 \pm 0.4\%$  (mean  $\pm$  SEM) reports of correctly perceiving one stimulus, SOA 100 ms:  $94.6 \pm 2.3\%$  reports of correctly perceiving two stimuli]. Individually determined, intermediate SOAs yielded correct perception of two stimuli in ~50% of the trials ( $58.0 \pm 3.1\%$  reports). For the condition intermediate – 10 ms, subjects perceived two stimuli in  $25.6 \pm 4.7\%$  reports, and for intermediate + 10 ms, subjects perceived two stimuli in  $79.1 \pm 4.7\%$  reports. A one-way repeated

## Significance

Our sensory system constantly receives multiple inputs, which are usually perceived as a seamless stream. Thus, perception is commonly regarded as a continuous process. Alternatively, a few phenomena and recent studies suggest that perception might work in a discrete and periodic sampling mode. In a human magnetoencephalography study, we challenged the common view of continuous perception. We demonstrate that neuronal oscillations in the alpha band and low beta band determine discrete perceptual sampling windows in primary somatosensory cortex. The current results elucidate how ongoing neuronal oscillations shape discrete perceptual cycles, which constitute the basis for a discontinuous and periodic nature of somatosensory perception.

Author contributions: J.L. designed research; T.J.B. performed research; T.J.B. and J.L. analyzed data; and T.J.B., A.S., and J.L. wrote the paper.

The authors declare no conflict of interest.

This article is a PNAS Direct Submission.

<sup>1</sup>To whom correspondence should be addressed. Email: thomas.baumgarten@med.uni-duesseldorf.de.

This article contains supporting information online at [www.pnas.org/lookup/suppl/doi:10.1073/pnas.1501438112/-DCSupplemental](http://www.pnas.org/lookup/suppl/doi:10.1073/pnas.1501438112/-DCSupplemental).

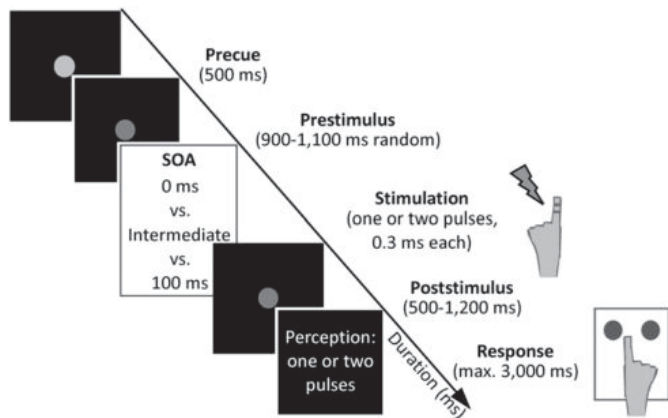


**Fig. 1.** Experimental paradigm. The sequence of events begins with presentation of a central fixation dot (500 ms). Luminance decrease signals start at the prestimulus epoch (900–1,100 ms), after which tactile stimulation is applied to the left index finger with varying SOAs (0 ms, intermediate – 10 ms, intermediate, intermediate + 10 ms, 100 ms). Stimulation is followed by a jittered poststimulus period (500–1,200 ms), after which written instructions signal subjects to report their respective perception of the stimulation by pressing a button.

measures ANOVA comparing average hit rates between conditions demonstrated a highly significant difference [ $F(4,60) = 141.25, P < 0.001$ ]. Post hoc  $t$  tests revealed significant differences between the condition 0 ms vs. intermediate – 10 ms [ $t(15) = 5.14, P < 0.01$ ], 0 ms vs. intermediate [ $t(15) = 18.34, P < 0.001$ ], 0 ms vs. intermediate + 10 ms [ $t(15) = 15.79, P < 0.001$ ], 0 ms vs. 100 ms [ $t(15) = -37.15, P < 0.001$ ], intermediate – 10 ms vs. intermediate [ $t(15) = 7.36, P < 0.001$ ], intermediate – 10 ms vs. intermediate + 10 ms [ $t(15) = -7.15, P < 0.001$ ], intermediate – 10 ms vs. 100 ms [ $t(15) = -13.1, P < 0.001$ ], intermediate vs. intermediate + 10 ms [ $t(15) = -5.35, P < 0.001$ ], intermediate vs. 100 ms [ $t(15) = -12.54, P < 0.001$ ], and intermediate + 10 ms vs. 100 ms [ $t(15) = -3.79, P < 0.01$ ].

**Phase Angle Contrast.** To study the influence of oscillatory phase angles on perception, we sorted trials with intermediate SOA according to perceptual response (perceived one or two stimuli), resulting in two perceptual conditions (intermediate1 vs. intermediate2). We computed phase angles for each condition in source space by means of a virtual channel in the primary somatosensory cortex (S1) (Fig. 2A) and contrasted the phases of intermediate2 with intermediate1 (Fig. S1). The analysis revealed a significant positive cluster ( $P < 0.05$ ; Fig. 2B) in the prestimulus epoch (–0.53 to –0.09 s) for frequencies in the alpha band and

lower beta band (8–20 Hz). Notably, the effect was more prominent and temporally extended in the beta band (14–20 Hz, –0.53 to –0.09 s) compared with the alpha band (8–12 Hz, –0.39 to –0.24 s). That is, the phase difference between perceptual conditions differed significantly more in this time-frequency range compared with randomly distributed phases. For frequencies in the lower beta band, phase difference fluctuated around maximum (i.e.,  $\pi$ ) in the prestimulus period (Fig. 2C). To exclude any bias due to power differences, we analyzed power differences between perceptual conditions for those time-frequency elements exhibiting significant phase differences (analysis parameters are provided in ref. 14). The results did not reveal any significant power differences ( $P > 0.05$ , uncorrected). Regarding phase angle differences, we found an additional significant negative cluster ( $P < 0.05$ ; Fig. 2B) between 2 and 28 Hz and between –0.1 and 0.24 s. Here, phase differences were significantly smaller compared with randomly distributed phases. This effect presumably resembles the phase resetting after stimulus presentation (18, 20).

**Phase Angles and Perception.** To analyze the extent by which perception was influenced by phase, we computed for each subject the momentary phase for each single trial for both perceptual conditions at the time point showing the largest statistical phase difference effect (*Materials and Methods*). Trials were placed in one of six different phase bins and aligned for each subject so that the highest probability for perceiving two stimuli corresponded to a zero phase angle. For each subject, we calculated the normalized perceptual response rate per bin, and we then averaged normalized response rates across subjects (Fig. 2D). Although this analysis resembles a post hoc test (because it is based on the time-frequency points of maximal phase difference determined in the previous analysis), it quantifies the magnitude by which phase influences perception, as well as the grade by which performance varies over different phase bins. A one-way repeated measures ANOVA comparing normalized perceptual response rates between bins demonstrated a highly significant difference [ $F(4,60) = 6.53, P < 0.001$ ]. Post hoc  $t$  tests revealed significant differences between bin 1 vs. bin 3 [ $t(5) = -4.17, P < 0.01$ ], bin 1 vs. bin 5 [ $t(5) = -4.21, P < 0.01$ ], bin 1 vs. bin 6 [ $t(5) = -4.13, P < 0.01$ ], bin 2 vs. bin 3 [ $t(5) = -2.77, P < 0.05$ ], and bin 2 vs. bin 5 [ $t(5) = -3.16, P < 0.01$ ]. The results indicate a monotonic decrease of mean response rate from zero phase angle to  $\pi$ , with the response rates differing by 13% points between the lowest ( $-\pi$ , 38%) and highest ( $1/3 \pi$ , 51%) phase bins (with exclusion of the zero phase bin).

**Beta-Band Cycles Determine Perceptual Cycles.** Fig. 3 illustrates a model derived from the analysis of phase angle contrasts and the theory of temporal framing (3, 19, 21). The model proposes that

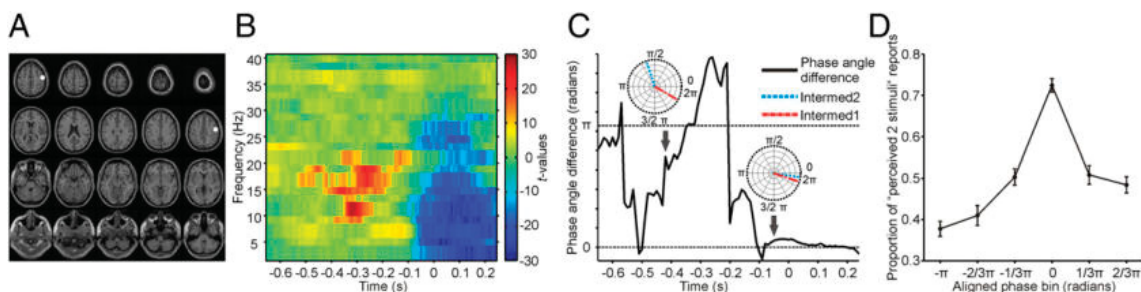


**Fig. 2.** Virtual sensor location and phase angle differences. (A) Virtual sensor location based on the voxel of maximum activity of the contrast M50 vs. prestimulus baseline. The voxel is highlighted on a slice plot of the Montreal Neurological Institute (MNI) template brain (MNI coordinates: 50 –10 50). (B) Time-frequency plot showing the results of the statistical analysis of phase angle differences between intermediate2 vs. intermediate1. Significant clusters ( $P < 0.05$ , corrected) are highlighted. Red colors indicate higher phase differences compared with randomly distributed phases.  $t = 0$  indicates onset of the first stimulus. (C) Phase angle difference (black solid line) between intermediate2 (Intermed2) and intermediate1 (Intermed1) for an exemplary 14-Hz band. The upper dashed line indicates the maximum phase angle difference ( $\pi$ ). (Insets) Phase angles for intermediate2 (blue lines) and intermediate1 (red lines) for exemplary time points (Left,  $t = -420$  ms; Right,  $t = -50$  ms) (D) Relationship between the momentary phase (*Materials and Methods*) and the normalized perceptual response rate. The probability of perceiving two stimuli significantly depends on the phase angle and differs maximally between opposite phase angles (ANOVA,  $P < 0.001$ ).

the temporal resolution of perception is defined by one cycle of a specific frequency. If presented within one cycle, the two stimuli are merged into one perceptual event and perceived as one single stimulus (Fig. 3A, white rectangles). If presented within two separate cycles, they will be perceived as two temporally separate perceptual events (Fig. 3A, black rectangles). Although the neural representation of the first stimulus can arrive at any point in the oscillatory cycle (21) for ongoing oscillations, the arrival of the second stimulus is determined by the SOA. For a cycle length twice as long as the respective SOA, a stimulus arriving in the first half of the cycle determines the arrival of the second stimulus in the same cycle (one perceived stimulus). Vice versa, a stimulus arriving in the second half of the cycle determines the arrival of the second stimulus in a subsequent cycle (two perceived stimuli). From the results of the phase angle contrast analysis, we derive that this critical frequency band lies in the alpha band and, particularly, the lower beta band between 8 and 20 Hz (Fig. 2B). Given these model preconditions, we can make two predictions. First, if the SOA between two stimuli equals half the length of the cycle of the critical frequency (e.g., 25 ms for a 20-Hz oscillation), mean phases for the perception of one stimulus (range: 0 to  $\pi$  for the example in Fig. 3A) and two stimuli (range:  $\pi$  to  $2\pi$ ) should differ maximally ( $\sim\pi$ ). More precisely, perception rates should critically depend on the phase at which the first stimulus arrives (Fig. 3B–D). That is, if the stimulus arrives at a given phase  $\phi$ , perception rates should differ significantly from  $\phi + \pi$ . Second, if the critical frequency is known, we can predict behavioral response rates for different SOAs. The first prediction is confirmed by the analysis of phase angle contrast (Fig. 2B and C). Based on these results, the post hoc phase binning analysis shows a monotonic decrease in perception over bins, and, thus, the dependence of perception rates on phase (Fig. 2D). The second prediction will be tested and presented below.

**Prediction of Perception.** Based on the model (Fig. 3), we predicted response rates for the different SOAs and computed linear regressions between predicted and behaviorally measured response rates. We computed predictions based on (i) group-level effect frequencies determined from MEG experimental data (8–20 Hz; Fig. 2B), (ii) based on single subject-level individual frequencies determined from MEG experimental data (Fig. S2 and Table S1), and (iii) based on frequencies determined from behavioral experimental data (i.e., the intermediate SOAs):

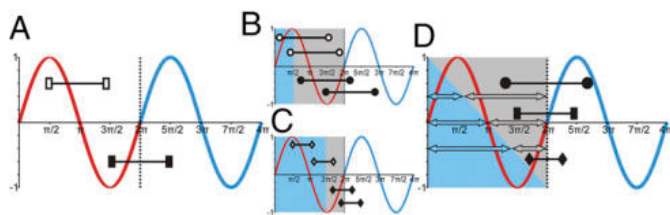


**Fig. 3.** Model for perceptual cycles. (A) Red and blue lines illustrate two perceptual cycles. Two stimuli can occur within one (white rectangles, one stimulus perceived) or two (black rectangles, two separate stimuli perceived) perceptual cycles. (B) Same as in A, but for stimulus pairs with a longer SOA. The blue background illustrates the time frame in which the occurrence of the first stimulus results in one perceived stimulus (○), and the gray background illustrates the time frame in which the occurrence of the first stimulus results in two perceived stimuli (●). (C) Same as in B, but for stimuli with a shorter SOA. Note different lengths of blue and gray time frames. (D) Same as in B, but for examples of three different SOAs. Intermediate SOAs (rectangles) result in time frames for one (blue arrows) or two (gray arrows) perceived stimuli of approximately equal length. For longer SOAs (●), the time frame for two perceived stimuli (gray arrows) is bigger than for one perceived stimulus (blue arrows). For shorter SOAs (◆), the time frame for two perceived stimuli (gray arrows) is smaller than for one perceived stimulus (blue arrows).

- i) Based on group-level effect frequencies (8–20 Hz; Fig. 2B), the linear regression analysis for behavioral response rates and predicted response rates (Fig. 4) resulted in a highly significant correlation coefficient ( $r = 0.93$ ,  $P < 0.01$ ). The resulting slope estimate ( $0.83 \pm 0.1$ ) did not differ significantly from 1 [ $t(4) = -1.8$ ,  $P > 0.05$ ].
- ii) Linear regression analysis of the individual behavioral and predicted individual response rates resulted in a significant correlation coefficient in all 16 subjects ( $r$  ranging from 0.69 to 0.96,  $P < 0.05$ ). For 12 of 16 subjects, the resulting slope estimate did not differ significantly from 1 [ $t(4)$  ranging from  $-2.6$  to  $2.4$ ,  $P > 0.05$ ; Fig. S2 and Table S1]. We additionally predicted group-level response rates by averaging the individual response rates over subjects. The resulting predictions were virtually similar to the predictions based on the averaging over group-level effect frequencies (i) (Fig. 4). The resulting slope estimate ( $0.78 \pm 0.1$ ) did not differ significantly from 1 [ $t(4) = -2.23$ ,  $P > 0.05$ ].
- iii) Predictions based on frequencies determined from behavioral experimental data yielded results highly similar to those results determined from MEG experimental data (details are provided in *SI Results*).

## Discussion

We investigated the neuronal mechanisms of varying conscious perception in the somatosensory domain. The results argue against a continuous perceptual mechanism and provide evidence that somatosensory perception operates in a discrete mode, with sensory input being sampled by discrete perceptual cycles in the alpha band and, in particular, the lower beta band (8–20 Hz).

**Beta-Band Cycles Determine Discrete Perceptual Sampling.** We found that phase angles in S1 in the alpha band and lower beta band (8–20 Hz) before stimulus onset predicted whether subjects perceived two constant electrical stimuli with an SOA of  $\sim 25$  ms as one or two stimuli (Fig. 2B). Notably, this effect was most prominent in the lower beta band (14–18 Hz). We put forward a model proposing that somatosensory stimulation is discretely sampled and that the underlying perceptual cycles are determined by ongoing oscillatory alpha and beta cycles (Fig. 3). If multiple discrete stimuli fall within one perceptual cycle, the temporally fine-grained information is lost and the distinct stimuli are fused to a single percept, a phenomenon that has been labeled perceptual or temporal framing in the visual domain (3, 19, 21). The model was confirmed by two theoretical predictions. First, beta oscillations were found to be antiphasic (phase difference of  $\pi$ ) for perception of one vs. two stimuli for intermediate SOAs ( $\sim 25$  ms; Fig. 2B–D). Based on these results, response rates were shown to depend on the specific phase at which the first stimulus arrives (Fig. 2D). Second, the model predicts behavioral performance on group (Fig. 4) and single-subject (Fig. S2) levels.

Based on behavioral response rates, the model predicted a theoretical critical sampling frequency of  $\sim 23$  Hz. The experimentally observed frequency range based on statistical analysis of phase angles revealed a significant effect between 8 and 20 Hz. Whereas the upper end of the experimental frequency range is close to the theoretically assumed frequency, the experimental frequency band also includes lower frequencies. A potential reason for this underestimation of the critical sampling frequency might be a decreased signal-to-noise ratio for higher frequencies. Noninvasive measurement (e.g., via EEG/MEG) of phase has been assumed to be especially susceptible to various interferences (e.g., delays in synaptic transmission) at higher frequencies (5). Likewise, phase differences in lower frequency bands could also resemble processes different than perceptual sampling (e.g., attentional processes) (22). This idea is in line with the different temporal distributions of phase angle differences for alpha- and beta-band frequencies. Finally, the presented model does not claim to cover all portions of the decision process determining the final response but, instead, focuses on early perceptual components. For example, the present data are derived

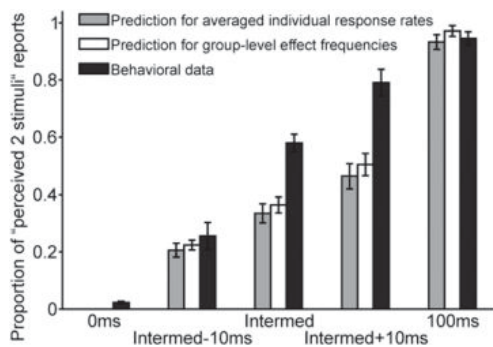


**Fig. 4.** Model prediction of response rates. Proportion of “perceived two stimuli” reports for conditions with different SOAs for model predictions based on averaged individual response rates (gray bars), significant group-level frequencies (8–20 Hz, white bars), and behavioral data (black bars). Predicted responses based on frequencies were calculated per frequency bin and then averaged over all respective frequencies. Hit rates are presented as mean  $\pm$  SEM.

from S1, thus not taking into account other cortical areas involved in the decisional process.

**Discrete Perceptual Sampling Is Not a Domain-Specific Mechanism.** The theory of discrete perceptual cycles was introduced decades ago (1, 2). However, it has been controversially discussed (8, 9). Recently, the discussion on discrete perceptual cycles has gained new momentum by studies using EEG, which allows one to study potential neuronal mechanisms of discrete perceptual cycles noninvasively (5, 17, 22). Nonetheless, empirical evidence to support the theory of discrete perceptual cycles remains scarce and focuses mainly on the visual domain (3, 17), whereas evidence for discrete cycles in other domains is largely missing (19). The present study is thus, to our knowledge, the first to demonstrate the existence of perceptual cycles in the somatosensory domain, indicating that the cyclic characteristic of perception is not a domain-specific visual mechanism (19).

**Modality-Specific Differences.** For the visual domain, EEG studies propose discrete cycles in perception and attentional updating defined by the alpha cycle (3, 17, 22). Our model agrees with these studies, albeit we propose perceptual cycles to be defined by alpha-band and, decisively, beta-band frequencies in the somatosensory domain. Although the significant group-level phase angle differences cover a rather broad band between 8 and 20 Hz, the major effect can be found in a narrower band between 14 and 18 Hz (Fig. 2B). Because subjects exhibit different individual intermediate SOAs, different individual frequencies for the discrete perceptual cycles are also to be expected (thereby blurring the group-level effect). In fact, the analyses based on individually determined frequencies confirmed that the individual narrow-band frequencies represent an appropriate predictor for individual response rates (Fig. S2). These domain-specific differences agree with a more prominent role of alpha oscillations in the visual domain for perception and neuronal processing (23, 24), whereas there is experimental evidence for a specific role of beta oscillations in the somatosensory domain (10, 13, 25–27). The present findings are in line with studies investigating steady-state somatosensory evoked potentials (SSSEPs). These studies found that the largest SSSEP amplitudes can be achieved by a stimulation frequency of  $\sim$ 18–26 Hz (i.e., in the beta band) (27–29). Stimulation at this frequency would place every stimulus in a separate beta cycle, therefore enhancing SSSEPs and, consequently, facilitating perceptual detection (26). Finally, the proportion perceiving two stimuli differed by 13% between the lowest ( $-\pi$ ) and the highest ( $1/3 \pi$ ) phase bins (with exclusion of the zero phase bin). This difference agrees with ranges reported for visual stimuli (5, 15). Thus, both visual and somatosensory

perception seems to be influenced by phase with a comparable magnitude.

**What About Absolute Phase Angles?** Varela et al. (3) reported that the phase of occipital alpha oscillations determines whether subjects perceive two sequential visual stimuli as one or two stimuli. The respective phase for perceiving one vs. two stimuli was anticyclic (i.e., the phase difference was  $\pi$ ). Although later studies failed to replicate this result (19, 30), our results support the finding by Varela et al. (3), because we find a phase difference of  $\pi$  between phases for perceiving one vs. two tactile stimuli. In contrast to Varela et al. (3), however, we do not claim that the specific phase (the peak or trough) is important for perception but, rather, whether two stimuli fall within a single cycle or separate cycles. The majority of studies investigating the influence of oscillatory phase on perception analyzed absolute phase angles within an oscillatory cycle at a specific moment, which are either favorable or unfavorable for subsequent perception (5, 11, 12, 15, 31). Thus, a potential concern might be that our results could be explained by favorable or unfavorable phases within one cycle. In such a framework, one stimulus might be presented at a favorable phase and the other stimulus might be presented at an unfavorable phase, thus leading to the erroneous perception of only one stimulus. The above-mentioned studies, however, used near-threshold stimuli. We presented stimuli with clearly suprathreshold intensities that are presumably perceived independent of the specific phase. Although a hypothesis proposing an influence of (un)favorable phases would predict that  $\sim$ 50% of the stimuli with SOA 0 ms would be missed, subjects correctly perceived almost all stimuli. Similarly, such a framework would predict a higher percentage of trials with SOA 100 ms to be perceived as one stimulus than found in our behavioral data. Therefore, the present results cannot be explained by favorable or unfavorable phases within one oscillatory cycle.

**Differentiating Effects of Phase and Power.** Recent studies demonstrated an influence of oscillatory power for perception of single (near-threshold) tactile stimuli, as well as for the temporal discrimination of two tactile stimuli (10, 25). The majority of these studies [including a previous study by our group on the dataset presented in this study (14)] found prestimulus power differences in the alpha band (8–12 Hz), whereas the present phase angles differed mostly in the lower beta band (14–18 Hz). Further, we found no significant power differences in those time-frequency elements showing significant phase angle differences between perceptual conditions. It is thus unlikely that the presented phase effect was biased by power differences. Indeed, there is experimental evidence for an influence of both oscillatory power (10) and phase (12, 31) for neuronal processing and perception, and recent studies could demonstrate that these measures act largely independently (5, 22). This differentiation is further supported by results showing that phase is able to transport more units of information per time than power changes (32) or spike counts (33), and represents a suitable candidate measure to encode fast-changing stimulus features (21).

**Contradicting Subjective Experience.** There is accumulating evidence that our brain processes incoming stimulus information in a phasic mode (3, 17). However, personal experience does not intuitively match with a discrete sequencing approach but, rather, resembles a seamlessly updated percept. This divergence might explain why relatively few studies address this topic, although the concept of discrete perceptual sampling has been put forward at least since the middle of the 20th century (1, 2). It remains an open question how the brain transforms discretely sampled sensory information into a subjectively seamless impression. Although the mechanisms for such perceptual “smoothing” are unknown, there are, at least for the visual domain, several reports where the mechanisms fail to work (34). For example, in akinetopsia, subjects report perceiving a sequence of snapshots rather than a continuous motion (35, 36). Similarly, the ingestion of lysergic acid diethylamide often results in a perceptual disturbance

wherein visual motion is perceived as a sequence of discrete stationary images (37, 38).

## Conclusions

The present study demonstrates an influence of oscillatory phase on the temporal perception of two stimuli. We propose the existence of discrete perceptual cycles for the conscious perception of subsequently presented tactile stimuli. The perceptual cycles are determined particularly by frequencies in the beta band acting as the specific physiological correlate for perceptual cycles for the somatosensory modality. In combination with previous studies investigating similar paradigms in the visual domain (3, 30), the present results support the theory of temporal framing (1–3, 19, 21) and indicate that perceptual cycles are no domain-specific visual phenomenon, albeit modality-specific frequencies that define perceptual cycles seem to be present.

## Materials and Methods

**Subjects.** The subjects, stimuli, paradigm, and MEG recording of the present study were previously reported in detail (14). Here, we present a comprehensive overview. Sixteen right-handed volunteers [seven males, age:  $26.1 \pm 4.7$  y (mean  $\pm$  SD)] participated in the study. Subjects provided written informed consent before the experiment in accordance with the Declaration of Helsinki and approved by the Ethical Committee of the Medical Faculty, Heinrich-Heine-University Düsseldorf.

**Experimental Paradigm.** Details on the paradigm can be found in the study by Baumgarten et al. (14). A comprehensive overview is provided in Fig. 1 and *SI Materials and Methods*.

**MEG Data Recording and Preprocessing.** Electromagnetic brain activity was continuously recorded using a 306-channel, whole-head MEG system (NeuroMag Elekta Oy). Analysis was restricted to the gradiometers. Individual structural MRI scans were acquired using a 3-T MRI scanner (Siemens). Offline analysis of the data was carried out using custom-made MATLAB (MathWorks) scripts and the MATLAB-based open-source toolboxes FieldTrip ([fieldtriptoolbox.org](http://fieldtriptoolbox.org)) (39), CircStat (40), and SPM8 (41). Continuously recorded data were segmented into trials. All trials were semiautomatically and visually inspected for artifacts, whereas artifacts caused by muscle activity, eye movements, or technical artifacts were removed semiautomatically using a z-score-based algorithm implemented in FieldTrip.

**Virtual Channel Construction.** To focus on S1, we analyzed oscillatory activity in a predefined region of interest in source space ("virtual sensor"). Details regarding the construction of the virtual sensor are provided in *SI Materials and Methods*.

**Phase Angle Contrast.** Oscillatory phase was calculated for the virtual sensor. We sorted trials with respect to the SOA for each subject separately, resulting in five different conditions defined by the length of the SOA (0 ms, intermediate – 10 ms, intermediate, intermediate + 10 ms, and 100 ms). Subsequently, we separated intermediate trials by perceptual response (perceived one vs. two stimuli, subsequently labeled intermediate1 vs. intermediate2). Because trial numbers are known to influence phase measures crucially (42), trial numbers were equated across conditions in each analysis by determining the condition with the lowest number of trials per subject and randomly selecting the same number of trials from the remaining conditions. To exclude potential effects due to a specific trial selection, we performed trial selection by means of random subsampling 100 times, and subsequently computed the median of the resulting phase parameters over these 100 repetitions (because  $F$  values were not normally distributed). The time point  $t = 0$  was defined as the onset of the first stimulus. The oscillatory phase was calculated for each time-frequency element (–650 to 240 ms, 2–40 Hz) of each single trial by applying a discrete Fourier transform (DFT) on fixed sliding time windows with a length of 500 ms, moved in steps of 10 ms. Data segments were tapered with a single Hanning taper, resulting in a spectral smoothing of 2 Hz. For each subject  $s$ , trial  $r$ , frequency  $f$ , and time point  $t$ , we normalized the complex outcome  $F_{s,r,f,t}$  of the DFT by dividing it by its absolute (abs) value, thus normalizing the signal by its amplitude:

$$F_{s,r,f,t}^{norm} = \frac{F_{s,r,f,t}}{\text{abs}(F_{s,r,f,t})} \quad [1]$$

From these normalized values, we computed for each subject  $s$ , trial  $r$ , frequency  $f$ , and time point  $t$ , the normalized phase:

$$\Phi_{s,r,f,t}^{norm} = \text{atan} \left( \frac{\text{Im}(F_{s,r,f,t}^{norm})}{\text{Re}(F_{s,r,f,t}^{norm})} \right) \quad [2]$$

where  $\text{Im}$  and  $\text{Re}$  are the imaginary part and real part, respectively, of the DFT.

To analyze statistically whether phase angles differed between perceptual conditions, we compared phase angles between the intermediate1 and intermediate2 conditions for each time-frequency element at the within-subject level by means of the Watson–Williams multisample test for equal means [CircStat toolbox (40)]. This test for circular data is equivalent to a two-sample  $t$  test for equal angular means. For each randomized trial selection, we compared phase angles for each subject independently for each time-frequency element, resulting in 100  $F$  values for each time-frequency element. We took for each time-frequency element the median of all 100  $F$  values, resulting in a time-channel map of  $F$  values for each subject, which constitutes the test distribution. To assess the consistency of phase angle differences over subjects, we performed a nonparametric randomization test identifying clusters in time-frequency space demonstrating a similarly directed phase angle difference relative to a null distribution (43). We computed this null distribution under the null hypothesis that phases are randomly and uniformly distributed, showing no difference between conditions. That is, for each subject, we assigned to each condition random phases (equaling the number of trials for each subject) and then repeated the above-mentioned statistical analysis. We compared (random) phase angles between both conditions for each time-frequency element at the within-subject level by applying the Watson–Williams test. This procedure was repeated 100 times (each time with new, randomly chosen phases), resulting in 100  $F$  values for each time-frequency element. Subsequently, we took the median of all 100  $F$  values for each time-frequency element, resulting in a time-channel map of  $F$  values for each subject, which constitutes the null distribution. We then statistically compared the  $F$  values of the test distribution with the  $F$  values of the null distribution for each time-frequency element by means of a dependent-samples  $t$  test, resulting in a time-frequency map of  $t$  values. Positive  $t$  values for a specific time-frequency element demonstrate a larger phase angle difference compared with randomly distributed phase angles, and vice versa for negative  $t$  values (44). To investigate whether the phase angle differences between perceptual conditions were significantly different from randomly distributed phases, we applied a cluster-based randomization approach (14). This statistical approach effectively controls for the type I error rate due to multiple comparisons across time points and channels (43).

To ensure that phase angle differences are not biased by power, we analyzed power differences between perceptual conditions for those time-frequency elements exhibiting significant phase differences. The respective analysis parameters are discussed in ref. 14. To visualize phase angle differences on the group level, we computed phase angle differences for each time-frequency element. We computed the circular distance between the over-trial averages of the intermediate2 and intermediate1 conditions for each subsampling run, and subsequently averaged circular distances over all subsampling runs on the single-subject level and over subjects (Fig. 2C).

**Phase Angles and Perception.** To determine to what extent perception of one or two stimuli is associated with different phase angles, we selected for each subject the time-frequency point showing the largest statistical phase angle effect (maximum Watson–Williams test  $F$  value) within the time-frequency range of the aforementioned phase contrast effect (8–20 Hz, –0.53 to –0.09 s; Fig. 2B). This analysis resembles a post hoc test based on previous results. For each subject, the momentary phase for the respective time-frequency point was computed for each single trial for both perceptual conditions. Subsequently, the trial was placed in one of six different, equally spaced phase bins (bin width =  $1/3 \pi$ ), ranging from  $-\pi$  to  $+\pi$ . For each subject, we calculated the normalized perceptual response rate per bin. We adjusted phase distributions for each subject so that the bin showing maximum perception of two distinct stimuli was aligned to a phase angle of zero (a similar procedure is described in refs. 5 and 11). This process was repeated for each of the 100 specific randomized trial selections. Subsequently, we computed the median of the normalized perceptual response rates for each bin across the 100 repetitions for random trial selection and averaged response rates over subjects (Fig. 2D). To assess an effect of phase angle on perceptual response rates, a one-way repeated measures ANOVA and post hoc paired sample  $t$  tests were conducted. Due to the realignment, we excluded the bin centered on zero from the statistical analyses.

**Prediction of Perception.** Based on the model (Fig. 3), we predicted response rates for the different SOAs and computed linear regressions between predicted and behaviorally measured response rates. We used different approaches to predict response rates, with each approach based on a slightly different method to determine the critical frequency: (i) based on group-level effect frequencies determined from MEG experimental data (Fig. 2B), (ii) based on single-subject individual frequencies determined from MEG

experimental data (Fig. S2 and Table S1), and (iii) based on frequencies determined from behavioral experimental data (i.e., the intermediate SOAs). The approaches are described in detail in *SI Materials and Methods*.

**ACKNOWLEDGMENTS.** We thank Erika Rädisch for help with the MRI recordings. J.L. was supported by the German Research Foundation (Grant LA 2400/4-1). T.J.B. was supported by the German Research Foundation (SFB 974, B07).

1. Stroud JM (1956) *Information Theory in Psychology*, ed Quastler H (Free Press, Chicago), pp 174–205.
2. Harter MR (1967) Excitability cycles and cortical scanning: A review of two hypotheses of central intermittency in perception. *Psychol Bull* 68(1):47–58.
3. Varela FJ, Toro A, John ER, Schwartz EL (1981) Perceptual framing and cortical alpha rhythm. *Neuropsychologia* 19(5):675–686.
4. VanRullen R, Koch C (2003) Is perception discrete or continuous? *Trends Cogn Sci* 7(5): 207–213.
5. Busch NA, Dubois J, VanRullen R (2009) The phase of ongoing EEG oscillations predicts visual perception. *J Neurosci* 29(24):7869–7876.
6. Jensen O, Gips B, Bergmann TO, Bonnefond M (2014) Temporal coding organized by coupled alpha and gamma oscillations prioritize visual processing. *Trends Neurosci* 37(7):357–369.
7. Schroeder CE, Lakatos P (2009) Low-frequency neuronal oscillations as instruments of sensory selection. *Trends Neurosci* 32(1):9–18.
8. Allport DA (1968) Phenomenal simultaneity and the perceptual moment hypothesis. *Br J Psychol* 59(4):395–406.
9. Kline KA, Eagleman DM (2008) Evidence against the temporal subsampling account of illusory motion reversal. *J Vis* 8(4):1–5.
10. Lange J, Halacz J, van Dijk H, Kahlbrock N, Schnitzler A (2012) Fluctuations of prestimulus oscillatory power predict subjective perception of tactile simultaneity. *Cereb Cortex* 22(11):2564–2574.
11. Ng BS, Schroeder T, Kayser C (2012) A precluding but not ensuring role of entrained low-frequency oscillations for auditory perception. *J Neurosci* 32(35):12268–12276.
12. Mathewson KE, Gratton G, Fabiani M, Beck DM, Ro T (2009) To see or not to see: Prestimulus alpha phase predicts visual awareness. *J Neurosci* 29(9):2725–2732.
13. Jones SR, et al. (2010) Cued spatial attention drives functionally relevant modulation of the mu rhythm in primary somatosensory cortex. *J Neurosci* 30(41):13760–13765.
14. Baumgarten TJ, Schnitzler A, Lange J (2014) Prestimulus alpha power influences tactile temporal perceptual discrimination and confidence in decisions. *Cereb Cortex*, 10.1093/cercor/bhu247.
15. Dugué L, Marque P, VanRullen R (2011) The phase of ongoing oscillations mediates the causal relation between brain excitation and visual perception. *J Neurosci* 31(33): 11889–11893.
16. Lange J, Keil J, Schnitzler A, van Dijk H, Weisz N (2014) The role of alpha oscillations for illusory perception. *Behav Brain Res* 271:294–301.
17. Chakravarthi R, Vanrullen R (2012) Conscious updating is a rhythmic process. *Proc Natl Acad Sci USA* 109(26):10599–10604.
18. Romei V, Gross J, Thut G (2012) Sounds reset rhythms of visual cortex and corresponding human visual perception. *Curr Biol* 22(9):807–813.
19. VanRullen R, Zoefel B, Ilhan B (2014) On the cyclic nature of perception in vision versus audition. *Philos Trans R Soc Lond B Biol Sci* 369(1641):20130214.
20. Lakatos P, Chen CM, O’Connell MN, Mills A, Schroeder CE (2007) Neuronal oscillations and multisensory interaction in primary auditory cortex. *Neuron* 53(2):279–292.
21. Vanrullen R, Busch NA, Drewes J, Dubois J (2011) Ongoing EEG phase as a trial-by-trial predictor of perceptual and attentional variability. *Front Psychol* 2:60.
22. Busch NA, VanRullen R (2010) Spontaneous EEG oscillations reveal periodic sampling of visual attention. *Proc Natl Acad Sci USA* 107(37):16048–16053.
23. Romei V, et al. (2008) Spontaneous fluctuations in posterior  $\alpha$ -band EEG activity reflect variability in excitability of human visual areas. *Cereb Cortex* 18(9):2010–2018.
24. Wyart V, Tallon-Baudry C (2009) How ongoing fluctuations in human visual cortex predict perceptual awareness: Baseline shift versus decision bias. *J Neurosci* 29(27): 8715–8725.
25. Linkenkaer-Hansen K, Nikulin VV, Palva S, Ilmoniemi RJ, Palva JM (2004) Prestimulus oscillations enhance psychophysical performance in humans. *J Neurosci* 24(45): 10186–10190.
26. Jones SR, Pritchett DL, Stufflebeam SM, Hämäläinen M, Moore CI (2007) Neural correlates of tactile detection: A combined magnetoencephalography and biophysically based computational modeling study. *J Neurosci* 27(40):10751–10764.
27. Haegens S, et al. (2011) Beta oscillations in the monkey sensorimotor network reflect somatosensory decision making. *Proc Natl Acad Sci USA* 108(26):10708–10713.
28. Snyder AZ (1992) Steady-state vibration evoked potentials: Descriptions of technique and characterization of responses. *Electroencephalogr Clin Neurophysiol* 84(3): 257–268.
29. Tobimatsu S, Zhang YM, Kato M (1999) Steady-state vibration somatosensory evoked potentials: Physiological characteristics and tuning function. *Clin Neurophysiol* 110(11):1953–1958.
30. Gho M, Varela FJ (1988-1989) A quantitative assessment of the dependency of the visual temporal frame upon the cortical rhythm. *J Physiol (Paris)* 83(2):95–101.
31. Neuling T, Rach S, Wagner S, Wolters CH, Herrmann CS (2012) Good vibrations: Oscillatory phase shapes perception. *Neuroimage* 63(2):771–778.
32. Schyns PG, Thut G, Gross J (2011) Cracking the code of oscillatory activity. *PLoS Biol* 9(5):e1001064.
33. Montemurro MA, Rasch MJ, Murayama Y, Logothetis NK, Panzeri S (2008) Phase-of-firing coding of natural visual stimuli in primary visual cortex. *Curr Biol* 18(5):375–380.
34. Dubois J, Vanrullen R (2011) Visual trails: Do the doors of perception open periodically? *PLoS Biol* 9(5):e1001056.
35. Horton JC, Trobe JD (1999) Akinetopsia from nefazodone toxicity. *Am J Ophthalmol* 128(4):530–531.
36. Tsai PH, Mendez MF (2009) Akinetopsia in the posterior cortical variant of Alzheimer disease. *Neurology* 73(9):731–732.
37. Abraham HD (1983) Visual phenomenology of the LSD flashback. *Arch Gen Psychiatry* 40(8):884–889.
38. Kawasaki A, Purvin V (1996) Persistent palinopsia following ingestion of lysergic acid diethylamide (LSD). *Arch Ophthalmol* 114(1):47–50.
39. Oostenveld R, Fries P, Maris E, Schoffelen JM (2011) FieldTrip: Open source software for advanced analysis of MEG, EEG, and invasive electrophysiological data. *Comput Intell Neurosci* 2011:156869.
40. Berens P (2009) CircStat: A MATLAB toolbox for circular statistics. *J Stat Softw* 31(10): 1–21.
41. Litvak V, et al. (2011) EEG and MEG data analysis in SPM8. *Comput Intell Neurosci* 2011:852961.
42. Hanslmayr S, Volberg G, Wimber M, Dalal SS, Greenlee MW (2013) Prestimulus oscillatory phase at 7 Hz gates cortical information flow and visual perception. *Curr Biol* 23(22):2273–2278.
43. Maris E, Oostenveld R (2007) Nonparametric statistical testing of EEG- and MEG-data. *J Neurosci Methods* 164(1):177–190.
44. Keil J, Müller N, Hartmann T, Weisz N (2014) Prestimulus beta power and phase synchrony influence the sound-induced flash illusion. *Cereb Cortex* 24(5):1278–1288.
45. Suk J, Ribary U, Cappel J, Yamamoto T, Llinás R (1991) Anatomical localization revealed by MEG recordings of the human somatosensory system. *Electroencephalogr Clin Neurophysiol* 78(3):185–196.
46. Iguchi Y, Hoshi Y, Tanosaki M, Taira M, Hashimoto I (2005) Attention induces reciprocal activity in the human somatosensory cortex enhancing relevant- and suppressing irrelevant inputs from fingers. *Clin Neurophysiol* 116(5):1077–1087.
47. Van Veen BD, van Drongelen W, Yuchtman M, Suzuki A (1997) Localization of brain electrical activity via linearly constrained minimum variance spatial filtering. *IEEE Trans Biomed Eng* 44(9):867–880.
48. Nolte G (2003) The magnetic lead field theorem in the quasi-static approximation and its use for magnetoencephalography forward calculation in realistic volume conductors. *Phys Med Biol* 48(22):3637–3652.
49. Schoffelen JM, Poort J, Oostenveld R, Fries P (2011) Selective movement preparation is subserved by selective increases in corticomuscular gamma-band coherence. *J Neurosci* 31(18):6750–6758.

10) **Lange, J.**, Pavlidou, A., & Schnitzler, A. (2015).

Lateralized modulation of beta-band power in sensorimotor areas during action observation.

*Frontiers in Integrative Neuroscience, 9.*

Impact factor (2018): 2.81

# Lateralized modulation of beta-band power in sensorimotor areas during action observation

Joachim Lange<sup>1\*</sup>, Anastasia Pavlidou<sup>1,2</sup> and Alfons Schnitzler<sup>1</sup>

<sup>1</sup> Medical Faculty, Institute of Clinical Neuroscience, Heinrich Heine-University, Düsseldorf, Germany, <sup>2</sup> Department of Medicine, John A. Burns Medical School and The Queens Medical Center, University of Hawaii, Honolulu, HI, USA

The cortical network for action observation includes areas of the visual cortex and non-visual areas, including areas of the motoric system. Parts of this network are known for their contralateral organization during motion execution, i.e., they predominantly control and respond to movements of the contralateral body side. We were interested whether this lateralized organization was also present during action observation. Human participants viewed point-light displays of human actors, where the actor was facing and moving either to the right or to the left, while participants' neuromagnetic activity was recorded using magnetoencephalography (MEG). We found that right and left facing movements elicited different activity in left and right motoric areas. This lateralization effect was found in two distinct spatio-temporal-spectral clusters: An early lateralization effect in medial sensors at 12–16 Hz and ~276–675 ms after stimulus onset, and a second cluster in more lateral sensors at 22–28 Hz and ~1275–1775 ms. Our results demonstrate that in addition to the known somatotopic organization of parts of the human motoric system, these areas also show a lateralization effect during action observation. Thus, our results indicate that the hemispheric organization of one's own body map known for motion execution extends to the visual observation of others' bodily actions and movements.

**Keywords:** mirror-neuron system, somatotopy, inferior frontal gyrus, premotor cortex, point-light displays

## OPEN ACCESS

### Edited by:

Sharon Gilaie-Dotan,  
University College London, UK

### Reviewed by:

Lars Michels,  
University Hospital Zurich, Switzerland  
Anat Perry,  
University of California, Berkeley, USA

### \*Correspondence:

Joachim Lange,  
Medical Faculty, Institute of Clinical  
Neuroscience, Heinrich  
Heine-University, Universitätsstr. 1,  
40225 Düsseldorf, Germany  
joachim.lange@  
med.uni-duesseldorf.de

**Received:** 30 March 2015

**Accepted:** 12 June 2015

**Published:** 25 June 2015

### Citation:

Lange J, Pavlidou A and Schnitzler A  
(2015) Lateralized modulation of  
beta-band power in sensorimotor  
areas during action observation.  
*Front. Integr. Neurosci.* 9:43.  
doi: 10.3389/fnint.2015.00043

## Introduction

The recognition of human movements is an important aspect of social interaction. Observing other individuals provides rich information about their actions, intentions, moods, etc. (see Blake and Shiffrar, 2007 for an overview). The recognition of human movements also shows remarkable characteristics which differentiate the recognition process of human movements from recognition processes of other, non-living objects. For example, human movements and their intrinsic characteristics can be quickly and accurately recognized even if the human body is depicted by only a handful of so-called point-lights attached on the otherwise invisible body (Johansson, 1973).

Imaging studies have revealed a widespread cortical network involved in the perception of human movements. This network includes visual areas, but also higher level cortical areas extending beyond the classical low level visual areas (e.g., Grossman et al., 2000; Saygin et al., 2004; Gilaie-Dotan et al., 2013; Pavlidou et al., 2014b,c). Among these areas is a network known as the mirror neuron system (MNS). The MNS has been first observed in monkeys and is known as a system of neurons which are activated during action execution but also during observation of the

action in the absence of active execution (see Rizzolatti and Craighero, 2004 for a review). Most prominent areas of the MNS are the premotor cortex, inferior frontal gyrus and inferior parietal lobule (Rizzolatti and Craighero, 2004). It is still debated whether a MNS analogous to the monkey MNS exists in humans.

An analogous system in the human brain has been supported by single cell recordings in humans (Mukamel et al., 2010) and indirectly by neurophysiological and neuroimaging studies, including EEG and MEG. Several EEG studies reported a suppression of alpha/mu-activity ( $\sim 8\text{--}13\text{ Hz}$ ) in sensors over central and motoric areas during action observation (e.g., Muthukumaraswamy et al., 2004; Ulloa and Pineda, 2007; Perry and Bentin, 2009; Frenkel-Toledo et al., 2013).

In addition, MEG studies have demonstrated that action observation leads to a desynchronization of activity in the beta-band ( $\sim 14\text{--}30\text{ Hz}$ ). It has been shown that execution, observation and imagination of a movement suppress alpha/beta-band activity, but at different degrees. For example, the suppression of beta-band activity has been shown to be less strong for observation and imagination compared to motion execution (e.g., Schnitzler et al., 1997; Hari et al., 1998; Babiloni et al., 2002). Furthermore, recent studies have demonstrated that beta-band power in sensorimotor areas correlates with the plausibility of the observed action (Pavlidou et al., 2014c).

In addition to the core parts of the MNS observed in monkeys, also other areas in the human brain are relevant for action observation. While these areas may not contain mirror neurons *per se*, they are connected anatomically and/or functionally to the core MNS. In addition, they often show desynchronization of alpha/beta activity in response to action observation, similar to the areas of the MNS. This has led to the notion of an “extended MNS” including, among others, the superior temporal sulcus and sensorimotor areas (Pineda, 2008).

Parts of this extended MNS—mainly the sensorimotor areas—are known for their somatotopic organization. That is, each part of the body is represented in a corresponding area in the sensorimotor cortex. In addition, the somatotopic representation is mainly contralateral, so that sensorimotor area resembles the human body of the contralateral side (Rizzolatti and Luppino, 2001).

While the knowledge of somatotopic organization and hemispheric lateralization is mainly derived from studies on motor execution, studies have shown that the somatotopic representation is also present during action observation. For example, an fMRI study revealed that observation of hand, foot or mouth movements activated different areas in the premotor cortex in accordance with the known somatotopic organization (Buccino et al., 2001).

A largely unresolved experimental question, however, is whether the hemispheric lateralization of sensorimotor areas is also present during action observation. Evidence for a lateralized organization during action observation comes mainly from studies investigating hand movements. For example, EEG and MEG studies reported that observation or imagination of hand movements induces lateralized alpha/beta-band suppression over frontal and central sites (de Lange et al., 2008; Frenkel-Toledo et al., 2013). In the present study, we aimed to

investigate whether such lateralized activation is also present during action observation involving the whole body. That is, we studied whether the activation of motoric areas by action observation depends on the observed body side of the actor. We hypothesized that this lateralization would be reflected in differential neuronal oscillatory power, especially in the beta-band. To this end, we employed different human actions depicted as point-light displays and recorded neuromagnetic brain activity while subjects viewed these actions either with the actor facing left or right.

## Methods

The present study uses data from a previously reported study (Pavlidou et al., 2014b,c). While subjects, stimuli and paradigm are thus identical to the previously reported studies, the present study, however, focuses on a different experimental questions and thus data analysis differs from our previous studies.

## Subjects

Twelve subjects (6 male, age:  $27.6 \pm 2.9\text{ y}$  [mean  $\pm$  SD]) with normal or corrected-to-normal vision participated in this study after giving written informed consent in accordance to the declaration of Helsinki and the Ethical Committee of the Medical Faculty, Heinrich Heine-University Düsseldorf.

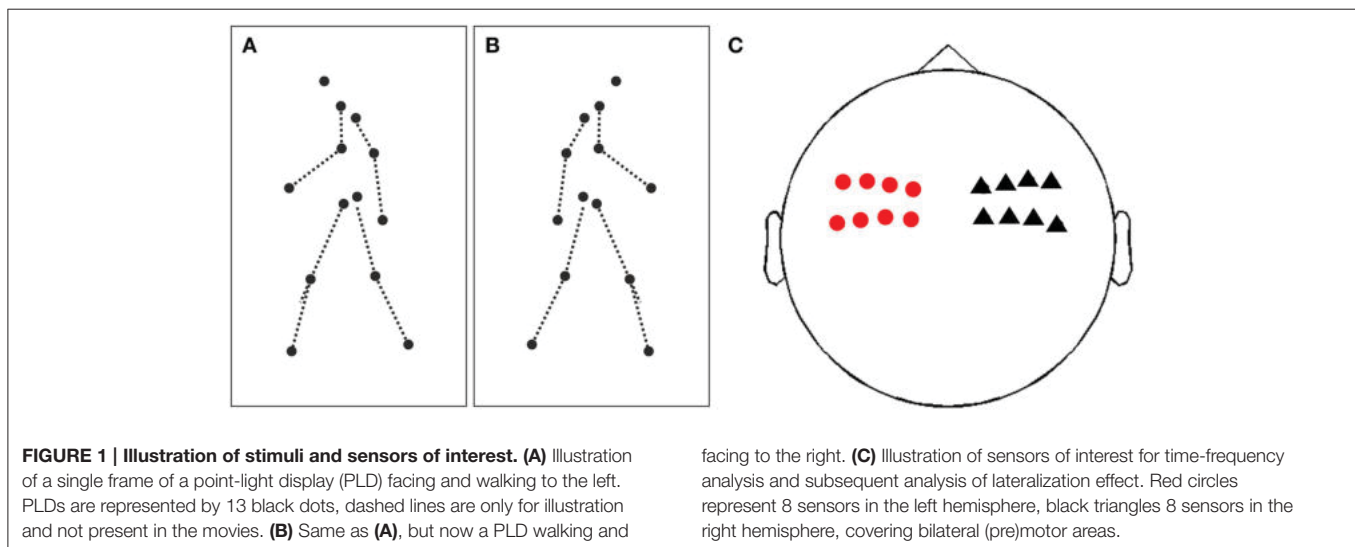
## Stimuli and Paradigm

Stimuli and paradigm of the present study were previously reported in detail (Pavlidou et al., 2014b,c). Here we report a concise overview.

Subjects fixated a central red cross for a jittered period (800–1300 ms). Then, additionally, a movie of point-light display (PLD) was presented centrally for 5 cycles (3600–5000 ms). After the PLD presentation, a black screen was presented for a jittered period (0–1000 ms). Finally, response instructions were presented for 2000 ms and subjects were asked to rate the PLD within this period. After the response or after 2000 ms the response text disappeared and the next trial started.

PLDs depicted either a natural action of a human figure or a modified, unnatural (implausible or scrambled) version of the action and subjects were asked to rate the plausibility of the action. All stimuli were presented in random order. Since in the present study data analysis will focus only on a subset of the natural actions, we will describe only natural actions in detail here. For a detailed description of the unnatural actions see Pavlidou et al. (2014b,c).

PLDs were generated by recording the movements of human actors with 13 sensors attached to their main joints (head, shoulders, elbows, wrists, hips, knees, and feet) using a motion tracking system [MotionStar; Ascension Technology, Burlington, VT; (Lange and Lappe, 2007)]. Movements consisted of natural actions (e.g., walking, skipping, throwing) viewed either from the left, right or frontal view. All translatory motion was subtracted offline so that the PLDs were walking in place. Since in the present study we were interested in the putative lateralization of neuronal activity in response to left and right movements, we used only the



stimuli facing left or right (see **Figures 1A,B** and Movies 1, 2 for examples).

### MEG Recordings and Data Analysis

While subjects viewed the stimuli, we recorded neuromagnetic activity with a 306-channel whole head MEG system (Elekta Neuromag Oy, Helsinki, Finland) with a sampling rate of 1000 Hz. Vertical and horizontal electrooculograms were recorded simultaneously for offline artifact rejection.

Data were offline analyzed using custom-made Matlab (The Mathworks, Natick, Massachusetts, USA) scripts and the Matlab-based open source toolboxes FieldTrip (Oostenveld et al., 2011) (<http://fieldtrip.fcdonders.nl>).

Continuously recorded MEG data were offline epoched in trials starting with the onset of the fixation cross and ending with the presentation of the response instructions. All trials were semi-automatically and visually inspected for artifacts. Artifacts caused by muscle activity, eye movements or SQUID jumps were removed semi-automatically using a *z*-score based algorithm implemented in FieldTrip. In a nutshell, data was filtered in a frequency band known to be sensitive for muscular (110–140 Hz) or ocular (1–14 Hz) artifact. Next, *z*-values for each channel were computed for each time point, resulting in a time course representing standardized deviations from the mean of all channels. Artifacts were identified and removed by applying a threshold and cutting out segments exceeding this threshold. The threshold was individually set for each subject and manually chosen, depending on individual noise levels and data quality (Lange et al., 2013). Excessively noisy channels were removed and reconstructed by an interpolation of neighboring channels. Additionally, power line noise was removed from the segmented data by using a band-stop filter encompassing the 50, 100, and 150 Hz components.

Spectral power for the frequency band 4–40 Hz was computed for each sensor separately by applying a discrete Fourier Transformation on sliding time windows of 500 ms length, moved in steps of 20 ms. Data segments were first multiplied with

Hanning window, resulting in an effective smoothing of  $\pm 2$  Hz. The two orthogonal channels of each gradiometer pair were combined by summing the power of the two channels.

For each subject, spectral power was averaged separately over trials depicting a PLD facing to the left or to the right, respectively. Next, we chose two sets of a priori defined sensors covering left and right (pre)motor areas (**Figure 1C**; eight left sensors: “MEG0212+0213,” “MEG0222+0223,” “MEG0232+0233,” “MEG0242+0243,” “MEG0412+0413,” “MEG0422+0423,” “MEG0432+0433,” “MEG0442+0443”; eight right sensors: “MEG1112+1113,” “MEG1122+1123,” “MEG1132+1133,” “MEG1142+MEG1143,” “MEG1312+1313,” “MEG1322+1323,” “MEG1332+1333,” “MEG1342+1343”). In each sensor set, we pooled for each time-frequency pixel spectral power for right and left facing PLDs across all sensors of interest and then computed a lateralization index (LI) for each time-frequency pixel in each sensor set (right or left sensors). The LI was defined as the differences of spectral power between right and left PLDs divided by their variance (i.e., equivalent to an independent sample *t*-test). This approach provided for each subject and each sensor set (right or left) a time-frequency map of LI.

To evaluate whether right and left hemispheres showed a differential activation by PLD, we finally statistically compared the LI for right and left sensor sets across subjects using a non-parametric randomization test (Maris and Oostenveld, 2007).

To this end, we compared the LI for right and left sensor sets by a time-frequency-wise dependent samples *t*-test. This approach led to a time-frequency map of *t*-values. To correct for multiple comparisons, we applied a cluster-based randomization approach (Maris and Oostenveld, 2007). To this end, *t*-values were thresholded at a value of  $t = 1.96$  (i.e.,  $p = 0.05$ ), and neighboring time-frequency-points exceeding this threshold were clustered. Values within a cluster were summed, giving our cluster-level test statistic. We generated a randomization distribution by randomly exchanging the *t*-maps of a random subset of subjects. The cluster-statistics were recomputed for

these new group-level pooled *t*-maps. By repeating this step 1000 times, a randomization distribution of cluster-level test-statistics was computed and the test statistics of the observed clusters were compared with this randomization distribution (for details see Lange et al., 2011, 2013). This non-parametric approach avoids assumptions about underlying distributions, implements a random effect analysis, and corrects for multiple comparisons across time and frequency (Maris and Oostenveld, 2007).

In summary, our approach results in a multiple-comparison corrected time-frequency map of values that indicate how strongly activation in response to left and right PLD differs between hemispheres.

In addition, we performed *post-hoc* ANOVAs and *t*-tests on the significant clusters found in the above mentioned analysis. To this end, we averaged spectral power over significant time-frequency pixels (as defined in Figure 2) separately for each condition (left or right PLD) and sensor set (left or right hemisphere). Averaged power values were log-transformed and then forwarded to a  $2 \times 2$  ANOVA with the factors PLD direction (left/right) and hemisphere (left/right).

To test an influence of body posture on lateralization of spectral power, we extracted for each action sequences of maximally and minimally informative body postures. Maximally informative postures were defined as postures which show the largest difference between a rightward oriented posture and its mirrored leftward counterpart. Hence, minimally informative postures show the smallest difference. The respective body postures were determined by subtracting for each point the horizontal positions of left and right postures and then summing up the differences of individual points. We averaged spectral power at the time point of maximal/minimal difference  $\pm 100$  ms. Averaged power values were log-transformed and then forwarded to a  $2 \times 2 \times 2$  ANOVA with the factors PLD direction (left/right), hemisphere (left/right), and body posture (maximal/minimal).

## Results

We found a significant negative cluster between 275 and 675 ms and 12–16 Hz ( $p = 0.045$ ) and second negative cluster between

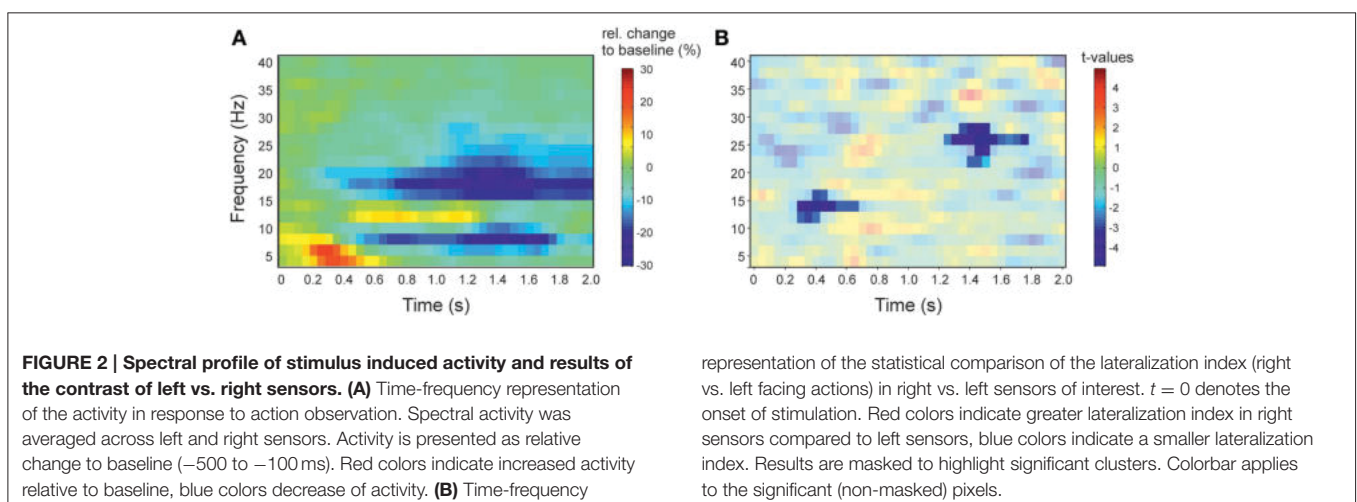
1225 and 1775 ms and 22–28 Hz ( $p = 0.004$ ), i.e., the difference between left and right facing point-light displays (PLD) showed the strongest lateralization effect in the beta-band (Figure 2).

To further elucidate the lateralization effect, we performed a *post-hoc* analysis on these significant time-frequency clusters. To this end, we performed a  $2 \times 2$  ANOVA with the factors direction (left/right) and hemisphere (left/right). For the early cluster (275–675 ms), the ANOVA revealed no significant main effects (factor direction:  $F = 0.03$ ,  $p = 0.87$ , factor hemisphere:  $F = 0.01$ ,  $p = 0.93$ ) but a highly significant interaction effect ( $F = 8.6$ ,  $p = 0.008$ ). For the late cluster (1225–1775 ms), the ANOVA revealed no significant main effects (factor direction:  $F = 2.31$ ,  $p > 0.14$ , factor hemisphere:  $F = 0.37$ ,  $p > 0.55$ ) but a highly significant interaction effect ( $F = 16.1$ ,  $p \leq 0.001$ ).

For the early cluster, *post-hoc t*-tests revealed a strong trend toward significance ( $p = 0.08$ ) for the comparison in the left hemisphere and a significant difference for the comparison in right sensors ( $p = 0.03$ ). That is, in right sensors, PLD facing to the left elicited stronger power in the beta-band compared to PLD facing to the right and in left sensors, PLD facing to the right elicited stronger power in the beta-band compared to PLD facing to the left (Figure 3A).

For the late cluster, *t*-tests revealed a very strong trend toward significance ( $p = 0.05$ ) in left sensors and a highly significant ( $p < 0.001$ ) difference in right sensors, i.e., in left sensors PLD facing to the right elicited stronger power in the beta-band compared to PLD facing to the left while in right sensors the opposite pattern was found: PLD facing to the left elicited stronger power in the beta-band than PLD facing to the right (Figure 3B).

To test whether the lateralization effect depended on body postures, we performed an additional  $2 \times 2 \times 2$  ANOVA with the factors direction (left/right), hemisphere (left/right), and body posture (maximal/minimal) (see Methods for details). The ANOVA revealed a significant main effect of the factors direction ( $F = 8.1$ ,  $p = 0.02$ ) and hemisphere ( $F = 15.2$ ,  $p = 0.002$ ). In addition, we found a significant interaction for direction  $\times$  hemisphere ( $F = 5.1$ ,  $p = 0.04$ ) and a highly significant effect for the Three-Way interaction direction  $\times$  hemisphere  $\times$  body posture ( $F = 30.1$ ,  $p < 0.001$ ). *Post-hoc t*-tests revealed



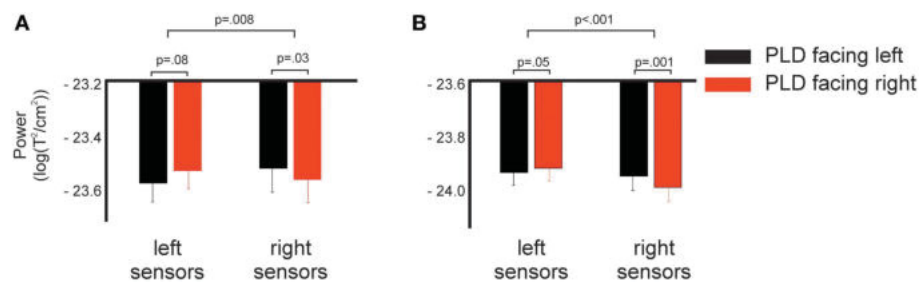


**FIGURE 3 | Spectral power in response to left and right facing actions for left and right sensors as shown in Figure 1C. (A)** Log-transformed spectral power averaged across time-frequency points of the early significant cluster shown in **Figure 2** (275–675 ms, 12–16 Hz).

**(B)** Same as **(A)**, but now for the late cluster (1225–1775 ms, 22–28 Hz). *p*-values indicate results of *post-hoc t*-tests (lower row) and interaction effect of the  $2 \times 2$  ANOVA (upper row, see Methods and Results for details).

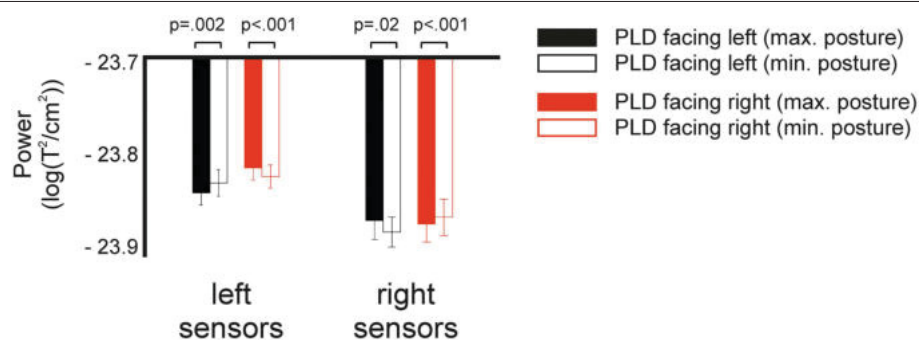


**FIGURE 4 | Spectral power in response to left and right facing actions at specific body postures.** Fully colored bars show power in response to body postures which maximally differentiate between left and right facing

bodies. White bars with colored outline show power in response to body postures which minimally differentiate. *P*-values indicate results of *post-hoc t*-tests between maximally and minimally differentiating postures.

a significant difference between maximal and minimal body postures for all four pairwise comparisons ( $p < 0.02$ , **Figure 4**).

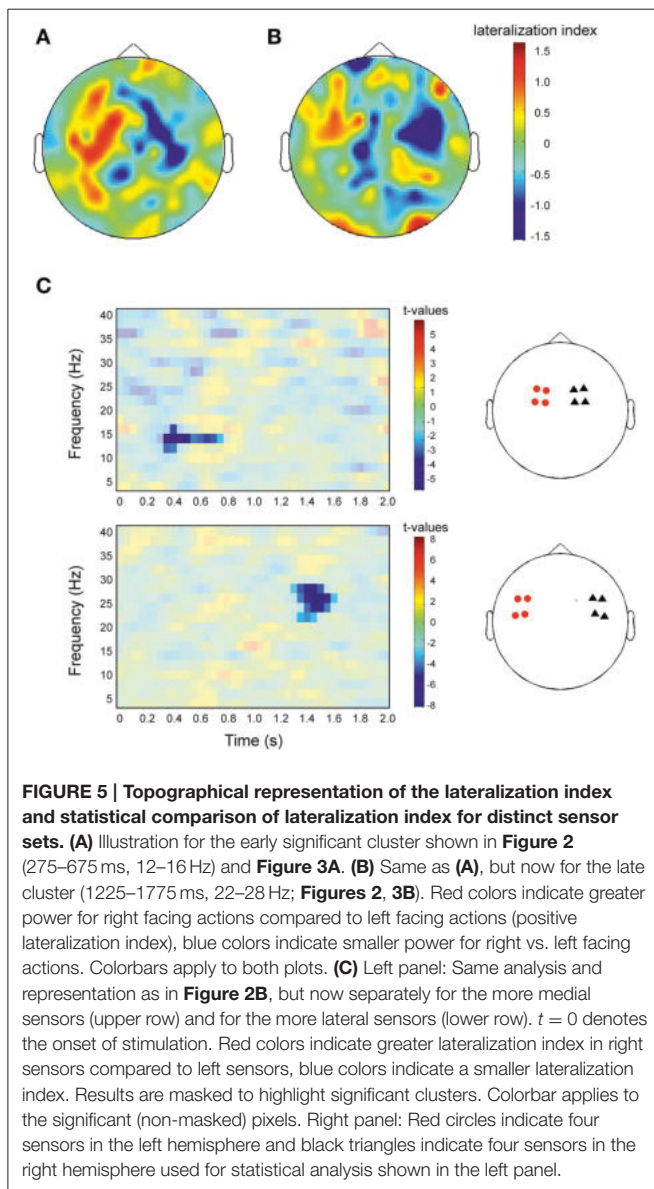
In accordance with the results shown in **Figures 2, 3**, the topographical representation of the lateralization effect showed a positive LI in the left hemisphere and a negative LI in the right hemisphere (**Figure 5**). Visual inspection indicated that both, early and late effects were mostly pronounced in motoric areas, with the early significant effect being more pronounced to medial sites (**Figure 5A**) compared to the late significant effect (**Figure 5B**). To test this observation, we repeated the analysis of **Figure 2**, but now separately for the eight lateral and the eight medial sensors. In medial sensors, only the early cluster reached significance ( $p = 0.044$ ), while in lateral sensors, only the late cluster reached significance ( $p = 0.001$ ; **Figure 5C**). This analysis, thus, confirmed that the early significant effect was more pronounced to medial sites while the late significant effect was more pronounced in lateral sites.

## Discussion

Suppression of neuronal activity, especially in the alpha- and beta-band, in motoric systems during action observation has been interpreted as an involvement of the respective areas in the process of action observation (e.g., Babiloni et al., 2002; Pineda, 2008; Kilner et al., 2009; Frenkel-Toledo et al., 2013). Here, we

found that human actions with the actor facing either to the right or to the left elicited lateralized activity in motoric areas: Right and left areas of the motoric system showed significantly different activation in response to right and left facing actions. This lateralization effect was found at two distinct time periods and spectral clusters: An early significant cluster between 275 and 675 ms and 12–16 Hz ( $p < 0.05$ ) and second cluster between 1225 and 1775 ms and 22–28 Hz ( $p < 0.01$ ). The topographical representation of both effects showed a spatial overlap covering presumably frontal, premotor and motor areas, with the early effect showing a stronger focus toward medial sites and the late effect a more lateralized location.

It is known from studies on action execution that suppression of beta-band power is mainly found in sensorimotor areas contralateral to the movement (Gross et al., 2005). Thus, one also might expect stronger suppression of beta band power in areas contralateral to the body side the actor displays toward the observer. In other words, viewing the actor facing to the right and thus mainly observing the right body side would be expected to elicit stronger suppression of beta-band power in the left hemisphere and vice versa. *Post-hoc* analysis of our data revealed, however, that beta-band power in left sensors was lowest for left facing actions and in right sensors for right facing actions. A potential reason for this effect might be that our point-light actors always displayed both body sides. That



is, although for each action there was always one body side directed to the observer, there was no occlusion of remote point-lights when they moved behind the body. In addition, there was no specific task regarding the body side. Since action direction and body side was irrelevant for the task, remote body sides might be included in the recognition process to produce a “whole-body” representation of the action. This might lead to overcompensation effects when the observer tried to embody the remote, ipsilateral body side or imagine the movement of the remote body side.

In a study by Kilner et al. (2009) subjects viewed whole body movements of human actors while EEG activity was recorded. The actor always faced toward the observer while performing an action either with the right or left arm. Similar to the results of our study, Kilner et al. reported that beta band suppression in sensorimotor areas was strongest in sensors ipsilateral to the arm

performing the action, i.e., movements of the left arm induced strongest suppression in the left hemisphere and vice versa for right arms. The authors argued that the observed pattern was driven mainly by the side of the screen on which the observed movement occurred and not by the hand that was observed moving. An influence of the side of the screen, however, cannot explain our results since actions were always presented centrally. Our results therefore argue that while the hemifield in which the action is presented certainly plays a role for the strength of the beta-band suppression, there is an additional effect of body side.

de Lange et al. (2008) studied beta-band suppression in sensorimotor areas during motor imagery of hand movements. The authors reported that the duration of beta-band suppression was correlated with the difficulty of the imagery task: The more complex a task or process, the longer beta-band suppression lasts. Observing actions might thus initially induce similar beta-band suppression in both hemispheres independent of the body side viewed. The duration of the beta-band suppression, however, might depend on the body side processed, leading to shorter beta-band suppression in left sensors if the right body side is viewed in comparison to viewing the right body side and vice versa for right sensors. The different duration of beta-band suppression might thus explain the results reported in our study (**Figure 3**).

In a recent study, Pavlidou et al. (2014b) analyzed the beta-band activity in response to normal (plausible) and biomechanically implausible human actions (using the same dataset as in the present study). The authors reported that beta band suppression was significantly stronger for implausible than plausible actions. The authors argued that the stronger suppression might result from stronger matching of incoming visual information to stored representations of the actions in (pre)motor areas. Thus, rather than reflecting an activation of the MNS *per se*, beta-band suppression might reflect the complexity of a task (Pavlidou et al., 2014a).

We found that the contrast between left and right facing actors was stronger in right than in left hemispheres. This finding is in line with results from studies on action observation and motor imagery. For example, Kilner et al. (2009) reported that the difference of beta-band power between observing left and right arm movements was stronger in right than in left hemispheres. In addition, de Lange et al. (2008) studied imagery of left and right hand movements. The authors reported for the contrast left vs. right hand a stronger suppression of beta-band power in right than in left hemispheres. Similarly, previous studies reported that the left parietal and premotor cortices are equally involved in imagined movements of left and right hands, while the right parietal and premotor cortices are preferentially involved in imagined movements of the contralateral left hand (Parsons et al., 1998; De Lange et al., 2006; Stinear et al., 2006).

In addition, we found that the contrast between left and right facing actors was stronger at the later time cluster. The timing of this later effect is in line with other studies investigating modulations of beta-band power in response to action observation and imagery. For example, Kilner et al. (2009) reported significant differences in beta-band power between observing left and right hand movements to peak at 1670 ms. Pavlidou et al. (2014b) studied the contrast between plausible

and implausible actions and reported that the difference in sensorimotor beta-band power was found at 2400–2650 ms. In addition, de Lange et al. (2008) reported differences in beta-band power between imagery of left and right hand movements around 1500 ms.

Early and late cluster differ also with regard of the frequency for which the lateralization effect was found. The early cluster was found to be significant between 12 and 16 Hz. Typically, this frequency band might be assigned to the beta-band (13–30 Hz). While the frequency bands between 6 and 10 Hz and 16–30 Hz show a suppression of activity in response to action observation, the frequency band between 12 and 16 Hz shows an increase of activity (**Figure 2A**). The spectral profile of the activation pattern in response to action observation, thus, argues for a separate frequency band between ~12 and 16 Hz (**Figure 2A**). There is evidence for a functional distinction of the alpha-frequency band in a lower and an upper alpha-band (Klimesch et al., 1997; Klimesch, 1999). In sensorimotor areas, the lower band (8–10 Hz) has been suggested to be somatotopically non-specific while a somatotopically specific oscillation is characteristically found in the upper alpha (10–13 Hz) frequency band (Pfurtscheller et al., 2000). The distinct profile of the 12–16 Hz band underlying the early cluster argues thus that the early cluster might be functionally separate from the late cluster which is clearly located in the beta-band. The early cluster might be related to the somatotopically specific upper alpha band (Pfurtscheller et al., 2000).

In addition to their temporal and spectral profile, the early and the late cluster seem to differ also with regard to their cortical origin. While both clusters spatially overlap, the late cluster clearly extends to more lateral sides than the early cluster (**Figure 5**). We can only speculate about the cortical sources. The early, more medial cluster might reflect activity in sensorimotor or (pre)motor areas. These areas are known to be somatotopically organized (Buccino et al., 2001). Therefore, the potential spectral overlap with the upper alpha-band, which is

thought to reflect somatotopically specific activity (Pfurtscheller et al., 2000), provides further evidence for the sensorimotor areas. The late cluster might originate from inferior frontal areas (Nishitani and Hari, 2000) or premotoric areas. Sensorimotor and premotor areas and inferior frontal gyrus are known to be involved in the process of action observation (Nishitani and Hari, 2000; Rizzolatti and Craighero, 2004; Molenberghs et al., 2012). Our results imply that in addition to their somatotopical organization, these areas show a lateralized organization with right and left hemispheres being differently activated by left or right facing actions.

In conclusion, we demonstrate that parts of the human motoric system show a lateralization effect with regard to action observation. That is, left and right hemispheres are activated differently by actions for which the actor was facing to the right or to the left. These effects are found for two sensor arrays, presumably covering sensorimotor areas, (pre)motor areas and/or inferior frontal areas. The lateralization effects are found in the beta-band, with the lateralization effect being more strongly pronounced at ~1500 ms after stimulus onset in putative inferior frontal areas. These results demonstrate that during action observation parts of the human MNS show in addition to the known somatotopic organization a lateralization.

## Acknowledgments

We thank Markus Lappe and Marc de Lussanet for providing us with the PLDs. This work was supported by a grant to JL from the research commission of the medical department at Heinrich Heine University, Düsseldorf, Germany.

## Supplementary Material

The Supplementary Material for this article can be found online at: <http://journal.frontiersin.org/article/10.3389/fnint.2015.00043>

## References

- Babiloni, C., Babiloni, F., Carducci, F., Cincotti, F., Ciozza, G., Del Percio, C., et al. (2002). Human cortical electroencephalography (EEG) rhythms during the observation of simple aimless movements: a high-resolution EEG study. *Neuroimage* 17, 559–572. doi: 10.1006/nimg.2002.1192
- Blake, R., and Shiffrar, M. (2007). Perception of human motion. *Annu. Rev. Psychol.* 58, 47–73. doi: 10.1146/annurev.psych.57.102904.190152
- Buccino, G., Binkofski, F., Fink, G. R., Fadiga, L., Fogassi, L., Gallese, V., et al. (2001). Action observation activates premotor and parietal areas in a somatotopic manner: an fMRI study. *Eur. J. Neurosci.* 13, 400–404. doi: 10.1111/j.1460-9568.2001.01385.x
- De Lange, F. P., Helmich, R. C., and Toni, I. (2006). Posture influences motor imagery: an fMRI study. *Neuroimage* 33, 609–617. doi: 10.1016/j.neuroimage.2006.07.017
- de Lange, F. P., Jensen, O., Bauer, M., and Toni, I. (2008). Interactions between posterior gamma and frontal alpha/beta oscillations during imagined actions. *Front. Hum. Neurosci.* 2:7. doi: 10.3389/fnro.09.007.2008
- Frenkel-Toledo, S., Bentin, S., Perry, A., Liebermann, D. G., and Soroker, N. (2013). Dynamics of the EEG power in the frequency and spatial domains during observation and execution of manual movements. *Brain Res.* 1509, 43–57. doi: 10.1016/j.brainres.2013.03.004
- Gilaie-Dotan, S., Kanai, R., Bahrami, B., Rees, G., and Saygin, A. P. (2013). Neuroanatomical correlates of biological motion detection. *Neuropsychologia* 51, 457–463. doi: 10.1016/j.neuropsychologia.2012.11.027
- Gross, J., Pollok, B., Dirks, M., Timmermann, L., Butz, M., and Schnitzler, A. (2005). Task-dependent oscillations during unimanual and bimanual movements in the human primary motor cortex and SMA studied with magnetoencephalography. *Neuroimage* 26, 91–98. doi: 10.1016/j.neuroimage.2005.01.025
- Grossman, E., Donnelly, M., Price, R., Pickens, D., Morgan, V., Neighbor, G., et al. (2000). Brain areas involved in perception of biological motion. *J. Cogn. Neurosci.* 12, 711–720. doi: 10.1162/089982900562417
- Hari, R., Forss, N., Avikainen, S., Kirveskari, E., Salenius, S., and Rizzolatti, G. (1998). Activation of human primary motor cortex during action observation: a neuromagnetic study. *Proc. Natl. Acad. Sci. U.S.A.* 95, 15061–15065. doi: 10.1073/pnas.95.25.15061

- Johansson, G. (1973). Visual perception of biological motion and a model for its analysis. *Percept. Psychophys.* 14, 201–211. doi: 10.3758/BF03212378
- Kilner, J. M., Marchant, J. L., and Frith, C. D. (2009). Relationship between activity in human primary motor cortex during action observation and the mirror neuron system. *PLoS ONE* 4:e4925. doi: 10.1371/journal.pone.0004925
- Klimesch, W. (1999). EEG alpha and theta oscillations reflect cognitive and memory performance: a review and analysis. *Brain Res. Rev.* 29, 169–195. doi: 10.1016/S0165-0173(98)00056-3
- Klimesch, W., Doppelmayr, M., Pachinger, T., and Russegger, H. (1997). Event-related desynchronization in the alpha band and the processing of semantic information. *Brain Res. Cogn. Brain Res.* 6, 83–94. doi: 10.1016/S0926-6410(97)00018-9
- Lange, J., Christian, N., and Schnitzler, A. (2013). Audio-visual congruency alters power and coherence of oscillatory activity within and between cortical areas. *Neuroimage* 79, 111–120. doi: 10.1016/j.neuroimage.2013.04.064
- Lange, J., and Lappe, M. (2007). The role of spatial and temporal information in biological motion perception. *Adv. Cogn. Psychol.* 3, 419–428. doi: 10.2478/v10053-008-0006-3
- Lange, J., Oostenveld, R., and Fries, P. (2011). Perception of the touch-induced visual double-flash illusion correlates with changes of rhythmic neuronal activity in human visual and somatosensory areas. *Neuroimage* 54, 1395–1405. doi: 10.1016/j.neuroimage.2010.09.031
- Maris, E., and Oostenveld, R. (2007). Nonparametric statistical testing of EEG- and MEG-data. *J. Neurosci. Methods* 164, 177–190. doi: 10.1016/j.jneumeth.2007.03.024
- Molenberghs, P., Cunnington, R., and Mattingley, J. B. (2012). Brain regions with mirror properties: a meta-analysis of 125 human fMRI studies. *Neurosci. Biobehav. Rev.* 36, 341–349. doi: 10.1016/j.neubiorev.2011.07.004
- Mukamel, R., Ekstrom, A. D., Kaplan, J., Iacoboni, M., and Fried, I. (2010). Single-neuron responses in humans during execution and observation of actions. *Curr. Biol.* 20, 750–756. doi: 10.1016/j.cub.2010.02.045
- Muthukumaraswamy, S. D., Johnson, B. W., and McNair, N. A. (2004). Mu rhythm modulation during observation of an object-directed grasp. *Brain Res. Cogn. Brain Res.* 19, 195–201. doi: 10.1016/j.cogbrainres.2003.12.001
- Nishitani, N., and Hari, R. (2000). Temporal dynamics of cortical representation for action. *Proc. Natl. Acad. Sci. U.S.A.* 97, 913–918. doi: 10.1073/pnas.97.2.913
- Oostenveld, R., Fries, P., Maris, E., and Schoffelen, J.-M. (2011). FieldTrip: open source software for advanced analysis of MEG, EEG, and invasive electrophysiological data. *Comput. Intell. Neurosci.* 2011:e156869. doi: 10.1155/2011/156869
- Parsons, L. M., Gabrieli, J. D., Phelps, E. A., and Gazzaniga, M. S. (1998). Cerebrally lateralized mental representations of hand shape and movement. *J. Neurosci.* 18, 6539–6548.
- Pavlidou, A., Schnitzler, A., and Lange, J. (2014a). Beta oscillations and their functional role in movement perception. *Transl. Neurosci.* 5, 286–292. doi: 10.2478/s13380-014-0236-4
- Pavlidou, A., Schnitzler, A., and Lange, J. (2014b). Distinct spatio-temporal profiles of beta-oscillations within visual and sensorimotor areas during action recognition as revealed by MEG. *Cortex* 54, 106–116. doi: 10.1016/j.cortex.2014.02.007
- Pavlidou, A., Schnitzler, A., and Lange, J. (2014c). Interactions between visual and motor areas during the recognition of plausible actions as revealed by magnetoencephalography. *Hum. Brain Mapp.* 35, 581–592. doi: 10.1002/hbm.22207
- Perry, A., and Bentin, S. (2009). Mirror activity in the human brain while observing hand movements: a comparison between EEG desynchronization in the mu-range and previous fMRI results. *Brain Res.* 1282, 126–132. doi: 10.1016/j.brainres.2009.05.059
- Pfurtscheller, G., Neuper, C., and Krausz, G. (2000). Functional dissociation of lower and upper frequency mu rhythms in relation to voluntary limb movement. *Clin. Neurophysiol.* 111, 1873–1879. doi: 10.1016/S1388-2457(00)00428-4
- Pineda, J. A. (2008). Sensorimotor cortex as a critical component of an ‘extended’ mirror neuron system: does it solve the development, correspondence, and control problems in mirroring? *Behav. Brain Funct.* 4:47. doi: 10.1186/1744-9081-4-47
- Rizzolatti, G., and Craighero, L. (2004). The mirror-neuron system. *Annu. Rev. Neurosci.* 27, 169–192. doi: 10.1146/annurev.neuro.27.070203.144230
- Rizzolatti, G., and Luppino, G. (2001). The cortical motor system. *Neuron* 31, 889–901. doi: 10.1016/S0896-6273(01)00423-8
- Saygin, A. P., Wilson, S. M., Hagler, D. J., Bates, E., and Sereno, M. I. (2004). Point-light biological motion perception activates human premotor cortex. *J. Neurosci.* 24, 6181–6188. doi: 10.1523/JNEUROSCI.0504-04.2004
- Schnitzler, A., Salenius, S., Salmelin, R., Jousmäki, V., and Hari, R. (1997). Involvement of primary motor cortex in motor imagery: a neuromagnetic study. *Neuroimage* 6, 201–208. doi: 10.1006/nimg.1997.0286
- Stinear, C. M., Fleming, M. K., and Byblow, W. D. (2006). Lateralization of unimanual and bimanual motor imagery. *Brain Res.* 1095, 139–147. doi: 10.1016/j.brainres.2006.04.008
- Ulloa, E. R., and Pineda, J. A. (2007). Recognition of point-light biological motion: mu rhythms and mirror neuron activity. *Behav. Brain Res.* 183, 188–194. doi: 10.1016/j.bbr.2007.06.007

**Conflict of Interest Statement:** The authors declare that the research was conducted in the absence of any commercial or financial relationships that could be construed as a potential conflict of interest.

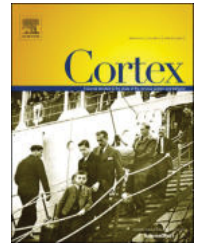
Copyright © 2015 Lange, Pavlidou and Schnitzler. This is an open-access article distributed under the terms of the Creative Commons Attribution License (CC BY). The use, distribution or reproduction in other forums is permitted, provided the original author(s) or licensor are credited and that the original publication in this journal is cited, in accordance with accepted academic practice. No use, distribution or reproduction is permitted which does not comply with these terms.

11) Pavlidou, A., Schnitzler, A., & **Lange, J.** (2014a).

Distinct spatio-temporal profiles of beta-oscillations within visual and sensorimotor areas during action recognition as revealed by MEG.

*Cortex*, 54, 106–116.

Impact factor (2014): 5.128



## Research report

# Distinct spatio-temporal profiles of beta-oscillations within visual and sensorimotor areas during action recognition as revealed by MEG



Anastasia Pavlidou\*, Alfons Schnitzler and Joachim Lange

Institute of Clinical Neuroscience and Medical Psychology, Medical Faculty, Heinrich-Heine-University Düsseldorf, Düsseldorf, Germany

## ARTICLE INFO

## Article history:

Received 7 March 2013

Reviewed 1 July 2013

Revised 27 September 2013

Accepted 10 February 2014

Action editor David Carey

Published online 24 February 2014

## Keywords:

Point-light displays

Oscillatory activity

Actions

Mirror neuron system

## ABSTRACT

The neural correlates of action recognition have been widely studied in visual and sensorimotor areas of the human brain. However, the role of neuronal oscillations involved during the process of action recognition remains unclear. Here, we were interested in how the plausibility of an action modulates neuronal oscillations in visual and sensorimotor areas. Subjects viewed point-light displays (PLDs) of biomechanically plausible and implausible versions of the same actions. Using magnetoencephalography (MEG), we examined dynamic changes of oscillatory activity during these action recognition processes. While both actions elicited oscillatory activity in visual and sensorimotor areas in several frequency bands, a significant difference was confined to the beta-band (~20 Hz). An increase of power for plausible actions was observed in left temporal, parieto-occipital and sensorimotor areas of the brain, in the beta-band in successive order between 1650 and 2650 msec. These distinct spatio-temporal beta-band profiles suggest that the action recognition process is modulated by the degree of biomechanical plausibility of the action, and that spectral power in the beta-band may provide a functional interaction between visual and sensorimotor areas in humans.

© 2014 Elsevier Ltd. All rights reserved.

## 1. Introduction

Recognizing others' actions is essential to communicate effectively with the people around us. The proposed mechanism of how the brain mediates recognition of actions is the combination of both visual and motor processes (Craigheo, Metta, Sandini, & Fadiga, 2007; Jeannerod, 2001; Rizzolatti &

Craigheo, 2004). The underlying cortical sources of this process have been studied by single-cell recordings in macaque monkeys (Di, Fadiga, Fogassi, Gallese, & Rizzolatti, 1992; Fadiga, Fogassi, Pavesi, & Rizzolatti, 1995; Oram & Perrett, 1994) and extensively in humans using haemodynamic and electrophysiological techniques (Buccino, Binkofski, & Riggio, 2004; Grossman et al., 2000; Kessler et al., 2006; Michels, Kleiser, de Lussanet, Seitz, & Lappe, 2009; Michels, Lappe, &

\* Corresponding author. Institute of Clinical Neuroscience and Medical Psychology, Medical Faculty, Heinrich-Heine-University, Universitätsstr. 1, 40225 Düsseldorf, Germany.

E-mail address: [pavlidou.anastasia@gmail.com](mailto:pavlidou.anastasia@gmail.com) (A. Pavlidou).

<http://dx.doi.org/10.1016/j.cortex.2014.02.007>

0010-9452/© 2014 Elsevier Ltd. All rights reserved.

Vaina, 2005; Nishitani & Hari, 2000; Pavlova, Lutzenberger, Sokolov, & Birbaumer, 2004; Saygin, Wilson, Hagler, Bates, & Sereno, 2004; Schippers & Keysers, 2011). In summary, these studies have identified two main areas to be involved in the observation/recognition of actions known as the superior temporal sulcus (STS) and premotor cortex (PMC). It has been suggested that patterns of neural activity in both STS and PMC are reflective of the existence of a dynamic network known as the mirror neuron system (MNS) similar to that observed in monkeys (Rizzolatti & Craighero, 2004; Schippers & Keysers, 2011).

Electrophysiological studies have demonstrated changes of neuronal oscillatory activity in visual and sensorimotor areas, during the observation of actions in the alpha (9–13 Hz) and the beta range (13–30 Hz) (Babiloni et al., 1999; Caetano, Jousmaki, & Hari, 2007; Cochin, Barthelemy, Roux, & Martineau, 1999; Hari et al., 1998; Kessler et al., 2006; de Lange, Jensen, Bauer, & Toni, 2008; Muthukumaraswamy, Johnson, Gaetz, & Cheyne, 2004, 2006; Muthukumaraswamy, Johnson, & McNair, 2004; Rossi et al., 2002). Such changes in oscillatory activity and in particular across the beta range have been associated with two processes: asynchrony or decrease of beta power occurs during the preparation and execution of movements, while synchrony or increase of beta power reflects active inhibition of the motor system (Pfurtscheller & Lopes da Silva, 1999; Pfurtscheller, Neuper, Brunner, & da Silva, 2005; Salmelin, Hamalainen, Kajola, & Hari, 1995).

While beta activity in sensorimotor areas is abundant, little is known, however, how oscillatory activity in sensorimotor areas is modulated by the plausibility or naturalness of an

observed action, and how sensorimotor areas interact with visual areas during the processing of such actions.

In a previous study, we examined how oscillatory activity in visual and sensorimotor areas is modulated by the presence or absence of a biological action (Pavlidou, Schnitzler, & Lange, 2014). Actions were represented by point-light displays (PLDs), a visual presentation method in which the human body is portrayed by just a handful of moving dots (Grossman et al., 2000; Johansson, 1973; Saygin et al., 2004). Subjects were asked to differentiate between plausible (e.g. walking) and scrambled (random assortment of dots) versions of different PLD action representations. We observed changes in gamma (~80 Hz), beta (~25 Hz) and alpha (~10 Hz) oscillatory activity between .5 and 1.3 sec in a widespread network of cortical areas, including STS and PMC. Further research however, is needed to determine whether sensorimotor areas are involved in higher form processing such as distinguishing between natural and unnatural forms of action movements when the degree of plausibility of an action is manipulated.

In the current study, we compare plausible human PLD actions to implausible human PLD actions. An implausible PLD action leaves the overall movement of the dots unchanged. In contrast to scrambled PLD however, overall visual information and human figure are only minimally altered to illustrate a somewhat biomechanically implausible or unnatural action. Subjects were asked to differentiate between plausible and implausible PLD actions. We were interested whether visual and motor areas will be engaged differently when we manipulate the biomechanical plausibility or naturalness of a human PLD action. More specifically, we were interested whether beta-band activity was sensitive to the

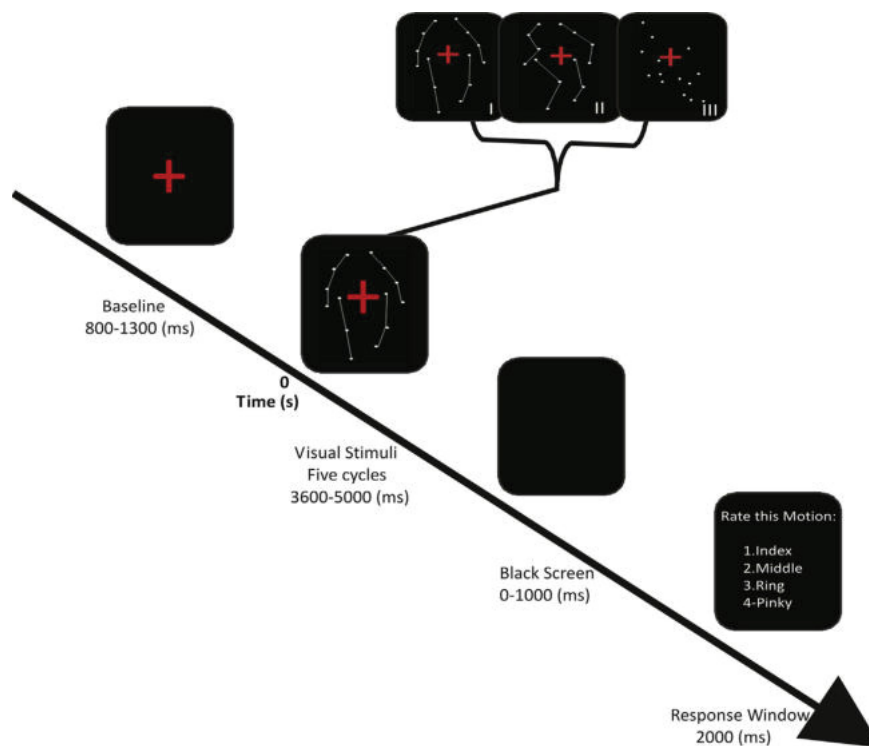


**Fig. 1 – Experimental setup.** Examples of stimuli used plausible (I), implausible (II), scrambled (III). Connecting lines were not present in the actual experiment. Participants first fixated on a red cross. PLD stimuli appeared at time point 0. After a black screen, response instructions visually appeared. See Subjects, experimental procedure and stimuli for details.

degree of plausibility of the observed action within and between visual and sensorimotor areas.

## 2. Methods

Data were collected in the same experiment with data from an earlier study (Pavlidou et al., 2014). Accordingly, the details of the stimuli and experimental procedures as well as the methods of data acquisition and data analysis have been described in great detail elsewhere (Pavlidou et al., 2014). Here, we provide a concise overview of the experimental procedure and analysis. All data were acquired in one session for each of our subjects. Data analysis in the present study, however, focuses on different experimental questions and uses different subsets of the data (the comparison between plausible and implausible PLD actions) than that from our previous study.

### 2.1. Subjects, experimental procedure and stimuli

Twelve right handed subjects with normal or corrected to normal vision [six males, mean age ( $\pm$  standard deviation – SD)  $27.6 \pm 2.87$  years] participated in the study. Each trial started with a presentation of a red fixation cross (visual angle  $.23^\circ$ ). After a jittered period (800–1300 msec), a PLD (visual angle  $4.81^\circ \times 1.95^\circ$ ) appeared for a period of 3600–5000 msec (five cycles of one action). After another randomized period (0–1000 msec), where only a black screen was visible, instructions were visually presented for a duration of 2000 msec. Subjects were asked to rate the PLD as either 1 - plausible, 2,3 - implausible and 4 - scrambled (Fig. 1). The total number of PLD stimuli employed during the experimental task was 31; 12 of which were plausible and 12 were implausible (and seven scrambled; see Movie 1 and 2 for example stimuli). All trials that were rated within the 2000 msec response window were included in the analysis. Stimuli were presented with a projector (PT-DW700E; Panasonic) with a refresh rate of 60 Hz. Stimulus presentation was controlled using Presentation Software (Neurobehavioral Systems, Albany, USA).

Supplementary video related to this article can be found at <http://dx.doi.org/10.1016/j.cortex.2014.02.007>.

### 2.2. Data acquisition and analysis

Neuronal activity was recorded with a 306-channel whole head magnetoencephalography (MEG) system (Neuromag Elekta Oy, Helsinki, Finland). Such a system contains 204 planar gradiometers and 102 magnetometers. Analysis in the present study was carried out only for the planar gradiometers. In addition, vertical and horizontal electrooculograms (EOGs) were recorded for offline artefact rejection. The subjects' head position relative to the sensor array was determined before the MEG recording. For source reconstruction, we obtained structural magnetic resonance images (MRI) from each subject using a 3 T MRI scanner (Siemens, Erlangen, Germany) and then co-registered the MRIs with the MEG data. The MEG data were analysed offline using the Fieldtrip toolbox

**Table 1 – Sensor selection based on stimulation effects observed during PLD visual stimulation pooled over all conditions. Sustained effects (0–4.5 sec) observed in our four regions of interest (parieto-occipital, sensorimotor, and bilateral temporal) in alpha (7–13 Hz), beta (13–23 Hz) and gamma (55–100 Hz).**

Regions of interest	Frequency range
Parieto-occipital	↑
	Gamma (55–100 Hz)
	↓
	Beta (13–23 Hz)
Sensorimotor	↓
	Alpha (7–13 Hz)
	↓
	Beta (15–23 Hz)
Left temporal	↑
	High alpha (11–13 Hz)
	↓
	Low alpha (7–11 Hz)
Right temporal	↓
	Beta (13–23 Hz)
	↑
	High alpha (11–13 Hz)
Right temporal	↓
	Low alpha (7–11 Hz)
	↑
	Gamma (90–100 Hz) <sup>a</sup>
	↓
	Gamma (50–80 Hz)
Right temporal	↓
	Beta (13–23 Hz)
	↑
	High alpha (11–13 Hz)
Right temporal	↓
	Low alpha (7–11 Hz)

<sup>a</sup> Gamma increase observed between 0 and 1.5 sec in right temporal.

[<http://www.ru.nl/donders/fieldtrip> (Oostenveld, Fries, Maris, & Schoffelen, 2011)]. Epochs with artifacts were discarded and power line noise was removed as previously described (Pavlidou et al., 2014).

### 2.3. Time–frequency analysis

Time–frequency representations (TFRs) of power were calculated using windows of 500 msec moved in steps of 50 msec for frequencies between 4 and 40 Hz. Time windows were tapered with a Hanning window with a spectral smoothing of  $\pm 2.0$  Hz. For frequencies between 40 and 100 Hz, we used windows of 400 msec moved in steps of 50 msec. Time windows were multiplied with seven tapers, resulting in a spectral smoothing of  $\pm 10$  Hz. Regions of interest were first determined on sensor level by pooling all conditions together irrespective of PLD movement and comparing it to a baseline ( $-400$  to  $-250$  msec). Sensors revealing the strongest perturbations in oscillatory activity were then selected for further analysis. Strong changes in alpha (7–13 Hz), beta (13–35 Hz) and gamma (55–100 Hz) oscillatory power were bilaterally observed in sensors over parieto-occipital, temporal, and sensorimotor areas, but varied within each area (for details of sensor selection see Table 1 and Pavlidou et al., 2014). These variations in alpha, beta and gamma power between the above-mentioned areas (parieto-occipital, sensorimotor, and bilateral temporal), suggest that each area processes the visual presentation of our PLD actions differently. To assess the different roles of the four regions of interest in action recognition, we measured differences in oscillatory activity between plausible and implausible PLD actions as described below.

### 2.4. Condition contrast

Differences in spectral power between plausible and implausible PLDs were assessed for parieto-occipital, temporal and sensorimotor areas. Per subject, we performed an independent samples t-test between power values of the plausible and implausible conditions averaged across sensors for each of the four regions of interest. This resulted in a time–frequency t-map for each subject. The consistency of t-values across subjects was analysed in a second step using a nonparametric randomization test. This statistical test effectively corrects for multiple comparisons (Maris & Oostenveld, 2007), and thresholds the individual time–frequency maps of t-values at a value of  $\pm 1.96$  (alpha = .05). Neighbouring t-values exceeding the threshold were combined to time–frequency clusters. For each time–frequency cluster the sum of the t-values was used in the second-level cluster-level test statistics (Maris & Oostenveld, 2007). The *p*-value of the cluster in the second-level test statistics was then estimated using the Monte Carlo approach by comparing cluster test statistic with a randomization null distribution. The null distribution was computed by randomly permuting the data 1000 times and calculating the maximum cluster test statistic (Lange, Oostenveld, & Fries, 2011). Statistical analysis was done for the first 3 sec following visual presentation of our PLD actions to minimize influence of motor preparation.

### 2.5. Temporal evolution of alpha/beta power

Based on the significant clusters found on sensor level (condition contrast analysis), we assessed changes in beta power separately for our plausible and implausible PLD conditions for left temporal (9–21 Hz), parieto-occipital (5–21 Hz) and sensorimotor areas (15–21 Hz). Since the clusters in parieto-occipital and left temporal areas were found in a broader frequency band, covering alpha- and beta-frequencies (5–21 Hz, 9–21 Hz, respectively), temporal evolution was effectively collapsed over alpha- and beta-frequency bands for these areas. We additionally computed temporal analysis separately for the alpha (8/9–12 Hz) and beta (13–21 Hz) bands. Since the results were highly similar in space and time for both frequency bands (please refer to Fig. S1), we will report only the results of the collapsed frequency band. Since no significant clusters were found for right temporal areas we did not assess changes in alpha/beta power in this area. Per subject, we averaged power across sensors for each of the three areas (parieto-occipital, left temporal and sensorimotor) and their respective significant frequency clusters, across all trials for each of our two conditions. This resulted in a temporal evolution of alpha/beta power change for each subject. Finally, we averaged the results across subjects.

### 2.6. Source analysis

Based on the significant clusters on sensor level, we determined neuronal sources by applying Dynamic Imaging of Coherent Sources (DICS), an adaptive spatial filtering technique (Gross et al., 2001). This takes into account the forward model at the location of interest (the leadfield matrix) and the crossspectral density (CSD) between all MEG sensor pairs for the frequency of interest determined by the significant time-clusters on sensor level. The leadfield matrix was calculated based on a realistically shaped single-shell volume conduction model (Nolte, 2003), derived from each individual subject's structural MRI. The headmodel was reduced to a regular three-dimensional grid (1 cm resolution) and spatial filters  $w(r, f)$  were constructed for each grid point using the following formula:

$$w(r, f) = (L'(r)C(f) + \lambda \times I)^{-1} L'(r)^{-1} L'(r)(C(f) + \lambda \times I)^{-1},$$

where  $L'(r)$  is the inverse of the leadfield matrix (forward model) at location of interest  $r$ ,  $C(f)$  is the CSD matrix between all MEG sensor pairs at frequency  $f$ ,  $\lambda$  is the regularization parameter, and  $I$  is the identity matrix (Gross et al., 2001; de Lange et al., 2008). Plausible and implausible conditions were pooled to compute common filters. Next, CSD matrices of single trials were projected through those filters, providing single trial estimates of source power ( $p$ ) using the following formula (Bauer, Oostenveld, Peeters, & Fries, 2006)

$$p(r, f) = w(r, f)C(f)'w^*(r, f).$$

In line with the analysis on sensor level, a between-condition t-value for condition contrasts was computed for each subject and overlaid to the corresponding anatomical MRI. Anatomical and functional data were then spatially normalized using SPM8 (Statistical Parametric Mapping; <http://www.fil.ion.ucl.ac.uk/spm>) to the Montreal

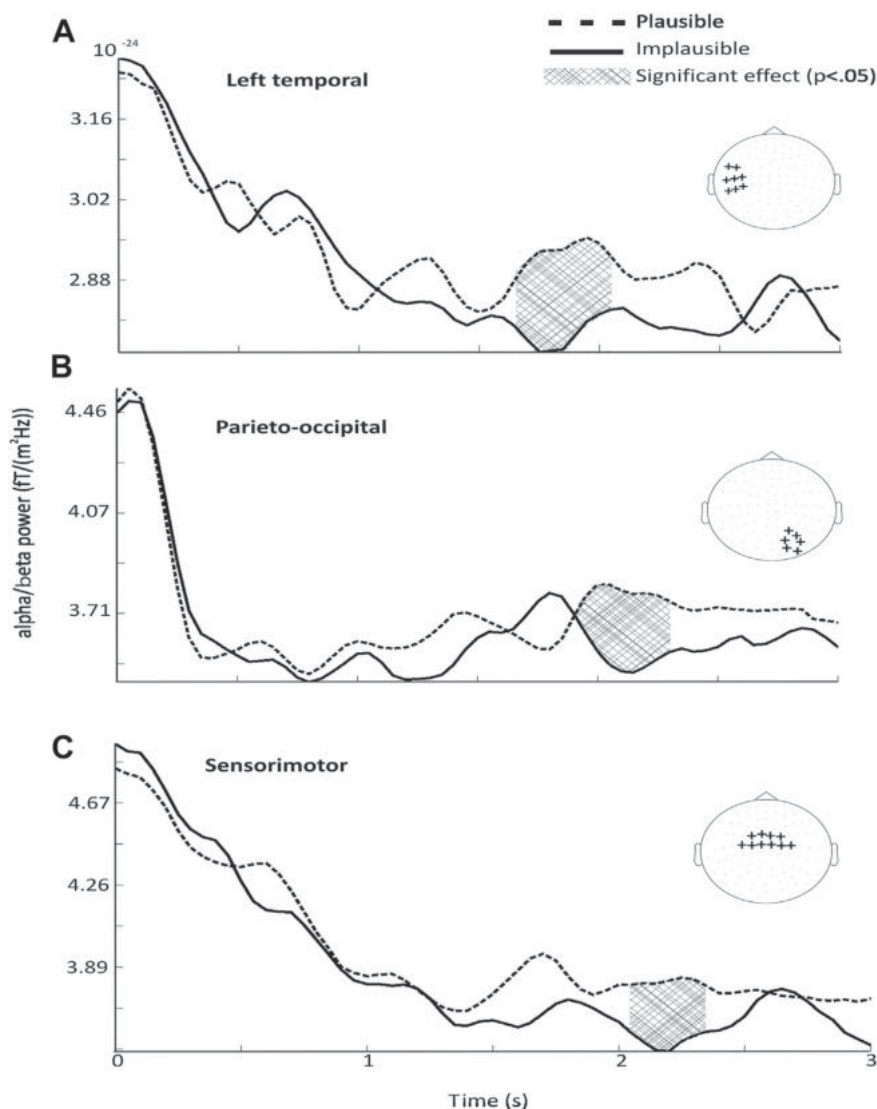


**Fig. 2 – Temporal evolution of alpha/beta power change for plausible (dotted line) and implausible (black line) for left temporal (A), parieto-occipital (B), and sensorimotor (C) sensors (+). Pattern area denotes the significant time points, i.e., highest differences between plausible and implausible. Power is represented on a log scale.**

Neurological Institute (MNI) template. Statistical testing on group level for condition contrasts was carried out in the same way as on sensor level (see above). For visual illustration of the significance effects found on sensor level (see above) results on group level ( $p < .05$  uncorrected) were displayed on the MNI template brain and neuronal sources were identified using the AFNI atlas (<http://afni.nimh.nih.gov/afni>), integrated into Fieldtrip.

### 2.7. Power correlations

We calculated power correlations between our areas of interest (Figs. 2 and 3A) to assess interactions between visual and sensorimotor areas during the processing of plausible and implausible actions. To this end, we averaged spectral power in each area of interest over time and frequency for each trial. Time and frequency were determined by the significant clusters found in the condition contrast (Fig. 3A). We

computed power correlations between areas on a trial-by-trial basis for each subject by computing the Pearson correlation coefficient. Correlation coefficients were transformed to  $z$ -values (Choi, 1977). Finally, we used a two-sided  $t$ -test to statistically test correlation coefficients across subjects against the null hypothesis of no correlation, i.e.,  $r = 0$ . To investigate whether the correlations were time-based specific, data windows were shifted  $\pm 100$  msec and correlations were recomputed in the same way as described above.

## 3. Results

### 3.1. Behavioural data

Subjects could easily distinguish between plausible and implausible PLDs with an average rating of  $1.5 (\pm 1.9)$  and  $2.3$

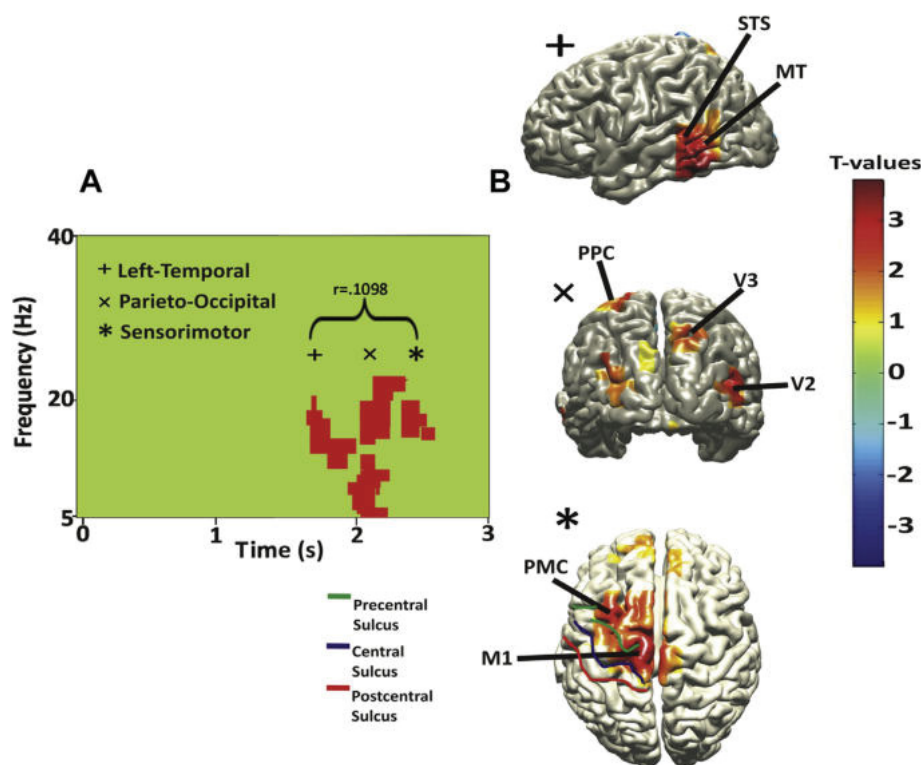


**Fig. 3 – Condition contrasts: plausible vs implausible actions. (A) Representations of significant clusters ( $p < .05$ ) found on sensor level for (chi) parieto-occipital, (cross) left temporal, and (star) sensorimotor areas. Red denotes positive clusters, i.e., higher power for plausible stimuli. Bracket and  $r$ -value represent a significant trial-by-trial correlation between left temporal and sensorimotor beta power for our plausible condition. (B) Source reconstruction of the significant clusters found on sensor level. The precentral (green), central (blue), and postcentral (red) sulci are displayed for reference. Colour maps illustrate  $t$ -values for the source reconstruction.**

( $\pm .34$ ) respectively. Statistical testing revealed highly significant differences between the two conditions ( $p < .001$ ).

### 3.2. Stimulation effects

Visual stimulation (pooling all conditions) of PLD showed clear perturbations of spectral activity in the low alpha (7–11 Hz), high alpha (11–13 Hz), beta (13–23 Hz) and gamma (55–100 Hz) frequency bands in four areas (parieto-occipital, bilateral temporal and sensorimotor) (see Table 1 and Pavlidou et al., 2014).

### 3.3. Temporal evolution of power

The temporal evolution of alpha/beta power change was assessed separately for plausible and implausible conditions in left temporal (Fig. 2A), parieto-occipital (Fig. 2B), and sensorimotor areas (Fig. 2C). For both conditions, we observed an initial strong decrease of power in all areas directly after stimulation onset. Stronger alpha/beta-suppression of power was observed for implausible versus plausible across left temporal, parieto-occipital and sensorimotor areas. Significant time point differences (where the difference between plausible and implausible conditions was greater;  $p < .05$ ) were observed for left temporal (Fig. 2A), parieto-occipital

(Fig. 2B) and sensorimotor areas (Fig. 2C). No significant effects were observed for right temporal areas.

### 3.4. Condition contrast

We assessed differences between plausible and implausible PLD actions in the four regions of interest on sensor level (sensors over parieto-occipital, left and right temporal, and sensorimotor areas; see Table 1 for details on sensor selection).

We found a significant increase in alpha/low beta (9–21 Hz,  $p = .012$ ) power at 1650–2050 msec post-stimulus onset in sensors over left temporal areas. In addition, we found a significant increase in alpha (5–11 Hz,  $p = .007$ ) and low beta (13–21 Hz,  $p = .010$ ) power, between 1950 and 2350 msec in sensors over parieto-occipital areas, and a significant increase in low beta (15–21 Hz,  $p = .044$ ) power at 2400–2650 msec in sensors over sensorimotor areas (Fig. 3A). No significant clusters were found in sensors over right temporal cortex. The observed increase of alpha/beta power in left temporal, parieto-occipital and sensorimotor areas indicates higher power for plausible than implausible PLD actions (see also Fig. 2).

Next, we identified the cortical sources of these significant clusters. For the increase in high alpha/low beta power

(9–21 Hz) between 1650 and 2050 msec, the sources were identified in the STS and middle temporal area (MT) (Fig. 3B, top panel).

The sources of the significant effects between 5 and 21 Hz and 1950 and 2350 msec were located in bilateral parieto-occipital regions of the brain and more specifically visual areas (V2, V3) and left posterior parietal cortex (PPC) (Fig. 3B, centre panel).

Finally, the sources of the significant cluster between 15 and 21 Hz and 2400 and 2650 msec were localized in bilateral primary motor cortex (M1) as well as left PMC (Fig. 3B, lower panel).

### 3.5. Power correlations

We assessed interactions between visual and motor areas by calculating trial-by-trial cross-frequency correlations between the significant time–frequency clusters reported above. We observed a significant positive trial-by-trial correlation for plausible conditions between sensorimotor beta (2400–2650 msec) and left temporal beta (1650–2050 msec) power ( $r = .1098$ ,  $p = .035$ ). This significant positive trial-by-trial correlation was still visible when the data windows for sensorimotor and left temporal were shifted by  $-100$  msec (2300–2550 msec and 1550–1950 msec respectively;  $r = .1596$ ,  $p = .032$ ). No significant trial-by-trial correlations were observed for other time windows nor for plausible or implausible conditions between sensorimotor and parieto-occipital or parieto-occipital and left temporal areas.

## 4. Discussion

We investigated the modulations of neuronal oscillatory activity elicited by two seemingly similar PLD actions (plausible vs implausible). Plausible and implausible PLD actions are highly similar in low-level visual information and both actions are clearly recognized as a human figure. The subtle modification, however, had an effective influence on the configural recognition so that subjects perceived the actions as biomechanically plausible or implausible action.

We found that PLD (pooled over all conditions) elicited power changes in alpha (7–13 Hz), beta (13–23 Hz) and gamma (55–100 Hz) bands in several cortical areas in visual and sensorimotor areas including STS and PMC. Activation of STS and PMC during the visual processing of PLD action representations is consistent with earlier studies of action observation (Buccino, Lui, et al., 2004; Calvo-Merino, Glaser, Grezes, Passingham, & Haggard, 2005; Dinstein, Hasson, Rubin, & Heeger, 2007; Gallese, Fadiga, Fogassi, & Rizzolatti, 1996; Grossman et al., 2000; Pelphrey, Viola, & McCarthy, 2004; Saygin et al., 2004).

Our main finding is that subtle changes in the configuration of the human PLD elicited modulations of beta-band power in distinct spatio-temporal profiles within the above-mentioned network of action recognition. Normal, plausible actions showed a significant increase of beta-band power relative to implausible actions in left temporal sensors between 1650 and 2050 msec, followed by an increase in parieto-occipital sensors between 1950 and 2350 msec, and finally in

sensorimotor sensors between 2400 and 2650 msec post-stimulus onset. We identified the left STS, and middle temporal area (V5/MT+), as the cortical sources of the effects found in left temporal sensors. As cortical sources of the effects in parieto-occipital sensors, we identified bilateral visual areas (V2, V3), and left PPC. Finally, the effects in sensorimotor sensors were localized to PMC, and primary motor area (M1).

These positive beta-clusters reflect a stronger suppression of power for implausible than plausible actions (Fig. 2). Stronger suppression of beta-band power in sensorimotor areas has been found for incorrect relative to correct button presses (Koelewijn, van Schie, Bekkering, Oostenveld, & Jensen, 2008). Implausible actions might therefore be processed similar to incorrect button presses. Another potential explanation for the stronger suppression of power for the implausible PLD might be increased internal motor imagery when differentiating between two very similar stimuli. Motor imagery has been found to suppress beta-band power in sensorimotor areas (Kessler et al., 2006; de Lange et al., 2008; Schnitzler, Salenius, Salmelin, Jousmaki, & Hari, 1997). The complexity of the imagery task correlates with the duration of the beta-suppression (de Lange et al., 2008). Recognition of an implausible action might therefore require more mental imagery, reflected in prolonged beta-suppression in sensorimotor areas. A previous study found suppression of alpha/beta power to correlate with the observation of actions belonging to the observer's motor repertoire (e.g., ballet dancing observed by professional ballet dancers) but not if ballet dancing was observed by non-professional dancers (Orgs, Dombrowski, Heil, & Jansen-Osmann, 2008). Orgs et al. (2008) reported their effects in the alpha (7.5–13 Hz) and low beta (13–18 Hz). Interestingly, our observed significant difference between plausible and implausible in parieto-occipital and left temporal areas was also found in the alpha- and beta-band (5–21 Hz and 9–21 Hz). The high similarity between both frequency bands in the temporal evolution (Fig. S1) suggests that both frequency bands have a similar role during the processing of plausible versus implausible and familiar versus unfamiliar actions respectively, in parieto-occipital areas. In addition to the study by Orgs et al. (2008), our results demonstrate that alpha/beta-band power is not only involved in the recognition of familiar actions (plausible) but also in the recognition of unfamiliar actions (implausible). Notably, our significant effects in sensorimotor and left temporal areas were more strongly confined to the beta-band.

Previous haemodynamic (Allison, Puce, & McCarthy, 2000; Grossman & Blake, 2002; Hirai, Fukushima, & Hiraki, 2003; Michels et al., 2009, 2005; Pelphrey, Morris, & McCarthy, 2004; Pelphrey, Viola, et al., 2004) and electrophysiological (Pavlova et al., 2004; Singh, Barnes, Hillebrand, Forde, & Williams, 2002) studies reported right-temporal activity in response to PLD. Activity in the right hemisphere reflects the processing of the global form of the PLD (Lamb & Robertson, 1988). In their global form both plausible and implausible PLDs appear very similar. The differences of the two PLDs exist in the spatial position of only a few of the overall number of dots that makes up the human form (four of 13 dots). This subtle manipulation of the human PLD form requires the process of the PLD local details, which is generally thought to be involved in the left hemisphere (Bonda, Petrides, Ostry, & Evans, 1996; Lamb & Robertson, 1988). The observed left temporal activity in our study when differentiating between

plausible and implausible stimuli might thus reflect the extraction of the local details of the PLD, when differentiating between two seemingly similar PLD forms.

Although alpha/beta responses in posterior regions are often regarded within the framework of attention (Kaminski, Brzezicka, Gola, & Wrobel, 2012; Thut, Nietzel, Brandt, & Pascual-Leone, 2006; Worden, Foxe, Wang, & Simpson, 2000; Wrobel, 2000; Wrobel, Ghazaryan, Bekisz, Bogdan, & Kaminski, 2007), it is highly unlikely that our observed effects are simply related to different attentional efforts between conditions. First, the PLD stimuli in our study were randomized so that subjects could not predict the upcoming stimulus. Thus they could not direct attention to one stimulus more than the other before stimulus onset. Second, during the experimental task, our participants were asked to rate each stimulus as it appeared on the screen. Therefore, all stimuli irrespective of movement type required the same attention. Third, if the effects were simply due to attentional differences between conditions then we would expect similar attentional effects in the contrast plausible versus scrambled actions (albeit maybe shifted in time). However, since these effects differed (Pavlidou et al., 2014), we are confident that the effects reveal different cortical processes rather than simply differences in attention. Finally, we did not observe any typical attention-related effects of oscillatory activity neither a differential decreases of pre-stimulus alpha (e.g. Thut et al., 2006; Worden et al., 2000) nor early poststimulus gamma increases in posterior regions (e.g. Fries, 2009; Kahlbrock, Butz, May, & Schnitzler, 2012; Pavlova, Birbaumer, & Sokolov, 2006). This implies that our stimuli required the same attention irrespective of movement.

Earlier studies found activity in visual cortices as early as ~200 msec after stimulus onset when observing a PLD walker relative to scrambled displays (Pavlova et al., 2004). Similarly, in our previous study, we observed first differences in gamma-band (55–90 Hz) power in parieto-occipital areas between 500 and 800 msec post-stimulus onset. This gamma difference suggests that plausible and scrambled stimuli are first distinguished on an early visual basis (Pavlidou et al., 2014). In the present study, we did not find early gamma-band differences between plausible and implausible movements. The reason might be that due to their highly similar low-level visual information, both plausible and implausible PLDs appear to be very similar, and thus there is no visual distinction between the two PLD actions. This lack of visual distinction is reflected in the absence of any significant differences in gamma-band activity, as observed e.g., for plausible versus scrambled PLD (Pavlidou et al., 2014; Pavlova et al., 2006, 2004).

In our previous study, we found significant differences between plausible and scrambled movements between 500 and 2000 msec. In contrast, the present study reveals significant differences between plausible and implausible at later time windows (1650–2650 msec). This suggests that the process of distinguishing between similar movements takes longer than distinguishing between movements and random dot patterns.

We found beta-band power to decrease in left temporal, parieto-occipital and sensorimotor areas for both, plausible and implausible actions. Notably, we found differences in beta power between both conditions which followed a distinct spatio-temporal profile across left temporal, parieto-occipital

and sensorimotor areas. These beta effects reveal that both plausible and biomechanically implausible human actions activate the visual and sensorimotor areas but do so at different spatio-temporal scales. Additionally, we found trial-by-trial power correlations in the beta-band between sensorimotor and left temporal areas for plausible actions. These findings provide supporting evidence that during action recognition the beta-band couples visual and sensorimotor areas into a functional network. This finding is in line with other studies emphasizing the role of beta-oscillations for long-range communication between spatially distinct areas (Bibbig, Traub, & Whittington, 2002; Engel & Fries, 2010; Gross et al., 2004; Kopell, Ermentrout, Whittington, & Traub, 2000; Schnitzler & Gross, 2005). In our earlier study, we observed significant positive trial-by-trial correlations between sensorimotor beta power and parieto-occipital gamma power as well as left temporal alpha power during the visual perception of plausible PLD actions that were specific to the significant time–frequency cluster (at ~500–1300 msec, Pavlidou et al., 2014). The power correlations in the beta-band in our present study reveal additional interactions between visual and sensorimotor areas acting at later time windows (between 1550 and 2650 msec). These interactions seem to be more specifically related to the differentiation between plausible and implausible actions. Similarly, studies of apparent motion also imply that possible and impossible human actions are analysed by processes that operate over large spatio-temporal scales, taking into account the biomechanics of the human figure (Shiffrar & Freyd, 1990, 1993).

When contrasting plausible and scrambled movements, we have found significant differences in sensorimotor beta-band activity between 700 and 1200 msec post-stimulus onset (Pavlidou et al., 2014). In the present study, the significant differences in sensorimotor areas in the beta-band were found between 2400 and 2650 msec. This suggests that sensorimotor areas are involved in differentiating between different kinds of movements. However, depending on the similarity between movements the differentiation process takes longer as reflected in the differential activation of sensorimotor cortex. The time window of significant differences between plausible and implausible movements (2400–2650 msec) is in line with studies that have used correct versus incorrect actions (Koelewijn et al., 2008). This suggests that sensorimotor areas are involved in higher form processes that include an evaluative component for the observed action operating at a slower rate. The involvement of the sensorimotor areas therefore, suggests that visual areas categorize the observed movements and work together with motor areas to further cultivate the observed movements (Borroni, Montagna, Cerri, & Baldissera, 2005; Craighero et al., 2007; Fadiga et al., 2006). Previously, we found for plausible versus scrambled actions differences in sensorimotor beta-band power between 700 and 1200 msec (Pavlidou et al., 2014). The process to distinguish two seemingly similar actions, however, requires more time to activate visual and sensorimotor areas and thus more time is required to interpret the observed action than a simple plausible versus scrambled action discrimination. An open question remains whether the beta-band effects in visual and sensorimotor areas are related specifically to unnatural plausible actions or whether similar results would be found for unusual, but still

plausible actions. For instance, due to their higher similarity to natural plausible actions, unnatural plausible actions might require a temporally longer processing window in sensorimotor areas than plausible actions, but shorter than that required for implausible movements. Future studies will shed light on such distinctions between implausible and unnatural but still plausible actions.

Another possible explanation to the present results is a reflection of motor imagery. Motor imagery is a process in which an internal formation of a movement plan takes place. de Lange et al. (2008) observed activity in visual and sensorimotor areas during motor imagery of hand movements. This observation of visual and sensorimotor activity suggests a similar network involvement to that observed during action recognition. Future research can produce a carefully designed paradigm in which both action recognition and motor imagery processes can be extracted independently, to further understand the MNS role in the recognition as well as the prediction of actions. MEG can be used to determine the time course and dynamic modulations involved in the frequency domain (e.g. beta power) of both processes.

In summary, we found distinct spatio-temporal profiles in the beta-band when subjects had to distinguish plausible and implausible actions. The beta-clusters revealed a sequential order suggesting a directed flow of information. Notably, the significant effects were mainly found in the beta-band, suggesting that the beta-band might provide a functional network of long-range communication between visual and sensorimotor areas in the differentiation of plausible and implausible action movements. The later activation of the sensorimotor areas in comparison to visual areas suggests their involvement in higher form processes when interpreting the plausibility of the observed actions, which further suggests that sensorimotor areas act more like an active interpreter than a submissive observer when recognizing an action.

---

## Acknowledgements

We thank Markus Lappe and Marc de Lussanet for providing us with the PLDs, and helpful comments; and Nienke Hoogenboom and Hanneke van Dijk for helpful discussions and suggestions. This work was supported by the research commission of the medical department at Heinrich Heine University, Düsseldorf, Germany.

---

## Supplementary data

Supplementary data related to this article can be found at <http://dx.doi.org/10.1016/j.cortex.2014.02.007>.

---

## REFERENCES

Allison, T., Puce, A., & McCarthy, G. (2000). Social perception from visual cues: role of the STS region. *Trends in Cognitive Sciences*, 4, 267–278.

- Babiloni, C., Carducci, F., Cincotti, F., Rossini, P. M., Neuper, C., Pfurtscheller, G., et al. (1999). Human movement-related potentials vs desynchronization of EEG alpha rhythm: a high-resolution EEG study. *NeuroImage*, 10, 658–665.
- Bauer, M., Oostenveld, R., Peeters, M., & Fries, P. (2006). Tactile spatial attention enhances gamma-band activity in somatosensory cortex and reduces low-frequency activity in parieto-occipital areas. *Journal of Neuroscience*, 26, 490–501.
- Bibbig, A., Traub, R. D., & Whittington, M. A. (2002). Long-range synchronization of gamma and beta oscillations and the plasticity of excitatory and inhibitory synapses: a network model. *Journal of Neurophysiology*, 88, 1634–1654.
- Bonda, E., Petrides, M., Ostry, D., & Evans, A. (1996). Specific involvement of human parietal systems and the amygdala in the perception of biological motion. *Journal of Neuroscience*, 16, 3737–3744.
- Borroni, P., Montagna, M., Cerri, G., & Baldissera, F. (2005). Cyclic time course of motor excitability modulation during the observation of a cyclic hand movement. *Brain Research*, 1065, 115–124.
- Buccino, G., Binkofski, F., Riggio, L. (2004). The mirror neuron system and action recognition. *Brain and Language*, 89, 370–376.
- Buccino, G., Lui, F., Canessa, N., Patteri, I., Lagravinese, G., Benuzzi, F., et al. (2004). Neural circuits involved in the recognition of actions performed by nonconpecifics: an FMRI study. *Journal of Cognitive Neuroscience*, 16, 114–126.
- Caetano, G., Jousmaki, V., & Hari, R. (2007). Actor's and observer's primary motor cortices stabilize similarly after seen or heard motor actions. *Proceedings of National Academy of Science USA*, 104, 9058–9062.
- Calvo-Merino, B., Glaser, D. E., Grezes, J., Passingham, R. E., & Haggard, P. (2005). Action observation and acquired motor skills: an FMRI study with expert dancers. *Cerebral Cortex*, 15, 1243–1249.
- Choi, S. C. (1977). Test of equality of dependent correlations. *Biometrika*, 64, 645–647.
- Cochin, S., Barthelemy, C., Roux, S., & Martineau, J. (1999). Observation and execution of movement: similarities demonstrated by quantified electroencephalography. *European Journal of Neuroscience*, 11, 1839–1842.
- Craigheo, L., Metta, G., Sandini, G., & Fadiga, L. (2007). The mirror-neurons system: data and models. *Progress in Brain Research*, 164, 39–59.
- Di, P. G., Fadiga, L., Fogassi, L., Gallese, V., & Rizzolatti, G. (1992). Understanding motor events: a neurophysiological study. *Experimental Brain Research*, 91, 176–180.
- Dinstein, I., Hasson, U., Rubin, N., & Heeger, D. J. (2007). Brain areas selective for both observed and executed movements. *Journal of Neurophysiology*, 98, 1415–1427.
- Engel, A. K., & Fries, P. (2010). Beta-band oscillations—signalling the status quo? *Current Opinion in Neurobiology*, 20, 156–165.
- Fadiga, L., Craighero, L., Destro, M. F., Finos, L., Cotillon-Williams, N., Smith, A. T., et al. (2006). Language in shadow. *Social Neurosciences*, 1, 77–89.
- Fadiga, L., Fogassi, L., Pavesi, G., & Rizzolatti, G. (1995). Motor facilitation during action observation – a magnetic stimulation study. *Journal of Neurophysiology*, 73, 2608–2611.
- Fries, P. (2009). Neuronal gamma-band synchronization as a fundamental process in cortical computation. *Annual Review of Neuroscience*, 32, 209–224.
- Gallese, V., Fadiga, L., Fogassi, L., & Rizzolatti, G. (1996). Action recognition in the premotor cortex. *Brain*, 119(Pt 2), 593–609.
- Gross, J., Kujala, J., Hamalainen, M., Timmermann, L., Schnitzler, A., & Salmelin, R. (2001). Dynamic imaging of coherent sources: studying neural interactions in the human brain. *Proceedings of National Academy of Science USA*, 98, 694–699.

- Gross, J., Schmitz, F., Schnitzler, I., Kessler, K., Shapiro, K., Hommel, B., et al. (2004). Modulation of long-range neural synchrony reflects temporal limitations of visual attention in humans. *Proceedings of National Academy of Science USA*, 101, 13050–13055.
- Grossman, E. D., & Blake, R. (2002). Brain areas active during visual perception of biological motion. *Neuron*, 35, 1167–1175.
- Grossman, E., Donnelly, M., Price, R., Pickens, D., Morgan, V., Neighbor, G., et al. (2000). Brain areas involved in perception of biological motion. *Journal of Cognitive Neuroscience*, 12, 711–720.
- Hari, R., Forss, N., Avikainen, S., Kirveskari, E., Salenius, S., & Rizzolatti, G. (1998). Activation of human primary motor cortex during action observation: a neuromagnetic study. *Proceedings of National Academy of Science USA*, 95, 15061–15065.
- Hirai, M., Fukushima, H., & Hiraki, K. (2003). An event related potentials study of biological motion perception in humans. *Neuroscience Letters*, 344, 41–44.
- Jeannerod, M. (2001). Neural simulation of action: a unifying mechanism for motor cognition. *NeuroImage*, 14, S103–S109.
- Johansson, G. (1973). Visual perception of biological motion and a model for its analysis. *Perception and Psychophysics*, 14, 201–211.
- Kahlbrock, N., Butz, M., May, E. S., & Schnitzler, A. (2012). Sustained gamma band synchronization in early visual areas reflects the level of selective attention. *NeuroImage*, 59, 673–681.
- Kaminski, J., Brzezicka, A., Gola, M., & Wrobel, A. (2012). Beta band oscillations engagement in human alertness process. *International Journal of Psychophysiology*, 85, 125–128.
- Kessler, K., Biermann-Ruben, K., Jonas, M., Siebner, H. R., Baumer, T., Munchau, A., et al. (2006). Investigating the human mirror neuron system by means of cortical synchronization during the imitation of biological movements. *NeuroImage*, 33, 227–238.
- Koelewijn, T., van Schie, H. T., Bekkering, H., Oostenveld, R., & Jensen, O. (2008). Motor-cortical beta oscillations are modulated by correctness of observed action. *NeuroImage*, 40, 767–775.
- Kopell, N., Ermentrout, G. B., Whittington, M. A., & Traub, R. D. (2000). Gamma rhythms and beta rhythms have different synchronization properties. *Proceedings of National Academy of Science USA*, 97, 1867–1872.
- Lamb, M. R., & Robertson, L. C. (1988). The processing of hierarchical stimuli: effects of retinal locus, locational uncertainty, and stimulus identity. *Perception and Psychophysics*, 44, 172–181.
- de Lange, F. P., Jensen, O., Bauer, M., & Toni, I. (2008). Interactions between posterior gamma and frontal alpha/beta oscillations during imagined actions. *Frontiers in Human Neuroscience*, 2, 7.
- Lange, J., Oostenveld, R., & Fries, P. (2011). Perception of the touch-induced visual double-flash illusion correlates with changes of rhythmic neuronal activity in human visual and somatosensory areas. *NeuroImage*, 54, 1395–1405.
- Maris, E., & Oostenveld, R. (2007). Nonparametric statistical testing of EEG- and MEG-data. *Journal of Neuroscience Methods*, 164, 177–190.
- Michels, L., Kleiser, R., de Lussanet, M. H., Seitz, R. J., & Lappe, M. (2009). Brain activity for peripheral biological motion in the posterior superior temporal gyrus and the fusiform gyrus: dependence on visual hemifield and view orientation. *NeuroImage*, 45, 151–159.
- Michels, L., Lappe, M., & Vaina, L. M. (2005). Visual areas involved in the perception of human movement from dynamic form analysis. *NeuroReport*, 16, 1037–1041.
- Muthukumaraswamy, S. D., Johnson, B. W., Gaetz, W. C., & Cheyne, D. O. (2004). Modulation of neuromagnetic oscillatory activity during the observation of oro-facial movements. *Neurology and Clinical Neurophysiology*, 2004, 2.
- Muthukumaraswamy, S. D., Johnson, B. W., Gaetz, W. C., & Cheyne, D. O. (2006). Neural processing of observed oro-facial movements reflects multiple action encoding strategies in the human brain. *Brain Research*, 1071, 105–112.
- Muthukumaraswamy, S. D., Johnson, B. W., & Mcnair, N. A. (2004). Mu rhythm modulation during observation of an object-directed grasp. *Cognitive Brain Research*, 19, 195–201.
- Nishitani, N., & Hari, R. (2000). Temporal dynamics of cortical representation for action. *Proceedings of National Academy of Science USA*, 97, 913–918.
- Nolte, G. (2003). The magnetic lead field theorem in the quasi-static approximation and its use for magnetoencephalography forward calculation in realistic volume conductors. *Physics in Medicine and Biology*, 21, 3637–3652.
- Oostenveld, R., Fries, P., Maris, E., & Schoffelen, J. M. (2011). FieldTrip: open source software for advanced analysis of MEG, EEG, and invasive electrophysiological data. *Computational Intelligence and Neuroscience*, 2011, 156869.
- Oram, M. W., & Perrett, D. I. (1994). Responses of anterior superior temporal polysensory area STPa neurons to 'biological motion' stimuli. *Journal of Cognitive Neuroscience*, 6, 99–116.
- Orgs, G., Dombrowski, J. H., Heil, M., & Jansen-Osmann, P. (2008). Expertise in dance modulates alpha/beta event-related desynchronization during action observation. *European Journal of Neuroscience*, 27, 3380–3384.
- Pavlidou, A., Schnitzler, A., & Lange, J. (2014). Interactions between visual and motor areas during the recognition of plausible actions as revealed by magnetoencephalography. *Human Brain Mapping*, 35(2), 581–592.
- Pavlova, M., Birbaumer, N., & Sokolov, A. (2006). Attentional modulation of cortical neuromagnetic gamma response to biological movement. *Cerebral Cortex*, 16, 321–327.
- Pavlova, M., Lutzenberger, W., Sokolov, A., & Birbaumer, N. (2004). Dissociable cortical processing of recognizable and non-recognizable biological movement: analysing gamma MEG activity. *Cerebral Cortex*, 14, 181–188.
- Pelphrey, K. A., Morris, J. P., & McCarthy, G. (2004). Grasping the intentions of others: the perceived intentionality of an action influences activity in the superior temporal sulcus during social perception. *Journal of Cognitive Neuroscience*, 16, 1706–1716.
- Pelphrey, K. A., Viola, R. J., & McCarthy, G. (2004). When strangers pass – processing of mutual and averted social gaze in the superior temporal sulcus. *Psychological Science*, 15, 598–603.
- Pfurtscheller, G., & Lopes da Silva, F. H. (1999). Event-related EEG/MEG synchronization and desynchronization: basic principles. *Clinical Neurophysiology*, 110, 1842–1857.
- Pfurtscheller, G., Neuper, C., Brunner, C., & da Silva, F. L. (2005). Beta rebound after different types of motor imagery in man. *Neuroscience Letters*, 378, 156–159.
- Rizzolatti, G., & Craighero, L. (2004). The mirror-neuron system. *Annual Review of Neuroscience*, 27, 169–192.
- Rossi, S., Tecchio, F., Pasqualetti, P., Olivelli, M., Pizzella, V., Romani, G. L., et al. (2002). Somatosensory processing during movement observation in humans. *Clinical Neurophysiology*, 113, 16–24.
- Salmelin, R., Hamalainen, M., Kajola, M., & Hari, R. (1995). Functional segregation of movement-related rhythmic activity in the human brain. *NeuroImage*, 2, 237–243.
- Saygin, A. P., Wilson, S. M., Hagler, D. J., Bates, E., & Sereno, M. I. (2004). Point-light biological motion perception activates human premotor cortex. *Journal of Neuroscience*, 24, 6181–6188.
- Schippers, M. B., & Keysers, C. (2011). Mapping the flow of information within the putative mirror neuron system during gesture observation. *NeuroImage*, 57, 37–44.
- Schnitzler, A., & Gross, J. (2005). Functional connectivity analysis in magnetoencephalography. *International Review of Neurobiology*, 68, 173–195.

- Schnitzler, A., Salenius, S., Salmelin, R., Jousmaki, V., & Hari, R. (1997). Involvement of primary motor cortex in motor imagery: a neuromagnetic study. *NeuroImage*, 6, 201–208.
- Shiffrar, M., & Freyd, J. J. (1990). Apparent motion of the human body. *Psychological Science*, 1, 257–264.
- Shiffrar, M., & Freyd, J. J. (1993). Timing and apparent motion path choice with human body photographs. *Psychological Science*, 4, 379–384.
- Singh, K. D., Barnes, G. R., Hillebrand, A., Forde, E. M., & Williams, A. L. (2002). Task-related changes in cortical synchronization are spatially coincident with the hemodynamic response. *NeuroImage*, 16, 103–114.
- Thut, G., Nietzel, A., Brandt, S. A., & Pascual-Leone, A. (2006). Alpha-band electroencephalographic activity over occipital cortex indexes visuospatial attention bias and predicts visual target detection. *Journal of Neuroscience*, 26, 9494–9502.
- Worden, M. S., Foxe, J. J., Wang, N., & Simpson, G. V. (2000). Anticipatory biasing of visuospatial attention indexed by retinotopically specific alpha-band electroencephalography increases over occipital cortex. *Journal of Neuroscience*, 20, RC63.
- Wrobel, A. (2000). Beta activity: a carrier for visual attention. *Acta Neurobiologiae Experimentalis*, 60, 247–260.
- Wrobel, A., Ghazaryan, A., Bekisz, M., Bogdan, W., & Kaminski, J. (2007). Two streams of attention-dependent beta activity in the striate recipient zone of cat's lateral posterior-pulvinar complex. *Journal of Neuroscience*, 27, 2230–2240.

12) Pavlidou, A., Schnitzler, A., & **Lange, J.** (2014b).

Interactions between visual and motor areas during the recognition of plausible actions as revealed by magnetoencephalography.

Human brain mapping, 35(2), 581-592.

Impact factor (2014): 5.969

# Interactions Between Visual and Motor Areas During the Recognition of Plausible Actions as Revealed by Magnetoencephalography

Anastasia Pavlidou,\* Alfons Schnitzler, and Joachim Lange

*Institute of Clinical Neuroscience and Medical Psychology, Medical Faculty,  
Heinrich-Heine-University Düsseldorf, Düsseldorf, Germany*



**Abstract:** Several studies have shown activation of the mirror neuron system (MNS), comprising the temporal, posterior parietal, and sensorimotor areas when observing plausible actions, but far less is known on how these cortical areas interact during the recognition of a plausible action. Here, we recorded neural activity with magnetoencephalography while subjects viewed point-light displays of biologically plausible and scrambled versions of actions. We were interested in modulations of oscillatory activity and, specifically, in coupling of oscillatory activity between visual and motor areas. Both plausible and scrambled actions elicited modulations of  $\theta$  (5–7 Hz),  $\alpha$  (7–13 Hz),  $\beta$  (13–35 Hz), and  $\gamma$  (55–100 Hz) power within visual and motor areas. When comparing between the two actions, we observed sequential and spatially distinct increases of  $\gamma$  (~65 Hz),  $\beta$  (~25 Hz), and  $\alpha$  (~11 Hz) power between 0.5 and 1.3 s in parieto-occipital, sensorimotor, and left temporal areas. In addition, significant clusters of  $\gamma$  (~65 Hz) and  $\alpha/\beta$  (~15 Hz) power decrease were observed in right temporal and parieto-occipital areas between 1.3 and 2.0 s. We found  $\beta$ -power in sensorimotor areas to be positively correlated on a trial-by-trial basis with parieto-occipital  $\gamma$  and left temporal  $\alpha$ -power for the plausible but not for the scrambled condition. These results provide new insights in the neuronal oscillatory activity of the areas involved in the recognition of plausible action movements and their interaction. The power correlations between specific areas underscore the importance of interactions between visual and motor areas of the MNS during the recognition of a plausible action. *Hum Brain Mapp* 35:581–592, 2014. © 2012 Wiley Periodicals, Inc.

**Key words:** MEG; mirror neurons; oscillatory activity; power correlations; point-light displays



## INTRODUCTION

Action recognition plays an important role for effective communication and interaction with other people [Blake-more and Frith, 2005; Kokal et al., 2009; Schippers and Keysers, 2011]. Action recognition occurs at different levels and over distinctive time scales. On a lower level and a shorter time period, sensory information will be processed [Blake and Shiffrar, 2007; Grossman et al., 2000; Michels et al., 2009; Pavlova and Sokolov, 2003]. This incorporates the ability to integrate form and motion but it can also rely on the ability to distinguish form from motion [Lange et al., 2006; Michels et al., 2005; Oram and Perrett, 1994]. Several recent studies have argued that action recognition also relies on higher, nonsensory areas of the mirror

Contract grant sponsor: The Research Commission Medical Department at Heinrich Heine University, Düsseldorf, Germany.

\*Correspondence to: Anastasia Pavlidou, Institute of Clinical Neuroscience and Medical Psychology, Medical Faculty, Heinrich-Heine-University, Universitätsstr. 1, Düsseldorf 40225, Germany. E-mail: Anastasia.Pavlidou@med.uni-duesseldorf.de

Received for publication 6 May 2012; Revised 3 September 2012; Accepted 3 September 2012

DOI: 10.1002/hbm.22207

Published online 1 November 2012 in Wiley Online Library (wileyonlinelibrary.com).

neuron system (MNS) [Schippers and Keysers, 2011; Urgesi et al., 2010]. Mirror neurons were first discovered in area F5 of the macaque monkey premotor cortex (PMC) [Di Pellegrino et al., 1992]. They are a particular class of neurons that fire when a monkey performs a goal-oriented action but also when it passively observes that same action [Gallese et al., 1996; Rizzolatti et al., 1996]. Areas frequently considered as being part of the MNS in humans are the PMC, supplementary motor area, somatosensory areas, the inferior parietal lobe, inferior frontal gyrus, and indirectly the superior temporal sulcus (STS), a visual area known to respond to biological actions without being a standard part of the MNS [Bonda et al., 1996; Buccino, 2004; Dinstein et al., 2007; Filimon et al., 2007; Gazzola et al., 2007; Pelphrey et al., 2005; Rizzolatti and Craighero, 2004; Schippers and Keysers, 2011].

The proposed mechanism of how mirror neurons mediate recognition of actions is to compare visual information of an action to one's own motor repertoire [Rizzolatti and Craighero, 2004]. In other words, when one observes an action performed by another person, neurons that represent that action in the observer's repertoire of possible actions are triggered in the PMC [Buccino et al., 2004a; Rizzolatti et al., 2001]. Actions belonging to the movement repertoire of the observer are mapped in their PMC. Actions that do not belong to this repertoire are recognized predominantly on a visual basis. In line with this model, studies have shown that the observers' ability to perform an observed action modulates activation in mirror neuron areas (e.g., Calvo-Merino et al., 2005; Orgs et al., 2008).

An effective and frequently used method for studying action recognition is the point-light display (PLD) method [Johansson, 1973]. Although PLD represents a human body and its action with only a handful of dots, observers can easily recognize the actions of these PLD (e.g., Grossman et al., 2000; Johansson, 1973). As PLDs are easy to present and manipulate, they are a useful tool in neuroimaging to study the cortical areas involved in action recognition. By changing the spatial configuration of the dots, while keeping the motion trajectories intact, the configural and holistic impression of the action can be destroyed while keeping low-level information such as motion signals, stimulus size, and number of point-light dots constant. Such "scrambled" PLDs are often used as control stimuli to unravel action recognition from basic low-level visual perception [Grossman et al., 2000; Michels et al., 2005; Pavlova et al., 2004]. Neuroimaging studies in human and nonhuman primates have identified the visual areas to be primarily involved in the process of PLD actions compared to scrambled PLD [Grossman et al., 2000; Michels et al., 2005; Oram and Perrett, 1994; Pavlova et al., 2004]. More recently, studies have also identified the PMC to be involved in the recognition of PLD actions compared to scrambled PLD [Candidi et al., 2008; Kemeade et al., 2012; Saygin et al., 2004]. These findings have led to the interpretation that visual as well as motor areas contribute to the recognition of actions. Most of these stud-

ies have been performed using functional magnetic resonance imaging (fMRI). Little is known, however, about the role of neuromagnetic oscillatory activity and how these cortical areas dynamically interact during the process of action recognition.

To investigate the dynamic modulations and interactions between visual and motor areas during the process of action recognition, we used the PLD method similar to the above-mentioned fMRI studies and magnetoencephalography (MEG). We created different PLD action representations and scrambled versions of these PLD actions. MEG's high temporal and good spatial resolution enabled us to examine the dynamics in the frequency domain within- and between-sensory and motor areas during the process of action recognition.

## METHODS

### Subjects

Twelve right-handed subjects with normal or corrected to normal vision (six males, mean age  $\pm$  SD = 27.6  $\pm$  2.87) and with no known neurological disorders participated in this study. All subjects gave informed consent in accordance to the declaration of Helsinki and the local Ethics Committee.

### Stimuli

Point-light biological motion animations were generated by recording the movements of human actors with sensors attached to their main joints (head, shoulders, elbows, wrists, hips, knees, and feet) using a motion tracking system (MotionStar; Ascension Technology, Burlington, VT; [Lange and Lappe, 2007]). The main joints were represented by 14 small white dots ( $5 \times 5$  pixels) against a black background.

Stimuli were offline manipulated using MATLAB (MathWorks, Natick, MA). First, actions were cut into segments representing one cycle of the action, lasting between 0.6 and 1.0 s. Next, cycles of each action were repeated five times. To compute a seemingly continuous movement of each action, transitions between cycles were smoothed [Lange et al., 2006]. We manipulated the different stimuli to create three different stimulus conditions with different degrees of action representation, whereas leaving low-level visual information as constant as possible (Fig. 1).

Originally 20 animations depicting a human action were recorded. In a pretest, we presented plausible, implausible, and scrambled versions of the animations and asked subjects to rate the stimuli as plausible, implausible, or scrambled. Eight animations, which were clearly distinguished based on the three-scale rating, were selected and used in the MEG experiment. The selected animations depicted eight actions: walking (viewed from the front, walking toward the screen), walking (viewed from the

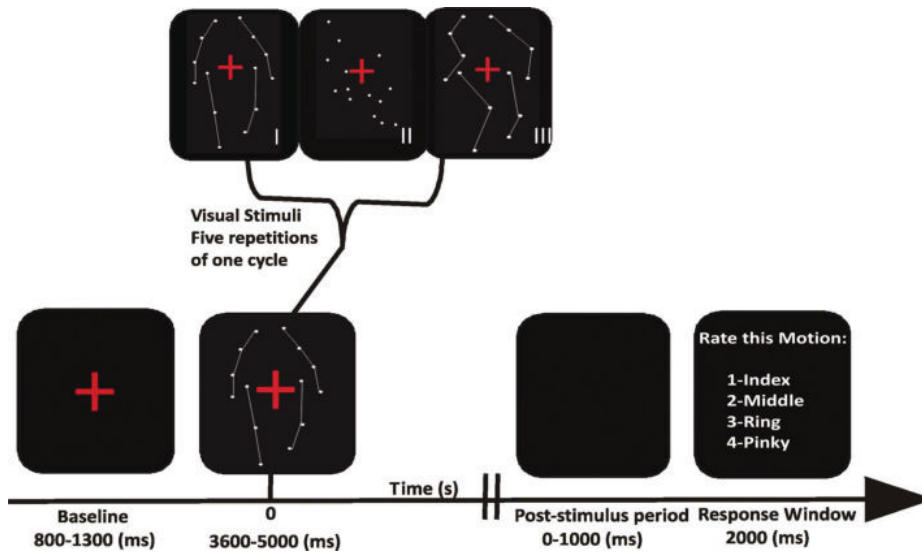


Figure 1.

Experimental setup. Examples of stimuli used (I) Plausible, (II) Scrambled, (III) Implausible. Connecting lines were not present in the actual experiment. For details, see **Experimental Procedures** section. [Color figure can be viewed in the online issue, which is available at [wileyonlinelibrary.com](http://wileyonlinelibrary.com).]

side walking either toward the left or toward the right), running, throwing, boxing, skipping (on one leg), skipping (side to side), and a high kick into the air.

*Plausible condition (I):* Each animation in its original form as recorded. In the pretest, subjects reported to perceive the stimuli as normal, biomechanically probable biological motion.

*Scrambled condition (II):* Scrambled versions of each animation were created by randomizing the spatial positions of all dots within the field of the original figure [Grossman et al., 2000; Pavlova and Sokolov, 2003; Saygin et al., 2004]. Again, the net movement of the dots is unchanged, whereas the spatial configuration of a human figure is completely destroyed. In the pretest, subjects rated these stimuli as meaningless movements of dots.

*Implausible condition (III):* Implausible versions of each animation were created by randomizing the starting positions of two dots from the upper body and two from the lower body, whereas leaving their motion paths unchanged. This manipulation leaves the overall movement of all dots unchanged and alters the configurational structure only minimally. In the pretest, subjects reported to perceive the stimuli as “somehow human” but the actions as biomechanically implausible.

### Experimental Procedure

Subjects were seated comfortably with their head placed inside the MEG helmet. Visual stimuli were projected on the backside of a translucent screen positioned 100 cm in

front of the subjects using a projector (PT-DW700E; Panasonic) with a refresh rate of 60 Hz placed outside the shielded room. Each trial started with the presentation of a central red cross ( $0.4 \times 0.4$  cm; visual angle.  $0.23^\circ$ ). After a randomized period of 800–1,300 ms, in which only the red fixation cross was visible, the point-light animation ( $8.4 \times 3.4$  cm; visual angle,  $4.81^\circ \times 1.95^\circ$ ) appeared for a period of 3,600–5,000 ms (five cycles). The red fixation cross was centrally present throughout the duration of the stimuli to minimize eye movements. After another random period of 0–1,000 ms, in which only a black screen was visible, response instructions were visually presented on the screen. Subjects were asked to rate the animation using a 1–4 rating scale as either plausible (1), implausible (2–3), or scrambled (4) by button presses. Once a response was given, a new trial started. The assignment of the four-fingers to the four configurations of the rating scale was randomized for each trial and response hands were balanced across subjects (Fig. 1). If no response was given within 2,000 ms, or if a response was given too quickly (before the response instructions appeared), the trial was discarded from analysis and repeated at the end of the block. No feedback was given. The *estimated* duration of a trial was 4,400–7,300 ms, followed by the individual response period (maximum of 2,000 ms). Stimuli were presented in pseudo-random order within a block. One block consisted of 31 trials, so that each block had an *estimated* duration of 136.4–226.3 s, respectively, without individual response times (max. 2,000 ms) taken into account (no. of trials  $\times$  duration). If response times are taken into account,

each block had an estimate duration of  $\sim 5$  min. Overall, five blocks were presented, with self-timed breaks of  $\sim 2$  min in between blocks. On the whole, the experiment lasted  $\sim 25$ – $30$  min. Subjects performed a training session of  $\sim 5$  min before the start of the MEG experiment. Stimulus presentation was controlled using Presentation Software (Neurobehavioral Systems, Albany, NY).

### Data Acquisition and Analysis

While subjects performed the task, neuromagnetic activity was recorded continuously at a sampling rate of 1,000 Hz with a 306-channel whole head MEG system (NeuroMag Elekta Oy, Helsinki, Finland). This system includes 204 planar gradiometers and 102 magnetometers arranged in a helmet configuration. In the present study, data analysis was carried out only with the planar gradiometers. In addition, vertical and horizontal electrooculograms were recorded simultaneously for offline artifact rejection. Subjects' head position within the MEG helmet was registered by four coils placed at subjects' forehead and behind the left and right ear. A 3T MRI scanner (Siemens, Erlangen, Germany) was used to obtain individual full brain high-resolution standard T1-weighted structural magnetic resonance images (MRIs). MRIs were offline aligned with the MEG coordinate system using the coils and anatomical landmarks (nasion, left, and right preauricular points).

Data were analyzed offline with the open source toolbox FieldTrip for Matlab (<http://www.ru.nl/donders/fieldtrip>) [Oostenveld et al., 2011]. Continuously recorded data were cut into epochs as defined by the trials. All epochs were first semi-automatically and then visually inspected for artifacts. Artifacts caused by eye movements or muscle activity were removed. Power line noise was removed by applying a Fourier transformation of 10-s long signal periods and subtracting the 50, 100, and 150 Hz components.

### Time–Frequency Analysis

Time–frequency representations were computed separately for two frequency windows: For frequencies ranging from 4 to 40 Hz (in steps of 2 Hz), we applied a Fourier transformation on 500-ms windows moved in steps of 50 ms. Data segments were tapered with a single Hanning taper, resulting in a spectral smoothing of  $\pm 2.0$  Hz. For the frequencies from 40 to 100 Hz (in steps of 5 Hz), a Fourier transformation was applied on 400-ms windows moved in steps of 50 ms, using the multitaper approach [Walden et al., 1995]. Data segments were tapered with seven tapers, resulting in a spectral smoothing of  $\pm 10.0$  Hz around each center frequency.

As we were interested in the development of power over time and power correlations across frequencies (for details, see correlation analysis), we used a Fourier transformation on constant time window and tapering for all frequencies within a frequency band. This approach

ensures that the same data set and same tapers are used within a frequency band. Any changes observed are thus attributed to the frequency components, rather than changes in time windows and/or tapers. We used different time windows and tapering for low and high frequencies because low-frequency bands are relatively narrow and closely spaced. We therefore aimed at a high spectral resolution in the low frequency range of roughly  $\pm 2$  Hz (i.e., 1/500 ms). In the higher frequency range, frequency bands are broader and spaced more far apart so that we applied a spectral smoothing of  $\pm 10.0$  Hz. This approach provided an acceptable trade-off between capture of physiological frequency bands and comparability within- and between-frequencies. Previous studies have identified parieto-occipital, left and right temporal, and sensorimotor areas as crucial areas in the recognition of PLD actions [Grossman et al., 2000; Michels et al., 2009; Saygin et al., 2004; Schippers and Keysers, 2011]. To identify these regions of interest in sensor space in our study, we applied a combined data driven and a priori approach. First, we pooled all trials together irrespective of stimulus conditions (plausible, implausible, and scrambled) and determined which sensors showed clear perturbations of oscillatory activity in response to PLD relative to baseline ( $-400$  to  $-250$  ms). Six sensors in the right hemisphere showing a sustained decrease in  $\alpha$  (7–13 Hz) and  $\beta$  (13–23 Hz) power as well as a selective sustained increase in  $\gamma$  (55–95 Hz) power were selected over parieto-occipital areas (Fig. 2A). In addition, 10 sensors, five in the left hemisphere and symmetrically five in the right hemisphere, showing a sustained decrease in low  $\alpha$  (7–11 Hz) and a selective increase in high  $\alpha$  (11–13 Hz) power as well as a sustained decrease in  $\beta$  (15–23 Hz) power were selected over the sensorimotor cortex (Fig. 2B). Finally, owing to the vast reports on the importance of STS and temporal areas in action recognition (e.g., Dinstein et al., 2007; Grossman and Blake, 2001, 2002; Grossman et al., 2000; Pavlova et al., 2004; Pelphrey et al., 2004), eight sensors in the left and symmetrically eight sensors in the right hemisphere were selected over the temporal cortices. Although temporal cortices showed similar effects in the lower range frequencies (4–40 Hz) as observed in parieto-occipital areas, the difference in the  $\gamma$ -band effects between the two suggests that both process action representations differently. To assess the different roles of the parieto-occipital, temporal, and sensorimotor areas in action recognition, we next investigated the contrasts between the conditions.

### Condition Contrasts

We assessed differences in spectral power between stimulus conditions in the four above-mentioned regions of interest (parieto-occipital, left and right temporal, sensorimotor). To this end, we averaged spectral power over the sensors of interest for each stimulus condition

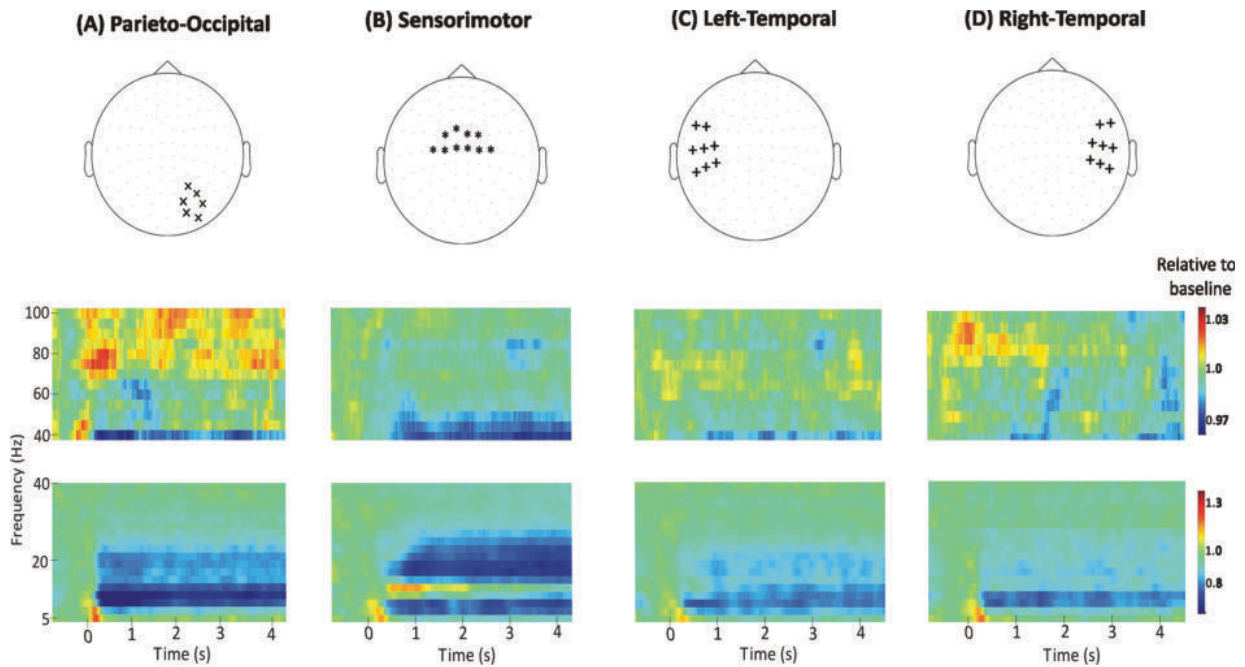


**Figure 2.**

Stimulation effects of PLDs. Top row shows our sensors of interest for (A) parieto-occipital (x), (B) sensorimotor (\*), (C) left-temporal (+), and (D) right-temporal (+) areas, respectively. Color maps illustrate changes in power relative to baseline

(−400 to −250 ms), which were calculated separately for low (4–40 Hz) and high frequencies (40–100 Hz) by pooling all trials together irrespective of conditions.

separately. Next, we compared stimulus conditions for each subject by subtracting power of both conditions and dividing the difference by the variance (equivalent to an independent-sample *t*-test). This step serves as a normalization of interindividual differences [Hoogenboom et al., 2010; Lange et al., 2011]. This comparison was carried out for each time–frequency sample independently, resulting in a time–frequency map of pseudo-*t*-values for each subject. To minimize influences of motor activity owing to response preparation, statistical analyses were restricted to the first 3 s. Next, we analyzed the consistency of pseudo-*t*-values over subjects by means of a nonparametric randomization test. This statistical test effectively corrects for multiple comparisons [Maris and Oostenveld, 2007]. To this end, time–frequency pseudo-*t*-values exceeding a threshold ( $P < 0.05$ ) were identified and neighboring significant time–frequency pseudo-*t*-values were combined to a cluster. For each cluster, the sum of the *t*-values was used in the second-level cluster-level test statistics. We used the Monte Carlo approach to estimate the permutation *P*-value of the cluster by comparing the cluster-level test statistic with a randomization null distribution. The null distribution was computed by randomly assigning data to different conditions, under the null hypothesis of no difference between conditions and thus exchangeability of the data. The random reassignment of the data to conditions was performed 1,000 times. For each of these 1,000

repetitions, a group *t*-value was calculated. Finally, a *P*-value was estimated for each cluster as the proportion of the elements in the randomization null distribution exceeding the observed maximum cluster-level test statistic (for details, see Lange et al., 2011). This group level statistics results in time–frequency clusters which reveal differences between conditions that were significant at the random effects level after correcting for multiple comparisons along both the time and the frequency dimension [Maris and Oostenveld, 2007].

In the present study, we were interested in how processing of plausible actions differs from processing of nonactions. As discussed in the **Introduction** section, most fMRI studies, to date, on PLD action recognition have dealt with a similar question by comparing actions to scrambled versions of these actions. Based on our main research question and for the sake of comparability, we will focus in our present study on the main contrast of plausible (actions) versus scrambled (nonactions) conditions. The comparison between plausible and implausible actions engages different research questions and thus presumably different cortical networks and mechanisms which lie beyond the scope of the present study.

### Source Analysis

To determine the neuronal sources, we applied dynamic imaging of coherent sources (DICS), an adaptive spatial

filtering beamforming technique [Gross et al., 2001]. To this end, a regular three-dimensional 1-cm grid in the Montreal Neurological Institute (MNI) template brain was created and the structural MRI of each subject was linearly warped onto this template brain. The inverse of this warp was applied to the template grid, resulting in individual grids. This approach allowed us to average source parameters over subjects by simply averaging over grid points. For each grid point then, a forward model based on a realistic single shell volume conductor based on the individual MRI was used to calculate the lead-field matrix [Nolte, 2003]. We next applied a Fourier transformation on time-windows of interest and computed the cross-spectral density (CSD) matrix between all MEG sensor pairs for the frequency bands of interest, which were determined by the significant time clusters on sensor level. Spatial filters were constructed for each individual grid point using the CSD and lead field matrix. These filters pass activity from the location of interest, whereas suppressing activity from all other locations. Spatial filters  $w(r,f)$  were computed from the following formula:

$$w(r, f) = (L'(r)C(f) + \lambda x I)^{-1}L'(r)^{-1}L'(r)C(f) + \lambda x I)^{-1},$$

where  $L'(r)$  is the inverse of lead-field matrix (forward model) at location of interest  $r$ ,  $C(f)$  is the CSD matrix between all MEG signals at frequency  $f$ ,  $\lambda$  is the regularization parameter, and  $I$  is the identity matrix [de Lange et al., 2008; Gross et al., 2001].

First, we pooled all conditions (pre- and post-stimulus period for stimulation effects; plausible and scrambled conditions for condition contrast) and computed common filters. Next, CSD matrices of single trials were projected through those filters, providing single trial estimates of source power [Hoogenboom et al., 2010; Lange et al., 2011]. In line with the analysis on sensor level, we computed a relative change to baseline for stimulation contrasts and a between-condition  $t$ -value for condition contrasts for each subject. Statistical testing on group level for time–frequency representations of stimulation effects ( $P < 0.05$ , cluster corrected) and condition contrasts ( $P < 0.05$ , uncorrected) was carried out in the same way as on sensor level (see above). Results were displayed on the MNI template brain and neuronal sources were identified using the AFNI atlas (<http://afni.nimh.nih.gov/afni>), integrated into FieldTrip.

### Cross-frequency Correlations

To investigate the interaction between visual and motor areas during the recognition of plausible actions, we calculated the crossfrequency coupling over the specific time course of our significant clusters. Cross-frequency coupling refers to the coupling of the neuronal signal between distinct frequency bands in the same or different cortical regions [Jensen and Colgin, 2007]. Here, we investigated the power correlation between the significant time–fre-

quency clusters of the above-mentioned time–frequency analysis. For each trial, we averaged spectral power across the time and frequency bins defined by the significant clusters on group level (Fig. 4A). Next, we computed correlations between sensorimotor  $\beta$ -power on the one hand and parieto-occipital  $\gamma$  and temporal  $\alpha$ -power on the other hand. Power correlations were determined per subject on a trial-by-trial basis by computing Pearson correlation coefficient. Individual correlation coefficients were converted to  $z$ -values using the Pearson's  $r$ -to- $z$  transform to attain a normally distributed variable [Choi, 1977]. The distribution of correlation coefficients across subjects was statistically tested against the null hypothesis of no correlation, that is,  $r = 0$  by using a two-sided  $t$ -test. To test for a temporal specificity of the correlations, frequency bands of interest were shifted in steps of  $\pm 100$  ms and correlations were recomputed as described above.

## RESULTS

### Behavioral Data

The subjects rating of the PLD motion as plausible or scrambled indicated that they could easily distinguish both stimuli with an average rating of 1.5 ( $\pm 0.19$ ) for all plausible, and 3.8 ( $\pm 0.14$ ) for all scrambled. Statistical testing revealed highly significant differences between both conditions ( $P < 0.001$ ).

### Stimulation Effects

We first determined the effects of stimulation by pooling all trials irrespective of condition (plausible, implausible, and scrambled) and computing time–frequency representations of neural oscillatory activity in response to the PLD relative to baseline ( $-400$  to  $-250$  ms). We focused on four main areas, which showed clear perturbations of spectral activity in response to visual stimulation:

*Parieto-occipital areas:* PLD elicited an increase of power in the  $\theta$ -band (5–7 Hz) immediately after stimulus onset (0–0.3 s). In addition, we observed a sustained decrease in the  $\alpha$  (7–13 Hz) and  $\beta$  (13–21 Hz) band power after stimulus onset (0.2–4.5 s), as well as a sustained increase in  $\gamma$ -power (70–95 Hz) between 0.1 and 4.5 s poststimulus onset. All stimulation effects showed a clear bilateral distribution in parieto-occipital areas, with the  $\gamma$ -band effect more strongly pronounced to the right hemisphere (Fig. 2A).

*Sensorimotor areas:* PLD elicited a weak increase in  $\theta$ -band (5–7 Hz) power after stimulus onset (0.0–0.3 s), which, however, is most likely owing to spatial smearing from the parieto-occipital areas. In addition, we observed a distinct and sustained increase in high  $\alpha$  (11–13 Hz) power between 0.4 and 4.0 s and a sustained decrease in low  $\alpha$  (7–11 Hz) and  $\beta$  (15–23 Hz) power between 0.5 and 4.5 s poststimulus onset in bilateral sensorimotor areas (Fig. 2B).

*Temporal areas:* PLD elicited a bilateral increase in  $\theta$ -band (5–7 Hz) power after stimulus onset (0.0–0.3 s). In addition, we observed a sustained bilateral decrease in low  $\alpha$

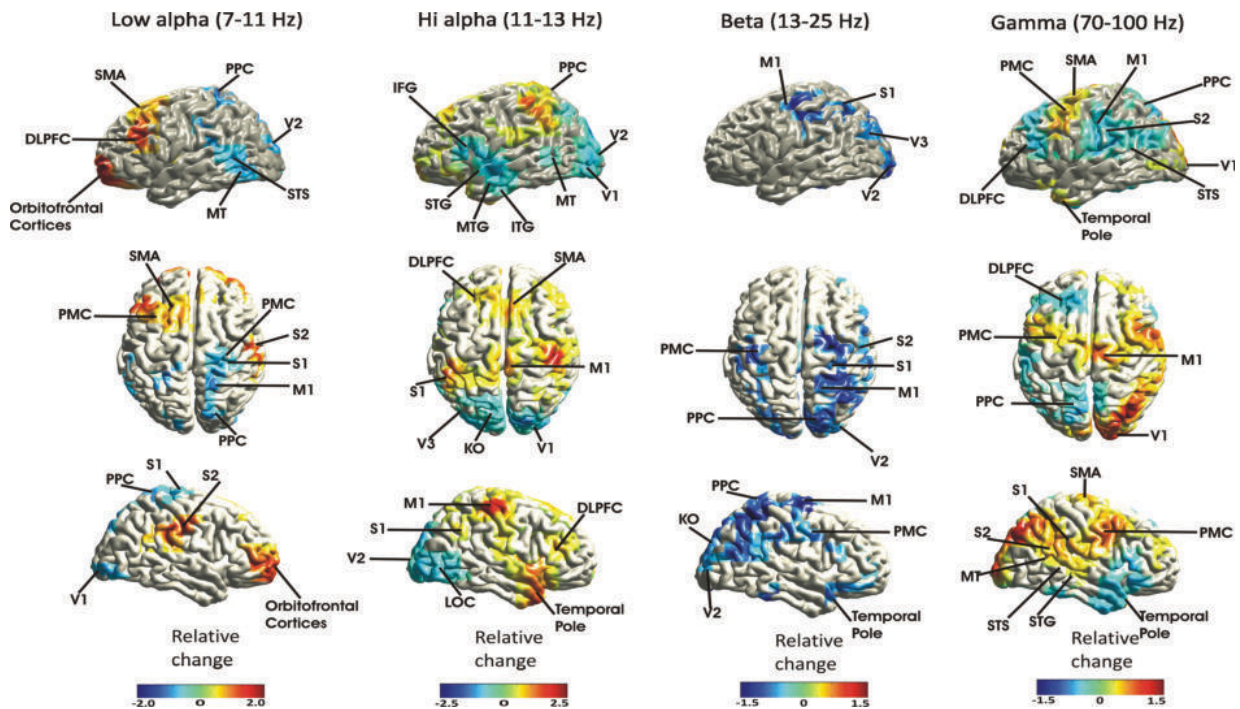


**Figure 3.**

Stimulation effects on source level. Cortical sources of relative change for low  $\alpha$  (7–11 Hz), high  $\alpha$  (11–13 Hz),  $\beta$  (13–25 Hz), and  $\gamma$  (70–100 Hz) power, respectively. Color maps illustrate changes in power relative to baseline. Only significant sources ( $P < 0.05$ ; cluster corrected) are shown.

(7–11 Hz) and  $\beta$ -power (13–23 Hz) between 0.5 and 4.5 s, as well as a bilateral increase in high  $\alpha$  (11–13 Hz) between 0.3 and 0.6 s (Fig. 2C,D). These effects are highly similar to the effects found in sensors over parieto-occipital and sensorimotor areas (see above) but with lower amplitude. In contrast to the results from parieto-occipital sensory, we observed a robust early increase (90–100 Hz) between 0 and 1.5 s and a sustained decrease in oscillatory  $\gamma$ -power (50–80 Hz) between 0 and 4.5 s poststimulus onset in right temporal cortex (Fig. 2D).

Next, we identified the cortical sources of the sustained effects, found in the time-frequency representations on sensor level. To this end, we performed source localization using a beamformer on four distinct frequency bands, based on the results on sensor level (i.e., for low  $\alpha$  [7–11 Hz], high  $\alpha$  [11–13 Hz],  $\beta$  [13–25 Hz], and  $\gamma$  [50–100 Hz] band). Strongest cortical sources were identified in visual as well as sensorimotor areas (for details, see Fig. 3).

### Condition Contrast

We assessed differences between plausible versus scrambled stimuli in the four regions of interest (parieto-occipital, left, and right temporal, and sensorimotor areas). We found a significant increase in  $\gamma$  (55–90 Hz) power at 500–800 ms poststimulus onset in parieto-occipital areas ( $P$

$< 0.05$ ), followed by a significant increase in  $\beta$  (20–35 Hz) power at 700–1,200 ms poststimulus onset in sensorimotor areas as well as a significant increase in high  $\alpha$  (9–13 Hz) power at 900–1,300 ms in left temporal areas (Fig. 4A). In addition, we found a significant decrease in  $\gamma$  (50–80 Hz) and  $\alpha$ /low  $\beta$  (10–22 Hz) power, between 1,300 and 2,000 ms in right temporal and parieto-occipital (Fig. 4A) areas ( $P < 0.05$ ), respectively.

Next, we identified the cortical sources of these significant clusters. For the increase in  $\gamma$ -power (55–90 Hz) between 500 and 800 ms, the sources were identified in the primary visual cortex (V1). Additional sources were identified in the right medial and inferior temporal gyrus, as well as right dorsolateral prefrontal cortex (DLPFC) (Fig. 4B).

The sources of the significant effects between 20–35 Hz and 700–1,200 ms were located in the bilateral sensorimotor areas of the brain and more specifically the PMC and right primary motor cortex (M1) (Fig. 4D).

The sources for the significant effects between 9–13 Hz and 900–1,300 ms were located in the left temporal areas of the brain and more specifically the STS. Additional sources were identified in the left somatosensory areas (Fig. 4F).

The sources for the significant effects between 50–80 Hz and 1,300–1,600 ms were located in the right temporal areas of the brain and more specifically the right medial

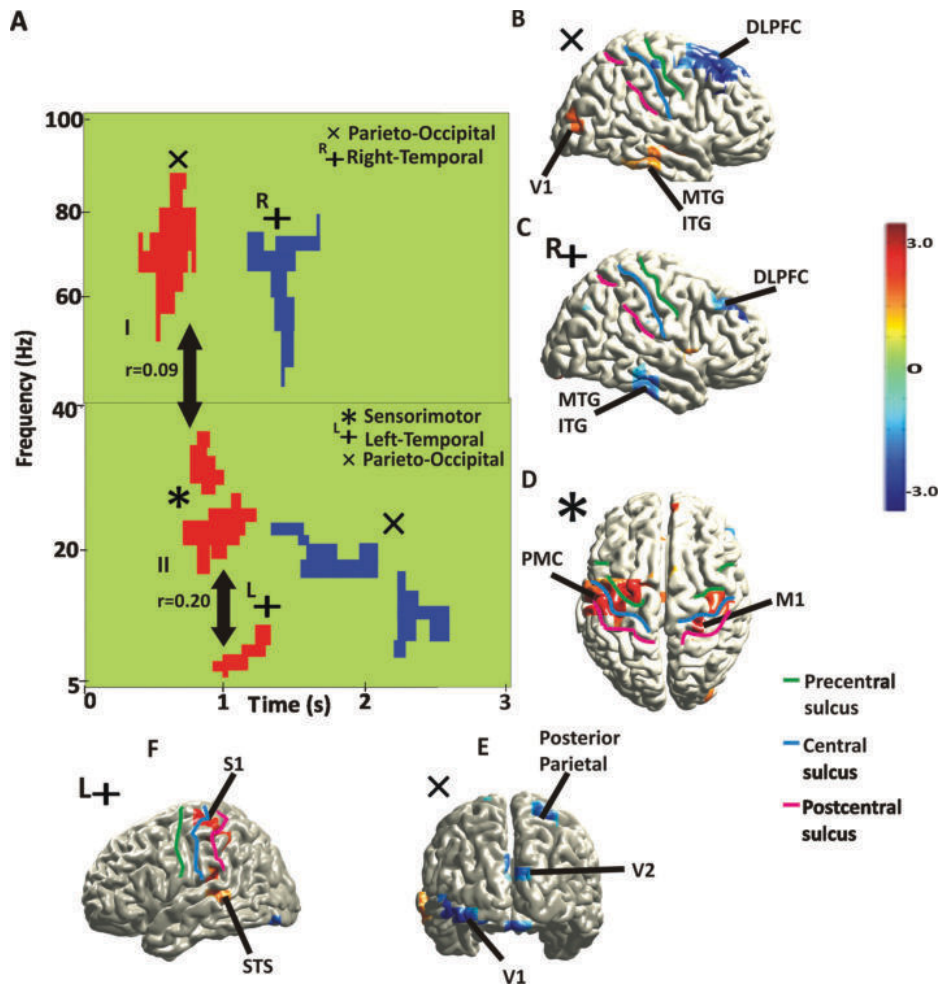


**Figure 4.**

Condition contrasts for plausible versus scrambled PLD: (A) Representations of significant clusters ( $P < 0.05$ ) found on sensor level for (x) parieto-occipital, (\*) sensorimotor cortex, and (+) left-temporal, and (+) right-temporal. Red denotes higher power for plausible, whereas blue denotes higher power for scrambled. Source reconstruction of the significant clusters found on sensor level for (B) parieto-occipital  $\gamma$  increase, (C) right temporal  $\gamma$  decrease, (D) sensorimotor  $\beta$ -increase, (E)

parieto-occipital  $\beta$ -decrease and, (F) left temporal  $\alpha$  increase. Color map represents  $t$ -values for source reconstruction. Red denotes higher power for plausible, whereas blue denotes higher power for scrambled. Arrows and  $r$ -values represent significant ( $P < 0.05$ ) positive trial-by-trial correlations for the plausible condition between sensorimotor  $\beta$  and (I) parieto-occipital  $\gamma$ -power as well as (II) left temporal  $\alpha$ -power.

and inferior temporal cortex. Additional sources were identified in the right DLPFC (Fig. 4C).

Finally, the sources of the significant cluster between 10–22 Hz and 1,600–2,000 ms were localized in bilateral parieto-occipital areas and more specifically visual areas V1 and V2 as well as right parietal posterior (Fig. 4E).

### Cross-frequency Correlations

To assess the interactions between visual and sensorimotor areas during the recognition of actions, we calculated

the trial-by-trial cross-frequency correlation between the significant time–frequency clusters (Fig. 4A). A significant positive correlation was observed between sensorimotor  $\beta$  (averaged between 20–35 Hz and 700–1,200 ms) and parieto-occipital  $\gamma$  (averaged between 55–75 Hz and 500–800 ms) power ( $r = 0.09$ ;  $P < 0.05$ ) as well as between sensorimotor  $\beta$  and left temporal  $\alpha$  (9–13 Hz and 900–1,300 ms) power ( $r = 0.20$ ;  $P < 0.05$ ) for the plausible action condition, but not for the scrambled one. No significant correlation was observed when the time windows of the significant clusters were moved in steps of  $\pm 100$  ms. In

addition, a significant positive trial-by-trial correlation was observed between parieto-occipital  $\beta$  (10–22 Hz and 1,600–2,000 ms) and right temporal  $\gamma$  (50–80 Hz and 1,300–1,600 ms) power ( $r = 0.16$ ;  $P < 0.05$ ) for the scrambled condition. A significant positive trial-by-trial correlation was still visible when the time windows of the significant clusters were simultaneously moved in steps of  $-100$  ms ( $r = 0.19$ ;  $P < 0.05$ ), but not for other time shifts. Finally, a significant negative trial-by-trial correlation was observed between sensorimotor  $\beta$  (20–35 Hz and 700–1,200 ms) and parieto-occipital  $\beta$  (10–22 Hz and 1,600–2,000 ms) power ( $r = 0.08$ ;  $P < 0.05$ ) for the scrambled condition that was not present when the time windows were moved in steps of  $\pm 100$  ms.

## DISCUSSION

The present study aimed at determining the dynamic modulations of neuronal oscillatory activity in the cortical networks involved in the recognition of plausible actions. PLDs elicited sustained effects in  $\theta$  (5–7 Hz),  $\alpha$  (7–13 Hz),  $\beta$  (15–25 Hz), and  $\gamma$  (50–100 Hz) power within cortical areas of the MNS. We were particularly interested how these dynamic modulations as well as the interactions between areas of MNS changed when we compared plausible and scrambled actions. We will first discuss the observed stimulation-induced effects with respect to earlier hemodynamic and electrophysiological reports. The main focus of this article is the comparison of our two conditions and their interactions between cortical areas of the MNS, which will then be applied to current theories of the action recognition process.

Presentation of PLD (pooled over all conditions) induced a sustained decrease of spectral power in the  $\alpha$ - and  $\beta$ -band in parieto-occipital regions. The decrease started at  $\sim 200$  ms poststimulus onset and was sustained throughout the trial. The decrease as well as its timing is in line with the previous reports on visual stimulation (e.g., de Lange et al., 2008; Hoogenboom et al., 2006; Koelewijn et al., 2008; Singh et al., 2002). The decrease of  $\alpha/\beta$ -power was also found in sensorimotor areas, starting at around  $\sim 500$  ms poststimulus and lasting until the end of the trial, in agreement with the earlier reports of  $\alpha/\beta$  suppression during action preparation, action execution, and motor imagery tasks (de Lange et al., 2008; Hari and Salmelin, 1997; Koelewijn et al., 2008; Oberman et al., 2005; Orgs et al., 2008; Schnitzler et al., 1997; Ulloa and Pineda, 2007). Moreover, somatosensory areas have been suggested to play a role in the internal simulation of the sensory consequences of observed actions or embodiment [Caetano et al., 2007; de Lussanet et al., 2008]. In contrast to the suppression of low  $\alpha$  band-power, sensorimotor areas revealed an increase of high  $\alpha$  (11–13 Hz) band power between 400 and 4,000 ms poststimulus. While a decrease of  $\alpha/\beta$ -band power has been linked to engagement of sensorimotor areas, an increase has been sug-

gested to reflect inhibition or disengagement of the sensorimotor system [Hummel et al., 2002; Jensen et al., 2002; Nachev et al., 2008; Neuper and Pfurtscheller, 2001]. The early observed increase in high  $\alpha$ -band power might thus reflect subjects' active inhibition of finger and/or eye movements during stimulus presentation or suppression of task-irrelevant areas during initial stimulus presentation. Finally, we observed a sustained increase of high  $\gamma$ -band power in a wide range of areas including frontal and posterior regions of the brain (for details, see Fig. 3). This increase of  $\gamma$ -power is visible between 100 and 4,500 ms, that is it starts slightly earlier than the other sustained effects, similar to the previous reports involving visuomotor tasks [Aoki et al., 1999; de Lange et al., 2008; Pavlova et al., 2004, 2006; Pfurtscheller and Neuper, 1992].

When comparing plausible to scrambled condition, we observed an early increase of  $\gamma$  (55–75 Hz) band power between 500 and 800 ms in right V1 and temporal cortex. Other electrophysiological studies report an increase in  $\gamma$ -power as early as 80–170 ms when subjects passively viewed point-light walkers [Pavlova et al., 2004, 2006]. One reason for the differences in timing might be owing to the different definition of  $\gamma$ -band activity: Although we observed  $\gamma$ -band effects between 55 and 75 Hz, Pavlova et al. found effects in the lower  $\gamma$ -band between 25 and 40 Hz. In addition, differences might be owing to the different experimental designs between Pavlova et al. (passive viewing of normal, scrambled, inverted PLD) and our study (active evaluation of normal, implausible, and scrambled PLD). This increase of  $\gamma$ -band, however, is in line with increased hemodynamic responses in parieto-occipital and temporal areas for plausible versus scrambled PLD (e.g. Grossman and Blake, 2002; Grossman et al., 2000; Michels et al., 2005, 2009; Pelphrey et al., 2004, 2005). Neuronal activity, especially  $\gamma$ -band activity, in right temporal areas reflects the processing of the global form of the PLD, which is only recognizable in the plausible condition [Michels et al., 2005, 2009; Pavlova et al., 2004]. As the  $\gamma$ -band effect was the earliest significant cluster, the result suggests that discrimination between plausible and scrambled PLD starts at early, low-, and high-level visual stages of the action recognition process (e.g. Pavlova et al., 2004).

The increase of  $\gamma$ -band power was followed by an increase of power in the  $\beta$  (20–35 Hz) band between 700 and 1,200 ms in bilateral sensorimotor areas (PMC and M1). Similar to the timing of the sensorimotor  $\beta$ -effect, previous electrophysiological studies reported sensorimotor  $\alpha/\beta$  decreases to differentiate during action observation or motor imagery in the time period of  $\sim 450$ – $1,500$  ms poststimulus onset [de Lange et al., 2008; Orgs et al., 2008; Schnitzler et al., 1997]. Previous fMRI studies demonstrated that sensorimotor areas and more specifically the PMC, responded to both human (plausible) and nonhuman (scrambled) actions, but much stronger for human actions belonging to the observer's own motor repertoire [Buccino et al., 2004b; Saygin et al., 2004]. In addition, Calvo-Merino et al. (2005) observed a stronger hemodynamic response in

STG, premotor, and parietal areas when capoeira and classical ballet dancers observed movements from their own repertoire. The observed positive  $\beta$ -cluster in sensorimotor areas reflects a stronger suppression of power for scrambled than plausible actions. In contrast to this observation, one previous study revealed a stronger suppression of sensorimotor  $\beta$ -power when subjects viewed actions within their own repertoire compared to other plausible, but clearly distinguishable movements [Orgs et al., 2008]. Interestingly however, stronger suppression of sensorimotor  $\beta$ -band power has been reported for the observation of incorrect versus correct button presses [Koelewijn et al., 2008]. Although subjects in the study by Koelewijn et al. had to distinguish between correct and incorrect button presses, subjects in our study had to distinguish between normal and scrambled actions. Despite these notable differences in the experimental setup, we observed a similar pattern of  $\beta$ -decrease as reported by Koelewijn et al. We therefore speculate that stronger  $\beta$ -band suppression in our study might thus be related to the recognition of the scrambled action movements as incorrect. Future studies, however, are needed to support this speculation.

The sensorimotor  $\beta$ -increase was followed by an  $\alpha$  (9–13 Hz) band increase between 900 and 1,300 ms in left S1 and STS. An increase in  $\alpha$  power might reflect suppression of task-irrelevant areas during initial stimulus presentation, as well as active inhibition or disengagement of the cortical areas involved (e.g. Jensen and Mazaheri, 2010; Jensen et al., 2002). The observed  $\alpha$ -power increase over left STS and somatosensory areas, two areas known to be involved in the processing [Allison et al., 2000] and internal simulation [de Lussanet et al., 2008] of biological actions, might thus reflect active inhibition of these areas. Previous electrophysiological studies reported  $\alpha$  activity of temporal areas peaking at around  $\sim$ 750 ms during a visual attention task [Pantazis et al., 2009]. The observed left hemisphere activity might reflect visual attention of the local details of the PLD when differentiating between plausible and scrambled conditions [Bonda et al., 1996; Fink et al., 1997; Lamb and Robertson, 1988].

Interestingly, we observed a significant positive trial-by-trial correlation between sensorimotor  $\beta$ -power and parieto-occipital  $\gamma$ -power as well as left temporal  $\alpha$ -power. This correlation was observed only for plausible PLD but not for scrambled PLD, and the correlation was observed only at specific time points, namely at time points where we found the significant power increase for plausible PLD. This finding illustrates a crossfrequency coupling between visual and motor areas during recognition of plausible actions operating at large spatio-temporal scales. The temporal profiles of the power changes suggest a functional interaction proceeding from visual areas to sensorimotor areas and back projecting to STS.

At a later time point, we observed an additional negative cluster in the  $\beta$ -band in parieto-occipital areas, reflecting a stronger  $\beta$ -band power for the scrambled than the plausible condition. This finding is in line with fMRI studies which

suggest that parieto-occipital areas are more sensitive to image scrambling (for review, see Grill-Spector and Malach, 2004). Trial-by-trial correlations between this late parieto-occipital  $\beta$ -band power and early sensorimotor power revealed a negative correlation for the scrambled PLD, but no significant correlation for the plausible PLD. This finding reveals crossfrequency coupling between sensorimotor and visual areas over several hundred milliseconds. We suggest that this effect reflects feedback projections from sensorimotor areas to visual areas, possibly updating visual processing [Schippers and Keysers, 2011]. Interestingly, all correlations have been observed between sensorimotor  $\beta$ -power and other frequencies in other areas. Oscillations in the  $\beta$ -band have been widely observed in sensorimotor areas in relation to motor behavior [Haegens et al., 2011; Salenius and Hari, 2003] and have been proposed as a mechanism for synchronization over long transmission delays and long ranges [Bibbig et al., 2002; Gross et al., 2004; Kopell et al., 2000; Schnitzler and Gross, 2005]. We suggest that  $\beta$ -oscillations supply a mechanism that combines visual and motor areas into a functional network [Brovelli et al., 2004].

The power correlations, although low in absolute value, are statistically significant and consistent across all subjects. Studies investigating working memory with intracranial EEG (iEEG) have reported correlation with absolute values  $>0.3$  (e.g. Axmacher et al., 2010). This difference might be owing to a higher signal-to-noise ratio for iEEG when compared to MEG. The absolute values of the correlation values (0.07–0.20) of our study, however, are in line with the previous MEG studies, reporting power correlations in the range of 0.01–0.07 (e.g., Hipp et al., 2012; Hoogenboom et al., 2010).

Interestingly, we also observed a much stronger  $\gamma$ -power for scrambled PLD in right DLPFC. DLPFC activity has been linked to the process of evaluating other people's behavior (e.g. Saygin, 2007; Saygin et al., 2004). It has been, therefore, suggested that DLPFC is an important contributor to cognitive control in a social domain, as its role is to maintain intentions of our actions in working memory, and subsequently using feedback to evaluate whether our actions match those intentions [Weissman et al., 2008]. The stronger suppression of  $\gamma$ -power for plausible than scrambled actions might thus reflect DLPFC efforts in trying to evaluate the intentions of the scrambled actions that do not match the intentions stored in working memory.

In summary, our results reveal a widespread cortical network involved in the recognition of plausible actions, including areas of the MNS operating at different frequency bands, extending previous fMRI and MEG studies. We demonstrate interactions between these areas by revealing power correlations between visual and motor areas during the recognition of plausible and scrambled actions at specific spatial-temporal scales. We propose that these results reveal a functional coupling of visual and motor areas, predominantly coupled to the sensorimotor  $\beta$ -frequency, in support to current models of motor control that propose the presence of internal models (inverse and forward) involving visual and motor interactions.

## ACKNOWLEDGMENTS

The authors thank Markus Lappe and Marc de Lussanet for providing them with the point-light displays (PLD), and helpful comments; and Nienke Hoogenboom and Hanneke van Dijk for helpful discussions and suggestions.

## REFERENCES

- Allison T, Puce A, McCarthy G (2000): Social perception from visual cues: role of the STS region. *Trends Cogn Sci* 4:267–278.
- Aoki F, Fetz, EE, Shupe L, Lettich E, Ojemann GA (1999): Increased gamma range activity in human sensorimotor cortex during performance of visuomotor tasks. *Clin Neurophysiol* 110:524–537.
- Axmacher N, Henseler MM, Jensen O, Weinreich I, Elger CE, Fell J (2010): Cross-frequency coupling supports multi-item working memory in the human hippocampus. *Proc Natl Acad Sci USA* 107:3228–3233.
- Bibbig A, Traub RD, Whittington MA (2002): Long-range synchronization of gamma and beta oscillations and the plasticity of excitatory and inhibitory synapses: A network model. *J Neurophysiol* 88:1634–1654.
- Blake R, Shiffrar M (2007): Perception of human motion. *Annu Rev Psychol* 58:47–73.
- Blakemore SJ, Frith C (2005): The role of motor contagion in the prediction of action. *Neuropsychologia* 43:260–267.
- Bonda E, Petrides M, Ostry D, Evans A (1996): Specific involvement of human parietal systems and the amygdala in the perception of biological motion. *J Neurosci* 16:3737–3744.
- Brovelli A, Ding M, Ledberg A, Chen Y, Nakamura R, Bressler SL (2004): Beta oscillations in a large-scale sensorimotor cortical network: Directional influences revealed by Granger causality. *Proc Natl Acad Sci USA* 101:9849–9854.
- Buccino G (2004): Neural substrates involved in executing, observing, and imagining actions. *Brain and Cognition* 56:118.
- Buccino G, Binkofski F, Riggio L (2004a): The mirror neuron system and action recognition. *Brain Lang* 89:370–376.
- Buccino G, Lui F, Canessa N, Patteri I, Lagravinese G, Benuzzi F, Porro CA, Rizzolatti G (2004b): Neural circuits involved in the recognition of actions performed by nonconspecifics: An FMRI study. *J Cogn Neurosci* 16:114–126.
- Calvo-Merino B, Glaser DE, Grezes J, Passingham RE, Haggard P (2005): Action observation and acquired motor skills: An FMRI study with expert dancers. *Cereb Cortex* 15:1243–1249.
- Caetano G, Jousmaki V, Hari R (2007): Actor's and observer's primary motor cortices stabilize similarly after seen or heard motor actions. *Proc Natl Acad Sci USA* 104:9058–9062.
- Candidi M, Urgesi C, Ionta S, Aglioti SM (2008): Virtual lesion of ventral premotor cortex impairs visual perception of biomechanically possible but not impossible actions. *Soc Neurosci* 3:388–400.
- Choi SC (1977): Test of equality of dependent correlations. *Biometrika* 64:645–647.
- de Lange FP, Jensen O, Bauer M, Toni I (2008): Interactions between posterior gamma and frontal alpha/beta oscillations during imagined actions. *Front Hum Neurosci* 2:7.
- de Lussanet MH, Fadiga L, Michels L, Kleiser R, Seitz RJ, Lappe M (2008): Interaction of visual hemifield and body view in biological motion perception. *Eur J Neurosci* 27:514–522.
- Di Pellegrino G, Fadiga L, Fogassi L, Gallese V, Rizzolatti G (1992): Understanding motor events: A neurophysiological study. *Exp Brain Res* 91:176–180.
- Dinstein I, Hasson U, Rubin N, Heeger DJ (2007): Brain areas selective for both observed and executed movements. *J Neurophysiol* 98:1415–1427.
- Filimon F, Nelson JD, Hagler DJ, Sereno MI (2007): Human cortical representations for reaching: Mirror neurons for execution, observation, and imagery. *Neuroimage* 37:1315–1328.
- Fink GR, Halligan PW, Marshall JC, Frith CD, Frackowiak RS, Dolan RJ (1997): Neural mechanisms involved in the processing of global and local aspects of hierarchically organized visual stimuli. *Brain* 120:1779–1791.
- Gallese V, Fadiga L, Fogassi L, Rizzolatti G (1996): Action recognition in the premotor cortex. *Brain* 119:593–609.
- Gazzola V, Rizzolatti G, Wicker B, Keysers C (2007): The anthropomorphic brain: The mirror neuron system responds to human and robotic actions. *Neuroimage* 35:1674–1684.
- Grill-Spector K, Malach R (2004): The human visual cortex. *Annu Rev Neurosci* 27:649–677.
- Gross J, Kujala J, Hamalainen M, Timmermann L, Schnitzler A, Salmelin R (2001): Dynamic imaging of coherent sources: Studying neural interactions in the human brain. *Proc Natl Acad Sci USA* 98:694–699.
- Gross J, Schmitz F, Schnitzler I, Kessler K, Shapiro K, Hommel B, Schnitzler A (2004): Modulation of long-range neural synchrony reflects temporal limitations of visual attention in humans. *Proc Natl Acad Sci USA* 101:13050–13055.
- Grossman ED, Donnelly M, Price R, Pickens D, Morgan V, Neighbor G, Blake R (2000): Brain areas involved in perception of biological motion. *J Cogn Neurosci* 12:711–720.
- Grossman ED, Blake R (2001): Brain activity evoked by inverted and imagined biological motion. *Vision Res* 41:1475–1482.
- Grossman ED, Blake R (2002): Brain areas active during visual perception of biological motion. *Neuron* 35:1167–1175.
- Haegens S, Nácher V, Hernández A, Luna R, Jensen O, Romo R (2011): Beta oscillations in the monkey sensorimotor network reflect somatosensory decision making. *Proc Natl Acad Sci USA* 108:10708–10713.
- Hari R, Salmelin R (1997): Human cortical oscillations: A neuro-magnetic view through the skull. *Trends Neurosci* 20:44–49.
- Hipp JF, Hawellek DJ, Corbetta M, Siegel M, Engel AK (2012): Large-scale cortical correlation structure of spontaneous oscillatory activity. *Nat Neurosci* 15:884–890.
- Hoogenboom N, Schoffelen JM, Oostenveld R, Parkes LM, Fries P (2006): Localizing human visual gamma-band activity in frequency, time and space. *NeuroImage* 29:764–773.
- Hoogenboom N, Schoffelen JM, Oostenveld R, Fries P (2010): Visually induced gamma-band activity predicts speed of change detection in humans. *Neuroimage* 51:1162–1167.
- Hummel F, Andres F, Altenmüller E, Dichgans J, Gerloff C (2002): Inhibitory control of acquired motor programmes in the human brain. *Brain* 125:404–420.
- Jensen O, Colgin LL (2007): Cross-frequency coupling between neuronal oscillations. *Trends Cogn Sci* 11:267–269.
- Jensen O, Gelfand J, Kounios J, Lisman JE (2002): Oscillations in the alpha band (9–12 Hz) increase with memory load during retention in a short-term memory task. *Cereb Cortex* 12:877–882.
- Jensen O, Mazaheri A (2010): Shaping functional architecture by oscillatory alpha activity: Gating by inhibition. *Front Hum Neurosci* 4:186. doi:10.3389/fnhum.2010.00186.
- Johansson G (1973): Visual perception of biological motion and a model for its analysis. *Percept Psychophys* 14:201–211.

- Kemenade BM, Muggleton N, Walsh V, Saygin AP (2012): The Effects of TMS over STS and premotor cortex on the perception of biological motion. *J Cogn Neurosci* 24:896–904.
- Koelwijn T, van Schie HT, Bekkering H, Oostenveld R, Jensen O (2008): Motor-cortical beta oscillations are modulated by correctness of observed action. *Neuroimage* 40:767–775.
- Kokal I, Gazzola V, Keysers C (2009): Acting together in and beyond the mirror neuron system. *Neuroimage* 47:2046–2056.
- Kopell N, Ermentrout GB, Whittington MA, Traub RD (2000): Gamma rhythms and beta rhythms have different synchronization properties. *Proc Natl Acad Sci USA* 97:1867–1872.
- Lamb MR, Robertson LC (1988): The processing of hierarchical stimuli: Effects of retinal locus, locational uncertainty, and stimulus identity. *Percept Psychophys* 44:172–181.
- Lange J, Georg K, Lappe M (2006): Visual perception of biological motion by form: A template-matching analysis. *J Vis* 6:836–849.
- Lange J, Lappe M (2007): The role of spatial and temporal information in biological motion perception. *Adv Cogn Psychol* 3:419–429.
- Lange J, Oostenveld R, Fries P (2011): Perception of the touch-induced visual double-flash illusion correlates with changes of rhythmic neuronal activity in human visual and somatosensory areas. *Neuroimage* 54:1395–1405.
- Maris E, Oostenveld R (2007): Nonparametric statistical testing of EEG- and MEG-data. *J Neurosci Methods* 164:177–190.
- Michels L, Kleiser R, de Lussanet MH, Seitz RJ, Lappe M (2009): Brain activity for peripheral biological motion in the posterior superior temporal gyrus and the fusiform gyrus: Dependence on visual hemifield and view orientation. *Neuroimage* 45:151–159.
- Michels L, Lappe M, Vaina LM (2005): Visual areas involved in the perception of human movement from dynamic form analysis. *Neuroreport* 16:1037–1041.
- Nachev P, Kennard C, Husain M (2008): Functional role of the supplementary and pre-supplementary motor areas. *Nat Rev Neurosci* 9:856–869.
- Neuper C, Pfurtscheller G (2001): Event-related dynamics of cortical rhythms: Frequency-specific features and functional correlates. *Int J Psychophysiol* 43:41–58.
- Nolte G (2003): The magnetic lead field theorem in the quasi-static approximation and its use for magnetoencephalography forward calculation in realistic volume conductors. *Phys Med Biol* 21:3637–3652.
- Oberman LM, Hubbard EM, McCleery JP, Altschuler EL, Ramachandran VS, Pineda JA (2005): EEG evidence for mirror neuron dysfunction in autism spectrum disorders. *Brain Res Cogn Brain Res* 24:190–198.
- Oostenveld R, Fries P, Maris E, Schoffelen JM (2011): FieldTrip: Open source software for advanced analysis of MEG, EEG, and invasive electrophysiological data. *Comput Intell Neurosci* 2011:156869.
- Oram MW, Perrett DI (1994): Responses of anterior superior temporal polysensory area STPa neurons to ‘biological motion’ stimuli. *J Cogn Neurosci* 6:99–116.
- Orgs G, Dombrowski JH, Heil M, Jansen-Osmann P (2008): Expertise in dance modulates alpha/beta event-related desynchronization during action observation. *Eur J Neurosci* 27:3380–3384.
- Pantazis D, Simpson GV, Weber DL, Dale CL, Nichols TE, Leahy RM (2009): A novel ANCOVA design for analysis of MEG data with application to a visual attention study. *NeuroImage* 44:164–174.
- Pavlova M, Sokolov A (2003): Prior knowledge about display inversion in biological motion perception. *Perception* 32:937–946.
- Pavlova M, Lutzenberger W, Sokolov A, Birbaumer N (2004): Dissociable cortical processing of recognizable and non-recognizable biological movement: Analysing gamma MEG activity. *Cerebral Cortex* 14:181–188.
- Pavlova M, Birbaumer N, Sokolov A (2006): Attentional modulation of cortical neuromagnetic gamma response to biological movement. *Cerebral Cortex* 16:321–327.
- Pelphrey KA, Morris JP, McCarthy G (2004): Grasping the intentions of others: The perceived intentionality of an action influences activity in the superior temporal sulcus during social perception. *J Cogn Neurosci* 16:1706–1716.
- Pelphrey KA, Morris JP, Michelich CR, Allison T, McCarthy G (2005): Functional anatomy of biological motion perception in posterior temporal cortex: An fMRI study of eye, mouth and hand movements. *Cerebral Cortex* 15:1866–1876.
- Pfurtscheller G, Neuper C (1992): Simultaneous EEG 10 Hz desynchronization and 40 Hz synchronization during finger movements. *Neuroreport* 3:1057–1060.
- Rizzolatti G, Craighero L (2004): The mirror-neuron system. *Annu Rev Neurosci* 27:169–192.
- Rizzolatti G, Fadiga L, Gallese V, Fogassi L (1996): Premotor cortex and the recognition of motor actions. *Brain Res Cogn Brain Res* 3:131–141.
- Rizzolatti G, Fogassi L, Gallese V (2001): Neurophysiological mechanisms underlying the understanding and imitation of action. *Nat Rev Neurosci* 2:661–670.
- Salenius S, Hari R (2003): Synchronous cortical oscillatory activity during motor action. *Curr Opin Neurobiol* 13:678–684.
- Saygin AP (2007): Superior temporal and premotor brain areas necessary for biological motion perception. *Brain* 130:2452–2461.
- Saygin AP, Wilson SM, Hagler DJ, Bates E, Sereno MI (2004): Point-light biological motion perception activates human premotor cortex. *J Neurosci* 24:6181–6188.
- Schippers MB, Keysers C (2011): Mapping the flow of information within the putative mirror neuron system during gesture observation. *Neuroimage* 57:37–44.
- Schnitzler A, Gross J (2005): Functional connectivity analysis in magnetoencephalography. *Int Rev Neurobiol* 68:173–195.
- Schnitzler A, Salenius S, Salmelin R, Jousmaki V, Hari R (1997): Involvement of primary motor cortex in motor imagery: A neuromagnetic study. *Neuroimage* 6:201–208.
- Singh KD, Barnes GR, Hillebrand A, Forde EM, Williams AL (2002): Task-related changes in cortical synchronization are spatially coincident with the hemodynamic response. *Neuroimage* 16:103–114.
- Ulloa ER, Pineda JA (2007): Recognition of point-light biological motion: mu rhythms and mirror neuron activity. *Behav Brain Res* 183:188–194.
- Urgesi C, Maieron M, Avenanti A, Tidoni E, Fabbro F, Aglioti SM (2010): Simulating the future of actions in the human cortico-spinal system. *Cereb Cortex* 20:2511–2521.
- Walden AT, McCoy EJ, Percival DB (1995): The effective bandwidth of a multitaper spectral estimator. *Biometrika* 82:201–214.
- Weissman DH, Perkins AS, Woldorff MG (2008): Cognitive control in social situations: The role of the dorsolateral prefrontal cortex. *NeuroImage* 40:955–962.

13) **Lange, J.**, Christian, N., & Schnitzler, A. (2013a).

Audio–visual congruency alters power and coherence of oscillatory activity within and between cortical areas.

*NeuroImage*, 79, 111–120.

Impact factor (2013): 6.132



## Audio–visual congruency alters power and coherence of oscillatory activity within and between cortical areas

Joachim Lange<sup>a,\*</sup>, Nadine Christian<sup>a</sup>, Alfons Schnitzler<sup>a,b</sup>

<sup>a</sup> Institute of Clinical Neuroscience and Medical Psychology, Medical Faculty, Heinrich-Heine-University Düsseldorf, Universitätsstraße 1, 40225 Düsseldorf, Germany

<sup>b</sup> Department of Neurology, Medical Faculty, Heinrich-Heine-University Düsseldorf, Universitätsstraße 1, 40225 Düsseldorf, Germany

### ARTICLE INFO

#### Article history:

Accepted 16 April 2013

Available online 2 May 2013

#### Keywords:

MEG  
Theta  
Beta  
Gamma  
Multisensory

### ABSTRACT

Dynamic communication between functionally specialized, but spatially distributed areas of the brain is essential for effective brain functioning. A candidate mechanism for effective neuronal communication is oscillatory neuronal synchronization. Here, we used magnetoencephalography (MEG) to study the role of oscillatory neuronal synchronization in audio–visual speech perception. Subjects viewed congruent audio–visual stimuli of a speaker articulating the vowels /a/ or /o/. In addition, we presented modified, incongruent versions in which visual and auditory signals mismatched. We identified a left hemispheric network for processing congruent audio–visual speech as well as network interaction between areas: low frequency (4–12 Hz) power was suppressed for congruent stimuli at auditory onset around auditory cortex, while power in the high gamma (120–140 Hz)-band was enhanced in the Broca's area around auditory offset. In addition, beta-power (20–30 Hz) was suppressed in supramarginal gyrus for incongruent stimuli. Interestingly, coherence analysis revealed a functional coupling between auditory cortex and Broca's area for congruent stimuli demonstrated by an increase of coherence. In contrast, coherence decreased for incongruent stimuli, suggesting a decoupling of auditory cortex and Broca's area. In addition, the increase of coherence was positively correlated with the increase of high gamma-power. The results demonstrate that oscillatory power in several frequency bands correlates with the processing of matching audio–visual speech on a large spatio-temporal scale. The findings provide evidence that coupling of neuronal groups can be mediated by coherence in the theta/alpha band and that low frequency coherence and high frequency power modulations are correlated in audio–visual speech perception.

© 2013 Elsevier Inc. All rights reserved.

### Introduction

The human brain is organized in functionally and spatially distributed areas, e.g. specialized in sensory processing or motor output. Effective interaction and integration of these distributed areas to a functional network are fundamental to perception, cognition, and action. Such effective interaction requires that the functional coupling of neurons in distributed areas to coherent neuronal groups is dynamically modulated depending on sensory information, task requirements or internal brain states. It has been proposed that communication and interaction between areas of the distributed network is shaped and coordinated by neuronal oscillatory synchronization (Fries, 2005; Fries, 2009; Gregoriou et al., 2009; Gross et al., 2004; Jensen and Mazaheri, 2010; Womelsdorf et al., 2007).

Here, we studied neuronal processes underlying audio–visual speech perception. Audio–visual speech perception provides an intriguing model to study cortical network interaction in multisensory integration and perception. It is well established that speech perception comprises a

network of several, spatially distributed functional areas showing a hierarchical organization that progresses from sensory processing in early sensory areas to more abstract linguistic and decision processes in e.g. the inferior frontal gyrus (IFG) or sensorimotor areas (Hickok and Poeppel, 2007; Nishitani and Hari, 2002; Pulvermuller, 2005; Sohoglu et al., 2012). It has been found that neuronal oscillations play a crucial role for the integration of audio–visual speech perception (Arnal et al., 2011; Chandrasekaran and Ghazanfar, 2009; Ghazanfar et al., 2008; Giraud and Poeppel, 2012; Schroeder et al., 2008). While several studies have demonstrated the functional role of neuronal oscillations in local nodes of the network (Chandrasekaran and Ghazanfar, 2009; Kaiser et al., 2005; Luo and Poeppel, 2007; Palva et al., 2002), few studies were able to provide evidence that neuronal oscillations are involved in the interaction and coupling of cortical areas during speech perception (Arnal et al., 2011; Canolty et al., 2007; Ghazanfar et al., 2008).

In the present study, we aimed to study the role of neuronal oscillations for coupling of cortical areas and formation of dynamic networks during perception of matching audio–visual speech. To this end, we presented audio–visual stimuli with either congruent, matching (e.g. audio: /a/; visual: /a/) or incongruent, non-matching

\* Corresponding author.

E-mail address: [joachim.lange@med.uni-duesseldorf.de](mailto:joachim.lange@med.uni-duesseldorf.de) (J. Lange).

(e.g. audio: /a/; visual: /o/) audio–visual information. Using magnetoencephalography (MEG), we studied neuronal oscillations in local neuronal groups and the interaction of specific cortical areas in terms of coherence. Our main hypothesis was that relevant neuronal groups should be coupled during congruent, but not during incongruent stimuli and that neuronal oscillations should reflect the dynamic coupling between neuronal groups of the speech processing network. Furthermore, several studies demonstrated a functional coupling of spatially distributed areas by coherence (e.g. Gross et al., 2004; Hirschmann et al., 2011; Keil et al., 2012; Womelsdorf et al., 2007). In the present study, we were therefore additionally interested, whether coherence provides a mechanism for defining cortical networks during audio–visual perception. If coherence provides a functional mechanism, the strength of intra- or inter-areal coherence should increase for congruent relative to incongruent audio–visual stimuli in or between relevant cortical areas.

## Methods

### Subjects

Eleven subjects (mean age 24.6 years, range 22–27 years, 6 males) participated in the study after giving written informed consent in accordance with the Declaration of Helsinki. All subjects were right-handed, had normal or corrected-to-normal vision and normal hearing and none of the subjects had a known history of neurological disorders.

### Stimuli

Video sequences of a female speaking vowels /a/ and /o/ in German were recorded using a digital camera (Canon, MV500i, Canon Inc., Japan). Video sequences were taken in frontal view showing the face in front of a gray background (16 × 14 cm, mouth region 2 × 1 cm). Video sequences included a variable baseline (760, 840, 920, or 1000 ms) before the start of the lip movement to minimize expectancy effects. After 526 (/a/) or 543 ms (/o/) the auditory signal started and lasted for 705 (/a/) or 661 ms (/o/), respectively. Lip movements finished 1600 (/a/) or 1640 ms (/o/) after the onset of the lip movement (Fig. 1).

Video sequences were modified using Video Studio 12 (Corel Corporation, Ottawa, Canada) to obtain four stimulus categories. AV<sub>C</sub>: natural, unmodified video sequences showing congruent combinations of visual and auditory signals. AV<sub>I</sub>: video sequences were modified to incongruent combinations of visual and auditory signals (visual: /a/ and auditory: /o/

and vice versa). Onset of the auditory signal was matched to the onset of the expected congruent auditory signal. A: visual information was replaced by a static picture taken from the period prior to the lip movement period (i.e. without any visual information about the vowel) so that information about the vowel was provided by the auditory signal only. V: auditory information was replaced by the residual background noise so that information about the vowel was provided by the visual signal only.

The time scale of all video sequences was realigned, so that  $t = 0$  denotes the onset of the auditory signal (in condition V this is the time point of expected onset of auditory signal).

To determine the on- and offset of the auditory signals, waveforms of the auditory signals were first rectified and each time sample was then smoothed using a 10 ms Gaussian kernel. Auditory signal were defined as time points where the rectified and smoothed signal exceeded the baseline (averaged signal between 400–500 ms after video onset, i.e. before onset of auditory signal and lip movements) by three standard deviations. Onset of auditory signal was defined as the first time point, offset as the last time point exceeding the threshold. Onset of articulatory lip movements was defined by visual inspection of the video frames.

### Experimental paradigm

Stimulus presentation was controlled using Presentation (Neurobehavioral Systems, Albany). Visual stimuli were presented via a projector located outside the magnetically shielded room and back-projected via a mirror-system onto a translucent screen 100 cm in front of the subjects. Auditory stimuli were presented via earphones (TIP-300 Tubal Insert Phone, Nicolet Biomedical, Inc., Fitchburg, Wisconsin) inserted into the subjects' ear. The volume was adjusted individually.

Each trial began with the presentation of a black screen for 600 ms followed by presentation of a fixation cross. The fixation cross was presented for 1000 ms at the position where the mouth will be presented in the following video sequence (center of the speaker's mouth). The fixation cross was presented to minimize eye movements and disappeared with the onset of the video sequence (Fig. 1). Next, one of the four video sequences was presented.

After the end of the stimulus, a black screen appeared for a random period between 0 and 1000 ms, followed by the response period (Fig. 1). Subjects were asked to report whether the video showed a congruent audio–visual sequence (condition AV<sub>C</sub>) or incongruent sequence (conditions AV<sub>I</sub>, A, or V). Subjects were explicitly instructed to rate conditions A and V as incongruent as audio and visual information were not

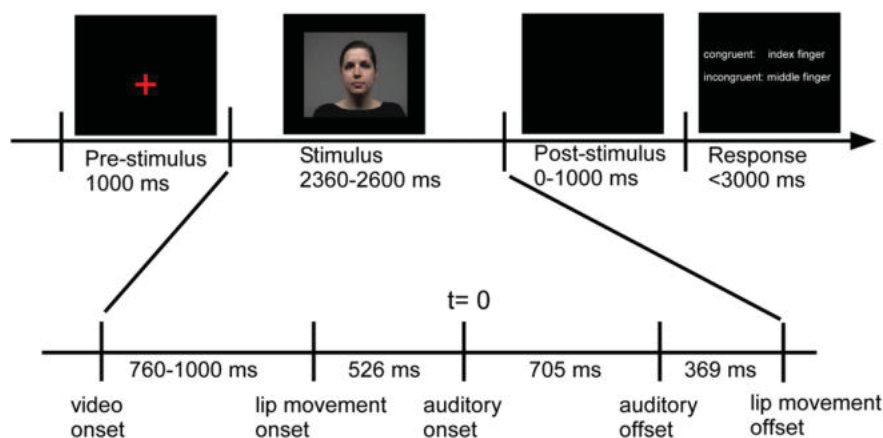


**Fig. 1.** Illustration of the experimental paradigm. Upper row: subjects fixated a cross centered at the position of the mouth position during following stimulus presentation. After a jittered time period, subjects were asked to report the (in)congruency of the stimulus. Lower row: detailed illustration of the stimulus period. Video sequences started with a baseline where the face was visible. After a random period, lip movements started, followed by onset of auditory signal. Auditory signal lasted for 705 ms followed by closing of lips 369 ms later. All time periods are for the condition /a/, slightly different values were presented for condition /o/ (see Methods for details). All trials were aligned to onset of auditory stimulation ( $t = 0$ ).

matching. Responses were given through button press: 5 subjects responded with the index and middle fingers of left hand, and 6 with the right hand. The allocation of finger and response was randomly changed each trial and the response configuration was presented at the beginning of the response period to minimize preparatory movement signals.

Subjects were instructed to respond within 3000 ms after presentation of response instructions and were informed that response speed was not taken into account. If no response was given after 3000 ms or subjects responded before the presentation of the instructions, a warning was visually presented. The respective trial was discarded from analysis and repeated at the end of the block. Except the warning signal, no feedback was given.

Each stimulus type (e.g. visual: /a/ and auditory: /o/) was repeated 48 times resulting in overall 384 trials (4 categories [AV<sub>C</sub>, AV<sub>I</sub>, A, V] × 2 stimulus types per category [e.g. visual: /a/ and auditory: /o/ and vice versa] × 48 repetitions) and all stimuli were presented in pseudorandom order. The experiment lasted ~30 min and subjects were allowed to have a break of ~2 min after half of the trials. Subjects performed a training session of ~5 min before the start of the MEG experiment.

#### Data acquisition

Neuromagnetic brain activity was continuously recorded using a 306-channel whole head MEG system (Neuromag Elekta Oy, Helsinki, Finland). For offline artifact rejection, we simultaneously recorded the vertical and horizontal electrooculogram (EOG). All data were recorded with a sampling frequency of 1000 Hz.

Subjects' head position within the MEG helmet was registered by 4 coils placed at subjects' forehead and behind both ears. Head position was recorded at the beginning of the recording session using four head position indicator (HPI) coils. A 3D digitizer (Fastrak Polhemus) was used to record the positions the HPI coils, three anatomical fiducial points (the nasion and left and right pre-auricular points) and ~12 additional points evenly distributed over the scalp. Individual full-brain high-resolution standard T1-weighted structural magnetic resonance images (MRIs) were obtained from a 3-T MRI scanner (Siemens, Erlangen, Germany) and offline aligned with the MEG coordinate system using the HPI coils, anatomical landmarks (nasion, left and right preauricular points) and additional points.

#### Data analysis

Data were offline analyzed using FieldTrip (Oostenveld et al., 2011), Matlab 7.13 (MathWorks, Natick, MA) and SPM8 (Litvak et al., 2011). For data analysis, only the 204 planar gradiometers (i.e. 102 pairs of orthogonal gradiometers) were taken into account. First, preprocessing was applied to all data (see below). Preprocessed data were then analyzed in independent processing steps (analysis of event related fields, spectral power, source analysis, coherence analysis) as described below.

#### Preprocessing

The power line artifact was removed from the MEG data using the following procedure: for each time epoch of interest (and each recording channel), we first took a 10 s epoch out of the continuous signal with the epoch of interest in the middle. Next, we calculated the discrete Fourier transform (DFT) of the 10 s epoch at 50, 100, and 150 Hz without any tapering. Because the power line is of a perfectly constant frequency, the 10 s epoch contains integer cycles of the artifact frequencies and nearly all the artifact energy is contained in those DFTs.

We then constructed 50, 100, and 150 Hz sine waves with the amplitudes and phases as estimated by the respective DFTs and subtracted those sine waves from the 10 s epoch. The epoch of interest was then

cut out of the cleaned 10 s epoch. Power spectra of the cleaned 10 s epochs demonstrated that all artifact energy was eliminated, leaving a notch of a bin width of 0.1 Hz (i.e. 1/10 s). The actual spectral analysis used the (multi)taper method, with a spectral smoothing  $\geq 2.5$  Hz (see below), so that the notch became invisible.

Next, continuous data were segmented into trials starting with the onset of video sequence and ending with the presentation of the response instructions. Muscle and ocular artifacts were removed using a semi-automatic routine implemented in FieldTrip. In a nutshell, a copy of the data was created and this copy of the data was filtered in a frequency band known to be sensitive for muscular (110–140 Hz) or ocular (1–14 Hz) artifact. Next, z-values for each channel were computed for each time point, resulting in a time course representing standardized deviations from the mean of all channels. Artifacts were identified and removed by applying a threshold and cutting out segments exceeding this threshold from the original, unfiltered data. Note that the filters were only applied to the copy of the data but do not affect the original data. Finally, the linear trend was removed from each trial.

#### Analysis of event-related fields (ERF) and definition of sensors of interest

First, we determined regions of interest in sensor space. Since we were interested in modulations of activity in regions involved in auditory processing, we pooled all conditions containing auditory signals (AV<sub>C</sub>, AV<sub>I</sub>, A) and computed event-related fields (ERF) in response to auditory stimulation. For each subject, ERF were computed by applying a bandpass filter between 0.4 and 30 Hz on the preprocessed data and averaging trials separately on each of the 204 gradiometers. Next, we averaged the signal over trials for each pair of orthogonal sensors separately. To avoid cancellation effects when averaging over subjects due to spatial smearing or differences in head size and/or position, the two orthogonal channels of each sensor pairs were combined by computing the root-mean-square, resulting in 102 sensors. Next, ERF were averaged over subjects and represented relative to a baseline (–300 to –100 ms). The grand average ERF over all sensors revealed two clear peaks at 130 and 200 ms. To define sensors of interest which cover these activation peaks, we averaged for each subject ERF over time. We chose a time window defined by the group peak latencies  $\pm 30$  ms (i.e. 100–230 ms) to cover the full width of the evoked components. We statistically compared the averaged ERF to the averaged ERF in the baseline (–300 to –100 ms) by means of the cluster-based randomization approach (Maris and Oostenveld, 2007; see below). In brief, in a first step this approach statistically tests for each sensor the consistency of the differences (peak vs. baseline) across subjects. In a second step, neighboring sensors exceeding a pre-defined threshold ( $p < .05$ ) were combined to a cluster and tested in a second-level cluster-statistics. This resulted in a significant cluster ( $p < .05$ ) of four sensors in the left and a significant cluster ( $p < .05$ ) of three sensors in the right hemisphere defining bilateral sensors of interest (Fig. 2).

To statistically compare ERF for conditions AV<sub>C</sub> and AV<sub>I</sub>, we first averaged ERF across sensors of interest (see above). The averaging was done separately for each condition and each hemisphere. Note that ERF were used directly, without subtracting a baseline. ERF for AV<sub>C</sub> and AV<sub>I</sub> were then statistically compared within each subject by computing the difference and normalizing the difference by the variance across trials (equivalent to an independent samples *t*-test). The comparison was done for each hemisphere separately. To statistically test the consistency of the difference across subjects, we applied a nonparametric permutation approach (Maris and Oostenveld, 2007). In brief, the difference values were pooled across subjects. Neighboring time-points exceeding a predefined threshold ( $p < .05$ ) were combined to a cluster and the summed cluster values were used as the test statistic. Next, a randomization approach, which randomly exchanged trials between conditions, was applied and the statistics were re-computed for the new distribution. This way, a randomization distribution was computed and the test statistics was

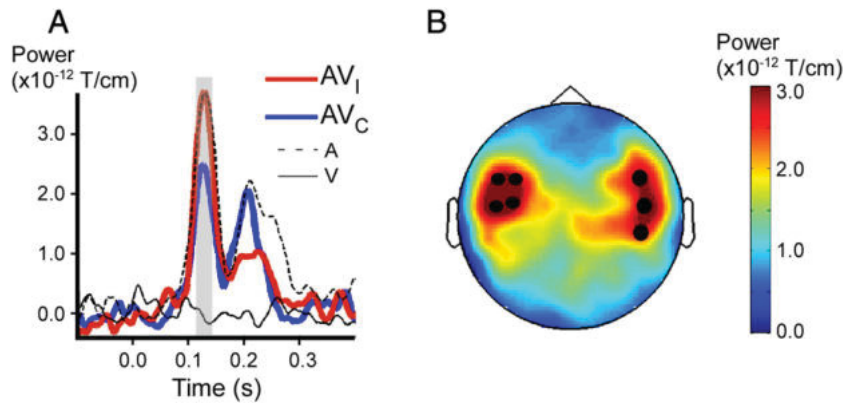


**Fig. 2.** Event related fields (ERF) for all conditions and definition of sensors of interest. A) Temporal profiles of ERF for conditions  $AV_C$  (thick blue line), and  $AV_I$  (thick red line), A (thin, dashed black line), and V (thin, solid black line) relative to an averaged baseline ( $-300$  to  $-100$  ms). ERFs are averaged across four sensors in the left hemisphere (see B). The shaded box indicates the area of statistically significant differences between the main conditions  $AV_C$  and  $AV_I$ . No significant differences were found for sensors in the right hemisphere. B) Topographical representation of the ERF of the first two peaks (i.e. ERF averaged between 100 and 230 ms relative to baseline of  $-300$  to  $-100$  ms; see A), averaged across all conditions containing auditory stimulation ( $AV_C$ ,  $AV_I$ , A). Two significant clusters showing significant increases of ERF were identified: Four sensors in the left and three sensors in the right hemisphere (black dots). Significant clusters were determined by cluster-based randomization approach (see Methods for details). The sensors of these significant clusters were chosen for subsequent analysis.

compared to the randomization distribution. This approach effectively corrects for multiple comparisons (Maris and Oostenveld, 2007) (see Lange et al., 2012 for details).

#### Spectral analysis

We computed time–frequency–representations (TFR) of the pre-processed MEG data. For each gradiometer and each trial separately, we applied fast Fourier Transformations (FFT) on short time windows. To compute the temporal evolution of spectral power, time windows were moved in steps of 25 ms across each trial.

We computed TFRs on two frequency ranges: 4–40 Hz and 40–150 Hz. For the low frequencies (4–40 Hz), we used a time window of 400 ms length. To minimize spectral leakage caused by using finite data segments, data segments were multiplied with a single Hanning window before applying the FFT, resulting in a smoothing of  $\sim \pm 2.5$  Hz (i.e.  $1/0.4$  s). For the high frequencies (40–150 Hz), we used a window of 200 ms length, multiplied with 3 Slepian tapers (Mitra and Pesaran, 1999), resulting in a spectral smoothing of  $\pm 10$  Hz. The choice of different time windows and smoothing for the low and high frequency ranges was motivated by two facts: low frequencies are relatively narrow and closely spaced. To separate physiological frequency bands, a small spectral resolution is needed. We chose a spectral smoothing of  $\pm 2.5$  Hz, which requires window lengths of 400 ms. For the high frequency ranges, physiological frequency bands are typically much broader, allowing more spectral smoothing. We chose a spectral smoothing for the high frequencies of  $\pm 10$  Hz. Secondly, the different time windows reflect the fact that the time window for a fixed number of cycles becomes smaller for higher frequencies. To capture also short lasting effects at high frequencies, we chose a shorter time window for the high frequencies. An even smaller window length would have been problematic because it might create problems in the group analysis when different subjects have short spectral perturbations at slightly different times.

The sensor system of the Neuromag MEG system contains 102 pairs of orthogonal gradiometers. Spectral power was first estimated for each trial and for each of the 204 gradiometers separately. For each trial, power of each gradiometer pair was then combined by summing power of the two orthogonal sensors of each pair, resulting in 102 sensors.

Statistical analysis between conditions  $AV_C$  and  $AV_I$  was done similar to the approach described for statistics on ERF. First, power was averaged for each condition across the sensors of interest (see above) and compared between conditions within each subject. We compared

power directly, without subtracting a baseline. Then the second-level cluster-statistics was applied. Clusters were now defined by neighboring pixels in the time and frequency (see Lange et al., 2012 for details).

The abovementioned statistical analysis was applied to statistically test differences between conditions  $AV_C$  and  $AV_I$ . The resulting significant clusters of this analysis reflect significant differences between conditions (Fig. 3). These clusters do not allow an interpretation as to whether differences are due to power increase or decreases of a condition. To interpret these clusters in terms of power changes of each condition, we performed an additional analysis (Fig. 4). To this end, we averaged spectral power across the four sensors of interest and additionally averaged power across time and frequency. Time and frequency were defined by the significant clusters (see Fig. 4 for respective time–frequency windows used for averaging power). Averaged power was then calculated as relative change to a baseline ( $-500$  to  $-100$  ms). To further characterize power changes, we repeated the abovementioned procedure of power averaging for the unimodal conditions. Please note that this analysis is not orthogonal to but biased by the abovementioned cluster analysis and the analysis serves mainly to further characterize the data. An ANOVA was applied to statistically test differences of relative change between conditions. Post-hoc pairwise tests were performed by means of a paired *t*-test. Additionally, the relative change of power was statistically tested against zero (i.e. no change relative to baseline) by means of a one-sample *t*-test.

#### Source analysis

To determine the cortical sources of the significant effects found in sensor space, we applied an adaptive spatial filtering technique in the frequency domain (DICS Gross et al., 2001). To estimate sources, spatial filters were constructed for a grid of discrete locations. To construct the grid for an individual subject, first a regular grid with a resolution of 1 cm was created in the Montreal Neurological Institute (MNI) template brain. Each subject's structural MRI was linearly warped into this template MRI and the inverse was applied to the template grid, resulting in individual grids. For each grid position, we constructed spatial filters based on leadfield and cross spectral density (CSD) matrices. Leadfield matrices were constructed for the individual grid locations using a realistic single-shell volume conduction model based on the individual MRIs (Nolte, 2003). CSD matrices were computed between all MEG gradiometer sensor pairs from the Fourier transforms of the tapered data epochs at the frequency of interest for each subject separately. The data epoch and the frequency of interest (theta [Fig. 3D]:  $6 \pm 3$  Hz; beta [Fig. 3C]:  $25 \pm 4$  Hz; gamma [Fig. 3B]:  $130 \pm 12$  Hz) were based on the

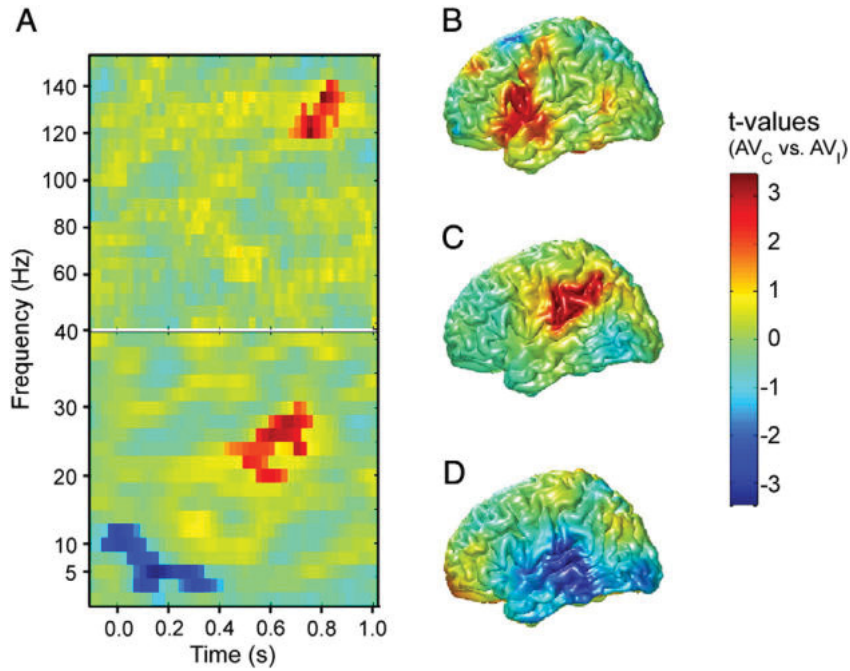


**Fig. 3.** Statistical comparison between  $AV_C$  and  $AV_I$  in the time–frequency domain and on source level. A) Time–frequency–representations of  $AV_C$  and  $AV_I$  were statistically compared by averaging spectral power across the four sensors in the left hemisphere (see Fig. 2) and comparing the averaged spectral power between  $AV_C$  and  $AV_I$  by means of a cluster-based randomization test. Red colors indicate higher spectral power for  $AV_C$ , blue colors higher power for  $AV_I$ . Non-significant values are masked to highlight significant time–frequency clusters. No statistically significant effects were found in sensors over right hemisphere. B) Source reconstruction for the significant cluster in the high-gamma band ( $130 \pm 12$  Hz) (see A). Non-significant voxels are masked to highlight significant areas. C) Source reconstruction for the cluster in the beta-band ( $25 \pm 4$  Hz). D) Source reconstruction for the cluster in the theta/alpha-band ( $6 \pm 3$  Hz). The color bar represents t-values and applies to all plots.

significant time–frequency clusters of the above mentioned group analysis on sensor level. Source parameters estimated in this way per subject were combined across subjects per grid position.

To statistically test the differences between conditions  $AV_C$  and  $AV_I$ , we first pooled trials of both conditions and computed a common spatial filter for each subject. For each subject, the CSD matrices of

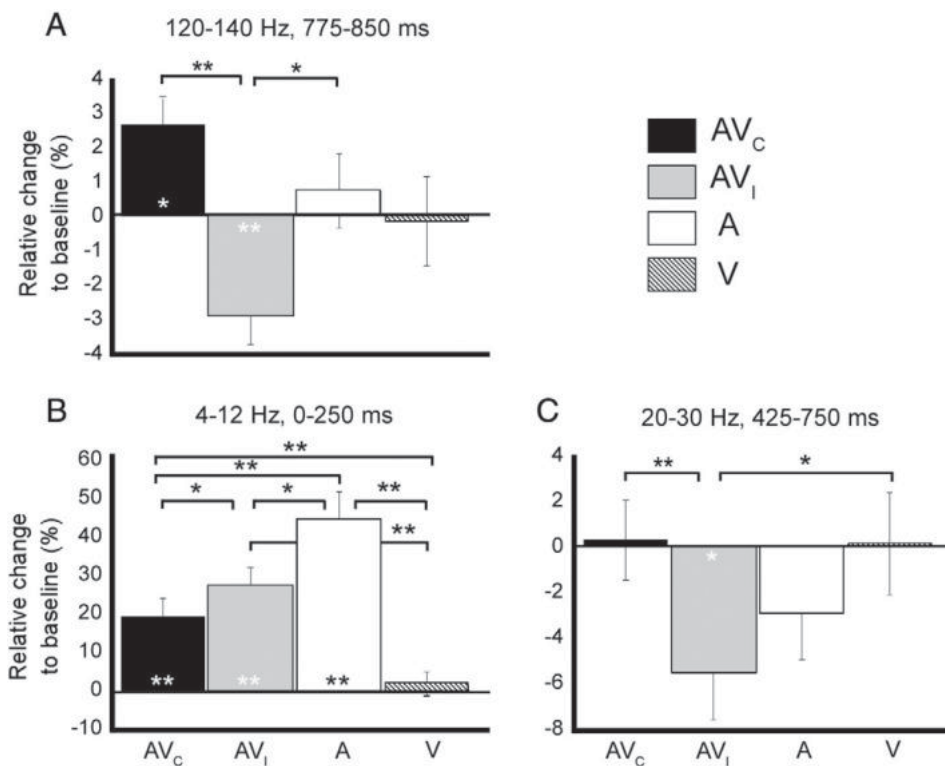


**Fig. 4.** Spectral power modulations for the four conditions ( $AV_C$ ,  $AV_I$ , A, V) relative to baseline. Spectral power is averaged across sensors of interest in the left hemisphere (see Fig. 2) and time–frequency bands (as shown by significant clusters in Fig. 3 and defined as indicated on top of each subfigure) and compared relative to baseline ( $-500$  to  $-100$  ms), separately for each condition. Power modulations are shown for the A) gamma-, B) theta, and C) beta-band. Significance was tested against zero (indicated by \* and \*\* inside each bar) and between conditions (indicated by \* and \*\* on top of bars). \*:  $p < 0.05$ ; \*\*:  $p < 0.01$ .

single trials were then projected through those individual filters, providing single trial estimates of source power for each grid point (Hoogenboom et al., 2010; Lange et al., 2011). Single trials were then sorted for conditions again and statistical testing on source level was performed in line with testing on sensor level (see above). Clusters were defined based on neighboring voxels in source space.

Results were displayed on the MNI template brain and significant cortical sources were identified using the AFNI atlas (<http://afni.nimh.nih.gov/afni>), integrated into FieldTrip.

#### Coherence analysis

Coherence was computed on source level using DICS (Gross et al., 2001). Coherence measures the consistency of the phase and amplitude between two signals for a given frequency band across trials and was computed according to the formula:

$$Coh_{x,y} = \frac{|\langle S_{x,y} \rangle|}{\sqrt{\langle S_{x,x} \rangle \times \langle S_{y,y} \rangle}}$$

with

$$S_{x,y} = F_x(f) \times F_y(f)^*$$

where  $F_x(f)$  denotes the Fourier Transform of a signal at location  $x$  for a specific frequency  $f$ ,  $*$  the complex conjugate and  $\langle \rangle$  the mean across trials (Schoffelen et al., 2011). Since coherence is non-uniformly distributed and biased by the number of trials, corrected  $z$ -Coherence-values were computed according to the formula:

$$zCoh = \operatorname{arctanh}(Coh) - \frac{1}{2N-2}$$

and normalized differences between conditions were computed following:

$$\Delta zCoh = \frac{zCoh_1 - zCoh_2}{\sqrt{\frac{1}{2N_1-2} + \frac{1}{2N_2-2}}}$$

with  $Coh_x$  and  $N_x$  denoting Coherence and number of trials for condition  $x$  (Schoffelen et al., 2011).

For each condition, Coherence was computed relative to a reference point in auditory cortex, which revealed the highest power differences for source localization of power differences. Statistical comparison for all voxels between conditions was performed on  $\Delta zCoh$ -values as described above.

We computed coherence relative to a voxel in left auditory cortex (MNI coordinates:  $[-50, -30, 0]$ ), which revealed the highest  $t$ -value during source localization of the early significant negative cluster found on source level. Similar to the computation of spectral power, coherence was computed by first cutting out data epochs in the time domain and then computing the Fourier Transformation. Fourier Transformation and thus coherence were computed on time window of 375 ms length. A coherence value at time point  $t$  in Fig. 5 reflects thus coherence computed on time windows from  $t - 187$  to  $t + 187$  ms. The data epochs were multiplied with three Slepian tapers before coherence computation, resulting in an effective frequency band of  $\sim 8 \pm 5$  Hz (i.e. very close to the frequency band 4–12 Hz for which we found significant effects in spectral power). For the temporal evolution of coherence (Fig. 5B), we computed coherence for sliding windows in steps of 50 ms.

## Results

Eleven subjects were presented with video sequences of a speaker articulating vowels /a/ and /o/. We presented four versions of the video sequence: videos could be presented in either in the original

version, i.e. with congruent audio–visual information ( $AV_C$ ), or in three modified versions. The three modified version consisted of incongruent audio–visual information ( $AV_I$ ), auditory information combined with uninformative static pictures (A), or visual information combined with uninformative auditory signals (V). Subjects were asked to rate whether auditory and visual information was congruent, i.e. portraying the same vowel, or incongruent. Crucially, pooled overall conditions, congruent and incongruent stimuli differed only in terms of congruency while net audio and visual information were identical. The main focus of our study was to investigate neuronal mechanisms and networks underlying neuronal processing of matching auditory and visual signals.

#### Behavioral data

Subjects recognized video sequences with high accuracy as congruent ( $AV_C$ :  $96.13 \pm 0.02\%$ ; Mean  $\pm$  SEM) and incongruent ( $AV_I$ :  $97.01 \pm 0.01\%$ ; A:  $98.90 \pm 0.01\%$ ; V:  $97.56 \pm 0.02\%$ ). For the subsequent analyses, only valid trials were taken into account.

#### Analysis of event related fields (ERF)

Incongruent audio–visual stimulation ( $AV_I$ ) elicited a significantly stronger N1 component than congruent stimulation ( $AV_C$ ) in sensors of interest in the left hemisphere between 117 and 146 ms after auditory onset ( $p < .01$ ; Fig. 2A). No significant differences were found in sensors of the right hemisphere.

#### Time–frequency analysis and source reconstruction

For sensors in the left hemisphere, we found three significant clusters in the time frequency representation revealing significant power differences between conditions: i) a negative cluster ( $p < .01$ ) between  $-50$  and  $400$  ms in the 4–12 Hz band revealing stronger spectral power for incongruent ( $AV_I$ ) than congruent ( $AV_C$ ) audio–visual stimulation, ii) a positive cluster ( $p < .05$ ) between 425 and 750 ms in the 20–30 Hz band, and iii) a positive cluster ( $p < .05$ ) between 675 and 875 ms in the high gamma band (120–140 Hz) indicating higher spectral power in condition  $AV_C$  compared to  $AV_I$  (Fig. 3A). Additional analyses revealed a sustained increase for gamma power in condition  $AV_C$  with two peaks around 100 and 700 ms (i.e. around on- and offset of auditory stimulation, Fig. S1A). For condition  $AV_I$ , we did not find an initial increase, but instead a decrease around offset of auditory stimulation (Figs. 1B and 4A). No statistically significant effects were found in sensors over right hemisphere.

To further study the modulatory effect of congruent and incongruent audio–visual signals, we additionally analyzed power changes relative to baseline ( $-500$  to  $-100$  ms before auditory onset) for all conditions, separately for the three significant time–frequency clusters. Note that these analyses are based on the results of the initial TFR contrast  $AV_C$  vs.  $AV_I$  (Fig. 3A) and thus not independent of these results. These analyses serve mainly to further characterize the results in terms of power increases and decreases and relate them to the unimodal conditions (A and V).

For the cluster in the theta-band (4–12 Hz, 0–250 ms; Fig. 4B), we found a significant main effect ( $F_{(3,43)} = 25.55$ ,  $p < 0.001$ ). Post hoc analysis revealed that congruent stimulus condition  $AV_C$  elicited significantly less power than incongruent  $AV_I$  ( $t_{(10)} = -2.49$ ;  $p = 0.032$ , paired  $t$ -test) and unimodal A ( $t_{(10)} = -5.77$ ;  $p < 0.001$ ), but more power than unimodal V ( $t_{(10)} = 4.17$ ;  $p = 0.002$ ). Condition  $AV_I$  elicited significantly less power than A ( $t_{(10)} = -3.08$ ;  $p = 0.012$ ) and more power than V ( $t_{(10)} = 6.59$ ;  $p < 0.001$ ). Finally, unimodal condition A elicited significantly more theta-power than unimodal condition V ( $t_{(10)} = 5.84$ ;  $p < 0.001$ ). Comparison of power against zero revealed a significant increase for  $AV_C$  ( $t_{(10)} = 3.88$ ;  $p = 0.003$ ;  $t$ -test against zero),  $AV_I$  ( $t_{(10)} = 5.88$ ;  $p < 0.001$ ), and A ( $t_{(10)} = 6.45$ ;  $p < 0.001$ ). No significant changes were found for condition V ( $p > .59$ ).

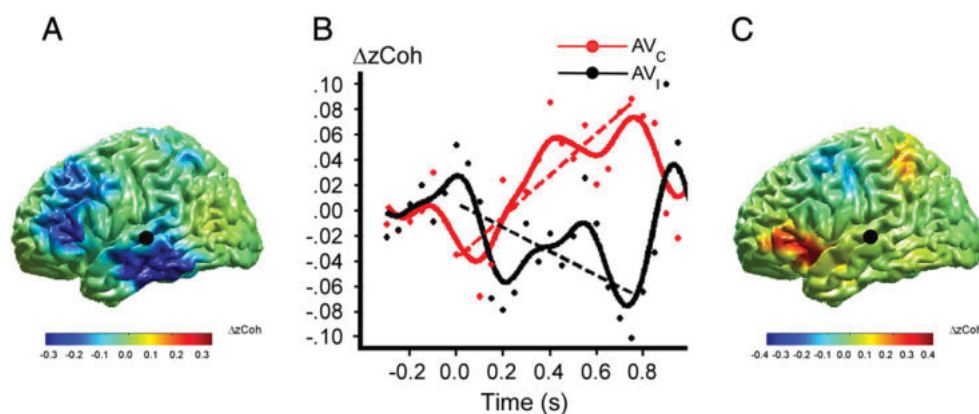


**Fig. 5.** Results of the coherence analysis for conditions  $AV_C$  and  $AV_I$ . A) Differences between coherence for  $AV_C$  and  $AV_I$ . Coherence was computed for all voxels of each condition relative to a reference voxel in auditory cortex (indicated by the black dot) at the onset of auditory stimulation and then statistically tested for coherence differences between  $AV_C$  and  $AV_I$ . The colorbar indicates differences in coherence. Red denotes higher coherence to auditory cortex for  $AV_C$ , and blue higher coherence for  $AV_I$ . Non-significant voxels are masked to highlight significant effects. B) Analysis of the temporal evolution of coherence. Coherence was averaged across significant voxels of Broca's area (see A) and computed relative to a baseline ( $-500$  to  $-100$  ms). Solid lines represent smoothed time courses (Gaussian kernel with FWHM of 100 ms) of coherence for  $AV_C$  (red) and  $AV_I$  (black). Dashed lines represent linear fits for  $AV_C$  and  $AV_I$  for all time points between on- and offset of auditory stimulation. C) Same as A), but now at offset of auditory stimulation.

For the beta-cluster (20–30 Hz, 425–750 ms; Fig. 4C), we found a significant main effect ( $F_{(3,43)} = 3.1$ ,  $p < 0.05$ ). Post hoc analysis revealed that power in condition  $AV_I$  was significantly lower than in  $AV_C$  ( $t_{(10)} = -3.13$ ;  $p < 0.01$ ) and than in V ( $t_{(10)} = -2.36$ ;  $p = 0.04$ ). None of the other comparisons revealed a significant effect ( $p > .13$ ). Only condition  $AV_I$  was significantly different from 0 ( $t_{(10)} = -2.74$ ;  $p = 0.021$ ), revealing a decrease in beta-power.

For the gamma-cluster (120–140 Hz, 775–850 ms; Fig. 4A), we found a significant main effect ( $F_{(3,43)} = 4.31$ ,  $p < 0.01$ ). Post hoc analysis revealed that power changes were significantly higher for  $AV_C$  vs  $AV_I$  ( $t_{(10)} = 4.38$ ,  $p = 0.001$ ) and lower for  $AV_I$  than for unimodal A ( $t_{(10)} = -2.91$ ,  $p = 0.016$ ). None of the other comparisons revealed a significant effect ( $p > 0.11$ ). Additionally, power increase for  $AV_C$  was significantly higher than 0 ( $t_{(10)} = 2.28$ ;  $p = 0.045$ ), while power for  $AV_I$  revealed a significant decrease ( $t_{(10)} = -3.38$ ,  $p = 0.007$ ). Unimodal conditions elicited no significant power changes ( $p > 0.51$ ).

We used a beamforming approach (DICS Gross et al., 2001) to identify the cortical sources of the three clusters identified on sensor level. Source reconstruction revealed that the three clusters originated from different sources in the left hemisphere: i) the negative cluster in the low frequencies (4–12 Hz) was localized mainly to auditory cortex and the middle and superior temporal gyri (Brodmann areas 21, 22, 41, 42) (Fig. 3D; frequency for source localization:  $6 \pm 3$  Hz), ii) the positive cluster in the beta-band (20–30 Hz) originated from the supramarginal gyrus (Brodmann area 40) (Fig. 3C; frequency for source localization:  $25 \pm 4$  Hz), iii) the positive cluster in the gamma-band (120–140 Hz) originated from the inferior frontal gyrus (Broca's area, Brodmann area 44) (Fig. 3B; frequency for source localization:  $130 \pm 12$  Hz).

#### Coherence analysis

Coherence is a measure of phase and amplitude consistency between neuronal groups across trials. Coherence is commonly interpreted as a measure of interaction or communication between neuronal groups. We were interested which cortical areas interact via coherence when processing congruent audio-visual information. To this end, we chose a voxel in left auditory cortex (MNI coordinates:  $[-50; -30; 0]$ ) as the reference voxel and computed coherence in the  $8 \pm 5$  Hz frequency band relative to all other voxels using DICS for conditions  $AV_C$  and  $AV_I$ . The reference voxel was chosen since it showed the maximum t-value during source localization of the early significant negative cluster (Fig. 3D).

We found coherence to be significantly enhanced for condition  $AV_I$  relative to  $AV_C$  directly after auditory onset in the middle and inferior temporal gyri (Fig. 5A). In addition, we found a second, spatially

distinct significant cluster located in inferior frontal gyrus (Broca's area, Brodmann area 44) and dorsal premotor cortex (Brodmann area 6) (Fig. 5A). To investigate the temporal evolution of coherence between auditory cortex and Broca's area, we computed coherence in sliding time windows and averaged coherence-values across the voxels in Broca's area showing significant interaction in the above mentioned analysis. Coherence increased between on- and offset of congruent audio-visual stimuli, indicated by a significant linear regression ( $AV_C$ :  $r = .82$ ,  $p < .001$ ; slope: 0.12; Fig. 5B) before it returned to baseline. Conversely, we found for incongruent audio-visual stimulation a decrease of coherence over time, indicated by a significant linear regression ( $AV_I$ :  $r = .49$ ,  $p < .05$ ; slope:  $-.06$ ; Fig. 5B) before it returned to baseline after offset of auditory stimulation. Consequently, the difference between  $AV_C$  and  $AV_I$  increased between on- and offset (linear regression:  $r = .78$ ,  $p < .001$ ; slope: 0.19; data not shown). Control analyses for unimodal conditions A and V showed a weak linear increase, which, however, did not reach statistical significance (A:  $r = .38$ ,  $p > .05$ ; slope: 0.03; V:  $r = .42$ ,  $p > .05$ ; slope: .05; data not shown). Source reconstruction of the difference between  $AV_C$  and  $AV_I$  at auditory offset revealed that coherence was confined to inferior frontal gyrus (Broca's area, Brodmann area 44) (Fig. 5C).

Interestingly, the main difference of coherence between  $AV_C$  and  $AV_I$  was found in the same area (i.e. Broca's area, Brodmann Area 44) as the significant cluster for gamma power (Fig. 3B, see time-frequency and source analysis above). To study a potential relation between theta/alpha-coherence and gamma-power, we correlated the difference of coherence between  $AV_C$  and  $AV_I$  and the difference in gamma-power between  $AV_C$  and  $AV_I$  during auditory stimulus presentation. We found gamma-power and theta/alpha-coherence to be positively correlated ( $r = .77$ ,  $p < .001$ ), with early time points around auditory onset revealing the lowest values and late time points shortly before auditory offset revealing the highest values (Fig. 6).

#### Discussion

We studied the role of oscillatory neuronal synchronization in an audio-visual match/mismatch task using magnetoencephalography (MEG). To this end, we present audio-visual stimuli that differed in their congruency of auditory and visual information. We found differences in spectral power and coherence in a distinct spatio-temporal cortical network. Interestingly, we found that the coherence in the theta-band was correlated to high gamma-power over time.

Normal, congruent audio-visual stimuli ( $AV_C$ ) revealed a suppression of the event related field (ERF) relative to incongruent stimuli

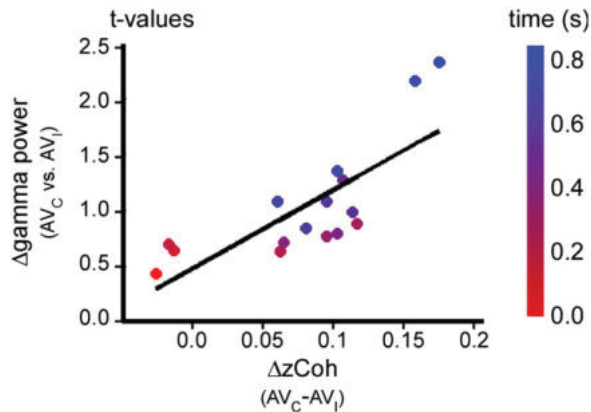


**Fig. 6.** Correlation of coherence and power differences between  $AV_C$  and  $AV_I$ . Differences in coherence between  $AV_C$  and  $AV_I$  (see Fig. 5B) were correlated with differences in high-gamma-power between  $AV_C$  and  $AV_I$  (see Fig. 3A). Solid line represents the best linear fit. Time points relative to auditory onset are color coded with red colors indicating early time points and blue colors late time points.

( $AV_I$ ) for the first auditory peak (M100). Suppression of the M100 has been interpreted as an index of audio–visual interaction (Besle et al., 2004). The early decrease of evoked activity suggests that auditory cortex is modulated by preceding visual information and auditory stimulation interacts with prior modulation (Arnal et al., 2011; Besle et al., 2004; Sohoglu et al., 2012; van Wassenhove et al., 2005). Previous studies reported a reduction of the M100 for audio–visual stimuli compared to unimodal auditory stimuli, independent of audio–visual congruency (Arnal et al., 2009; van Wassenhove et al., 2005). The lack of M100 suppression for  $AV_I$  might suggest that visual information is simply ignored and rendering  $AV_I$  effectively similar to unimodal condition A. However, peak amplitudes of second peak are modulated qualitatively differently by congruency than the M100, revealing a clear distinction between conditions  $AV_I$  and A following the relation  $AV_I < AV_C < A$ . This relation is in line with previous studies showing the strongest suppression of the second peak by incongruent audio–visual signals (Stekelenburg and Vroomen, 2007).

In addition,  $AV_C$  showed a significant suppression of low frequency (4–12 Hz) spectral power relative to  $AV_I$  around auditory onset in early auditory cortex. Moreover, theta-band power after onset of auditory stimulation (~200 ms) shows the relation  $AV_C < AV_I < A$ , again strongly suggesting that incongruent visual information is not simply ignored, but selectively modulates theta-band power. Given the spatio-temporal profiles, it is likely that this effect in low frequency oscillations corresponds to the differences found for components in the ERF. Low frequency oscillations have been suggested to play a role as an integration window as well as for cortical gating of information or sensory selection (Fries, 2005; Mizuseki et al., 2009; Schroeder and Lakatos, 2009; Schroeder et al., 2008). We found neuronal oscillations in the theta/alpha-band to be coherent between auditory cortex and Broca's area. Coherence was stronger for  $AV_I$  than  $AV_C$  directly after auditory onset, but decreased thereafter for  $AV_I$ , while coherence increased for  $AV_C$  until auditory offset. We propose that the coherence in the theta/alpha-band provides a mechanism for efficient gating of information from early to higher stages of speech processing. During congruent audio–visual stimulation ( $AV_C$ ), auditory cortex and Broca's area are coupled and coupling increases over time as evidenced by an increase of coherence. In contrast, during incongruent audio–visual stimulation ( $AV_I$ ), the two areas are continuously decoupled. Potential reasons for the initial high coherence for condition  $AV_I$  might be attentional effects due to unexpected bimodal stimulation or an initial forwarding of the task-relevant bimodal information for a cognitive evaluation. Future studies, however, are needed to shed more light on this initial effect. One might wonder why we did not find increasing

coherence for unimodal conditions A and V. Both conditions also provide information that might be processed to higher stages for cognitive evaluation. One potential reason might be that the lack of bimodal information renders cognitive evaluation of this stimulus in higher cortical areas unnecessary. Missing lip movements and missing auditory information might already provide sufficient information to evaluate the stimuli as incongruent. Future studies forcing subjects to cognitively evaluate such unimodal stimuli might find similar coherence effects as we found for congruent audio–visual stimuli.

In addition, we found a sustained increase of high-gamma band power in Broca's area with two peaks around on- and offset of auditory stimulation for  $AV_C$ . In contrast, there was no gamma power increase for incongruent stimuli at auditory onset, but even a decrease around offset. The difference between congruent and incongruent stimuli in gamma power became significant around auditory offset. Most interestingly, this difference in gamma power was positively correlated to the difference in coherence over time. We suggest that information flow from auditory cortex to Broca's area is provided by coherence in the low frequencies. Broca's area evaluates audio–visual congruency (Noppeney et al., 2010), reflected in an increase or decrease of gamma power. Gamma power for congruent stimuli peaked particularly around on- and offset of auditory stimulation. We propose that these peaks are caused by the fact that our stimuli show the strongest modulations at on- and offset of auditory stimulation. Modulation of the input might provoke a re-evaluation of the audio–visual signal leading to modulations of gamma band activity. In line with absent coherence for unimodal conditions A and V, we did not find any modulations of gamma-band activity for these unimodal conditions in Broca's area, further suggesting that the observed gamma-band increase reflects evaluation of matching audio–visual information.

Coherence in the theta-band has also been reported in a word processing study using intracranial EEG (Canolty et al., 2007). The authors reported increased phase-locking of sensors specifically in the theta-band over several centimeters, however, without reporting whether phase-locking was specific for electrode pairs. Theta-band phase in auditory cortex was also found in an MEG study to code intelligible speech (Luo and Poeppel, 2007). Coherence in the low frequencies has been found to be modulated in deep layers of the cortex, while gamma-coherence has been found in superficial layers (Buffalo et al., 2011). Deep layers are thought to play a role in cortico-cortical feedback connections and receive input from subcortical areas, while superficial areas are thought to mediate feedforward processes (Buffalo et al., 2011; Lakatos et al., 2007). Coherence in the theta/alpha-band might therefore reflect feedback processing between early and higher stages of cortical processing and thus shaping and establishing the functional interaction of these areas in the case of congruent stimuli and, conversely, continuously disjointing the cortical interaction for incongruent stimuli. In contrast, the increase in gamma band power in higher areas might reflect integration of accumulated information and effective feedforward processing of information (Fries, 2005; Jensen and Mazaheri, 2010).

Coherence is potentially confounded by power. Since the early decrease of coherence in auditory cortex is paralleled in time, frequency, and space by a power decrease, we cannot fully exclude that the negative coherence in middle and inferior temporal gyri is confounded by power modulations. It should be noted, however, that power modulations were also found in auditory cortex, while the coherence difference was not. This lack of local coherence argues against the possibility that coherence differences can be fully explained by power differences. For three reasons it is unlikely that the coherence differences measured in Broca's area are confounded by power. First, no power differences in the theta band were observed in Broca's area and the gap between the two significant clusters in middle and inferior temporal gyri and in Broca's area (Fig. 5A) makes it unlikely that the cluster in Broca's area is confounded by spatially smeared power differences

around auditory cortex. Secondly, we observe a temporal evolution of coherence that is not paralleled by power differences neither in auditory cortex nor Broca's area. Finally, the difference in coherence reverses in sign between on- and offset of auditory stimulation. Again, this effect is not accompanied by power changes and cannot be explained by spatial or temporal smearing of coherence or power effects.

In addition, we found decreased beta-band power for incongruent audio–visual signal around offset of auditory stimulation in supramarginal gyrus, while it was not significantly modulated by congruent audio–visual or unimodal stimuli. Together with inferior frontal gyrus and (pre)motor areas, supramarginal gyrus has been suggested to be part of a dorsal stream of audio–visual speech perception, dominant to the left hemisphere (Hickok and Poeppel, 2007). Supramarginal gyrus was not linked to auditory cortex by coherence in the low frequencies. It remains speculative whether coupling of supramarginal area to the other areas might be mediated in other frequency bands, e.g. coherence in the beta-band (Arnal et al., 2011) or whether this area is coupled to other areas via feedback connections. While auditory cortex and Broca's area were significantly activated by congruent stimuli ( $AV_C$ ), supramarginal gyrus showed responses (i.e. decrease of beta-power) only for incongruent stimuli ( $AV_I$ ). This finding suggests a different role for supramarginal gyrus in our match/mismatch task. One possible role might be error monitoring of incongruent, non-matching stimuli. This interpretation is in line with previous studies showing activity in supramarginal gyrus for deviant or mismatching stimuli (Celsis et al., 1999; Guenther, 2006; Xu et al., 2001). Future studies have to shed light on the role of supramarginal gyrus and its connections to the network of congruent speech integration.

In summary, our results might also be interpreted in the context of predictive coding. In predictive coding it is assumed that higher cognitive areas modulate activity in lower sensory areas by conveying top-down predictions about upcoming sensory events (e.g. Bastos et al., 2012). Due to the top-down signal, activity in response to predicted stimuli is suppressed in early cortical areas. Violating expectations causes enhanced responses in lower levels due to an inability to predict and suppress cortical activity.

Since visual information predicts a congruent auditory signal, the enhanced early evoked/theta-band activity in early sensory areas to incongruent stimuli might be interpreted as a violation of predictions leading to an enhanced response, a prediction error. In predictive coding, prediction errors are forwarded to higher areas to update higher-level representations. This might be reflected by the observed initial increase of theta-band coherence between auditory cortex and Broca's area. After the initial increase, predictions might be updated to suppress the incongruent auditory information. We also found high gamma-band activity in Broca's area around stimulus on- and offset. Gamma-band activity is assumed to reflect feedforward processing to higher areas. The differences in gamma-band power around auditory offset might thus reflect different feedforward signals for congruent and incongruent stimuli. The temporal coincidence with differences in beta-band activity in supramarginal gyrus suggests a correlation of both signals. But since connectivity and correlation analyses for gamma-band power were beyond the scope of the present study, we can only speculate about the direction of the feedforward process.

While we found significant differences between conditions  $AV_C$  and  $AV_I$  in auditory ROI, no significant effects were found in visual ROI (data not shown). In contrast, other studies have reported modulations of visual responses by congruent audio–visual information in visual or multisensory areas, e.g. in STS (Arnal et al., 2011; Dahl et al., 2010; Ghazanfar et al., 2008). One potential reason for the lack of significant differences in visual areas in our study might be that overall visual signals as well as their modulations by auditory signals might be too small to be detected by our design, e.g. due to the pre-selection of ROI. Additionally, choice of task and method (single cell recordings or MEG) might strongly influence the sensitivity to

detect congruency effects in STS or other areas. More detailed focus on STS or other areas, which are typically considered as visual areas, e.g. by a different definition of ROI, might reveal additional effects. However, this was beyond the scope of the present study and might be investigated in future studies.

In summary, we have demonstrated that processing of congruent and incongruent audio–visual speech differs in a widespread network that is characterized by neuronal oscillatory activity in several frequency bands. Parts of this network are functionally coupled by coherence in the low frequencies. Moreover, low frequency coherence and high-gamma power are coupled in higher areas of the speech perception network. We propose that low frequency coherence constitutes functional coupling between primary sensory and higher order cortical areas. Recent studies suggest that such coupling might be mediated by feedback connections (Buffalo et al., 2011). Finally, we provide evidence that coupling of low-frequency coherence and high frequency power reflects a functional mechanism for dynamic integration of neuronal networks.

Supplementary data to this article can be found online at <http://dx.doi.org/10.1016/j.neuroimage.2013.04.064>.

## Acknowledgments

We are most grateful to Anja Zimmermann and Christian Dobel for recording and providing the stimulus material.

## Conflict of Interest

The authors declare no conflict of interest.

## References

- Arnal, L.H., Morillon, B., Kell, C.A., Giraud, A.L., 2009. Dual neural routing of visual facilitation in speech processing. *J. Neurosci.* 29, 13445–13453.
- Arnal, L.H., Wyart, V., Giraud, A.L., 2011. Transitions in neural oscillations reflect prediction errors generated in audiovisual speech. *Nat. Neurosci.* 14, 797–801.
- Bastos, A.M., Usrey, W.M., Adams, R.A., Mangun, G.R., Fries, P., Friston, K.J., 2012. Canonical microcircuits for predictive coding. *Neuron* 76 (4), 695–711.
- Besle, J., Fort, A., Delpuech, C., Giard, M.H., 2004. Bimodal speech: early suppressive visual effects in human auditory cortex. *Eur. J. Neurosci.* 20, 2225–2234.
- Buffalo, E.A., Fries, P., Landman, R., Buschman, T.J., Desimone, R., 2011. Laminar differences in gamma and alpha coherence in the ventral stream. *Proc. Natl. Acad. Sci. U. S. A.* 108, 11262–11267.
- Canolty, R.T., Soltani, M., Dalal, S.S., Edwards, E., Dronkers, N.F., Nagarajan, S.S., Kirsch, H.E., Barbaro, N.M., Knight, R.T., 2007. Spatiotemporal dynamics of word processing in the human brain. *Front. Neurosci.* 1, 185–196.
- Celsis, P., Boulanouar, K., Doyon, B., Ranjeva, J.P., Berry, I., Nespoulous, J.L., Chollet, F., 1999. Differential fMRI responses in the left posterior superior temporal gyrus and left supramarginal gyrus to habituation and change detection in syllables and tones. *NeuroImage* 9, 135–144.
- Chandrasekaran, C., Ghazanfar, A.A., 2009. Different neural frequency bands integrate faces and voices differently in the superior temporal sulcus. *J. Neurophysiol.* 101, 773–788.
- Dahl, C.D., Logothetis, N.K., Kayser, C., 2010. Modulation of visual responses in the superior temporal sulcus by audio–visual congruency. *Front. Integr. Neurosci.* 4, 10.
- Fries, P., 2005. A mechanism for cognitive dynamics: neuronal communication through neuronal coherence. *Trends Cogn. Sci.* 9, 474–480.
- Fries, P., 2009. Neuronal gamma-band synchronization as a fundamental process in cortical computation. *Annu. Rev. Neurosci.* 32, 209–224.
- Ghazanfar, A.A., Chandrasekaran, C., Logothetis, N.K., 2008. Interactions between the superior temporal sulcus and auditory cortex mediate dynamic face/voice integration in rhesus monkeys. *J. Neurosci.* 28, 4457–4469.
- Giraud, A.L., Poeppel, D., 2012. Cortical oscillations and speech processing: emerging computational principles and operations. *Nat. Neurosci.* 15, 511–517.
- Gregoriou, G.G., Gotts, S.J., Zhou, H., Desimone, R., 2009. High-frequency, long-range coupling between prefrontal and visual cortex during attention. *Science* 324, 1207–1210.
- Gross, J., Kujala, J., Hamalainen, M., Timmermann, L., Schnitzler, A., Salmelin, R., 2001. Dynamic imaging of coherent sources: Studying neural interactions in the human brain. *Proc. Natl. Acad. Sci. U. S. A.* 98, 694–699.
- Gross, J., Schmitz, F., Schnitzler, I., Kessler, K., Shapiro, K., Hommel, B., Schnitzler, A., 2004. Modulation of long-range neural synchrony reflects temporal limitations of visual attention in humans. *Proc. Natl. Acad. Sci. U. S. A.* 101, 13050–13055.
- Guenther, F.H., 2006. Cortical interactions underlying the production of speech sounds. *J. Commun. Disord.* 39, 350–365.
- Hickok, G., Poeppel, D., 2007. The cortical organization of speech processing. *Nat. Rev. Neurosci.* 8, 393–402.

- Hirschmann, J., Ozkurt, T.E., Butz, M., Homburger, M., Elben, S., Hartmann, C.J., Vesper, J., Wojtecki, L., Schnitzler, A., 2011. Distinct oscillatory STN-cortical loops revealed by simultaneous MEG and local field potential recordings in patients with Parkinson's disease. *NeuroImage* 55, 1159–1168.
- Hoogenboom, N., Schoffelen, J.M., Oostenveld, R., Fries, P., 2010. Visually induced gamma-band activity predicts speed of change detection in humans. *NeuroImage* 51, 1162–1167.
- Jensen, O., Mazaheri, A., 2010. Shaping functional architecture by oscillatory alpha activity: gating by inhibition. *Front. Hum. Neurosci.* 4, 186.
- Kaiser, J., Hertrich, I., Ackermann, H., Mathiak, K., Lutzenberger, W., 2005. Hearing lips: gamma-band activity during audiovisual speech perception. *Cereb. Cortex* 15, 646–653.
- Keil, J., Muller, N., Ihssen, N., Weisz, N., 2012. On the variability of the McGurk effect: audiovisual integration depends on prestimulus brain states. *Cereb. Cortex* 22 (1), 221–231.
- Lakatos, P., Chen, C.M., O'Connell, M.N., Mills, A., Schroeder, C.E., 2007. Neuronal oscillations and multisensory interaction in primary auditory cortex. *Neuron* 53, 279–292.
- Lange, J., Oostenveld, R., Fries, P., 2011. Perception of the touch-induced visual double-flash illusion correlates with changes of rhythmic neuronal activity in human visual and somatosensory areas. *NeuroImage* 54, 1395–1405.
- Lange, J., Halacz, J., van, D.H., Kahlbrock, N., Schnitzler, A., 2012. Fluctuations of prestimulus oscillatory power predict subjective perception of tactile simultaneity. *Cereb. Cortex* 22, 2564–2574.
- Litvak, V., Mattout, J., Kiebel, S., Phillips, C., Henson, R., Kilner, J., Barnes, G., Oostenveld, R., Daunizeau, J., Flandin, G., Penny, W., Friston, K., 2011. EEG and MEG data analysis in SPM8. *Comput. Intell. Neurosci.* 2011, 852961.
- Luo, H., Poeppel, D., 2007. Phase patterns of neuronal responses reliably discriminate speech in human auditory cortex. *Neuron* 54, 1001–1010.
- Maris, E., Oostenveld, R., 2007. Nonparametric statistical testing of EEG- and MEG-data. *J. Neurosci. Methods* 164, 177–190.
- Mitra, P.P., Pesaran, B., 1999. Analysis of dynamic brain imaging data. *Biophys. J.* 76, 691–708.
- Mizuseki, K., Sirota, A., Pastalkova, E., Buzsaki, G., 2009. Theta oscillations provide temporal windows for local circuit computation in the entorhinal-hippocampal loop. *Neuron* 64, 267–280.
- Nishitani, N., Hari, R., 2002. Viewing lip forms: cortical dynamics. *Neuron* 36, 1211–1220.
- Nolte, G., 2003. The magnetic lead field theorem in the quasi-static approximation and its use for magnetoencephalography forward calculation in realistic volume conductors. *Phys. Med. Biol.* 21, 3637–3652.
- Noppeney, U., Ostwald, D., Werner, S., 2010. Perceptual decisions formed by accumulation of audiovisual evidence in prefrontal cortex. *J. Neurosci.* 30 (21), 7434–7446.
- Oostenveld, R., Fries, P., Maris, E., Schoffelen, J.M., 2011. FieldTrip: open source software for advanced analysis of MEG, EEG, and invasive electrophysiological data. *Comput. Intell. Neurosci.* 2011, 156869.
- Palva, S., Palva, J.M., Shtyrov, Y., Kujala, T., Ilmoniemi, R.J., Kaila, K., Naatanen, R., 2002. Distinct gamma-band evoked responses to speech and non-speech sounds in humans. *J. Neurosci.* 22, RC211.
- Pulvermuller, F., 2005. Brain mechanisms linking language and action. *Nat. Rev. Neurosci.* 6, 576–582.
- Schoffelen, J.M., Poort, J., Oostenveld, R., Fries, P., 2011. Selective movement preparation is subserved by selective increases in corticomuscular gamma-band coherence. *J. Neurosci.* 31, 6750–6758.
- Schroeder, C.E., Lakatos, P., 2009. Low-frequency neuronal oscillations as instruments of sensory selection. *Trends Neurosci.* 32, 9–18.
- Schroeder, C.E., Lakatos, P., Kajikawa, Y., Partan, S., Puce, A., 2008. Neuronal oscillations and visual amplification of speech. *Trends Cogn. Sci.* 12, 106–113.
- Sohoglu, E., Peelle, J.E., Carlyon, R.P., Davis, M.H., 2012. Predictive top-down integration of prior knowledge during speech perception. *J. Neurosci.* 32, 8443–8453.
- Stekelenburg, J.J., Vroomen, J., 2007. Neural correlates of multisensory integration of ecologically valid audiovisual events. *J. Cogn. Neurosci.* 19, 1964–1973.
- van Wassenhove, V., Grant, K.W., Poeppel, D., 2005. Visual speech speeds up the neural processing of auditory speech. *Proc. Natl. Acad. Sci. U. S. A.* 102, 1181–1186.
- Womelsdorf, T., Schoffelen, J.M., Oostenveld, R., Singer, W., Desimone, R., Engel, A.K., Fries, P., 2007. Modulation of neuronal interactions through neuronal synchronization. *Science* 316, 1609–1612.
- Xu, B., Grafman, J., Gaillard, W.D., Ishii, K., Vega-Bermudez, F., Pietrini, P., Reeves-Tyer, P., DiCamillo, P., Theodore, W., 2001. Conjoint and extended neural networks for the computation of speech codes: the neural basis of selective impairment in reading words and pseudowords. *Cereb. Cortex* 11, 267–277.

14) **Lange, J.**, Oostenveld, R., & Fries, P. (2013b).

Reduced occipital alpha power indexes enhanced excitability rather than improved visual perception.

*The Journal of Neuroscience: The Official Journal of the Society for Neuroscience*, 33(7), 3212–3220.

Impact factor (2013): 6.747

# Reduced Occipital Alpha Power Indexes Enhanced Excitability Rather than Improved Visual Perception

Joachim Lange,<sup>1,2</sup> Robert Oostenveld,<sup>1</sup> and Pascal Fries<sup>1,3</sup>

<sup>1</sup>Donders Institute for Brain, Cognition and Behaviour, Radboud University Nijmegen, 6525 HR Nijmegen, The Netherlands, <sup>2</sup>Medical Faculty, Institute of Clinical Neuroscience and Medical Psychology, Heinrich-Heine-University Düsseldorf, 40225 Düsseldorf, Germany, and <sup>3</sup>Ernst Strüngmann Institute (ESI) for Neuroscience in Cooperation with Max Planck Society, 60528 Frankfurt, Germany

Several studies have demonstrated that prestimulus occipital alpha-band activity substantially influences subjective perception and discrimination of near-threshold or masked visual stimuli. Here, we studied the role of prestimulus power fluctuations in two visual phenomena called double-flash illusion (DFI) and fusion effect (FE), both consisting of suprathreshold stimuli. In both phenomena, human subjects' perception varies on a trial-by-trial basis between perceiving one or two visual stimuli, despite constant stimulation. In the FE, two stimuli correspond to veridical perception. In the DFI, two stimuli correspond to an illusory perception. This provides for a critical test of whether reduced alpha power indeed promotes veridical perception in general. We find that in both, DFI and FE, reduced prestimulus occipital alpha predicts the perception of two stimuli, regardless of whether this is veridical (FE) or illusory (DFI). Our results suggest that reduced alpha-band power does not always predict improved visual processing, but rather enhanced excitability. In addition, for the DFI, enhanced prestimulus occipital gamma-band power predicted the perception of two visual stimuli. These findings provide new insights into the role of prestimulus rhythmic activity for visual processing.

## Introduction

Despite physically constant sensory stimulation, subjective perception can vary substantially across subjects. Subjective perception can also vary within individual subjects on a trial-by-trial basis or over time, for example in ambiguous, bistable visual stimuli. It has been shown that peristimulus fluctuations of rhythmic neuronal activity are related to changes of subjective perception (Rodriguez et al., 1999; Parkkonen et al., 2008). In recent years, there has been cumulative evidence that also modulations of ongoing rhythmic neuronal activity before sensory stimulation can influence perception of the subsequent stimulus (van Dijk et al., 2008; Hipp et al., 2011; Keil et al., 2012). Especially ongoing rhythmic activity in the alpha-band (~10 Hz) has drawn much attention recently. Some studies have found the power of prestimulus alpha-band activity in parieto-occipital areas to correlate negatively with the subjective perception in visual detection and discrimination tasks (Worden et al., 2000; Hanslmayr et al., 2007; van Dijk et al., 2008; Wyart and Tallon-Baudry, 2009; Romei et al., 2010). Other studies have found pre-

stimulus alpha-power in the visual and somatosensory domain to correlate to perception and poststimulus evoked responses as an inverted-U function: intermediate levels of alpha-power enhance perception and evoked responses while low and high levels have a negative effect (Linkenkaer-Hansen et al., 2004; Zhang and Ding, 2010; Rajagovindan and Ding, 2011; Lange et al., 2012). In addition, prestimulus gamma-band power has been shown to influence perception (Wyart and Tallon-Baudry, 2009).

Alpha-band power is modulated by attention (Worden et al., 2000; Thut et al., 2006; Haegens et al., 2011; Rajagovindan and Ding, 2011; van Ede et al., 2011) and has been linked to inhibition of task irrelevant areas (Händel et al., 2011; Jensen and Mazaheri, 2010). Similarly, gamma-band power is modulated by attention (Fries et al., 2001b, 2008; Bauer et al., 2006; Buffalo et al., 2011; Kahlbrock et al., 2012). Both processes are believed to gate neuronal processing and thus increase neuronal stimulus processing in task related neuronal groups (Fries, 2005; Fries et al., 2007; Romei et al., 2008a; Schroeder and Lakatos, 2009; Jensen and Mazaheri, 2010). Specifically, decreased prestimulus alpha-band power has been interpreted by some studies to improve visual perception in the sense that it leads to better detection performance of near threshold stimuli or more veridical perception in visual discrimination tasks (Hanslmayr et al., 2007; van Dijk et al., 2008; Mathewson et al., 2009; Wyart and Tallon-Baudry, 2009; Romei et al., 2010).

Here, we study prestimulus rhythmic neuronal activity in two phenomena called double-flash illusion (DFI) and fusion effect (FE). In the visuotactile DFI, subjects receive one visual stimulus accompanied by two tactile stimuli, and this stimulation is misperceived as two visual stimuli (Violentsev et al., 2005; Lange et al., 2011). By contrast, the FE occurs when two visual stimuli are

Received Aug. 2, 2012; revised Nov. 30, 2012; accepted Dec. 19, 2012.

Author contributions: J.L. and P.F. designed research; J.L. performed research; R.O. contributed unpublished reagents/analytic tools; J.L., R.O., and P.F. analyzed data; J.L. and P.F. wrote the paper.

J.L. was supported by the German Research Foundation (LA 2400/1-1), P.F. was supported by a European Young Investigator Award from the European Science Foundation. We thank Paul Gaaman and Pieter Buur for help with the MRI recordings. We are most grateful to Sander Berends for recording parts of the MEG data.

The authors declare no competing financial interests.

This article is freely available online through the *JNeurosci* Open Choice option.

Correspondence should be addressed to Joachim Lange, Medical Faculty, Institute of Clinical Neuroscience and Medical Psychology, Heinrich-Heine-University Düsseldorf, Universitätsstrasse 1, 40225 Düsseldorf, Germany. E-mail: Joachim.lange@med.uni-duesseldorf.de.

DOI:10.1523/JNEUROSCI.3755-12.2013

Copyright © 2013 the authors 0270-6474/13/333212-09\$15.00/0

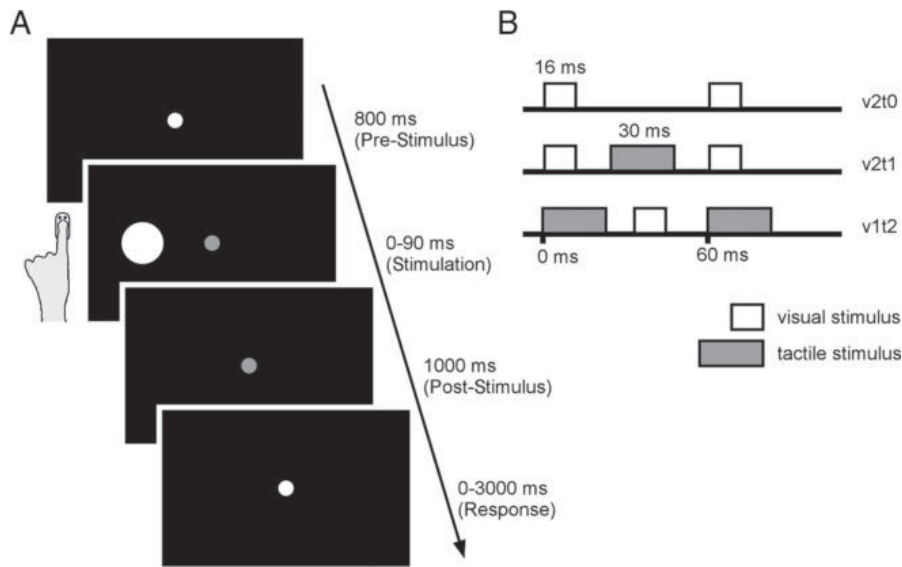


**Figure 1.** Illustration of the paradigm. **A**, Each trial started with the presentation of a central fixation. The luminance of the dot decreased and 800 ms later, visuotactile stimulation followed. The visual stimulus was a white disc (2.5° diameter) that appeared at 17° eccentricity in the left hemifield. Tactile stimulation was applied to the left index finger. After stimulation, only the fixation dot was visible for another 1000 ms before subjects were allowed to respond with their right hand. **B**, Illustration of stimulation sequences for the critical conditions v2t0, v2t1, and v1t2. Visual stimuli (white rectangles) were presented for 16 ms, tactile stimuli (gray rectangles) for 30 ms.

presented with no or one tactile stimulus, and this stimulation is misperceived as a single visual stimulus (McCormick and Mamassian, 2008). In both the FE and the DFI, varying perception occurs in the face of constant physical stimulation. The comparison of the DFI and the FE provides for a critical test: If reduced prestimulus alpha-band activity indeed promotes veridical perception in general, it should reduce illusory misperception in both the DFI and the FE. Here, we test this prediction using MEG recordings in 33 subjects.

## Materials and Methods

### Subjects

Thirty-three right-handed volunteers [15 male, mean age ( $\pm$  SD) 22.2  $\pm$  2.8 years] participated in this study. All participants had normal or corrected-to-normal vision and no known history of neurological disorders. The experiment was approved by the local ethics committee, and each subject gave written informed consent before the experiment, according to the Declaration of Helsinki.

### Paradigm and stimuli

Paradigm and stimuli were reported in detail previously (Lange et al., 2011). Here, we will present a comprehensive overview; for details, see the study Lange et al. (2011).

Subjects were lying in supine position with their head placed inside the MEG helmet while they received visuotactile stimulation. Visual stimuli were presented via a projector (60 Hz refresh rate) placed outside the magnetic shielded room and backprojected via a mirror system on a translucent screen. The visual stimulus consisted of a gray disc (2.5° diameter) presented 17° left of the center of the screen. The luminance of the disc was adjusted individually (average across subjects 2.3 cd/m<sup>2</sup>) to obtain balanced responses during illusion trials (see below). Visual stimuli were presented for one monitor frame (16 ms). Tactile stimuli were presented via a piezoelectric stimulation device (Metec) that was taped to the subjects' left index finger. The device consisted of 4  $\times$  2 pins that were raised simultaneously for 30 ms. To mask clicking sounds produced by the stimulator, subjects' hands and the stimulator were covered by sound attenuating foam and subjects received white noise via headphones.

Each trial began with the presentation of a central gray fixation dot (Gaussian of diameter 0.5°, luminance 7 cd/m<sup>2</sup>). A decrease of lumi-

nance served as a warning cue and after 800 ms visuotactile stimulation began (Fig. 1A). Stimulation consisted of 0, 1, or 2 visual stimuli, accompanied by 0, 1, or 2 tactile stimuli. We will address the different conditions as "vxty" for a condition with x visual and y tactile stimuli, e.g., conditions potentially showing the DFI effect are labeled v1t2. We applied all nine combinations of visuotactile stimulations in random order. In the critical condition v2t0 the onset of both visual stimuli was separated by 60 ms (Fig. 1B). In the bimodal conditions v1t2 and v2t1, stimuli were presented in the order t-v-t (v-t-v, respectively), with the onset of the two tactile (visual) separated by 60 ms and the visual (tactile) stimulus presented in between. We used only the stimulation order t-v-t for v1t2 trials (Fig. 1B). This choice was motivated by a previous study on the auditory-visual DFI (Shams et al., 2002). This study had shown that perception of the DFI occurs if the visual stimulus is presented in between the two auditory stimuli (or simultaneous to one auditory stimulus) and that the gap of the onsets of visual and auditory stimuli needs to be within  $\pm$ 70 ms.

After stimulation, only the fixation dot was visible for 1000 ms before its luminance increased, indicating the start of the response period (Fig. 1A). Subjects were asked to report

how many visual stimuli they perceived while ignoring tactile stimulation. Responses were given by button presses with the thumb, index, and middle finger of right hand. After button press or maximally 3000 ms, the next trial started.

Overall, each condition was presented in 100 trials. To increase statistical power, the condition v1t2 was presented 200 times. The trials were presented in 10 blocks with each block containing all nine conditions (v1t2 twice) in pseudorandom order. After 10 blocks, subjects were allowed to take a short self-paced break.

The experiment was controlled using the software "Presentation" (Neurobehavioral Systems).

### MEG and MRI recordings

Electromagnetic brain activity was recorded using a 151-channel MEG system for 22 subjects and a 275-channel MEG system for the other 11 subjects (both CTF Systems). Data from the 275-channel system were interpolated to a common 151-channel template using a procedure that was also used to compensate for differences in subjects' head position (for details, see Preprocessing, below) (Lange et al., 2011).

Subjects were measured in supine position. An electro-oculogram (EOG) was recorded for offline detection of eye-movements. MEG/EOG data were low-pass filtered at 300 Hz and sampled continuously at a rate of 1200 Hz. Subjects' head position relative to the sensor array was determined before and after the recording session by measuring the position of reference coils placed at the subjects' nasion and at the left and right ear canals.

Structural MR images were acquired using standard T1-weighted sequences on a 1.5 T or 3 T whole-body scanner (Siemens). MRI and MEG data were aligned according to reference coils at nasion and at the left and right ear canals.

### Data analysis

**Preprocessing.** Data were analyzed using FieldTrip (Oostenveld et al., 2011), Matlab (MathWorks), and SPM8 (Litvak et al., 2011).

To average the data from the 275-channel and the 151-channel system, the individual subjects' MEG data were interpolated to a common 151-channel-template position for the MEG sensors with respect to the head (for details, see Lange et al., 2011). Power line noise was removed using a Fourier transformation of 10-s-long signal periods and subtracting the

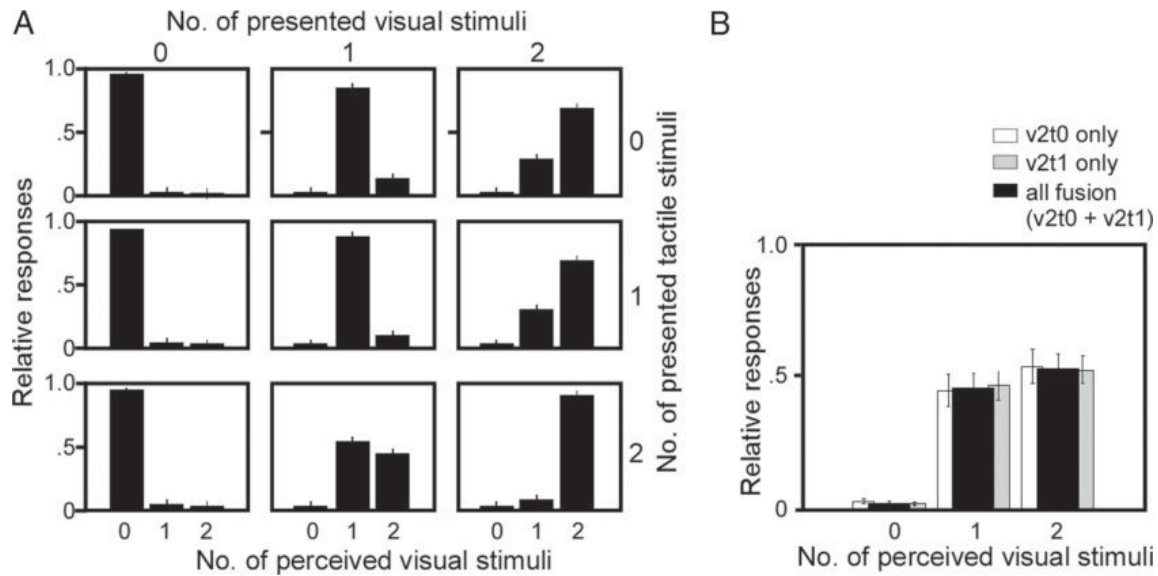


**Figure 2.** Behavioral results. *A*, Relative proportion of subjective reports for all nine conditions, averaged across all 33 subjects. *B*, Subjective reports for conditions v2t0 (white bars), v2t1 (gray bars), and pooled across both conditions (fusion trials, black bars), averaged across all 17 subjects showing a reliable fusion effect.

50, 100, and 150 Hz components. Artifacts caused by eye-movements, muscle activity, or sensor jumps were removed using a semiautomatic procedure. Trials shorter than 800 ms were completely rejected. Trials in which subjects gave no response or the response was given too early (i.e., within the 1000 ms poststimulus period) were also rejected.

**Time-frequency analysis.** We analyzed spectral power in two distinct frequency ranges. For the low-frequency range (4–40 Hz), we applied a discrete Fourier transformation on sliding temporal windows with a length of 400 ms, shifted in steps of 20 ms. Data segments were tapered with a single Hanning window resulting in a spectral smoothing of  $\sim \pm 2.5$  Hz. For the high-frequency range (40–150 Hz), we used time windows of 200 ms length, shifted in steps of 20 ms. We applied a multitaper approach to the respective analysis windows to optimize spectral concentration over the frequency of interest (Mitra and Pesaran, 1999). We applied 11 Slepian tapers resulting in a spectral smoothing of  $\pm 30$  Hz. Spectral power was first estimated per trial and taper and then averaged across trials and tapers.

The focus of the present study was on the effect of prestimulus rhythmic neuronal activity on visual perception. We defined regions of interest (ROIs) in sensor space for the visual domain as defined in our previous study (Lange et al., 2011): The ROI for visual processing was defined by taking the 10 occipital MEG sensors overlying visual cortex centrally and contralaterally to stimulus presentation that revealed the strongest post-stimulus effects in the alpha-, beta-, and gamma-band in response to visual stimulation (sensors RO21, RO22, RO31, RO32, RO33, RO41, RO42, ZO01, LO31, LO32).

Additionally, we studied effects in the somatosensory domain. We defined sensors of interest as defined in our previous study (Lange et al., 2011), i.e. by taking the 10 sensors over somatosensory areas contralateral to tactile stimulation showing the strongest poststimulus effects in response to tactile stimulation (sensors RC13, RC14, RC15, RC21, RC22, RC23, RC24, RC31, RC32, RP34).

**Statistical analysis of spectral power.** Subjects frequently misperceived trials of the condition v1t2 as two visual stimuli (DFI trials). In addition, subjects frequently reported only one visual stimulus in the conditions v2t0 and v2t1 (FE trials, Fig. 2).

We performed two statistical analyses. First, we sorted all trials of the condition v1t2 into DFI (2 stimuli perceived) and non-DFI (1 perceived) trials. Second, we pooled trials of the conditions v2t0 and v2t1 and sorted the trials into fusion (1 perceived) and nonfusion (2 perceived) trials. Pooling the two conditions was motivated by the fact that they showed very similar proportions of perceptual fusions (Fig. 2) and very similar effects in the time-frequency analyses. Statistical comparison was performed by first pooling spectral power over sensors of interest for each

subject individually. This was done separately for DFI, non-DFI, FE, and non-FE trials. Next, we compared DFI to non-DFI and non-FE to FE trials, i.e., we always compared conditions with two perceived stimuli to conditions with one perceived stimulus. Within each subject, we computed a time-frequency-wise independent samples *t* test between the conditions compared in a given contrast, leading to a time-frequency *t*-map. For the actual statistical inference, these *t*-maps were forwarded to a group-level statistics where the consistency of the effect across subjects was tested by using a nonparametric randomization test (Maris and Oostenveld, 2007). The *t*-maps were pooled across subjects. Pooled values were thresholded at a value of  $t = 1.96$ , and neighboring time-frequency-points exceeding this threshold were clustered. Values within a cluster were summed, giving our cluster-level test statistic. Under the null hypothesis, the conditions compared in the *t*-maps can be randomly exchanged. Therefore, we generated a randomization distribution by inverting the *t*-map sign of a random subset of subjects before pooling. The cluster-statistics were recomputed for these new group-level pooled *t*-maps. By repeating this step 1000 times, a randomization distribution of cluster-level test-statistics was computed and the test statistics of the observed clusters were compared with this randomization distribution (for details, see Lange et al., 2011). This nonparametric approach avoids assumptions about underlying distributions, implements a random effect analysis, and corrects for multiple comparisons across time and frequency (Maris and Oostenveld, 2007).

For significant time-frequency clusters, we further studied the relation of prestimulus rhythmic activity to subjective perception. For each subject separately, we averaged prestimulus power over the sensor-ROI, and over the significant time-frequency bins. Based on these averages and separately per subject, we sorted the trials and divided into quartiles. Averaged perception rates were calculated for each quartile and normalized per subject by subtracting the mean perception rate across all trials [similar to the studies by van Dijk et al., 2008; Lange et al., 2012]. To study linear trends, a linear regression was fitted to the data. Detection rates in quartiles were statistically compared by repeated-measures ANOVA and *post hoc t* tests. The comparison was performed separately for the condition v1t2 and the combined conditions v2t0 and v2t1.

**Source reconstruction.** To determine the cortical sources of the significant time-frequency clusters identified on sensor level, we applied a beamforming approach in the frequency domain (Gross et al., 2001).

To this end, the brain was discretized into a three-dimensional grid. Leadfield matrices were computed for each grid location using a realistic single-shell volume conduction model based on the individual MRIs (Nolte, 2003). The grid locations were determined for individual subjects by the following procedure: First, a regular grid with a resolution of 1 cm

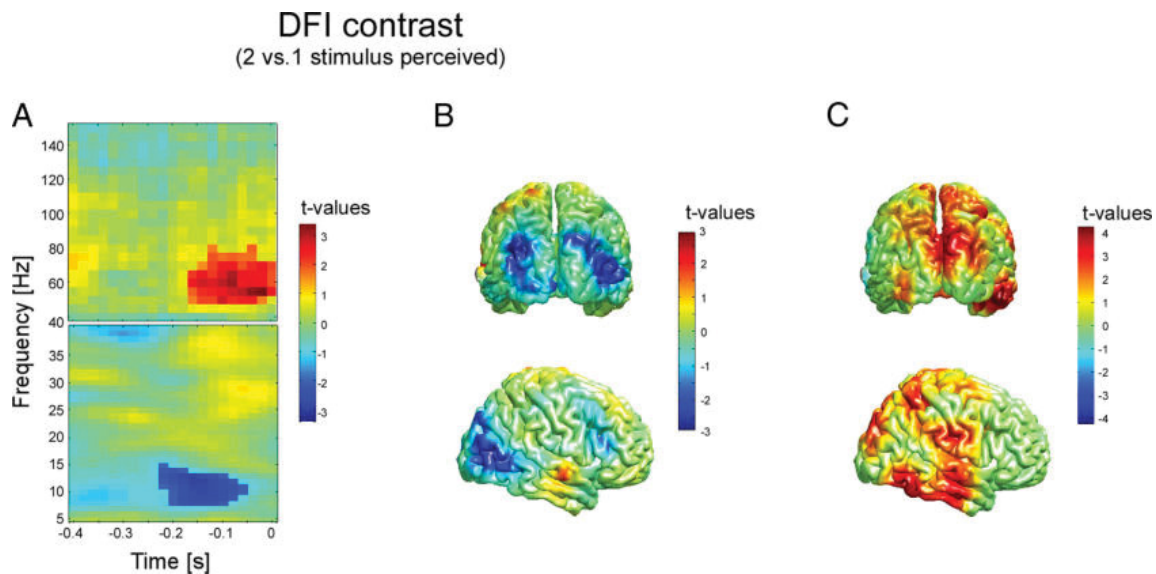


**Figure 3.** Results of the DFI contrast in visual sensors. **A**, Time-frequency representations on sensor level.  $t = 0$  indicates the onset of the first stimulation. **B**, Source reconstruction projected on the MNI template brain for the significant effect in the alpha-band ( $\sim 10$  Hz in **A**) viewed from the back (top row) and right (bottom row). **C**, Same as in **B** but now for the significant effect in the gamma-band ( $\sim 60$  Hz in **A**). Time-frequency representations and source plots are masked to highlight significant clusters. Red colors indicate greater spectral power in trials when subjects perceived two visual stimuli (i.e., the DFI) compared with trials in which they perceived one stimulus. Color bars apply to the significant (nonmasked) pixels/voxels.

was created in the Montreal Neurological Institute (MNI) template brain. Individual subject's structural MRIs were linearly warped into this template MRI and the inverse was applied to the template grid, resulting in individual grids. The advantage of this approach is that group level results can be computed by averaging results per grid point. Spatial filters were constructed for each grid location based on leadfield and cross spectral density (CSD) matrices. CSD matrices were computed between all MEG pairs for the time period and frequency of interest. Time-frequency bands of interest were determined by the significant clusters of the abovementioned time-frequency analysis on sensor level. For each contrast (DFI vs non-DFI and nonfusion vs fusion), we first pooled all trials of the respective condition (v1t2 or v2t0 and v2t1) and computed a common filter per subject and condition. Next, the single trials of each condition were projected through the respective filter and sorted according to subjective perception. Statistical comparison was performed in line with the statistical comparison on the sensor level except that clusters were now based on spatiotemporal proximity rather than on time-frequency proximity. Source parameters estimated this way per subject were statistically tested across subjects (see above) and group results were plotted on the MNI template brain.

**Inter-trial coherence.** To study the role of phase entrainment, we computed intertrial coherence (ITC). ITC is a measure of phase consistency across trials. We measured ITC in the prestimulus period separately for trials in which subjects perceived two stimuli and for trials in which subjects perceived one stimulus. At each time  $t$  and frequency  $f$ , the we computed ITC following the formula (Busch et al., 2009):

$$ITC_{t,f} = \frac{1}{k} \sum_{n=1}^k e^{-i\varphi_{n(t,f)}},$$

with  $k$  the number of trials. The number of trials was stratified between conditions. ITC was computed in two ways: averaged across the whole prestimulus period or in sliding time windows of 300 ms length in steps of 20 ms. Differences of ITC between conditions (two vs one stimulus perceived) were statistically tested using the randomization approach described above.

**Interaction metrics: coherence and power correlation.** To quantify interactions between visual and somatosensory channels, we calculated two metrics: coherence and power correlation.

Coherence quantifies the consistency of phase differences between two signals and across multiple trials (Siegel et al., 2008; Schoffelen et al.,

2011). If phase differences are random, coherence tends toward zero. If all trials have the same phase difference, coherence can reach one. Power correlation is the Pearson correlation coefficient between the trial-by-trial fluctuations in the power (at the same frequency) of two signals (Nieuwenhuis et al., 2012).

## Results

### Behavioral data

Subjects made only negligible errors when reporting the number of visual stimuli in six of the nine conditions (Fig. 2A). However, in trials with one visual stimulus paired with two tactile stimuli (v1t2), subjects perceived a second, illusory visual stimulus in  $43.0 \pm 3.3\%$  (mean  $\pm$  SEM) of the trials, which constitutes the double flash illusion (DFI). By contrast, in trials with two visual stimuli paired with no (v2t0) or one tactile stimulus (v2t1), subjects missed one visual stimulus (the fusion trials) in  $29.3 \pm 5.8\%$  and  $30.8 \pm 4.5\%$ , respectively, which constitutes the FE. Closer inspection of the behavioral data revealed that 16 out of 33 subjects did not experience an FE, i.e., they reliably perceived two visual stimuli in the majority of trials ( $>90\%$ ). For the remaining 17 subjects who experienced a reliable FE, the fusion occurred on  $44.3 \pm 6.2\%$  (v2t0) and  $46.2 \pm 5.4\%$  (v2t1) of the trials. Since the stimulation conditions v2t0 and v2t1 revealed highly similar FEs, we pooled both conditions to a common "fusion" condition (Fig. 2B).

### DFI contrast

To study the effect of prestimulus rhythmic activity on the perception of the DFI, we sorted trials of the condition v1t2 according to the subjective perception. We contrasted trials in which subjects reported two visual stimuli versus trials in which subjects reported one visual stimulus, despite physically constant stimulation.

In the time-frequency analysis of power in occipital MEG sensors (see Materials and Methods for details), we found a significant negative cluster between 8–15 Hz and  $-220$  to  $-60$  ms ( $p < 0.05$ ), i.e., alpha-power was significantly decreased in the prestimulus period if subjects perceived the DFI after the subse-

quent stimulation (Fig. 3A). The cortical sources of this effect were localized to bilateral visual areas (Brodmann areas 17, 18, 19), extending on the right hemisphere (contralateral to stimulus presentation) to more ventrolateral sites (Fig. 3B).

In addition, we found prestimulus gamma-band (50–80 Hz) power to be significantly enhanced for DFI trials compared with non-DFI-trials between –180 and 0 ms (Fig. 3A). Source localization of this effect revealed a widespread network of cortical areas, covering bilateral occipitoparietal areas, right inferior temporal gyrus, as well as parts of middle and superior temporal gyrus, and finally right primary and secondary somatosensory cortex (Fig. 3C).

Prestimulus alpha-power (averaged between –200 and –80 ms and 8–12 Hz, sensor level) was negatively correlated with subjective perception rates ( $r = 0.98$ ,  $p < 0.05$ ), i.e., lower prestimulus alpha power predicted a higher probability to perceive the DFI (see Fig. 5C). An ANOVA revealed a significant difference between power bins ( $p < 0.05$ ). *Post hoc* analysis revealed that perception rates were significantly larger in the first bin than in the third and fourth bin (both  $p < 0.05$ ). In addition, prestimulus gamma-power (averaged between –180 and 0 ms and 50–70 Hz) showed a strong trend toward a positive correlation with subjective perception rates ( $r = 0.94$ ,  $p = 0.055$ ), i.e., higher prestimulus gamma-power tended to predict a higher probability to perceive the DFI. An ANOVA revealed a significant difference between power bins ( $p < 0.05$ ). *Post hoc* analysis revealed that perception rates were significantly larger in the fourth bin than in the second ( $p < 0.05$ ) and an almost significant trend between the fourth and first bin ( $p = 0.055$ ) (see Fig. 5A).

Because the interval between warning signal and stimulus was fixed (800 ms), it was conceivable that some kind of phase entrainment may occur, which in turn might impact stimulus processing. Therefore, we quantified phase entrainment by computing intertrial coherence (Busch et al., 2009). No significant differences were found.

Time-frequency analysis in the somatosensory sensors (see Materials and Methods for sensor selection details) did not reveal any significant DFI effect (see Fig. 6A).

We also analyzed two different metrics of interaction between visual and somatosensory channels: coherence and power-power correlation. First, we calculated the average coherence between all possible pairs of visual and somatosensory channels in the same time-frequency range for which we had analyzed power. This did not reveal any significant DFI effect. Next, we calculated the average correlation between power fluctuations in all possible pairs of

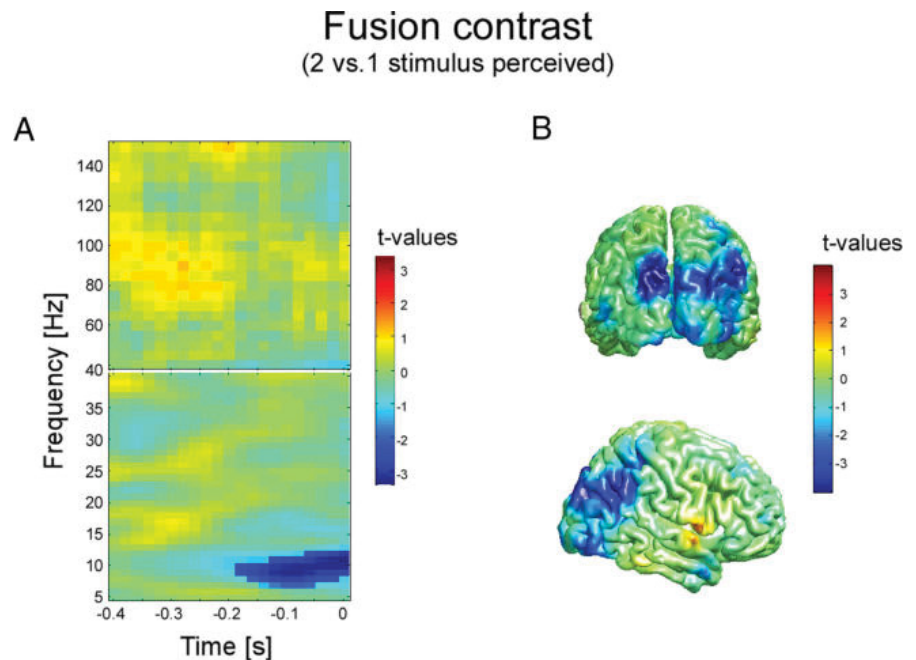


**Figure 4.** Results of the fusion contrast in visual sensors. **A**, Same as in Figure 2A but now for the contrast two versus one stimulus perceived in the pooled fusion trials conditions (v2t0 and v2t1). **B**, Source reconstruction of the significant effect in the alpha-band ( $\sim 10$  Hz in **A**). All formats as in Figure 2.

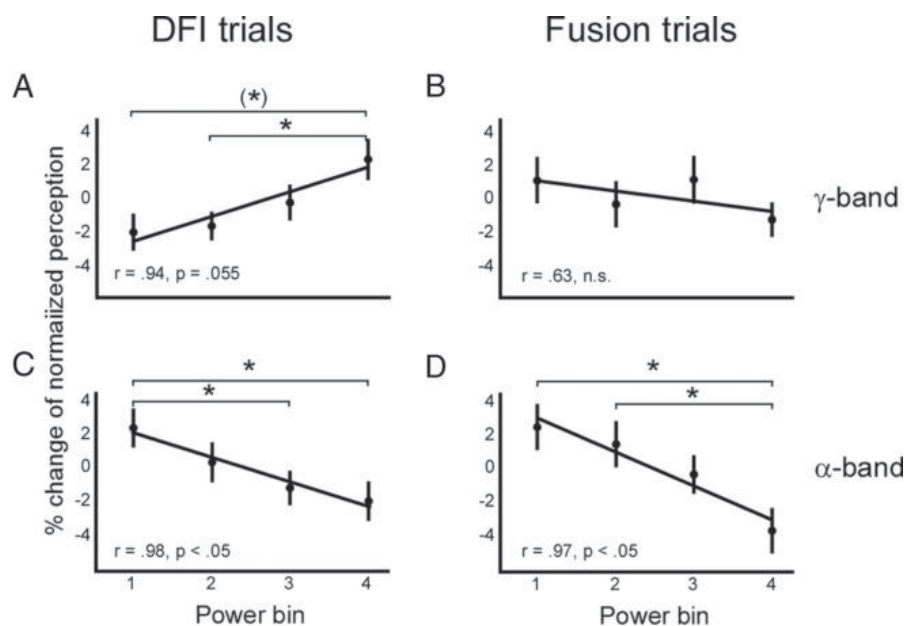


**Figure 5.** Results of the correlation analysis of spectral power and normalized subjective perception. Power was averaged for DFI trials in the gamma- (**A**) and alpha-band (**C**) or for the fusion trials in the gamma- (**B**) and alpha-band (**D**). \* $p < 0.05$ ; (\*\*) $p = 0.055$ ; n.s., not significant ( $p > 0.05$ ). Insets show results of the regression analysis. Higher bin numbers indicate higher spectral power.

visual and somatosensory channels. This was again for the same time-frequency range and always considering somatosensory and visual sensor power of the same frequency. This analysis revealed a significant DFI effect: When subjects perceived two as compared to one flash, there was enhanced power correlation  $\sim 180$  and 0 ms before stimulation and ranging from  $\sim 14$ – $26$  Hz (see Fig. 7A).

#### FE contrast

To study the effect of prestimulus rhythmic activity on the perception of the FE, we pooled trials of the conditions v2t0 and v2t1

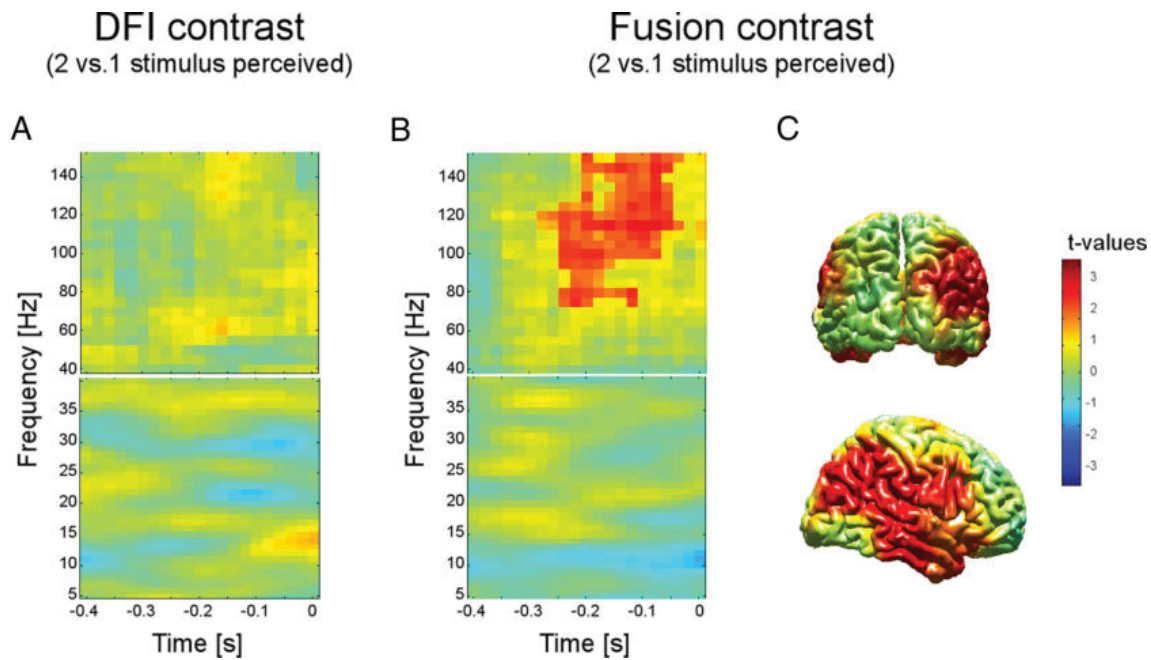


**Figure 6.** Results of the DFI and FE contrast in somatosensory sensors. **A**, Time-frequency representations for the DFI contrast on sensor level.  $t = 0$  indicates the onset of the first stimulation. **B**, Time-frequency representations for the FE contrast on sensor level. **C**, Source reconstruction projected on the MNI template brain for the significant effect in the gamma-band (70–150 Hz in **B**) viewed from the back (top row) and right (bottom row). All formats as in Figure 3.

and sorted all trials according to the subjective perception. We contrasted trials in which subjects reported two visual stimuli versus trials in which subjects reported one visual stimulus. Analysis was restricted to the 17 subjects that showed a reliable fusion effect.

The time-frequency analysis of power in the same occipital MEG sensors as used for the DFI analysis revealed a significant negative cluster between  $-180$  and  $0$  ms and  $7$ – $12$  Hz ( $p < 0.05$ ), i.e., alpha-power was significantly decreased in the prestimulus period if subjects perceived no fusion effect after the subsequent stimulation (Fig. 4A). The cortical sources of this effect were localized to bilateral visual areas (Brodmann areas 17, 18, 19), with the effect slightly lateralized to the right hemisphere (Fig. 4B). No significant effect was found for the high frequencies.

Prestimulus alpha-power (averaged between  $-180$  and  $0$  ms and  $8$ – $12$  Hz, sensor level) was negatively correlated with perception rates ( $r = 0.97$ ,  $p < 0.05$ ), i.e., lower prestimulus alpha power correlated with higher probability to perceive no FE (Fig. 5D). An ANOVA revealed a significant difference between power bins ( $p < 0.05$ ). *Post hoc* analysis revealed that perception rates were significantly larger in the first and second bin than in the fourth bin (both  $p < 0.05$ ). Gamma-band power (averaged between  $-180$  and  $0$  ms and  $50$ – $70$  Hz, see above analysis for DFI trials) showed no significant correlation to perception rates in the FE (Fig. 5B).

As for the DFI contrast, we tested for potential differences in intertrial coherence, but found no significant difference also for the FE contrast.

In somatosensory channels, a time-frequency analysis for the fusion effect revealed a significant positive cluster between  $-240$  and  $-50$  ms and  $70$ – $150$  Hz, i.e., gamma-power was significantly increased in the prestimulus period if subjects perceived no fusion effect after the subsequent stimulation (Fig. 6B). The source reconstruction revealed that this effect was not specific to the somatosensory domain, but spread over a large right hemispheric network covering temporal, visual, and parietal areas (Fig. 6C).

Additionally, we analyzed average coherence and power correlation between all possible pairs of visual and somatosensory channels. This did not reveal any significant difference in the FE contrast (Fig. 7B).

Finally, we compared prestimulus alpha-power (averaged between  $-180$  and  $0$  ms and  $8$ – $12$  Hz) between the 17 subjects with FE and the 16 subjects without reliable FE. Prestimulus alpha-power was lower in subjects without FE than with FE ( $p < 0.05$ ). This difference held when non-FE subjects were compared with FE subjects in trials with ( $p < 0.01$ ) or without FE ( $p < 0.05$ ) occurring (Fig. 8).

## Discussion

We studied the influence of prestimulus rhythmic activity on subjective perception in two perceptual phenomena called DFI and FE. In both phenomena, subjective perception can vary on a trial-by-trial basis despite constant physical stimulation. In DFI trials, one visual stimulus was paired with two tactile stimuli, but subjects frequently perceived two visual stimuli. In FE trials, two visual stimuli were paired with zero or one tactile stimulus, but subjects frequently “fused” the two physical stimuli to one perceived stimulus. For both phenomena, we found that prestimulus power in visual areas in the alpha-band directly before the stimulation ( $\sim -200$ – $0$  ms) correlated with subjective perception, i.e., decreased alpha-power increased the likelihood to perceive two visual stimuli during constant physical stimulation. Interestingly, while in DFI trials, a power decrease predicted an illusory perception, in FE trials, a power decrease predicted a veridical perception. In addition, prestimulus ( $\sim -200$ – $0$  ms) gamma-band power correlated positively with perception in DFI trials.

Several studies have reported an inverted-U relationship between on the one hand prestimulus alpha power and on the other hand stimulus evoked responses and/or behavioral performance, with intermediate alpha levels leading to largest responses and best performance (Linkenkaer-Hansen et al., 2004; Zhang and Ding, 2010; Rajagovindan and Ding, 2011; Lange et al., 2012).

Other studies have found that an enhanced detection performance for single visual stimuli is monotonically related to occipital prestimulus alpha-band power, with lower alpha levels leading to better performance (Thut et al., 2006; Hanslmayr et al., 2007; van Dijk et al., 2008; Mathewson et al., 2009). The precise reason for the discrepancy between these results is not yet known and requires future research. Our results from the FE analysis are in line with the studies reporting a monotonic relationship by demonstrating that trial-by-trial fluctuations of occipital prestimulus alpha-band power predict the temporal resolution of visual perception. Low temporal resolution (i.e., the fusion effect) was predicted by high alpha-power, while high temporal resolution (i.e., perception of two visual stimuli) was predicted by low alpha-power. This effect was visible both when we compared in individual subjects the trials with and without FE, and also when we compared subjects with FE to subjects not experiencing the FE: For a subgroup of subjects, which did not perceive FEs, we found absolute levels of alpha-power to be significantly decreased relative to subjects frequently experiencing the fusion effect. These findings are in line with previous studies arguing that reduced prestimulus alpha-power improves visual perception (van Dijk et al., 2008; Mathewson et al., 2009; Wyart and Tallon-Baudry, 2009; Jensen and Mazaheri, 2010; Jensen et al., 2012).

Our analysis of the DFI effect revealed that reduced prestimulus alpha-band activity is not always related to improved perceptual performance in the sense of a more veridical perception. Rather, in trials with one visual stimulus paired with two tactile stimuli (v1t2, DFI trials), decreased occipital alpha-power promotes the perception of a visual illusion. We propose that reduced alpha-band power in general indexes enhanced excitability of visual cortex rather than improved visual perception per se. This hypothesis is in line with recent TMS-studies showing that a larger number of TMS-induced phosphenes are perceived when pre-TMS alpha-band power is reduced (Romei et al., 2008a,b, 2012). We suggest that enhanced excitability might render visual cortex in general more susceptible to input, including heteromodal input, e.g., from somatosensory cortex. If somatosensory activity induced by two tactile stimuli merges with low alpha-power in visual cortex, it is more likely to induce two visual sensations during the DFI, showing that increased excitability is not always related to more veridical visual perception.

Our analyses revealed also two effects in the gamma-frequency band. The time-frequency analyses of occipital sensors revealed that the perception of two flashes during DFI trials was predicted by enhanced prestimulus power in the gamma-band. The corresponding analysis of somatosensory sensors revealed that the perception of two flashes as compared with one in the fusion contrast was predicted by enhanced gamma-band power. The precise temporal and spectral extensions of these effects differed and the spatial extensions overlapped only partly. Yet, in both cases, prestimulus gamma power predicted the per-

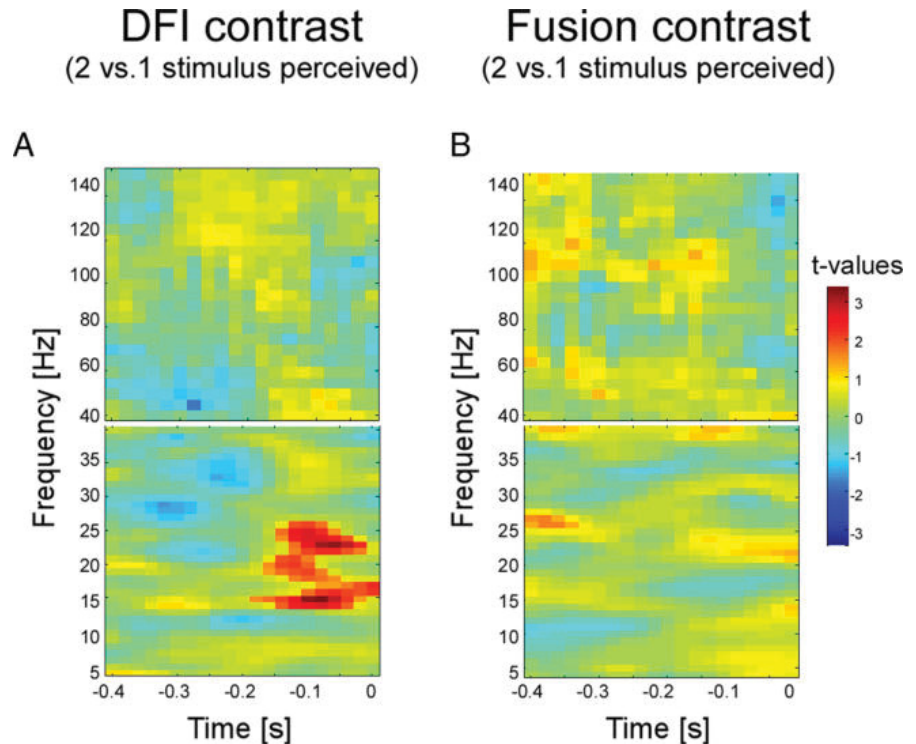


**Figure 7.** Results of the power correlation analyses. **A**, Averaged difference in power correlation for the DFI contrast on the sensor level. Power correlation was computed between all predefined somatosensory and visual sensors (see Materials and Methods for sensor selection).  $t = 0$  indicates the onset of the first stimulus. **B**, Averaged difference in power correlation for the FE contrast. Time-frequency representation plots are masked to highlight significant clusters. Red colors indicate greater power correlation in trials in which subjects perceived two visual stimuli (i.e., the DFI) compared with trials in which they perceived one stimulus. Color bars apply to the significant (nonmasked) pixels.

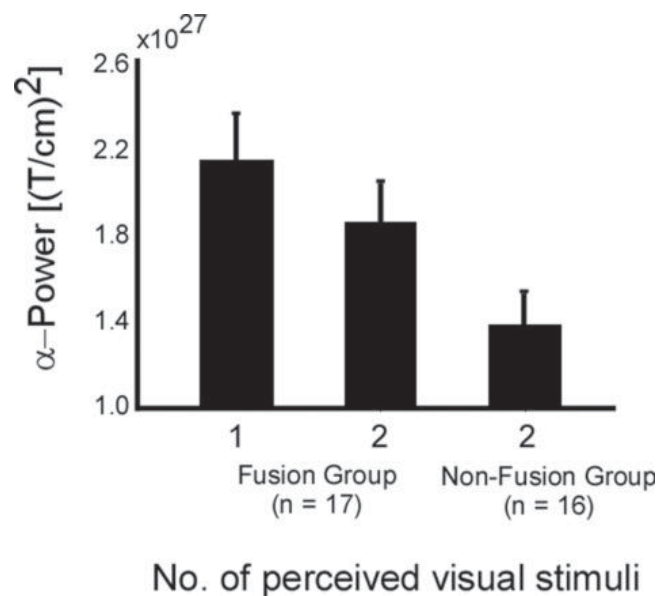


**Figure 8.** Absolute power levels in the alpha-band for subjects ( $n = 17$ ) showing a reliable fusion effect (left and middle bar) and subjects ( $n = 16$ ) showing no fusion effect. The fusion group was split into perceived 1 (left bar) and perceived 2 stimuli (middle bar). All bars are significantly different from each other ( $p < 0.05$ ).

ception of two flashes. This is in line with previous studies linking prestimulus gamma-band activity to attention, enhanced excitability, and reduced neuronal and behavioral response times (Engel et al., 2001; Fries et al., 2001a,b; Gonzalez Andino et al., 2005). Prestimulus occipital gamma-band power is also posi-

tively related to detection performance in a unimodal visual task (Wyart and Tallon-Baudry, 2008, 2009). The prestimulus gamma increase reported in these studies was highly similar in time and frequency to our observed gamma-band increase in the DFI contrast.

Our analysis of correlations between power fluctuations in somatosensory and visual regions revealed that the perception of two flashes in DFI trials was predicted by higher interareal power correlations in the beta-frequency band. This supports the hypothesis that the perception of the DFI is mediated by an interaction between visual and somatosensory cortex.

In summary, our results complement recent studies demonstrating that fluctuations of prestimulus rhythmic activity and interareal interactions are more than mere background noise, but substantially influence subjective perception despite constant physical stimulation. Our study critically extends previous studies in three aspects. First, we demonstrate within and across subjects that prestimulus alpha-power in visual cortex predicts the temporal resolution of visual perception: The lower the prestimulus alpha-power the more likely subjects perceive the veridical two stimuli. Second, we demonstrate that low prestimulus alpha-power is not always correlated to more veridical perception. During DFI trials, low prestimulus alpha-power correlated with an illusory perception of a second stimulus. We propose that prestimulus alpha power indexes excitability of visual cortex rather than improved perception per se. Low alpha-power renders visual cortex more susceptible to unimodal, but also heteromodal input, leading to improved perception in most cases, but to illusory perception in the case of DFI. In addition, we report fluctuations of prestimulus gamma-band power in a widespread network. Gamma-band power correlates with the perception of two flashes in both, the DFI and the FE contrast. Finally, we show that the DFI is preceded by enhanced beta-power correlation between visual and somatosensory regions. Taking these results together, we conclude that prestimulus fluctuations in power and power correlations play a functional role in unimodal and heteromodal perception.

## References

- Bauer M, Oostenveld R, Peeters M, Fries P (2006) Tactile spatial attention enhances gamma-band activity in somatosensory cortex and reduces low-frequency activity in parieto-occipital areas. *J Neurosci* 26:490–501. [CrossRef Medline](#)
- Buffalo EA, Fries P, Landman R, Buschman TJ, Desimone R (2011) Laminar differences in gamma and alpha coherence in the ventral stream. *Proc Natl Acad Sci U S A* 108:11262–11267. [CrossRef Medline](#)
- Busch NA, Dubois J, VanRullen R (2009) The phase of ongoing EEG oscillations predicts visual perception. *J Neurosci* 29:7869–7876. [CrossRef Medline](#)
- Engel AK, Fries P, Singer W (2001) Dynamic predictions: oscillations and synchrony in top-down processing. *Nat Rev Neurosci* 2:704–716. [CrossRef Medline](#)
- Fries P (2005) A mechanism for cognitive dynamics: neuronal communication through neuronal coherence. *Trends Cogn Sci* 9:474–480. [CrossRef Medline](#)
- Fries P, Neuenschwander S, Engel AK, Goebel R, Singer W (2001a) Rapid feature selective neuronal synchronization through correlated latency shifting. *Nat Neurosci* 4:194–200. [CrossRef Medline](#)
- Fries P, Reynolds JH, Rorie AE, Desimone R (2001b) Modulation of oscillatory neuronal synchronization by selective visual attention. *Science* 291:1560–1563. [CrossRef Medline](#)
- Fries P, Nikolić D, Singer W (2007) The gamma cycle. *Trends Neurosci* 30:309–316. [CrossRef Medline](#)
- Fries P, Womelsdorf T, Oostenveld R, Desimone R (2008) The effects of visual stimulation and selective visual attention on rhythmic neuronal synchronization in macaque area v4. *J Neurosci* 28:4823–4835. [CrossRef Medline](#)
- Gonzalez Andino SL, Michel CM, Thut G, Landis T, Grave de Peralta R (2005) Prediction of response speed by anticipatory high-frequency (gamma band) oscillations in the human brain. *Hum Brain Mapp* 24:50–58. [CrossRef Medline](#)
- Gross J, Kujala J, Hamalainen M, Timmermann L, Schnitzler A, Salmelin R (2001) Dynamic imaging of coherent sources: studying neural interactions in the human brain. *Proc Natl Acad Sci U S A* 98:694–699. [CrossRef Medline](#)
- Haegens S, Händel BF, Jensen O (2011) Top-down controlled alpha band activity in somatosensory areas determines behavioral performance in a discrimination task. *J Neurosci* 31:5197–5204. [CrossRef Medline](#)
- Händel BF, Haarmeier T, Jensen O (2011) Alpha oscillations correlate with the successful inhibition of unattended stimuli. *J Cogn Neurosci* 23:2494–2502. [Medline](#)
- Hanslmayr S, Aslan A, Staudigl T, Klimesch W, Herrmann CS, Bäuml KH (2007) Prestimulus oscillations predict visual perception performance between and within subjects. *Neuroimage* 37:1465–1473. [CrossRef Medline](#)
- Hipp JF, Engel AK, Siegel M (2011) Oscillatory synchronization in large-scale cortical networks predicts perception. *Neuron* 69:387–396. [CrossRef Medline](#)
- Jensen O, Mazaheri A (2010) Shaping functional architecture by oscillatory alpha activity: gating by inhibition. *Front Hum Neurosci* 4:186. [Medline](#)
- Jensen O, Bonnefond M, VanRullen R (2012) An oscillatory mechanism for prioritizing salient unattended stimuli. *Trends Cogn Sci* 16:200–206. [CrossRef Medline](#)
- Kahlbrock N, Butz M, May ES, Schnitzler A (2012) Sustained gamma band synchronization in early visual areas reflects the level of selective attention. *Neuroimage* 59:673–681. [CrossRef Medline](#)
- Keil J, Müller N, Ihssen N, Weisz N (2012) On the variability of the McGurk effect: audiovisual integration depends on prestimulus brain states. *Cereb Cortex* 22:221–231. [Medline](#)
- Lange J, Oostenveld R, Fries P (2011) Perception of the touch-induced visual double-flash illusion correlates with changes of rhythmic neuronal activity in human visual and somatosensory areas. *Neuroimage* 54:1395–1405. [CrossRef Medline](#)
- Lange J, Halacz J, van Dijk H, Kahlbrock N, Schnitzler A (2012) Fluctuations of prestimulus oscillatory power predict subjective perception of tactile simultaneity. *Cereb Cortex* 22:2564–2574. [CrossRef Medline](#)
- Linkenkaer-Hansen K, Nikulin VV, Palva S, Ilmoniemi RJ, Palva JM (2004) Prestimulus oscillations enhance psychophysical performance in humans. *J Neurosci* 24:10186–10190. [CrossRef Medline](#)
- Litvak V, Mattout J, Kiebel S, Phillips C, Henson R, Kilner J, Barnes G, Oostenveld R, Daunizeau J, Flandin G, Penny W, Friston K (2011) EEG and MEG data analysis in SPM8. *Comput Intell Neurosci* 2011:852961. [Medline](#)
- Maris E, Oostenveld R (2007) Nonparametric statistical testing of EEG- and MEG-data. *J Neurosci Methods* 164:177–190. [CrossRef Medline](#)
- Mathewson KE, Gratton G, Fabiani M, Beck DM, Ro T (2009) To see or not to see: prestimulus alpha phase predicts visual awareness. *J Neurosci* 29:2725–2732. [CrossRef Medline](#)
- McCormick D, Mamassian P (2008) What does the illusory-flash look like? *Vision Res* 48:63–69. [Medline](#)
- Mitra PP, Pesaran B (1999) Analysis of dynamic brain imaging data. *Biophys J* 76:691–708. [CrossRef Medline](#)
- Nieuwenhuis IL, Takashima A, Oostenveld R, McNoughton BL, Fernández G, Jensen O (2012) The neocortical network representing associative memory reorganizes with time in a process engaging the anterior temporal lobe. *Cereb Cortex* 22:2622–2633. [CrossRef Medline](#)
- Nolte G (2003) The magnetic lead field theorem in the quasi-static approximation and its use for magnetoencephalography forward calculation in realistic volume conductors. *Phys Med Biol* 48:3637–3652. [CrossRef Medline](#)
- Oostenveld R, Fries P, Maris E, Schoffelen JM (2011) FieldTrip: open source software for advanced analysis of MEG, EEG, and invasive electrophysiological data. *Comput Intell Neurosci* 2011:156869. [Medline](#)
- Parkkonen L, Andersson J, Hämäläinen M, Hari R (2008) Early visual brain areas reflect the percept of an ambiguous scene. *Proc Natl Acad Sci U S A* 105:20500–20504. [CrossRef Medline](#)
- Rajagovindan R, Ding M (2011) From prestimulus alpha oscillation to visual-evoked response: an inverted-U function and its attentional modulation. *J Cogn Neurosci* 23:1379–1394. [CrossRef Medline](#)

- Rodriguez E, George N, Lachaux JP, Martinerie J, Renault B, Varela FJ (1999) Perception's shadow: long-distance synchronization of human brain activity. *Nature* 397:430–433. [CrossRef Medline](#)
- Romei V, Brodbeck V, Michel C, Amedi A, Pascual-Leone A, Thut G (2008a) Spontaneous fluctuations in posterior alpha-band EEG activity reflect variability in excitability of human visual areas. *Cereb Cortex* 18:2010–2018. [Medline](#)
- Romei V, Rihs T, Brodbeck V, Thut G (2008b) Resting electroencephalogram alpha-power over posterior sites indexes baseline visual cortex excitability. *Neuroreport* 19:203–208. [CrossRef Medline](#)
- Romei V, Gross J, Thut G (2010) On the role of prestimulus alpha rhythms over occipito-parietal areas in visual input regulation: correlation or causation? *J Neurosci* 30:8692–8697. [CrossRef Medline](#)
- Romei V, Gross J, Thut G (2012) Sounds reset rhythms of visual cortex and corresponding human visual perception. *Curr Biol* 22:807–813. [CrossRef Medline](#)
- Schoffelen JM, Poort J, Oostenveld R, Fries P (2011) Selective movement preparation is subserved by selective increases in corticomuscular gamma-band coherence. *J Neurosci* 31:6750–6758. [CrossRef Medline](#)
- Schroeder CE, Lakatos P (2009) Low-frequency neuronal oscillations as instruments of sensory selection. *Trends Neurosci* 32:9–18. [CrossRef Medline](#)
- Shams L, Kamitani Y, Shimojo S (2002) Visual illusion induced by sound. *Brain Res Cogn Brain Res* 14:147–152. [CrossRef Medline](#)
- Siegel M, Donner TH, Oostenveld R, Fries P, Engel AK (2008) Neuronal synchronization along the dorsal visual pathway reflects the focus of spatial attention. *Neuron* 60:709–719. [CrossRef Medline](#)
- Thut G, Nietzel A, Brandt SA, Pascual-Leone A (2006) Alpha-band electroencephalographic activity over occipital cortex indexes visuospatial attention bias and predicts visual target detection. *J Neurosci* 26:9494–9502. [CrossRef Medline](#)
- van Dijk H, Schoffelen JM, Oostenveld R, Jensen O (2008) Prestimulus oscillatory activity in the alpha band predicts visual discrimination ability. *J Neurosci* 28:1816–1823. [CrossRef Medline](#)
- van Ede F, de Lange F, Jensen O, Maris E (2011) Orienting attention to an upcoming tactile event involves a spatially and temporally specific modulation of sensorimotor alpha- and beta-band oscillations. *J Neurosci* 31:2016–2024. [CrossRef Medline](#)
- Violentyev A, Shimojo S, Shams L (2005) Touch-induced visual illusion. *Neuroreport* 16:1107–1110. [CrossRef Medline](#)
- Worden MS, Foxe JJ, Wang N, Simpson GV (2000) Anticipatory biasing of visuospatial attention indexed by retinotopically specific alpha-band electroencephalography increases over occipital cortex. *J Neurosci* 20:RC63. [Medline](#)
- Wyart V, Tallon-Baudry C (2008) Neural dissociation between visual awareness and spatial attention. *J Neurosci* 28:2667–2679. [CrossRef Medline](#)
- Wyart V, Tallon-Baudry C (2009) How ongoing fluctuations in human visual cortex predict perceptual awareness: baseline shift versus decision bias. *J Neurosci* 29:8715–8725. [CrossRef Medline](#)
- Zhang Y, Ding M (2010) Detection of a weak somatosensory stimulus: role of the prestimulus mu rhythm and its top-down modulation. *J Cogn Neurosci* 22:307–322. [CrossRef Medline](#)

- 15) **Lange, J.**, Halacz, J., van Dijk, H., Kahlbrock, N., & Schnitzler, A. (2012).  
Fluctuations of prestimulus oscillatory power predict subjective perception of tactile simultaneity.  
*Cerebral Cortex (New York, N.Y.: 1991)*, 22(11), 2564–2574.  
Impact factor (2012): 6.828

# Fluctuations of Prestimulus Oscillatory Power Predict Subjective Perception of Tactile Simultaneity

Joachim Lange, Johanna Halacz, Hanneke van Dijk, Nina Kahlbrock and Alfons Schnitzler

Institute of Clinical Neuroscience and Medical Psychology, Medical Faculty, Heinrich-Heine-University Düsseldorf, 40225 Düsseldorf, Germany

Address correspondence to Joachim Lange, Institute of Clinical Neuroscience and Medical Psychology, Medical Faculty, Heinrich-Heine-University Düsseldorf, Universitätsstrasse 1, 40225 Düsseldorf, Germany. Email: joachim.lange@med.uni-duesseldorf.de.

**Oscillatory activity is modulated by sensory stimulation but can also fluctuate in the absence of sensory input. Recent studies have demonstrated that such fluctuations of oscillatory activity can have substantial influence on the perception of subsequent stimuli. In the present study, we employed a simultaneity task in the somatosensory domain to study the role of prestimulus oscillatory activity on the temporal perception of 2 events. Subjects received electrical stimulations of the left and right index finger with varying stimulus onset asynchronies (SOAs) and reported their subjective perception of simultaneity, while brain activity was recorded with magnetoencephalography. With intermediate SOAs (30 and 45 ms), subjects frequently misperceived the stimulation as simultaneously. We compared neuronal oscillatory power in these conditions and found that power in the high beta band (~20 to 40 Hz) in primary and secondary somatosensory cortex prior to the electrical stimulation predicted subjects' reports of simultaneity. Additionally, prestimulus alpha-band power influenced perception in the condition SOA 45 ms. Our results indicate that fluctuations of ongoing oscillatory activity in the beta and alpha bands shape subjective perception of physically identical stimulation.**

**Keywords:** alpha, beta, MEG, oscillation, somatosensory

## Introduction

Depending on the surrounding or internal brain states, physically identical sensory stimulation can be perceived quite differently. For example, subjective perception of ambiguous and bistable stimuli fluctuates over time despite identical and constant sensory input to the brain. Moreover, absolute detection thresholds for sensory perception can vary over time or over stimulus presentations. Several studies have shown that fluctuations of oscillatory neuronal activity can predict at least some of the perceptual variability. The state of oscillatory activity just prior to the onset of a stimulus influences whether the subsequent stimulation will be perceived, especially when stimuli are weak and near perceptual threshold. Among all frequency bands, alpha-band (~8 to 12 Hz) activity has gained much attention in recent years. It has been shown that prestimulus alpha-band power and phase in human parieto-occipital areas are correlated with conscious perception of visual stimuli (Thut et al. 2006; Hanslmayr et al. 2007; van Dijk et al. 2008; Mathewson et al. 2009; Mazaheri et al. 2009; Wyart and Tallon-Baudry 2009; Romei et al. 2010). Similarly in human somatosensory cortex, it has been shown that attentional or spontaneous fluctuations of prestimulus alpha-band activity influences perception of tactile stimuli. Linkenkaer-Hansen et al. (2004) showed that prestimulus amplitude of ongoing

alpha and beta oscillations in human somatosensory cortex correlates with subjects' ability to detect a subsequent weak tactile stimulus, with intermediate levels of amplitudes showing the highest detection rates. Moreover, it has been shown that the phase of alpha oscillations before stimulus onset influences subsequent perception (Palva et al. 2005). Recent studies have demonstrated that cued attention to somatosensory stimuli modulates prestimulus alpha- and beta-band activity in human somatosensory cortex in a spatially (Jones et al. 2010; van Ede et al. 2010, 2011; Anderson and Ding 2011) and temporally specific way (van Ede et al. 2011). In addition, prestimulus alpha- and beta-band amplitudes modulate the amplitude of the early stimulus-evoked M50 component of the event-related field (ERF) (Jones et al. 2009; Anderson and Ding 2011) and are correlated to behavioral detection rates of subsequent stimuli (Linkenkaer-Hansen et al. 2004; Jones et al. 2010), similar to findings in human visual cortex for alpha-band amplitudes (van Dijk et al. 2008). In summary, these results are in line with the hypothesis that ongoing fluctuations of oscillatory neuronal synchronization in the prestimulus period modulates the gain of neuronal assemblies and thus facilitates subsequent processing of sensory stimulation (Fries 2005, 2009; van Dijk et al. 2008).

Similar to the perception of a single stimulus, simultaneous perception of 2 tactile stimuli shows a considerable variation. Perception of simultaneity is a powerful cue for determining whether 2 events define a single or multiple objects. Perception of the relative timing of 2 events tolerates a moderate degree of temporal delays between sensory stimulations. However, this tolerance of temporal delays introduces a substantial degree of variability. For example, when 2 tactile stimuli are presented with a stimulus onset asynchrony (SOA) of ~30 to 70 ms, subjects show a considerable variation in their trial-by-trial responses when asked to judge whether the 2 stimulations were simultaneous or not, that is, asynchronously nonsimultaneously presented stimuli are frequently misperceived as simultaneous (Geffen et al. 2000; Kopinska and Harris 2004; Harrar and Harris 2005, 2008). The neurophysiological basis of this variability is not well understood.

In the present study, we used magnetoencephalography (MEG) to investigate the role of oscillatory neuronal activity for subjective perception of simultaneity and its variability. We employed a simultaneity task to study the role of prestimulus oscillatory activity for subjective perception. We focused on the somatosensory domain and compared conditions in which identical stimuli can lead to variable subjective perceptions on a trial-by-trial basis. These conditions offer an intriguing possibility to study the role of oscillatory neuronal synchronization under constant conditions of sensory stimulation (Rodriguez et al. 1999; Leopold et al. 2002).

## Materials and Methods

### Subjects

Twenty subjects participated in this study ( $24.9 \pm 3.8$  years [mean  $\pm$  standard deviation], 7 males). None of the subjects had a known history of neurological disorders, and subjects gave written informed consent in accordance with the Declaration of Helsinki.

### Paradigm and Stimuli

Subjects were seated comfortably with their head placed inside an MEG helmet and fixated a central gray dot on a screen positioned 60 cm in front of them. Each trial started with a decrease of luminance of the fixation dot, which served as the start cue (Fig. 1). After a randomized period of 800–1000 ms, subjects received short (0.3 ms) electrical pulses between the 2 distal joints of the left and right index finger to stimulate the cutaneous end branches of the digital nerves. The amplitude of the electric pulses was set to 60% of the individually determined subjective (mild) pain threshold level as measured prior to the recordings (mean amplitude  $5.5 \pm 0.7$  mA). Notably, subsequent analyses were performed on within-subject levels, that is, we always compared conditions of identical stimulation amplitudes (for details, see Data Analysis). Stimulation of the fingers was applied with varying SOAs of  $\pm 200$ ,  $\pm 45$ ,  $\pm 30$ , or 0 ms with negative SOA indicating that stimulation was first on the left finger. The condition of 0 ms was presented twice as often as the other SOA. SOA were chosen based on behavioral pilot experiments to ensure a balanced distribution of difficulty levels. After another random period of 800–1200 ms, in which only the fixation dot was visible, the fixation dot increased luminance indicating the start of the response window. Subjects were asked to report whether they had perceived the stimulation as simultaneous or nonsimultaneous by button presses. Button configurations were balanced within and between subjects: Half of the subjects responded with the middle fingers of both hands and half of the subjects responded with the index and middle finger of one hand (5 with the right hand and 5 with the left hand). For each subject, the button configuration was switched blockwise, that is, allocation of response finger and subjective report was balanced within and across subjects. Subjects were instructed to respond within 2000 ms after presentation of response instructions and that response speed was not taken into account. If no response was given after 2000 ms or subjects responded before the presentation of the instructions, a warning was visually presented. The respective trial was discarded from analyses and repeated at the end of the block. Except the warning signal, no feedback was given, and subjects were naïve to the different SOA used. Five repetitions of each SOA (i.e., 40 trials) constituted one block with stimuli within one block presented in pseudorandom order. Each block was repeated 10 times with self-paced breaks of  $\sim 2$  min in between. Response instructions for each block were visually presented on the screen before the start of each block. The experimental run was controlled using Presentation software (Neurobehavioral Systems,

Albany, NY). Subjects performed a training session of  $\sim 5$  min before the start of the MEG experiment.

### Data Acquisition and Analysis

#### Data Recording and Preprocessing

Neuromagnetic brain activity was continuously recorded using a 306-channel whole head MEG system (Neuromag Elekta Oy, Helsinki, Finland). Simultaneously, electrooculogram were recorded by placing electrodes above and below the left eye and on the outer sides of each eye. The data were recorded at a rate of 1000 Hz. Subjects' head position within the MEG helmet was registered by 4 coils placed at subjects' forehead and behind both ears. Individual full-brain high-resolution standard  $T_1$ -weighted structural magnetic resonance images (MRIs) were obtained from a 3-T MRI scanner (Siemens, Erlangen, Germany) and offline aligned with the MEG coordinate system using the coils and anatomical landmarks (nasion, left and right preauricular points).

MEG data were offline analyzed using FieldTrip (<http://www.ru.nl/donders/fieldtrip>), an open source matlab toolbox for neurophysiological data analysis (Oostenveld et al. 2011). Power line noise was removed from the continuous data using a discrete Fourier transformation of 10-s long signal periods to estimate the amplitudes and the phases of the 50, 100, and 150 Hz components. These components were subtracted from the continuous data as described earlier (Hoogenboom et al. 2006; van Ede et al. 2010, 2011; Lange et al. 2011). This was done separately for all 10-s periods around all periods of interest. Continuous data were segmented into trials, starting with the first appearance of the fixation dot and ending with appearance of instruction text. Artifacts caused by eye movements or muscle activity were removed using a semiautomated algorithm, and the linear trend was removed from each trial.

#### Time-Frequency Analysis

Time-frequency representations (TFRs) were computed applying a Fourier transformation on adaptive sliding time windows containing 5 full cycles of the respective frequency  $f$  ( $\Delta t = 5/f$ ), moved in steps of 25 ms (similar to Mazaheri et al. 2009; van Dijk et al. 2010; Haegens et al. 2011). Data segments were tapered with a single Hanning taper, resulting in a spectral smoothing of  $1/\Delta t$ .

Next, we determined regions of interest in sensor space. We chose 4 sensors in the left and 4 sensors in the right hemisphere covering bilateral primary somatosensory cortex (SI) and 4 sensors in the left and 4 sensors in the right hemisphere covering secondary somatosensory cortex (SII) (Fig. 3). The choice of sensors was based on previous studies (Bauer et al. 2006; Haegens et al. 2010; Hagiwara et al. 2010; van Ede et al. 2010, 2011). This set of sensors defined the somatosensory region of interest for subsequent analyses for all subjects. The set of sensors in the left and in the right hemisphere

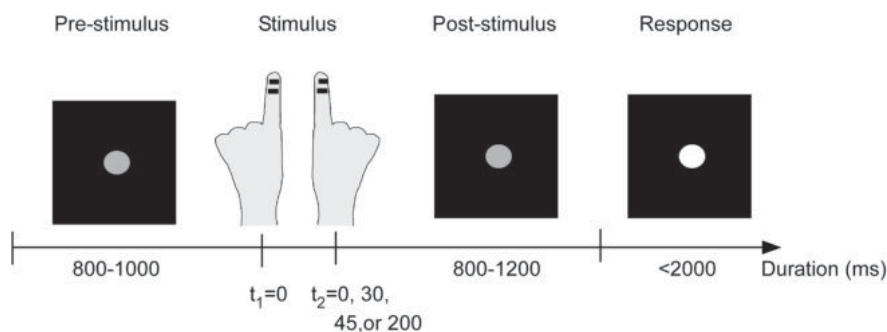


**Figure 1.** Schematic illustration of the paradigm. Subjects fixated a central gray dot throughout the entire trial. After 800–1000 ms, tactile stimulation was given to one index finger (right or left), followed by stimulation of the other finger after a randomized SOA (0, 30, 45, or 200 ms). After a jittered period (800–1200 ms), the luminance of the fixation dot increased, and subjects reported their subjective perception of simultaneity by pressing a button, upon which the next trial began (indicated by a luminance decrease of the fixation dot).

were symmetrically distributed with respect to the midline of the sensor array (Fig. 3*B,E,H,K*).

For each subject separately, we sorted trials with respect to the SOA. Within each SOA-bin, we compared trials with reports of subjective simultaneity to trials in which the stimulation was perceived as nonsimultaneous. Thus, we compared 2 conditions with identical physical stimulation that only differed with respect to the subjective perception. To this end, we averaged spectral power over the sensors of interest (see above) for each perceptual condition and compared both conditions by independent samples *t*-tests. This comparison was done independently for each time-frequency sample and thus resulted in a time-frequency *t*-map for each subject. Note that this comparison is not an actual statistical test but serves as a normalization of interindividual differences. This comparison was done separately for sensors in the left and right SI and SII. Only conditions with SOA of 30 and 45 ms were included in the analysis as only these conditions revealed a reasonably high number of trials for both perceptual conditions (simultaneous and nonsimultaneous). Behavioral and neuro-magnetic data revealed highly symmetrical patterns for positive and negative SOA (e.g., Fig. 2 for behavioral data), that is, no statistically significant differences were found when restricting the analyses to contra- or ipsilateral sites with respect to the site of the first stimulation. To increase statistical power, we pooled data regarding the site of the stimulation, that is, we report data in terms of contra- and ipsilateral to the site of the first stimulation. All *t* values of the time-frequency *t*-map were transformed to *z* values using SPM2 resulting in time-frequency *z*-maps (e.g., van Dijk et al. 2008; Mazaheri et al. 2009). For group-level statistics, we used the *z*-maps obtained for single subjects as inputs and determined their consistency across subjects. We used a nonparametric permutation approach that identifies clusters in time-frequency with significant changes. This effectively corrects for multiple comparisons (Maris and Oostenveld 2007; for details, see Lange et al. 2011). For statistical testing, the entire time window (–500 to 800 ms) was used. To generate topographical representations of statistically significant effects, we repeated the above-mentioned statistical comparison, but this time for each sensor independently, resulting in time-frequency *z*-maps for each sensor separately (instead of averaging over sensors). For each sensor, we averaged the *z* values over all individual time-frequency samples that correspond to the statistically significant time-frequency clusters in the above-mentioned analysis (as can be seen in, e.g., Fig. 3*A,B*). Finally, we plotted the averaged *z* values in a topographical representation (Fig. 3*B,E,H,K*).

#### Correlation of Prestimulus Power and Detection Rates

Next, we aimed to further investigate the correlation of prestimulus power to perception of simultaneity. First, we averaged spectral power over time, frequency, and sensors. Sensors of interest were defined as mentioned above (left and right SI and SII). Time-frequency bands of

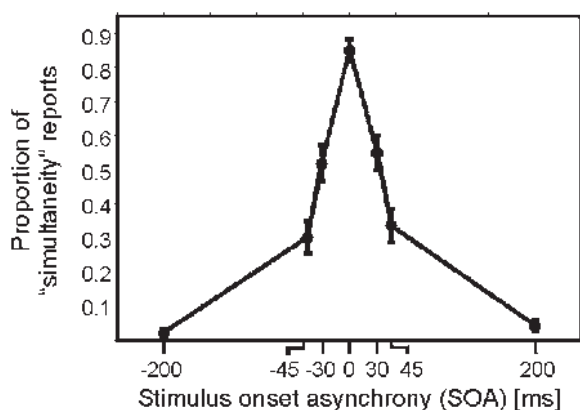


**Figure 2.** Behavioral results presented as proportion of simultaneity reports depending on SOA of left and right index finger stimulations. Negative SOA indicate that stimulation was applied first to the left index finger. Data are presented as mean  $\pm$  1 SEM.

interest were determined by the significant time-frequency clusters in the above-mentioned cluster-based statistical analysis on group level (Fig. 3*A,D,G,J*), resulting in 4 different time-frequency bands in the beta band. Since the significant clusters slightly differed in time and frequency for the different sensors of interest, time-frequency bands used to compute prestimulus power for the correlation analysis differed for each set of sensors of interest. The exact time-frequency bands for each analysis can be found in Figure 4.

Due to the relevance of prestimulus alpha-band power in somatosensory perception (Linkenkaer-Hansen et al. 2004; Jones et al. 2009, 2010; Anderson and Ding 2011; van Ede et al. 2011), we also included the alpha band into the analyses. The exact time-frequency bands used for each correlation analysis can be found in Figure 4. The averaging was done for each subject separately (with a common and fixed time-frequency-sensor triplet for all subjects, based on the group-level statistics). Subsequently, we sorted the single trials of each subject according to averaged power and divided all trials into 6 bins with equal number of trials. For each bin, we calculated the mean number of simultaneity reports and normalized the result for each subject. Finally, we computed the mean and standard error of the mean (SEM) over subjects and fitted linear and quadratic functions to the data to determine the best fit (Linkenkaer-Hansen et al. 2004; van Dijk et al. 2008; Jones et al. 2010).

#### Correlation of Prestimulus Power and ERFs

To study a potential relation between prestimulus alpha- and beta-band power and poststimulus ERFs (Jones et al. 2009, 2010; Anderson and Ding 2011), we correlated prestimulus power and ERFs in line with the above-mentioned analysis of prestimulus power and detection rates. To this end, we averaged power over time, frequency, and sensors. Sensors were chosen as defined above. Time-frequency bands were based on the significant clusters found in Figure 3*A,D,G,J*. Since the significant clusters slightly differed in time and frequency for the different sensors of interest, time-frequency bands used to compute prestimulus power differed for each set of sensors of interest. The exact time-frequency bands for each analysis can be found in Figure 5. Time-frequency bands were defined on group level, and the same time-frequency band was used for all subjects. Subsequently, we divided trials in 2 bins (low and high prestimulus alpha/beta power) and then computed the ERFs in the poststimulus period over the same sensors used for the power analyses (Jones et al. 2009, 2010). ERFs were computed by first applying a low-pass filter of 30 Hz, rectifying the signals by taking the root mean square of the signal in the time domain (e.g., Bauer et al. 2006; van Dijk et al. 2008; Mazaheri et al. 2009) and then averaging ERFs over trials and subjects. Statistical analysis was performed by applying dependent sample *t*-test between low and high power conditions for each time point.

#### Source Reconstruction

To determine the cortical sources of the significant effects on sensor level, we applied an adaptive spatial filtering technique in the frequency domain (Gross et al. 2001).

The leadfield matrix was computed for grid points in a realistically shaped single-shell volume conduction model, derived from the individual subject's structural MRI (Nolte 2003). To this end, a regular 3D 1-cm grid in the Montreal Neurological Institute template brain was created, and each subject's structural MRI was linearly warped onto this template. The inverse of this warp was applied to the template grid, resulting in individual grids based on individual subject's volume conduction model. The individual source parameters estimated in this way were combined across subjects per grid position. We aimed to determine the sources for the statistically significant effects revealed on sensor level (Fig. 3). To this end, we computed cross-spectral density (CSD) matrices between all MEG sensor pairs from the Fourier transforms of the tapered data epochs at the frequency of interest for each subject separately. The data epoch and the frequency of interest were based on the significant time-frequency clusters of the above-mentioned group analysis on sensor level (Fig. 3*A,D,G,J*). Since the significant clusters differed in time and frequency for the different sensors of interest, time-frequency bands used for source reconstruction differed for each condition. The exact time-frequency bands for

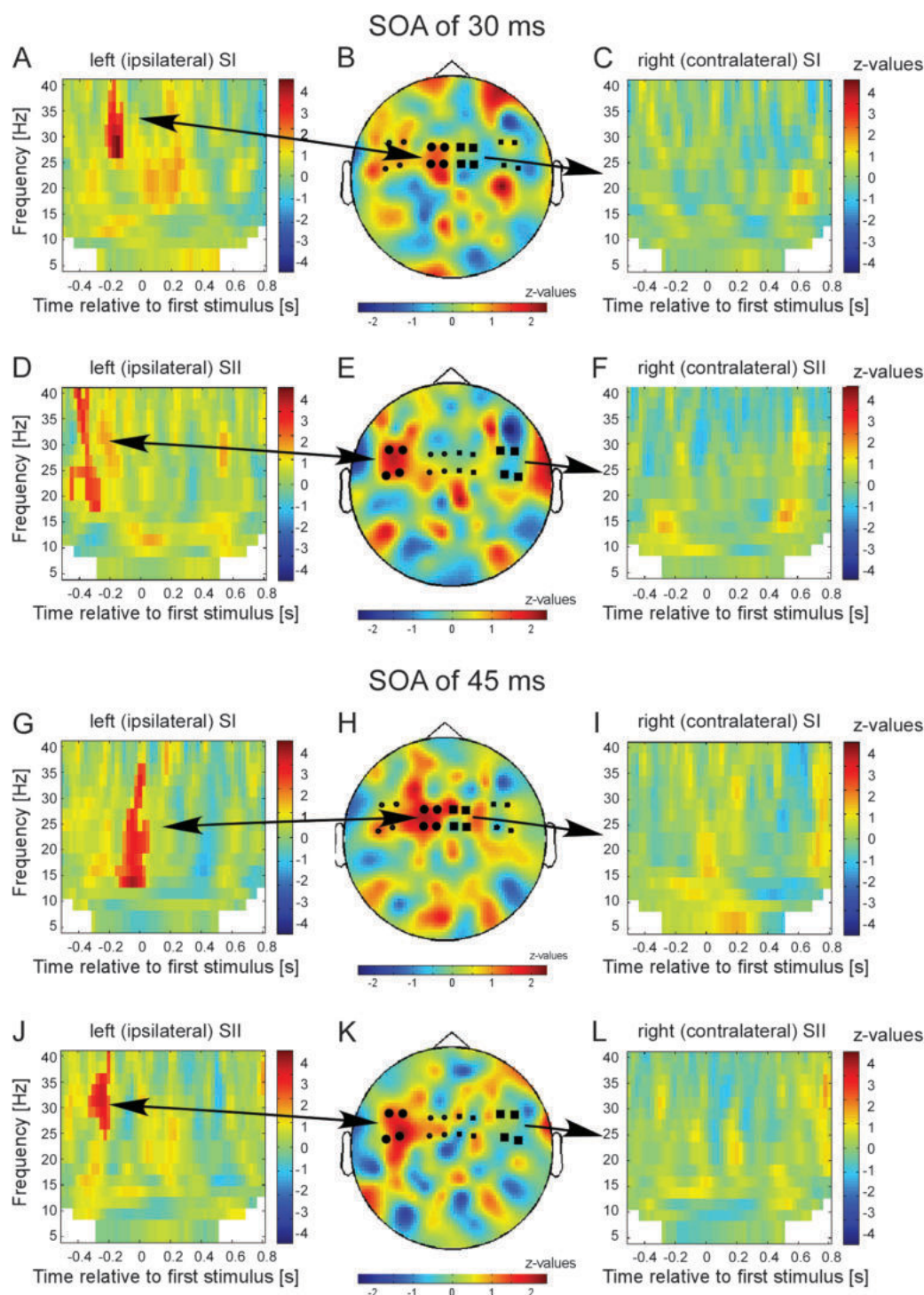


**Figure 3.** Results of the statistical comparison of trials with subjective simultaneity versus nonsimultaneity for conditions SOA 30 ms (A–F) and SOA 45 ms (G–L) for different sensor groups: (A) TFR for the 4 sensors over the left (ipsilateral) primary somatosensory cortex (SI) as indicated by the larger black circles in B. z values in nonsignificant pixels are lowered by 60% in order to highlight significant clusters. Color bars represent z values. Positive z values indicate higher power if subsequent stimulation was misperceived as simultaneously. (B) Topographical representation of the significant cluster as highlighted in A. Only time-frequency samples that correspond to the statistically significant time-frequency clusters in A were averaged to generate the topographical representation (for details, see Materials and Methods). (C) TFR for the 4 sensors over the right (contralateral) SI (as indicated by larger black squares). No significant clusters were found. (D) Same representation as in A but for 4 sensors over left (ipsilateral) secondary somatosensory cortex (SII). (E) Topographical representation for the significant cluster as highlighted in D. (F) TFR for the 4 sensors over the right (contralateral) SII (as indicated by larger black squares). (G–L) Same representation as in A–F but now for condition SOA of 45 ms.

each analysis can be found in Figure 6. Common spatial filters for each subject were computed using the CSD between all MEG sensor pairs, averaged over all trials of a given condition for the respective subject (pooled over subjective perceptions). For each subject, the CSD

matrices of single trials were then projected through those individual filters, providing single trial estimates of source power (Hoogenboom et al. 2010). Statistical testing on source level was performed in line with testing on sensor level (see above). Results were displayed on the

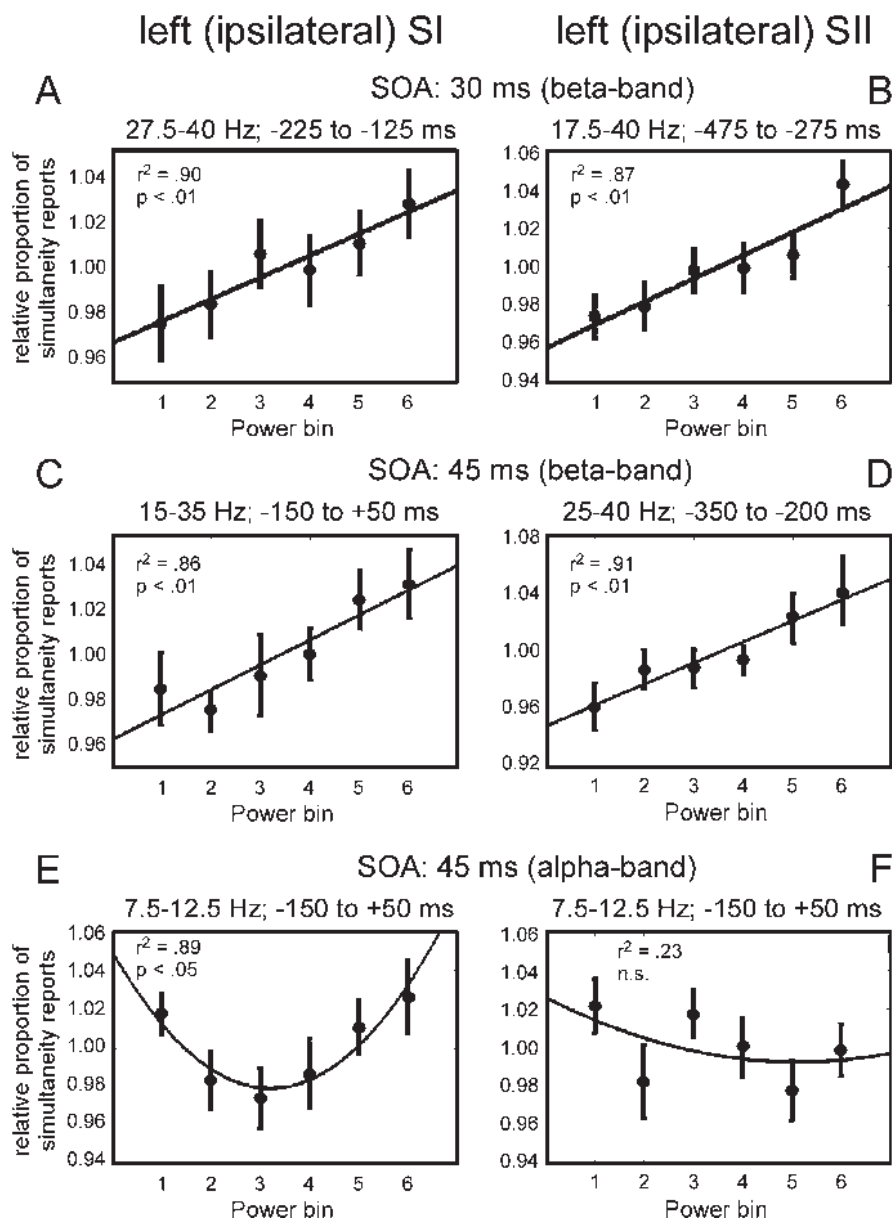


**Figure 4.** Regression analyses of the dependence of subjective perception on prestimulus oscillatory activity for the 4 significant clusters in the beta band (as shown in Fig. 3) and for the alpha band. The exact time–frequency bands to determine averaged prestimulus power bins are based on significant clusters in Figure 3 and are presented at the top of each figure. (A) Results for the significant cluster in the beta band for condition SOA 30 ms in sensors over ipsilateral SI (as highlighted in Fig. 3A). (B) Same analysis as in A but for the significant cluster in sensors over SII (as highlighted in Fig. 3D). (C–D) Same analysis as in A,B but for the significant clusters in the beta band for condition SOA 45 ms (as highlighted in Fig. 3G,J). For all regression analyses, a significant linear relationship was found ( $P < 0.01$ ). (E) Same analysis for the alpha band for condition SOA 45 ms in sensors over ipsilateral SI. A significant quadratic relationship was found. (F) Same analyses as in E but for sensors over SII. No significant relationship was found.

template brain, and cortical sources were identified using the AFNI atlas (<http://afni.nimh.nih.gov/afni>), integrated into FieldTrip.

## Results

### Behavioral Results

Subjects were asked to report their subjective percept of simultaneity for electrical stimuli delivered to their left and right index finger with different SOAs. They made negligible errors for SOA of 0 and 200 ms (Fig. 2). However, intermediate SOA were perceived as simultaneous in some trials and as not simultaneous in other trials (SOA of  $-30$  ms:  $51.8 \pm 5.5\%$  (mean  $\pm$  SEM) simultaneity reports; SOA of  $+30$  ms:  $54.9 \pm 5.2\%$ ; SOA of  $-45$  ms:  $30.2 \pm 4.8\%$ ; and SOA of  $+45$  ms:  $33.6 \pm 4.8\%$ ).

### Condition Contrasts

Next, we studied the role of oscillatory activity for the perception of simultaneity. Within each SOA we sorted trials with respect to subjects' perceptual reports. We compared spectral power between reports of simultaneity and reports of nonsimultaneity in sensors over sensorimotor areas.

For SOA of 30 ms, we found spectral power in sensors over ipsilateral primary somatosensory cortex (SI) to be statistically significantly enhanced in the frequency band 27.5–40 Hz if subjects perceived the stimulation erroneously as simultaneous. Notably, this effect occurred between  $-225$  and  $-125$  ms, that is, the effect appeared already before any electrical stimulation was delivered, and the effect was only present in ipsilateral sensors (Fig. 3A). In line with these findings, the

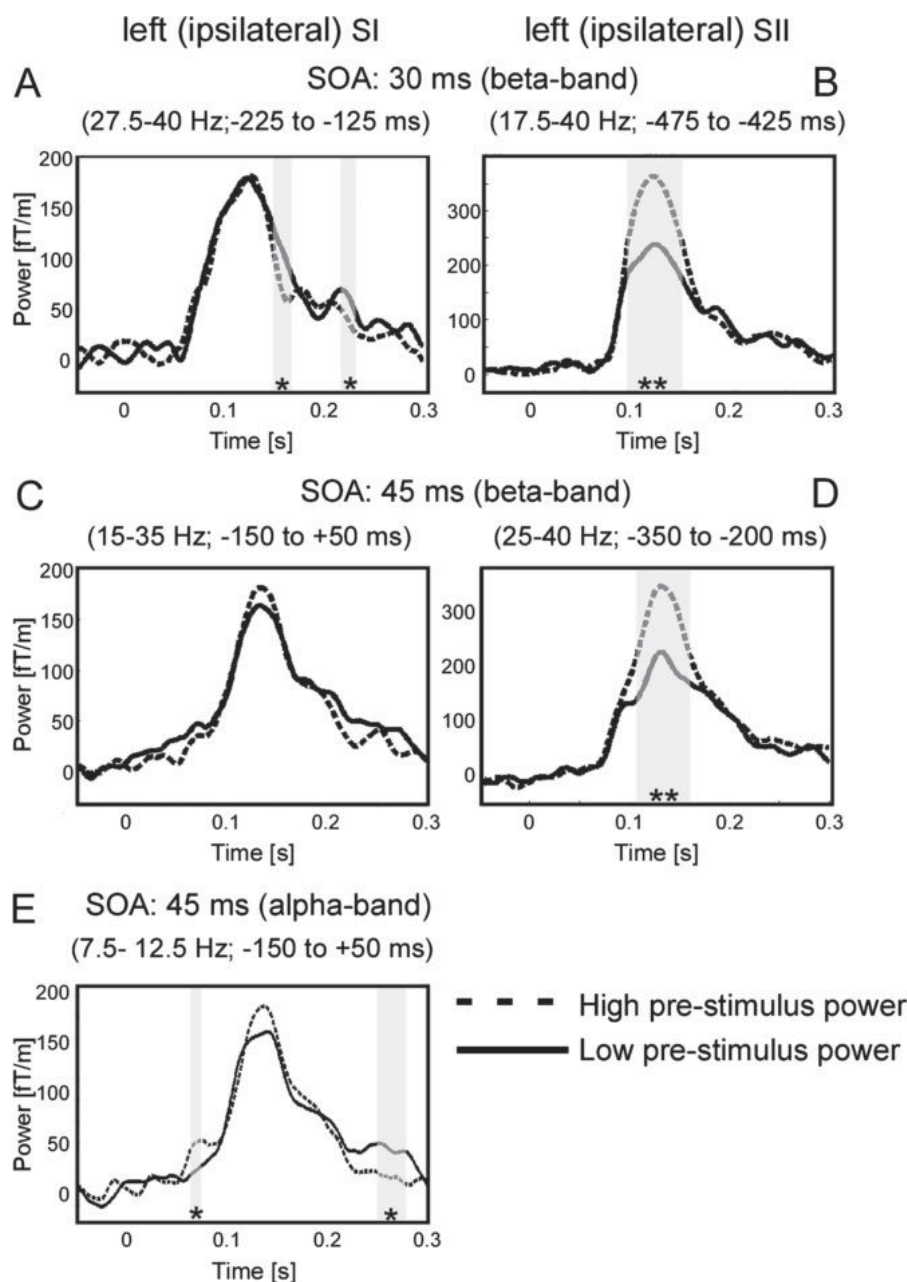


**Figure 5.** Dependence of poststimulus ERF amplitudes on prestimulus power for the 4 significant clusters in the beta band (as shown in Fig. 3) and for the alpha band. The exact time–frequency bands to determine averaged prestimulus power bins are based on significant clusters in Figure 3 and are presented at the top of each figure. (A) Results for the significant cluster in the beta band for condition SOA 30 ms in sensors over ipsilateral SI (as highlighted in Fig. 3A). (B) Same analysis as in A, but for the significant cluster in sensors over SII (as highlighted in Fig. 3D). (C–D) Same analysis as in A,B but for the significant clusters in the beta band for condition SOA 45 ms (as highlighted in Fig. 3G,J). (E) Same analysis for the alpha band for condition SOA 45 ms in sensors over ipsilateral SI. Significant differences ( $*P < 0.05$ ,  $**P < 0.01$ ) are indicated by gray shaded areas.

topographical representation of this effect revealed a focus on sensors over ipsilateral SI (Fig. 3B). In sensors over secondary somatosensory cortex (SII), power was statistically significantly enhanced in the frequency band 17.5–40 Hz between –475 and –275 ms (Fig. 3D). The topographical representation revealed a focus over ipsilateral SII (Fig. 3E). No significant differences were observed in contralateral sensors (Fig. 3C,F).

For SOA of 45 ms, a similar finding was observed. In sensors over ipsilateral SI, oscillatory activity between 15–35 Hz and –150 to 50 ms was enhanced if subjects perceived the following stimulation erroneously as simultaneous (Fig. 3G,H). In sensors over ipsilateral SII, oscillatory activity between 25–40 Hz and

–350 to –200 ms was significantly enhanced (Fig. 3J,K). Contralateral sensors did not show any significant differences (Fig. 3I,L).

#### **Correlation of Prestimulus Power and Detection Rates**

We found spectral power in alpha- and beta-frequency bands to be enhanced before and around the onset of stimulation, when subjects incorrectly perceived the 2 subsequent stimuli as simultaneous. To study the relation between subjective perception of stimuli and prestimulus oscillatory activity, we performed a correlation analysis. To this end, in each trial spectral power was averaged over sensors, time, and

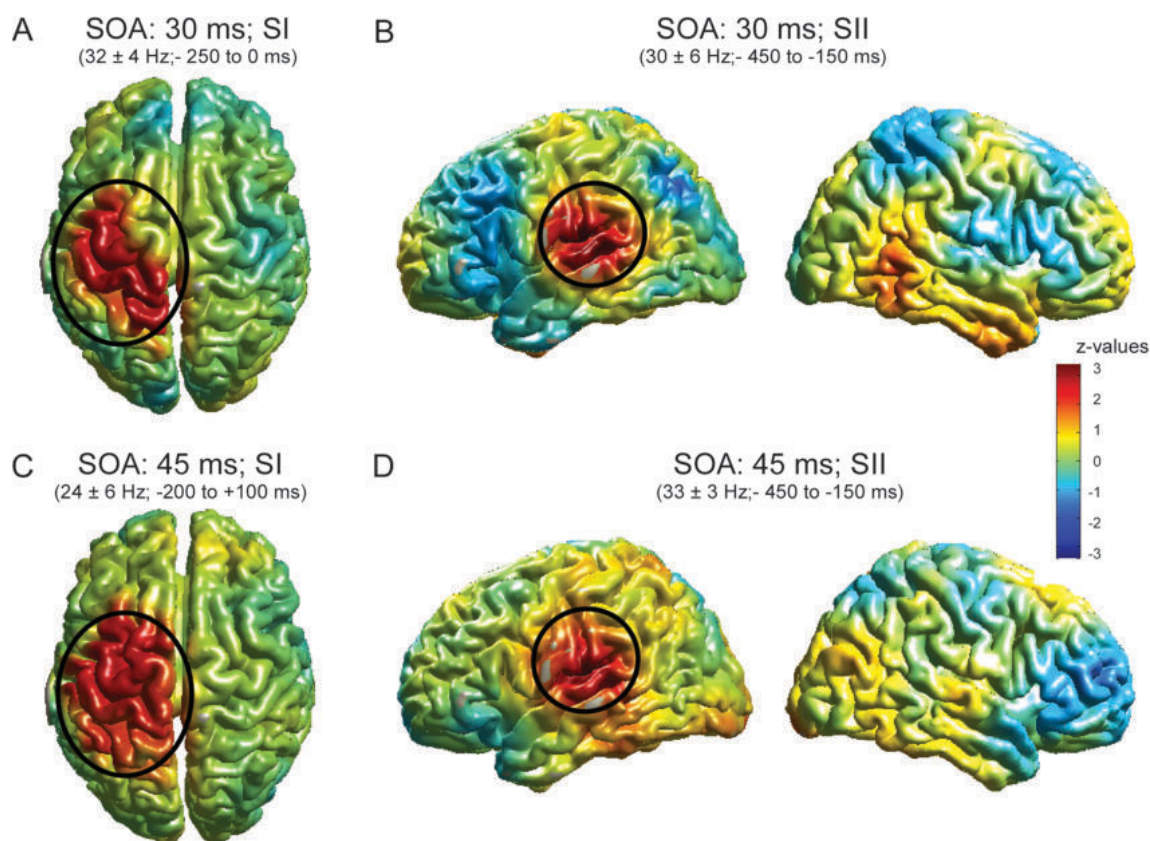


**Figure 6.** Source analysis of significant clusters as found in Figure 3. The exact time–frequency bands used for source reconstruction are based on significant clusters in Figure 3 and are presented at the top of each figure. (A) Results for the significant cluster in the beta band for condition SOA 30 ms (as highlighted in Fig. 3A). z values in nonsignificant regions are lowered by 60% in order to highlight significant clusters. Additionally, significant clusters are highlighted by ovals. (B) Same as in A but for beta-band effect as highlighted in Figure 3D. Left column: view of the left hemisphere, right column: view of the right hemisphere. (C, D) Same as in A and B but for beta-band effect in SOA 45 ms (as highlighted in Fig. 3G,J). The color bar applies to all figures.

frequencies. Next, trials were sorted for spectral power and divided into 6 bins (Linkenkaer-Hansen et al. 2004; van Dijk et al. 2008; Jones et al. 2010). The perceptual reports were normalized per subject and then averaged over subjects. For the 4 cluster in the beta range in ipsilateral SI and SII (see Fig. 3A,D,G,J), we found a significant linear relationship between prestimulus power and subjects' perceptual reports in ipsilateral sensors for all conditions (SOA of 30 ms: SI:  $r^2 = 0.90$ ,  $P < 0.01$ ; SII:  $r^2 = 0.87$ ,  $P < 0.01$ ; SOA of 45 ms: SI:  $r^2 = 0.86$ ,  $P < 0.01$ ; SII:  $r^2 = 0.91$ ,  $P < 0.01$ ; Fig. 4A–D), that is, high prestimulus power was correlated with a high number of erroneous simultaneity reports. In contrast, we did not find a significant correlation in contralateral sensors (Supplementary Fig. S1). Additionally, we performed the same analysis for the alpha band in the condition SOA of 45 ms. We observed a quadratic relationship between subjective perception and prestimulus oscillatory activity in SI, with intermediate power bins showing the lowest probability of simultaneity reports ( $r^2 = 0.89$ ,  $P < 0.05$ ; Fig. 4E). In other words, intermediate alpha amplitudes were associated with a more veridical perception of non-simultaneity. No significant correlation was found in contralateral sensors (Supplementary Fig. S1).

#### Correlation of Prestimulus Power and ERFs

We additionally analyzed the correlation between prestimulus alpha-/beta-band activity and poststimulus ERFs (Jones et al. 2009, 2010; Anderson and Ding 2011).

First, we sorted trials in the condition SOA of 30 ms for power in ipsilateral sensors over SI in the time–frequency band between 27.5–40 Hz and –225 to –125 ms (i.e., the significant cluster in Fig. 3A). Trials with low prestimulus beta-band power revealed a significant increase of the ERFs between 150–168 and 216–232 ms (Fig. 5A). Trials with high prestimulus beta-band power in sensors over SII revealed increased ERFs between 93 and 148 ms (Fig. 5B).

For the condition SOA of 45 ms, we found no significant effects of prestimulus beta-band power on ERFs for sensors over SI (Fig. 5C). Sensors over SII revealed increased ERFs for trials with high beta-band power between 107 and 162 ms (Fig. 5D). Additionally, we sorted trials for prestimulus power in the alpha band. Sensors over SI revealed increased ERFs for trials with high prestimulus power between 64 and 75 ms. Furthermore, trials with low prestimulus power revealed increased ERFs between 250 and 278 ms (Fig. 5E).

#### Source Localization

To identify the cortical sources of the significant effects found in TFRs on sensor level (Fig. 3), we applied a beamforming approach. For both conditions (SOA of 30 and 45 ms), the comparatively late (–200 to 0 ms) significant components (Fig. 3A,G) revealed a significant source in ipsilateral sensorimotor areas with the peak located in ipsilateral SI (SOA of 30 ms:  $P < 0.05$ ; SOA of 45 ms:  $P < 0.05$ , Fig. 6A,C). For both conditions, the earlier component (–450 to –250 ms) was

located in ipsilateral SII (SOA of 30 ms:  $P < 0.05$ ; SOA of 45 ms:  $P < 0.05$ , Fig. 6B,D).

## Discussion

We studied the contribution of oscillatory neuronal activity to subjective perception of brief electrical stimuli applied bilaterally to the index fingers with varying SOAs. We were interested whether fluctuations of spectral power predict subjective perception. Crucially, the paradigm enabled us to study the role of neuronal oscillatory under conditions of constant physical stimulation while only the subjective perception was changed intrinsically.

When SOA was 30 or 45 ms, subjects frequently misperceived the stimulation as simultaneous. Erroneous perception of simultaneity was associated in both conditions (SOA 30 and 45 ms) with an increase of power in the beta band (~20 to 30 Hz) in sensors over primary (SI) and secondary (SII) somatosensory cortex. The increase was evident in the cortical hemisphere ipsilateral to the site of the first stimulation but not in contralateral sites. Notably, this increase was visible before the onset of stimulation and the significant differences appeared earlier in sensors over SII than in sensors over SI. Source reconstruction confirmed a priori sensor selection by revealing significant cortical sources of the earlier effects (found in sensors presumably over SII at ~-450 to -250 ms) in ipsilateral SII. The relatively later effects (~-200 to 0 ms, observed in sensors presumably over SI) were located in ipsilateral sensorimotor areas with the peak located in SI. It should be noted that the source reconstruction was performed on prestimulus data, that is, in the absence of any stimulation. Without stimulation, absolute power levels have a smaller signal-to-noise ratio than power values in response to stimulation. Low signal-to-noise ratios naturally limit beamforming results by making also the sources noisier and thus spatially smeared. Furthermore, the observed significant effects are relatively short lived which also limits beamforming techniques. Despite these limitations and although the significant sources appear spatially smeared, their origins can be clearly assigned to SI and SII and are in good agreement in terms of location and quality with other findings of prestimulus power changes (Haegens et al. 2010, 2011; van Ede et al. 2011). In addition, the topographical representations imply weak activations in other cortical areas, presumably frontal and parietal areas (Fig. 3). However, none of these areas was found to be significantly activated in the source analysis. Reasons for the lack of significance might be that the effects in these areas were less strong than in the somatosensory areas or less consistent over subjects. Further studies need to unravel the contribution of nonsensory areas to the perception of simultaneity.

Notably, all reported effects were observed prior to onset of stimulation. We found prestimulus power in the beta (~20 to 30 Hz) band in both ipsilateral SI and SII to be linearly correlated to perceptions of nonsimultaneity, that is, veridical perception was highest for low prestimulus amplitudes. In addition, alpha-band power in ipsilateral SI revealed a quadratic relation to perception of simultaneity for condition SOA of 45 ms, that is, veridical perception was highest for intermediate states of prestimulus alpha power.

One potential concern in the interpretation of the results might be that the effects are caused by motor preparation. It is well known that alpha- and beta-band power in sensorimotor

cortex can be modulated by motor preparation and execution (e.g., Hari and Salmelin 1997). For several reasons, however, it is unlikely that our reported effects are related to motor preparation:

To minimize the influence of premovement power changes, we had included a jittered interval of 800–1200 ms after stimulus presentation before occurrence of the response cue. Subjects responded on average  $539 \pm 36$  ms after the response cue. Thus, while subjects responded on average ~1500 ms after stimulus presentation, significant differences in oscillatory activity were found ~0 to 400 ms before stimulus presentation. In contrast, no significant differences were found in the poststimulus period prior to button presses. Consequently, we did not find any correlation between prestimulus power and reaction times (data not shown). Furthermore, response configurations were balanced across and within subjects so that the response hand and the site of the first stimulation were unrelated. Taken together, due to the setup and the timing of the significant effects, it is highly unlikely that the observed effects are due to motor preparation.

Recent studies investigated the influence of attention on prestimulus alpha- and beta-band power and their impact on tactile detection (Linkenkaer-Hansen et al. 2004; Jones et al. 2009, 2010; van Ede et al. 2010, 2011; Anderson and Ding 2011). These studies reported prestimulus effects to be lateralized contralaterally to the side of the stimulation. While in these studies, stimulation was applied unilaterally, and the side of stimulation was cued, we applied stimulation bilaterally, and the site of the first stimulation was unknown (i.e., randomized from trial to trial). Therefore, we did not expect attention to be lateralized. In line with this, we found prestimulus power modulations bilaterally rather than lateralized. In addition, fluctuations of prestimulus power modulations do significantly affect perception of subsequent stimuli and that these effects are lateralized with respect to the site of the first stimulation. While there are also poststimulus modulations of oscillatory activity in both hemispheres in response to bilateral stimulation, Figure 3 reveals that these modulations do not differ for the 2 subjective reports. In other words, poststimulus modulations of spectral power do not correlate with subjective perception of simultaneity.

In line with our findings, Jones et al. (2010) reported a linear relationship for veridical perception of tactile stimuli and prestimulus alpha-/beta-band power. While Jones et al. explicitly studied the effects in SI, we observed the effects in both, SI and SII. While we and Jones et al. found a linear relationship, Linkenkaer-Hansen et al. (2004) reported a quadratic relationship between prestimulus beta-band activity in sensorimotor areas and subjects' performance in a tactile detection task. A possible reason for these different findings of Linkenkaer-Hansen et al. might be that they used much broader time and frequency bands for their analyses.

In addition, studies reported that intermediate amplitudes of prestimulus alpha-band oscillations in sensorimotor areas were optimal for perception of weak tactile stimuli (Linkenkaer-Hansen et al. 2004; Zhang and Ding 2010). In line with these studies, we found a quadratic relationship between prestimulus alpha-band activity and simultaneity reports in sensors over SI, that is, veridical perception of simultaneity was highest for intermediate states of prestimulus alpha-band activity. In contrast, a linear relationship between prestimulus alpha-band activity and detection probabilities of tactile stimuli has been

reported by Jones et al. (2010). Differences might be attributable to different tasks: While Jones et al. employed a cued attention task, subjects in our study were asked to report subjective simultaneity.

Several studies reported a correlation of prestimulus power and poststimulus ERFs (Jones et al. 2009, 2010; Zhang and Ding 2010; Anderson and Ding 2011). In line with previous studies (Jones et al. 2009, 2010; Anderson and Ding 2011), we found that trials with a high prestimulus power in the alpha band revealed increased ERFs between 64 and 75 ms in ipsilateral SI, which is likely to represent the early evoked M20/M50 component to electrical or mechanical stimulation. Note that the time scale is always presented relative to the presentation of the first stimulus, while the reported effects are always in the hemisphere contralateral to the site of the second stimulation. Due to this shift in stimulation parameters, we expect ERFs to be shifted by 30 or 45 ms, respectively. In their computational study, Jones et al. (2009) suggested that an increased M50 component might be caused by greater levels of recruited inhibition, subsequently decreasing the effect of excitatory cells. Notably, we found an increased early ERF component only in ipsilateral SI and only for the condition SOA of 45 ms, suggesting that the proposed inhibition processes induced by prestimulus alpha-band power influence only the (interhemispheric) processing of stimuli spaced 45 ms but not stimuli spaced 30 ms. We suggest that with higher prestimulus power, that is, with early inhibiting poststimulus processes, the second stimulus might be processed less efficiently, leading to a lower temporal precision and thus more incorrect reports in the perception of simultaneity.

In addition, we found that trials with low prestimulus beta-band power revealed a lower M100 peak (at ~130 ms for SOA of 30 ms and at ~145 ms for SOA of 45 ms, for discussion of the temporal shift of the M100 component, see above). Studies in human and nonhuman primates have demonstrated subsequent attenuation of ipsilateral somatosensory responses after contralateral tactile stimulation (Simões and Hari 1999; Simões et al. 2001; Hlushchuk and Hari 2006; Tommerdahl et al. 2006; Reed et al. 2011; Wühle et al. 2011) with the maximum attenuation for peaks at ~100 ms (Simões et al. 2001; Wühle et al. 2011). Our results suggest that the attenuation is mediated by prestimulus states of the beta band. The correlation of beta-band power and ERFs was only found in sensors over ipsilateral SII but not in SI. Since SII receives input from both body sides and bilateral SI, it is a likely candidate for integration of bilateral sensory input. One potential explanation might be that the stronger attenuation of the M100 component reflects stronger interhemispheric interaction, which in turn is modulated by prestimulus states in the beta band.

The above-mentioned studies (Linkenkaer-Hansen et al. 2004; Jones et al. 2010) have argued that prestimulus alpha- and beta-band activity influences the perception and detection of tactile stimuli. In line with this hypothesis, we suggest that subjective perception of simultaneity strongly depends on the veridical perception of the second stimulus. If prestimulus alpha- and beta-band activity is at optimal states, the likelihood to detect the second stimulus is high. This in turn promotes veridical perception of the 2 stimuli as temporally separate. We report beta-band effects in SI and SII, while most previous studies reported prestimulus effects mainly in SI (Linkenkaer-Hansen et al. 2004; Jones et al. 2009, 2010; van Ede et al. 2010, 2011; Zhang and Ding 2010; Anderson and Ding 2011). One

crucial difference is that we used bilateral stimulation, while the above-mentioned studies always used unilateral stimulation. Prestimulus activity in SII might therefore be relevant for bilateral integration of tactile stimuli or gating of information but less crucial for unilateral perception. However, it should be mentioned that prestimulus effects in the beta band have been reported also in SII before (Linkenkaer-Hansen et al. 2004). Another crucial difference is that previous studies explicitly or implicitly incorporated a spatial attention task where subjects had to direct attention to one body side. It might be possible that spatial attention is more strongly confined to SI, while bilateral interaction is more strongly relying on SI and SII.

Our main finding was that for both conditions (SOA of 30 and 45 ms) prestimulus beta-band activity was increased in SI and SII when stimulation was erroneously perceived as simultaneously. Several studies have reported involvement of beta-band oscillations in top-down modulations of attention or the perception of bistable stimuli (von Stein et al. 2000; Engel et al. 2001; Gross et al. 2004; Buschman and Miller 2007; Kranczioch et al. 2007; Pesaran et al. 2008; van Elswijk et al. 2010). In their computational study, Jones et al. (2010) suggested that prestimulus alpha-band activity modulates feedforward bottom-up processing, while beta-band activity reflects both feedforward and feedback modulations of cortical processes. Similarly, Engel and Fries (2010) suggested that beta-band activity plays a role in endogenous top-down modulation of cognitive processes. According to this hypothesis, low amplitudes of beta-band oscillations should promote bottom-up stimulus-driven processing, while high amplitudes should increase the threshold for the responses to novel unexpected stimuli. In line with this hypothesis, we suggest that fluctuations of prestimulus beta oscillations determine the threshold for detecting stimuli. An increase of beta activity impairs bottom-up processing, therefore renders distinct temporal detection of the first and the second stimulus more unlikely and thus biases (incorrect) simultaneous reports. Several studies also found interareal coherence mainly in the beta band (Gross et al. 2004; Kranczioch et al. 2007; Hipp et al. 2011). A recent study found increased prestimulus beta-band activity in superior temporal gyrus associated with the (incorrect) perception of the bistable McGurk illusion (Keil et al. 2011). We suggest that the perception of bistable stimuli (such as McGurk effect, attentional blink or our paradigm of simultaneity perception) is strongly influenced by ongoing network fluctuations in the beta band.

Similar to the attentional blink paradigm, in our paradigm the second of 2 subsequent stimuli is frequently misperceived. Both paradigms require thus a high temporal resolution of sensory perception. We propose that low states of beta oscillations prior to the sensory stimulation promote a processing of stimuli, while states of high beta amplitudes increase the threshold for sensory processing and make perception less accurate, especially for weak near-threshold stimuli (Engel and Fries 2010). In our case, less accurate (temporal) perception might bias simultaneity reports.

Prolonged SOA will lead to more veridical reports, that is, prolonged SOA will decrease the degree of ambiguity or bistability (Fig. 2). Subjective perception for prolonged SOA thus might be less influenced by small fluctuations of ongoing fluctuations of oscillatory activity. Additional components might thus be necessary to further increase perceptual threshold. One component might be inhibited bottom-up

processing of sensory input in SI by alpha-band activity (Jones et al. 2009). In line with this hypothesis, we additionally found increased prestimulus alpha power for subjective perception of simultaneity in condition with SOA of 45 ms.

In summary, we found that prestimulus activity in the alpha and high beta band predicts the subjective perception of electrical simultaneity. We propose that states of prestimulus alpha- and beta-band activity determine perceptual detection thresholds for tactile and electrical stimuli (Engel and Fries 2010). Modulations in the beta band were found in SI and SII, while alpha-band modulations were found in SI. We suggest that these regions communicate in the respective frequency bands and thus control bottom-up and top-down information flow. The results mount on recent evidence and extend findings emphasizing the role of prestimulus oscillatory activity for perception.

### Supplementary Material

Supplementary material can be found at: <http://www.cercor.oxfordjournals.org/>

### Notes

*Conflict of Interest* : None declared.

### References

- Anderson KL, Ding M. 2011. Attentional modulation of the somatosensory mu rhythm. *Neuroscience*. 180:165–180.
- Bauer M, Oostenveld R, Peeters M, Fries P. 2006. Tactile spatial attention enhances gamma-band activity in somatosensory cortex and reduces low-frequency activity in parieto-occipital areas. *J Neurosci*. 26:490–501.
- Buschman TJ, Miller EK. 2007. Top-down versus bottom-up control of attention in the prefrontal and posterior parietal cortices. *Science*. 315:1860–1862.
- Engel AK, Fries P. 2010. Beta-band oscillations—signalling the status quo? *Curr Opin Neurobiol*. 20:156–165.
- Engel AK, Fries P, Singer W. 2001. Dynamic predictions: oscillations and synchrony in top-down processing. *Nat Rev Neurosci*. 2:704–716.
- Fries P. 2005. A mechanism for cognitive dynamics: neuronal communication through neuronal coherence. *Trends Cogn Sci*. 9:474–480.
- Fries P. 2009. Neuronal gamma-band synchronization as a fundamental process in cortical computation. *Annu Rev Neurosci*. 32:209–224.
- Geffen G, Rosa V, Luciano M. 2000. Sex differences in the perception of tactile simultaneity. *Cortex*. 36:323–335.
- Gross J, Kujala J, Hamalainen M, Timmermann L, Schnitzler A, Salmelin R. 2001. Dynamic imaging of coherent sources: studying neural interactions in the human brain. *Proc Natl Acad Sci U S A*. 98:694–699.
- Gross J, Schmitz F, Schnitzler I, Kessler K, Shapiro K, Hommel B, Schnitzler A. 2004. Modulation of long-range neural synchrony reflects temporal limitations of visual attention in humans. *Proc Natl Acad Sci U S A*. 101:13050–13055.
- Haegens S, Handel BF, Jensen O. 2011. Top-down controlled alpha band activity in somatosensory areas determines behavioral performance in a discrimination task. *J Neurosci*. 31:5197–5204.
- Haegens S, Osipova D, Oostenveld R, Jensen O. 2010. Somatosensory working memory performance in humans depends on both engagement and disengagement of regions in a distributed network. *Hum Brain Mapp*. 31:26–35.
- Hagiwara K, Okamoto T, Shigetoh H, Ogata K, Somehara Y, Matsushita T, Kira J, Tobimatsu S. 2010. Oscillatory gamma synchronization binds the primary and secondary somatosensory areas in humans. *Neuroimage*. 51:412–420.
- Hanslmayr S, Aslan A, Staudigl T, Klimesch W, Herrmann CS, Bauml KH. 2007. Prestimulus oscillations predict visual perception performance between and within subjects. *Neuroimage*. 37:1465–1473.
- Hari R, Salmelin R. 1997. Human cortical oscillations: a neuromagnetic view through the skull. *Trends Neurosci*. 20:44–49.
- Harrar V, Harris LR. 2005. Simultaneity constancy: detecting events with touch and vision. *Exp Brain Res*. 166:465–473.
- Harrar V, Harris LR. 2008. The effect of exposure to asynchronous audio, visual, and tactile stimulus combinations on the perception of simultaneity. *Exp Brain Res*. 186:517–524.
- Hipp JF, Engel AK, Siegel M. 2011. Oscillatory synchronization in large-scale cortical networks predicts perception. *Neuron*. 69:387–396.
- Hlushchuk Y, Hari R. 2006. Transient suppression of ipsilateral primary somatosensory cortex during tactile finger stimulation. *J Neurosci*. 26:5819–5824.
- Hoogenboom N, Schoffelen JM, Oostenveld R, Fries P. 2010. Visually induced gamma-band activity predicts speed of change detection in humans. *Neuroimage*. 51:1162–1167.
- Hoogenboom N, Schoffelen JM, Oostenveld R, Parkes LM, Fries P. 2006. Localizing human visual gamma-band activity in frequency, time and space. *Neuroimage*. 29:764–773.
- Jones SR, Kerr CE, Wan Q, Pritchett DL, Hamalainen M, Moore CI. 2010. Cued spatial attention drives functionally relevant modulation of the mu rhythm in primary somatosensory cortex. *J Neurosci*. 30:13760–13765.
- Jones SR, Pritchett DL, Sikora MA, Stufflebeam SM, Hamalainen M, Moore CI. 2009. Quantitative analysis and biophysically realistic neural modeling of the MEG mu rhythm: rhythmogenesis and modulation of sensory-evoked responses. *J Neurophysiol*. 102:3554–3572.
- Keil J, Muller N, Ihssen N, Weisz N. Forthcoming 2011. On the variability of the McGurk effect: audiovisual integration depends on prestimulus brain states. *Cereb Cortex*. doi: 10.1093/cercor/bhr125.
- Kopinska A, Harris LR. 2004. Simultaneity constancy. *Perception*. 33:1049–1060.
- Kranzloch C, Debener S, Maye A, Engel AK. 2007. Temporal dynamics of access to consciousness in the attentional blink. *Neuroimage*. 37:947–955.
- Lange J, Oostenveld R, Fries P. 2011. Perception of the touch-induced visual double-flash illusion correlates with changes of rhythmic neuronal activity in human visual and somatosensory areas. *Neuroimage*. 54:1395–1405.
- Leopold DA, Wilke M, Maier A, Logothetis NK. 2002. Stable perception of visually ambiguous patterns. *Nat Neurosci*. 5:605–609.
- Linkenkaer-Hansen K, Nikulin VV, Palva S, Ilmoniemi RJ, Palva JM. 2004. Prestimulus oscillations enhance psychophysical performance in humans. *J Neurosci*. 24:10186–10190.
- Maris E, Oostenveld R. 2007. Nonparametric statistical testing of EEG- and MEG-data. *J Neurosci Methods*. 164:177–190.
- Mathewson KE, Gratton G, Fabiani M, Beck DM, Ro T. 2009. To see or not to see: prestimulus alpha phase predicts visual awareness. *J Neurosci*. 29:2725–2732.
- Mazaheri A, Nieuwenhuis IL, van DH, Jensen O. 2009. Prestimulus alpha and mu activity predicts failure to inhibit motor responses. *Hum Brain Mapp*. 30:1791–1800.
- Nolte G. 2003. The magnetic lead field theorem in the quasi-static approximation and its use for magnetoencephalography forward calculation in realistic volume conductors. *Phys Med Biol*. 21:3637–3652.
- Oostenveld R, Fries P, Maris E, Schoffelen JM. 2011. FieldTrip: open source software for advanced analysis of MEG, EEG, and invasive electrophysiological data. *Comput Intell Neurosci*. 2011:156869.
- Palva S, Linkenkaer-Hansen K, Näätänen R, Palva JM. 2005. Early neural correlates of conscious somatosensory perception. *J Neurosci*. 25:5248–5258.
- Pesaran B, Nelson MJ, Andersen RA. 2008. Free choice activates a decision circuit between frontal and parietal cortex. *Nature*. 453:406–409.
- Reed JL, Qi HX, Kaas JH. 2011. Spatiotemporal properties of neuron response suppression in owl monkey primary somatosensory cortex when stimuli are presented to both hands. *J Neurosci*. 31:3589–3601.

- Rodriguez E, George N, Lachaux JP, Martinerie J, Renault B, Varela FJ. 1999. Perception's shadow: long-distance synchronization of human brain activity. *Nature*. 397:430-433.
- Romei V, Gross J, Thut G. 2010. On the role of prestimulus alpha rhythms over occipito-parietal areas in visual input regulation: correlation or causation? *J Neurosci*. 30:8692-8697.
- Simões C, Hari R. 1999. Relationship between responses to contra- and ipsilateral stimuli in the human second somatosensory cortex SII. *Neuroimage*. 10:408-416.
- Simões C, Mertens M, Forss N, Jousmäki V, Lütkenhöner B, Hari R. 2001. Functional overlap of finger representations in human SI and SII cortices. *J Neurophysiol*. 86:1661-1665.
- Thut G, Nietzel A, Brandt SA, Pascual-Leone A. 2006. Alpha-band electroencephalographic activity over occipital cortex indexes visuospatial attention bias and predicts visual target detection. *J Neurosci*. 26:9494-9502.
- Tommerdahl M, Simons SB, Chiu JS, Favorov O, Whitsel BL. 2006. Ipsilateral input modifies the primary somatosensory cortex response to contralateral skin flutter. *J Neurosci*. 26:5970-5977.
- van Dijk H, Schoffelen JM, Oostenveld R, Jensen O. 2008. Prestimulus oscillatory activity in the alpha band predicts visual discrimination ability. *J Neurosci*. 28:1816-1823.
- van Dijk H, van der Werf J, Mazaheri A, Medendorp WP, Jensen O. 2010. Modulations in oscillatory activity with amplitude asymmetry can produce cognitively relevant event-related responses. *Proc Natl Acad Sci U S A*. 107:900-905.
- van Ede F, de Lange F, Jensen O, Maris E. 2011. Orienting attention to an upcoming tactile event involves a spatially and temporally specific modulation of sensorimotor alpha- and beta-band oscillations. *J Neurosci*. 31:2016-2024.
- van Ede F, Jensen O, Maris E. 2010. Tactile expectation modulates pre-stimulus beta-band oscillations in human sensorimotor cortex. *Neuroimage*. 51:867-876.
- van Elswijk G, Maj F, Schoffelen JM, Overeem S, Stegeman DF, Fries P. 2010. Corticospinal beta-band synchronization entails rhythmic gain modulation. *J Neurosci*. 30:4481-4488.
- von Stein A, Chiang C, König P. 2000. Top-down processing mediated by interareal synchronization. *Proc Natl Acad Sci U S A*. 97:14748-14753.
- Wühle A, Preissl H, Braun C. 2011. Cortical processing of near-threshold tactile stimuli in a paired-stimulus paradigm—an MEG study. *Eur J Neurosci*. 34:641-651.
- Wyart V, Tallon-Baudry C. 2009. How ongoing fluctuations in human visual cortex predict perceptual awareness: baseline shift versus decision bias. *J Neurosci*. 29:8715-8725.
- Zhang Y, Ding M. 2010. Detection of a weak somatosensory stimulus: role of the prestimulus mu rhythm and its top-down modulation. *J Cogn Neurosci*. 22:307-322.

right (contralateral) SI

right (contralateral) SII

**A**

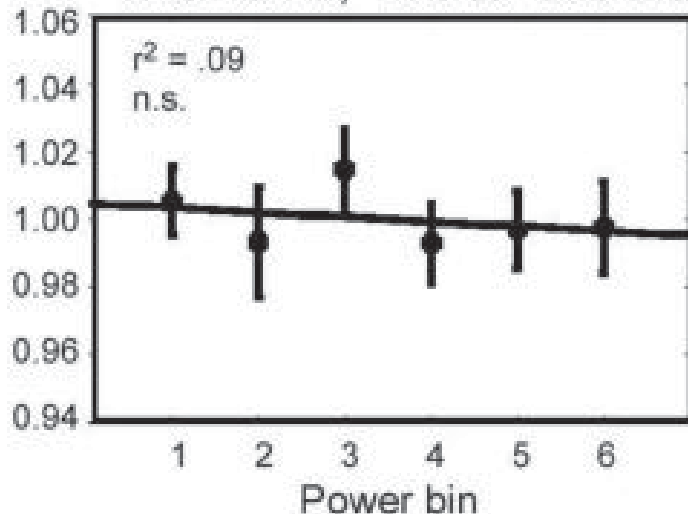
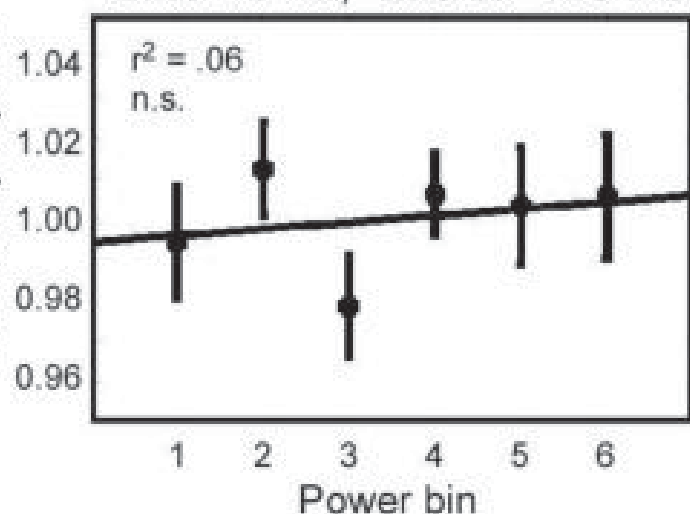
SOA: 30 ms (beta-band)

**B**

relative proportion of  
simultaneity reports

27.5-40 Hz; -225 to -125 ms

17.5-40 Hz; -475 to -275 ms



**C**

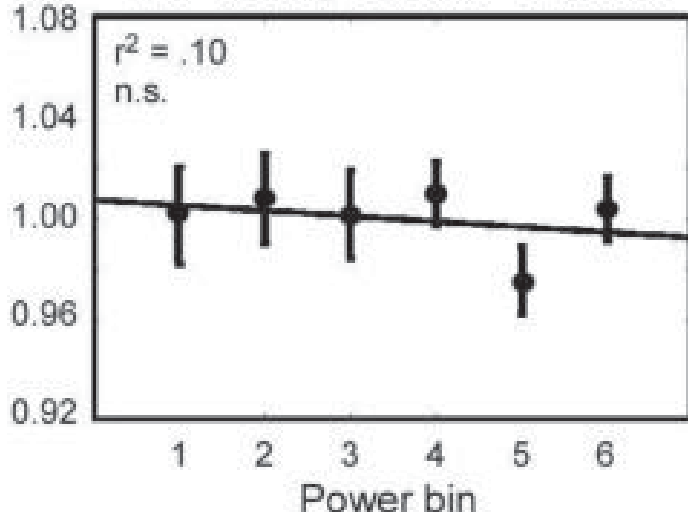
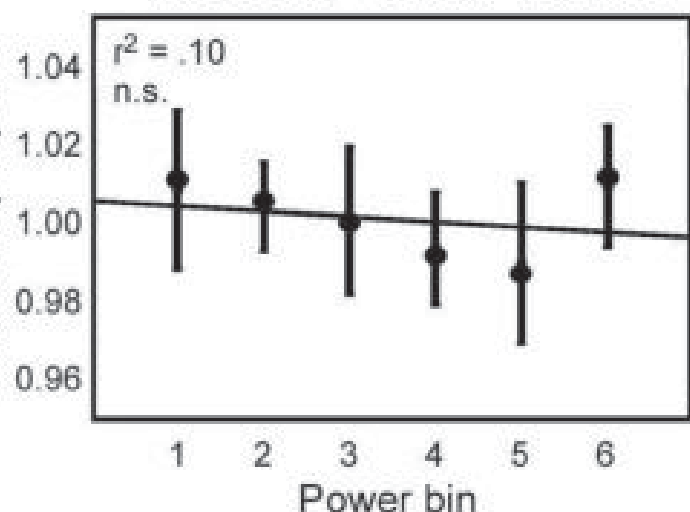
SOA: 45 ms (beta-band)

**D**

relative proportion of  
simultaneity reports

15-35 Hz; -150 to +50 ms

25-40 Hz; -350 to -200 ms



**E**

SOA: 45 ms (alpha-band)

**F**

relative proportion of  
simultaneity reports

7.5-12.5 Hz; -150 to +50 ms

7.5-12.5 Hz; -150 to +50 ms

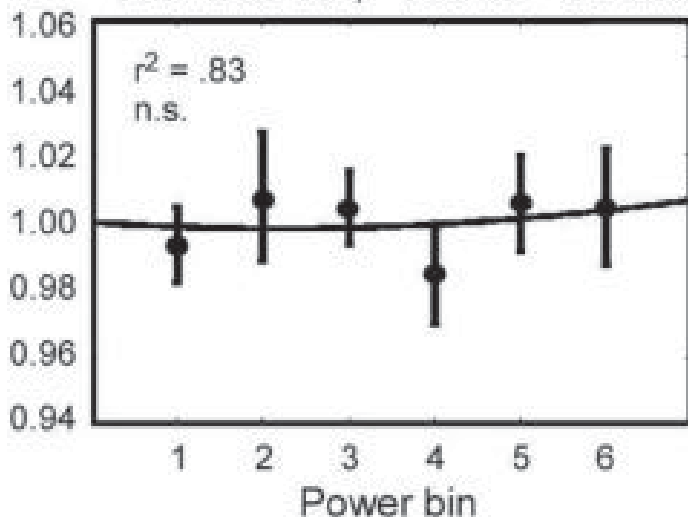
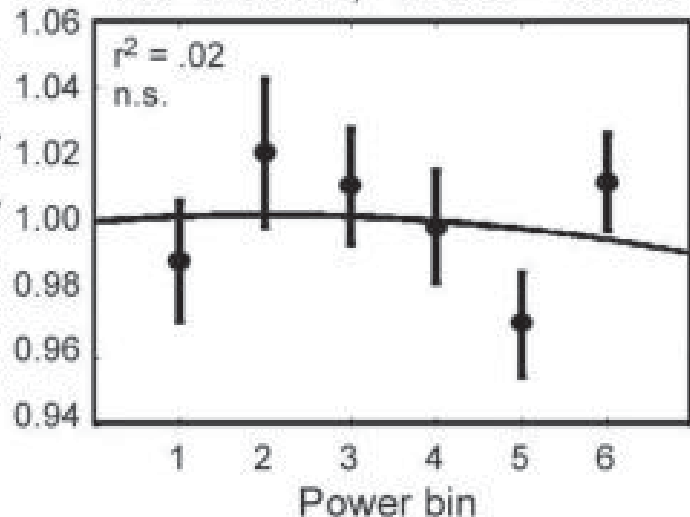


Fig. S1: Same analyses as in Fig. 4 but for contralateral sensors. No significant correlations were found.

16) **Lange, J.**, Oostenveld, R., & Fries, P. (2011).

Perception of the touch-induced visual double-flash illusion correlates with changes of rhythmic neuronal activity in human visual and somatosensory areas.

*NeuroImage*, 54(2), 1395–1405.

Impact factor: 5.895



## Perception of the touch-induced visual double-flash illusion correlates with changes of rhythmic neuronal activity in human visual and somatosensory areas

Joachim Lange<sup>a,b,\*</sup>, Robert Oostenveld<sup>a,c</sup>, Pascal Fries<sup>a,c</sup>

<sup>a</sup> Donders Institute for Brain, Cognition and Behaviour, Radboud University Nijmegen, Kapittelweg 29, 6525 EN Nijmegen, The Netherlands

<sup>b</sup> Medical Faculty, Institute for Clinical Neuroscience and Medical Psychology, Heinrich-Heine-University Düsseldorf, Universitätsstr. 1, 40225 Düsseldorf, Germany

<sup>c</sup> Ernst Strüngmann Institute (ESI) in Cooperation with Max Planck Society, Deutschordenstr. 46, 60528 Frankfurt, Germany

### ARTICLE INFO

#### Article history:

Received 20 May 2010

Revised 24 August 2010

Accepted 13 September 2010

Available online 18 September 2010

#### Keywords:

Illusion

Oscillation

MEG

Somatosensory

Visual

### ABSTRACT

A single brief visual stimulus accompanied by two brief tactile stimuli is frequently perceived incorrectly as two flashes, a phenomenon called double-flash illusion (DFI). We investigated whether the DFI is accompanied by changes in rhythmic neuronal activity, using magnetoencephalography in human subjects. Twenty-two subjects received visuo-tactile stimulation and reported the number of perceived visual stimuli. We sorted trials with identical physical stimulation according to the reported subjective percept and assessed differences in spectral power in somatosensory and occipital sensors. In DFI trials, occipital sensors displayed a contralateral enhancement of gamma-band (80–140 Hz) activity in response to stimulation. In somatosensory sensors, the DFI was associated with an increase of spectral power for low frequencies (5–17.5 Hz) around stimulation and a decrease of spectral power in the 22.5–30 Hz range between 450 and 750 ms post-stimulation. In summary, several components of rhythmic activity predicted variable subjective experience for constant physical stimulation. Notably, the enhanced occipital gamma-band activity during DFI was similar in time and frequency extent to the somatosensory gamma-band response to tactile stimulation. We speculate that the DFI might therefore occur when the somatosensory gamma-response is transmitted to visual cortex. This transmission might be supported by the observed modulations in low-frequency activity.

© 2010 Elsevier Inc. All rights reserved.

### Introduction

Rhythmic neuronal activity has been proposed as a crucial factor for communication among neuronal groups (Canolty et al., 2006; Fries, 2005; Lachaux et al., 2005; Salinas and Sejnowski, 2001; Tallon-Baudry et al., 2004, 2005; Womelsdorf et al., 2007). Putative specific roles of coherent rhythmic activity include top-down modulation (Engel et al., 2001) or the effective long-range communication of neuronal groups (Gross et al., 2004; Lachaux et al., 2005; Varela et al., 2001). Synchronization of rhythmic activity has been found in cortico-cortical (Gross et al., 2004) and cortico-spinal networks (Schiffman et al., 2005).

Several studies argue that long-range communication through rhythmic neuronal activity might provide a mechanism also for cross-modal interaction. Multisensory stimuli evoke stronger rhythmic activity in the gamma-band than unisensory stimuli (Sakowitz et al., 2001; Senkowski et al., 2007). A recent intracranial study in monkeys revealed that somatosensory input in auditory cortex resets the phase of ongoing auditory cortical oscillations which leads to enhanced proces-

sing capabilities of audio-tactile stimuli (Lakatos et al., 2007). Evidence for a role of rhythmic neuronal activity for cross-sensory interaction has also been found in a cross-modal illusion (Bhattacharya et al., 2002; Mishra et al., 2007). The authors presented a briefly flashed visual stimulus accompanied by two brief auditory stimuli. This stimulation triggers, in a subset of trials, the illusory perception of a second visual stimulus, i.e. the double-flash illusion (DFI) (Shams et al., 2000). Recently, it has been demonstrated that the perception of a visual stimulus can also be altered by tactile stimulation in a similar way (Violentev et al., 2005). Both, the auditory induced and the tactile induced DFI, do not merely shift unimodal perception quantitatively (e.g. to a higher perceived luminance), but rather alter the phenomenological quality of the percept. Such illusions in which identical stimulation can lead to categorically different visual perception are rare but offer an intriguing opportunity to study cross-modal interactions and perception in general (Haynes et al., 2005; Leopold et al., 2002; Wilke et al., 2006).

The neurophysiological basis of the DFI has been investigated for the audio-visual DFI. These EEG studies found among other results that gamma band activity in occipital areas was enhanced for trials in which subjects perceived the illusion (Bhattacharya et al., 2002; Mishra et al., 2007). The neurophysiological basis of the touch-induced visual DFI has so far not been investigated. Since rhythmic neuronal activity has been proposed as a general mechanism for

\* Corresponding author. Medical Faculty, Institute for Clinical Neuroscience and Medical Psychology, Universitätsstraße 1, 40225 Düsseldorf, Germany. Fax: +49 2118113015.

E-mail address: [joachim.lange@med.uni-duesseldorf.de](mailto:joachim.lange@med.uni-duesseldorf.de) (J. Lange).

cross-modal integration, the objective of the present study was to investigate its putative role for the dynamic interaction of somato-sensory and visual areas in the visuo-tactile DFL.

**Methods**

*Subjects*

Twenty-two right-handed volunteers (12 female, mean age ( $\pm$  SD)  $22.3 \pm 2.7$  years) without any known history of neurological disorders participated in this study. All participants had normal or corrected-to-normal vision. The experiment was approved by the local ethics committee, and each subject gave written informed consent prior to the experiment, according to the Declaration of Helsinki.

*Stimuli, tasks, and procedure*

Subjects were lying comfortably in supine position with their head placed in the horizontally positioned MEG helmet. Visual stimuli were presented using an LCD projector located outside the magnetically shielded room and back-projected onto a translucent screen via a mirror-system. The vertical refresh rate of the LCD projector was 60 Hz. The screen was positioned 70 cm in front of the subjects so that they could comfortably view the visual stimuli.

The experimental paradigm and the stimuli are illustrated in Fig. 1. Each trial started with the presentation of a fixation point (Gaussian of diameter  $0.5^\circ$ , luminance  $7 \text{ cd/m}^2$ ) in the middle of the screen. Subjects maintained fixation on this dot throughout the entire trial. After 700 ms, a stimulation period of 90 ms started in which subjects received visual and/or tactile stimulation. Visual stimulation consisted of uniform gray discs ( $2.5^\circ$  diameter, average luminance over subjects  $2.3 \text{ cd/m}^2$ , see below for details about the luminance of the visual stimuli) presented for 16 ms,  $17^\circ$  left of the fixation dot. Visual stimuli were presented eccentrically because this increased the likelihood to experience the visual illusion (Shams et al., 2000).

Tactile stimulation was given through a piezoelectrical Braille stimulator (Metec, Stuttgart, Germany) (Bauer et al., 2006) that was taped to the subjects' left index finger. The Braille stimulator consisted

of a  $2 \times 4$  matrix of pins and was driven using custom-built electronic circuitry. For the tactile stimulation, all eight pins were lifted simultaneously by 2 mm, stayed elevated for 30 ms, and were then lowered again.

The number of visual and/or tactile stimuli could be zero, one, or two. All nine possible visuo-tactile combinations were used (Fig. 1B). We will address the different conditions as "vxty" for a condition with x visual and y tactile stimuli. Thus, stimuli could be either single unimodal (v1t0, v0t1), double unimodal (v2t0, v0t2) with onsets of both stimuli separated by 60 ms, or bimodal combinations of tactile and visual stimuli. Bimodal visuo-tactile stimuli could either appear synchronously (v1t1, v2t2). In the latter condition (v2t2) the onsets of both pairs of visuo-tactile stimuli were separated by 60 ms. Or one tactile stimulus was presented between two visual stimuli (v2t1) or vice versa (v1t2). Finally, one condition did not contain any stimulation at all (v0t0).

The stimulation period was followed by a post-stimulus period of 1000 ms in which only the fixation dot was visible. Then, the contrast of the fixation dot was increased by 40% indicating the response period. Subjects were asked to report the number of perceived visual stimuli and to ignore the tactile stimulations. Responses were given by pressing one of three buttons with fingers of the right hand (Fig. 1A) on an optical button box (Lumitouch, Photon Control Inc., Burnaby, Canada). Button presses were counterbalanced for the critical responses (i.e. one or two stimuli). For half of the subjects the button configuration was: thumb press: zero stimuli; index finger: one stimulus; middle finger: two stimuli; for the other half of the subjects the button configuration was: thumb press: zero stimuli; middle finger: one stimulus; index finger: two stimuli. Additionally, subjects reported their confidence by pressing the respective button once (confident) or twice (not confident). The fraction of not-confident trials was below 5%. Thus, confident and not-confident trials were collapsed for the analysis. Since confidence ratings were high for each subject, we conclude that the results express subjects' subjective perception rather than indecisiveness in a two-alternative choice task, in agreement with a recent direct investigation of this issue (McCormick and Mamassian, 2008).

After the subject's response, or maximally 3000 ms after the increase in fixation dot luminance, the next trial started. Only

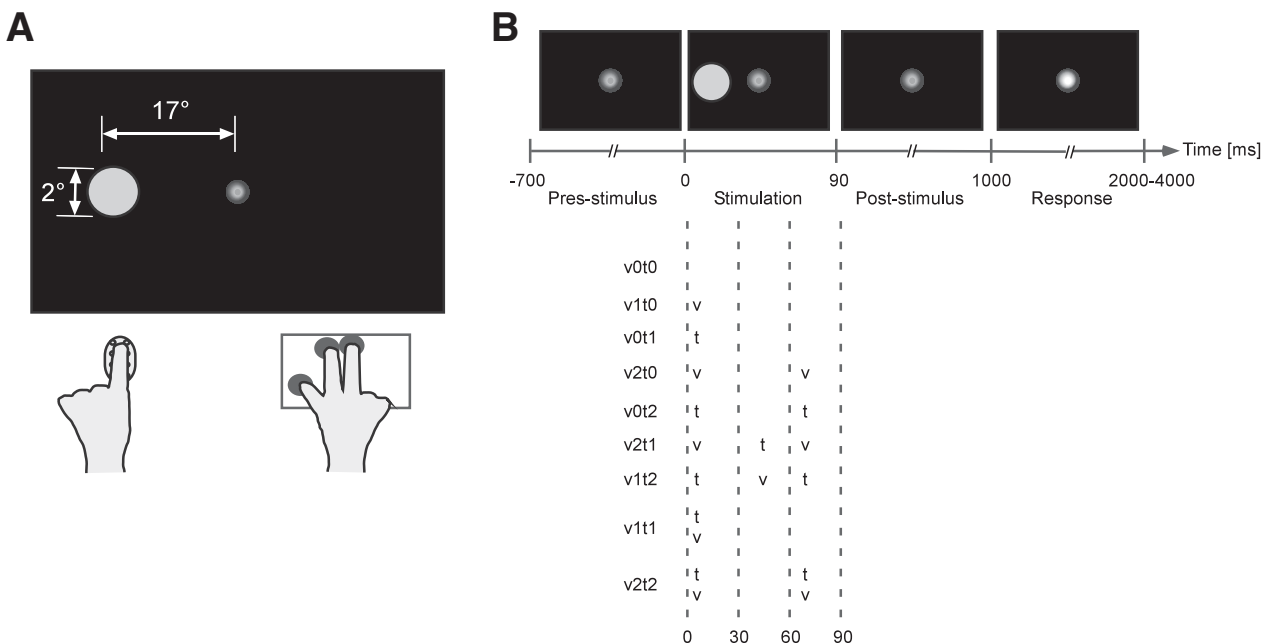


**Fig. 1.** Schematic illustration of the experimental paradigm and setup. A, schematic overview of the setup. Subjects fixated a central dot while they received tactile stimulation on their left index finger and/or visual stimulation. Visual stimuli consisted of a gray disc presented at  $17^\circ$  eccentricity in the left visual hemifield, on the horizontal meridian. Subjects responded by pressing one of three buttons with their right hand. B, illustration of a single trial and of the different experimental conditions. All nine conditions were presented in random order within a block. The entire experiment consisted of 100 blocks.

responses given during the response period were analyzed. Trials in which the response was given before the response period were discarded from analysis.

Both, the prestimulus and the post-stimulus intervals were constant for the following reasons:

- 1) The study focuses on spectral power. Since power is a rectified quantity, anticipatory perturbations would be visible in the average with both, a constant and a varying stimulus/response timing.
- 2) By varying the time of stimulus onset, we would have created a time-varying hazard rate and corresponding expectation and thereby had created more variance of neuronal activity at stimulus onset.
- 3) The main focus of our study was on illusion effects, i.e. on perceptual contrasts between conditions of identical physical stimulation. A fixed time interval minimizes variance due to anticipation.

For the analysis of the effects of sensory stimulation *per se*, a post-stimulus period is compared to a pre-stimulus baseline. This comparison is not immune to anticipatory signals. However, the stimulation contrasts are not central to the study. They are only used to constrain the sensors (regions of interest) for the subsequent investigation of the illusion contrasts. Furthermore, the stimulation contrasts basically confirm existing findings and are thus very unlikely caused purely by expectation.

Previous studies reported a high inter-subject variability of illusory trials despite identical stimulations for all subjects (Mishra et al., 2007; Shams et al., 2000; Violyentev et al., 2005). To ensure a balanced ratio of illusory and non-illusory trials within each subject, we adapted the luminance of the visual stimuli for each subject individually prior to the experiment by a staircase method. These pre-tests also served as training trials for the subjects and lasted about 5 min. The resulting luminance of the visual stimuli was  $2.3 \pm 0.2$  cd/m<sup>2</sup> (mean  $\pm$  SEM).

To increase statistical power for the investigation of the illusory effect, the condition v1t2 was presented twice as often as the other conditions. One pseudorandom sequence of all conditions (including two times v1t2) constituted one block. After ten blocks, subjects were allowed to take a short break. Overall, the experiment consisted of 100 blocks, resulting in 100 trials for each condition (200 trials for condition v1t2) and a recording session of  $\sim 1$  h. Subjects were instructed to blink only during the response period or during the breaks and to press the buttons only during the response periods.

The sound generated by the Braille cells was strongly attenuated by encapsulating them into foam. Additionally, a very weak residual sound was masked by presenting subjects with auditory white noise via pneumatic earphones. Behavioral tests preceding the experiment confirmed that subjects did not hear the clicking of the Braille cells.

Stimuli were controlled using the software "Presentation" (Neurobehavioral Systems, Albany).

#### Data acquisition

##### MEG recordings

Electromagnetic brain activity was recorded using a whole head 151-channel or 275-channel MEG system (CTF systems Inc., Port Coquitlam, Canada). Data from the 275-channel system were interpolated to a common 151-channel template using a procedure that was also used to compensate for differences in subjects' head position (see paragraph 2.4.1 on Preprocessing for details). The system was moved to a horizontal position and subjects were recorded in supine position. We recorded vertical and horizontal eye movements simultaneously, by measuring the electrooculogram (EOG) through electrodes placed below and above the left eye and on the outer sides of each eye. MEG/EOG data were low-pass filtered at 300 Hz and sampled continuously at a rate of 1200 Hz. Subjects' head position relative to the gradiometer array was determined before and after the recording session by measuring the position of reference coils placed at the subjects' nasion and at the left and right ear canals.

##### Structural MRI

For each subject, a full-brain high-resolution anatomical MR image was acquired on a 1.5T or 3T whole-body scanner (Siemens, Erlangen, Germany) using a volume head coil for radio frequency transmission and signal reception. We applied standard T1-weighted sequences. MRI reference markers were placed at the subjects' nasion and at the left and right ear canals for alignment of the MEG and MRI coordinate systems.

##### Data analysis

##### Preprocessing

Data were analyzed using the FieldTrip software (<http://fieldtrip.fcdonders.nl>), an open source Matlab toolbox for neurophysiological data analysis developed at the Donders Institute for Brain, Cognition and Behaviour, Nijmegen.

Power line noise was removed from the continuous data using a Fourier transformation of 10-s long signal periods and subtracting the 50, 100 and 150 Hz components. This was done separately for all 10-s periods around all periods of interest.

Using a semi-automated routine, segments contaminated by eye movements or blinks, artifacts caused by muscle activity, and jump artifacts in the MEG signal caused by the SQUID electronics were removed. If the length of a trial was smaller than 800 ms, the entire trial was removed. All trials in which subjects responded too early (i.e. during the 1000 ms post-stimulus period after stimulus presentation, see Fig. 1), or trials in which no response was given, were discarded.

Differences in subjects' head positions with respect to the MEG sensors may cause smearing of activity when constructing the grand-average topography over subjects. To compensate for this and to interpolate the data from the 275-channel and the 151-channel system, the individual subjects' MEG data were interpolated to a common 151-channel-template position for the MEG sensors with respect to the head. Each subjects' head shape was reconstructed from the MRI and a superficial layer of dipoles was placed 1 cm beneath the inner skull surface, approximately in the sulcal gray matter. This dipole layer consisted of 642 evenly spaced nodes covering the whole surface, with a regional source (i.e. free orientation) at every node. The leadfield matrix for all combined sources was computed using an individual forward model for every subject (Nolte, 2003). The strength of each of the  $3 \times 642$  dipole components was estimated using a minimum norm estimate (MNE). The MNE was done using the More-Penrose pseudoinverse of the leadfield matrix by computing the singular value decomposition and regularized by truncating the singular values of the leadfield matrix at 1/1000 of the maximal singular value. The estimated strength of these dipoles in the gray matter was subsequently used to compute the field distribution at the location of each sensor in the template gradiometer array, again using the individual forward model. The placement of the dipole layer in grey matter ensures that the forward computed field distribution resembles the actual distribution of the field of the true underlying sources. This method is robust and yields accurate results, regardless of the position of the field generator (Knösche, 2002). Subsequently, planar gradients for a given sensor were estimated from the axial field distribution and computed separately in vertical and horizontal direction by comparing the field at that sensor with its neighbors (Bastiaansen and Knösche, 2000). An advantage of the planar gradient transformation over axial gradient data is that the signal amplitude is largest directly above a source. This is particularly advantageous when interpreting distributions of spectral power at the sensor level.

##### Spectral analysis

We analyzed the data in the frequency domain. Power spectra were computed by using a short time discrete Fourier transform on temporal windows sliding in 25-ms steps. Two frequency ranges were analyzed separately: A low-frequency band (5–40 Hz) was analyzed

with analysis windows of 400 ms length, tapered with a single Hanning window resulting in a spectral smoothing of roughly  $\pm 2.5$  Hz. A high-frequency band (40–150 Hz) was analyzed with analysis windows of 200 ms length. For the high-frequency band, we applied a multi-taper approach to the respective analysis windows to optimize spectral concentration over the frequency of interest (Mitra and Pesaran, 1999). We applied eleven Slepian tapers resulting in a spectral smoothing of  $\pm 30$  Hz. Spectral power was first estimated per trial and taper and then averaged across trials and tapers.

The long window for the low-frequency band was chosen, because known, physiological low-frequency bands are relatively narrow and closely spaced. We therefore aimed at a spectral resolution in the low-frequency range of roughly  $\pm 2.5$  Hz. A spectral resolution of 2.5 Hz requires analysis windows of at least the inverse of 2.5 Hz, i.e. 0.4 s.

In the higher frequency range, frequency bands of physiological rhythms are broader and spaced more far apart. We could therefore afford to use a window that was half the size used for the low frequencies, i.e. 0.2 s. A further reduction in window length would have been problematic. (1) It would have rendered the windows of temporal support for low and high frequencies even more disparate. (2) It would have created problems in the group analysis when different subjects had slightly different times of spectral perturbations.

We defined regions of interest (ROIs) in sensor space, in which we analyzed the spectral power. The choice of ROIs was motivated by our focus on sensory representations. We therefore defined the ROIs as the region showing the most consistent spectral perturbations of rhythmic activity in response to tactile/visual stimulation. First, all trials with purely tactile stimulation (v0t1 and v0t2) were pooled. These trials showed clear spectral components in the low-, mid- and high-frequency bands (Fig. 3A). For each time–frequency band, we determined the topographical distribution (Fig. 3B). We normalized and rectified the amplitudes of the three resulting patterns (i.e. response amplitudes were normalized to values between 0 and 1), averaged these patterns, and determined the 10 sensors which captured the maxima of the averaged pattern. The spectral patterns overlapped in 10 MEG sensors in the right central region, contralateral to tactile stimulation (RC13, RC14, RC15, RC21, RC22, RC23, RC24, RC31, RC32, RP34). This set of sensors defined the somatosensory region of interest.

Secondly, all trials with purely visual stimulation (v1t0 and v2t0) were pooled. These trials showed four clear spectral components in the low-, mid- and high-frequency bands (Fig. 4A). In line with the analysis of the somatosensory ROI, we averaged the normalized and rectified the four resulting topographical representations and determined the 10 sensors which captured the maxima of the averaged pattern (Fig. 4B). The spectral patterns overlapped in 10 MEG sensors in the right and central occipital region, contralateral to visual stimulation (RO21, RO22, RO31, RO32, RO33, RO41, RO42, ZO01, LO31, LO32). This set of sensors defined the occipital region of interest.

#### Statistical analysis

We tested for effects of sensory stimulation and for effects of subjective perception.

To test for the overall effect of tactile and visual stimulation, all trials with purely tactile stimulation (v0t1 and v0t2) were pooled into a new tactile-only condition, and all trials with purely visual stimulation (v1t0 and v2t0) were pooled into a new visual-only condition. The response to sensory stimulation was assessed by comparing, within those unimodal stimulation conditions, the post-stimulus period to the pre-stimulus baseline period (–300 ms to –100 ms before stimulus onset, collapsed across time). To test for an effect of the DFI, we sorted the v1t2 trials into trials with DFI and without DFI.

For each subject separately, we averaged the spectral power over the sensors of interest (see Spectral analysis). We visually inspected the power spectra and defined broad time–frequency regions of

interest that captured visible perturbations, but restricted the time–frequency range over which multiple comparison correction was performed later. Those broad time–frequency regions correspond to the time–frequency ranges shown in the figures. The two conditions were compared with an independent samples *t*-test (i.e. “post-stimulus versus baseline,” or “DFI versus non-DFI”). This was done for each subject and each time–frequency pixel and therefore resulted in time–frequency *t*-maps. The subsequent group level statistic determined whether inside those regions of interest, there were time–frequency clusters with effects that were significant at the random effects level after correcting for multiple comparisons along both the time and the frequency dimension.

The group level statistic used those *t*-maps as inputs and determined their consistency across subjects. The null hypothesis was that the data from the two conditions were not different and could therefore be exchanged. We therefore tested exchangeability using a non-parametric permutation approach (Maris and Oostenveld, 2007). We choose this approach for several reasons: First, it is free of assumptions about the underlying distributions. Second, it is not affected by the fact that there was partial dependence (due to overlap) between neighboring time–frequency pixels. Third, it offers an elegant way to correct for multiple comparisons. The procedure was as follows:

- 1) We defined the test-statistic to be the *t*-value pooled across subjects, i.e. the sum of the individual subjects' *t*-values divided by the square root of the number of subjects. This test-statistic was determined per time–frequency pixel.
- 2) The pooled *t*-map was thresholded with a non-multiple comparison corrected a priori *t*-value threshold of 1.96, corresponding to a parametric two-sided paired *t*-test with 5% false positives.
- 3) This resulted in clusters of adjacent time–frequency pixels for which we determined the sum of the test statistic. This sum was defined to be our cluster-level test statistic.
- 4) We performed 5000 randomizations. In each randomization, we selected a random subset of subjects. For those subjects, the *t*-values were inverted, i.e. all time–frequency *t*-values were multiplied with minus one. This is equivalent to an exchange of the two conditions and therefore implements a new dataset under the null-hypothesis of exchangeability (Maris and Oostenveld, 2007).
- 5) For each of the 5000 randomization, steps (1) through (3) were repeated.
- 6) For each randomization, only the maximal and the minimal cluster-level test statistic across all clusters were retained and placed into two histograms, which we address as maximum (or minimum, respectively) cluster-level test statistic histograms.
- 7) After all 5000 randomizations, we determined, for each cluster from the observed data, the fraction of the maximum (minimum) cluster-level test statistic histogram that was greater (smaller) than the cluster-level test statistic from the observed cluster. The smaller of the two fractions was retained and divided by 5000, giving the multiple comparisons corrected significance thresholds for a two-sided test.

Please note that this procedure implements a random effect analysis, because the randomization (condition exchange, i.e. *t*-value inversion) was done at the level of subjects. Had we simply thresholded the pooled *t*-values, this had implemented a fixed effect analysis, but rather we used those pooled *t*-values only as a well normalized input to the group level random effect analysis.

To analyze the contribution of time-locked (evoked) components, we sorted the v1t2 trials into DFI and non-DFI trials and averaged the trials in the time-domain. To optimize the analysis of time-locked data, averaging was performed before computation of planar fields. Additionally, we computed the spectral power of these time-locked data. Statistical testing was performed separately in the time and frequency domain.

### Correlation analysis

The main, early post-stimulus DFI effects were found to be enhancements of somatosensory low-frequency and visual gamma-band activity. For those effects, we tested whether the somatosensory and visual effects were correlated across trials. For each of the effects, those time–frequency points were selected that showed significant DFI effects on the group level. Subsequently, for each subject and trial, the power in those time–frequency regions was expressed as percent change relative to baseline. Within each subject, we then determined the Spearman rank correlation between visual gamma and somatosensory low-frequency across trials. The resulting correlation coefficients were tested against a null hypothesis of no correlation, using a one-sample *t*-test across subjects.

### Eye movements

Although trials contaminated by eye movements have been discarded during preprocessing, we tested for residual eye movements. To analyze directly whether eye-movements differed between DFI trials and non-illusory trials, we applied the procedure described in the section *Statistical analysis* for MEG-channels to the EOG-channels in the time domain. To this end, we first computed eye movements in horizontal and vertical direction and then combined them to assess overall eye movements. For the combination, we used an Euclidian measure ( $EOG_{comb} = \sqrt{EOG_{vert}^2 + EOG_{hor}^2}$ ), with  $EOG_{comb}$  denoting combined EOG channels and  $EOG_{vert}$  and  $EOG_{hor}$  the vertical and horizontal channels, respectively. Statistical analysis was performed separately for horizontal, vertical and overall eye movements.

## Results

### Behavioral results

Subjects made negligible errors when judging the number of presented visual stimuli in six out of nine conditions (Fig. 2). These were the conditions without visual stimulation, the conditions in

which the number of visual and tactile stimuli was the same and the condition in which only one visual stimulus was presented. However, trials with one visual and two tactile stimuli (v1t2 condition), were perceived as two visual stimuli in  $45.8 \pm 0.4\%$  (mean  $\pm$  SEM). Statistical analysis revealed that the presence of a second tactile stimulus in condition v1t2 significantly increased the proportion of incorrect responses (i.e. perception of illusory second flashes) compared to condition v1t1 ( $t(21) = 11.9$ ,  $p < .0001$ ), i.e. confirming previous results that subjects experienced the double flash illusion (DFI) (Mishra et al., 2007; Shams et al., 2000; Violentev et al., 2005). To confirm that the DFI is caused by perceptual processes, we performed an additional analysis based on signal detection theory. For this analysis, we denoted correctly perceived double flashes as “hits”, correctly perceived single flashes as “correct rejections.” Trials with a single flash that were erroneously perceived as two flashes were denoted as “false alarms,” and trials with two flashes that were erroneously reported as a single flash as “misses” (McCormick and Mamassian, 2008; Violentev et al., 2005; Watkins et al., 2006). The presence of two tactile stimuli significantly decreased sensitivity ( $d' = 1.78 \pm 0.16$ ; mean  $\pm$  SEM) by 19.8% compared to the presence of one tactile stimulus ( $d' = 2.19 \pm 0.20$ ,  $t(21) = 2.24$ ,  $p = 0.036$ ). This confirms previous results showing that the DFI is a perceptual effect and not caused by a simple shift of criterion bias (McCormick and Mamassian, 2008; Violentev et al., 2005; Watkins et al., 2006).

### Stimulation contrast

To study the effect of tactile stimulation per se, all trials with purely tactile stimulation (v0t1 and v0t2) were pooled. We focused on the effects of stimulation, thus, we averaged over all (artifact free) trials irrespective of perceptual report, and we contrasted to the pre-stimulation baseline. The same procedure was applied to the purely visual stimuli (v1t0 and v2t0). Fig. 3A shows the time–frequency analysis for tactile stimulation averaged over the somatosensory sensors (see *Spectral analysis* for details). We found that tactile stimulation induced a highly significant reduction ( $p < 0.001$ ) of

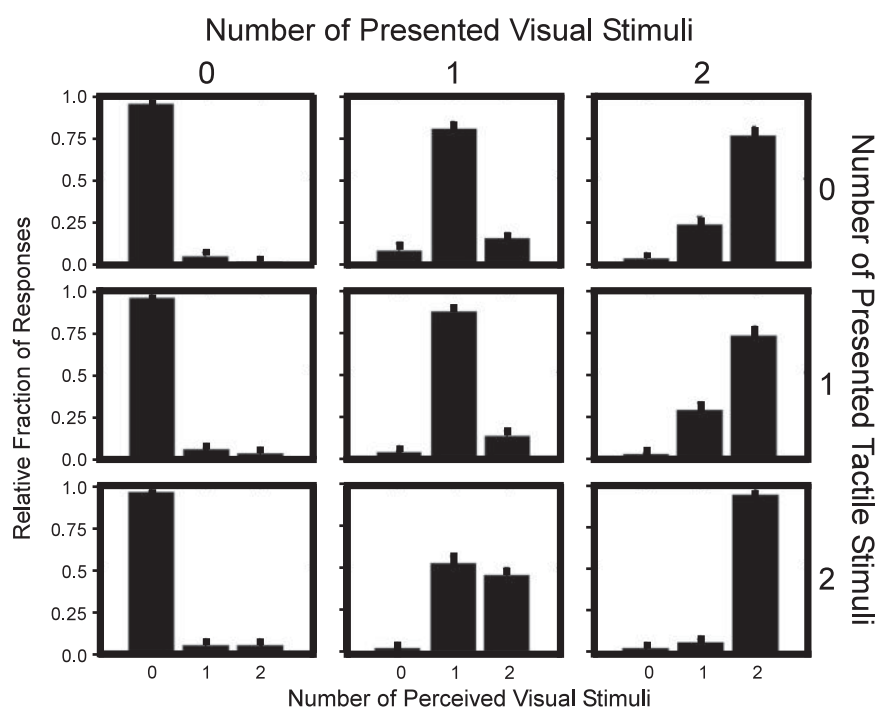
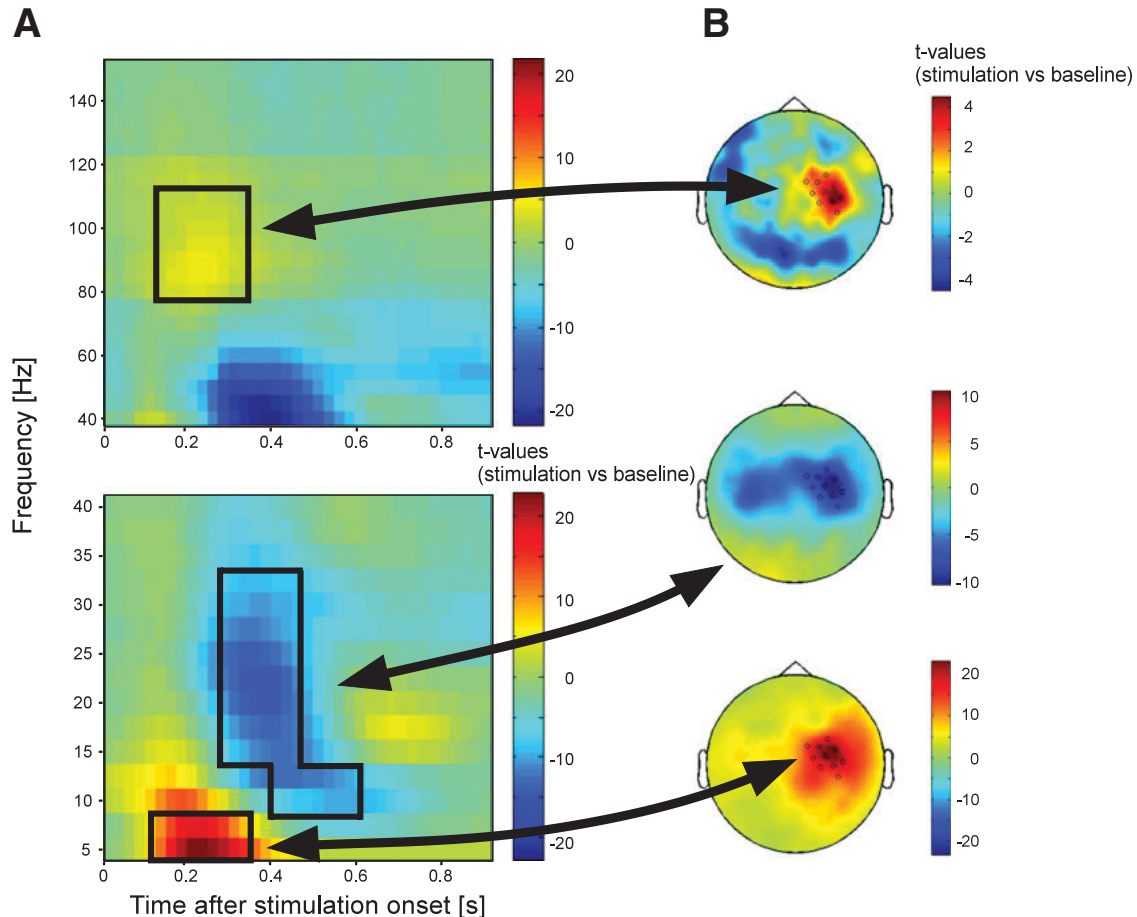


Fig. 2. Behavioral data of the experimental conditions. Bar plots show the relative fractions of behavioral responses indicating whether subjects perceived 0, 1, or 2 visual stimuli. The different panels show the results for the different stimulation conditions, comprising 0, 1, or 2 visual and/or tactile stimuli. Data are presented as mean  $\pm$  1 SEM.



**Fig. 3.** The effect of tactile stimulation of the left index finger. A, TFRs for the sensors indicated in B (black dots).  $t$ -Values were calculated separately for low and high frequencies by pooling all trials of purely tactile conditions (v0t1 and v0t2). Positive  $t$ -values indicate greater power after stimulation as compared to the pre-stimulus baseline. The negative cluster in the high frequency analysis corresponds to the negative cluster in the frequency analysis. B, separate topographies for the three clusters as highlighted in A (see Spectral analysis for details on choice of time-frequency clusters in (A) and sensors in (B)).

rhythmic activity in a time–frequency cluster that had three major lobes: One between 200 and 550 ms after stimulation and in a frequency band of 15–40 Hz, a second between 300 and 700 ms and in a frequency band of 7.5–15 Hz, and a third, although less prominent lobe between 800 and 950 ms and in a frequency band of 25–40 Hz (Fig. 3A).

Significant increases of rhythmic activity were found in two time–frequency clusters: one cluster ( $p < 0.05$ ) ranging from 75 to 500 ms and from 5 to 12.5 Hz and a second cluster ( $p < 0.05$ ), from 100 to 300 ms and ranging from 80 to 120 Hz, i.e. in the gamma-frequency band. The upper panel of Fig. 3A also shows a strong reduction in rhythmic activity from 200 to 600 ms and for the frequencies from 40 to 70 Hz. This cluster corresponds most likely to the negative cluster observed for the low frequencies (7.5–40 Hz) and becomes visible in the high-frequency analysis because of the spectral smoothing. Therefore, we will not further discuss this effect.

We averaged the  $t$ -values of all time–frequency pixels inside significant clusters to compile topographic plots. The topographies of the significant clusters reveal that the effects peak over somatosensory areas contralateral to stimulus presentation. The stimulation effect is most spatially focused for the gamma-band. The remaining two clusters reveal in addition weak ipsilateral responses.

Fig. 4 shows the effects of visual stimulation. There was a significant enhancement of rhythmic activity ( $p < 0.05$ ) with two prominent lobes: one between 200 and 400 ms and from 5 to 15 Hz, and a second lobe between 400 and 700 ms in the frequency band 12.5–40 Hz. There is a significant decrease of rhythmic activity

( $p < 0.05$ ) between 400 and 900 ms and from 65 to 150 Hz. There is also a significant increase of activity between 400 and 600 ms in the frequency band 40–60 Hz. Similar to the tactile condition, this cluster corresponds most likely to the cluster observed for the low frequencies and becomes visible in the high-frequency analysis because of the spectral smoothing. Therefore, we will not further discuss this effect.

The topographies of the significant clusters reveal that the increase in the low frequencies is spatially restricted to the occipital sensors and peaks over the contralateral side. The decrease of activity in the high frequencies has a widespread topography.

#### The double flash illusion (DFI) effect

Next, we investigated the role of rhythmic activity for the perception of a second (illusory) flash. All trials with one visual and two tactile stimuli (condition v1t2) were sorted according to the perceptual report of the subjects. We compared the spectral power in the somatosensory and occipital regions for trials in which subjects reported to perceive two flashes (on average 76 trials per subject) vs. trials in which one flash was reported (on average 88 trials). Power estimates were used for further analyses directly, without subtracting a baseline. We will address results of this comparison as DFI effects. If not mentioned otherwise, statistical tests were performed over the entire time–frequency range. For sensors overlying somatosensory areas, we found significant DFI effects in two time–frequency clusters (Fig. 5A): One cluster

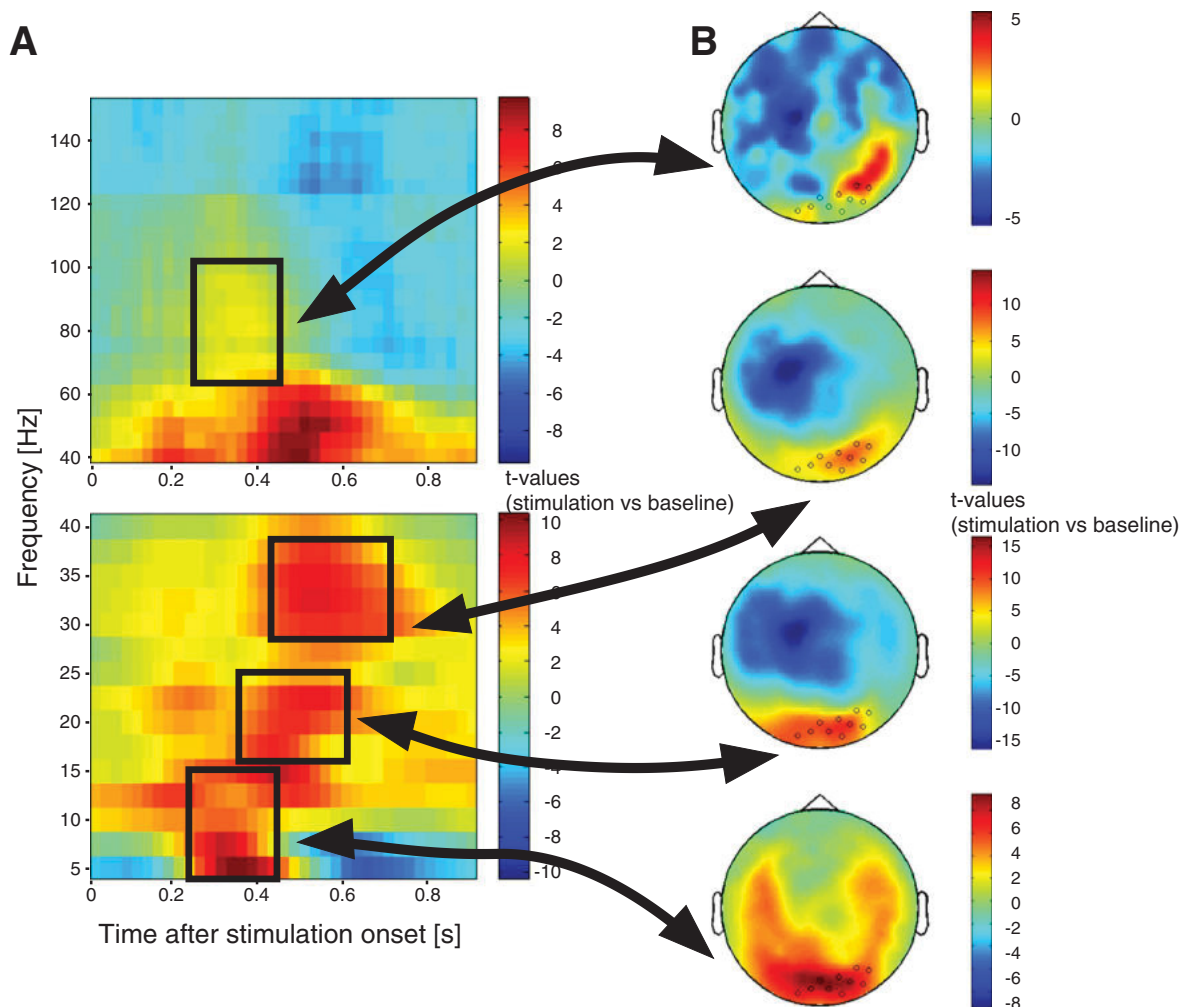


**Fig. 4.** The effect of visual stimulation. Same format as Fig. 3, but comparing visual stimulation to baseline. A, TFRs for sensors indicated in B. B, separate topographies for clusters as highlighted in A.

( $p < 0.05$ ) of increased rhythmic activity extending from  $-50$  to  $400$  ms and between  $5$  and  $17.5$  Hz, and a second cluster ( $p < 0.05$ ) of reduced rhythmic activity between  $450$ – $750$  ms and  $22.5$ – $30$  Hz. Topographical plots of both effects revealed clear spatial foci over contralateral somatosensory sensors (Fig. 5B). We tested whether these effects were attributable to stimulus-locked components. To this end, we first averaged the signals in the time domain and then performed the spectral and statistical analysis in the time- and the spectral domain as before. This did not reveal any significant DFI effects for the stimulus-locked components (Figs. S3 and S4, see Methods (section 2.4.3.)). No significant DFI effect was observed in somatosensory sensors for higher frequencies.

By contrast, in sensors over visual cortex, the main DFI effect was an increase of rhythmic activity between  $75$  and  $300$  ms and in the frequency range  $80$ – $140$  Hz, i.e. in the high gamma-band (Fig. 6A). Visual inspection of the power spectra revealed that high-frequencies were dominated by a strong decrease in the range  $40$ – $70$  Hz and that high gamma-band effects were only visible in the post-stimulus period (Fig. S1). Therefore, the statistical analysis of the high-frequency effects in the visual cortex was restricted to  $0$ – $900$  ms after stimulation and to the frequency band  $70$ – $150$  Hz. The topography of this effect revealed a focus over contralateral visual cortex, with additional peaks over parietal and left frontal areas (Fig. 6B). As in the analysis over somatosensory areas, there was no significant DFI effect for the stimulus-locked components (Figs. S3 and S5, see Statistical analysis).

Visual inspection of the increase of gamma-band activity for DFI-trials (Fig. 6) and the stimulus-driven gamma-band activity (Fig. 4) revealed that the DFI-effect occurred slightly earlier in time, in a slightly higher frequency-band, and also topographically more central than the stimulus-driven gamma effect in response to unimodal visual stimulation.

In conditions v2t0 and v2t1 subjects frequently missed one visual stimulus, i.e. they reported seeing only one flash (Fig. 2). Similar to the analyses of the DFI effect, we sorted the trials in conditions v2t0 and v2t1 sorted according to the perceptual report of the subjects and compared the spectral power in the somatosensory and occipital regions for trials in which subjects reported to perceive two flashes vs. trials in which one flash was reported. We did not find any significant differences between both perceptual reports.

The main early DFI effects were enhancements of somatosensory low-frequency and visual gamma-band activity. To test for a potential relation between those processes, we calculated the correlation across trial-by-trial variations in those effects (see Methods for details). We found the power enhancements in somatosensory low-frequency and visual gamma-band activity to be positively correlated (positive Spearman rank correlation in 21 of 22 subjects ( $t$ -test across subjects:  $t(21) = 8.4, p < 0.001$ ).

Additional analyses compared DFI and non-DFI trials in the EOG-signals but did not show any significant differences in either horizontal, vertical or overall eye-movements (Fig. S2; see Eye movement for details).

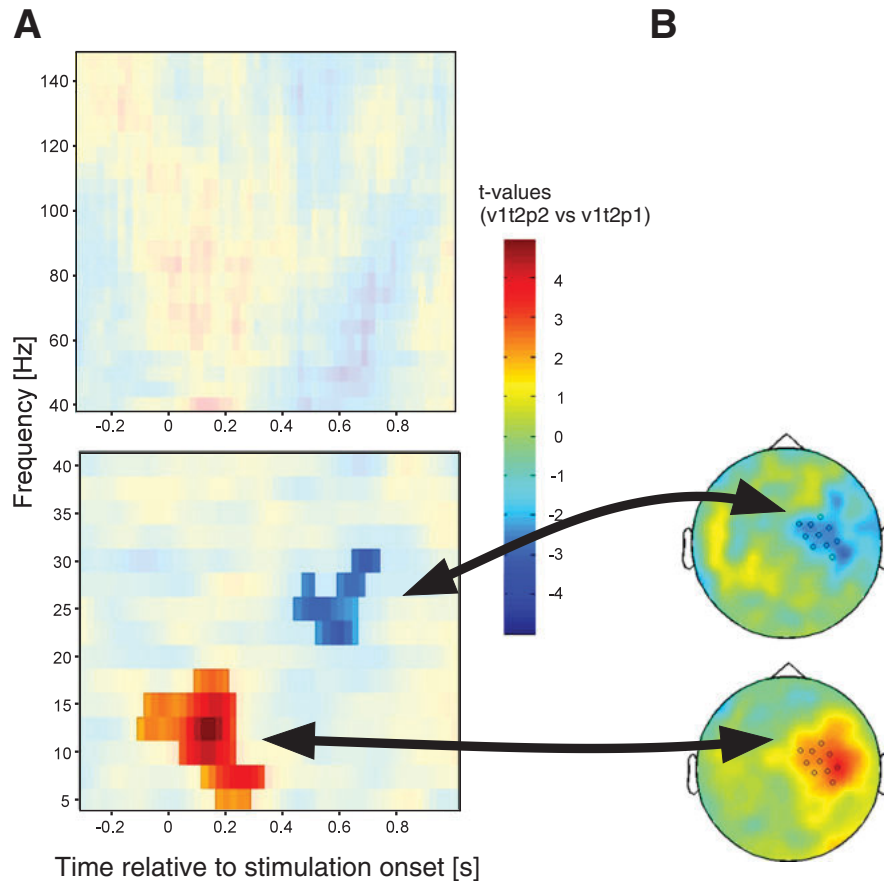


**Fig. 5.** The double flash illusion effect in somatosensory sensors. The stimulation condition was v1t2. Positive  $t$ -values indicate greater power in trials in which subjects perceived an illusory second flash as compared to trials in which they perceived the veridical single flash. Time–frequency regions that are revealed by the semitransparent white mask were significant after multiple comparison correction. Otherwise, the format is as in Fig. 3. A, TFRs for sensors indicated in B. B, separate topographies for both significant clusters as highlighted in A. The colorbar applies to both topographies.

## Discussion

We studied rhythmic neuronal activity in humans during visual and/or tactile stimulation and in relation to the induced visual percept. Isolated tactile stimulation induced enhanced low-frequency and high-gamma frequency activity, as well as reduced alpha- and beta-band activity over somatosensory cortex contralateral to stimulation and very similar to previous reports (Bauer et al., 2006; Trenner et al., 2008). The relatively weak and peripheral visual stimulus induced an earlier enhanced activity in low frequencies, a weak enhanced gamma-band activity, and a later reduced high-gamma band activity. When one visual stimulus was paired with two tactile stimuli, subjects often experienced the double-flash illusion (DFI). In trials with the DFI, occipital sensors showed enhanced gamma-band activity. Also, during the DFI, somatosensory sensors showed enhanced low-frequency activity and a reduced beta-rebound. The DFI-related enhancements in visual gamma- and somatosensory low-frequency activity were correlated across trials.

Recently, Mishra et al. (2010) have shown that directing attention to the visual stimulus increases the likelihood of perceiving the DFI. Based on this study one might speculate that also spontaneous fluctuations of ongoing attentional processes might influence the perception of the DFI-effect. Our results are in line with this hypothesis: attention has been found to (1) reduce the beta rebound in somatosensory cortex (Bauer et al., 2006; Trenner et al., 2008) and (2) enhance gamma-band activity in visual cortex (e.g. Fries et al., 2008). This interpretation proposes spontaneous fluctuations of attention as the underlying cause of both somatosensory and visual effects. In support of this, we found the DFI-related enhancements in

somatosensory low-frequency and visual gamma-band activity to be correlated across trials. Notably, states of putatively enhanced attention were not always related to more veridical perception, in agreement with previous studies (Yeshurun and Carrasco, 1998).

We find DFI effects and effects to purely visual stimulation in occipital sensors at rather high frequencies. Previous studies using MEG have reported initial high gamma response to visual stimulation before the response settles to a lower and sustained frequency band (Hoogenboom et al., 2006). Since our stimuli were presented for a short duration (16 ms), the observed effects at high frequencies might reflect the previously reported initial high gamma response before the responses settles to lower frequencies. Given the rather long latency of the somatosensory DFI effect in the beta-band, it seems unlikely that it is purely driven by bottom-up stimulus processing. Rather, it might be related to stimulus replay or other top-down mechanisms. For four reasons, however, it is unlikely that this effect is related to motor responses or response preparation: First, the effect is observed contralateral to stimulus presentation but ipsilateral to the response hand. An effect related to response preparation should have a spatial maximum contralateral to the response hand. By contrast, the observed maximum contralateral to stimulation suggests an effect at the sensory stage. Second, a control analysis of rhythmic activity contralateral to the response hand (mirroring the somatosensory ROI across the midline), did not reveal any significant effects (data not shown). Third, if the DFI effect had been due to response preparation then it should also have been visible in the analysis of the other conditions for which subjects sometimes reported one and sometimes two stimuli (i.e. conditions v2t0 and v2t1), because the response patterns (i.e. button presses)

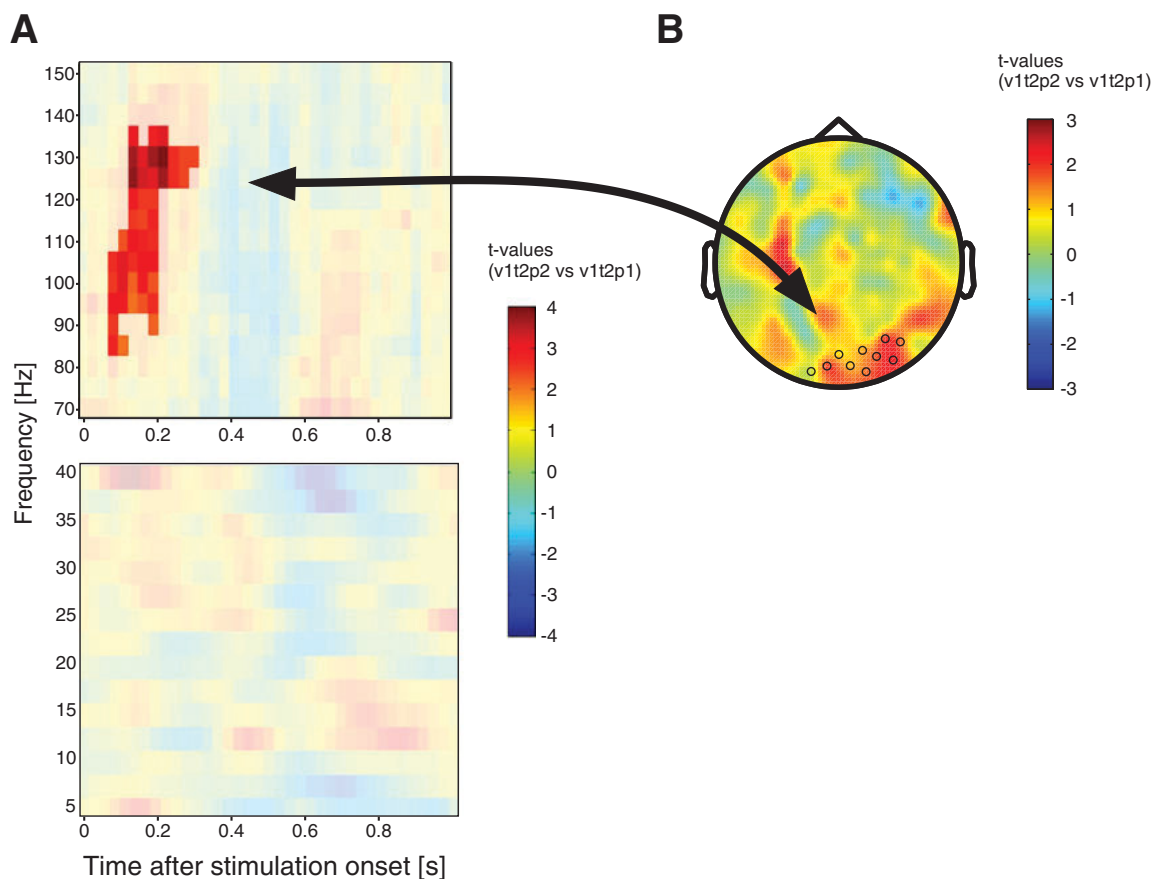


**Fig. 6.** The double flash illusion effect in visual sensors. Same analysis and format as Fig. 5. A, TFRs for sensors indicated in B. B, separate topography for significant cluster as highlighted in A.

for these conditions and DFI trials were similar. However, the analysis of these conditions did not reveal any significant effects over somatosensory cortex. Finally, the response buttons relevant for the DFI contrast (one and two stimuli) were counterbalanced across subjects. Therefore, it is unlikely that the effects were due to different preparatory signals to different fingers.

One potential concern in the interpretation of neuronal correlates of the DFI is that the DFI might be based on an ambiguity that might in principle as well be related to perception as to decision. Signal detection theory provides a measure ( $d'$ ) of the difference in subjects' perceptual representations between two conditions, independent of the subjects' response bias. In agreement with previous studies on both the audio-visual and visuo-tactile DFI, our  $d'$ -analysis revealed that the DFI cannot be explained solely as a consequence of shift in response bias (McCormick and Mamassian, 2008; Mishra et al., 2007; Violentyev et al., 2005; Watkins et al., 2006). In addition, the perceptual nature of the phenomenon is clearly favored by the phenomenological experience during the illusion. This is supported by the confidence ratings of our subjects, which were very high throughout, in agreement with a recent study addressing this issue in detail (McCormick and Mamassian, 2008).

Several previous studies have investigated the role of rhythmic neuronal activity in cross-modal integration, and to the best of our knowledge, they all investigated the integration of a visual stimulus with an auditory one. Some of those studies compared unimodal visual stimulation with bimodal stimulation and reported supra-additive responses in the bimodal condition (Sakowitz et al., 2001; Senkowski et al., 2007). Two EEG studies used the audio-visual DFI and found that the illusion is related to an enhanced activity in a lower gamma-band between 30 and 50 Hz in occipital electrodes (Bhatta-

charya et al., 2002; Mishra et al., 2007). The timing of these effects was very similar to the high-gamma DFI effect described here. By contrast, the frequency range was lower and this could be due to differences between EEG and MEG, between the analyses, and/or between the paradigms. Any of these differences might also explain why these previous studies did not report two of our central findings: (1) The similarity between the DFI effect and the tactile stimulation effect in the high gamma-frequency range; (2) DFI effects on rhythmic activity over somatosensory areas, or more generally the non-visual areas involved in the induction of the illusion.

Although Mishra et al. (2007) did not report any changes in rhythmic activity over non-visual (i.e. auditory) areas, they found an enhanced evoked component in the ERPs in sensors over auditory cortex ranging from 92 to 124 ms if subjects perceive the illusion. For DFI trials, we found a significant enhancement of low-frequencies over somatosensory areas. While the timing suggests that this effect might be related to the effect described by Mishra et al. for the audio-visual DFI, we did not find any significant contribution of stimulus-locked effects.

Our results suggest that the DFI occurred during states of enhanced attention and previous studies would suggest that in this case, the DFI should also have been associated with enhanced somatosensory gamma-band activity (Bauer et al., 2006). While somatosensory gamma-band activity was indeed enhanced at a similar time range as described by Bauer et al., this did not reach statistical significance (Fig. 5A), probably due to insufficient signal-to-noise-ratio or statistical power. However, we did find that the DFI is related to significantly enhanced gamma-band activity over visual areas. This DFI related gamma-band activity over visual areas had a strong similarity to the tactile stimulation induced gamma-band activity over

somatosensory areas and it occurred ~100–200 ms earlier in time and topographically more central than the gamma-band increase in response to isolated visual stimulation. We therefore propose that the DFI is related to a somatosensory-to-visual transmission of gamma-band activity, which occurs more likely during spontaneously enhanced attention. The consequently enhanced gamma-band activity in visual cortex during DFI will most likely enhance the impact of visual cortex on other brain areas.

It should be noted that in this hypothesis somatosensory gamma-band activity does not need to be enhanced. Rather, we speculate the DFI occurs when a given amount of somatosensory gamma-band activity is more effectively transmitted to visual cortex. While the interpretation of a transmission of gamma-band activity from somatosensory to visual cortex remains speculative, there are several studies that might propose a framework for this hypothesis. A functional interaction of somatosensory and visual cortex has been reported previously. For example, studies using transcranial magnetic stimulation provided evidence for a functional role of visual cortex for tactile discrimination tasks (Merabet et al., 2004; Zangaladze et al., 1999). Macaluso et al. (2002) reported an increased BOLD response in visual cortex if visual stimuli are accompanied by spatially congruent tactile stimuli. Also, ERP studies reported a functional modulation of visual cortex by attention to tactile stimuli (Eimer and Driver, 2000; Eimer and Van Velzen, 2002). Recently, it has been shown that selective spatial attention to tactile stimuli modulates rhythmic activity in low frequencies in occipital areas (Bauer et al., 2006).

We can only speculate about the anatomical framework that might underlie the transmission of rhythmic activity from somatosensory areas to visual areas. While there is evidence for direct connections between early visual cortex and auditory cortex (Bizley et al., 2007; Falchier et al., 2002; Rockland and Ojima, 2003) and studies indicate the possibility of direct connections of auditory and somatosensory cortices (Fu et al., 2003; Hackett et al., 2007), there is to our knowledge no evidence for similar connections from somatosensory cortex to visual cortex. Alternatively, the transmission might be relayed by higher-level multimodal areas (e.g. the superior temporal sulcus, STS) which control information transfer between sensory cortices. Such a mechanism has been suggested in fMRI studies on visuo-tactile attention tasks (Macaluso et al., 2000) as well as on audio-visual integration (Noesselt et al., 2007). In line with this hypothesis, a recent study found interactions of neurons in the STS and auditory cortex for face-voice integration (Ghazanfar et al., 2008). A third possible mechanism might be an information transfer via subcortical areas. Several studies found multimodal thalamo-cortical projections in rats (e.g. Barth et al., 1995; Nicolelis et al., 1997) and recent studies on monkeys have suggested a role of the thalamic system in audio-tactile integration by rhythmic neural activity (Lakatos et al., 2007).

Lakatos and colleagues found in their study that somatosensory inputs modulated auditory responses by changing the phase of ongoing auditory cortical oscillations. Low frequent rhythmic activity was phase reset by somatosensory stimulation which subsequently enhanced auditory induced responses when auditory inputs fell on peaks of low-frequency activity and vice versa. A similar mechanism might account for the findings in our study. However, due to the technical limitations of our method, this remains speculative.

In summary, our results elucidate some of the mechanisms behind the double flash illusion. They add to the growing evidence for a functional role of rhythmic neuronal synchronization in cognition. We hypothesize that the double flash illusion occurs when tactile induced gamma-band activity is transmitted to visual cortex. During ongoing fluctuations in attention, this transmission is more likely during patterns of rhythmic activity associated with states of enhanced attention. Further studies will be needed to confirm this hypothesis.

Supplementary materials related to this article can be found online at [doi:10.1016/j.neuroimage.2010.09.031](https://doi.org/10.1016/j.neuroimage.2010.09.031).

## Acknowledgments

We are most grateful to Sander Berends for collecting parts of the MEG data. We also thank Pieter Buur and Paul Gaalman for help with MRI recordings. JL is supported by the German Research Foundation (LA 2400/1-1), PF is supported by the Human Frontier Science Program Organization, The Netherlands Organization for Scientific Research, The Volkswagen Foundation, and the European Science Foundation's European Young Investigator Award Program.

## References

- Barth, D.S., Goldberg, N., Brett, B., Di, S., 1995. The spatiotemporal organization of auditory, visual and auditory-visual evoked-potentials in rat cortex. *Brain Res.* 678, 177–190.
- Bastiaansen, M.C., Knösche, T.R., 2000. Tangential derivative mapping of axial MEG applied to event-related desynchronization research. *Clin. Neurophysiol.* 111, 1300–1305.
- Bauer, M., Oostenveld, R., Peeters, M., Fries, P., 2006. Tactile spatial attention enhances gamma-band activity in somatosensory cortex and reduces low-frequency activity in parieto-occipital areas. *J. Neurosci.* 26, 490–501.
- Bhattacharya, J., Shams, L., Shimojo, S., 2002. Sound-induced illusory flash perception: role of gamma band responses. *NeuroReport* 13, 1727–1730.
- Bizley, J.K., Nodal, F.R., Bajo, V.M., Nelken, I., King, A.J., 2007. Physiological and anatomical evidence for multisensory interactions in auditory cortex. *Cereb. Cortex* 17, 2172–2189.
- Canolty, R.T., Edwards, E., Dalal, S.S., Soltani, M., Nagarajan, S.S., Kirsch, H.E., Berger, M.S., Barbaro, N.M., Knight, R.T., 2006. High gamma power is phase-locked to theta oscillations in human neocortex. *Science* 313, 1626–1628.
- Eimer, M., Driver, J., 2000. An event-related brain potential study of cross-modal links in spatial attention between vision and touch. *Psychophysiology* 37, 697–705.
- Eimer, M., Van Velzen, J., 2002. Crossmodal links in spatial attention are mediated by supramodal control processes: evidence from event-related potentials. *Psychophysiology* 39, 437–449.
- Engel, A.K., Fries, P., Singer, W., 2001. Dynamic predictions: oscillations and synchrony in top-down processing. *Nat. Rev. Neurosci.* 2, 704–716.
- Falchier, A., Clavagnier, S., Barone, P., Kennedy, H., 2002. Anatomical evidence of multimodal integration in primate striate cortex. *J. Neurosci.* 22, 5749–5759.
- Fries, P., 2005. A mechanism for cognitive dynamics: neuronal communication through neuronal coherence. *Trends Cogn. Sci.* 9, 474–480.
- Fries, P., Womelsdorf, T., Oostenveld, R., Desimone, R., 2008. The effects of visual stimulation and selective visual attention on rhythmic neuronal synchronization in macaque area v4. *J. Neurosci.* 28, 4823–4835.
- Fu, K.M.G., Johnston, T.A., Shah, A.S., Arnold, L., Smiley, J., Hackett, T.A., Garraghty, P.E., Schroeder, C.E., 2003. Auditory cortical neurons respond to somatosensory stimulation. *J. Neurosci.* 23, 7510–7515.
- Ghazanfar, A.A., Chandrasekaran, C., Logothetis, N.K., 2008. Interactions between the superior temporal sulcus and auditory cortex mediate dynamic face/voice integration in rhesus monkeys. *J. Neurosci.* 28, 4457–4469.
- Gross, J., Schmitz, F., Schnitzler, I., Kessler, K., Shapiro, K., Hommel, B., Schnitzler, A., 2004. Modulation of long-range neural synchrony reflects temporal limitations of visual attention in humans. *Proc. Natl. Acad. Sci. U.S.A.* 101, 13050–13055.
- Hackett, T.A., Smiley, J.F., Ulbert, I., Karmos, G., Lakatos, P., de la Mothe, L.A., Schroeder, C.E., 2007. Sources of somatosensory input to the caudal belt areas of auditory cortex. *Perception* 36, 1419–1430.
- Haynes, J.D., Deichmann, R., Rees, G., 2005. Eye-specific effects of binocular rivalry in the human lateral geniculate nucleus. *Nature* 438, 496–499.
- Hoogenboom, N., Schoffelen, J.M., Oostenveld, R., Parkes, L.M., Fries, P., 2006. Localizing human visual gamma-band activity in frequency, time and space. *Neuroimage* 29, 764–773.
- Knösche, T.R., 2002. Transformation of whole-head MEG recordings between different sensor positions. *Biomed. Technol. (Berl.)* 47, 59–62.
- Lachaux, J.P., George, N., Tallon-Baudry, C., Martinerie, J., Hugueville, L., Minotti, L., Kahane, P., Renault, B., 2005. The many faces of the gamma band response to complex visual stimuli. *Neuroimage* 25, 491–501.
- Lakatos, P., Chen, C.M., O'Connell, M.N., Mills, A., Schroeder, C.E., 2007. Neuronal oscillations and multisensory interaction in primary auditory cortex. *Neuron* 53, 279–292.
- Leopold, D.A., Wilke, M., Maier, A., Logothetis, N.K., 2002. Stable perception of visually ambiguous patterns. *Nat. Neurosci.* 5, 605–609.
- Macaluso, E., Frith, C.D., Driver, J., 2000. Modulation of human visual cortex by crossmodal spatial attention. *Science* 289, 1206–1208.
- Macaluso, E., Frith, C.D., Driver, J., 2002. Crossmodal spatial influences of touch on extrastriate visual areas take current gaze direction into account. *Neuron* 34, 647–658.
- Maris, E., Oostenveld, R., 2007. Nonparametric statistical testing of EEG- and MEG-data. *J. Neurosci. Methods* 164, 177–190.
- McCormick, D., Massarian, P., 2008. What does the illusory-flash look like? *Vis. Res.* 48, 63–69.
- Merabet, L., Thut, G., Murray, B., Andrews, J., Hsiao, S., Pascual-Leone, A., 2004. Feeling by sight or seeing by touch? *Neuron* 42, 173–179.
- Mishra, J., Martinez, A., Sejnowski, T.J., Hillyard, S.A., 2007. Early cross-modal interactions in auditory and visual cortex underlie a sound-induced visual illusion. *J. Neurosci.* 27, 4120–4131.

- Mishra, J., Martínez, A., Hillyard, S.A., 2010. Effect of attention on early cortical processes associated with the sound-induced extra flash illusion. *J. Cogn. Neurosci.* 8, 1714–1729.
- Mitra, P.P., Pesaran, B., 1999. Analysis of dynamic brain imaging data. *Biophys. J.* 76, 691–708.
- Nicolelis, M.A.L., Lin, R.C.S., Chapin, J.K., 1997. Neonatal whisker removal reduces the discrimination of tactile stimuli by thalamic ensembles in adult rats. *J. Neurophysiol.* 78, 1691–1706.
- Noesselt, T., Rieger, J.W., Schoenfeld, M.A., Kanowski, M., Hinrichs, H., Heinze, H.J., Driver, J., 2007. Audiovisual temporal correspondence modulates human multisensory superior temporal sulcus plus primary sensory cortices. *J. Neurosci.* 27, 11431–11441.
- Nolte, G., 2003. The magnetic lead field theorem in the quasi-static approximation and its use for magnetoencephalography forward calculation in realistic volume conductors. *Phys. Med. Biol.* 21, 3637–3652.
- Rockland, K.S., Ojima, H., 2003. Multisensory convergence in calcarine visual areas in macaque monkey. *Int. J. Psychophysiol.* 50, 19–26.
- Sakowitz, O.W., Quiroga, R.Q., Schürmann, M., Basar, E., 2001. Bisensory stimulation increases gamma-responses over multiple cortical regions. *Cogn. Brain Res.* 11, 267–279.
- Salinas, E., Sejnowski, T.J., 2001. Correlated neuronal activity and the flow of neural information. *Nat. Rev. Neurosci.* 2, 539–550.
- Schoffelen, J.M., Oostenveld, R., Fries, P., 2005. Neuronal coherence as a mechanism of effective corticospinal interaction. *Science* 308, 111–113.
- Senkowski, D., Talsma, D., Grigutsch, M., Herrmann, C.S., Woldorff, M.G., 2007. Good times for multisensory integration: effects of the precision of temporal synchrony as revealed by gamma-band oscillations. *Neuropsychologia* 45, 561–571.
- Shams, L., Kamitani, Y., Shimojo, S., 2000. Illusions. What you see is what you hear. *Nature* 408, 788.
- Tallon-Baudry, C., Mandon, S., Freiwald, W.A., Kreiter, A.K., 2004. Oscillatory synchrony in the monkey temporal lobe correlates with performance in a visual short-term memory task. *Cereb. Cortex* 14, 713–720.
- Tallon-Baudry, C., Bertrand, O., Hénaff, M.A., Isnard, J., Fischer, C., 2005. Attention modulates gamma-band oscillations differently in the human lateral occipital cortex and fusiform gyrus. *Cereb. Cortex* 15, 654–662.
- Trenner, M.U., Heekeren, H.R., Bauer, M., Rössner, K., Wenzel, K., Villringer, A., Alchier, A., 2008. What happens in between? Human oscillatory brain activity related to crossmodal spatial cueing. *PLoS ONE* 23.
- Varela, F., Lachaux, J.P., Rodriguez, E., Martinerie, J., 2001. The brainweb: phase synchronization and large-scale integration. *Nat. Rev. Neurosci.* 2, 229–239.
- Violyentsev, A., Shimojo, S., Shams, L., 2005. Touch-induced visual illusion. *NeuroReport* 16, 1107–1110.
- Watkins, S., Shams, L., Tanaka, S., Haynes, J.D., Rees, G., 2006. Sound alters activity in human V1 in association with illusory visual perception. *Neuroimage* 31, 1247–1256.
- Wilke, M., Logothetis, N.K., Leopoldt, D.A., 2006. Local field potential reflects perceptual suppression in monkey visual cortex. *Proc. Natl. Acad. Sci. USA* 103, 17507–17512.
- Womelsdorf, T., Schoffelen, J.M., Oostenveld, R., Singer, W., Desimone, R., Engel, A.K., Fries, P., 2007. Modulation of neuronal interactions through neuronal synchronization. *Science* 316, 1609–1612.
- Yeshurun, Y., Carrasco, M., 1998. Attention improves or impairs visual performance by enhancing spatial resolution. *Nature* 396, 72–75.
- Zangaladze, A., Epstein, C.M., Grafton, S.T., Sathian, K., 1999. Involvement of visual cortex in tactile discrimination of orientation. *Nature* 401, 587–590.